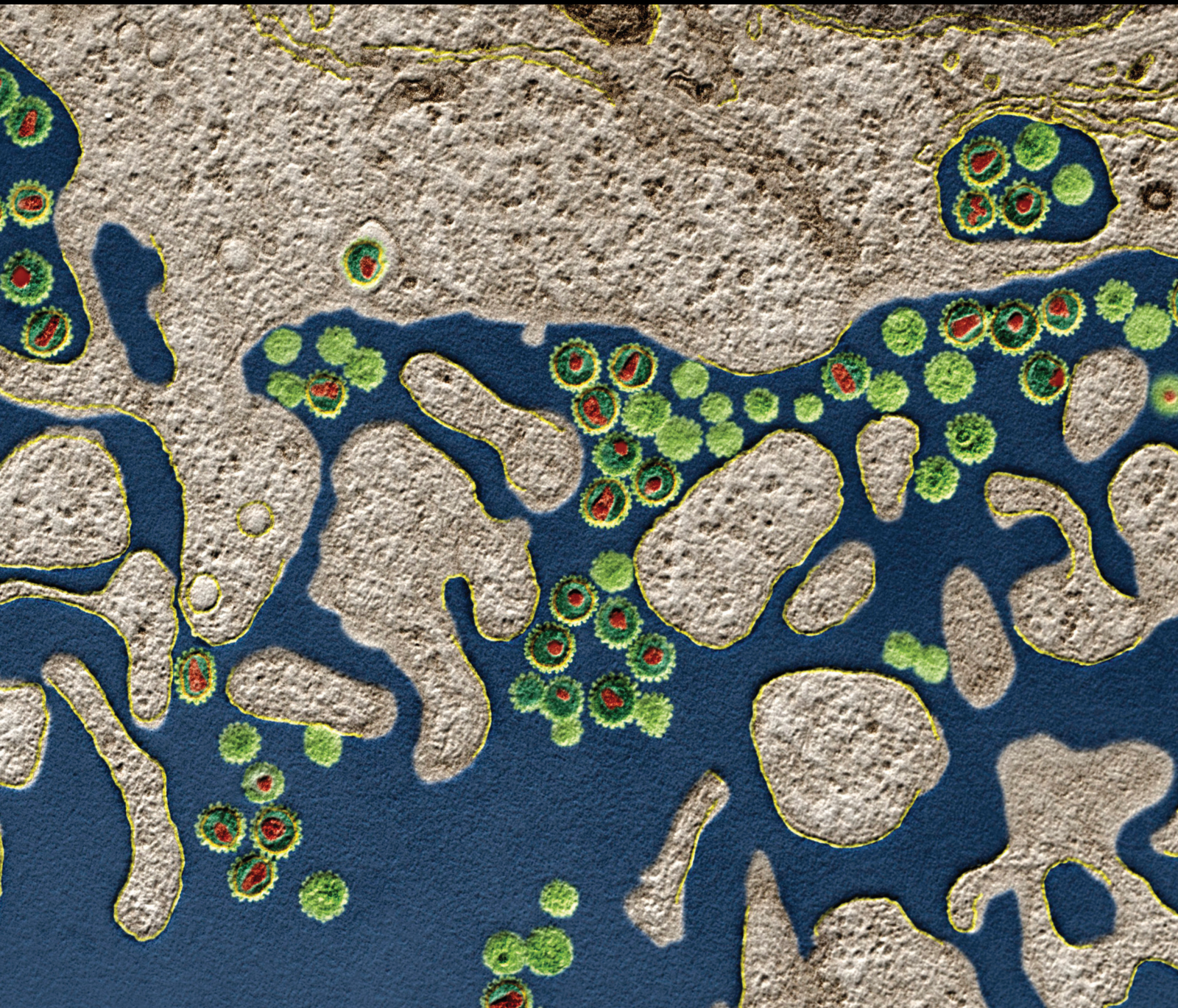


Immunopathogenesis of Neglected Tropical Diseases

Lead Guest Editor: Luiz Felipe Passero

Guest Editors: Márcia Laurenti and Gabriela Santos-Gomes





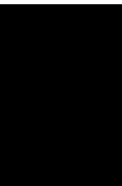
Immunopathogenesis of Neglected Tropical Diseases

Journal of Immunology Research

Immunopathogenesis of Neglected Tropical Diseases

Lead Guest Editor: Luiz Felipe Passero





Guest Editors: Márcia Laurenti and Gabriela
Santos-Gomes





Copyright © 2022 Hindawi Limited. All rights reserved.

This is a special issue published in "Journal of Immunology Research." All articles are open access articles distributed under the Creative Commons Attribution License, which permits unrestricted use, distribution, and reproduction in any medium, provided the original work is properly cited.

Associate Editors

Douglas C. Hooper , USA
Senthamil R. Selvan , USA
Jacek Tabarkiewicz , Poland
Baohui Xu , USA

Academic Editors








Nitin Amdare , USA
Lalit Batra , USA
Kurt Blaser, Switzerland
Dimitrios P. Bogdanos , Greece
Srinivasa Reddy Bonam, USA
Carlo Cavaliere , Italy
Cinzia Ciccacci , Italy
Robert B. Clark, USA
Marco De Vincentiis , Italy
M. Victoria Delpino , Argentina
Roberta Antonia Diotti , Italy
Lihua Duan , China
Nejat K. Egilmez, USA
Theodoros Eleftheriadis , Greece
Eyad Elkord , United Kingdom
Weirong Fang, China
Elizabeth Soares Fernandes , Brazil
Steven E. Finkelstein, USA
JING GUO , USA
Luca Gattinoni , USA
Alvaro González , Spain
Manish Goyal , USA
Qingdong Guan , Canada
Theresa Hautz , Austria
Weicheng Hu , China
Giannicola Iannella , Italy
Juraj Ivanyi , United Kingdom
Ravirajsinh Jadeja , USA
Peirong Jiao , China
Youmin Kang , China
Sung Hwan Ki , Republic of Korea
Bogdan Kolarz , Poland
Vijay Kumar, USA
Esther Maria Lafuente , Spain
Natalie Lister, Australia

Daniele Maria-Ferreira, Saint Vincent and the Grenadines





Eiji Matsuura, Japan
Juliana Melgaço , Brazil
Cinzia Milito , Italy
Prasenjit Mitra , India
Chikao Morimoto, Japan
Paulina Niedźwiedzka-Rystwej , Poland
Enrique Ortega , Mexico
Felipe Passero, Brazil
Anup Singh Pathania , USA
Keshav Raj Paudel, Australia
Patrice Xavier Petit , France
Luis Alberto Ponce-Soto , Peru
Massimo Ralli , Italy
Pedro A. Reche , Spain
Eirini Rigopoulou , Greece
Ilaria Roato , Italy
Suyasha Roy , India
Francesca Santilli, Italy
Takami Sato , USA
Rahul Shivahare , USA
Arif Siddiqui , Saudi Arabia
Amar Singh, USA
Benoit Stijlemans , Belgium
Hiroshi Tanaka , Japan
Bufu Tang , China
Samanta Taurone, Italy
Mizue Terai, USA
Ban-Hock Toh, Australia
Shariq M. Usmani , USA
Ran Wang , China
Shengjun Wang , China
Paulina Wlasiuk, Poland
Zhipeng Xu , China
Xiao-Feng Yang , USA
Dunfang Zhang , China
Qiang Zhang, USA
Qianxia Zhang , USA
Bin Zhao , China
Jixin Zhong , USA
Lele Zhu , China

Contents

Low Activation of CD8⁺ T Cells in response to Viral Peptides in Mexican Patients with Severe Dengue

Tania Estrada-Jiménez , Lilian Flores-Mendoza , Laura Ávila-Jiménez , Carlos Francisco Vázquez-Rodríguez , Gilma Guadalupe Sánchez-Burgos , Verónica Vallejo-Ruiz , and Julio Reyes-Leyva 
Research Article (13 pages), Article ID 9967594, Volume 2022 (2022)


















Increased TNF- α Initiates Cytoplasmic Vacuolization in Whole Blood Coculture with Dengue Virus

Rahmat Dani Satria, Tzu-Wen Huang , Ming-Kai Jhan, Ting-Jing Shen , Po-Chun Tseng, Yun-Ting Wang, Zhen-Yu Yang, Chung-Hsi Hsing , and Chiou-Feng Lin 
Research Article (10 pages), Article ID 6654617, Volume 2021 (2021)











Pleiotropic Effect of Hormone Insulin-Like Growth Factor-I in Immune Response and Pathogenesis in Leishmaniases

Luiza C. Reis , Eduardo Milton Ramos-Sanchez , Fernanda N. Araujo , Ariane F. Leal, Christiane Y. Ozaki , Orlando R. Sevellano , Bernardina A. Uscata , and Hiro Goto 
Review Article (17 pages), Article ID 6614475, Volume 2021 (2021)











Improved Performance of ELISA and Immunochromatographic Tests Using a New Chimeric A2-Based Protein for Human Visceral Leishmaniasis Diagnosis

Maria Marta Figueiredo , Anna R. R. dos Santos , Lara C. Godoi , Natália S. de Castro , Bruno C. de Andrade , Sarah A. R. Sergio , Selma M. B. Jerônimo , Edward J. de Oliveira , Ruth T. Valencia-Portillo , Lucilândia M. Bezerra , Hiro Goto , Maria C. A. Sanchez , Caroline Junqueira , Santuza M. R. Teixeira , Flávio G. da Fonseca , Ricardo T. Gazzinelli , and Ana Paula Fernandes 
Research Article (15 pages), Article ID 5568077, Volume 2021 (2021)


Invariant Natural Killer T Cells as Key Players in Host Resistance against *Paracoccidioides brasiliensis*

Joés Nogueira-Neto , Flavio V. Loures , Alessandra S. Schanoski , David A. G. Andrade , Michelangelo B. Gonzatti , Tania A. Costa, Bruno C. Vivanco , Patrícia Xander , Daniela S. Rosa , Vera L. G. Calich , and Alexandre C. Keller 
Research Article (11 pages), Article ID 6673722, Volume 2021 (2021)




Macrophage Polarization in the Skin Lesion Caused by Neotropical Species of *Leishmania* sp

Carmen M. Sandoval Pacheco , Gabriela V. Araujo Flores , Kadir Gonzalez , Claudia M. de Castro Gomes , Luiz F. D. Passero , Thaise Y. Tomokane , Wilfredo Sosa-Ochoa, Concepción Zúniga , Jose Calzada , Azael Saldaña , Carlos E. P. Corbett, Fernando T. Silveira, and Marcia D. Laurenti 
Research Article (8 pages), Article ID 5596876, Volume 2021 (2021)




Effect of Prophylactic Vaccination with the Membrane-Bound Acid Phosphatase Gene of *Leishmania mexicana* in the Murine Model of Localized Cutaneous Leishmaniasis

María Angélica Burgos-Reyes, Lidia Baylón-Pacheco, Patricia Espíritu-Gordillo, Silvia Galindo-Gómez, Víctor Tsutsumi, and José Luis Rosales-Encina 
Research Article (13 pages), Article ID 6624246, Volume 2021 (2021)





Biomarkers and Their Possible Functions in the Intestinal Microenvironment of Chagasic Megacolon: An Overview of the (Neuro)inflammatory Process

José Rodrigues do Carmo Neto , Yarlla Loyane Lira Braga, Arthur Wilson Florêncio da Costa, Fernanda Hélia Lucio, Thais Cardoso do Nascimento, Marlene Antônia dos Reis, Mara Rubia Nunes Celes, Flávia Aparecida de Oliveira, Juliana Reis Machado , and Marcos Vinícius da Silva 
Review Article (17 pages), Article ID 6668739, Volume 2021 (2021)







Antiviral Efficacy of the Anesthetic Propofol against Dengue Virus Infection and Cellular Inflammation

Ting-Jing Shen , Chia-Ling Chen, Ming-Kai Jhan, Po-Chun Tseng, Rahmat Dani Satria, Chung-Hsi Hsing , and Chiou-Feng Lin 
Research Article (8 pages), Article ID 6680913, Volume 2021 (2021)






Nanoemulsified Butenafine for Enhanced Performance against Experimental Cutaneous Leishmaniasis

Adriana Bezerra-Souza, Jéssica A. Jesus , Márcia D. Laurenti , Aikaterini Lalatsa , Dolores R. Serrano, and Luiz Felipe D. Passero 
Research Article (13 pages), Article ID 8828750, Volume 2021 (2021)



Dual Role of Insulin-Like Growth Factor (IGF)-I in American Tegumentary Leishmaniasis

Carolina de O Mendes-Aguiar , Camilla Lopes-Siqueira, Fabrício Pettito-Assis , Márcia Pereira-Oliveira , Manoel Paes de Oliveira-Neto, Claude Pirmez , Alda Maria Da-Cruz , and Hiro Goto 
Research Article (7 pages), Article ID 6657785, Volume 2021 (2021)

Evaluation of the PE Δ III-LC3-KDEL3 Chimeric Protein of *Entamoeba histolytica*-Lectin as a Vaccine Candidate against Amebic Liver Abscess

Sandra L. Martínez-Hernández , Viridiana M. Becerra-González, Martín H. Muñoz-Ortega , Víctor M. Loera-Muro, Manuel E. Ávila-Blanco , Marina N. Medina-Rosales , and Javier Ventura-Juárez 
Research Article (12 pages), Article ID 6697900, Volume 2021 (2021)



Related Pentacyclic Triterpenes Have Immunomodulatory Activity in Chronic Experimental Visceral Leishmaniasis

Jéssica Adriana de Jesus, Márcia Dalastra Laurenti , Leila Antonangelo, Caroline Silvério Faria, João Henrique Ghilardi Lago, and Luiz Felipe Domingues Passero 
Research Article (15 pages), Article ID 6671287, Volume 2021 (2021)

***Schistosoma japonicum* Infection in Treg-Specific USP21 Knockout Mice**

Youxiang Zhang, De-Hui Xiong, Yangyang Li, Guina Xu, Baoxin Zhang, Yang Liu, Shan Zhang, Qing Huang, Simin Chen, Fansheng Zeng, Jingyi Guo, Bin Li, Zhiqiang Qin , and Zuping Zhang 
Research Article (15 pages), Article ID 6613162, Volume 2021 (2021)

New Biomarker in Chagas Disease: Extracellular Vesicles Isolated from Peripheral Blood in Chronic Chagas Disease Patients Modulate the Human Immune Response

Rafael Pedro Madeira , Lavínia Maria Dal'Mas Romera, Paula de Cássia Buck, Charles Mady, Barbara Maria Ianni, and Ana Claudia Torrecilhas 
Research Article (14 pages), Article ID 6650670, Volume 2021 (2021)

Research Article

Low Activation of CD8⁺ T Cells in response to Viral Peptides in Mexican Patients with Severe Dengue

Tania Estrada-Jiménez ^{1,2} **Lilian Flores-Mendoza** ^{1,3} **Laura Ávila-Jiménez** ⁴
Carlos Francisco Vázquez-Rodríguez ⁵ **Gilma Guadalupe Sánchez-Burgos** ⁶
Verónica Vallejo-Ruiz ¹ and **Julio Reyes-Leyva** ^{1,7}

¹Centro de Investigación Biomédica de Oriente, HGZ5, Instituto Mexicano del Seguro Social, Km 4.5 Carretera Atlixco-Metepec, CP 74360 Metepec, Puebla, Mexico

²Facultad de Medicina, Decanato de Ciencias Médicas, Universidad Popular Autónoma del Estado de Puebla, 21 Sur 1103, Puebla, CP 72410 Puebla, Mexico

³Departamento de Ciencias Químico Biológicas y Agropecuarias, División de Ciencias e Ingeniería, Universidad de Sonora, Unidad Regional Sur, C.P. 85880 Navojoa, Sonora, Mexico

⁴Coordinación Auxiliar de Investigación en Salud, Morelos, Instituto Mexicano del Seguro Social, Boulevard Juárez No. 18, Col. Centro C.P., 62000 Cuernavaca, Morelos, Mexico

⁵Coordinación Auxiliar de Investigación en Salud, Veracruz Sur, Instituto Mexicano del Seguro Social, Calle Poniente 7 # 1350, Col. Centro, C.P., 94300 Orizaba, Veracruz, Mexico

⁶Unidad de Investigación Médica Yucatán, Instituto Mexicano del Seguro Social, Mérida, Yucatán, Mexico

⁷Posgrado en Ciencias Químicas, Facultad de Ciencias Químicas, Benemérita Universidad Autónoma de Puebla, 18 Sur y Avenida San Claudio, Colonia San Manuel, 72570 Puebla, Puebla, Mexico

Correspondence should be addressed to Julio Reyes-Leyva; julio.reyesleyva@viep.com.mx

Received 27 March 2021; Revised 23 December 2021; Accepted 18 February 2022; Published 25 March 2022

Academic Editor: Luiz Felipe Domingues Passero

Copyright © 2022 Tania Estrada-Jiménez et al. This is an open access article distributed under the Creative Commons Attribution License, which permits unrestricted use, distribution, and reproduction in any medium, provided the original work is properly cited.

It is acknowledged that antiviral immune response contributes to dengue immunopathogenesis. To identify immunological markers that distinguish dengue fever (DF) and dengue hemorrhagic fever (DHF), 113 patients with confirmed dengue infection were analyzed at 6 or 7 days after fever onset. Peripheral blood mononuclear cells (PBMC) were isolated, lymphocyte subsets and activation biomarkers were identified by flow cytometry, and differentiation of T helper (Th) lymphocytes was achieved by the relative expression analysis of *T-bet* (Th1), *GATA-3* (Th2), *ROR-γ* (Th17), and *FOXP-3* (T regulatory) transcription factors quantified by real-time PCR. CD8⁺, CD40L⁺, and CD45⁺ cells show higher numbers in DF compared to DHF patients, whereas CD4⁺, CD19⁺, and CD25⁺ cells show higher numbers in DHF than DF patients. High expression of *GATA-3* accompanied by low expression of *T-bet* indicates predominance of Th2 response. In addition, higher expression of *FOXP-3* and reduced functional cytotoxic T cells (CD8⁺perforin⁺) were observed in DHF patients. In further experiments, PBMC were stimulated ex vivo with dengue virus E, NS3, NS4, and NS5 peptides, and proliferating T cell subsets were determined. Lower proliferative responses to NS3 and NS4 peptides and reduced CD8⁺ cytotoxic T cells were observed in DHF patients. Our results suggest that immune response to dengue is dysregulated with predominance of CD4⁺ T cells, low activation of Th1 cells, and downregulation of the antiviral cytotoxic activity during severe dengue, likely induced by regulatory T cells.

1. Introduction

Dengue is one of the most important viral diseases worldwide and frequently causes outbreaks of high morbidity and economic impact in underdeveloped countries [1, 2]. Dengue virus (DENV) belongs to the Flaviviridae family, genus *Flavivirus*; it is transmitted by mosquitos of the *Aedes aegypti* and *Aedes albopictus* species. DENV possesses an RNA genome that encodes a polyprotein that is posttranslationally processed into three structural proteins (capsid (C), precursor membrane (prM), and envelope (E)) and seven nonstructural (NS) proteins (NS1, NS2A, NS2B, NS3, NS4A, NS4B, and NS5) [3]. There are four DENV serotypes (DENV-1, DENV-2, DENV-3, and DENV-4) [2].

The global incidence of dengue has shown important changes in recent decades; the World Health Organization (WHO) estimates there are 100-400 million dengue infections each year [4]. Reported number of dengue cases increased more than 8-fold in the last two decades, from 505,430 cases in 2000 to 5.2 million in 2019. Reported deaths also increased from 960 to 4032 between the year 2000 and 2015 [4]. For the Pan American Health Organization (PAHO), the largest epidemics recorded in the Region of the Americas occurred in 2015 and 2019, with more than 2.7 million dengue cases reported in 2019 [5]. In particular, Mexico had 213,822 dengue cases in 2019 [5]; Torres-Galicia et al. reported a notable increase in the incidence of DHF in Mexico since the previous decade [6].

Dengue has a wide spectrum of clinical manifestations starting with fever and a mild flu-like syndrome [7]. Febrile phase usually lasts from 2 to 7 days; fever can rise to more than 40°C accompanied by other symptoms such as intense headache, retroocular pain, myalgia, arthralgia, nausea, and rash. Patients can spontaneously recover or progress to severe dengue, which includes DHF and dengue shock syndrome (DSS). DHF is characterized by coagulopathy, increased vascular fragility, and permeability. A patient can enter the critical phase about 3-7 days after fever onset. At this time, fever is dropping (below 38°C) but signs associated with severe disease can manifest, such as intense bleeding, plasma loss, and led in some cases to organ failure and potentially fatal complications [4, 7]. Currently, the WHO classifies dengue into 2 major categories: dengue (with or without warning signs) and severe dengue, but in medical practice, it still used the 1997 classification in DF and DHF [4, 8].

Evolution of febrile to severe dengue seems to be correlated with establishment of the immune response in both primary and secondary infections. Altered immune processes include proliferation of dysfunctional effector T cells induced by cross-reactivity between DENV serotypes, antibody-dependent enhancement (ADE) of infection that increases virus replication in phagocytic cells, dysregulation of complement and coagulation cascades, and overproduction of cytokines, chemokines, and other mediators of inflammation that contribute to clinical manifestations of severe disease [2, 9-11].

Diverse immune cells are targets of DENV infection, including monocytes/macrophages and dendritic cells [2]. Early after infection, these cells contribute to establish a proin-

flammatory state by overproduction of several cytokines such as TNF- α , IL-1 β , IL-2, IL-6, and type I IFNs. This leads to activation of CD4⁺ Th2 cells that produce IL-2, IL-4, IL-5, and IL-13 that consolidate the inflammatory process, as well as IL-10 and TGF- β that induce differentiation of regulatory T cells (Treg) and contribute to downregulate the antiviral response [2, 11-15]. In contraposition, IL-12 and IFN- γ induce activation of Th1 cells that promote activation of CD8⁺ cells and the cytotoxic antiviral response necessary to clear out infection [12]. Diverse transcription factors are the main regulators of T cell differentiation; they control the type of cytokines secreted and the route that will follow the immune response; indeed T-bet, GATA-3, ROR- γ , and FOXP-3 are involved in the control of the differentiation process of Th1, Th2, Th17, and Treg cells, respectively [16, 17].

The protective role of T cells in dengue is controversial; some reports showed that early activation of CD8⁺ T cells is crucial to restrict DENV infection [18, 19]; indeed, higher proliferation and cytotoxic activity of CD8⁺ T cells with production of IFN- γ have been associated with protection against secondary infections, regardless of DENV serotype [18-22]. In contrast, high levels of CD4⁺ cells were found in severe and fatal dengue cases [21, 23, 24], even with increased numbers of CD8⁺ T cells in patients with DHF [18, 25, 26]. At respect, the proinflammatory response induced by CD4⁺ cells to heterotypic secondary infections seems to be associated with proliferation of low-affinity memory CD8⁺ T lymphocytes that are not as functional as high-affinity memory cells to control DENV infection [24, 25, 27, 28].

Specific T cell response can be induced by different epitopes of structural and nonstructural DENV proteins [13, 14, 20, 29-32]. Kurane and Mathew studied the immune response to attenuated viruses in vaccinees as well as in patients with natural infection in Thailand; they showed that NS3 have multiple antigenic sites recognized by T cells [33, 34]. Rivino et al. evaluated the reactivity of T cells by using a library of overlaid peptides that cover all DENV-2 proteome in adult patients from Singapore that suffer a secondary infection. They found a higher proportion of CD8⁺ T cells induced by NS3 and NS5 peptides; meanwhile, E and C peptides induced CD4⁺ T cells [35]. Tian et al. showed that CD4⁺ T cells were predominantly directed against the capsid protein followed by E, NS3, and NS2 proteins, while the activation of CD8⁺ T cells was induced by NS3, followed by capsid, NS5, and NS4/B proteins [31]. Weiskopf et al. made a complete analysis of CD8⁺ T cells in a hyperendemic region of Sri Lanka. They measured the response of IFN- γ -producing cells ex vivo; the most antigenic proteins were NS3, NS4B, and NS5 [20]. Other authors showed that induction of CD4⁺ or CD8⁺ T cells depends on dengue virus serotype and the patient's HLA haplotypes [32, 33]. Thus, genetic factors and geographic location of infected people have an important influence on the specificity and intensity of cellular immune response and its role in protection [15, 20, 25, 28, 36, 37].

In this work, cellular parameters of the immune response were examined in patients during a dengue outbreak that occurred at the central region of Mexico, phenotyping of T cells and their transcription factors, and the proliferative response of immune cells induced by dengue peptides were correlated with disease severity.

2. Materials and Methods

2.1. Ethical Statement. This study was conducted in accordance with international ethical principles and the Declaration of Helsinki (last update Brazil 2013). The research protocol was approved by the Committee of Ethics in Health Research of the Mexican Institute of Social Security (IMSS) and recorded under registration numbers R-2011-2103-29 and R-2012-2104-2. All patients (and their relatives) were informed about the study, and written consent to participate was obtained from each participant. Parents or legal tutors authorized the participation and signed informed consent of patients lower than 18 years old. Patients' confidentiality was assured by assigning a progressive study number to their data and blood samples.

2.2. Clinical Procedures. The study was done with patients admitted at IMSS "HGZ5" General Hospital located at Metepec, Puebla, Mexico. Healthy blood donors from a geographical zone free of dengue were enrolled at IMSS High Specialty Medical Unit located at Puebla City. Confirmatory dengue diagnosis was done by means of IgM and IgG ELISA kits (PanBio Diagnostic) and/or detection of NS1 antigen (Platelia Bio-Rad). The 1997 WHO classification of dengue, still in practice at this hospital, was used to classify cases into DF and DHF [9].

Blood samples were obtained from all patients and submitted to hematological and biochemical laboratory tests, including hematic biometry, platelet and differential leukocyte counts, and the concentrations of hepatic enzymes aspartate (AST) and alanine (ALT) aminotransferases. Other tests such as abdominal ultrasounds were requested for medical purposes only.

For immunological tests, 3 to 5 ml blood samples were obtained in heparinized tubes at 6 or 7 days after fever onset. Samples were centrifuged at 1700 rpm at 4°C for 7 minutes; plasma was separated and stored in aliquots at -70°C until use. Ex vivo PBMC were separated by Ficoll-Histopaque density gradient centrifugation and analyzed by flow cytometry. Their mRNA was isolated for qPCR assays.

2.3. Flow Cytometry. The following monoclonal antibodies were used for flow cytometry: CD3-FITC (clone UCHT1), CD4-APC (clone OKT-4), CD8-APC-Cy7 (clone SK1), CD19-PE (clone HIB19), CD69-PE (clone FN-50), CD45-PE (clone UCHC1), CD40L-PE (clone 24-31), and CD25-PE (clone PC61.5) all from eBioscience (currently Thermo Fisher Scientific, Waltham, MA, USA). Anti-perforin antibody (clone dG9, sc-33655) and anti-IgG2b-PE (both of Santa Cruz Biotechnology, Dallas TX, USA) were used for intracellular staining. All antibodies used in multiparametric flow cytometry were tested and conditions calibrated before their use in samples.

Ex vivo PBMC were thawed and resuspended at 1×10^6 cells/ml, and lymphocyte subsets were identified by flow cytometry using the BD FACSCanto II Flow Cytometry System and the FACSDiva Software (BD Biosciences, San Jose CA, USA). Bicolor panels were analyzed as follows: for helper T cells, CD3/CD4; for cytotoxic T cells, CD3/CD8;

for B cells, CD3(-)/CD19; and for activated T cells, CD3 coupled with either CD69, CD45, CD40L, or CD25.

2.4. T Cell Proliferation Assays. Peptides of dengue virus NS3, NS4, NS5, and E proteins [38–40] were synthesized by GenScript (NJ, USA) at >90% purity. The peptide sequences and characteristics are shown in Table 1. Peptides were reconstituted at 10 mg/ml following the manufacturer's specifications: P1, P2, P4, P5, P6, P8, P9, P12, P13, and P14 in 10% DMSO in water, while P3, P7, and P11 peptides in 3% ammonia in water. Peptides were stored at -20°C until use. Mixtures of peptides corresponding to each viral protein were prepared as follows: E (P1, P2, and P3), NS3 (P4, P5, and P6), NS4 (P7, P8, P9, and P10), and NS5 (P11, P12, P13, and P14). The final concentration of each peptide in a mixture was 10 µg/ml.

For microplate priming, 96-well microplates were incubated overnight with 1 µg/ml suspensions of monoclonal antibodies with functional assay activity CD28 (clone 37.51) and CD3 (clone HIT3a) both of eBioscience, which induce costimulatory signals that increase the response to synthetic peptides [41]. The next day, PBMC of patients and controls (1.8×10^6 cells) were labelled with 5 µM CFSE (eBioscience) 5 minutes at 37°C in centrifuge tubes. After that, cells were washed with PBS and resuspended in RPMI 1640 containing 10% FBS, 1% HEPES, 1% L-glutamine, and 1% penicillin-streptomycin. Then, 1×10^5 PBMC were added to each well of a primed microplate and stimulated with the mixture of peptides mentioned previously (E, NS3, NS4, or NS5). All experiments were done by triplicate. DMSO (10%) and ammonia (3%) solutions in conditioned RPMI medium without peptides were used as negative controls. Cells stimulated with Phaseolus vulgaris hemagglutinin (PHA, SIGMA, 20 ng/ml) were included as positive proliferation controls. Microplates were incubated at 37°C, 5% CO₂ for 120 hours. After that time, proliferation of CD4⁺ and CD8⁺ cells was determined by flow cytometry using the BD FACSCanto II Flow Cytometry System and the FACSDiva Software (BD Biosciences, San Jose CA, USA).

2.5. Ex Vivo Relative Gene Expression Analysis. Total RNA was extracted directly from ex vivo PBMC using TRIzol (Invitrogen) following manufacturer's instructions. cDNA was synthesized by using random primers and the RevertAid H Minus Reverse Transcriptase Kit (Thermo Fisher Scientific, USA) at 25°C for 10 min, 42°C for 60 min, and 70°C for 10 min. Expression of *T-bet*, *GATA-3*, *ROR-γ*, and *FOXP-3* genes was determined by qPCR using the SYBR Green/ROX-PCR Master Mix (Thermo Fisher Scientific, USA) and the following primers: *T-bet* forward 5'-CAC GCA CTT CCG CAC ATT CC-3', *T-bet* reverse 5'-TCC AGC AGC TCG AAG AGG CA-3', *GATA-3* forward 5'-ACA ATC TGC CTC AAT CAC TCT G 3', *GATA-3* reverse 5'-TTG ACT TGG ATT GGG ATT TTG-3', *ROR-γ* forward 5'-GTC CAA CAA TGT GAC CCA G-3', *ROR-γ* reverse 5'-CTT TCC ACA TGC TGG CTA CA-3', *FOXP-3* forward 5'-AAG CAG CGG ACA CTC AAT-3', and *FOXP-3* reverse 5'-AGG TGG CAG GAT GGT TTC-

TABLE 1: Characteristics of dengue virus peptides used in this study.

Peptide ID	Protein	Sequence	Position	Induced response	Reference
P1	E	FKNPHAKKQDVV	519-530	CD4 ⁺ and CD8 ⁺	Sánchez-Burgos et al., 2010
P2	E	RGARRMAIL	687-695	CD8 ⁺ and antibodies	Sánchez-Burgos et al., 2010
P3	E	DFGSVGGVL	699-707	Mostly antibodies	Sánchez-Burgos et al., 2010
P4	NS3	WITDFKGTQVW	1824-1834	CD4 ⁺⁺	Zeng et al., 1996
P5	NS3	TPEGITPAL	1975-1983	CD4 ⁺ and CD8 ⁺	Livingston et al., 1995
P6	NS3	GTSGSPIVNR	1608-1617	CD8 ⁺	Friberg et al., 2011
P7	NS4a	ASILEFFL	2199-2207	Low CD4 ⁺ and CD8 ⁺ and antibodies	Sánchez-Burgos et al., 2010
P8	NS4a	LRPASAWTL	2271-2279	Mostly antibodies	Sánchez-Burgos et al., 2010
P9	NS4a	CYSQVNPTTL	2337-2346	CD8 ⁺ and antibodies	Sánchez-Burgos et al., 2010
P10	NS4b	GSYLAGAGL	2469-2477	High CD4 ⁺ and CD8 ⁺	Sánchez-Burgos et al., 2010
P11	NS5	VIPMVTQIAMTDTP	2826-2840	CD4 ⁺ and CD8 ⁺ and antibodies	Sánchez-Burgos et al., 2010
P12	NS5	YMWLGARFL	2967-1975	Mostly antibodies	Sánchez-Burgos et al., 2010
P13	NS5	SYSGVEGEG	3003-3012	Low CD4 ⁺ and high CD8 ⁺	Sánchez-Burgos et al., 2010
P14	NS5	YFHRRDLRL	3257-3265	Mid CD4 ⁺ and high CD8 ⁺	Sánchez-Burgos et al., 2010

Most peptide sequences were obtained from Sánchez-Burgos et al. (2010). P4, P5, and P6 were selected from Zeng et al., Livingston et al., and Friberg et al., respectively [38–40]. Position refers to the first and last amino acid in the polyprotein. Peptides that induced IFN- γ production in mouse or human CD4 and CD8 cells were selected for the present study. *Some peptides that induced antibody production and low CD4 and CD8 cell activity were selected as controls of activation. **CD8 cells were not tested.

3'. *HPRT* was included as endogenous control in all experiments using the primers *HPRT* forward 5'-CCT GGC GTC GTG ATT AGT GAT GAT-3' and *HPRT* reverse 5'-CGA GCA AGA CGT TCA GTC CTG TC-3'. All reactions were run in the StepOne Real-Time PCR system (Applied Biosystems). Before the analysis of gene expression in samples, dynamic ranges were calculated and dissociation curves corresponding to each gene were depicted to determine assay specificity. Relative gene expression between the control and patient groups was calculated using the $2^{-\Delta\Delta CT}$ method, where ΔCT is the difference in the threshold between any target gene (*T-bet*, *GATA-3*, *ROR- γ* , and *FOXP-3*) and the endogenous gene (*HPRT*). Expression of each mRNA transcription factor was arbitrarily assigned a value of 1 in uninfected controls, and relative expression changes were calculated in patients.

2.6. *Statistical Analysis.* Normality of data distribution was tested by the Kolmogorov–Smirnov test. The data were represented as means with standard deviations (SD). The non-parametric Mann–Whitney test, *T* test, or χ^2 test was used to compare independent groups as applicable. All analyses were done in GraphPad Prism v7.0 software; differences between groups were considered significant at $p < 0.05$.

3. Results

3.1. *Demographic Characteristics and Clinical Parameters.* According to hospital's archives, 189 patients were admitted with diagnosis of dengue from July 1 to October 1, 2015; of these, 113 patients were included in the study after completing their clinical tests and agreed to participate voluntarily by signing the informed consent. Sixty-three patients presented DF and fifty have DHF. Plasma values of NS1, IgM, and IgG confirmed dengue infection. Dengue serotype was

not determined. The median age was 48 and 41 years for DHF and DF patients, respectively, with a variation between 4 and 71 years. Table 2 summarizes the main characteristics of the study groups.

3.2. *Clinical Signs.* The most frequent signs and symptoms present in dengue patients were fever, headache, back pain, arthralgia, and rash. The hemorrhagic signs were variable; a high number of patients presented petechiae (46/113), epistaxis (35/113), and gingival hemorrhage (16/113). Hematemesis and melena were less frequent (7/113 and 4/113, respectively). Among the 50 patients with DHF, 26 presented both petechiae and epistaxis, and 10 presented simultaneously petechiae, epistaxis, and gingival hemorrhage. One patient with DHF presented ascites.

3.3. *Hematic Changes.* No significant differences were found between groups regarding hematocrit, hemoglobin, creatinine, and the proportion of leukocytes, lymphocytes, monocytes, or neutrophils. Significant differences were found between DF and DHF patients for platelet counts and serum albumin concentrations (see Table 2). Most patients showed platelet values $< 10,000$ cells/mm³ in both DF and DHF patients (6765 ± 2642 and 2624 ± 1830 cells/mm³, respectively; $p < 0.0001$). AST and ALT values were higher than the reference in both DF and DHF patients, but only two DHF patients presented values > 1000 UI/ml for both hepatic enzymes (see Table 2).

3.4. *Lymphocyte Proportions in Dengue Patients.* The proportion of CD3⁺CD4⁺ T cells was higher in DHF than in DF patients ($29.59 \pm 7.56\%$ and $21.03 \pm 8.18\%$, respectively, $p = 0.022$) (Figure 1). The proportion of B cells (CD3⁻CD19⁺) was almost twofold higher in DHF than in DF patients ($23.43 \pm 7.32\%$ vs. $12.2 \pm 5.59\%$, $p < 0.0001$).

TABLE 2: Clinical and laboratory features of patients with dengue fever (DF) and dengue hemorrhagic fever (DHF).

Clinical finding	DF (<i>n</i> = 63)	DHF (<i>n</i> = 50)	<i>p</i> value
Pleural effusion or ascites ¹	0	1 (2%)	—
Tourniquet (+) ¹	2 (3%)	5 (10%)	—
Bleeding manifestations ¹	12 (19%)	34 (68%)	0.0001
Hematocrit ²	39.75 ± 4.9%	37.8 ± 5.42%	—
Hemoglobin ³	13.55 ± 5.42 g/dl	12.6 ± 1.87 g/dl	—
Creatinine ³	0.88 ± 0.33 mg/dl	0.77 ± 0.26 mg/dl	0.2724
<0.6 mg/dl	7 (11%)	11 (22%)	0.0556
Albumin ²	3.23 ± 0.54	2.97 ± 0.5	0.0046
<2.5 mg/dl	6 (9%)	8 (16%)	0.1989
2.5-3.4 mg/dl	32 (51%)	33 (66%)	0.0314
Platelet counts ² (cells/mm ³)	67,660 ± 26,430	26,240 ± 18,180	0.0001
<25,000 cells/mm ³	19 (30%)	27 (54%)	0.0005
25,000–49,000 cells/mm ³	16 (25%)	17 (34%)	0.2146
50,000–99,000 cells/mm ³	12 (19%)	6 (12%)	0.2408
>100,000 cells/mm ³	17 (27%)	0	—
WBC count ² , cells × 10 ³ /μl	5.246 ± 2.589	6.325 ± 3.511	0.2225
WBC differential counts ² (% of total cells)			
Lymphocytes	41.384 ± 13.232	32.5 ± 15.382	0.1149
MID cells	15 ± 6.976	9.833 ± 5.373	0.0508
Neutrophils	43.548 ± 14.063	57.333 ± 19.075	0.0696
Hepatic enzymes			
ALT ²	114 ± 76 UI/ml	113 ± 107 UI/ml	0.9403
>80 UI/ml	37 (59%)	30 (60%)	0.4757
>200 UI/ml	6 (9%)	8 (16%)	0.1989
AST ²	159 ± 128 UI/ml	178 ± 209 UI/ml	0.7119
>80 UI/ml	43 (68%)	40 (80%)	0.0756
>200 UI/ml	14 (22%)	15 (30%)	0.2590

¹Number of patients with the symptom (and percentage). ²Mean value ± SD. ³Mean concentration ± SD. *p* values were determined by the Mann–Whitney *U* test for continuous variables and by the χ^2 test for categorical variables; **p* < 0.05 indicates significance between DF and DHF.

In contrast, a smaller number of CD3⁺CD8⁺ T cells were found in DHF compared to DF patients (15.45 ± 7.67% vs. 25.54 ± 11.19%; *p* = 0.0045) (see Figure 1). In addition, significant reduction of activated cytotoxic T cells (CD3⁺CD8⁺ perforin⁺) was found in DHF patients compared to DF patients (4.17 ± 1.75% vs. 14.65 ± 5.47%, respectively; *p* < 0.001) (Figure 2).

Activation of T cells was analyzed by the identification of CD3 together with CD40L, CD45, CD69, and CD25 markers (Figure 3). Proportions of total CD40L⁺ cells were significantly higher in DF than in DHF patients either in whole PBMC (19.06 ± 13.54 vs. 4.02 ± 2.96) or CD3⁺ cells (3.19 ± 1.98 vs. 1.65 ± 1.29) (*p* = 0.0009 and *p* = 0.0053, respectively) (Table 3). CD45⁺ cells were more abundant in DF than DHF (53.02 ± 16.09 vs. 35.73 ± 10.4; *p* < 0.0004), but they did not differ between T cells. In contrast, CD25 expression was higher in DHF than in DF patients, either analyzing whole PBMC (18.36 ± 8.15 vs. 7.49 ± 3.49%; *p* = 0.0001) or CD3⁺ T cells (3.0 ± 2.02 vs. 1.24 ± 0.81, *p* = 0.0018), respectively. No difference was observed in CD69 expression either in PBMC or T cells.

3.5. Relative Expression of T Cell Transcription Factors. T-bet (Th1), GATA-3 (Th2), ROR- γ (Th17), and FOXP-3 (Treg) transcription factors associated with helper T cell subpopulations were directly analyzed *ex vivo* in PBMC. Both DF and DHF patients showed low expression of *T-bet* mRNA (0.4 ± 0.17 and 0.6 ± 0.2-fold) which indicates low levels of Th1 cells and negative values of *ROR- γ* expression (0.0009 ± 0.0006 and 0.04 ± 0.05-fold), which suggest down-regulation of Th17 cells (Figure 4). The absence of Th17 cells (*ROR- γ*) was corroborated by the lack of IL-17 in the sera of DENV patients (limit of detection 20 pg/ml; data not shown).

In contrast, DENV patients showed higher expression of *GATA-3* and *FOXP-3* mRNA that indicate the presence of Th2 and Treg cells, respectively. *GATA-3* was significantly higher in DHF than in DF patients (24.3 ± 13.8 vs. 4.1 ± 3.5 -fold, respectively; *p* < 0.001). *FOXP-3* showed the highest differences in expression between DHF and DF (205 ± 191 vs. 1.8 ± 0.9-fold, respectively; *p* < 0.0001) (Figure 4).

3.6. T Cell Response to Viral Peptides. Proliferative responses induced *ex vivo* by viral peptides were analyzed by flow

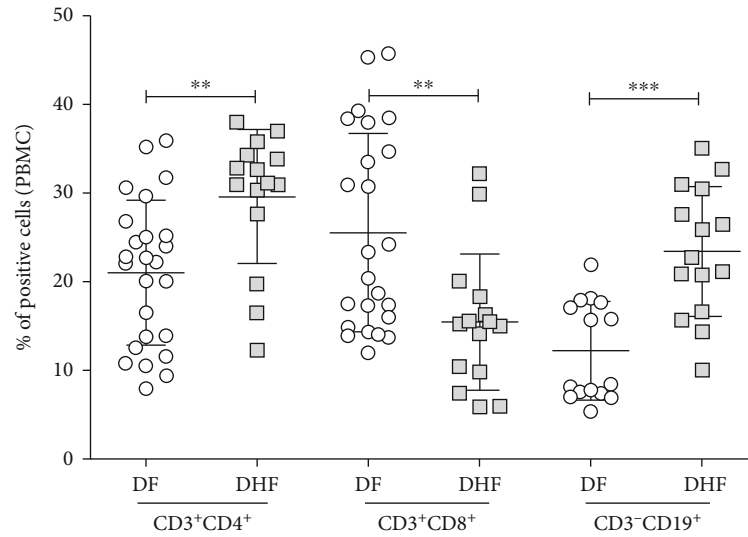


FIGURE 1: Proportion of CD4⁺ T cells (CD3⁺CD4⁺), cytotoxic T cells (CD3⁺CD8⁺), and B cells (CD3⁻CD19⁺) determined by flow cytometry in *ex vivo* PBMC of patients with dengue fever (DF) and dengue hemorrhagic fever (DHF). The error bars represent mean \pm SD. ** $p < 0.01$ and *** $p < 0.001$ by the Mann-Whitney U test.

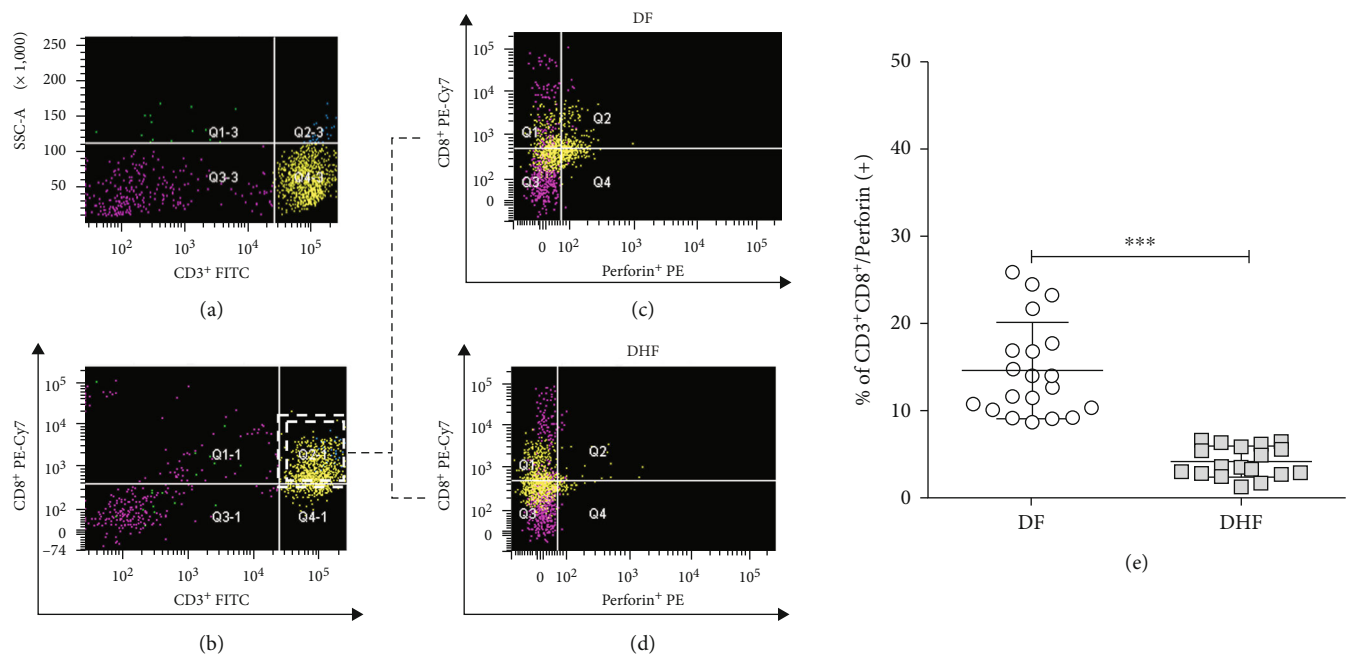


FIGURE 2: Analysis of functional cytotoxic T lymphocytes in *ex vivo* PBMC of patients with dengue fever (DF) and dengue hemorrhagic fever (DHF) by flow cytometry. Representative plots of the gating strategy for the analysis of CD3⁺/CD8⁺/perforin⁺ T cells (a-d). First, singlets and live cells were selected. (a) CD3⁺ and (b) CD3⁺/CD8⁺ double positive cells were gated and used to determine perforin expression in (c) DF and (d) DHF patients. (e) Percentages of activated CD3⁺CD8⁺perforin⁺ cells in patients with DF ($n = 23$) and DHF patients ($n = 20$). The error bars represent mean \pm SD. *** $p < 0.001$ determined by the Mann-Whitney U test.

cytometry using CFSE to label T cells. The strategy to analyze CD4 and CD8 proliferating T cells is shown in Figure 5; the objective was to evaluate the relative frequency of proliferating (CFSE low) and nonproliferating (CFSE high) in CD4⁺ and CD8⁺ cells. The proportion of proliferating CD4 and CD8 cells induced by viral peptides in DF and DHF is shown in Figure 6.

In general, T cell responses were higher in DF than in DHF patients; indeed, the proportion of CD4⁺ cells induced by E, NS3, NS4, and NS5 was 3.6 ± 1.8 vs. $1.1 \pm 0.8\%$ ($p = 0.0003$), 7.2 ± 4.3 vs. $1.6 \pm 1.3\%$ ($p = 0.0006$), 4.3 ± 3.2 vs. $0.9 \pm 0.6\%$ ($p = 0.0032$), and 2.6 ± 2.3 vs. $0.8 \pm 0.7\%$ ($p = 0.21$), respectively. The proportion of CD8⁺ cells induced by E, NS3, NS4, and NS5 peptides was 2.3 ± 1.7

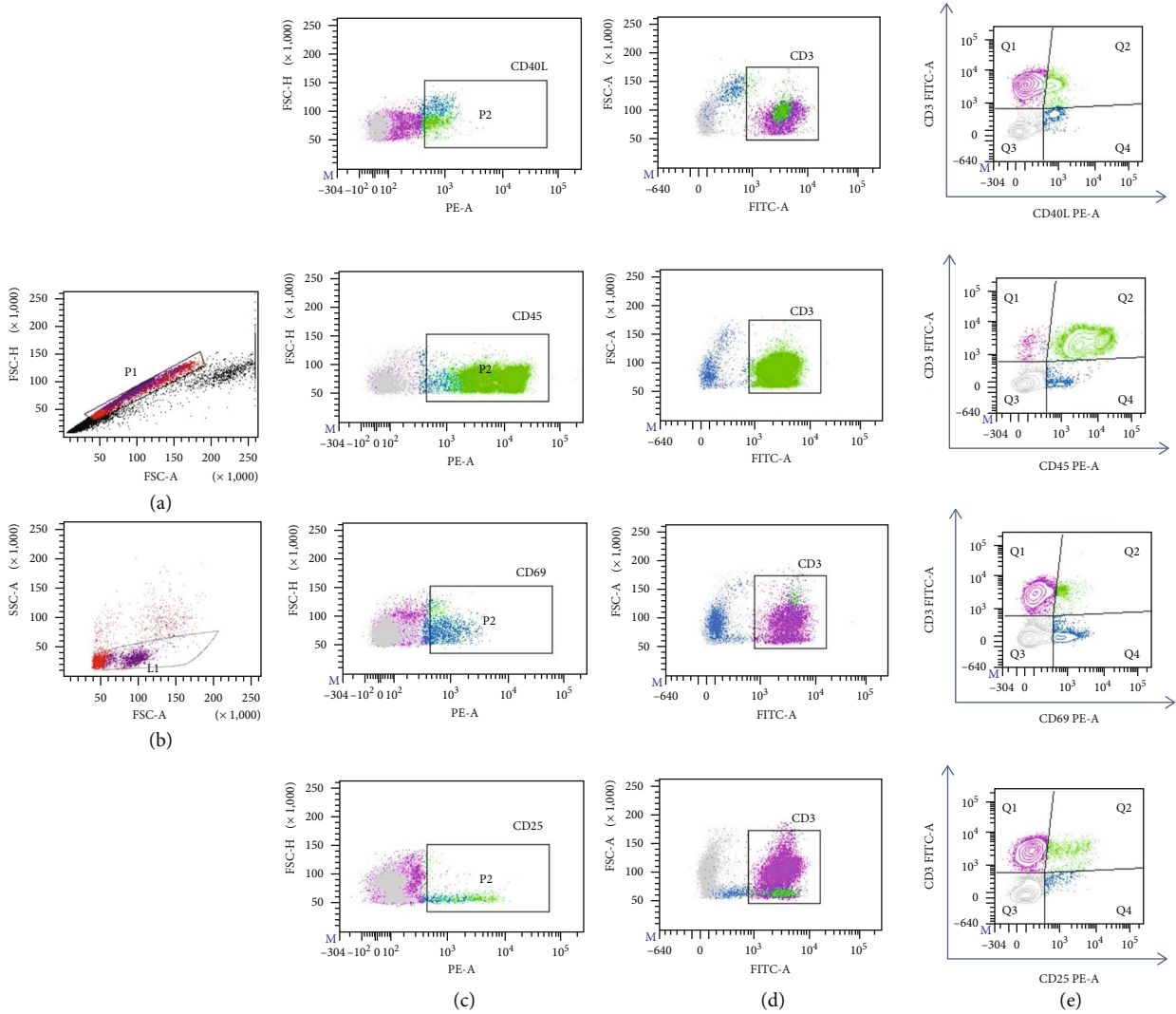


FIGURE 3: Strategy for the analysis of activation molecules on ex vivo PBMC and CD3⁺ population in patients with dengue fever (DF) and dengue hemorrhagic fever (DHF). (a, b) First, singlets (P1) and live (L1) cells were selected. (c) Activation molecules were identified in the PBMC population (P2): CD40L⁺, CD45⁺, CD69⁺, and CD25⁺ subsets are represented from top to bottom. (d) CD3⁺ cells were gated and used to determine double positive cells. (e) Representative plots of activation molecules (CD40⁺, CD45⁺, CD69⁺, and CD25⁺) expressed in T cells. Q1 represents CD3⁺ cells; Q2 represents double positive cells.

TABLE 3: Analysis of activation molecules on immune cells of dengue patients by flow cytometry.

	DF (n = 23)	DHF (n = 20)	p value
CD40L ⁺	19.06 ± 13.54	4.02 ± 2.96	0.0009*
CD45 ⁺	53.02 ± 16.09	35.73 ± 10.4	0.0004*
CD69 ⁺	7.84 ± 4.15	9.79 ± 4.04	0.0987
CD25 ⁺	7.49 ± 3.49	18.36 ± 8.15	0.0001*
CD3 ⁺ CD40L ⁺	3.19 ± 1.98	1.65 ± 1.29	0.0053*
CD3 ⁺ CD45 ⁺	36.46 ± 12.75	32.21 ± 9.15	0.8184
CD3 ⁺ CD69 ⁺	4.94 ± 2.01	4.54 ± 1.31	0.8901
CD3 ⁺ CD25 ⁺	1.24 ± 0.81	3.01 ± 2.02	0.0018*

Data are from flow cytometry experiments shown in Figure 3; numbers represent percentages. p values were determined by the Mann-Whitney U test; * mean significance between DF and DHF, p < 0.05.

vs. $1.03 \pm 0.7\%$ ($p = 0.28$), 5.7 ± 5.2 vs. $1.8 \pm 1.2\%$ ($p = 0.029$), 3.03 ± 2.1 vs. $0.7 \pm 0.4\%$ ($p = 0.0034$), and 1.4 ± 1.2 vs. $0.8 \pm 0.5\%$ ($p = 0.21$) either in DF or DHF, respectively. NS3 peptides were more immunogenic than the other peptides. Positive control stimulus (PHA) induced proliferation of both CD4⁺ and CD8⁺ T cells (around 15%) in both DF and DHF patients. Negative controls increased less than 0.1% for both groups.

4. Discussion

The balance between Th1 and Th2 cells is crucial to orchestrate an immune response that protects against virus infection but maintains homeostasis [42]. Differentiation of CD4⁺ naive T cells into Th1, Th2, Th17, and Treg cell lineages depends on the expression of T-bet, GATA-3, ROR-γ, and FOXP-3 transcription factors, respectively. T-bet and

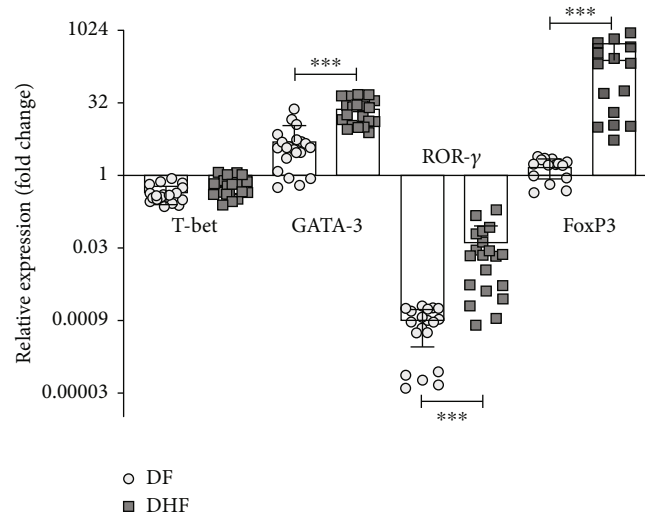


FIGURE 4: Relative gene expression analysis of T cell transcription factors. The expression of *T-bet* (Th1), *GATA-3* (Th2), *ROR- γ* (Th17), and *FOXP-3* (Treg) was analyzed ex vivo in PBMC of DF and DHF patients; data are expressed as fold increments compared with the expression level of the control group, which was assigned an arbitrary value of 1. Error bars represent mean \pm SD. Significant differences * $p < 0.05$, ** $p < 0.01$, and *** $p < 0.001$ by the Mann-Whitney U test.

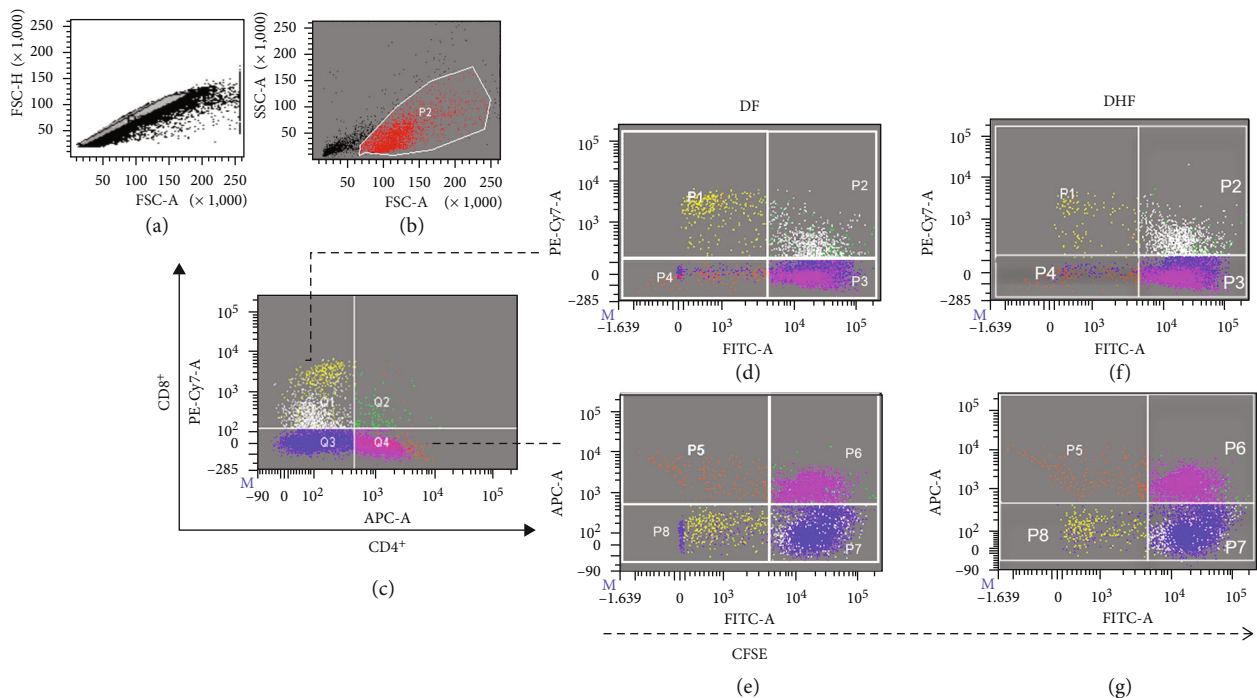


FIGURE 5: Strategy for the analysis of proliferating T cells labelled with CFSE. Singlets and live cells were selected (a, b). $CD4^+$ and $CD8^+$ positive cells were defined with APC or PE-Cy7, respectively (c). Representative plots show $CD8^+$ and $CD4^+$ cells in (d, e) DF and (f, g) DHF patients; P1 and P5 represent $CD8^+$ and $CD4^+$ proliferating cells (low CFSE), respectively. These data in cells stimulated with dengue virus peptides are shown in Figure 6. P2 and P6 represent $CD8^+$ and $CD4^+$ nonproliferating cells (high CFSE), respectively.

GATA-3 rival each other for activation; GATA-3 prevents the polarization of Th1 and Th17 response by promoting T-bet and ROR- γ downregulation and controls the secretion of their related cytokines [16, 43–45]. In this work, we found that patients with dengue did not significantly express *T-bet* and ROR- γ , but they showed higher expression of *GATA-3* and *FOXP-3*, particularly in patients that worsen to DHF. Higher expression of GATA-3 is in accor-

dance with its ability to promote the proinflammatory response that is mediated by IL-4, IL-5, IL-6, and IL-13 [16, 46, 47]. Their presence is also indicative of persistent inflammation and severity in other Flavivirus infections and dengue [21, 24, 48, 49].

Increased expression of FOXP-3 in patients with DHF suggests the differentiation of regulatory T cells involved in the secretion of IL-10. According to this, we have previously

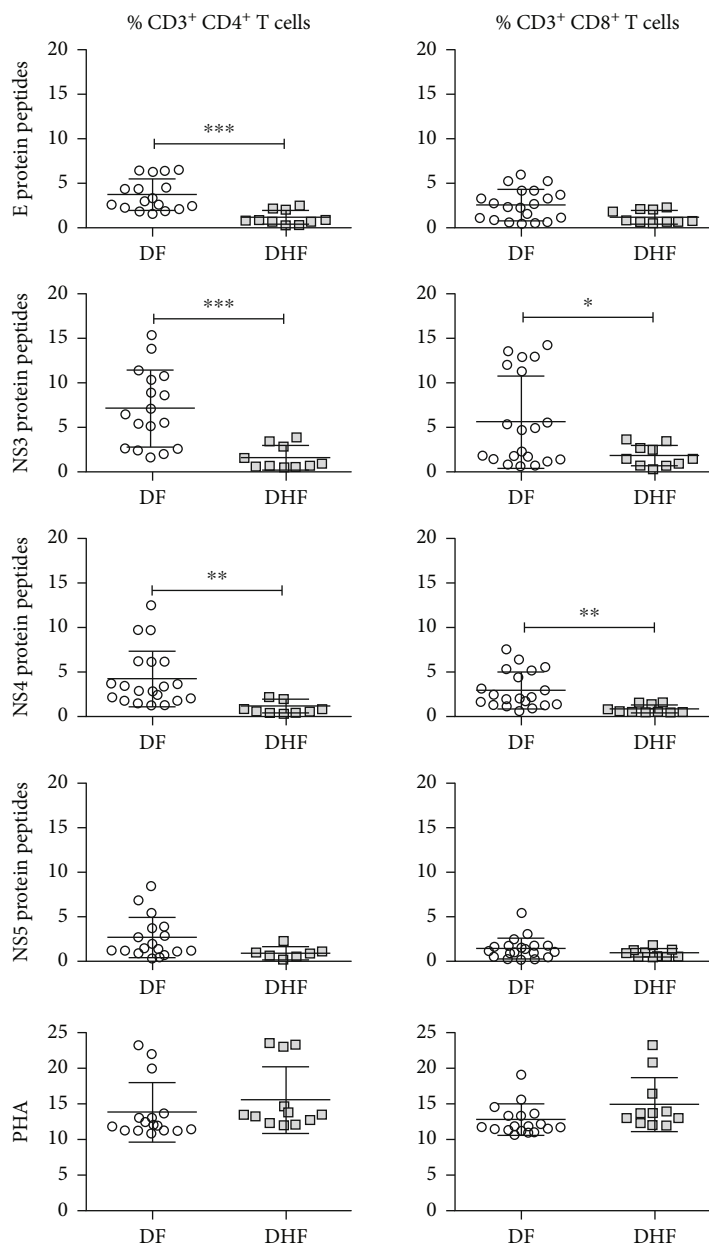


FIGURE 6: CD4⁺ and CD8⁺ proliferating cells stimulated with dengue virus peptides in dengue fever DF ($n = 23$) or dengue hemorrhagic fever DHF ($n = 20$) patients. Plots show the proportion of CD4⁺ and CD8⁺ cells induced by peptides of E, NS3, NS4, and NS5 viral proteins and the positive control stimulated with PHA. Error bars represent the mean \pm SD. Significant differences * $p < 0.05$, ** $p < 0.01$, and *** $p < 0.001$ by the Mann–Whitney U test.

found high levels of IL-10 in the serum of patients with DHF [50].

Several studies showed that CD8⁺ cells play important roles in the control of DENV infection [18–20]. Our results showed that CD8⁺ cells were more abundant in DF than in DHF patients. In accordance, an increased proportion of IFN- γ -producing CD8⁺ T cells has been found in patients with subclinical dengue infections [21, 22]. Other reports showed that CD8⁺ cells contribute to protect against homotypic and heterotypic DENV reinfection [13, 21, 51].

However, it has been proposed that cell immunity might be incompletely activated during the febrile phase of dengue

due to an altered cytokine production, decreased CD8⁺ T cell proliferation, and augmented T cell apoptosis [18, 26, 52]. Reduced cytotoxic function has been reported for mild and severe dengue during defervescence [53]. In our study, reduction in functional cytotoxic T cells was revealed by the lower proportion of CD8⁺perforin⁺ cells in DHF and reduced response to several viral peptides. Low CD4⁺ and CD8⁺ cell proliferation was observed both in DF and DHF; however, the lowest response was found in patients with hemorrhagic symptomatology. This could be associated with immune exhaustion observed in some studies on dengue [9, 41, 54, 55]. Exhausted T cells are characterized by specific

markers such as PD-1, IL-7R, and ICOS, reduced capacity to secrete IFN- γ , IL-2, or effector molecules (granzymes, perforin), and limited expansion capacity [41, 56].

The low levels of CD8⁺ T cells and reduced cytotoxic function observed in DHF patients may be related with kinetics of T cell responses on primary and secondary infection and not necessarily with the clinical outcome. During secondary heterologous DENV infection, an early and stronger T cell response was observed [9, 42]. It is also probable that the low levels of CD8⁺ cells are the consequence of previous activation that occurred early during infection and that negative feedback signals (IL-10, TGF- β) downregulated the activity of T cells and reduced their numbers. Therefore, we could be observing this phenomenon in a late phase after activation, when T cell numbers are reduced again. Other clues of higher activation of CD8⁺ cells are apparent increase in CD25 expression and lower frequency of perforin found by flow cytometry in DHF. This hypothesis is not contradictory to that of cell exhaustion, proposed previously; both include activation and downregulation phases. It is probable that DENV activates downregulatory signals (IL-10) to reduce the antiviral immune response as an evasion strategy to persist in the organism [50]. Notably, the clinical worsening of dengue patients could be associated with reduced activity of cytotoxic T cells induced by Treg cells [57].

Preservation of homeostasis after the activation of the antiviral cytotoxic response requires the development of regulatory T cells that are induced under the control of FOXP-3 [57]. A notable polarization of Treg response in DHF patients was indicated by the high proportion of CD3⁺ CD25⁺ cells and the 200-fold increase in FOXP-3 transcription that was not found in DF patients. Although FOXP-3 expression is not exclusive of the Treg lineage [58], expansion of Treg cells in acute dengue suggests that these cells suppressed the proliferative response of DENV-specific cytotoxic T cells, as what occurred *in vitro* and in a mouse model [59, 60].

By other side, our results show that a Th17 response was not involved in the pathogenesis of dengue in these patients; this is indicated by the low expression of ROR- γ and the lack of IL-17 both in DHF and DF patients. This is contrary to other studies that showed increased concentrations of IL-17 in dengue patients [61–63], including a study in Mexican patients that showed high levels of TH17 cells and IL-17 might be induced by PMA and ionomycin used to promote *in vitro* proliferation and differentiation of Th17 cells [63]. Reduced expression of ROR- γ in our study indicates that an intense downregulation process occurred in this gene associated with Th17 cells and IL-17 secretion. ROR- γ downregulation has been associated with T cell maturation in the thymus and differentiation of helper T cells in peripheral lymphoid organs; it is also related to several disorders, including infections. ROR- γ is downregulated by the presence of IL-10 in the microenvironment. Therefore, it is probable that reduced levels of ROR- γ is also consequence of FOXP3 expression and IL-10 secretion. In addition, ROR- γ is also susceptible to downregulation by GATA-3.

We also analyzed the presence of activation biomarkers on lymphocytes and other cells. CD40L expression

was significantly lower in patients with DHF, but the proportion of CD25⁺ (associated with Tregs and other cells) was significantly higher. CD40L is involved in the secretion of IL-12 as well as in the activation and differentiation of Th1 cells. Reduced numbers of Th1 cells have been reported in patients with severe dengue [64] and are associated with the presence of Treg cells, production of IL-10, and downregulation of CD40L [65, 66]. We and others have found the association of IL-10 levels with dengue severity [22, 50, 64].

Although patients were clinically classified in DF or DHF, our results should be taken with some reserve because most patients have reduced platelet counts. Platelet counts < 100,000 cells/mm³ are indicative of high risk for hemorrhage, and almost all patients in our study have < 10,000 cells/ml and any kind of hemorrhagic manifestations that indicates a severe hematological compromise. In addition, all patients were hospitalized; this reflects dengue complications, although patients classified as DF stay fewer days in hospitalization than DHF patients.

5. Conclusions

In this study, we analyzed the phenotype and functionality of immune cells in patients with dengue. Reduced amounts of functional cytotoxic CD8⁺ T cells and low expression of T-bet involved in Th1 differentiation were found in DHF patients that in contrast showed high levels of Th2 responses of CD4⁺ (GATA-3) and regulatory (Foxp3) T lymphocytes. These confluent characteristics determine the low antigenic response induced by viral peptides on immune cells of DHF patients and reveal the imbalance of Th1/Th2/Treg cells induced by dengue infection.

Data Availability

The clinical and laboratory data used to support the findings of this study are restricted by the Local Committees of Ethics and Research in Health of the Mexican Institute of Social Security, in order to protect patient privacy. Data are available from the corresponding author upon request for researchers who meet the criteria for access to confidential data.

Conflicts of Interest

The authors declare that there is no conflict of interest regarding the publication of this paper.

Authors' Contributions

Tania Estrada-Jiménez and Lilian Flores-Mendoza are the first authors. These authors contributed equally to the paper.

Acknowledgments

Julio Reyes-Leyva had a research fellowship from Fundación IMSS A.C. Tania Estrada-Jiménez had a scholarship from CONACYT (no. 209881) and IMSS (98220625). A special acknowledgement is due for the personnel of General Hospital of Zone #5 (HGZ5), IMSS, Q.F.B. María del Consuelo

Manjarrez, Q.F.B. Patricia Garrido, and Q.F.B. Erica Plata for their technical support. This study was supported by the Mexican Institute for Social Security (IMSS, grant FIS/IMSS/PROT/G15/1454 and infrastructure funds CTFIS/10RD/12/2011).

References

- [1] S. Bhatt, P. W. Gething, O. J. Brady et al., "The global distribution and burden of dengue," *Nature*, vol. 496, no. 7446, pp. 504–507, 2013.
- [2] B. E. Martina, P. Koraka, and A. D. Osterhau, "Dengue virus pathogenesis: an integrated view," *Clinical Microbiology Reviews*, vol. 22, no. 4, pp. 564–581, 2009.
- [3] A. N. Bäck and A. Lundkvist, "Dengue viruses - an overview," *Infection Ecology & Epidemiology*, vol. 3, 2013.
- [4] World Health Organization, "Dengue and severe dengue," 2020, <https://www.who.int/news-room/fact-sheets/detail/dengue-and-severe-dengue>.
- [5] Pan American Health Organization, "Media center "dengue in the Americas reaches highest number of cases recorded" recovered from," 2020, https://www3.paho.org/hq/index.php?option=com_content&view=article&id=15593:dengue-in-the-americas-reaches-highest-number-of-cases-recorded&Itemid=1926&lang=en.
- [6] I. Torres-Galicia, D. Cortés-Poza, and I. Becker, "Dengue in Mexico: an analysis of two decades," *Gaceta Medica*, vol. 150, no. 2, pp. 122–127, 2014.
- [7] N. Uno and T. M. Ross, "Dengue virus and the host innate immune response," *Emerging Microbes & Infections*, vol. 7, no. 1, pp. 1–11, 2018.
- [8] World Health Organization, *Dengue: Guidelines for Diagnosis, Treatment, Prevention and Control: New Edition*, Epidemiology, Burden of Disease and Transmission, Geneva, 2009.
- [9] A. L. St John and A. P. S. Rathore, "Adaptive immune responses to primary and secondary dengue virus infections," *Nature Reviews. Immunology*, vol. 19, no. 4, pp. 218–230, 2019.
- [10] G. Screaton, J. Mongkolsapaya, S. Yacoub, and C. Roberts, "New insights into the immunopathology and control of dengue virus infection," *Nature Reviews. Immunology*, vol. 15, no. 12, pp. 745–759, 2015.
- [11] A. L. Rothman, "Immunity to dengue virus: a tale of original antigenic sin and tropical cytokine storms," *Nature Reviews. Immunology*, vol. 11, no. 8, pp. 532–543, 2011.
- [12] F. Annunziato, C. Romagnani, and S. Romagnani, "The 3 major types of innate and adaptive cell-mediated effector immunity," *Journal of Allergy and Clinical Immunology*, vol. 135, no. 3, pp. 626–635, 2015.
- [13] D. Weiskopf and A. Sette, "T-cell immunity to infection with dengue virus in humans," *Frontiers in Immunology*, vol. 5, 2014.
- [14] S. J. Gagnon, F. A. Ennis, and A. L. Rothman, "Bystander target cell lysis and cytokine production by dengue virus-specific human CD4+cytotoxic T-lymphocyte clones," *Journal of Virology*, vol. 73, no. 5, pp. 3623–3629, 1999.
- [15] H. S. Bashyam, S. Green, and A. L. Rothman, "Dengue virus-reactive CD8+T cells display quantitative and qualitative differences in their response to variant epitopes of heterologous viral serotypes," *Journal of Immunology*, vol. 176, no. 5, pp. 2817–2824, 2006.
- [16] A. W. Lim and A. N. McKenzie, "Deciphering the transcriptional switches of innate lymphoid cell programming: the right factors at the right time," *Genes and Immunity*, vol. 16, no. 3, pp. 177–186, 2015.
- [17] J. Ren and B. Li, "The functional stability of FOXP3 and ROR γ t in Treg and Th17 and their therapeutic applications," *Advances in Protein Chemistry and Structural Biology*, vol. 107, pp. 155–189, 2017.
- [18] L. E. Yauch, R. M. Zellweger, M. F. Kotturi et al., "A protective role for dengue virus-specific CD8+T cells," *Journal of Immunology*, vol. 182, no. 8, pp. 4865–4873, 2009.
- [19] L. Rivino, E. A. Kumaran, T. L. Thein et al., "Virus-specific T lymphocytes home to the skin during natural dengue infection," *Science Translational Medicine*, vol. 7, no. 278, 2015.
- [20] D. Weiskopf, M. A. Angelo, E. L. de Azeredo et al., "Comprehensive analysis of dengue virus-specific responses supports an HLA-linked protective role for CD8+ T cells," *Proceedings of the National Academy of Sciences of the United States of America*, vol. 110, no. 22, pp. E2046–E2053, 2013.
- [21] S. Hatch, T. P. Endy, S. Thomas et al., "Intracellular cytokine production by dengue virus-specific T cells correlates with subclinical secondary infection," *The Journal of Infectious Diseases*, vol. 203, no. 9, pp. 1282–1291, 2011.
- [22] G. N. Malavige and G. S. Ogg, "T cell responses in dengue viral infections," *Journal of Clinical Virology*, vol. 58, no. 4, pp. 605–611, 2013.
- [23] R. F. Chen, K. D. Yang, L. Wang, J. W. Liu, C. C. Chiu, and J. T. Cheng, "Different clinical and laboratory manifestations between dengue haemorrhagic fever and dengue fever with bleeding tendency," *Transactions of the Royal Society of Tropical Medicine and Hygiene*, vol. 101, no. 11, pp. 1106–1113, 2007.
- [24] F. Perdomo-Celis, M. S. Salvato, S. Medina-Moreno, and J. C. Zapata, "T-cell response to viral hemorrhagic fevers," *Vaccines*, vol. 7, no. 1, 2019.
- [25] J. Mongkolsapaya, W. Dejnirattisai, X. N. Xu et al., "Original antigenic sin and apoptosis in the pathogenesis of dengue hemorrhagic fever," *Nature Medicine*, vol. 9, no. 7, pp. 921–927, 2003.
- [26] P. Sun and T. J. Kochel, "The battle between infection and host immune responses of dengue virus and its implication in dengue disease pathogenesis," *The Scientific World Journal*, vol. 2013, Article ID 843469, 11 pages, 2013.
- [27] J. Mongkolsapaya, T. Duangchinda, W. Dejnirattisai et al., "T cell responses in dengue hemorrhagic fever: are cross-reactive T cells suboptimal?," *Journal of Immunology*, vol. 176, no. 6, pp. 3821–3829, 2006.
- [28] C. M. Beaumier, A. Mathew, H. S. Bashyam, and A. L. Rothman, "Cross-reactive memory CD8+T cells alter the immune response to heterologous secondary dengue virus infections in mice in a sequence-specific manner," *The Journal of Infectious Diseases*, vol. 197, no. 4, pp. 608–617, 2008.
- [29] D. Weiskopf, D. J. Bangs, J. Sidney et al., "Dengue virus infection elicits highly polarized CX3CR1+cytotoxic CD4+T cells associated with protective immunity," *Proceedings of the National Academy of Sciences of the United States of America*, vol. 112, no. 31, pp. E4256–E4263, 2015.
- [30] T. Duangchinda, W. Dejnirattisai, S. Vasanawathana et al., "Immunodominant T-cell responses to dengue virus NS3 are associated with DHF," *Proceedings of the National Academy of Sciences of the United States of America*, vol. 107, no. 39, pp. 16922–16927, 2010.

- [31] Y. Tian, A. Grifoni, A. Sette, and D. Weiskopf, "Human T cell response to dengue virus infection," *Frontiers of Immunology*, vol. 10, 2019.
- [32] C. P. Simmons, T. Dong, N. V. Chau et al., "Early T-cell responses to dengue virus epitopes in Vietnamese adults with secondary dengue virus infections," *Journal of Virology*, vol. 79, no. 9, pp. 5665–5675, 2005.
- [33] I. Kurane, L. Zeng, M. A. Brinton, and F. A. Ennis, "Definition of an epitope on NS3 recognized by human CD4⁺ cytotoxic T lymphocyte clones cross-reactive for dengue virus types 2, 3, and 4," *Virology*, vol. 240, no. 2, pp. 169–174, 1998.
- [34] A. Mathew, I. Kurane, S. Green et al., "Predominance of HLA-restricted cytotoxic T-lymphocyte responses to serotype-cross-reactive epitopes on nonstructural proteins following natural secondary dengue virus infection," *Journal of Virology*, vol. 72, no. 5, pp. 3999–4004, 1998.
- [35] L. Rivino, E. A. Kumaran, V. Jovanovic et al., "Differential targeting of viral components by CD4⁺ versus CD8⁺ T lymphocytes in dengue virus infection," *Journal of Virology*, vol. 87, no. 5, pp. 2693–2706, 2013.
- [36] D. T. Wijeratne, S. Fernando, L. Gomes et al., "Association of dengue virus-specific polyfunctional T-cell responses with clinical disease severity in acute dengue infection," *Immunity, Inflammation and Disease*, vol. 7, no. 4, pp. 276–285, 2019.
- [37] A. Mathew, E. Townsley, and F. A. Ennis, "Elucidating the role of T cells in protection against and pathogenesis of dengue virus infections," *Future Microbiology*, vol. 9, no. 3, pp. 411–425, 2014.
- [38] G. Sánchez-Burgos, J. Ramos-Castañeda, R. Cedillo-Rivera, and E. Dumonteil, "Immunogenicity of novel dengue virus epitopes identified by bioinformatic analysis," *Virus Research*, vol. 153, no. 1, pp. 113–120, 2010.
- [39] L. Zeng, I. Kurane, Y. Okamoto, F. A. Ennis, and M. A. Brinton, "Identification of amino acids involved in recognition by dengue virus NS3-specific, HLA-DR15-restricted cytotoxic CD4⁺ T-cell clones," *Journal of Virology*, vol. 70, no. 5, pp. 3108–3117, 1996.
- [40] P. G. Livingston, I. Kurane, L. C. Dai et al., "Dengue virus-specific, HLA-B35-restricted, human CD8⁺ cytotoxic T lymphocyte (CTL) clones. Recognition of NS3 amino acids 500 to 508 by CTL clones of two different serotype specificities," *The Journal of Immunology*, vol. 154, no. 3, pp. 1287–1295, 1995.
- [41] A. Chandele, J. Sewatanon, S. Gunisetty et al., "Characterization of human CD8 T cell responses in dengue virus-infected patients from India," *Journal of Virology*, vol. 90, no. 24, pp. 11259–11278, 2016.
- [42] H. Friberg, H. Bashyam, T. Toyosaki-Maeda et al., "Cross-reactivity and expansion of dengue-specific T cells during acute primary and secondary infections in humans," *Scientific Reports*, vol. 1, no. 1, 2011.
- [43] F. Yu, S. Sharma, J. Edwards, L. Feigenbaum, and J. Zhu, "Dynamic expression of transcription factors T-bet and GATA-3 by regulatory T cells maintains immunotolerance," *Nature Immunology*, vol. 16, no. 2, pp. 197–206, 2015.
- [44] T. Usui, J. C. Preiss, Y. Kanno et al., "T-bet regulates Th1 responses through essential effects on GATA-3 function rather than on IFNG gene acetylation and transcription," *The Journal of Experimental Medicine*, vol. 203, no. 3, pp. 755–766, 2006.
- [45] R. Yagi, J. Zhu, and W. E. Paul, "An updated view on transcription factor GATA3-mediated regulation of Th1 and Th2 cell differentiation," *International Immunology*, vol. 23, no. 7, pp. 415–420, 2011.
- [46] U. C. Chaturvedi, R. Agarwal, E. A. Elbishbishi, and A. S. Mustafa, "Cytokine cascade in dengue hemorrhagic fever: implications for pathogenesis," *FEMS Immunology and Medical Microbiology*, vol. 28, no. 3, pp. 183–188, 2000.
- [47] P. Li, R. Spolski, W. Liao, and W. J. Leonard, "Complex interactions of transcription factors in mediating cytokine biology in T cells," *Immunological Reviews*, vol. 261, no. 1, pp. 141–156, 2014.
- [48] U. C. Chaturvedi, R. Shrivastava, R. K. Tripathi, and R. Nagar, "Denguevirus-specific suppressor T cells: current perspectives," *FEMS Immunology and Medical Microbiology*, vol. 50, no. 3, pp. 285–299, 2007.
- [49] U. C. Chaturvedi, R. Raghupathy, A. S. Pacsa et al., "Shift from a Th1-type response to Th2-type in dengue haemorrhagic fever," *Current Science*, vol. 76, no. 1, pp. 63–69, 1999.
- [50] L. K. Flores-Mendoza, T. Estrada-Jiménez, V. Sedeño-Monge et al., "IL-10 and socs3 are predictive biomarkers of dengue hemorrhagic fever," *Mediators of Inflammation*, vol. 2017, Article ID 5197592, 10 pages, 2017.
- [51] A. M. de Matos, K. I. Carvalho, D. S. Rosa et al., "CD8⁺ T lymphocyte expansion, proliferation and activation in dengue fever," *PLoS Neglected Tropical Diseases*, vol. 9, no. 2, 2015.
- [52] K. S. Myint, T. P. Endy, D. Mongkolsirichaikul et al., "Cellular immune activation in children with acute dengue virus infections is modulated by apoptosis," *The Journal of Infectious Diseases*, vol. 194, no. 5, pp. 600–607, 2006.
- [53] D. H. Manh, L. N. Weiss, N. V. Thuong et al., "Kinetics of CD4⁺ T helper and CD8⁺ effector T cell responses in acute dengue patients," *Frontiers in Immunology*, vol. 11, no. 11, 2020.
- [54] M. Singla, M. Kar, T. Sethi et al., "Immune response to dengue virus infection in pediatric patients in New Delhi, India—association of viremia, inflammatory mediators and monocytes with disease severity," *PLoS Neglected Tropical Diseases*, vol. 10, 2016.
- [55] K. Haltaufderhyde, A. Srikiatkachorn, S. Green et al., "Activation of peripheral T follicular helper cells during acute dengue virus infection," *The Journal of Infectious Diseases*, vol. 218, no. 10, pp. 1675–1685, 2018.
- [56] C. U. Blank, W. N. Haining, W. Held et al., "Defining 'T cell exhaustion,'" *Nature Reviews. Immunology*, vol. 19, no. 11, pp. 665–674, 2019.
- [57] A. McNally, G. R. Hill, T. Sparwasser, R. Thomas, and R. J. Steptoe, "CD4⁺CD25⁺ regulatory T cells control CD8⁺ T-cell effector differentiation by modulating IL-2 homeostasis," *Proceedings of the National Academy of Sciences of the United States of America*, vol. 108, no. 18, pp. 7529–7534, 2011.
- [58] V. Pillai, S. B. Ortega, C. K. Wang, and N. J. Karandikar, "Transient regulatory T-cells: a state attained by all activated human T-cells," *Clinical Immunology*, vol. 123, no. 1, pp. 18–29, 2007.
- [59] J. A. George, S. O. Park, J. Y. Choi, E. Uyangaa, and S. K. Eo, "Double-faced implication of CD4⁺Foxp3⁺ regulatory T cells expanded by acute dengue infection via TLR2/MyD88 pathway," *European Journal of Immunology*, vol. 50, no. 7, pp. 1000–1018, 2020.
- [60] K. Luhn, C. P. Simmons, E. Moran et al., "Increased frequencies of CD4⁺CD25^{high} regulatory T cells in acute dengue

- infection,” *The Journal of Experimental Medicine*, vol. 204, no. 5, pp. 979–985, 2007.
- [61] T. Furuta, L. A. Murao, N. T. Lan et al., “Association of mast cell-derived VEGF and proteases in dengue shock syndrome,” *PLoS Neglected Tropical Diseases*, vol. 6, 2012.
- [62] A. Jain, N. Pandey, R. K. Garg, and R. Kumar, “IL-17 level in patients with dengue virus infection & its association with severity of illness,” *Journal of Clinical Immunology*, vol. 33, no. 3, pp. 613–618, 2013.
- [63] L. A. Sánchez-Vargas, K. G. Hernández-Flores, P. Thomas-Dupont et al., “Characterization of the IL-17 and CD4+ Th17 cells in the clinical course of dengue virus infections,” *Viruses*, vol. 12, no. 12, 2020.
- [64] R. F. Chen, J. W. Liu, W. T. Yeh et al., “Altered T helper 1 reaction but not increase of virus load in patients with dengue hemorrhagic fever,” *FEMS Immunology and Medical Microbiology*, vol. 44, no. 1, pp. 43–50, 2005.
- [65] M. Grazia Roncarolo, S. Gregori, M. Battaglia, R. Bacchetta, K. Fleischhauer, and M. K. Levings, “Interleukin-10-secreting type 1 regulatory T cells in rodents and humans,” *Immunological Reviews*, vol. 212, no. 1, pp. 28–50, 2006.
- [66] A. O’Garra and P. Vieira, “Regulatory T cells and mechanisms of immune system control,” *Nature Medicine*, vol. 10, no. 8, pp. 801–805, 2004.

Research Article

Increased TNF- α Initiates Cytoplasmic Vacuolization in Whole Blood Coculture with Dengue Virus

Rahmat Dani Satria,^{1,2,3,4} Tzu-Wen Huang ^{4,5} Ming-Kai Jhan,^{4,5} Ting-Jing Shen ^{4,5}
Po-Chun Tseng,^{4,6} Yun-Ting Wang,⁴ Zhen-Yu Yang,^{4,5} Chung-Hsi Hsing ^{7,8}
and Chiou-Feng Lin ^{4,5,6}

¹International Ph.D. Program in Medicine, College of Medicine, Taipei Medical University, Taipei 110, Taiwan

²Department of Clinical Pathology and Laboratory Medicine, Faculty of Medicine, Public Health and Nursing, Universitas Gadjah Mada, Yogyakarta 55281, Indonesia

³Clinical Laboratory Installation, Dr. Sardjito Central General Hospital, Yogyakarta 55281, Indonesia

⁴Department of Microbiology and Immunology, School of Medicine, College of Medicine, Taipei Medical University, Taipei 110, Taiwan

⁵Graduate Institute of Medical Sciences, College of Medicine, Taipei Medical University, Taipei 110, Taiwan

⁶Core Laboratory of Immune Monitoring, Office of Research & Development, Taipei Medical University, Taipei 110, Taiwan

⁷Department of Medical Research, Chi Mei Medical Center, Tainan 710, Taiwan

⁸Department of Anesthesiology, Chi Mei Medical Center, Tainan 710, Taiwan

Correspondence should be addressed to Chung-Hsi Hsing; hsing@mail.chimei.org.tw and Chiou-Feng Lin; cflin2014@tmu.edu.tw

Received 12 November 2020; Revised 9 April 2021; Accepted 26 April 2021; Published 7 May 2021

Academic Editor: Luiz Felipe Domingues Passero

Copyright © 2021 Rahmat Dani Satria et al. This is an open access article distributed under the Creative Commons Attribution License, which permits unrestricted use, distribution, and reproduction in any medium, provided the original work is properly cited.

During the acute febrile phase of dengue virus (DENV) infection, viremia can cause severe systemic immune responses accompanied by hematologic disorders. This study investigated the potential induction and mechanism of the cytopathic effects of DENV on peripheral blood cells *ex vivo*. At one day postinfection, there was viral nonstructural protein NS1 but no further virus replication measured in the whole blood culture. Notably, DENV exposure caused significant vacuolization in monocytic phagocytes. With a minor change in the complete blood cell count, except for a minor increase in neutrophils and a significant decrease in monocytes, the immune profiling assay identified several changes, particularly a significant reduction in CD14-positive monocytes as well as CD11c-positive dendritic cells. Abnormal production of TNF- α was highly associated with the induction of vacuolization. Manipulating TNF- α expression resulted in cytopathogenic effects. These results demonstrate the potential hematological damage caused by *ex vivo* DENV-induced TNF- α .

1. Introduction

Dengue virus (DENV) infection is one of the most critical global health problems, especially in subtropical regions. Unfortunately, DENV causes disease in 50–100 million individuals per year [1]. Dengue-infected patients have different manifestations ranging from mild acute febrile illness, dengue fever, and dengue hemorrhagic fever to severe dengue

shock syndrome, leading to plasma leakage hypovolemic shock, causing death [2]. In addition to hematologic disorders, patients with severe dengue infection may display various diseases, including multiple organ dysfunction and neurological complications [3]. According to clinicopathological studies, hematologic changes, such as leukopenia and thrombocytopenia, are possibly involved in the coagulopathy and vasculopathy of dengue-infected patients

following the acute febrile phase of infection [4]. In dengue-related hematological pathogenesis initiation, a direct viral attack and indirect host effects are generally involved [5–8].

The complex interaction between the host and viral factors makes it challenging to explain the pathogenesis of DENV infection. However, it is believed that the main factors causing disease severity are typically due to numerous host factors. Several hypotheses have been formulated to explain severe dengue causes, including genetic involvement, underlying disorders, viral load, viral virulence, and immune responses [9–12]. Antibody-dependent enhancement is assumed to be pathogenic, mainly in the secondary infection of DENV, when patients are infected with a different serotype from the previous one [13]. Also, the imbalance of cytokines in some patients, namely, the cytokine storm, was related to dengue disease severity [14, 15]. Clinical studies have shown that tumor necrosis factor- α (TNF- α) is associated with increased severity and progression of DENV infection due to exacerbated proinflammatory cytokine production leading to instability in vascular endothelial cell function [16–18]. The impact of serum TNF- α on immune cells remains undefined.

Innate immune cells, such as neutrophils and monocytes, are believed to have an essential role in dengue pathogenesis [19, 20]. There is increased neutrophil degranulation in patients with DENV infection, as indicated by an increase in the levels of interleukin-8 (IL-8), elastase, and lactoferrin [21]. Following degranulation, in the acute febrile phase of DENV infection, there is a significant reduction in neutrophil counts, namely, neutropenia, in most patients with dengue disease [22]. Moreover, DENV infection triggers neutrophil activation and degranulation during the febrile phase, associated with increased plasma levels of proinflammatory mediators, such as IL-8 and TNF- α . Upon hematological immunity, activated neutrophils and monocytes can destroy microbes by releasing various toxic components, such as reactive oxygen species and granular enzymes [20, 21, 23]. The establishment of vacuolization is caused by the fusion process of endosomes, autophagosomes, and secretory vesicles [24]. In this study, we investigated the induction of cellular vacuolization and its possible regulation by TNF- α in an *ex vivo* whole blood (WB) model of DENV infection.

2. Materials and Methods

2.1. Antibodies and Reagents. The reagents and antibodies (Abs) used were as follows: recombinant human TNF- α (hTNF- α , PeproTech, Rocky Hill, NJ); crystal violet (Sigma-Aldrich Co., St. Louis, MO, USA); neutralizing antibodies against TNF- α (Abcam, Cambridge, MA); PerCP-conjugated anti-CD4 (Catalog# MA119775); PE-Cyanine 7-conjugated anti-CD8 (Catalog# 25-0086-42); PE-conjugated anti-CD11c (Catalog# 12-0116-42); APC-conjugated anti-CD14 (Catalog# 17-0149-42); eFluor 506-conjugated anti-CD19 (Catalog# 69-0199-42); APC-eFluor 780-conjugated anti-CD25 (Catalog# 47-0257-42); Super Bright 600-conjugated anti-CD56 (Catalog# 63-0566-42); Qdot 705-conjugated anti-HLA-DR (Catalog# Q22159) (Invitrogen, Thermo Fisher Scientific, Waltham, MA); Alexa Fluor 488-

conjugated anti-CD16 (Catalog# 302019); and Alexa Fluor 700-conjugated anti-CD62L (Catalog# 304820) (BioLegend, San Diego, CA).

2.2. Cell Culture and Virus Culture. Baby hamster kidney- (BHK-) 21 cells (ATCC® CCL-10™) and *Aedes albopictus* clone C6/36 cells (ATCC® CRL-1660™) were cultured in Dulbecco's Modified Eagle's Medium (DMEM, Invitrogen Life Technologies) containing 10% heat-inactivated fetal bovine serum (FBS) (Sigma-Aldrich). The DENV serotype (DENV2 PL046) was maintained in C6/36 cells. C6/36 cell monolayers were seeded in a 75 cm² tissue culture flask with DENV coculture at a multiplicity of infection (MOI) of 0.01 and incubated at 28°C in 5% CO₂ for 5 days. The virus supernatant was concentrated and filtered with Amicon Ultra centrifugal filters (Millipore, Billerica, MA, USA) and then stored at -80°C before use.

2.3. Human Blood Collection. The human study was performed according to guidelines established by the Taipei Medical University- (TMU-) Joint Institutional Review Board (TMU-JIRB). Informed consent from all participants, as approved by TMU-JIRB, was obtained. All five participants were volunteers with confirmed functional health status and good physical condition who were free from medication and had no current infectious disease. All samples were collected at the same time by sodium heparin BD vacutainer collection tubes (5 ml; Becton Drive Vacutainer, Franklin Lakes, USA). All blood collection tubes were gently inverted to mix additives with the blood after collection.

2.4. DENV *Ex Vivo* Infection. One hundred microliters of WB was seeded in a 24-well plate supplemented with 100 μ l of Roswell Park Memorial Institute (RPMI) 1640 medium containing DENV (MOI = 1). For infection, the total number of WB leukocytes was calculated using a hematology analyzer as described below. The WB was incubated with the calculated plaque-forming units of DENV at 37°C for 24 h. The culture supernatants were collected for measuring viral replication and protein expression.

2.5. DENV and Antigen Detection. For the plaque assay, BHK-21 cells were plated in a 12-well plate (2×10^5 cells/well) and cultured in DMEM at 28°C in 5% CO₂. After adsorption with serially diluted culture supernatants for 1 h, the solution was replaced with fresh DMEM containing 2% FBS and 0.5% methylcellulose (Sigma-Aldrich). Five days postinfection, the medium was removed, and the cells were fixed and stained with a crystal violet solution containing 1% crystal violet, 0.64% NaCl, and 2% formalin. To calculate the viral titer, the formation of plaques was counted at each dilution. For the DENV nonstructural protein NS1 detection, NS1 Antigen Rapid Test Cassette obtained from AsiaGen (Tainan, Taiwan) was used according to the manufacturer's instructions.

2.6. Wright-Giemsa Staining. Following DENV *ex vivo* infection for 24 and 48 h, a drop of WB approximately 3 mm in diameter on each sample was placed at one end of the slide and then spread across the width of the slide. All smears of

blood were air-dried and stained with Wright-Giemsa stain (Tonyar Biotech, Taipei, Taiwan). Cells were photographed and counted under an optical microscope (Olympus CX23; Olympus, Tokyo, Japan).

2.7. Complete Blood Counts (CBCs). A complete blood count (CBC) test was conducted on heparinized peripheral WB following DENV infection for 24 h by using a DxH 500 hematology analyzer (Beckman Coulter, Clare, Ireland).

2.8. Immune Profiling. Following DENV (MOI = 1) infection in 200 μ l of WB *ex vivo* for 24 h, representative flow cytometric analysis was conducted using an Attune NxT Flow Cytometer (Thermo Fisher Scientific) and performed by no-wash no-lyse staining for specific cell surface markers (CD4, CD8, CD11c, CD14, CD16, CD19, CD25, CD56, CD62L, and HLA-DR) according to the manufacturer's instructions (<https://www.thermofisher.com/order/catalog/product/100022776#/100022776>).

2.9. Enzyme-Linked Immunosorbent Assay (ELISA). According to the manufacturer's instructions, the concentration of human TNF- α in the plasma samples was determined using DuoSet ELISA Development System kits (R&D Systems, Minneapolis, MN). In brief, we coated microwells with capture Abs against TNF- α and then blocked the wells with 1% bovine serum albumin in phosphate-buffered saline (PBS). We added the tested serum, added the hTNF- α detection Abs, and then developed the signal with HRP-conjugated detection Abs against human IgG. The relative optical density was determined using a microplate reader set to 450 nm.

2.10. Statistical Analysis. Values are expressed as the mean \pm standard deviation (SD). Groups were compared by using Student's two-tailed unpaired *t*-test. These analyses were performed using GraphPad Prism 4 software (GraphPad Software, La Jolla, CA). Statistical significance was set at $p < 0.05$.

3. Results

3.1. DENV Causes Infection but Not Replication in the Blood Ex Vivo. To mimic a circulation situation during the acute febrile phase of DENV infection with viremia as demonstrated previously [25, 26], we created a novel *ex vivo* model of WB infection without peripheral blood mononuclear cell (PBMC) isolation. DENV was inoculated in the WB culture *ex vivo*. At 24 h postinfection of the coculture system, as summarized in the experimental flowchart (Figure 1(a)), in addition to analyzing the viral infection and antigen expression, several approaches were conducted to evaluate the induction of cytopathology, immune cell number and population changes, and cytokine response. For detecting DENV replication and release, the supernatant of the WB culture was harvested, and a plaque assay was then performed in a standard BHK-21 cell system [27]. Simultaneously, a commercial NS1-based rapid test cassette was performed to measure viral protein secretion [28]. Compared with the positive control (DENV-containing supernatant), DENV (Figure 1(b)) was not detectable, but viral NS1 (Figure 1(c)) was significantly

detected in all five tests (Cases 1-5). The results showed that DENV could cause infection but failed to release the virion in WB culture *ex vivo*.

3.2. DENV Coculture Causes Mononuclear Phagocytic Cell Vacuolization in the Blood Ex Vivo. After DENV coculture caused infection in the WB culture, we evaluated the morphological changes that occurred in leukocytes after viral incubation. In the DENV-WB coculture *ex vivo*, the suspected targets of DENV infection are the myeloid lineage's immune cells, such as neutrophils and monocytes [20, 29, 30]. Following DENV (MOI = 1) coculture in 100 μ l of WB *ex vivo* for 24 and 48 h, Wright-Giemsa staining showed histopathological changes significantly in mononuclear cells in all five tests (Figure 2(a)). There was an increase in the percentage of vacuolated cells after inoculation with DENV at 24 h (DENV, $82.53 \pm 4.84\%$; mock, $24.06 \pm 12.07\%$; $p = 0.001$) (Figure 2(b)). While DENV was able to cause infection in WB culture *ex vivo*, the results showed intracellular vacuolization in monocytes.

3.3. Complete Blood Count (CBC) Results Display a Decrease in Monocytes in the Blood Coculture with DENV Ex Vivo. To determine whether there was a change in the number of leukocytes, we next examined CBCs after DENV-WB coculture for 24 h. We found an increase in the number of neutrophils in the DENV group (DENV, $56.80 \pm 7.37\%$; mock, $44.52 \pm 9.26\%$) and a decrease in the number of monocytes in the DENV group (DENV, $0.908 \pm 0.30\%$; mock, $4.37 \pm 1.66\%$) (Figure 3). Monocytes are the most critical blood mononuclear phagocyte and one of the leading cell targets of DENV [31, 32]. The results showed a decrease in the number of monocytes caused by DENV *ex vivo*.

3.4. Immune Profiling Shows Cell Changes in the Blood Coculture with DENV Ex Vivo. In response to infection, alterations in blood cells are dependent on the viral load and duration of the disease [33]. Since the CBC showed a minor change in leukocytes, we evaluated blood cells by using an immune profiling approach. Multiparameter flow cytometric analysis was utilized to assess the subpopulations of immune cells, including those in the DENV-inoculated group (Figure 4(a)) and the mock control group (Figure 4(b)). In this analysis, DENV infection decreased the frequency of blood monocytes (CD14⁺) and dendritic cells (CD11c⁺) but increased total T (Th+Tc), Th (CD4⁺CD56⁻), naïve and memory Tc (CD4⁺CD56⁻), and total NK (CD56⁺) cells (Figure 4(c)). The findings indicate that DENV decreases monocytes and dendritic cells in *ex vivo* conditions of infection.

3.5. The Generation of TNF- α Is Correlated with Vacuolization in Blood Coculture with DENV Ex Vivo. Based on our findings, the blood monocytes' change was consistent with increasing numbers of cytoplasmic vacuoles in blood cells *ex vivo*. It is hypothesized that the cause of vacuolization is proinflammatory cytokines secreted by blood cells [24]. Therefore, we measured TNF- α production by ELISA. We found abnormal production of TNF- α in the DENV-inoculated groups at 24 h (DENV, 263.30 ± 180.08 pg/ml)

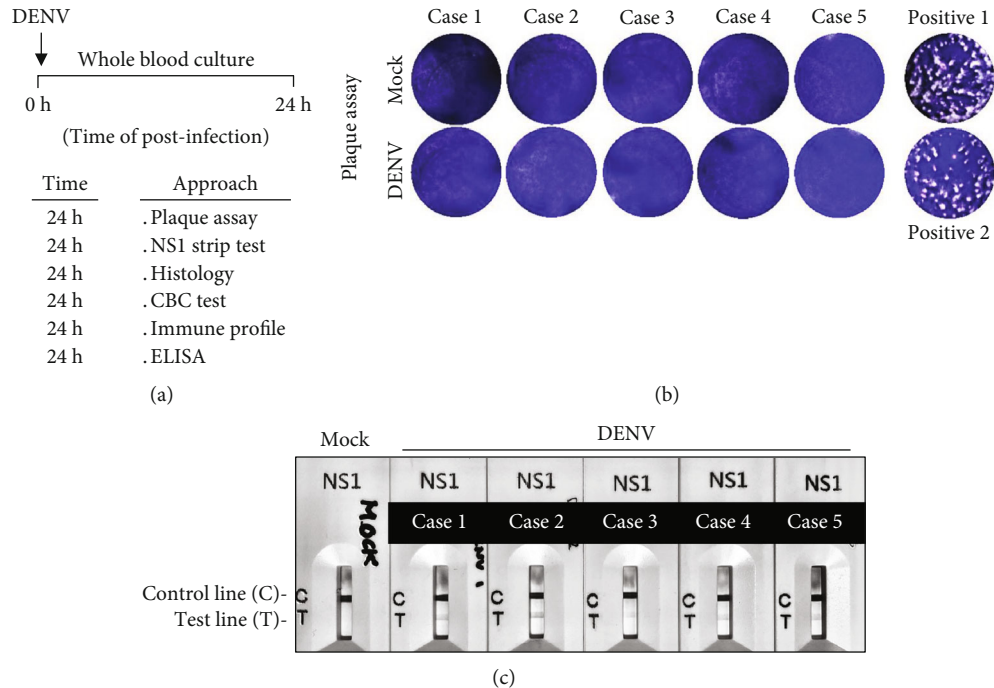


FIGURE 1: DENV infection of whole blood (WB) cells 24 h postincubation. (a) Experimental flowchart of this study. Following DENV (MOI = 1) infection in $100 \mu\text{l}$ of WB *ex vivo* for 24 h, five plasma samples were harvested to detect DENV infection. (b) The images (10x objectives) of plaque assay showed no viral replication. (c) An NS1 rapid test showed the expression of the NS1 dengue antigen in the plasma samples. Two positive controls were also performed for the plaque assay.

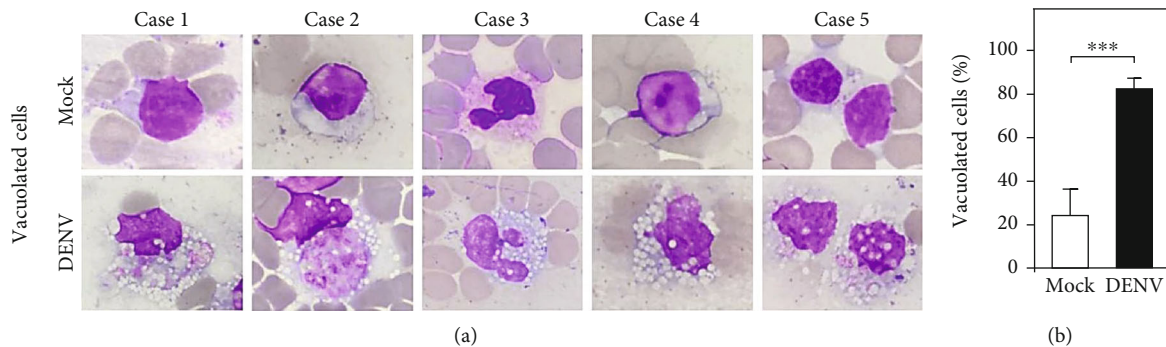


FIGURE 2: Wright-Giemsa staining images of whole blood (WB) cells 24 h postincubation. Following DENV (MOI = 1) coculture in $100 \mu\text{l}$ of WB *ex vivo* for 24 h, Wright-Giemsa staining, shown by an oil immersion field (100x objectives), presented histopathological changes in mononuclear cells (a). The percentages of vacuolated cells are shown (b). The quantitative data are depicted as the mean \pm SD obtained from five cases. *** $p < 0.001$, compared to the mock group.

postincubation (Figure 5(a)). Notably, we found a strong correlation between TNF- α production and the number of vacuolated cells ($r = 0.738$; $p = 0.015$) (Figure 5(b)). These results indicate that the occurrence of vacuolization is highly correlated with DENV-induced TNF- α .

3.6. TNF- α Determines Vacuolization in Blood Coculture with DENV *Ex Vivo*. To explore the mechanisms of induction of vacuolization by TNF- α , we added human TNF- α (hTNF- α , 100 ng/ml) to the WB culture *ex vivo*. After 24 h of treatment, Wright-Giemsa staining showed histopathological changes in mononuclear and polymorphonuclear cells in both tests (Figure 6(a)). After quantification, there was an increase in the percentage of vacuolated cells after cotreatment with

hTNF- α for 24 h (TNF- α , $64.83 \pm 13.77\%$; mock, $7.90 \pm 2.83\%$; $p = 0.01$) (Figure 6(b)). To ensure that TNF- α caused vacuolization, we administered anti-TNF- α to DENV-WB coculture, and the results showed a large decrease in the number of vacuolated cells after cotreatment with anti-TNF- α (DENV, $82.53 \pm 4.84\%$; DENV+ anti-TNF- α , $30.70 \pm 15.26\%$; and mock, $24.06 \pm 12.08\%$) (Figure 6(c)). These results demonstrated that the vacuolization is not caused by viral replication but is caused by DENV-induced TNF- α .

4. Discussion

In the acute febrile phase of dengue-infected patients, the viral load in circulation is associated with disease severity

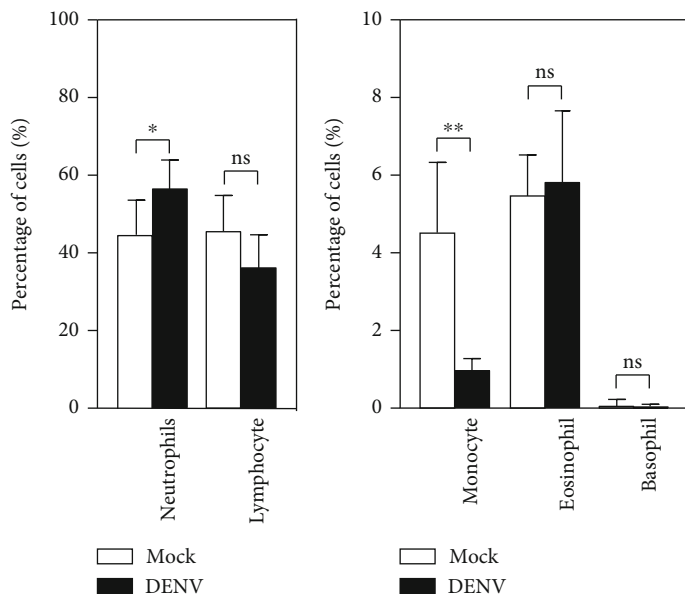


FIGURE 3: CBC results of whole blood (WB) cells 24 h postincubation. Following DENV (MOI = 1) coculture in 100 μ l of WB *ex vivo* for 24 h, the CBC test showed the percentages of specific cell populations as noted. The quantitative data are depicted as the mean \pm SD obtained from five cases. * $p < 0.05$ and ** $p < 0.01$, compared to the mock group. ns: not significant.

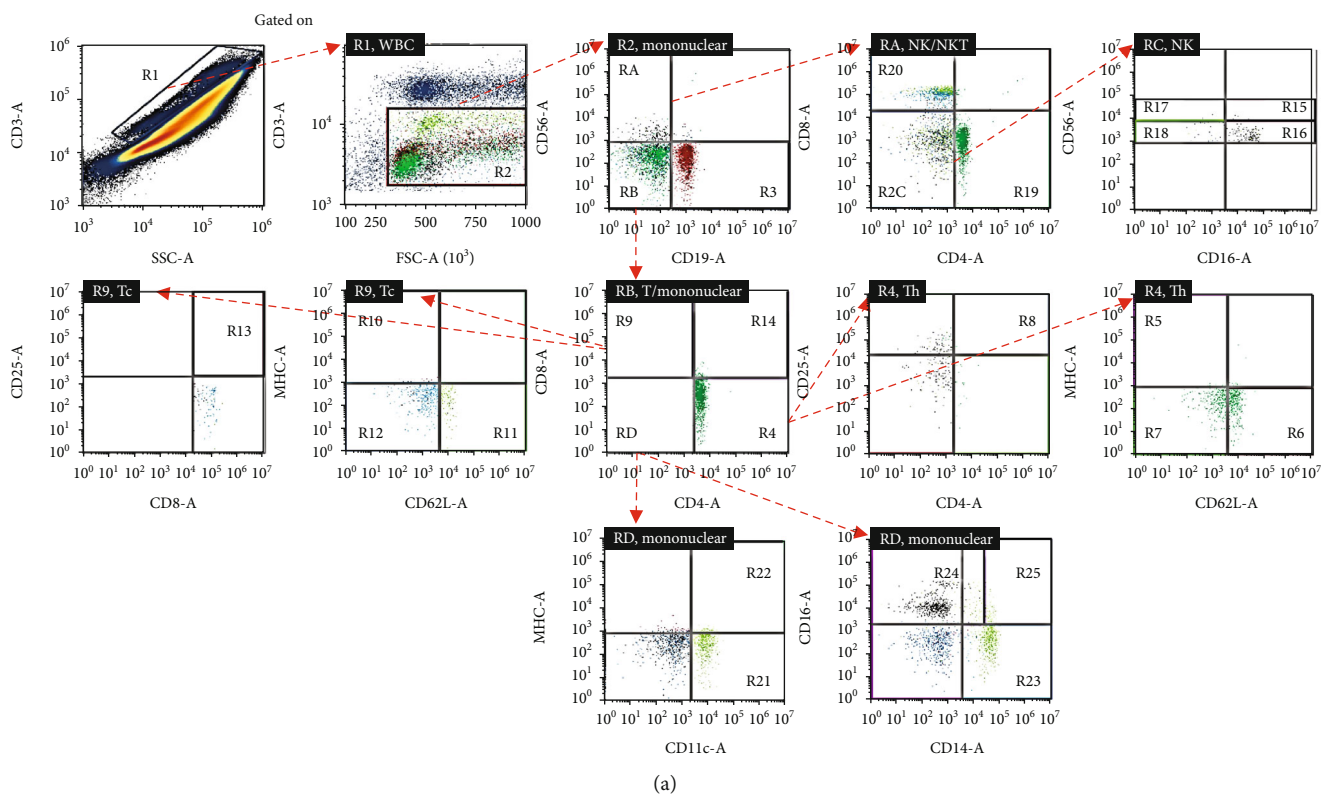


FIGURE 4: Continued.

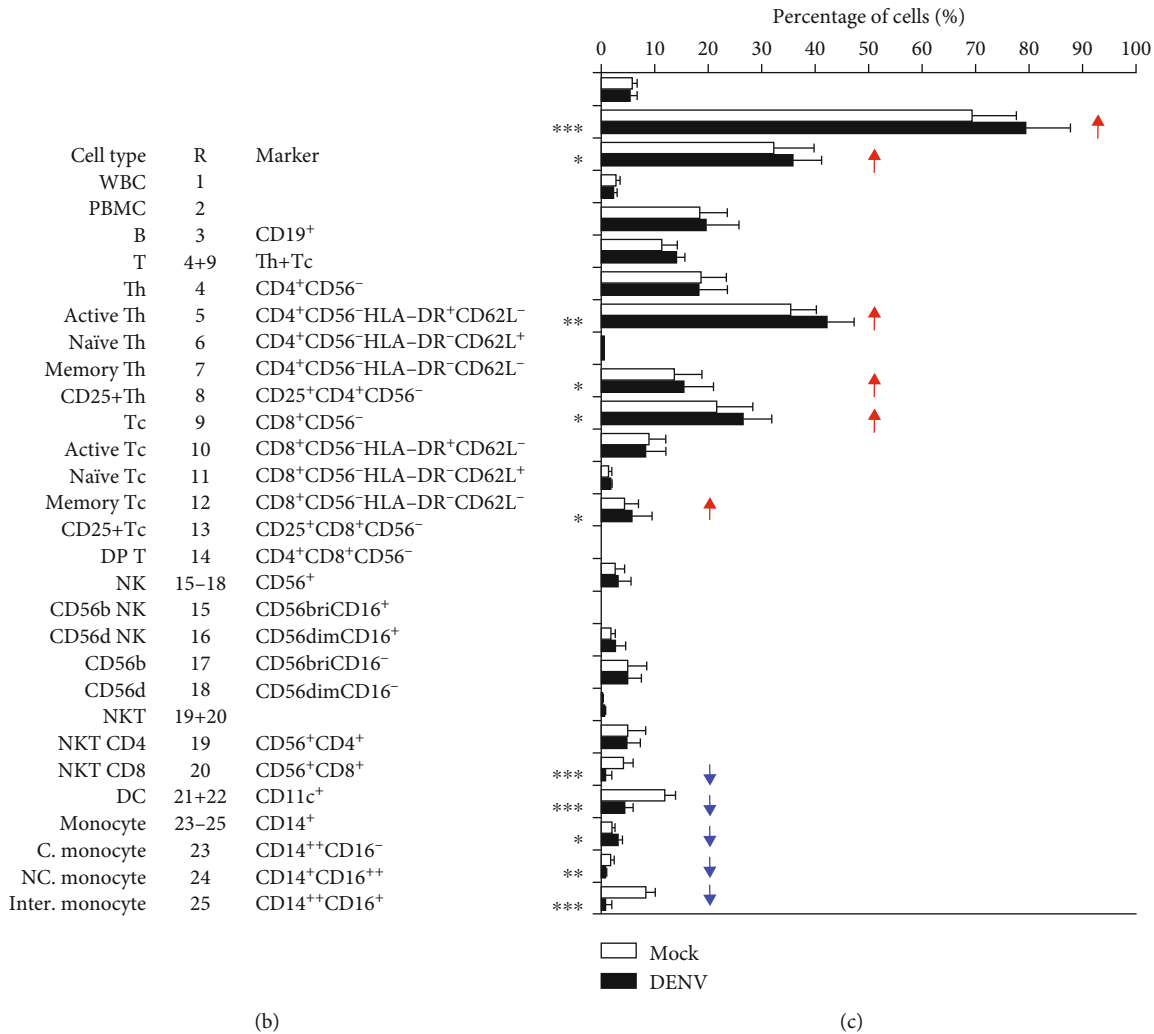


FIGURE 4: Immune profiling in DENV-treated whole blood cells 24 h postincubation. Following DENV (MOI = 1) coculture in 100 μ l of WB *ex vivo* for 24 h, (a) representative flow cytometric analysis and gating of various cells obtained from five cases, performed by staining for specific cell surface markers (CD4, CD8, CD11c, CD14, CD16, CD19, CD25, CD56, CD62L, and HLA-DR), in the DENV-infected and mock groups showed (b) the changes in the expression of specific immune cell populations as noted. (c) The results are shown as a percentage of the mean \pm SD obtained from five cases. * p < 0.05, ** p < 0.01, and *** p < 0.001, compared to the mock group. R: region; WBC: white blood cell; bri: bright.

[10]. However, the cytopathogenic effects of DENV in WB cells have not yet been clearly defined, particularly in well-known hematological conditions, such as leukopenia and thrombocytopenia, as found in dengue-infected patients [34]. In this study, we created an *ex vivo* model of DENV infection in WB culture to examine the possible conditions and effects of viremia during the disease's acute febrile phase. Following DENV infection, decreases in monocytes and dendritic cells following the induction of intracellular vacuolization in monocytic cells were identified in the WB culture with DENV incubation. Moreover, we demonstrated that DENV-induced TNF- α determines the cytopathogenic effect. Although the limited viral load and antiviral serum factors may affect the infectivity of DENV in our model, the findings of this study indicate the possible impacts of DENV infection on causing TNF- α production to induce intracellular vacuolization in phagocytes.

Dengue viremia is defined as the presence of DENV that can be detected in peripheral blood, including plasma and blood cells [26, 35]. In contrast to previous works, DENV could infect isolated human PBMCs *in vitro* and *in vivo* [26, 36, 37]. However, in our *ex vivo* model of infection in the human WB culture, no further newly assembled DENV could be detected, suggesting a limited microenvironment for virion release, probably due to antiviral immunity induction accompanied by a decrease in host factors to support the viral life cycle. Therefore, direct contact with host cells and its viral NS1 protein may cause TNF- α production, and then the indirect DENV-induced TNF- α may cause cytopathological changes in the targeted cells. The *ex vivo* model could be utilized for investigating the viral effects, including DENV and NS1, particularly at the acute febrile phase of DENV infection.

Upon the initial disease onset characterized by high fever, vomiting, and viremia, the hematological examination

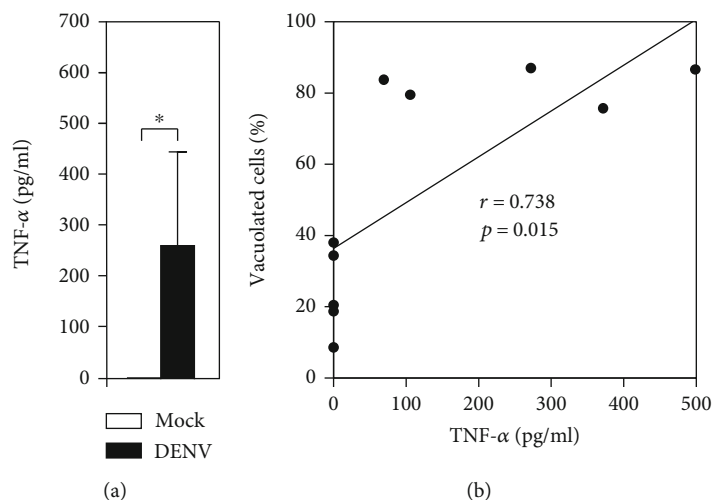


FIGURE 5: Abnormal production of TNF- α caused by DENV infection correlates with the cytopathological effects 24 h postincubation. (a) Following DENV (MOI = 1) coculture in 100 μ l of WB *ex vivo* for 24 h, TNF- α production was measured in the plasma by ELISA. The quantitative data are depicted as the mean \pm SD obtained from five cases. * $p < 0.05$, compared to the mock group. (b) Furthermore, correlation analysis showed the strength of the relationship between TNF- α production and the induction of vacuolization, which is expressed numerically based on the r and p values.

usually shows increased hemoglobin and hematocrit, lower white blood cell counts, lower platelet counts, and higher monocyte counts [2–4, 22]. Inconsistent with the clinical observation, our *ex vivo* model showed a decrease in the monocyte level, as demonstrated by using the CBC assay and immune profiling analysis, suggesting possible limitations on hematological manifestation and replacement compared with blood circulation. However, our *ex vivo* model identified the potential effects of DENV-induced TNF- α on cellular vacuolization in monocytic cells, indicating these cells' physiopathological stimulation for hematological manifestations. Accordingly, further investigations are needed to clarify the effectors involved in DENV-induced vacuolization, the possible regulatory effects caused by endocytosis, phagocytosis, autophagy, and cellular changes on cell survival and death, which are all involved in dengue pathogenesis.

This study found that DENV induces massive vacuolization of human leukocyte cells *ex vivo*, indicating this process is associated with DENV infection. However, the cytopathic effects of the DENV are less well known. Another flavivirus, ZIKV, also induces massive cytoplasmic vacuolization in human epithelial cells, primary skin fibroblasts, and astrocytes and then causes large-scale endoplasmic reticulum (ER) rearrangements and unfolded protein response (UPR) activation, namely, pyroptosis, a form of cell death characterized by swelling of the ER and mitochondria as well as cytoplasmic vacuolization [38]. When the UPR is inadequate to maintain the ER in a steady state, autophagy and cell death programs are activated [39]. Accumulated evidence shows that autophagy plays a vital role in controlling neutrophil and monocyte function when fighting off infections, including the processes of degranulation, metabolism, and the formation of neutrophil extracellular traps [40]. It is speculated that DENV may also cause large-scale ER rearrangements

followed by the generation of cytoplasmic vacuoles, which come from the ER membrane.

The CBC assay results only identified a change in monocyte counts in the *ex vivo* model of DENV infection. However, by using an immune profiling approach, this study also identified a partial increase in total NK (CD56⁺) cells and a decrease in monocytes (CD14⁺) and DCs (CD11c⁺). While the approach of immune profiling confirmed the results of CBC on monocyte expression, changes in the other identified cell populations are needed to compare with previous works [41] while NK cells are activated [42] and DCs are decreased [43] in dengue-infected patients. A decrease in monocytes may indicate the effects of DENV-induced TNF- α for cellular activation followed by cytopathological changes, including cell adhesion and cell death. Regarding their potential roles in controlling both infections, the *ex vivo* model of DENV infection in peripheral blood may provide a different investigative strategy for verifying the mechanisms of viral immunity and immunopathogenesis in response to DENV infection.

Cytokine storms can be present at the acute febrile phase of DENV infection and are involved in dengue diseases' immunopathogenesis [14, 15]. Among these immune parameters, TNF- α was shown to be positively linked to dengue-associated hematological changes in thrombocytopenia and vascular dysfunction [16–18]. Targeting TNF- α has been used as an immunotherapy strategy for suppressing DENV-induced peripheral and tissue-specific inflammatory disorders and mortality [44–46]. In this study, we found an increase in TNF- α in the *ex vivo* model of DENV infection, which may contribute to the induction of cellular vacuolization in monocytic cells. Because monocytes are innate immune cells that probably produce antiviral and proinflammatory cytokines, it is speculated that vacuolization of

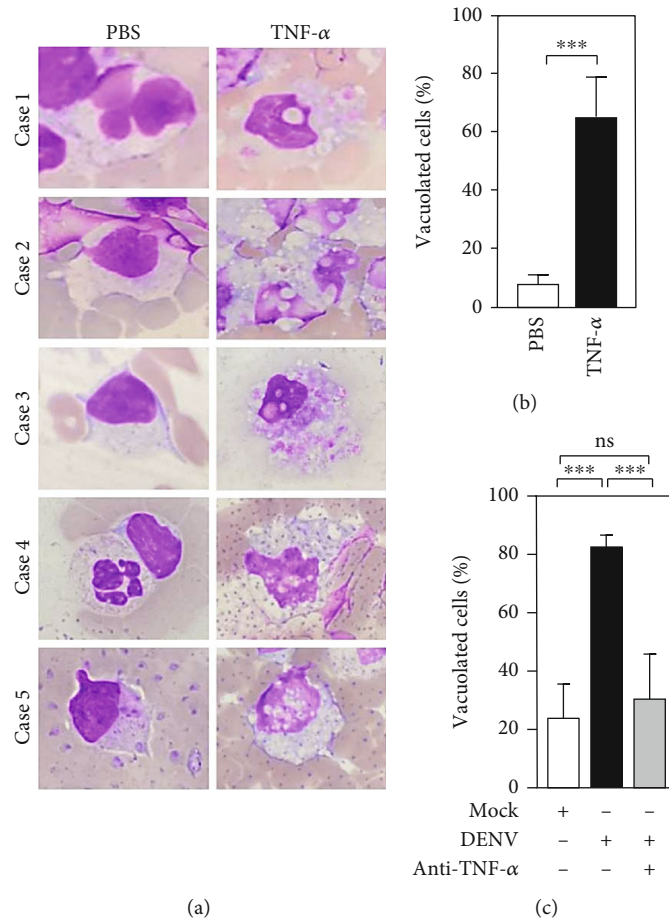


FIGURE 6: Abnormal TNF- α determines the cytopathological effects 24 h postincubation. Without DENV coculture, hTNF- α (100 ng/ml) was added to the *ex vivo* culture of WB for 24 h. (a) Image analysis, shown by an oil immersion field (100x objectives), was performed using the Wright-Giemsa stain to show the induction of vacuolization in five cases. (b) The percentages of vacuolated cells were calculated in the counting area with a high-power field (40x objectives). The quantitative data are depicted as the mean \pm SD obtained from five cases. *** p < 0.001, compared to the PBS group. PBS was used as a control. (c) With or without hTNF- α neutralizing antibody (Ab; 50 μ g/ml) cotreatment, DENV (MOI = 1)-induced vacuolization was monitored. The percentages of vacuolated cells were calculated in three different visible areas. *** p < 0.001, compared to the mock group. ns: not significant.

phagocytes is an immunological process that restricts or promotes microbial pathogenesis in infected patients.

Our study has several limitations. First, this study's *ex vivo* model reflects the cytopathological effects of DENV infection in circulation, particularly at the acute phase of infection during viremia. However, dissimilar with circulation, the closed system in the *ex vivo* model of WB culture may affect different cell populations' expression patterns. Notably, the induction of monocyte activation may be followed by functional changes, while the full expression of suspended monocyte numbers is significantly decreased. Monocytes are the primary cells probably targeted by DENV infection and may adhere to the disk culture. The response may increase the relative expression of neutrophils and NK cells in this experimental model system. Immune profiling in clinical blood samples of dengue patients is needed for validation. Second, in the immune profiling approach, more markers are needed to analyze the classification of specific immune cell populations. Finally, to explore the possible cytopathological effects caused by DENV and dengue NS1

protein, it is essential to investigate the infectivity of DENV in WB culture and the TNF- α -producing cells, particularly in circulating immune cell populations.

5. Conclusions

In conclusion, by using an *ex vivo* model of DENV-WB coculture, we found that the induction of proinflammatory TNF- α expression was followed by TNF- α -regulated cellular vacuolization in monocytic cells. Additionally, we identified the changes in immune cell subpopulations related to the immunopathogenesis of DENV infection. Monitoring cytokine response, cellular vacuolization, and immune cell changes may help the clinical diagnosis of DENV-induced systemic inflammation. While the pathogenesis of DENV infection and disease progression is complicated, the *ex vivo* model may provide an experimental strategy for further exploring peripheral blood immunity against DENV infection.

Data Availability

The data used to support the findings of this study are available from the corresponding authors upon request.

Conflicts of Interest

The authors declare that there is no conflict of interest.

Authors' Contributions

R.-D.S. and M.-K.J. performed most of the experiments and interpreted the results. T.-W.H., C.-H.H., and C.-F.L. participated in the design and supervision of the projects. M.-K.J. and T.-J.S. conducted the virus experiments. T.-J.S., P.-C.T., Y.-T.W., and Z.-Y.Y. contributed to flow cytometric analysis. R.-D.S., C.-H.H., and C.-F.L. designed the concept of the project and wrote the manuscript. All authors reviewed and approved the manuscript.

Acknowledgments

This work was supported by the Ministry of Science and Technology (MOST107-2321-B-038-001, 108-2320-B-038-026, 109-2320-B-038-050, and 109-2327-B-006-010) and Chi Mei Medical Center and Taipei Medical University (105CM-TMU-03, 106CM-TMU-09, and 107CM-TMU-10), Taiwan. We thank the Core Facility Center of Taipei Medical University (TMU) for providing technical support. We also appreciate the Office of Research and Publication, Universitas Gadjah Mada, Indonesia, for editing the manuscript.

References

- [1] I. A. Rodenhuis-Zybert, J. Wilschut, and J. M. Smit, "Dengue virus life cycle: viral and host factors modulating infectivity," *Cellular and Molecular Life Sciences*, vol. 67, no. 16, pp. 2773–2786, 2010.
- [2] World Health Organization and UNICEF, *Handbook for Clinical Management of Dengue*, p. 114, 2012.
- [3] C. M. Chen, K. S. Chan, W. L. Yu et al., "The outcomes of patients with severe dengue admitted to intensive care units," *Medicine (Baltimore)*, vol. 95, no. 31, article e4376, 2016.
- [4] J. Chaloeuwong, A. Tantiworawit, T. Rattanathamthee et al., "Useful clinical features and hematological parameters for the diagnosis of dengue infection in patients with acute febrile illness: a retrospective study," *BMC Hematology*, vol. 18, no. 1, p. 20, 2018.
- [5] M. Kotepui, B. PhunPhuech, N. Phiwklam, and K. Uthaisar, "Differentiating between dengue fever and malaria using hematological parameters in endemic areas of Thailand," *Infectious Diseases of Poverty*, vol. 6, no. 1, p. 27, 2017.
- [6] M. S. Diamond, D. Edgil, T. G. Roberts, B. Lu, and E. Harris, "Infection of human cells by dengue virus is modulated by different cell types and viral strains," *Journal of Virology*, vol. 74, no. 17, pp. 7814–7823, 2000.
- [7] D. M. Morens, M. C. Chu, N. J. Marchette, and S. B. Halstead, "Growth of dengue type 2 virus isolates in human peripheral blood leukocytes correlates with severe and mild dengue disease," *The American Journal of Tropical Medicine and Hygiene*, vol. 45, no. 5, pp. 644–651, 1991.
- [8] P. Sun, K. Bauza, S. Pal et al., "Infection and activation of human peripheral blood monocytes by dengue viruses through the mechanism of antibody-dependent enhancement," *Virology*, vol. 421, no. 2, pp. 245–252, 2011.
- [9] X. Fang, Z. Hu, W. Shang, J. Zhu, C. Xu, and X. Rao, "Genetic polymorphisms of molecules involved in host immune response to dengue virus infection," *FEMS Immunology and Medical Microbiology*, vol. 66, no. 2, pp. 134–146, 2012.
- [10] R. Ben-Shachar, S. Schmidler, and K. Koelle, "Drivers of inter-individual variation in dengue viral load dynamics," *PLoS Computational Biology*, vol. 12, no. 11, article e1005194, 2016.
- [11] C. Zou, C. Huang, J. Zhang et al., "Virulence difference of five type I dengue viruses and the intrinsic molecular mechanism," *PLoS Neglected Tropical Diseases*, vol. 13, no. 3, article e0007202, 2019.
- [12] N. Uno and T. M. Ross, "Dengue virus and the host innate immune response," *Emerging Microbes & Infections*, vol. 7, no. 1, p. 167, 2018.
- [13] J. Flipse, M. A. Dios-Toro, T. E. Hoornweg, D. P. I. van de Pol, S. Urcuqui-Inchima, and J. M. Smit, "Antibody-dependent enhancement of dengue virus infection in primary human macrophages; balancing higher fusion against antiviral responses," *Scientific Reports*, vol. 6, no. 1, p. 29201, 2016.
- [14] A. R. K. Patro, S. Mohanty, B. K. Prusty et al., "Cytokine signature associated with disease severity in dengue," *Viruses*, vol. 11, no. 1, p. 34, 2019.
- [15] A. L. Rothman, "Immunity to dengue virus: a tale of original antigenic sin and tropical cytokine storms," *Nature Reviews Immunology*, vol. 11, no. 8, pp. 532–543, 2011.
- [16] S. Inyoo, A. Suttitheptumrong, and S. N. Pattanakitsakul, "Synergistic effect of TNF- α and dengue virus infection on adhesion molecule reorganization in human endothelial cells," *Japanese Journal of Infectious Diseases*, vol. 70, no. 2, pp. 186–191, 2017.
- [17] K. I. Masood, B. Jamil, M. Rahim, M. Islam, M. Farhan, and Z. Hasan, "Role of TNF α , IL-6 and CXCL10 in dengue disease severity," *Iranian Journal of Microbiology*, vol. 10, no. 3, pp. 202–207, 2018.
- [18] A. A. Meena, A. Murugesan, S. Sopnajothi et al., "Increase of plasma TNF- α is associated with decreased levels of blood platelets in clinical dengue infection," *Viral Immunology*, vol. 33, no. 1, pp. 54–60, 2020.
- [19] E. D. Hottz, I. M. Medeiros-de-Moraes, A. Vieira-de-Abreu et al., "Platelet activation and apoptosis modulate monocyte inflammatory responses in dengue," *Journal of Immunology*, vol. 193, no. 4, pp. 1864–1872, 2014.
- [20] A. Opasawatchai, P. Amornsapawat, N. Jiravejchakul et al., "Neutrophil activation and early features of NET formation are associated with dengue virus infection in human," *Frontiers in Immunology*, vol. 9, p. 3007, 2019.
- [21] M. Juffrie, G. M. van der Meer, C. E. Hack et al., "Inflammatory mediators in dengue virus infection in children: interleukin-8 and its relationship to neutrophil degranulation," *Infection and Immunity*, vol. 68, no. 2, pp. 702–707, 2000.
- [22] J. G. X. Wong, T. L. Thein, D. C. Lye, Y. Hao, A. Wilder-Smith, and Y. S. Leo, "Severe neutropenia in dengue patients: prevalence and significance," *The American Journal of Tropical Medicine and Hygiene*, vol. 90, no. 6, pp. 984–987, 2014.
- [23] M. Kunder, V. Lakshmaiah, and A. V. Moideen Kutty, "Plasma neutrophil elastase, α 1-antitrypsin, α 2-macroglobulin and

- neutrophil elastase- α 1-antitrypsin complex levels in patients with dengue fever," *Indian Journal of Clinical Biochemistry*, vol. 33, no. 2, pp. 218–221, 2018.
- [24] C. C. Mihalache, S. Yousefi, S. Conus, P. M. Villiger, E. M. Schneider, and H. U. Simon, "Inflammation-associated autophagy-related programmed necrotic death of human neutrophils characterized by organelle fusion events," *Journal of Immunology*, vol. 186, no. 11, pp. 6532–6542, 2011.
- [25] S. Thiemmecca, A. Songjang, N. Punyadee, K. Kongmanas, J. Atkinson, and P. Avirutnan, "Infection of whole blood with dengue virus," *Molecular Immunology*, vol. 102, pp. 132–133, 2018.
- [26] A. P. Durbin, M. J. Vargas, K. Wanionek et al., "Phenotyping of peripheral blood mononuclear cells during acute dengue illness demonstrates infection and increased activation of monocytes in severe cases compared to classic dengue fever," *Virology*, vol. 376, no. 2, pp. 429–435, 2008.
- [27] T. T. Tsai, C. L. Chen, Y. S. Lin et al., "Microglia retard dengue virus-induced acute viral encephalitis," *Scientific Reports*, vol. 6, no. 1, p. 27670, 2016.
- [28] L. Osorio, M. Ramirez, A. Bonelo, L. A. Villar, and B. Parra, "Comparison of the diagnostic accuracy of commercial NS1-based diagnostic tests for early dengue infection," *Virology Journal*, vol. 7, no. 1, p. 361, 2010.
- [29] Z. Kou, M. Quinn, H. Chen et al., "Monocytes, but not T or B cells, are the principal target cells for dengue virus (DV) infection among human peripheral blood mononuclear cells," *Journal of Medical Virology*, vol. 80, no. 1, pp. 134–146, 2008.
- [30] S. Noisakran, N. Onlamoon, P. Songprakhon, H. M. Hsiao, K. Chokephaibulkit, and G. C. Perng, "Cells in dengue virus infection in vivo," *Advances in Virology*, vol. 2010, Article ID 164878, 15 pages, 2010.
- [31] J. A. Aguilar-Briseño, V. Upasani, B. M. . Ellen et al., "TLR2 on blood monocytes senses dengue virus infection and its expression correlates with disease pathogenesis," *Nature Communications*, vol. 11, no. 1, p. 3177, 2020.
- [32] S. W. Wan, B. A. Wu-Hsieh, Y. S. Lin, W. Y. Chen, Y. Huang, and R. Anderson, "The monocyte-macrophage-mast cell axis in dengue pathogenesis," *Journal of Biomedical Science*, vol. 25, no. 1, p. 77, 2018.
- [33] M. Kwissa, H. I. Nakaya, N. Onlamoon et al., "Dengue virus infection induces expansion of a CD14⁺CD16⁺ monocyte population that stimulates plasmablast differentiation," *Cell Host & Microbe*, vol. 16, no. 1, pp. 115–127, 2014.
- [34] H. K. Jayanthi and S. K. Tulasi, "Correlation study between platelet count, leukocyte count, nonhemorrhagic complications, and duration of hospital stay in dengue fever with thrombocytopenia," *Journal of Family Medicine and Primary Care*, vol. 5, no. 1, pp. 120–123, 2016.
- [35] G. Añez, D. A. R. Heisey, C. Chancey et al., "Distribution of dengue virus types 1 and 4 in blood components from infected blood donors from Puerto Rico," *PLoS Neglected Tropical Diseases*, vol. 10, no. 2, article e0004445, 2016.
- [36] L. Jiang and Q. Sun, "The expression profile of human peripheral blood mononuclear cell miRNA is altered by antibody-dependent enhancement of infection with dengue virus serotype 3," *Virology Journal*, vol. 15, no. 1, p. 50, 2018.
- [37] Y. L. Chen, N. Abdul Ghafar, R. Karuna et al., "Activation of peripheral blood mononuclear cells by dengue virus infection depotentiates balapiravir," *Journal of Virology*, vol. 88, no. 3, pp. 1740–1747, 2014.
- [38] B. Monel, A. A. Compton, T. Bruel et al., "Zika virus induces massive cytoplasmic vacuolization and paraptosis-like death in infected cells," *The EMBO Journal*, vol. 36, no. 12, pp. 1653–1668, 2017.
- [39] A. B. Blazquez et al., "Stress responses in flavivirus-infected cells: activation of unfolded protein response and autophagy," *Frontiers in Microbiology*, vol. 5, 2014.
- [40] Y. Yu and B. Sun, "Autophagy-mediated regulation of neutrophils and clinical applications," *Burns Trauma*, vol. 8, 2020.
- [41] K. Lühn, C. P. Simmons, E. Moran et al., "Increased frequencies of CD4⁺ CD25(high) regulatory T cells in acute dengue infection," *The Journal of Experimental Medicine*, vol. 204, no. 5, pp. 979–985, 2007.
- [42] C. Petitdemange, N. Wauquier, H. Devilliers et al., "Longitudinal analysis of natural killer cells in dengue virus-infected patients in comparison to Chikungunya and Chikungunya/dengue virus-infected patients," *PLoS Neglected Tropical Diseases*, vol. 10, no. 3, article e0004499, 2016.
- [43] S. Lertjuthaporn, L. Khowawisetsut, R. Keawwichit et al., "Identification of changes in dendritic cell subsets that correlate with disease severity in dengue infection," *PLoS One*, vol. 13, no. 7, article e0200564, 2018.
- [44] A. Atrasheuskaya, P. Petzelbauer, T. M. Fredeking, and G. Ignatyev, "Anti-TNF antibody treatment reduces mortality in experimental dengue virus infection," *FEMS Immunology and Medical Microbiology*, vol. 35, no. 1, pp. 33–42, 2003.
- [45] E. Branche, W. W. Tang, K. M. Viramontes et al., "Synergism between the tyrosine kinase inhibitor sunitinib and anti-TNF antibody protects against lethal dengue infection," *Antiviral Research*, vol. 158, pp. 1–7, 2018.
- [46] M. K. Jhan, W. C. HuangFu, Y. F. Chen et al., "Anti-TNF- α restricts dengue virus-induced neuropathy," *Journal of Leukocyte Biology*, vol. 104, no. 5, pp. 961–968, 2018.

Review Article

Pleiotropic Effect of Hormone Insulin-Like Growth Factor-I in Immune Response and Pathogenesis in Leishmaniasis

Luiza C. Reis ¹, Eduardo Milton Ramos-Sanchez ^{1,2}, Fernanda N. Araujo ¹,
Ariane F. Leal ¹, Christiane Y. Ozaki ¹, Orlando R. Sevillano ¹, Bernardina A. Uscata ¹,
and Hiro Goto ^{1,3}

¹Instituto de Medicina Tropical de São Paulo, Faculdade de Medicina, Universidade de São Paulo (IMTSP-USP), São Paulo, Brazil

²Departamento de Salud Publica, Facultad de Ciencias de La Salud, Universidad Nacional Toribio Rodriguez de Mendoza de Amazonas, Chachapoyas, Peru

³Departamento de Medicina Preventiva, Faculdade de Medicina, Universidade de São Paulo, São Paulo, Brazil

Correspondence should be addressed to Hiro Goto; hgoto@usp.br

Luiza C. Reis and Eduardo Milton Ramos-Sanchez contributed equally to this work.

Received 24 December 2020; Revised 3 April 2021; Accepted 11 April 2021; Published 5 May 2021

Academic Editor: Gabriela Santos-Gomes

Copyright © 2021 Luiza C. Reis et al. This is an open access article distributed under the Creative Commons Attribution License, which permits unrestricted use, distribution, and reproduction in any medium, provided the original work is properly cited.

Leishmaniasis are diseases caused by several *Leishmania* species, and many factors contribute to the development of the infection. Because the adaptive immune response does not fully explain the outcome of *Leishmania* infection and considering that the initial events are crucial in the establishment of the infection, we investigated one of the growth factors, the insulin-like growth factor-I (IGF-I), found in circulation and produced by different cells including macrophages and present in the skin where the parasite is inoculated. Here, we review the role of IGF-I in leishmaniasis experimental models and human patients. IGF-I induces the growth of different *Leishmania* species in vitro and alters the disease outcome increasing the parasite load and lesion size, especially in *L. major*- and *L. amazonensis*-infected mouse leishmaniasis. IGF-I affects the parasite interacting with the IGF-I receptor present on *Leishmania*. During *Leishmania*-macrophage interaction, IGF-I acts on the arginine metabolic pathway, resulting in polyamine production both in macrophages and *Leishmania*. IGF-I and cytokines interact with reciprocal influences on their expression. IL-4 is a hallmark of susceptibility to *L. major* in murine leishmaniasis, but we observed that IGF-I operates astoundingly as an effector element of the IL-4. Approaching human leishmaniasis, patients with mucosal, disseminated, and visceral diseases presented surprisingly low IGF-I serum levels, suggesting diverse effects than parasite growth. We observed that low IGF-I levels might contribute to the inflammatory response persistence and delayed lesion healing in human cutaneous leishmaniasis and the anemia development in visceral leishmaniasis. We must highlight the complexity of infection revealed depending on the *Leishmania* species and the parasite's developmental stages. Because IGF-I exerts pleiotropic effects on the biology of interaction and disease pathogenesis, IGF-I turns up as an attractive tool to explore biological and pathogenic processes underlying infection development. IGF-I pleiotropic effects open further the possibility of approaching IGF-I as a therapeutic target.

1. Introduction

Leishmaniasis are considered neglected tropical diseases caused by parasites of the order Kinetoplastida, family Trypanosomatidae, and genus *Leishmania*, affecting one million people globally each year and endemic in 98 countries. The

transmission occurs through a sandfly bite that inoculates promastigotes into the skin, which transform into amastigotes and proliferate within phagocytic mononuclear cells. The infection can be asymptomatic or symptomatic, leading to a wide spectrum of clinical manifestations ranging from localized, disseminated, or diffuse cutaneous lesions or

mucosal lesions to viscera involvement such as the liver and spleen [1]. The establishment of these different clinical forms depends on the parasite's species and on the vector, in addition to the epidemiological characteristics and genetic and immunological constitution of the host [2], where both innate and adaptive immune responses can drive the development or control of infection.

The beginning of our studies on insulin-like growth factors on *Leishmania* and leishmaniasis goes back to the nineties when the main focus on leishmaniasis research was the cell-mediated immune response. At the end of the eighties, T helper 1 (Th1) was related to resistance and T helper 2 (Th2) to susceptibility to *Leishmania major* infection in studies using inbred mouse strains. The susceptibility was attributed to early Th2 cell activation present in BALB/c mice and the resistance to Th1 cells in C57BL/6 mice by the infection. Subsequent studies using different approaches as cytokine neutralization, specific cell response induction, or inhibition of the immune system's elements through molecular deletions confirmed this view, but others pointed flaws in this model. Similar studies using other *Leishmania* species also showed that the adaptive immune response does not explain the infection's resistance and susceptibility profiles. Further, human leishmaniasis' pathogenesis cannot be explained only based on resistance and susceptibility to parasite growth.

In this review, we initially present some data related to the involvement of adaptive immune response on *Leishmania major* and *Leishmania donovani/Leishmania infantum* infections that do not fully clarify infection development to justify the focus here on nonspecific factors. Then, we present data including studies on the innate immune response that points out our research on the IGF-I growth factor as an element that may contribute to *Leishmania* infection.

2. Adaptive Immune Response in Leishmaniasis: Flaws

2.1. *Leishmania major*. The experimental model using *L. (L.) major* has been used to characterize the immune response on resistance or susceptibility to infection related to the Th1 and Th2 cell activation, respectively [3]. The role of cytokines in the Th1 and Th2 paradigm has been questioned by results suggesting that the resistance and susceptibility regulation are much more complex, involving cytokine production and other factors [4–9]. Studies have demonstrated that the interferon- (IFN-) γ and interleukin- (IL-) 4 production are similar in susceptible and resistant mice in the early stage of infection [3, 10, 11]. Further, IL-4 production in resistant mice does not alter the evolution towards progressive disease, similarly seen in C3H mice treated with IL-4 or anti-IL-12 at the beginning of infection. These mice presented a solid but transient increase in the IL-4 level, with no change in their resistant phenotype [12–14]. Another study showed that the transfer of BALB/c T cells with high IL-4 expression to genetically resistant chimeric mice having a C57BL/6 background did not result in susceptibility [15]. These questions on the Th1 and Th2 paradigm in leishmaniasis also become evident in infections caused by other *Leishmania* species.

2.2. *Leishmania donovani/Leishmania infantum*. In contrast to the *L. major*-infected mouse model's immune response very much scrutinized, the immune mechanisms in experimental visceral leishmaniasis (VL) are less explored. Resistance in VL involves CD4⁺ and CD8⁺ T cells, IL-2, IFN- γ , and IL-12, the latter in an IFN- γ -independent mechanism and linked to transforming growth factor β (TGF- β) production. Susceptibility involves IL-10 but not IL-4 and B cells [16]. Studies on *L. donovani* and *L. infantum* infections in mice and humans [17–20] suggest that control of infection was independent of the Th1 and Th2 cytokine differential production (IFN- γ /IL-4 balance) [20]. The resistance to *L. donovani* and induction of granuloma formation are dependent on the generation of an IFN- γ response by both CD4⁺ and CD8⁺ T cells. IFN- γ activates macrophages to produce antimicrobial reactive nitrogen and oxygen intermediates [21], also important in driving granuloma maturation. Most *L. donovani*-infected mouse strains control infection spontaneously, becoming immune for subsequent infections. In these immune animals, upon reinfection, the elements involved in resistance are different, i.e., CD8⁺ T cells and IL-2 [16]. These experimental VL findings do not contribute substantially to understand active human VL where the disease is progressive and lethal if not treated.

In active human VL, the patients present fever, hepatosplenomegaly, hypergammaglobulinemia, pancytopenia, and significant weight loss [1]. Most of the studies focus on the suppression of the T cell responses [22]. Immunosuppression is characterized as *Leishmania* antigen-specific, where T cells, Th2 cells, and adherent antigen-presenting cells are involved [16]. Cytotoxic T-lymphocyte-associated protein 4 (CTLA-4) and programmed cell death protein 1 (PD-1) are negative regulators of T cells and are expressed on exhausted or anergic T cells in active infection, taking part in immunosuppression. The evoked mechanism is the induction of an increased level of TGF- β and apoptosis of CD4⁺ T cells and inhibition of macrophage apoptosis by *Leishmania* infection [23]. T cell apoptosis, mainly CD4⁺ T cells, accompanied by a significant decrease in IL-2 and IFN- γ secretion and unaltered IL-4 secretion, was observed during *L. donovani* infection and was also related to immunosuppression [16]. Other immunosuppressive mechanisms established during VL may be mediated through regulatory T cells, secreting regulatory cytokines like IL-10 and TGF- β and expressing inhibitory molecules such as CTLA-4 and IL-35 [23].

In contrast to the studies on immunosuppression, other data suggest intense immune activation in active VL [24]. Studies on peripheral blood mononuclear cells raised data that suggest immunosuppression. However, findings in lymphoid organ samples such as bone marrow and spleen show high expression of tumor necrosis factor α (TNF- α) and IFN- γ mRNA levels and high IFN- γ serum level as a consequence [25, 26]. A study showing exhaustion of the immune system [27] reinforces this view. All these studies focusing on the balance between elements of adaptive immune mechanisms are aimed at explaining the active disease's development. Still, no clear answer was achieved, demanding the investigation on other components as the nonspecific factors.

3. Growth Factors in the Innate Response in Leishmaniasis

As the adaptive immune response does not fully explain the control or development of *Leishmania* infection and the initial events that occur immediately after the vector's promastigote inoculation are crucial, we chose to investigate growth factors present on the inoculation site. Once inoculated into the skin, the parasites immediately encounter innate immune elements, including growth factors such as TGF- β and granulocyte-macrophage colony-stimulating factor (GM-CSF).

The role of TGF- β as an important immune regulator in leishmaniasis has been demonstrated in vitro [28–31] and in vivo [32–34]. TGF- β can inhibit macrophage activation through the blockage of nitric oxide (NO) production, leading to an increase in the parasitic load. Further, a synergistic effect between TGF- β and EB1-3 (Epstein Barr virus-induced gene 3 or IL-27 β) on suppression of BALB/c mouse immune response infected by *L. donovani* was observed [35]. Interestingly, TGF- β homolog found in *Lutzomyia longipalpis* was suggested to contribute to the *L. infantum* survival within the vector [36].

In addition to TGF- β , GM-CSF can interact with *L. amazonensis* promastigotes, promoting their growth and protecting them from death by thermal shock [37, 38]. In accordance, the rGM-CSF (recombinant GM-CSF) treatment in *L. major*-infected BALB/c mice promoted an enlargement in lesions and increased parasite load, as well as *L. major*-infected macrophages incubated with rGM-CSF presented an increased parasite load [39]. Further, the GM-CSF was used topically during Miltefosine treatment in American tegumentary leishmaniasis without success [40, 41]. In a multiomic study in cutaneous leishmaniasis patients, diminished concentrations of GM-CSF, IFN- α 2, IL-6, and IL-3 and increased eotaxin levels were related to treatment failure [42]. However, other studies show opposite results; parasites are eliminated in *L. tropica*-, *L. mexicana*-, and *L. donovani*-infected macrophages upon activation with GM-CSF [43–45]. Moreover, mice with a null mutation in the gene for the beta common (β c) chain of the receptors for GM-CSF, IL-3, and IL-5 infected with *L. major* presented resistance to infection [46].

In this context, we have started studying another growth factor, the insulin-like growth factor-I (IGF-I). Its role in *Leishmania* infection was considered because it is produced by different cell types, including macrophages that harbor the parasites. Also, it is present in the skin, where the parasite initiates the infection [47].

The IGF-I is a hormone that presents a molecular structure relatively similar to insulin, being produced primarily by the liver under the control of growth hormone (GH). As a polypeptide phylogenetically well preserved, the IGF-I presents a molecular mass of approximately 7.5 kDa. It is present in the circulation bound to a complex of carrier proteins called insulin-like growth factor-binding proteins (IGFBPs). Since its affinity for IGFBPs is greater than for its receptor, in the extracellular environment, most IGFs bind to IGFBP, of which IGFBP-3 is the most abundant in human serum

[48]. As mentioned before, different cell types produce IGF-I, including macrophages that produce and harbor the IGF-I with 26 kDa that will be cleaved in a 7.5 kDa molecule to be secreted. IGF-I exhibits pleiotropic properties, including the ability to promote cellular proliferation, differentiation, nutrient transport, energy storage, gene transcription, protein synthesis, modulation of the immune response and inflammation, and epigenetic modifications [47, 49, 50]. Of note, IGF-I can trigger and/or modulate more than 200 genes depending on cell types, tissues, development stages, among others [51, 52]. In addition to insulin, the IGF-II is another molecule that presents considerable similarity with IGF-I, and its effect was observed on the stimulation of *Giardia lamblia* trophozoite growth [53]. Despite the substantial similarity between IGF-I and IGF-II, only IGF-I presented effect on *Leishmania* infection and proliferation [54–56]. The same was observed on the development of infection caused by other pathogens, like *Mycobacterium leprae*, *Schistosoma mansoni*, and *Schistosoma japonicum* [57, 58].

The IGF-I exerts its biological effects binding to its receptor (IGF-IR), which is present in several cell types, mainly in macrophages, activating the intracellular signaling cascade. The phosphoinositide-3 kinase/protein kinase-B (PI3K/AKT) and the mitogen-activated protein kinase (Ras/MAPK/ERK) are two main pathways activated by IGF-I. Their stimulation may also occur by binding to the insulin receptor (IR) when its free form is present in excess. Since IGF-IR and IR are highly homologous tyrosine kinase receptors sharing many signaling pathway components and inducing insulin receptor substrates 1 and 2 (IRS1/2) in addition to AKT and MAPK phosphorylation [59–61], the IGF-I binding to IR can result in a signaling cascade comparable to the one triggered by the IGF-IR, generating similar effects.

It has been demonstrated that some physiological processes are controlled by the immune and endocrine systems reciprocally, through cytokine and hormone-regulated actions [62–64]. Regarding IGF-I, some factors such as cytokines can regulate its expression in macrophages. Macrophage stimulation, in vitro, by IFN- γ results in a decrease and by IL-4 and IL-13 in an increase of IGF-I expression [65–67]. On the other hand, IGF-I can also regulate cytokine production. Phytohemagglutinin- (PHA-) stimulated human peripheral blood mononuclear cells (PBMC) in the IGF-I presence showed an increase in IL-10 and IL-4 and decrease in IFN- γ secretion. In accordance, the IL-10 mRNA level increased, as well as IL-10 secretion in PBMC-derived T cells under the same conditions [68]. Further data showing expression of IGF-I receptor expression upon T cell activation or modulation of adaptive immune elements by IGF-I [69–72] suggest an important role of IGF-I in immunity.

This review will present the IGF-I as an active participant both in experimental infection by *Leishmania spp* and human leishmaniasis.

4. IGF-I in Experimental Leishmaniasis

4.1. Effect of IGF-I on *Leishmania* Promastigotes and Amastigotes. The IGF-I likely interacts with *Leishmania*

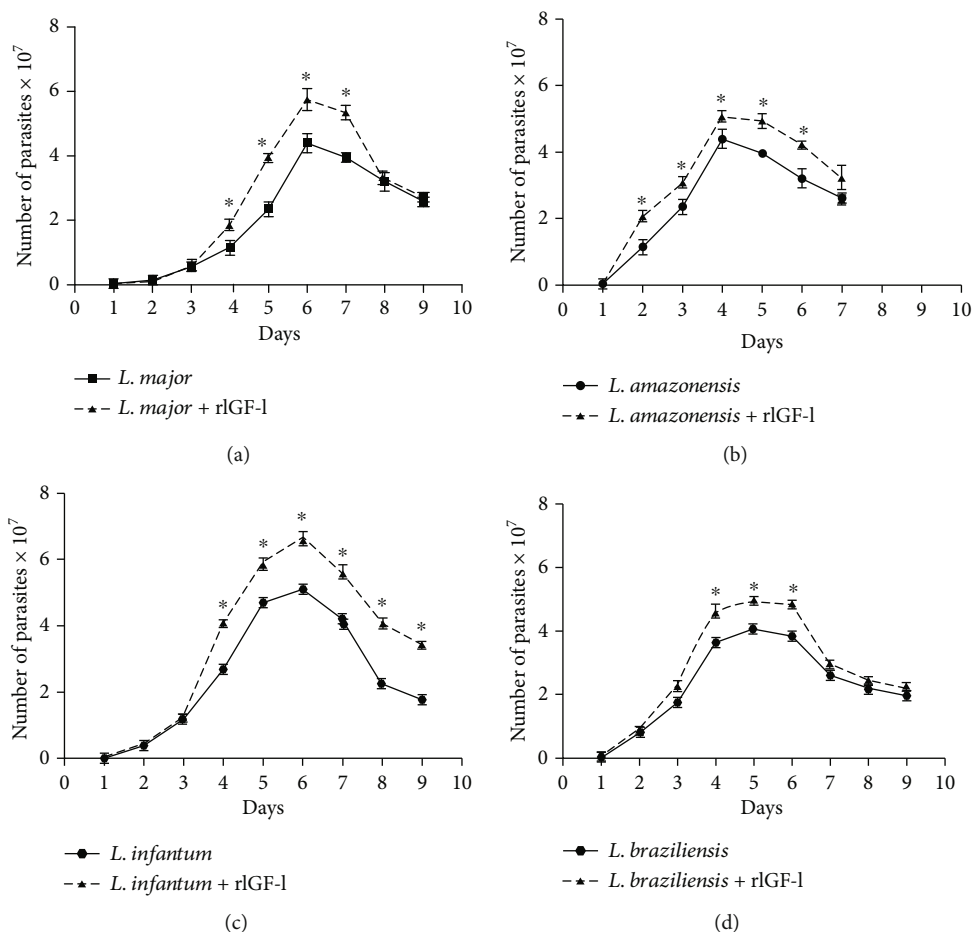


FIGURE 1: Growth curves of *Leishmania* spp promastigotes upon IGF-I stimulus. *L. major*, *L. amazonensis*, *L. infantum*, and *L. braziliensis* promastigotes (5×10^5 /mL) were cultured in 199 medium (Cultilab, Brazil) and Schneider's Insect medium (Sigma-Aldrich, USA), respectively, supplemented with 5% heat-inactivated fetal calf serum (FCS) (Cultilab, Brazil) at 26°C, with or without 50 ng/mL IGF-I (rIGF-I, R&D Systems, USA). The growth of parasites was monitored by daily counting, for 10 days, in a Neubauer chamber, and the results are presented as the number of parasites $\times 10^7$ /mL (mean \pm standard deviation) from three independent cultures with or without 50 ng/mL IGF-I. * $p < 0.05$ (one-way ANOVA) compared with the culture without IGF-I (adapted from Reis et al. [65]).

immediately after its inoculation into the host's skin and after being phagocytized by macrophages. For years, we studied the participation of this growth factor directly on *Leishmania* spp promastigotes and amastigotes in experimental in vitro and in vivo infection and human infection.

We initially evaluated the IGF-I effect on promastigotes and axenic amastigotes of different *Leishmania* species by adding extrinsic IGF-I (i.e., recombinant human IGF-I) in physiological concentrations [54–56]. Analyzing the IGF-I effect throughout the promastigote growth curves of each species, we observed increased proliferation of the parasites in the presence of IGF-I. Its effect was more evident when they reached the stationary growth phase (Figure 1). Thus, the promastigotes' response to extrinsic IGF-I suggests that their contact with the host's IGF-I when inoculated into the skin can substantially affect them at the initial stage of infection.

Subsequently, binding of IGF-I was shown to induce phosphorylation of tyrosine (185 kDa and 60 to 40 kDa proteins) and serine-threonine residues (110 kDa and 120 and 95 kDa proteins) in promastigotes and axenic amastigotes,

in a stage-specific effect [73]. When analyzing the interaction between IGF-I and parasites, it was shown that IGF-I binds specifically to a single-site putative receptor at the parasite membrane. The receptor is a monomeric glycoprotein with a molecular mass of 65 kDa and is antigenically related to the α chain of human type 1 IGF-I receptor [74]. This specific IGF-I receptor found on the surface of *Leishmania* promastigotes and amastigotes differs considerably from those found on mammalian cells. In human cells, the IGF-I receptor is constituted by two alpha and two beta chains with a molecular mass of 135 and 93 kDa, respectively [74, 75]. Upon IGF-I stimulation, the receptor goes through autophosphorylation on tyrosine residues, activating the signaling pathway. Activation of the IGF-I receptor on *Leishmania* also leads to the phosphorylation of a 185 kDa molecule that is homologous to the insulin receptor substrate present in human cells, the IRS-1. IRS-1 is a critical adapter protein involved in IGF-I signaling and is considered a docking protein, playing a central role in the intracellular signaling network [74, 76]. We may speculate that the receptor functions as part of an array of adaptive responses developed by the parasite to survive

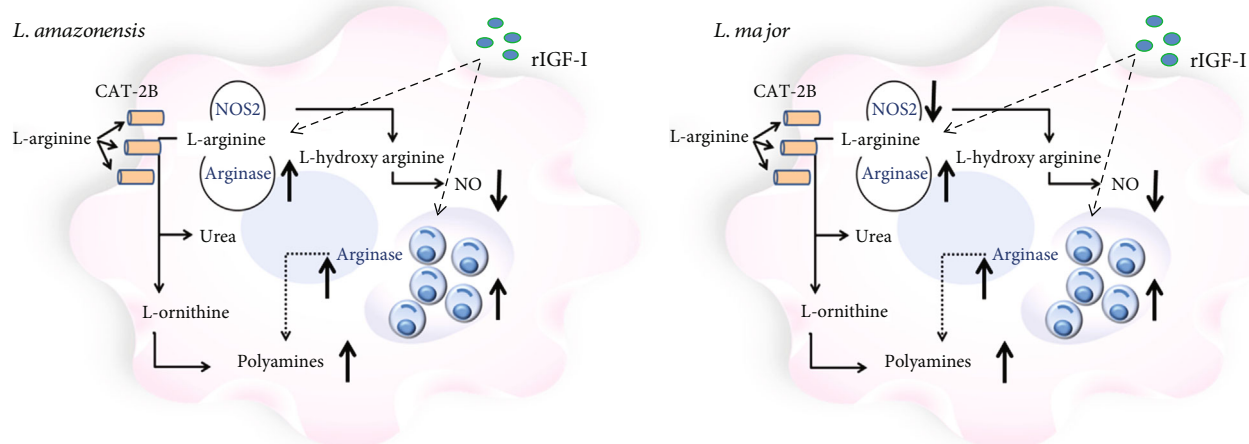


FIGURE 2: Scheme of the effect of extrinsic IGF-I (rIGF-I) in the L-arginine metabolic pathway activation in macrophages infected by *L. amazonensis* and *L. major*. In RAW 264.7 cells or BALB/c mouse peritoneal macrophages infected with *L. amazonensis* or *L. major* promastigotes and stimulated with 50 ng/mL recombinant IGF-I (rIGF-I, R&D Systems, USA), the parasitism, arginase mRNA expression, and arginase activity, nitric oxide synthase 2 (NOS2) mRNA expression, and nitric oxide production (Griess reaction) were evaluated. Extrinsic IGF-I induced an increase in arginase expression and arginase activity in both parasites and macrophages, decreased the production of NO, and increased the parasitism in *L. amazonensis*- and *L. major*-infected cells, comparably.

within the host. Thus, it may be considered a possible vaccine target. In fact, it has been approached in schistosomiasis since the IR in *Schistosoma mansoni* and *S. japonicum* were discovered. These worms like *Leishmania* use the host's hormones and nutrients for their development. Their insulin receptors have been studied as a vaccine target in animal models to prevent transmission [57].

4.2. Effect of IGF-I on Leishmania-Macrophage Interaction.

Moving to in vivo studies using a cutaneous leishmaniasis model in BALB/c mice, we have shown that the preincubation of *L. amazonensis* promastigotes with IGF-I promotes a significant increase in the footpad lesion size, 21 days post-infection. We observed an increase in the number of parasites in the lesion accompanied by an inflammatory infiltrate. These results suggest that IGF-I has a significant role in the innate immune response during the infection, favoring the parasite growth within macrophages [77].

Since IGF-I favors the macrophage's parasite growth, this growth factor probably affects the macrophage's metabolic machinery. The macrophages are key cells in the establishment of *Leishmania* infection. Depending on the cells' activation stimuli, *Leishmania* infection's development will result in progression or cure. One of the mechanisms involved in these processes is the L-arginine metabolic pathway. The L-arginine enters the cells from the extracellular milieu by the cationic amino acid transporter 2 (CAT-2B), a member of the classical amino acid cationic transporter system γ^+ (SLC7) [78]. When this amino acid is oxidized by the nitric oxide synthase 2 (NOS2), it generates nitric oxide (NO), one of the main leishmanicidal elements. However, when the enzyme arginase hydrolyzes L-arginine, polyamines are generated, promoting *Leishmania* proliferation [79–81]. Thus, we addressed the study of extrinsic IGF-I's effect on the parasite-macrophage interaction in vitro, evaluating the

L-arginine metabolic pathway in macrophages' infection with *L. amazonensis*.

In this approach, we observed that IGF-I favored parasite growth in *L. amazonensis*-infected macrophages. It occurred through an increase in arginase mRNA expression and arginase activity in both parasites and macrophages and decreased the production of NO by macrophages [55]. As each species of *Leishmania* behaves differently, we analyzed the role of extrinsic IGF-I on *L. major*. Similarly to those results obtained with *L. amazonensis*, in *L. major*-infected macrophages, IGF-I favored the parasite proliferation within the macrophage inducing the arginase activation with an increase of arginase mRNA expression and arginase activity in both parasites and macrophages and a decrease in the *Nos2* mRNA expression and the production of NO by macrophages [65, 82] (Figure 2). These results showed the effect of extrinsic IGF-I on L-arginine metabolism leading to the parasite's proliferation within the macrophage.

It is worth mentioning that in *Leishmania* infection, the fate of host-parasite interaction depends on the *Leishmania* species involved. With this in mind, we evaluated the effect of IGF-I on the macrophage infection with other species, *L. infantum*, which causes visceral leishmaniasis (VL) and *L. braziliensis*, which is responsible for the cutaneous (CL), disseminated (DL), and mucosal (ML) forms of the disease.

For the evaluation of the IGF-I effect on *L. infantum* infection, we used the THP-1 human monocytic cell line and murine macrophages. In *L. infantum*-infected THP-1 cells upon IGF-I stimulus, the increase in parasitism was not evident, only a slight tendency, accompanied by an increase in NO production and no difference in arginase activity (Figures 3(a)–3(c)). We observed similar results in *L. infantum*-infected bone marrow-derived murine macrophages enquiring whether the cell type influences these results. We noted an increasing trend in parasitism, accompanied by

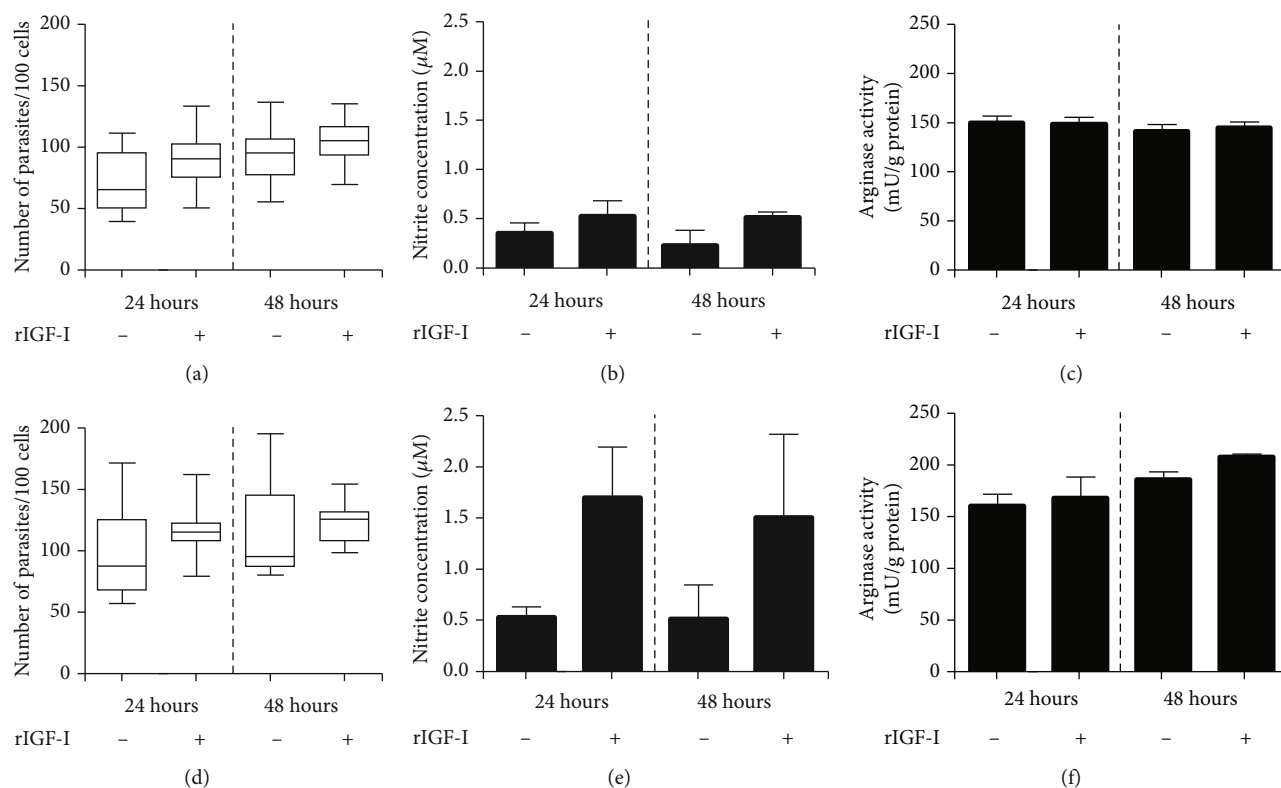


FIGURE 3: Parasitism and nitric oxide production in *L. infantum*-infected cells upon extrinsic IGF-I stimulus. THP-1 cells (a–c) or BALB/c mouse bone marrow-derived macrophages (d–f) were infected with *L. infantum* promastigotes and stimulated with recombinant IGF-I (rIGF-I, 50 ng/mL; R&D Systems, USA) for 24 and 48 hours. One representative experiment from three independent assays is shown. THP-1 cells were differentiated into macrophages with 20 ng/mL phorbol 12-myristate 13-acetate (PMA; Sigma-Aldrich, USA) for 24 hours. Then, the cells were washed and allowed to rest in a fresh medium for 48 hours before infection with *L. infantum* promastigotes. The parasitism (median number of parasites per 100 cells), nitric oxide production (Griess Reagent), and arginase activity (urea production) were determined after 24 and 48 hours of incubation.

increased NO production upon stimulation with IGF-I and no difference in arginase activity (Figures 3(d)–3(f)). Thus, unlike *L. major* and *L. amazonensis* infection, these data suggest that IGF-I does not significantly influence *L. infantum* amastigote proliferation. It may be related to the difference in the L-arginine metabolic pathway in this *Leishmania* species, where arginase does not seem essential for polyamine production. In studies with *L. donovani*, a related species that cause VL, arginase-deleted amastigotes survive within the cell without polyamine supplement but not promastigotes [83–85].

Further, in *L. infantum*-infected BALB/c and Swiss Webster mice, in the presence of spleen and liver cells producing high NO levels but with low arginase activity, the parasites continue multiplying within the host cells [86]. In vitro, *L. infantum* survives in the presence of high amounts of NO added in the culture medium [87]. Altogether, these data support the view that viscerotropic strains show differences in L-arginine metabolism.

As observed with other *Leishmania* species, the extrinsic IGF-I promoted *L. braziliensis* promastigote proliferation (Figure 1). However, this effect was not evident in *L. braziliensis* amastigotes within THP-1 cells upon stimulation with IGF-I. Analyzing the parasitism upon IGF-I stimulus in THP-1 cells infected with parasites isolated from patients

presenting different clinical manifestations, CL, ML, and DL, no differences were observed. We noted only a slight tendency to increase and decrease parasitism in cells infected with parasites derived from ML and DL patients, respectively. We also investigated the involvement of IGF-I on arginase activation in both *L. braziliensis* promastigote-infected THP-1 cells. In promastigotes isolated from CL and DL patients, the arginase activity was increased after IGF-I stimulation, while in parasites isolated from ML patients, a decrease was observed. It is worth mentioning that the ML-derived parasites presented a higher arginase activity when compared with CL- and DL-derived parasites. Besides the alteration in arginase activity in promastigotes, no difference in arginase activity was detected in macrophages infected with those parasites derived from different disease manifestations [88, 89]. Besides, no differences were observed on NO production between the groups stimulated or not with IGF-I (personal communication). Macrophage metabolism in *L. braziliensis* derived from diverse clinical manifestations is poorly understood, demanding more studies on the role of IGF-I.

4.3. Effect of Macrophage Intrinsic IGF-I on Intracellular *Leishmania* Growth. As macrophages contain endogenous IGF-I in the cytoplasm, we decided to evaluate IGF-I's role

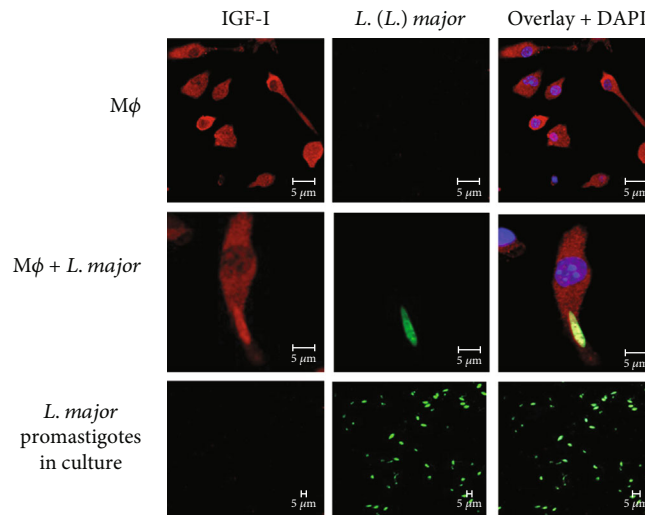


FIGURE 4: Detection of IGF-I within RAW 264.7 macrophages following infection with *Leishmania major* promastigotes. Colocalization of IGF-I and *Leishmania* was analyzed using immunofluorescence. Following a 24 h in vitro infection, cells were fixed in 4% paraformaldehyde (Sigma-Aldrich, USA), washed in 0.01 M phosphate-buffered saline, pH 7.2 (PBS), blocked for one hour with 2% bovine serum albumin (BSA; Sigma-Aldrich, USA) in PBS, and incubated overnight with monoclonal goat anti-mouse IGF-I antibody (1:75; R&D Systems, USA) and a polyclonal mouse anti-*Leishmania* antibody (1:400) [136]. Anti-goat IgG Alexa Fluor-546 (1:200, Invitrogen, USA—shown in red) and anti-mouse IgG Alexa Fluor-488 (1:400, Invitrogen, USA—shown in green) were used as secondary antibodies. 4,6-Diamidino-2-phenylindole (DAPI, Invitrogen, USA—shown in blue) was used to stain nuclei. Images were captured using a Leica LSM510 confocal microscope with a 63x objective and oil immersion (adapted from Reis et al. [82]).

produced by the macrophages (intrinsic IGF-I) in *Leishmania* infection. Under confocal microscopy, we showed that the intrinsic IGF-I interacts with intracellular *Leishmania* parasites [82] (Figure 4).

Since the interaction occurs between intrinsic IGF-I and intracellular parasites, we evaluate the parasitism upon inactivation of intrinsic IGF-I. Using a knockdown strategy, the *Igf-I* mRNA was silenced with IGF-I small interfering RNA (siRNA) in *L. major*-infected macrophages. In the siRNA-transfected group, we observed a significant decrease in parasitism, accompanied by decreased arginase mRNA expression and arginase activity in both parasites and macrophages and an increase in the *Nos-2* mRNA expression and NO production, when compared with the control group without siRNA transfection. This effect was reversed by the addition of recombinant IGF-I (rIGF-I), which induced an increase in the number of parasites and increased the levels of *Leishmania* arginase mRNA expression and arginase activity, accompanied by a decrease in the *Nos-2* mRNA expression and NO production [65].

We observed similar results when the IGF-I silencing strategy was employed in *L. amazonensis*-infected macrophages. We observed a significant decrease in parasitism accompanied by an increase in the NO production in the groups treated with siRNA compared with the control without siRNA (Figure 5). In another study, macrophages from growth hormone (GH)/IGF-I-deficient individuals, due to the growth hormone-releasing hormone receptor gene mutation, were assayed in vitro for *L. amazonensis* infection. It was observed that the macrophages isolated from these individuals were less prone to infection than healthy control

macrophages [90]. These data certainly confirmed the role of intrinsic IGF-I in intracellular parasite growth.

5. IGF-I and Cytokines

In *Leishmania* infection, the cytokines produced by macrophages and lymphocytes have an important participation in the interplay between parasite and the host involving IGF-I. In *L. amazonensis*-infected macrophages, the mechanisms leading to parasite growth upon IGF-I stimulus differed depending on the parasite life cycle stage used for infection. When cells were infected by promastigotes, upon IGF-I stimulus, this activation likely occurred through modulation of cytokine production, inducing a decrease in TNF- α and an increase in TGF- β and IFN- γ [55]. In cells infected by amastigotes, the mechanism was diverse. IGF-I induced phosphatidylserine exposure on the parasite surface that likely activated the macrophage arginase [91].

Other cytokines can act on the IGF-I expression like IFN- γ which promotes a reduction in the IGF-I expression, while IL-4 and IL-13 promote an increase in IGF-I expression [65–67]. These data suggest that IGF-I is involved in the development of the adaptive immune response in leishmaniasis.

The idea of immune-endocrine cross-talk has been described in other studies examining the roles of prolactin, GH, IGF-I, and thyroid-stimulating hormone in the development, maintenance, and function of the immune system, which in turn cause changes in the endocrine system [92–94]. The interaction between the endocrine

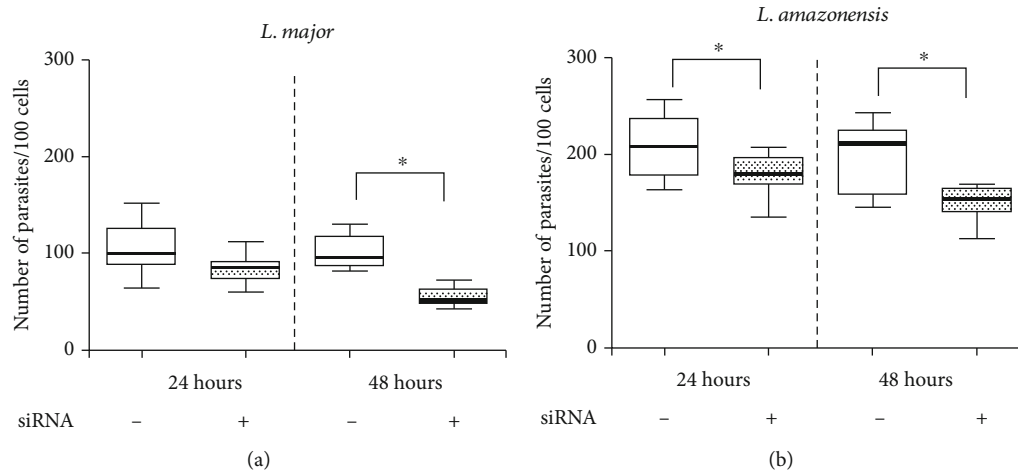


FIGURE 5: Parasitism in *L. major*- or *L. amazonensis*-infected macrophages upon IGF-I siRNA transfection. RAW 264.7 cells infected with *L. major* or *L. amazonensis* promastigotes transfected with or without 150 μ M IGF-I siRNA for 6 hours. The parasitism (median number of parasites per 100 cells) was evaluated after 24 and 48 hours. One representative experiment from three independent assays is shown. * $p < 0.05$ (ANOVA and Tukey's tests).

and immune systems is somewhat expected, as they share several ligands and receptors in their signaling pathways [65].

Interactions between IGF-I and the immune system are complex, bidirectional, and not fully explained. IGF-I could modulate the inflammatory response and the activity of systemic inflammation [95]. Studies have indicated that chronic inflammation could suppress the IGF-I axis via several mechanisms such as downregulation of IGF-I receptors, disruption in the IGF-I signaling pathways, dysregulation of IGF-BPs, reduced IGF bioavailability, and modified gene regulation through the changes in the microRNA expression [95, 96]. Proinflammatory cytokines such as IL-6, TNF- α , and IL-1 β impair the activity of the IGF-I axis by dysregulation of its intracellular mediators, such as mitogen-activated protein kinase (MAPK)/extracellular signal-regulated kinases and PI3K [97]. IGF-I can reduce inflammation induced by oxidized low-density lipoprotein treatment by reducing high-mobility group box 1 (HMGB1) release, a potent stimulator of tissue damage and inflammation, after stimulation with pathogens or a factor passively released by necrotic cells, activating nuclear factor kappa B (NF- κ B) [98, 99]. In another study on postmyocardial infarction, IGF-I decreased myocardium cell apoptosis and inhibited gene expression and production of proinflammatory cytokines, such as TNF- α , IL-1 β , and IL-6 [100]. Overall, most of the data appoint the effect of IGF-I on the innate inflammatory response.

In leishmaniasis, the specific immune response is well established in the *L. major*-infected mouse model, where Th1 and Th2 cytokines were, respectively, related to resistance and susceptibility to the infection. When Th1 cells are predominantly activated, the cytokines IL-2, IFN- γ , TNF- β , and IL-12 will be produced. Then, macrophages are activated and NOS2 induced, which metabolizes L-arginine, generating citrulline and NO associated with increased microbicidal activity. However, when Th2 cells are predominantly activated, mainly IL-4, IL-10, TGF- β , and IL-13 will be produced. Again, macrophages are activated alternatively, and arginase I expression and arginase activity are induced, lead-

ing to polyamine production that contributes to parasite proliferation [3].

When we analyzed IGF-I expression and the parasitism of *L. major* infection in vitro, macrophages stimulated with IFN- γ exhibited a reduction in the parasite load, accompanied by a parallel reduction in IGF-I expression and arginase activity and an increase in NO production. Further, IL-4 and IL-13 stimuli increased the parasitism, followed by a parallel increase in IGF-I expression and arginase activity and reduced NO production [65]. These data showing the similar effects of those cytokines on IGF-I expression and parasitism compelled us to explore this hormone's interference on the effects of cytokines during *Leishmania* infection.

As shown above, the Th1 and Th2 paradigm defined in the murine model with *L. major* infection has imperfections, and IL-4 related to susceptibility cannot be considered valid in any situation. Recently, in another *Leishmania* species, IL-4 was considered cytokine determining resistance in a *L. donovani*-infected BALB/c mouse [20]. Since the studies suggest that the susceptibility profile is not exclusively due to IL-4, and analyzing the signaling pathways of IL-4/IL-13 compared with the IGF-I pathway, we noticed shared components, suggesting that IGF-I and IL-4 may reciprocally interfere during *Leishmania* infection [65]. Thus, we proceeded with the study on the interference of IGF-I on IL-4 effect in *L. major*-macrophage interaction.

In *L. major*-infected macrophages stimulated with cytokines upon *Igf-I* mRNA expression silencing, the parasitism did not show the specific cytokine effect's expected result. Increased parasitism would be anticipated with IL-4 and IL-13 stimuli. However, they were utterly ineffective when the *Igf-I* mRNA was silenced. The effects of IL-4 and IL-13 on *Igf-I* mRNA-silenced cells were restored by the addition of rIGF-I in the culture, in a mechanism dependent on *Leishmania* arginase production [65].

Our results showed that IGF-I is necessary for IL-4 to exert its effect on parasite proliferation in macrophages. IGF-I and the cytokines IL-4 and IL-13 share common

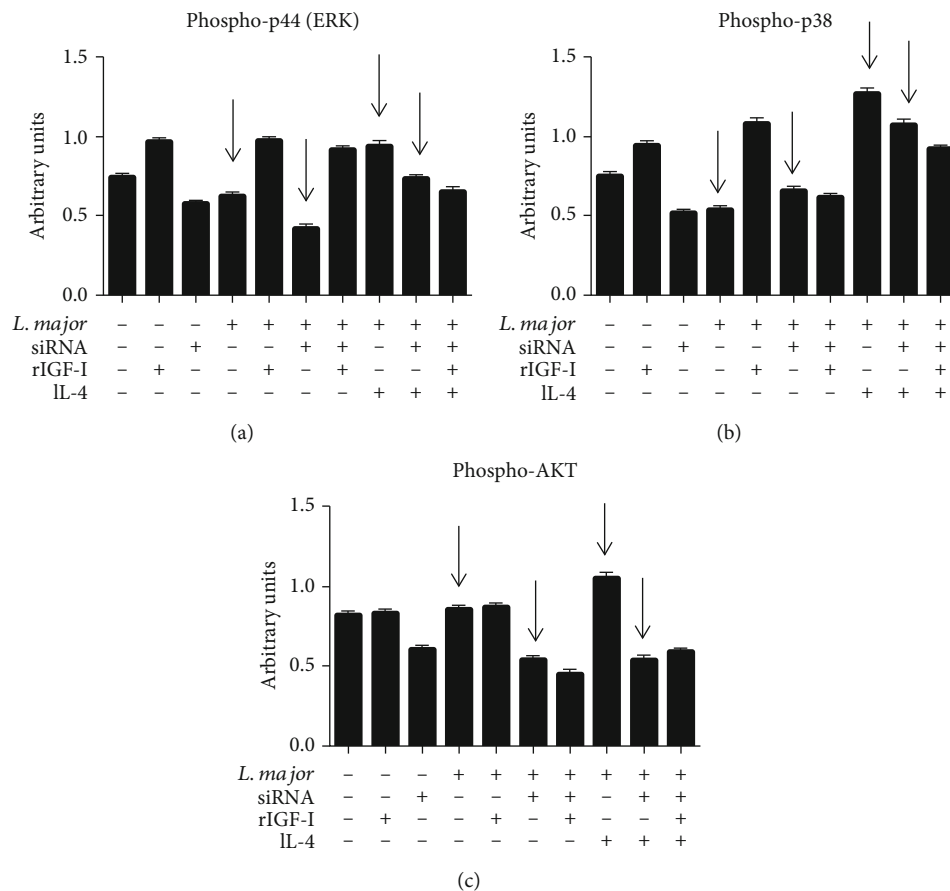


FIGURE 6: The effects of IGF-I siRNA and IL-4 on components of the IGF-I signaling pathways: levels of phosphorylated p44 (ERK), p38 (MAPK), and AKT proteins. *L. major* promastigote-infected or noninfected RAW 264.7 cells transfected with or without IGF-I siRNA were stimulated for 30 minutes with IL-4 (2 ng/mL; R&D Systems, EUA) and recombinant IGF-I (50 ng/mL; R&D Systems, EUA). Cells were lysed, the proteins were separated in 10% SDS-PAGE, and subsequently, a Western blotting was performed using anti-phospho-p44 (137F5, Cell Signaling Technology, USA), anti-phospho-p38 (D13E1, Cell Signaling Technology, USA), and anti-phospho-AKT (Ser473, Cell Signaling Technology, USA) antibodies. Protein bands corresponding to protein expression levels were submitted to a densitometric analysis (AlphaEaseFC™ software 3.2 beta version; Alpha Innotech Corporation, USA), and data are expressed in arbitrary units (adapted from Reis et al. [65]).

components in their intracellular signaling pathways. IGF-I triggers MAPK (ERK) and PI3K pathways [59, 101], and IL-4 sequentially activates IRS-2 and the PI3K/Akt and Ras-MAPK pathways [61, 102]. We observed an increase in the levels of these phosphorylated proteins in all groups treated with IL-4. Upon *Igf-I* mRNA silencing, we observed a decrease in the expression of all phosphoproteins, and interestingly, IL-4 stimulation did not completely restore the decreased expression of phospho-p44 (ERK), phospho-p38 (MAPK), and phospho-AKT [65] (Figure 6). We thus considered IGF-I as the effector element for the IL-4 effect in promoting susceptibility in *L. major* infection.

The participation of both Th1 and Th2 cytokines in resistance and susceptibility was defined on *L. major*-infected murine model infection, but it may not work in other *Leishmania* species such as *L. amazonensis*. IFN- γ promotes parasite growth in *L. amazonensis* amastigote-infected macrophages [103]. In our study with *L. amazonensis*-infected macrophages, IFN- γ induced increased parasitism and NO production and decreased IGF-I expression, with no correla-

tion with the parasitism. The IL-4 and IL-13 stimuli also promoted an increase in parasitism associated with an increase in IGF-I expression and an increase in arginase activity. Silencing *Igf-I* mRNA using IGF-I siRNA, the IL-4 and IL-13 stimuli led to decreased parasitism compared with their controls without siRNA. These data suggested that in the infection by *L. amazonensis*, IGF-I is also needed to promote susceptibility to infection (Figure 7). However, the effect of IFN- γ and interplay with IGF-I on *L. amazonensis* proliferation need further studies.

Thus, the susceptibility and resistance observed in *L. major*- and *L. amazonensis*-infected mouse strains may be due to cytokines to some extent, but the susceptibility essentially depends on the presence of IGF-I.

6. IGF-I in Susceptible and Resistant Leishmaniasis Mouse Models

In light of our findings showing IGF-I ruling susceptibility and resistance to *L. major* infection in vitro, we proceeded

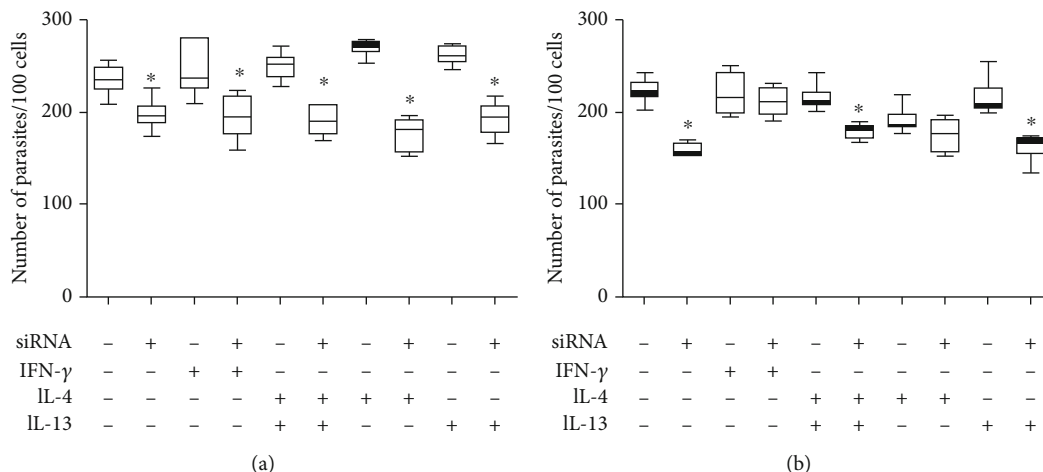


FIGURE 7: Parasitism in response to cytokine treatments and IGF-I siRNA transfection. Parasitism (median number of parasites per 100 cells) in *L. amazonensis*-infected RAW 264.7 cells transfected with or without 150 μ M IGF-I siRNA for 6 hours and then were stimulated with IFN- γ (200 U/mL; R&D Systems, EUA), IL-4 (2 ng/mL; R&D Systems, EUA), or IL-13 (5 ng/mL; R&D Systems, EUA) for 24 (a) and 48 (b) hours. One representative experiment from three independent assays is shown. * $p < 0.05$ (ANOVA and Tukey's tests).

to evaluate the participation of IGF-I in vivo in *L. major*-infected susceptible (BALB/c) and resistant (C57BL/6) mouse strains. In control BALB/c mice, the lesion continuously progressed as expected, while in those animals injected with parasites preincubated with IGF-I, the lesion development was accelerated, becoming larger when compared with the control. In contrast, in control C57BL/6 mice, the lesions progressed for three weeks and then stabilized and tended to diminish, but in those animals infected with parasites preincubated with IGF-I, the lesion interestingly progressed continuously, and it was significantly greater than that in the control, although smaller than that in the BALB/c mouse.

The previous data, showing that the transfer of BALB/c highly expressing IL-4 cells to genetically resistant chimeric mice on a C57BL/6 background did not result in susceptibility [15], suggested that the infection outcome is not governed only by the type of cytokine produced. Then, we asked whether IGF-I expression in mouse strains may explain the *L. major* infection outcome. The IGF-I expression in susceptible BALB/c mice and resistant C57BL/6 mice infected with *L. major* was indeed different. We evaluated the *Igf-I* mRNA by qPCR and IGF-I expression in anti-IGF-I labeled cells under confocal microscopy. By both approaches, IGF-I was detected in higher levels in BALB/c mice-derived peritoneal macrophages than in C57BL/6 mice-derived cells [65], suggesting that background expression of IGF-I may count determining susceptibility to *L. major* infection in mice.

Remarkably, in the *L. braziliensis*-infected mice, the disease development is not tangible, with tiny lesions [104]. The same is observed in a visceral leishmaniasis murine model using *L. donovani* or *L. infantum* that presents self-controlled disease [105, 106]. Coincidentally, the IGF-I in vitro effect on these *Leishmania* species was different from that observed with *L. major* and *L. amazonensis*. Whether these features are somehow related to IGF-I is an open question that deserves further studies.

7. IGF-I in Human Leishmaniasis

In human leishmaniasis, the infection development is related to the host's genetic and immunological characteristics and the *Leishmania* species' characteristics. We should emphasize the differences presented here on the IGF-I effect on the infection development, depending on the *Leishmania* species. We should also consider the sizable differences between the diseases seen in human patients and murine models.

In murine CL, in the mouse strains susceptible to *L. major* and *L. amazonensis*, the lesions' development is progressive. In these lesions, we find macrophages full of *Leishmania* amastigotes in proliferation [105]. In human active CL caused by these *Leishmania* species, the lesion presents different chronic inflammatory processes and scanty amastigotes [106, 107]. Only in rare diffuse cutaneous leishmaniasis, caused by *L. amazonensis*, the lesions are in some way similar to those observed in the susceptible murine CL model with abundant amastigotes in the lesion [107].

We addressed the VL caused by *L. infantum* and tegumentary leishmaniasis caused by *L. braziliensis* to study the participation of IGF-I in human leishmaniasis in Brazil.

7.1. IGF-I in Human Visceral Leishmaniasis. As shown above, the disease progression was initially attributed to *Leishmania* antigen-specific immunosuppression in active VL, but what we notice is an immune activation and imbalance of the immune response. Immunopathogenesis of VL is still not clear, and recently, CD8⁺ T cells were characterized by a gene signature observing the increased expression of specific cytolytic (granzymes A, B, and H and perforin), cytokine signaling (SOCS3, STAT1, JAK2, and JAK3), and immune checkpoint genes (LAG-3, TIM-3, and CTLA-4) [108].

When we evaluated both IGF-I and IGF-binding protein-3 (IGFBP3) serum levels in samples collected from active VL patients, we observed low levels of both IGF-I and IGFBP3 [109]. Based on these unexpected data, mainly in VL, where

we observe massive parasite proliferation in inner organs and considering experimental data showing no evident IGF-I effect on parasite growth, we should consider the participation of IGF-I in another way in the biology of *Leishmania*. Further IGF-I low levels in active VL were also seen in canine VL [109, 110] and human VL patients [111]. We do not have any element to envisage whether an IGF-I low level seen in active VL cases influences nonspecific processes related to parasite growth or adaptive immune response.

Alternatively, considering IGF-I's pleiotropic effect, we regarded it as IGF-I participation in other aspects of disease pathogenesis. High levels of IFN- γ and TNF- α in active VL may explain low IGF-I serum levels [66, 112]. We noticed that IGF-I is linked to hematopoiesis and anemia [113, 114]. Both IGF-I and IGFBP3 serum levels showed a positive correlation with hemoglobin levels in active human VL and canine VL. Thus, we suggested that IGF-I has a pathogenic role in VL anemia without any correlation with cytokine levels. IFN- γ was shown negatively correlated with anemia; thus, we suggested that both IFN- γ and IGF-I contribute to the pathogenesis of anemia in active VL but independently [109]. The experimental data in murine VL showing CD4⁺ T cells producing IFN- γ with alteration in the stromal microenvironment in bone marrow linked to anemia development reinforced the importance of IFN- γ in the pathogenesis of anemia in active VL [115].

7.2. IGF-I in Human Tegumentary Leishmaniasis. Tegumentary leishmaniasis in Brazil is mostly caused by *L. (Viannia) braziliensis*, which presents as CL, ML, and DL. Studies on pathogenesis show that immune response participates not only in parasite growth control but also in lesion development [116]. In CL, there is a strong T cell response with Th1 cytokine production, such as IFN- γ and IL-12, related to infection control, but if uncontrolled, it may cause tissue damage [117]. The ML has a high specific T cell response, both Th1 and Th2, directed to a Th1-type response. High levels of proinflammatory cytokines, TNF- α and IFN- γ , are produced, which are poorly regulated by IL-10 and TGF- β [118, 119].

Further, comparing infected asymptomatic, CL, and ML cases, a higher level of TNF- α was seen in CL and ML lesions than in asymptomatic individuals. This higher level of TNF- α is involved in lesion development even though it has known anti-*Leishmania* effect [120]. Another study showed that both CD8⁺ T cells and granzyme were related to lesion development [121]. In a more recent study, transcriptomic analysis in skin samples compared gene expression in cured and noncured CL patients after 90 days of treatment. Gene sets related to cytolytic machinery were significantly more expressed, with higher expression of granzyme (*GZMB gene*), perforin (*PRF1 gene*), and granulysin (*GNLY gene*) [122] in noncured CL patients. Thinking on the participation of IGF-I in the pathogenesis of *L. braziliensis*-caused CL, the role of IGF-I would be more related to inflammatory and healing processes than to parasite growth.

We initially addressed IGF-I in human cases of leishmaniasis, measuring both IGF-I and IGFBP3 serum levels in patients presenting different clinical forms, CL, ML, and DL. In this analysis, both IGF-I and IGFBP3 levels were lower

in ML and DL than CL and healthy controls [89]. Considering the pleiotropic effects of IGF-I and observing a low level of IGF-I in patients with worse clinical presentations such as ML and DL, we may speculate on IGF-I's role in the modulation of the inflammatory process and the maintenance of epidermis and healing process [123–127].

Searching the role of IGF-I by immunohistochemistry in the lesion of 51 human CL caused by *L. braziliensis*, IGF-I was seen related to chronicity and good response to treatment, but not parasite growth, and we relate the findings to the efficient anti-inflammatory response and the known action of IGF-I in wound repair [128].

8. Perspectives on the Use of IGF-I in Therapeutic Interventions in Human Leishmaniasis

IGF-I was associated with other skin diseases where delayed wound healing was related to IGF-I's low production at the injury sites. In conditions like diabetes mellitus, IGF-I has been used in skin ulcer treatment observing the healing with an increase in the IGF-I local level upon hyperbaric oxygen therapy or using IGF-I cream locally [129, 130].

Interference on the IGF-I pathway has been proposed to address treatment strategies in diseases such as cancer, autoimmune diseases, and atherosclerosis [131–133]. One of the suggested targets is the Th17/Treg axis. Th17 cells were associated with protection in VL but were associated with infiltration and disease pathology in human CL and ML [134]. In autoimmune disorders with the participation of Th17 cells, beneficial effects of a systemic recombinant IGF-I treatment were seen through an increase of regulatory T cell levels in affected tissues. Regulation of Th17 cells by IGF-I may occur through modulation of AKT-mTOR and STAT3 signalings [72]. Another target is the Vascular Endothelial Growth Factor A (VEGFA), a key factor in angiogenesis and wound healing process [135].

The possibility to explore the therapeutic use of IGF-I encourages us to proceed with the studies on IGF-I in the pathogenesis of different forms of leishmaniasis.

9. Conclusions

In leishmaniasis, because the adaptive immune response does not fully explain *Leishmania* infection's outcome, we addressed the participation of IGF-I in infection and disease outcome. Here, we reviewed the role of IGF-I in leishmaniasis experimental models and human patients. IGF-I's effect extends over the biology of *Leishmania*, *Leishmania*-macrophage interaction hitting arginine metabolic pathway in both cells, cytokine modulation, and pathogenic mechanisms of different disease manifestations. The direct effect of IGF-I on *Leishmania* results in its growth in vitro at a specific parasite stage. It influences the disease's course inducing an increase in the skin lesion size and parasite load, especially with *L. major*- and *L. amazonensis*-infected mouse cutaneous leishmaniasis. With other species of *Leishmania*, *L. braziliensis* and *L. infantum*, parasite growth is not evident, bringing

question on the differences in arginine metabolic pathway activation dependent on the parasite species.

IGF-I interacts with cytokines where IFN- γ inhibits, while IL-4 and IL-13 increase its expression in macrophages. In the interaction with IL-4, a cytokine that is a hallmark of susceptibility to *L. major* in murine leishmaniasis, we show IGF-I as an effector element of the IL-4, an unprecedented finding.

Moving to human leishmaniasis, IGF-I was not proven as a factor promoting parasite growth in cutaneous leishmaniasis caused by *L. braziliensis* and visceral leishmaniasis by *L. infantum*. Since patients with more severe diseases such as mucosal, disseminated, and visceral forms presented low IGF-I serum levels, alternative roles were searched. We observed that low IGF-I levels might contribute to the inflammatory response persistence and delayed lesion healing in human cutaneous leishmaniasis and the anemia development in visceral leishmaniasis. We must highlight the complexity of infection revealed depending on the *Leishmania* species and the parasite's developmental stages. Because IGF-I exerts pleiotropic effects on the biology of interaction and disease pathogenesis and can trigger and/or modulate more than 200 genes in certain cells and tissues, IGF-I turns up an interesting tool to explore biological and pathogenic processes underlying infection development. Further, IGF-I pleiotropic effects open the possibility to approach IGF-I as a therapeutical target.

Conflicts of Interest

The authors declare no conflicts of interest.

Authors' Contributions

LCR, EMRS, and HG contributed to the conceptualization, literature search, critical review, data analysis, and manuscript preparation; FNA, AFL, CYO, ORS, and BAU contributed with experimental data and data interpretation, literature search, and manuscript preparation. Luiza C. Reis and Eduardo Milton Ramos-Sanchez contributed equally to this work.

Acknowledgments

We specially acknowledge Magnus Gidlund for the insight to approach IGF-I in leishmaniasis and Claudia M.C. Gomes and Célia M. V. Vendrame for the initial great experimental contributions in the IGF-I leishmaniasis project. This work was supported by grants from the Fundação de Amparo à Pesquisa do Estado de São Paulo (grant 2018/14398-0 and fellowships 2019/25393-1 to LCR, 2017/02959-4 to FNA, and 2014/08340-8 to AFL), Medical Research Council (grant MR/P024661/1), Conselho Nacional de Pesquisa (research fellowship to HG), Coordenação de Aperfeiçoamento de Pessoal de Nível Superior (CAPES) (fellowships 1747829 and 88887.572142/2020-00 to BAU and 88882.376675/2019-01 to ORS), Programa Nacional de Bercas y Crédito Educativo de Perú (PRONABEC, fellowship to ORS), and LIM 38 (Hospital das Clínicas, Faculdade de Medicina da Universidade de São Paulo).

References

- [1] S. Burza, S. L. Croft, and M. Boelaert, "Leishmaniasis," *Lancet*, vol. 392, no. 10151, pp. 951–970, 2018.
- [2] K. A. Rogers, G. K. DeKrey, M. L. Mbow, R. D. Gillespie, C. I. Brodskyn, and R. G. Titus, "Type 1 and type 2 responses to *Leishmania major*," *FEMS Microbiology Letters*, vol. 209, no. 1, pp. 1–7, 2002.
- [3] A. Gummy, J. A. Louis, and P. Launois, "The murine model of infection with *Leishmania major* and its importance for the deciphering of mechanisms underlying differences in Th cell differentiation in mice from different genetic backgrounds," *International Journal for Parasitology*, vol. 34, no. 4, pp. 433–444, 2004.
- [4] D. Sacks and N. Noben-Trauth, "The immunology of susceptibility and resistance to *Leishmania major* in mice," *Nature Reviews. Immunology*, vol. 2, no. 11, pp. 845–858, 2002.
- [5] R. Hurdal and F. Brombacher, "The role of IL-4 and IL-13 in cutaneous *Leishmaniasis*," *Immunology Letters*, vol. 161, no. 2, pp. 179–183, 2014.
- [6] D. Liu and J. E. Uzonna, "The early interaction of *Leishmania* with macrophages and dendritic cells and its influence on the host immune response," *Frontiers in Cellular and Infection Microbiology*, vol. 2, p. 83, 2012.
- [7] C. F. Anderson, S. Mendez, and D. L. Sacks, "Nonhealing infection despite Th1 polarization produced by a strain of *Leishmania major* in C57BL/6 mice," *Journal of Immunology*, vol. 174, no. 5, pp. 2934–2941, 2005.
- [8] D. Artis, L. M. Johnson, K. Joyce et al., "Cutting edge: early IL-4 production governs the requirement for IL-27-WSX-1 signaling in the development of protective Th1 cytokine responses following *Leishmania major* infection," *Journal of Immunology*, vol. 172, no. 8, pp. 4672–4675, 2004.
- [9] S. Nylén and S. Gautam, "Immunological perspectives of leishmaniasis," *Journal of Global Infectious Diseases*, vol. 2, no. 2, pp. 135–146, 2010.
- [10] P. Launois, K. G. Swihart, G. Milon, and J. A. Louis, "Early production of IL-4 in susceptible mice infected with *Leishmania major* rapidly induces IL-12 unresponsiveness," *Journal of Immunology*, vol. 158, no. 7, pp. 3317–3324, 1997.
- [11] P. Launois, S. Pingel, H. Himmelrich, R. Locksley, and J. Louis, "Different epitopes of the LACK protein are recognized by V beta 4 V alpha 8 CD4+ T cells in H-2b and H-2d mice susceptible to *Leishmania major*," *Microbes and Infection*, vol. 9, no. 11, pp. 1260–1266, 2007.
- [12] B. D. Hondowicz, T. M. Scharton-Kersten, D. E. Jones, and P. Scott, "Leishmania major-infected C3H mice treated with anti-IL-12 mAb develop but do not maintain a Th2 response," *Journal of Immunology*, vol. 159, no. 10, pp. 5024–5031, 1997.
- [13] D. B. Stetson, M. Mohrs, V. Mallet-Designé, L. Teyton, and R. M. Locksley, "Rapid expansion and IL-4 expression by *Leishmania*-specific naive helper T cells in vivo," *Immunity*, vol. 17, no. 2, pp. 191–200, 2002.
- [14] P. Scott, A. Eaton, W. C. Gause, X. di Zhou, and B. Hondowicz, "Early IL-4 production does not predict susceptibility to *Leishmania major*," *Experimental Parasitology*, vol. 84, no. 2, pp. 178–187, 1996.
- [15] A. H. Shankar and R. G. Titus, "T cell and non-T cell compartments can independently determine resistance to *Leishmania major*," *The Journal of Experimental Medicine*, vol. 181, no. 3, pp. 845–855, 1995.

- [16] H. Goto and J. A. Lindoso, "Immunity and immunosuppression in experimental visceral leishmaniasis," *Brazilian Journal of Medical and Biological Research*, vol. 37, no. 4, pp. 615–623, 2004.
- [17] P. M. Kaye, A. J. Curry, and J. M. Blackwell, "Differential production of Th1- and Th2-derived cytokines does not determine the genetically controlled or vaccine-induced rate of cure in murine visceral leishmaniasis," *Journal of Immunology*, vol. 146, no. 8, pp. 2763–2770, 1991.
- [18] C. L. Karp, S. H. el-Safi, T. A. Wynn et al., "In vivo cytokine profiles in patients with kala-azar. Marked elevation of both interleukin-10 and interferon-gamma," *The Journal of Clinical Investigation*, vol. 91, no. 4, pp. 1644–1648, 1993.
- [19] K. Kemp, "Cytokine-producing T cell subsets in human leishmaniasis," *Archivum Immunologiae et Therapiae Experimentalis (Warsz)*, vol. 48, no. 3, pp. 173–176, 2000.
- [20] E. McFarlane, T. Mokgethi, P. M. Kaye et al., "IL-4 mediated resistance of BALB/c mice to visceral leishmaniasis is independent of IL-4R α signaling via T cells," *Frontiers in Immunology*, vol. 10, p. 1957, 2019.
- [21] H. W. Murray and C. F. Nathan, "Macrophage microbicidal mechanisms in vivo: reactive nitrogen versus oxygen intermediates in the killing of intracellular visceral *Leishmania donovani*," *The Journal of Experimental Medicine*, vol. 189, no. 4, pp. 741–746, 1999.
- [22] D. L. Sacks, S. L. Lal, S. N. Shrivastava, J. Blackwell, and F. A. Neva, "An analysis of T cell responsiveness in Indian kala-azar," *Journal of Immunology*, vol. 138, no. 3, pp. 908–913, 1987.
- [23] R. Kumar, S. B. Chauhan, S. S. Ng, S. Sundar, and C. R. Engwerda, "Immune checkpoint targets for host-directed therapy to prevent and treat leishmaniasis," *Frontiers in Immunology*, vol. 8, p. 1492, 2017.
- [24] H. Goto and M. Prianti, "Immunoactivation and immunopathogeny during active visceral leishmaniasis," *Revista do Instituto de Medicina Tropical de São Paulo*, vol. 51, no. 5, pp. 241–246, 2009.
- [25] I. M. de Medeiros, A. Castelo, and R. Salomao, "Presence of circulating levels of interferon-gamma, interleukin-10 and tumor necrosis factor-alpha in patients with visceral leishmaniasis," *Revista do Instituto de Medicina Tropical de São Paulo*, vol. 40, no. 1, pp. 31–34, 1998.
- [26] M. Samant, U. Sahu, S. C. Pandey, and P. Khare, "Role of cytokines in experimental and human visceral Leishmaniasis," *Frontiers in Cellular and Infection Microbiology*, vol. 11, article 624009, 2021.
- [27] S. Gautam, R. Kumar, N. Singh et al., "CD8 T cell exhaustion in human visceral leishmaniasis," *The Journal of Infectious Diseases*, vol. 209, no. 2, pp. 290–299, 2014.
- [28] F. Hamidi, S. Mohammadi-Yeganeh, M. Haji Molla Hoseini et al., "Inhibition of anti-inflammatory cytokines, IL-10 and TGF- β , in *Leishmania* major infected macrophage by miRNAs: a new therapeutic modality against leishmaniasis," *Microbial Pathogenesis*, vol. 153, article 104777, 2021.
- [29] M. Barral-Netto, A. Barral, C. Brownell et al., "Transforming growth factor-beta in leishmanial infection: a parasite escape mechanism," *Science*, vol. 257, no. 5069, pp. 545–548, 1992.
- [30] A. Barral, M. Barral-Netto, E. C. Yong, C. E. Brownell, D. R. Twardzik, and S. G. Reed, "Transforming growth factor beta as a virulence mechanism for *Leishmania braziliensis*," *Proceedings of the National Academy of Sciences of the United States of America*, vol. 90, no. 8, pp. 3442–3446, 1993.
- [31] B. J. Nelson, P. Ralph, S. J. Green, and C. A. Nacy, "Differential susceptibility of activated macrophage cytotoxic effector reactions to the suppressive effects of transforming growth factor-beta 1," *Journal of Immunology*, vol. 146, no. 6, pp. 1849–1857, 1991.
- [32] K. R. Gantt, S. Schultz-Cherry, N. Rodriguez et al., "Activation of TGF- β by *Leishmania chagasi*: importance for parasite survival in macrophages," *Journal of Immunology*, vol. 170, no. 5, pp. 2613–2620, 2003.
- [33] V. Rodrigues Jr., "Transforming growth factor β and immunosuppression in experimental visceral leishmaniasis," *Infection and Immunity*, vol. 66, no. 3, pp. 1233–1236, 1998.
- [34] A. Barral, M. Teixeira, P. Reis et al., "Transforming growth factor-beta in human cutaneous leishmaniasis," *The American Journal of Pathology*, vol. 147, no. 4, pp. 947–954, 1995.
- [35] M. Asad, A. Sabur, M. Shadab et al., "EBI-3 chain of IL-35 along with TGF- β synergistically regulate anti-leishmanial immunity," *Frontiers in Immunology*, vol. 10, p. 616, 2019.
- [36] T. di-Blasi, E. L. Telleria, C. Marques et al., "*Lutzomyia longipalpis* TGF- β has a role in *Leishmania infantum* chagasi survival in the vector," *Frontiers in Cellular and Infection Microbiology*, vol. 9, p. 71, 2019.
- [37] M. A. Barcinski, D. Schechtman, L. G. Quintao et al., "Granulocyte-macrophage colony-stimulating factor increases the infectivity of *Leishmania amazonensis* by protecting promastigotes from heat-induced death," *Infection and Immunity*, vol. 60, no. 9, pp. 3523–3527, 1992.
- [38] R. Charlab, C. Blaineau, D. Schechtman, and M. A. Barcinski, "Granulocyte-macrophage colony-stimulating factor is a growth-factor for promastigotes of *Leishmania mexicana amazonensis*," *The Journal of Protozoology*, vol. 37, no. 5, pp. 352–357, 1990.
- [39] J. Greil, B. Bodendorfer, M. R. Ö. L. And, and W. Solbach, "Application of recombinant granulocyte-macrophage colony-stimulating factor has a detrimental effect in experimental murine leishmaniasis," *European Journal of Immunology*, vol. 18, no. 10, pp. 1527–1534, 1988.
- [40] P. R. L. Machado, F. V. O. Prates, V. Boaventura et al., "A double-blind, randomized trial to evaluate Miltefosine and topical granulocyte macrophage colony-stimulating factor in the treatment of cutaneous leishmaniasis caused by *Leishmania braziliensis* in Brazil," *Clinical Infectious Diseases*, 2020.
- [41] L. Mendes, J. O. Guerra, B. Costa et al., "Association of miltefosine with granulocyte and macrophage colony-stimulating factor (GM-CSF) in the treatment of cutaneous leishmaniasis in the Amazon region: a randomized and controlled trial," *International Journal of Infectious Diseases*, vol. 103, pp. 358–363, 2021.
- [42] H. Malta-Santos, K. F. Fukutani, C. A. Sorgi et al., "Multi-omic analyses of plasma cytokines, lipidomics, and transcriptomics distinguish treatment outcomes in cutaneous leishmaniasis," *iScience*, vol. 23, no. 12, article 101840, 2020.
- [43] E. Handman and A. W. Burgess, "Stimulation by granulocyte-macrophage colony-stimulating factor of *Leishmania tropica* killing by macrophages," *Journal of Immunology*, vol. 122, no. 3, pp. 1134–1137, 1979.
- [44] J. L. Ho, S. G. Reed, E. A. Wick, and M. Giordano, "Granulocyte-macrophage and macrophage colony-stimulating

- factors activate intramacrophage killing of *Leishmania mexicana amazonensis*,” *The Journal of Infectious Diseases*, vol. 162, no. 1, pp. 224–230, 1990.
- [45] W. Y. Weiser, A. van Niel, S. C. Clark, J. R. David, and H. G. Remold, “Recombinant human granulocyte/macrophage colony-stimulating factor activates intracellular killing of *Leishmania donovani* by human monocyte-derived macrophages,” *The Journal of Experimental Medicine*, vol. 166, no. 5, pp. 1436–1446, 1987.
- [46] C. L. Scott, L. Roe, J. Curtis et al., “Mice unresponsive to GM-CSF are unexpectedly resistant to cutaneous *Leishmania* major infection,” *Microbes and Infection*, vol. 2, no. 10, pp. 1131–1138, 2000.
- [47] J. I. Jones and D. R. Clemmons, “Insulin-like growth factors and their binding proteins: biological actions,” *Endocrine Reviews*, vol. 16, no. 1, pp. 3–34, 1995.
- [48] L. A. Bach, “IGF-binding proteins,” *Journal of Molecular Endocrinology*, vol. 61, no. 1, pp. T11–T28, 2018.
- [49] A. D. Bakker and R. T. Jaspers, “IL-6 and IGF-1 signaling within and between muscle and bone: how important is the mTOR pathway for bone metabolism?,” *Current Osteoporosis Reports*, vol. 13, no. 3, pp. 131–139, 2015.
- [50] W. S. Cohick and D. R. Clemmons, “The insulin-like growth factors,” *Annual Review of Physiology*, vol. 55, no. 1, pp. 131–153, 1993.
- [51] F. Alvarez-Nava and R. Lanes, “GH/IGF-1 signaling and current knowledge of epigenetics; a review and considerations on possible therapeutic options,” *International Journal of Molecular Sciences*, vol. 18, no. 10, p. 1624, 2017.
- [52] J. Palsgaard, A. E. Brown, M. Jensen, R. Borup, M. Walker, and P. de Meyts, “Insulin-like growth factor I (IGF-I) is a more potent regulator of gene expression than insulin in primary human myoblasts and myotubes,” *Growth Hormone & IGF Research*, vol. 19, no. 2, pp. 168–178, 2009.
- [53] H. D. Luján, M. R. Mowatt, L. J. Helman, and T. E. Nash, “Insulin-like growth factors stimulate growth and L-cysteine uptake by the intestinal parasite *Giardia lamblia*,” *The Journal of Biological Chemistry*, vol. 269, no. 18, pp. 13069–13072, 1994.
- [54] H. Goto, C. M. C. Gomes, C. E. P. Corbett, H. P. Monteiro, and M. Gidlund, “Insulin-like growth factor I is a growth-promoting factor for *Leishmania* promastigotes and amastigotes,” *Proceedings of the National Academy of Sciences of the United States of America*, vol. 95, no. 22, pp. 13211–13216, 1998.
- [55] C. M. Vendrame, M. D. T. Carvalho, F. J. O. Rios, E. R. Manuli, F. Petitto-Assis, and H. Goto, “Effect of insulin-like growth factor-I on *Leishmania amazonensis* promastigote arginase activation and reciprocal inhibition of NOS2 pathway in macrophage in vitro,” *Scandinavian Journal of Immunology*, vol. 66, no. 2-3, pp. 287–296, 2007.
- [56] C. M. Gomes, H. Goto, C. E. P. Corbett, and M. Gidlund, “Insulin-like growth factor-I is a growth promoting factor for *Leishmania* promastigotes,” *Acta Tropica*, vol. 64, no. 3-4, pp. 225–228, 1997.
- [57] H. You, G. N. Gobert, M. G. Duke et al., “The insulin receptor is a transmission blocking veterinary vaccine target for zoonotic *Schistosoma japonicum*,” *International Journal for Parasitology*, vol. 42, no. 9, pp. 801–807, 2012.
- [58] L. S. Rodrigues, E. da Silva Maeda, M. E. C. Moreira et al., “*Mycobacterium leprae* induces insulin-like growth factor and promotes survival of Schwann cells upon serum withdrawal,” *Cellular Microbiology*, vol. 12, no. 1, pp. 42–54, 2010.
- [59] L. Laviola, A. Natalicchio, S. Perrini, and F. Giorgino, “Abnormalities of IGF-I signaling in the pathogenesis of diseases of the bone, brain, and fetoplacental unit in humans,” *American Journal of Physiology. Endocrinology and Metabolism*, vol. 295, no. 5, pp. E991–E999, 2008.
- [60] M. F. White, “The IRS-signaling system: a network of docking proteins that mediate insulin and cytokine action,” *Recent Progress in Hormone Research*, vol. 53, pp. 119–138, 1998.
- [61] L. Soon, L. Flechner, J. S. Gutkind et al., “Insulin-like growth factor I synergizes with interleukin 4 for hematopoietic cell proliferation independent of insulin receptor substrate expression,” *Molecular and Cellular Biology*, vol. 19, no. 5, pp. 3816–3828, 1999.
- [62] J. Frystyk, “Free insulin-like growth factors – measurements and relationships to growth hormone secretion and glucose homeostasis,” *Growth Hormone & IGF Research*, vol. 14, no. 5, pp. 337–375, 2004.
- [63] T. Hehlgans and K. Pfeffer, “The intriguing biology of the tumour necrosis factor/tumour necrosis factor receptor superfamily: players, rules and the games,” *Immunology*, vol. 115, no. 1, pp. 1–20, 2005.
- [64] A. M. Valverde, M. Benito, and M. Lorenzo, “The brown adipose cell: a model for understanding the molecular mechanisms of insulin resistance,” *Acta Physiologica Scandinavica*, vol. 183, no. 1, pp. 59–73, 2005.
- [65] L. C. Reis, E. M. Ramos-Sanchez, F. Petitto-Assis et al., “Insulin-like growth factor-I as an effector element of the cytokine IL-4 in the development of a *Leishmania* major infection,” *Mediators of Inflammation*, vol. 2018, Article ID 9787128, 17 pages, 2018.
- [66] S. Arkins, N. Rebeiz, D. L. Brunke-Reese, A. Biragyn, and K. W. Kelley, “Interferon-gamma inhibits macrophage insulin-like growth factor-I synthesis at the transcriptional level,” *Molecular Endocrinology*, vol. 9, no. 3, pp. 350–360, 1995.
- [67] M. W. Wynes and D. W. Riches, “Induction of macrophage insulin-like growth factor-I expression by the Th2 cytokines IL-4 and IL-13,” *Journal of Immunology*, vol. 171, no. 7, pp. 3550–3559, 2003.
- [68] R. Kooijman and A. Coppens, “Insulin-like growth factor-I stimulates IL-10 production in human T cells,” *Journal of Leukocyte Biology*, vol. 76, no. 4, pp. 862–867, 2004.
- [69] E. W. Johnson, L. A. Jones, and R. W. Kozak, “Expression and function of insulin-like growth factor receptors on anti-CD3-activated human T lymphocytes,” *Journal of Immunology*, vol. 148, no. 1, pp. 63–71, 1992.
- [70] M. E. Segretin, A. Galeano, A. Roldán, and R. Schillaci, “Insulin-like growth factor-1 receptor regulation in activated human T lymphocytes,” *Hormone Research*, vol. 59, no. 6, pp. 276–280, 2003.
- [71] P. T. Walsh and R. O’Connor, “The insulin-like growth factor-I receptor is regulated by CD28 and protects activated T cells from apoptosis,” *European Journal of Immunology*, vol. 30, no. 4, pp. 1010–1018, 2000.
- [72] D. DiToro, S. N. Harbour, J. K. Bando et al., “Insulin-like growth factors are key regulators of T helper 17 regulatory T cell balance in autoimmunity,” *Immunity*, vol. 52, no. 4, pp. 650–667.e10, 2020.
- [73] C. M. Gomes, H. P. Monteiro, M. Gidlund, C. E. P. Corbett, and H. Goto, “Insulin-like growth factor-I induces


















- phosphorylation in *Leishmania (Leishmania) mexicana* promastigotes and amastigotes,” *The Journal of Eukaryotic Microbiology*, vol. 45, no. 3, pp. 352–355, 1998.
- [74] C. M. Gomes, H. Goto, A. C. Magnanelli et al., “Characterization of the receptor for insulin-like growth factor on *Leishmania* promastigotes,” *Experimental Parasitology*, vol. 99, no. 4, pp. 190–197, 2001.
- [75] K. Drakenberg, V. R. Sara, S. Falkmer, S. Gammeltoft, C. Maahe, and M. Reinecke, “Identification of IGF-1 receptors in primitive vertebrates,” *Regulatory Peptides*, vol. 43, no. 1–2, pp. 73–81, 1993.
- [76] I. Navarro, B. Leibush, T. W. Moon et al., “Insulin, insulin-like growth factor-I (IGF-I) and glucagon: the evolution of their receptors,” *Comparative Biochemistry and Physiology. Part B, Biochemistry & Molecular Biology*, vol. 122, no. 2, pp. 137–153, 1999.
- [77] C. M. Gomes, H. Goto, V. L. Ribeiro da Matta, M. D. Laurenti, M. Gidlund, and C. E. Corbett, “Insulin-like growth factor (IGF)-I affects parasite growth and host cell migration in experimental cutaneous leishmaniasis,” *International Journal of Experimental Pathology*, vol. 81, no. 4, pp. 249–255, 2000.
- [78] N. Wanasen, C. L. MacLeod, L. G. Ellies, and L. Soong, “L-arginine and cationic amino acid transporter 2B regulate growth and survival of *Leishmania amazonensis* amastigotes in macrophages,” *Infection and Immunity*, vol. 75, no. 6, pp. 2802–2810, 2007.
- [79] F. Y. Liew, S. Millott, C. Parkinson, R. M. Palmer, and S. Moncada, “Macrophage killing of *Leishmania* parasite in vivo is mediated by nitric oxide from L-arginine,” *Journal of Immunology*, vol. 144, no. 12, pp. 4794–4797, 1990.
- [80] S. C. Roberts, M. J. Tancer, M. R. Polinsky, K. M. Gibson, O. Heby, and B. Ullman, “Arginase plays a pivotal role in polyamine precursor metabolism in *Leishmania*,” *The Journal of Biological Chemistry*, vol. 279, no. 22, pp. 23668–23678, 2004.
- [81] M. F. da Silva and L. M. Floeter-Winter, “Arginase in *Leishmania*,” *Sub-Cellular Biochemistry*, vol. 74, pp. 103–117, 2014.
- [82] L. C. Reis, E. M. Ramos-Sanchez, and H. Goto, “The interactions and essential effects of intrinsic insulin-like growth factor-I on *Leishmania (Leishmania)* major growth within macrophages,” *Parasite Immunology*, vol. 35, no. 7–8, pp. 239–244, 2013.
- [83] Y. Jiang, S. C. Roberts, A. Jardim et al., “Ornithine decarboxylase gene deletion mutants of *Leishmania donovani*,” *The Journal of Biological Chemistry*, vol. 274, no. 6, pp. 3781–3788, 1999.
- [84] J. M. Boitz, C. A. Gilroy, T. D. Olenyik et al., “Arginase is essential for survival of *Leishmania donovani* promastigotes but not intracellular amastigotes,” *Infection and Immunity*, vol. 85, no. 1, 2017.
- [85] C. C. Stempin, L. R. Dulgerian, V. V. Garrido, and F. M. Cerban, “Arginase in parasitic infections: macrophage activation, immunosuppression, and intracellular signals,” *Journal of Biomedicine & Biotechnology*, vol. 2010, Article ID 683485, 10 pages, 2010.
- [86] T. Ferreira-Paes, K. S. Charret, M. R. S. Ribeiro, R. F. Rodrigues, and L. L. Leon, “Comparative analysis of biological aspects of *Leishmania infantum* strains,” *PLoS One*, vol. 15, no. 12, article e0230545, 2020.
- [87] F. Marques, S. Vale-Costa, T. Cruz et al., “Studies in the mouse model identify strain variability as a major determinant of disease outcome in *Leishmania infantum* infection,” *Parasites & Vectors*, vol. 8, no. 1, p. 644, 2015.
- [88] C. M. Vendrame, L. D. Souza, M. D. T. Carvalho, K. Salgado, E. M. Carvalho, and H. Goto, “Insulin-like growth factor-I induced and constitutive arginase activity differs among isolates of *Leishmania* derived from patients with diverse clinical forms of *Leishmania braziliensis* infection,” *Transactions of the Royal Society of Tropical Medicine and Hygiene*, vol. 104, no. 568, pp. 566–568, 2010.
- [89] L. D. de Souza, C. M. V. Vendrame, A. R. de Jesus et al., “Insulin-like growth factor-I serum levels and their biological effects on *Leishmania* isolates from different clinical forms of American tegumentary leishmaniasis,” *Parasites & Vectors*, vol. 9, no. 1, p. 335, 2016.
- [90] M. R. Barrios, V. C. Campos, N. T. A. Peres et al., “Macrophages from subjects with isolated GH/IGF-I deficiency due to a GHRH receptor gene mutation are less prone to infection by *Leishmania amazonensis*,” *Frontiers in Cellular and Infection Microbiology*, vol. 9, p. 311, 2019.
- [91] C. M. Vendrame, M. D. T. Carvalho, A. G. Tempone, and H. Goto, “Insulin-like growth factor-I induces arginase activity in *Leishmania amazonensis* amastigote-infected macrophages through a cytokine-independent mechanism,” *Mediators of Inflammation*, vol. 2014, Article ID 475919, 13 pages, 2014.
- [92] R. Kooijman, E. L. Hooghe-Peters, and R. Hooghe, “Prolactin, growth hormone, and insulin-like growth factor-I in the immune system,” *Advances in Immunology*, vol. 63, pp. 377–454, 1996.
- [93] K. W. Kelley, D. A. Weigent, and R. Kooijman, “Protein hormones and immunity,” *Brain, Behavior, and Immunity*, vol. 21, no. 4, pp. 384–392, 2007.
- [94] J. C. O’Connor, R. H. McCusker, K. Strle, R. W. Johnson, R. Dantzer, and K. W. Kelley, “Regulation of IGF-I function by proinflammatory cytokines: at the interface of immunology and endocrinology,” *Cellular Immunology*, vol. 252, no. 1–2, pp. 91–110, 2008.
- [95] E. Witkowska-Sedek and B. Pyrzak, “Chronic inflammation and the growth hormone/insulin-like growth factor-1 axis,” *Central European Journal of Immunology*, vol. 45, no. 4, pp. 469–475, 2020.
- [96] Francesca Cirillo, Pietro Lazzeroni, C. Sartori, and M. E. Street, “Inflammatory diseases and growth: effects on the GH-IGF axis and on growth plate,” *International Journal of Molecular Sciences*, vol. 18, no. 9, p. 1878, 2017.
- [97] D. Choukair, U. Hügel, A. Sander, L. Uhlmann, and B. Tönshoff, “Inhibition of IGF-I-related intracellular signaling pathways by proinflammatory cytokines in growth plate chondrocytes,” *Pediatric Research*, vol. 76, no. 3, pp. 245–251, 2014.
- [98] X. Yu, C. Xing, Y. Pan, H. Ma, J. Zhang, and W. Li, “IGF-1 alleviates ox-LDL-induced inflammation via reducing HMGB1 release in HAECs,” *Acta Biochimica et Biophysica Sinica Shanghai*, vol. 44, no. 9, pp. 746–751, 2012.
- [99] H. Zatorski, M. Marynowski, and J. Fichna, “Is insulin-like growth factor 1 (IGF-1) system an attractive target inflammatory bowel diseases? Benefits and limitation of potential therapy,” *Pharmacological Reports*, vol. 68, no. 4, pp. 809–815, 2016.
- [100] J. Guo, D. Zheng, W. F. Li, H. R. Li, A. D. Zhang, and Z. C. Li, “Insulin-like growth factor 1 treatment of MSCs attenuates inflammation and cardiac dysfunction following MI,” *Inflammation*, vol. 37, no. 6, pp. 2156–2163, 2014.

- [101] J. B. C. Carvalheira, H. G. Zecchin, and M. J. A. Saad, "Vias de Sinalização da Insulina," *Arquivos Brasileiros de Endocrinologia e Metabologia*, vol. 46, no. 4, pp. 419–425, 2002.
- [102] J. P. Barrett, A. M. Minogue, A. Falvey, and M. A. Lynch, "Involvement of IGF-1 and Akt in M1/M2 activation state in bone marrow-derived macrophages," *Experimental Cell Research*, vol. 335, no. 2, pp. 258–268, 2015.
- [103] H. Qi, J. Ji, N. Wanasen, and L. Soong, "Enhanced replication of *Leishmania amazonensis* amastigotes in gamma interferon-stimulated murine macrophages: implications for the pathogenesis of cutaneous leishmaniasis," *Infection and Immunity*, vol. 72, no. 2, pp. 988–995, 2004.
- [104] T. R. de Moura, F. O. Novais, F. Oliveira et al., "Toward a novel experimental model of infection to study American cutaneous leishmaniasis caused by *Leishmania braziliensis*," *Infection and Immunity*, vol. 73, no. 9, pp. 5827–5834, 2005.
- [105] C. Loeuillet, A. L. Banuls, and M. Hide, "Study of *Leishmania* pathogenesis in mice: experimental considerations," *Parasites & Vectors*, vol. 9, no. 1, p. 144, 2016.
- [106] O. E. Akilov, A. Khachemoune, and T. Hasan, "Clinical manifestations and classification of old world cutaneous leishmaniasis," *International Journal of Dermatology*, vol. 46, no. 2, pp. 132–142, 2007.
- [107] F. T. Silveira, R. Lainson, C. M. de Castro Gomes, M. D. Laurenti, and C. E. P. Corbett, "Immunopathogenic competences of *Leishmania* (V.) *braziliensis* and L. (L.) *amazonensis* in American cutaneous leishmaniasis," *Parasite Immunology*, vol. 31, no. 8, pp. 423–431, 2009.
- [108] B. Singh, S. Bhushan Chauhan, R. Kumar et al., "A molecular signature for CD8⁺ T cells from visceral leishmaniasis patients," *Parasite Immunology*, vol. 41, no. 11, article e12669, 2019.
- [109] F. A. Pinho, C. M. V. Vendrame, B. L. L. Maciel et al., "Association between insulin-like growth factor-I levels and the disease progression and anemia in visceral leishmaniasis," *The American Journal of Tropical Medicine and Hygiene*, vol. 100, no. 4, pp. 808–815, 2019.
- [110] F. A. Pinho, N. A. Magalhães, K. R. Silva et al., "Divergence between hepatic insulin-like growth factor (IGF)-I mRNA expression and IGF-I serum levels in *Leishmania* (Leishmania) infantum chagasi-infected dogs," *Veterinary Immunology and Immunopathology*, vol. 151, no. 1-2, pp. 163–167, 2013.
- [111] C. M. Gomes, D. Giannella-Neto, M. E. A. Gama, J. C. R. Pereira, M. B. Campos, and C. E. P. Corbett, "Correlation between the components of the insulin-like growth factor I system, nutritional status and visceral leishmaniasis," *Transactions of the Royal Society of Tropical Medicine and Hygiene*, vol. 101, no. 7, pp. 660–667, 2007.
- [112] J. Fan, D. Char, G. J. Bagby, M. C. Gelato, and C. H. Lang, "Regulation of insulin-like growth factor-I (IGF-I) and IGF-binding proteins by tumor necrosis factor," *The American Journal of Physiology*, vol. 269, 5 Part 2, pp. R1204–R1212, 1995.
- [113] W. Zumkeller, "The insulin-like growth factor system in hematopoietic cells," *Leukemia & Lymphoma*, vol. 43, no. 3, pp. 487–491, 2002.
- [114] M. A. Marini, G. C. Mannino, T. V. Fiorentino, F. Andreozzi, F. Perticone, and G. Sesti, "A polymorphism at IGF1 locus is associated with anemia," *Oncotarget*, vol. 8, no. 20, pp. 32398–32406, 2017.
- [115] O. Preham, F. A. Pinho, A. I. Pinto et al., "CD4(+) T cells alter the stromal microenvironment and repress medullary erythropoiesis in murine visceral Leishmaniasis," *Frontiers in Immunology*, vol. 9, p. 2958, 2018.
- [116] K. J. Gollob, A. G. Viana, and W. O. Dutra, "Immunoregulation in human American leishmaniasis: balancing pathology and protection," *Parasite Immunology*, vol. 36, no. 8, pp. 367–376, 2014.
- [117] M. G. Vieira, F. Oliveira, S. Arruda et al., "B-cell infiltration and frequency of cytokine producing cells differ between localized and disseminated human cutaneous leishmaniasis," *Memórias do Instituto Oswaldo Cruz*, vol. 97, no. 7, pp. 979–983, 2002.
- [118] V. S. Amato, H. F. de Andrade, and M. I. Duarte, "Mucosal leishmaniasis: in situ characterization of the host inflammatory response, before and after treatment," *Acta Tropica*, vol. 85, no. 1, pp. 39–49, 2003.
- [119] O. Bacellar, H. Lessa, A. Schriefer et al., "Up-regulation of Th1-type responses in mucosal leishmaniasis patients," *Infection and Immunity*, vol. 70, no. 12, pp. 6734–6740, 2002.
- [120] A. Giudice, C. Vendrame, C. Bezerra et al., "Macrophages participate in host protection and the disease pathology associated with *Leishmania braziliensis* infection," *BMC Infectious Diseases*, vol. 12, no. 1, p. 75, 2012.
- [121] T. M. Cardoso, Á. Machado, D. L. Costa et al., "Protective and pathological functions of CD8⁺ T cells in *Leishmania braziliensis* infection," *Infection and Immunity*, vol. 83, no. 3, pp. 898–906, 2015.
- [122] C. F. Amorim, F. O. Novais, B. T. Nguyen et al., "Variable gene expression and parasite load predict treatment outcome in cutaneous leishmaniasis," *Science Translational Medicine*, vol. 11, no. 519, article eaax4204, 2019.
- [123] G. Kratz, M. Lake, and M. Gidlund, "Insulin like growth factor-1 and -2 and their role in the re-epithelialisation of wounds; interactions with insulin like growth factor binding protein type 1," *Scandinavian Journal of Plastic and Reconstructive Surgery and Hand Surgery*, vol. 28, no. 2, pp. 107–112, 1994.
- [124] A. Tavakkol, J. Varani, J. T. Elder, and C. C. Zouboulis, "Maintenance of human skin in organ culture: role for insulin-like growth factor-1 receptor and epidermal growth factor receptor," *Archives of Dermatological Research*, vol. 291, no. 12, pp. 643–651, 1999.
- [125] L. L. Sharp, J. M. Jameson, G. Cauvi, and W. L. Havran, "Dendritic epidermal T cells regulate skin homeostasis through local production of insulin-like growth factor 1," *Nature Immunology*, vol. 6, no. 1, pp. 73–79, 2005.
- [126] P. N. Rocha, R. P. Almeida, O. Bacellar et al., "Down-regulation of Th1 type of response in early human American cutaneous leishmaniasis," *The Journal of Infectious Diseases*, vol. 180, no. 5, pp. 1731–1734, 1999.
- [127] A. Ribeiro-de-Jesus, R. P. Almeida, H. Lessa, O. Bacellar, and E. M. Carvalho, "Cytokine profile and pathology in human leishmaniasis," *Brazilian Journal of Medical and Biological Research*, vol. 31, no. 1, pp. 143–148, 1998.
- [128] C. de O Mendes-Aguiar, C. Lopes-Siqueira, F. Pettito-Assis et al., "Dual role of insulin-like growth factor (IGF)-I in American tegumentary leishmaniasis," *Journal of Immunology Research*, vol. 2021, Article ID 6657785, 7 pages, 2021.
- [129] F. Aydin, A. Kaya, L. Karapinar et al., "IGF-1 increases with hyperbaric oxygen therapy and promotes wound healing in

- diabetic foot ulcers,” *Journal Diabetes Research*, vol. 2013, article 567834, 6 pages, 2013.
- [130] R. A. Achar, T. C. Silva, E. Achar, R. B. Martines, and J. L. M. Machado, “Use of insulin-like growth factor in the healing of open wounds in diabetic and non-diabetic rats,” *Acta Cirúrgica Brasileira*, vol. 29, no. 2, pp. 125–131, 2014.
- [131] D. Leroith, H. Werner, D. Beitner-Johnson, and A. T. Roberts JR., “Molecular and cellular aspects of the insulin-like growth factor I receptor,” *Endocrine Reviews*, vol. 16, no. 2, pp. 143–163, 1995.
- [132] D. Sachdev and D. Yee, “Inhibitors of insulin-like growth factor signaling: a therapeutic approach for breast cancer,” *Journal of Mammary Gland Biology and Neoplasia*, vol. 11, no. 1, pp. 27–39, 2006.
- [133] D. R. Clemmons, “Modifying IGF1 activity: an approach to treat endocrine disorders, atherosclerosis and cancer,” *Nature Reviews. Drug Discovery*, vol. 6, no. 10, pp. 821–833, 2007.
- [134] G. K. Katara, A. Raj, R. Kumar et al., “Analysis of localized immune responses reveals presence of Th17 and Treg cells in cutaneous leishmaniasis due to *Leishmania tropica*,” *BMC Immunology*, vol. 14, no. 1, p. 52, 2013.
- [135] M. Huang, X. Huang, B. Jiang et al., “linc00174-EZH2-ZNF24/Runx1-VEGFA regulatory mechanism modulates post-burn wound healing,” *Molecular Therapy–Nucleic Acids*, vol. 21, pp. 824–836, 2020.
- [136] F. A. Costa, H. Goto, L. C. B. Saldanha et al., “Histopathologic patterns of nephropathy in naturally acquired canine visceral leishmaniasis,” *Veterinary Pathology*, vol. 40, no. 6, pp. 677–684, 2003.

Research Article

Improved Performance of ELISA and Immunochromatographic Tests Using a New Chimeric A2-Based Protein for Human Visceral Leishmaniasis Diagnosis

Maria Marta Figueiredo ^{1,2}, Anna R. R. dos Santos ³, Lara C. Godoi ^{1,3,4},
Natália S. de Castro ¹, Bruno C. de Andrade ¹, Sarah A. R. Sergio ¹,
Selma M. B. Jerônimo ⁵, Edward J. de Oliveira ⁶, Ruth T. Valencia-Portillo ⁷,
Lucilândia M. Bezerra ⁸, Hiro Goto ^{7,9}, Maria C. A. Sanchez ⁷, Caroline Junqueira ^{1,6},
Santuza M. R. Teixeira ^{1,10}, Flávio G. da Fonseca ^{1,11}, Ricardo T. Gazzinelli ^{1,6,10},
and Ana Paula Fernandes ^{1,12}

¹Centro de Tecnologia em Vacinas da Universidade Federal de Minas Gerais, Belo Horizonte, Minas Gerais, Brazil

²Universidade Estadual de Minas Gerais, Divinópolis, Minas Gerais, Brazil

³Detechta Biotecnologia S.A, Brazil

⁴Colégio Técnico da Universidade Federal de Minas Gerais, Belo Horizonte, Minas Gerais, Brazil

⁵Departamento de Bioquímica, Universidade Federal do Rio Grande do Norte, Natal, Brazil

⁶Instituto René Rachou, Fundação Oswaldo Cruz, Belo Horizonte, Minas Gerais, Brazil

⁷Instituto de Medicina Tropical da Faculdade de Medicina, Universidade de São Paulo, São Paulo, São Paulo, Brazil

⁸Departamento de Pós-Graduação em Ciência Animal, Universidade Federal de Goiás, Goiânia, Goiás, Brazil

⁹Departamento de Medicina Preventiva, Faculdade de Medicina, Universidade de São Paulo, São Paulo, São Paulo, Brazil

¹⁰Departamento de Bioquímica e Imunologia, Universidade Federal de Minas Gerais, Belo Horizonte, Minas Gerais, Brazil

¹¹Departamento de Microbiologia, Instituto de Ciências Biológicas (ICB/UFMG), Belo Horizonte, Minas Gerais, Brazil

¹²Departamento de Análises Clínicas e Toxicológicas, Faculdade de Farmácia, Universidade Federal de Minas Gerais, Belo Horizonte, Minas Gerais, Brazil

Correspondence should be addressed to Ana Paula Fernandes; apfernandes.ufmg@gmail.com

Received 12 January 2021; Revised 22 March 2021; Accepted 30 March 2021; Published 29 April 2021

Academic Editor: Gabriela Santos-Gomes

Copyright © 2021 Maria Marta Figueiredo et al. This is an open access article distributed under the Creative Commons Attribution License, which permits unrestricted use, distribution, and reproduction in any medium, provided the original work is properly cited.

Summary. Human visceral leishmaniasis (VL) is a major public health problem worldwide, leading to significant mortality rates if not properly treated and controlled. Precise identification of infected patients is essential to establish treatment and control measures. Although several VL serological diagnosis advances have been accomplished lately, mainly using recombinant antigens and immunochromatographic tests (ICTs), improvements may still be achieved using multiepitope chimeric proteins in different test platforms. Here, we reported on the evaluation of ELISA and an ICT developed with a new chimeric protein, named DTL-4, based on repetitive antigenic sequences, including those present in the A2 protein. **Methods.** A total of 1028 sera samples were used for the development and validation of ELISA (321 samples from *L. infantum*-infected patients, 62 samples from VL/AIDS coinfecting patients, 236 samples from patients infected with other diseases, and 409 samples from healthy donors). A total of 520 sera samples were used to develop and validate ICT (249 samples from *L. infantum*-infected patients, 46 samples from VL/AIDS coinfecting patients, 40 samples from patients infected with other diseases, and 185 samples from healthy donors). **Findings.** Using the validation sera panels, DTL-4-based ELISA displayed an overall sensitivity of 94.61% (95% CI: 89.94-97.28), a specificity of 99.41% (95% CI: 96.39-99.99), and an accuracy of 97.02% (95% CI: 94.61-98.38), while for ICT, sensitivity, specificity, and accuracy values corresponded to 91.98% (95% CI: 86.65-95.39), 100.00% (95% CI: 96.30-100.00), and 95.14% (95% CI: 91.62-97.15), respectively. When testing sera samples from VL/AIDS coinfecting patients, DTL-4-ELISA

displayed a sensitivity of 77.42% (95% CI: 65.48-86.16), a specificity of 99.41% (95% CI: 96.39-99.99), and an accuracy of 93.51% (95% CI: 89.49%-96.10%), while for DTL-4-ICT, sensitivity was 73.91% (95% CI: 59.74-84.40), specificity was 90.63% (95% CI: 81.02-95.63), and accuracy was 82.00% (95% CI: 73.63-90.91). **Conclusion.** DTL-4 is a promising candidate antigen for serodiagnosis of VL patients, including those with VL/AIDS coinfection, when incorporated into ELISA or ICT test formats.

1. Introduction

Human visceral leishmaniasis (VL) is one of the world's most neglected diseases, largely affecting low-socioeconomic-level individuals, mainly in developing countries [1, 2, 3]. When not treated, VL is fatal in 90%-100% of cases [4, 5]. According to the World Health Organization (WHO) estimates, 50,000 to 90,000 new VL cases occur each year worldwide [6]. The zoonotic VL caused by *Leishmania (Leishmania) infantum* occurs in Mediterranean countries (North Africa and Europe); Southeast Europe; Middle East; Central Asia; and North, Central, and South America (Mexico, Venezuela, Brazil, and Bolivia) [7]. The zoonotic VL transmission areas have expanded lately due to the migration of people from rural to urban areas [8]. In 2018, more than 95% of new VL cases occurred in Brazil and nine countries of Asia and Africa [6], and 90% of VL cases in America occurred in Brazil [4].

Progress towards noninvasive, easy-to-perform, and highly accurate diagnosis of leishmaniasis depends on discovering suitable biomarkers and their use in sensitive, specific, and amenable diagnostic platforms to both laboratory and field conditions. Anti-*Leishmania* antibodies' detection is an important diagnostic alternative and may be achieved using several different test platforms. The most used serological methods are enzyme-linked immunosorbent assay (ELISA) and immunochromatographic tests [9–12]. Nevertheless, on serological assays, the diagnosis of cases with low or undetectable anti-*Leishmania* antibodies is a drawback and causes a drop in the test sensitivity. Another limitation of serological tests is cross-reactivity with other pathogens, which decreases the specificity. The low positive and negative predictive values resulting from these deficiencies generate uncertainties in the diagnostic accuracy [13].

To overcome the limitations in serological diagnosis, several groups have proposed the use of recombinant antigens comprising mapped and repetitive epitopes that can improve specificity and sensitivity of antibody detection [9, 11, 14–18]. In agreement, incorporating the recombinant rK39 or K28 antigens on immunochromatography platforms for VL serological diagnosis (rapid tests) represented a significant improvement since besides being faster and easier to perform, rapid tests with recombinant antigens are more accurate compared with assays based on total antigens [19, 20].

The recombinant protein A2 has also emerged as a promising antigen for VL serodiagnosis, which could be, in part, attributed to the repetitive structure of B cell epitopes present in A2 [9, 21–24]. Based on these previous studies, we designed a new chimeric protein containing part of the repetitive epitopes from A2 and other repetitive proteins expressed only by the visceralizing species of *Leishmania*, named DTL-4. Here, we report this chimeric recombinant antigen's performance in ELISA and immunochromatographic tests, using samples of patients from Brazilian

endemic areas presenting confirmed clinical and laboratory diagnosis of VL. The results show that DTL-4, regardless of the diagnostic platform used, is a reliable and efficient antigen capable of detecting human VL cases with improved accuracy.

2. Methods

2.1. Study Design. The performance of the DTL-4 chimeric protein was evaluated for the development of kits for serological diagnosis, ELISA, and immunochromatographic tests (ICTs). According to good clinical practice principles, the study was approved by local authorities and was carried out between 2016 and 2019.

2.2. Ethics Statement. This study complied with Ethical Principles in Human Research and resolutions CNS 466 of 12/12/2012 and CNS 441 of 05/12/2011 and was approved by the Research Ethics Committee/UFGM (CAAE: 67820516.8.1001.5149). The samples collected in Aracaju (Sergipe State), Bauru (São Paulo State), Campo Grande (Mato Grosso do Sul State), and Natal (Rio Grande do Norte State) are part of Research Protocol no. 490/11. The samples from Palmas (Tocantins State) and Belo Horizonte (Minas Gerais State) were approved for this project (CAAE: 67820516.8.1001.5149). The samples from São Paulo (São Paulo State) are part of Protocol no. 529.638 of 01/22/2014. Samples from patients with HIV/*Leishmania* coinfection, collected in Campo Grande (Mato Grosso do Sul State) and Rio de Janeiro (Rio de Janeiro State), are part of Research Protocol no. 1021/09. Samples from patients with other infectious diseases are part of Research Protocol no. 339/08.

2.3. Patients and Healthy Donors. The healthy donors included in the study did not display any symptoms suggestive of leishmaniasis when the blood samples were collected. Also, they showed no suggestive signs of any other infectious disease. VL patients consisted of women and men over 18 years old. All *L. infantum*-infected patients presented clinical symptoms of VL. Controls with possible cross-reactivity consisted of patients with a confirmed diagnosis of other diseases (Figure 1). Patients coinfecting with *Leishmania*/HIV were also studied. These samples were obtained at several centers and were characterized at each center using routine diagnostic methods.

Initially, to develop ELISA and ICT using DTL-4, sera samples (Figure 1) were obtained at the Central Public Health Laboratory (CPHL) in Palmas (Tocantins State), CPHL in Natal (Rio Grande do Norte State), and UFGM in Belo Horizonte (Center for Vaccine Technology (CT-Vacinas) from Universidade Federal de Minas Gerais (Belo Horizonte, Minas Gerais State) and Fundação Oswaldo Cruz (Centro de Pesquisas René Rachou, Belo Horizonte, Minas Gerais State)). A total of 154 samples of patients with a

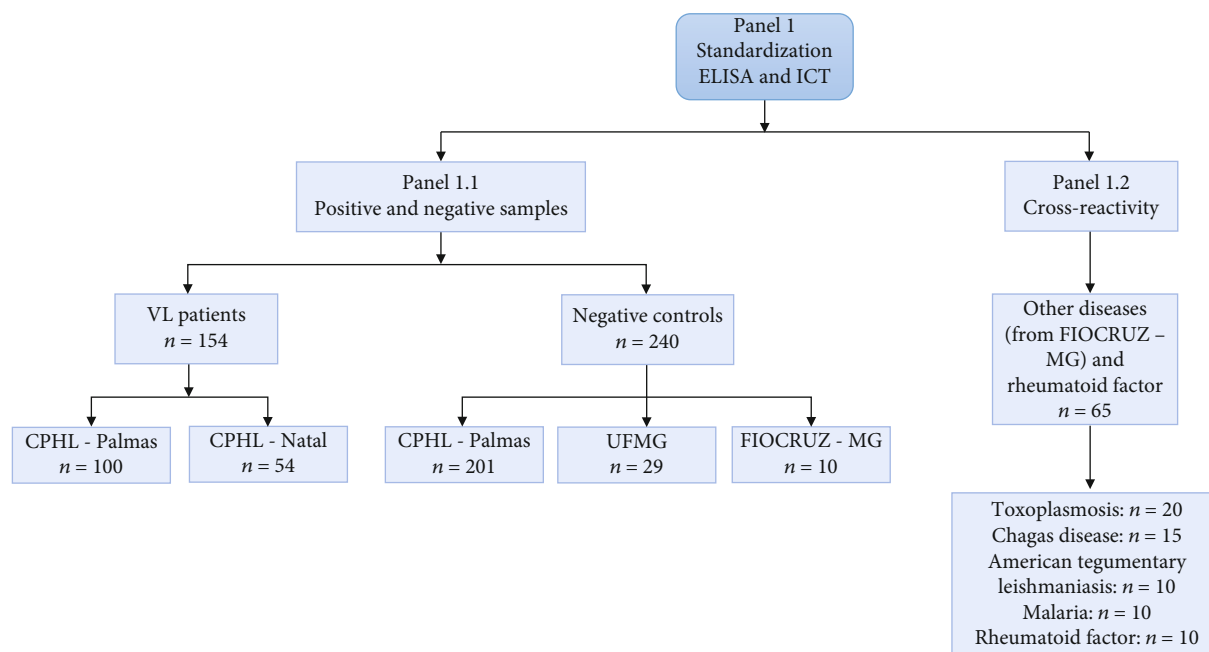


FIGURE 1: Sera samples used to standardize ELISA and ICT and the origin of the samples (panel 1.1 and panel 1.2). *n*: number of samples; VL: visceral leishmaniasis; CPHL-Palmas: Central Public Health Laboratory of Palmas (Tocantins State); CPHL-Natal: Central Public Health Laboratory of Natal (Rio Grande do Norte State); UFMG: Universidade Federal de Minas Gerais of Belo Horizonte (Minas Gerais State); FIOCRUZ, MG: René Rachou Institute (FIOCRUZ, Minas Gerais State).

confirmed VL diagnosis by either direct parasite microscopic or molecular detection, whose characteristics are described in the flowchart presented in Figure 1, were employed. Samples from patients from CPHL-Palmas were submitted to an indirect immunofluorescence (IFI) assay with *Leishmania* promastigotes, and samples from CPHL-Natal were assayed with both a house soluble leishmania promastigote antigen and rK39-based ELISA (Figure 1, panel 1.1). Negative sera samples from 240 healthy controls, with no symptoms of VL, also composed panel 1. To investigate cross-reactivity, 55 sera samples from subjects with a previously confirmed diagnosis of other parasitic diseases (toxoplasmosis, *n* = 20; Chagas' Disease, *n* = 15; American tegumentary leishmaniasis, *n* = 10, and malaria, *n* = 10) and rheumatoid factor (*n* = 10) were used (Figure 1, panel 1.2).

All positive and negative samples were further tested by in-house ELISA with a total extract of *L. infantum* (ELISA_{EXT}) performed at René Rachou Institute (FIOCRUZ, Minas Gerais), and with ELISA recombinant protein (rK39 Rekom Biotech®) provided by BioClin Quibasa Ltda. (Belo Horizonte, Minas Gerais), and the commercial immunochromatographic test IT-LEISH® (Bio-Rad Laboratories, Inc.), performed at the CT-Vacinas.

After the establishment of the conditions for the best performance of DTL-4-ELISA and ICT, the tests were submitted to external validation at the Instituto de Medicina Tropical da Faculdade de Medicina, Universidade de São Paulo (IMT-FMUSP), São Paulo State, Brazil, with another sample panel (Figure 2, panel 2) with 569 samples. Panel 2.1 included sera from 167 *L. infantum*-infected patients from distinct localities in Brazil (Aracaju, Sergipe State; Piauí State; Bauru, São Paulo State; Campo Grande, Mato Grosso do Sul State;

and Natal, Rio Grande do Norte State), and sera of 169 healthy individuals, living in an endemic area and negative by DAT (Aracaju, Sergipe State; Bauru, São Paulo State; Campo Grande, Mato Grosso do Sul State; Natal, Rio Grande do Norte State). The levels of DTL-4 antibodies were also assessed in a panel of sera from 62 patients previously diagnosed with VL/AIDS coinfection (Bauru, São Paulo State; Campo Grande, Mato Grosso do Sul State; Natal, Rio Grande do Norte State; Rio de Janeiro, Rio de Janeiro State; and São Paulo, São Paulo State). The *L. infantum* infection was diagnosed using the microscopic examination of the lymph node or bone marrow aspirate for *Leishmania* detection [25] and by direct agglutination test (DAT) [26]. The confirmation of HIV infection was made according to the Ministry of Health of Brazil [27].

To assess the interference of antibodies against other diseases with DTL-4-ELISA and ICT, 167 positive samples (Figure 2, panel 2.1) and 311 negative samples for VL (140 samples from panel 2.1 and 171 samples from panel 2.2—see Figure 2) were submitted to the interference test. Panel 2.2 was composed of seven positive samples for tegumentary leishmaniasis, 63 samples positive for Chagas disease (*Trypanosoma cruzi*), 12 positive samples for malaria (*Plasmodium vivax/Plasmodium falciparum*), 20 samples positive for toxoplasmosis (*Toxoplasma gondii*), 10 samples positive for tuberculosis, 20 samples positive for syphilis, ten samples positive for lupus erythematosus, 20 samples positive for paracoccidioidomycosis, and nine samples with increased levels of rheumatoid factor.

2.4. Cloning, Expression, and Purification of Recombinant DTL-4 Protein. The DTL-4 gene synthesized and cloned into

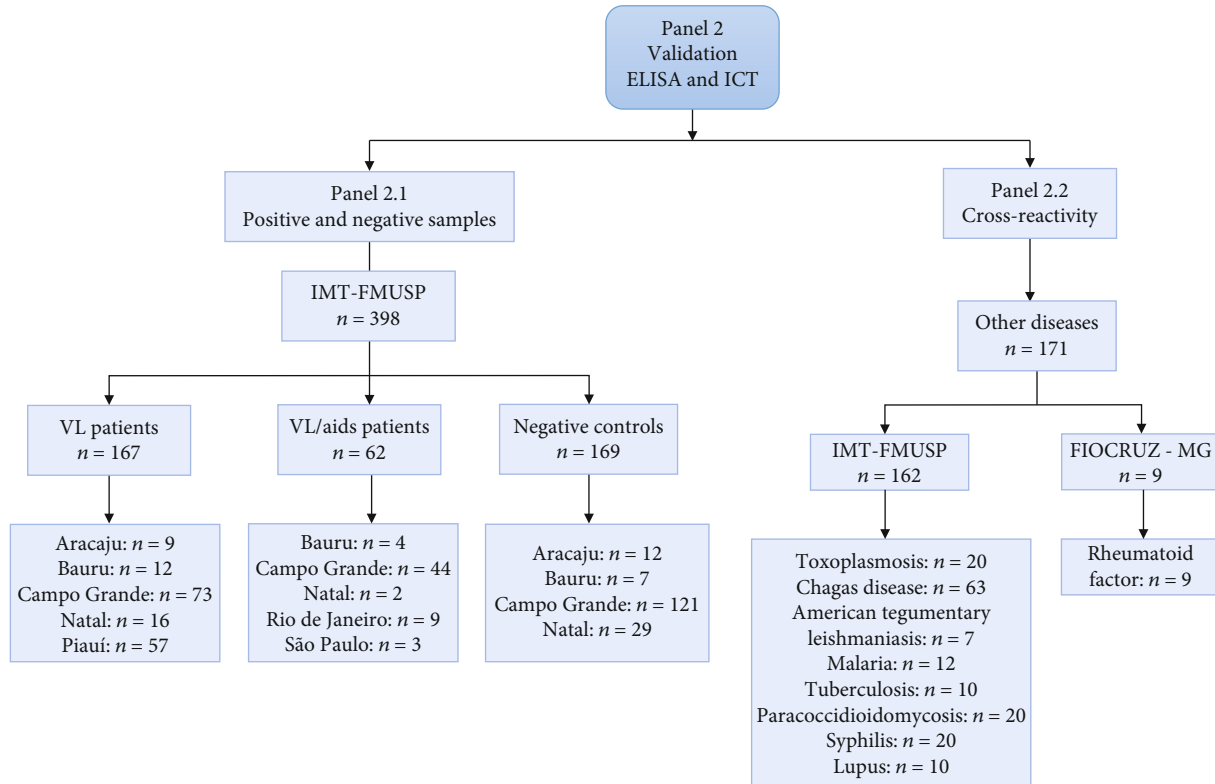


FIGURE 2: Sera samples used to validate the ELISA and ICT kits and the origin of the samples (panel 2.1 and panel 2.2). *n*: number of samples; VL: visceral leishmaniasis; VL/AIDS: coinfecting patients; FIOCRUZ-MG: René Rachou Institute (FIOCRUZ, Minas Gerais State); IMT-FMUSP: Instituto de Medicina Tropical da Faculdade de Medicina, Universidade de São Paulo (São Paulo State). Aracaju, Bauru, Campo Grande, Natal, Rio de Janeiro, São Paulo are Brazilian cities; Piauí is a Brazilian state.

the *E. coli* expression vector pET24a was purchased from GenScript (Piscataway, NJ, EUA). *E. coli* BL21 (DE3) cells transformed with pET24a/DTL-4 were grown at 37°C in 2 L of Luria-Bertani's medium (LB) with 50 µg/mL kanamycin until the optical density of 600 nm reached 0.6 before adding isopropyl beta-D-thiogalactopyranoside (IPTG). After 3 hours of incubation, the cells were harvested by centrifugation, and the bacterial cell pellet was resuspended in a solution containing 20 mM Tris-HCl (pH 8), 100 mM NaCl, 5 mM dithiothreitol (DTT), 5 mM benzamidine, and 1 mM phenylmethylsulfonyl fluoride (PMSF) and lysed in a homogenizer. Aliquots of total cell extracts were collected and analyzed by 12% sodium dodecyl sulfate-polyacrylamide gel electrophoresis (12% SDS-PAGE). The his-tagged protein was purified using the AKTA Prime Plus System (GE Healthcare). The suspension was loaded onto a Ni²⁺-charged chelating Sepharose HisTrap HP (GE Healthcare). Contaminants were washed away with a solution containing 20 mM Tris-HCl (pH 8) and 100 mM NaCl. The recombinant protein was then eluted with a solution containing 20 mM Tris-HCl (pH 8), 100 mM NaCl, and increasing amounts of imidazole, starting from 0 to 500 mM. Purified protein samples were analyzed by 12% SDS-PAGE. The protein was extensively dialyzed against 20 mM Tris-HCl (pH 8), 100 mM NaCl, and 10% glycerol at 4°C and frozen. Further detailing of the protein and its amino acid sequence will not be revealed due to pending patent issues. Table 1

TABLE 1: Physicochemical evaluation of the DTL-4 protein.

Parameters	Results
Number of amino acids	403
Estimated molecular weight (kDa)	40501.09
Theoretical isoelectric point	4.85

describes some characteristics of the recombinant DTL-4 protein.

The A2 recombinant protein (rA2) was produced as previously described [28]. The rK39 protein was purchased at Rekom Biotech® (Spain) and kindly provided by BioClin Quibasa Ltda. (Brazil).

2.5. DTL-4-ELISA. The presence of anti-DTL-4 IgG antibodies in plasma and serum was evaluated by the indirect ELISA method (enzyme-linked immunosorbent assay), using the purified recombinant DTL-4 antigen. ELISA plates (Costar®) were coated with 0.2 µg/well of recombinant protein diluted in carbonate-bicarbonate buffer (pH 9.6) (100 µL/well). The plates were incubated at 4°C for 18 hours and blocked with 1% BSA (280 µL/well) at 25°C for 2 hours. Plasma or serum samples were added to each well at a final dilution of 1:100. The antibody-antigen binding was detected by the addition of peroxidase-conjugated goat anti-human IgG FAPON® (1:100,000). The presence of bound IgG was detected using tetramethylbenzidine (MOSS), and the

reaction stopped by the addition of 0.5 M H₂SO₄. The optical density (OD) was measured at 450 nm using a Multiskan GO microplate spectrophotometer (Thermo Fisher Scientific). The results were expressed as optical density (OD). The cut-off points were set at three standard deviations above the mean optical density read at 450 nm. RI values > 1.1 were considered positive [9].

Initially, a titration was performed to determine the best amount of protein and serum dilution to be applied in individual serum evaluations by ELISA, using pools of samples with ten VL-positive sera and ten negative sera. We also compared the antibody levels against rA2, rK39, and rDTL-4 with the same sample pools, using in-house ELISA, since DTL-4 contains A2 epitopes, while rK39 is widely used as a recombinant antigen in several commercial tests. Next, we evaluated DTL-4-ELISA using 459 samples (positive and negatives samples from Figure 1, panel 1).

2.6. Repeatability, Reproducibility, Homogeneity, and Stability of DTL-4-ELISA. The DTL-4-ELISA intra-assay repeatability was determined using one positive and one negative sample in eight determinations to establish the coefficient of variation (% CV is equal to the standard deviation divided by the mean multiplied by 100) among measurements, within the same plate. A second test was performed to evaluate the test reproducibility, determining the inter-assay CV. To determine that, three samples were evaluated in three consecutive days, in eight measurements. A third test was carried out to evaluate the solid phase's homogeneity, applying the same samples in different plate wells. A fourth test was carried out to assess the reagents' stability in the solid phase, and each test solution, separately, at 37°C [29], to predict the shelf life of the kits stored under appropriate conditions. The cut-off was determined using one hundred samples from healthy donors from panel 1.1, and the cut-off points were defined as the mean plus three standard deviations.

2.7. Immunochromatographic Test (ICT). A lateral flow-based doubled antigen immunochromatographic test (ICT) for antibody detection was assembled using the DTL-4 protein. The purified DTL-4 antigen was dispensed as the test line (T), and the *Staphylococcus aureus* protein A was dispensed as the control line (C), both in the detection zone of the nitrocellulose membrane. Protein A labeled with a signal generator colloidal gold was used to detect the samples' antibodies as a control test line. For conjugation, either the DTL-4 protein or protein A were mixed with colloidal gold (Sigma-Aldrich) and incubated at room temperature. To detect specific antibodies, we immobilized the DTL-4 protein onto the nitrocellulose membrane. The conjugate was adsorbed to the glass fiber and dried in a low humidity room. When in contact with sera, plasma, or peripheral blood containing anti-*L. infantum* antibodies, these first reacted with the colloidal gold conjugates on the conjugation pad. As the colloidal gold complex flows through the capture site, antibodies reacted with the antigens at the test line site, leading to the formation of a visible colored line. In the absence of specific antibodies (negative samples), no reactivity is

observed at this site (Figure 3). The test was considered valid only if the control line could be clearly seen. Several tests were carried out to define the membranes' best control and test lines' location, type of plastic support, size of gold particles, sample volume, and buffer for lateral flow.

The sensitivity, specificity, and accuracy of the developed ICT test were evaluated against 520 samples, composed of 185 samples from healthy donors, from panels 1 and 2 (Figure 1 and 2) and 249 samples from *L. infantum*-infected patients from the Central Public Health Laboratory of Palmas (87 samples from panel 1.1—see Figure 1) and Instituto de Medicina Tropical of São Paulo (162 samples from panel 2.1—see Figure 2), and 46 samples from VL / AIDS coinfecting patients (panel 2.1—see Figure 2). Cross-reactivity was evaluated with ten samples of each disease (Chagas disease, American tegumentary leishmaniasis, and malaria) and of rheumatoid factor (40 samples from panel 1.2—see Figure 1). The strip stability after the unpacking was assessed by holding the cassettes at room temperature for two hours and testing them with positive and negative samples. The accelerated aging stability was assessed, keeping the strips at 37°C for 7, 14, 21, and 28 days and testing them on days 0, 7, 14, 21, and 28 days before the test.

2.8. Statistical Analysis. The results were analyzed using GraphPad Prism (version 7.0 for Windows). The lower limits of positivity (cut-off) for DTL-4-ELISA were established for optimal sensitivity, specificity, and accuracy using ROC (receiver operating characteristic) analysis. The D'Agostino-Pearson normality test, the Shapiro-Wilk normality test, and the Kolmogorov-Smirnov normality test were used to determine whether a variable was normally distributed. The Mann-Whitney test and ANOVA were also used, and significant differences were considered when $p < 0.05$. The diagnostic capacity of DTL-4 was measured by assessing its sensitivity, specificity, and accuracy with 95% confidence intervals (CI). Kappa index was calculated according to Cohen [30] and interpreted according to Landis and Koch [31] to assess the agreement between ELISA and ICT with the serological reference methods: 1.00–0.81 = excellent; 0.80–0.61 = good; 0.60–0.41 = moderate; 0.40–0.21 = weak; and 0.20–0.00 = negligible agreement. McNemar's test was used to estimate the statistical differences between ELISA and ICT. The significance of the difference between proportions was tested using the chi-square with Yate's correction test. In all tests, a significance level of 0.05 was considered.

3. Results

3.1. High Levels of Expression and Purification of DTL-4 from *Escherichia coli* Soluble Fraction. The recombinant DTL-4 protein was expressed in *E. coli* BL21 (DE3) and purified from the soluble fraction on a Ni²⁺-charged Sepharose column using single-step chromatography. As shown in Figure 4, the protein migrated in SDS-PAGE as a single band with an apparent molecular weight of 40 kDa, as expected according to bioinformatic projections.

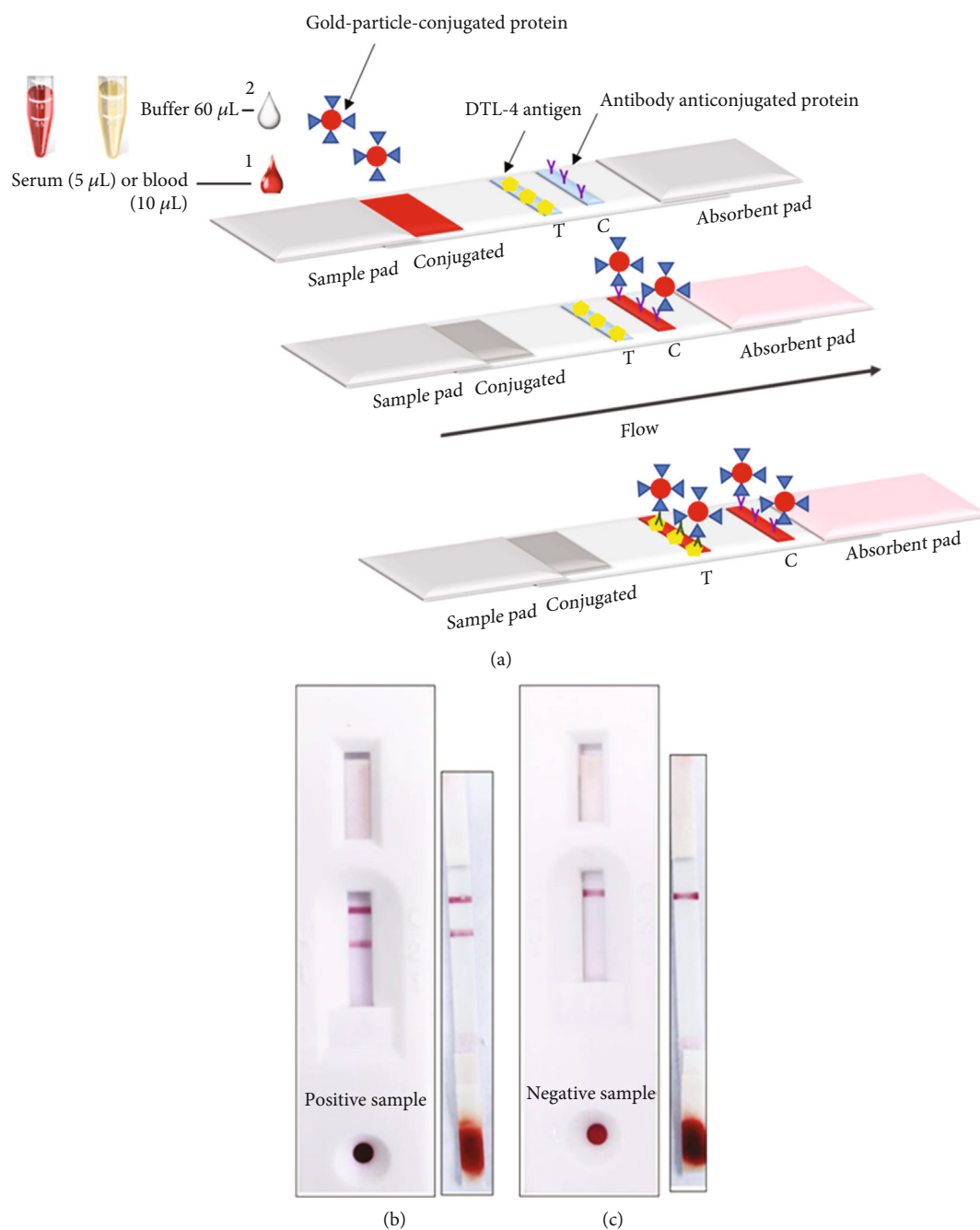


FIGURE 3: Representation of the ICT to detect IgG anti-*Leishmania* antibody. (a) The rapid test scheme developed for the detection of IgG anti-*L. infantum*. (b) Positive sample and (c) negative sample.

3.2. *The DTL-4 Protein-Based ELISA Has High Accuracy for the Diagnosis of Human VL.* The protein concentration to coat the ELISA plates was determined by a titration curve performed with pools containing ten positive and ten negative VL serum samples (Figure 5(a)). Moreover, since DTL-4 contains A2 epitopes and rK39 is the most widely used recombinant antigen for VL serodiagnosis, we have compared the antibody titers in the same sample pools against rA2, rK39, and DTL-4, using an ELISA made in-house. As shown in Figure 5(a), DTL-4 discriminates with high-precision positive and negative VL pools of sera, even

when small amounts of protein were used to coat the ELISA plates. The DTL-4 concentration of 0.1 $\mu\text{g}/\text{mL}$ (10 ng/well) was then selected to coat the ELISA plates for further analyses.

A serum titration curve was also performed with the same pools of sera (Figure 5(b)). As seen in Figure 5(b), positive sera's reactivity with DTL-4 remains high, even at 1:1280 sera dilutions, while antibody titers against rA2 or rK39 dropped significantly after 1:80 or 1:320, respectively. The serum dilution of 1:100 was selected for the DTL-4-ELISA.

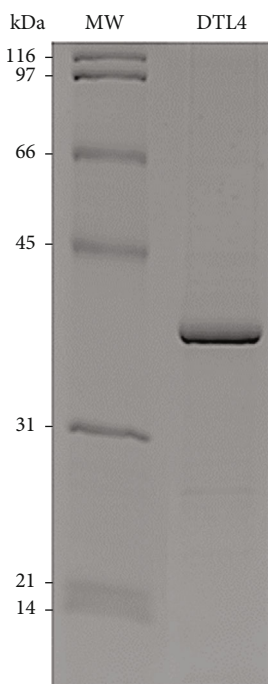


FIGURE 4: Dodecyl sulfate-polyacrylamide gel electrophoresis analysis of recombinant protein DTL-4. DTL-4 (~40 kDa) was purified in nickel affinity chromatography and submitted to SDS-PAGE analysis. Molecular weight markers are shown on the left.

3.3. The DTL-4 Protein-Based ELISA Is Highly Sensitive for Serological Diagnosis of VL and Did Not Present Cross-Reactivity with Antibodies Present in Sera of Patients with Other Diseases. After determining the protein concentration and sera dilution to be used for best performance, DTL-4-ELISA was tested against 228 individual samples (128 positive and 100 negative) from sera panel 1.1 (Figure 1). In this assay, eleven samples out of the 128 positive ones did not react with DTL-4, corresponding to a sensitivity of 91.27% (95% CI: 84.92–95.56%), while eight samples among the negative ones reacted with DTL-4, leading to a specificity value of 92.00% (95% CI: 84.84%–96.48%) (Figure 6). This result indicated that DTL-4 efficiently discriminates negative and from positive samples ($p < 0.0001$; Mann–Whitney test).

Because it has been described that sensitivity may vary depending on the test used for the previous diagnosis and origin of the samples assayed, we tested the DTL-4-ELISA considering these parameters. Accordingly, when using ELISA rK39 as reference (51 samples from the State of Rio Grande do Norte, an endemic area for VL), the sensitivity was 93.90%. When the reference diagnostic test was the IT-LEISH® rapid test (150 samples from the State of Tocantins, endemic for VL), the sensitivity was 90.00%. When using the reference ELISA with *L. infantum* total extract (272 samples from the State of Tocantins, endemic for VL), the sensitivity was 83.30% (Table 2).

Several conditions may lead to antibodies that cross-react in serological tests for VL, including other parasitic infections, whose transmission areas overlap with VL areas in Brazil. Thus, we tested the DTL-4 protein-based ELISA for

specificity using sera of patients diagnosed with inflammatory disorders (lupus and rheumatoid factor) and other infectious diseases. As shown in Figure 7, there is no significant reactivity of the DTL-4 protein-based DTL-4-ELISA with sera of the selected inflammatory diseases. No significant reactivity was also detected by testing sera of patients diagnosed with syphilis, tuberculosis, paracoccidiodomycosis, or other parasitic diseases, including tegumentary leishmaniasis, Chagas' disease, malaria, and toxoplasmosis (panel 2.2, Figure 2), which are also highly prevalent in Brazil.

3.4. The DTL-4 Protein-Based ELISA Fulfills the Requirements for a Prototype of a Commercial Kit. To test the stability, repeatability, reproducibility, and homogeneity of DTL-4-ELISA, we used the biological samples from panel 1, described in Figure 1. After performing eight readings of two samples under the same conditions, they presented an average intra-assay coefficient of variation (CV %) of 3.8% and 4.6%, with the positive and negative samples, respectively. The test's reproducibility, evaluated by assaying three samples (one positive and two negative) for three consecutive days, presented a CV% of 0.6% with the positive sample and 7.1% and 8.0% with the negative ones. ELISA stability was assessed by accelerated aging at 37°C for 28 days, which corresponds to stability for 18 months if maintained under refrigeration (4 to 8°C).

3.5. External Validation of the DTL-4-ELISA for the Diagnosis of Human Visceral Leishmaniasis. To further validate the sensitivity and specificity of the DTL-4-ELISA prototype, additional sera, including a very well-characterized sera panel (panel 2, Figure 2), were used, including the samples with previous results of DAT and parasitological tests and samples from different geographical localities in Brazil. As shown in Table 3, high overall values for sensitivity (94.61%; 95% CI: 89.94%–97.38%), specificity (99.41%; 95% CI: 96.39%–99.99%), and accuracy (97.02%; 95% CI: 94.61%–98.38%) were obtained.

We also compared anti-DTL-4 IgG in sera from patients with VL with those from patients coinfecting with VL/AIDS (samples from panel 2.1, Figure 2). The evaluation of IgG anti-DTL-4 showed that the median absorbance of sera of patients previously diagnosed with VL/AIDS coinfection (median = 1.050) is lower than that of VL patients not coinfecting (median = 3.430) (Mann–Whitney test, $p < 0.0001$) (Figure 8). The sensitivity of DTL-4-ELISA in 62 VL +/AIDS+ patients was 77.42% (95% CI: 65.48%–86.16%), while in 167 patients with VL, as detected by the parasitological method, but without HIV (VL+/AIDS), the sensitivity was 94.61% (95% CI: 89.94%–97.28%) (Fisher's exact test, $p < 0.0001$). Considering the results obtained in healthy donors, the accuracy of the DTL-4-ELISA in 62 VL +/AIDS+ patients was 93.51% (89.49%–96.10%).

We also evaluated the performance of the DTL-4-ELISA detection of VL in sera samples of VL and VL/AIDS patients from different localities in Brazil, according to the patients' origin (Table 4). DTL-4-ELISA displayed high sensitivity to detect VL infection in patients either from Campo Grande (97.26%) or Bauru (100.00%) localities. Overall sensitivity

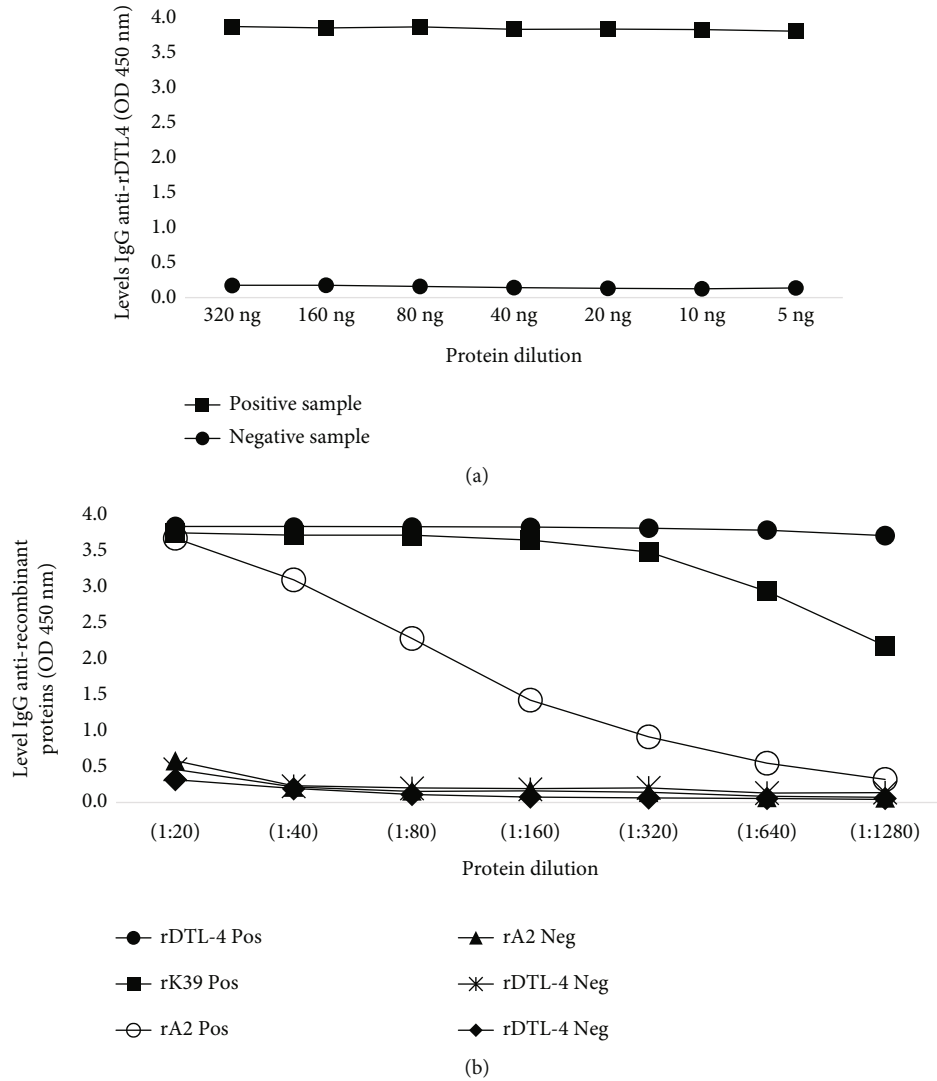


FIGURE 5: Titration curves for the determination of protein concentration and sera dilutions for DTL-4-ELISA. Pools of ten VL-positive and ten negative sera were assayed. (a) Titration of DTL-4 concentration by adding successive decreasing amounts of protein to wells on ELISA plates. (b) Titration of anti-DTL-4, anti-A2, and anti-K39 antibodies in pools of sera, using 10 ng of each protein per well.

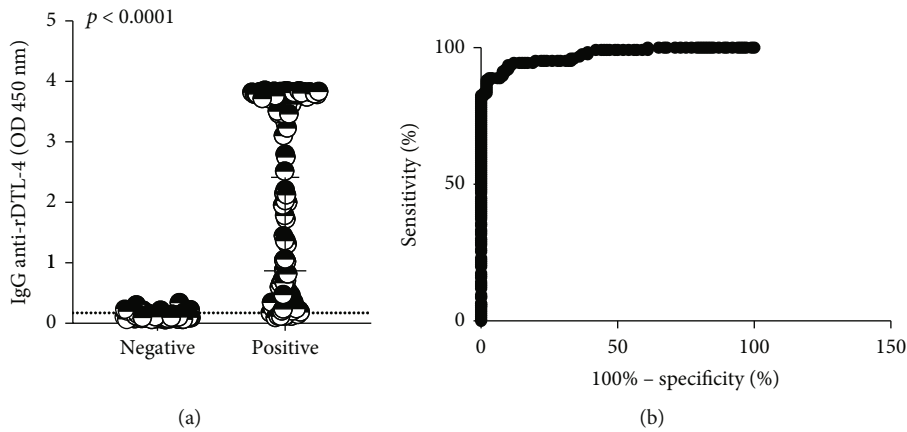


FIGURE 6: ELISA was performed to detect anti-DTL-4 IgG antibodies of sera. Sera from patients previously diagnosed with visceral leishmaniasis and healthy donors (panel 1.1). (a) DTL-4 discriminates significantly negative and positive samples ($p < 0.0001$; Mann-Whitney test). (b) ROC curve constructed from the absorbance values calculated for the 126 samples from patients with confirmed VL and 100 samples from healthy controls from the endemic area. Cut - off = 0.173. Area under the curve = 0.9727.

TABLE 2: Performance of DTL-4-ELISA in the diagnosis of VL according to the reference diagnostic test, like rK39-ELISA, IT-LEISH® rapid test, and *L. infantum*-ELISA (total extract).

	DTL-4-ELISA	
	Sensitivity% (<i>n</i>)	Specificity% (<i>n</i>)
rK39-ELISA	93.90 (51)	90.40 (100)
IT-LEISH® rapid test	90.00 (150)	94.00 (100)
<i>L. infantum</i> -ELISA	83.30 (272)	95.30 (100)

corresponded to 97.65% ($n = 85$). The test was also able to discriminate a significant proportion of VL/AIDS coinfecting patients, either from Campo Grande (81.82%) or Bauru (100.00%). Considering both localities, overall sensitivity among VL/AIDS coinfecting patients was 83.33% ($n = 48$). However, it should be noted that the number of VL/AIDS coinfecting patients' sera from Bauru City was low, which may have impacted the sensitivity values observed.

3.6. Evaluation of the Performance of DTL-4 on Immunochromatographic Tests (ICT) for Human VL. Based on the performance of the DTL-4-ELISA developed, we tested the DTL-4 protein on an ICT test to detect antibodies in serum, peripheral blood, or plasma samples (Figures 9(a) and 9(c)). The ideal sample volume was 5 μ L of serum or plasma and 10 μ L of blood, both with reading times between 10 and 15 minutes. The ICT's test stability was assessed by accelerated aging at 37°C for 28 days, corresponding to stability for 18 months, under adequate storage conditions.

As an initial evaluation, the ICT was tested against sera from panel 1 (Figure 1). The results were considered positive only if the test and control lines' reactivities were observed and negative only if the control line's reactivity was observed, indicating the absence of specific antibodies (Figure 9(a)). The sensitivity, specificity, and accuracy values obtained with sera panel 1 were 91.95% (84.12 - 96.70), 97.65% (91.76 - 99.71), and 94.80% (95% CI: 90.21 - 99.65), respectively (Table 5).

Then, the ICT was tested against sera samples from validation panel 2 (Figure 2). The sensitivity, specificity, and accuracy values obtained with this panel were 91.98 (95% CI: 86.65 - 95.39%), 100% (95% CI: 96.30 - 100.00), and 95.14% (95%CI: 91.62 - 97.15), respectively (Table 5).

The results of DTL-4-ICT were then compared with the results of DTL-4-ELISA. Among the 154 samples positive by ELISA (HVL), nine samples were negative by DTL-4-ICT, while all the 100 samples negative by DTL-4-ELISA were also negative by DTL-4-ICT. Thus, the tests presented excellent agreement, with $k = 0.898$. The McNemar test results indicated no statistically significant difference between the methods ($p = 0.2673$).

On the other hand, when samples from coinfecting VL/AIDS patients (all positive in VL-ELISA) were tested ($n = 46$), the sensitivity of DTL-4-ICT was lower (73.91%) as compared to DTL-4-ELISA 77.42%. A good concordance of $k = 0.657$ was observed between ELISA and ICT sensitivity (Table 5).

The evaluation of the interference of antibodies against other diseases (Chagas' disease, tegumentary leishmaniasis, malaria, and rheumatoid factor) that potentially would cross-react with DTL-4-ICT showed no cross-reactivity with antibodies raised against these other diseases (Figure 9). When sera samples of VL patients spiked with peripheral blood were tested ($n = 67$), the sensitivity determined for the ICT was 90% and the specificity was 100%. An illustration of the reactivity of a sera sample spiked with blood is seen in Figure 9(c).

4. Discussion

This study is aimed at evaluating a new chimeric recombinant protein, named DTL-4, as a potential antigen for accurate serological diagnosis of VL. DTL-4 contains epitopes from A2 and other proteins expressed by visceralizing species of *Leishmania*, which have been identified in previous immunoproteomic studies [21, 32, 33]. A2 has been consistently shown to discriminate symptomatic and asymptomatic VL individuals, either among human or dog populations [9, 16, 21, 34]. As shown for other antigens such as the *Leishmania* kinesins, the repetitive amino acid structure may amplify antibody detection, improving diagnosis sensitivity [22, 35]. On the other hand, the fact that A2 is present only in visceralizing *Leishmania* species also improves diagnosis specificity [23]. Besides its antigenic properties, DTL-4 is a recombinant antigen that is easily purified as a soluble protein and displays a low isoelectric point and significant amounts of positive and negative amino acids, which are highly desirable aspects for antibody reactivity and scaling up production, enabling cheaper and faster production in industrial settings and its further assembling of diagnostic tests in different formats.

By using well-characterized sera panels, the DTL-4-based ELISA specifically discriminated negative from positive samples in a ratio of 25 and displayed an improved performance (sensitivity, specificity, and accuracy of 94.61%, 99.41%, and 97.02%, respectively), when compared to other commercial ELISA kits for VL serodiagnosis available in Brazil, as reported by Freire et al. [36]. DTL-4 also performed better than rK39-based ELISA [37] in samples from Minas Gerais and Mato Grosso states, with 90.67% accuracy ($p = 0.0033$).

In general, ICT is a test format easier to perform than ELISA or other diagnosis platforms and can be applied individually, at the bedside, and in outpatient clinics. ICT has also been proven to be a versatile test format for use in field conditions. Although ICT is regarded as a more suitable format for serological screening, high sensitivity and specificity can be achievable and, in some cases, may replace more complex diagnostic tests. Boelaert et al. [38] claims that an ideal VL diagnostic test should perform with a sensitivity $\geq 95\%$ and a specificity $\geq 98\%$. Compared with these parameters, the DTL-4 antigen displayed a more than satisfactory performance in both test formats, ELISA and ICT. It is noteworthy that a minimum accuracy of 90% is required for ICT tests to be selected for the Brazilian Government's purchase through public calls to supply the public health system with commercial tests for VL diagnosis [39]. In 2019, Freire et al. [36] reported an accuracy of 96.2% (92.0–98.3) using IT-LEISH

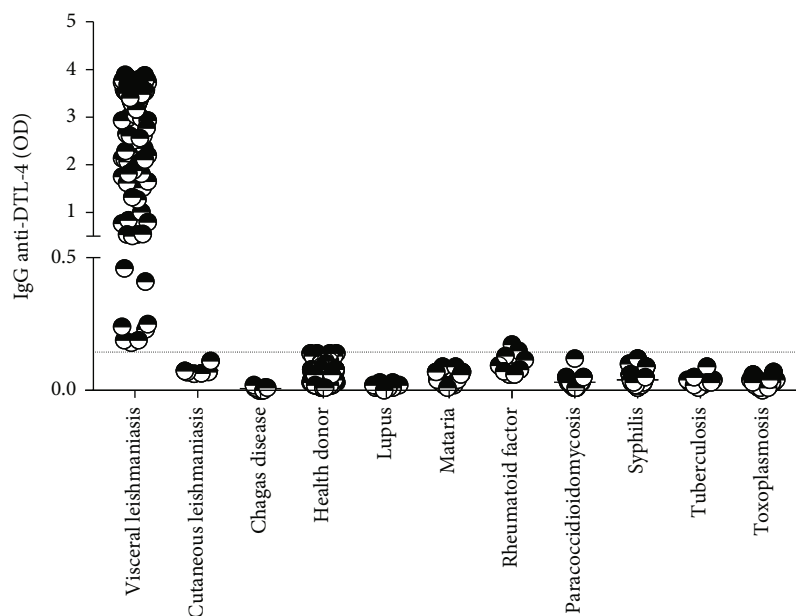


FIGURE 7: Cross-reactivity of DTL-4-ELISA with sera from patients diagnosed with other diseases. Sera from patients previously diagnosed with tegumentary leishmaniasis, Chagas' disease, malaria, toxoplasmosis, rheumatoid factor, lupus, tuberculosis, syphilis, and paracoccidioidomycosis were submitted for DTL-4-ELISA assay. Sera from VL patients ($n = 155$) and healthy donors ($n = 140$) were also included in this assay. The dotted line represents the cut-off.

TABLE 3: Performance of the DTL-4-ELISA in samples from patients with visceral leishmaniasis and negative controls from different geographical regions in Brazil.

Locality	Sensitivity% (n)	95% CI	Specificity% (n)	95% CI
Aracaju, SE	100.00 (9)	65.54-100.00	91.67 (12)	62.47-100.00
Campo Grande, MS	97.26 (73)	89.98-99.82	100.00 (121)	96.30-100.00
Bauru, SP	100.00 (12)	71.80-100.00	100.00 (7)	59.56-100.00
Natal, RN	93.75 (16)	69.69-99.99	100.00 (29)	88.13-100.00
Piauí state	89.47 (57)	78.53-95.44	—	—
Total	94.61 (167)	89.94-97.28	99.41 (169)	96.39-99.99

SE: Sergipe state; MS: Mato Grosso do Sul state; SP: São Paulo state; RN: Rio Grande do Norte state; n : number of samples; 95% CI: 95% confidence interval.

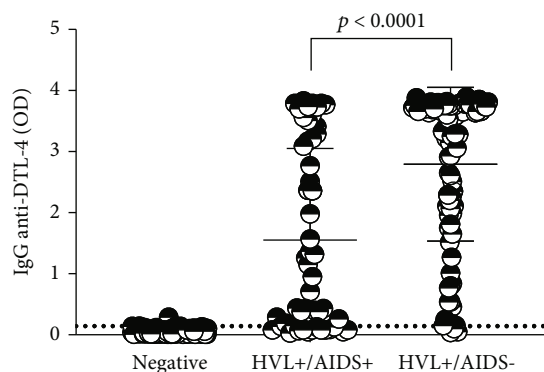


FIGURE 8: Evaluation of the reactivity of samples from coinfecting patients from different locations assayed with DTL-4-ELISA. Sera from HVL+/AIDS- patients ($n = 167$), sera from HVL+/AIDS+ patients ($n = 62$), and sera from healthy donors ($n = 169$) were included in this assay. Sera samples were diluted at 1:100. The dotted line represents the cut-off.

and 93.7% (88.8–96.6) with Kalazar Detect. Therefore, it may be considered that DTL-4-ICT displayed excellent performance, with an accuracy of 95.14%.

The majority of the ICTs available worldwide for active VL serodiagnosis, including the Kalazar Detect (InBios International, Seattle, WA) [23], IT-LEISH (Bio-Rad Laboratories, Inc.) [40], and Onsite *Leishmania* IgG/IgM Combo Rapid Test (CTK Biotech) [39] are based mainly on the same kinsin antigens also used in available ELISA. In a recent and comprehensive study, WHO reported that five different RDTs based on rK39 or rKE performed with high specificity (>95%) in all the different regions of the globe tested; however, sensitivity varied between tests (range, 36.8%–100%) and between regions. In ISC, all tests had a high sensitivity (>93%); in East Africa and Brazil, sensitivity results were variable, but no test exceeded 92% sensitivity (95% CI: 87.8–94.8%) [20].

The Brazilian Ministry of Health currently provides the OnSite *Leishmania* IgG/IgM Combo Rapid Test kit to diagnose suspected VL patients attending the public health

TABLE 4: Performance of DTL-4-ELISA to diagnosis of VL in samples of AIDS patients from different locations in Brazil.

Location	Subjects	Diagnostic accuracy (95% CI)		
		Sensitivity% (n) 95% CI	Specificity% (n) 95% CI	Accuracy% 95% CI
Campo Grande (Mato Grosso do Sul state)	VL	97.26 (73) 89.98-99.82	—	98.84 95.61-99.95
	VL/AIDS	81.82 (44) 67.78-90.75	—	94.44 89.26-97.32
	Healthy		100.00 (121) 96.30-100.00	—
Bauru (São Paulo state)	VL	100.00 (12) 71.80-100.00	—	100.00 80.21-100.00
	VL/AIDS	100.00 (04) 45.41-100.00	—	100.00 69.98-100.00
	Healthy		100.00 (07) 59.56-100.00	—
Total	VL	97.65 (85) 91.32-99.86	—	99.06 96.42-99.97
	VL/AIDS	83.33 (48) 70.16-91.57	—	95.48 91.20-97.83
	Healthy		100.00 (128) 96.50-100.00	—

VL: visceral leishmaniasis; VL/AIDS: coinfection; healthy donors; n: number of samples; 95% CI: 95% confidence interval.

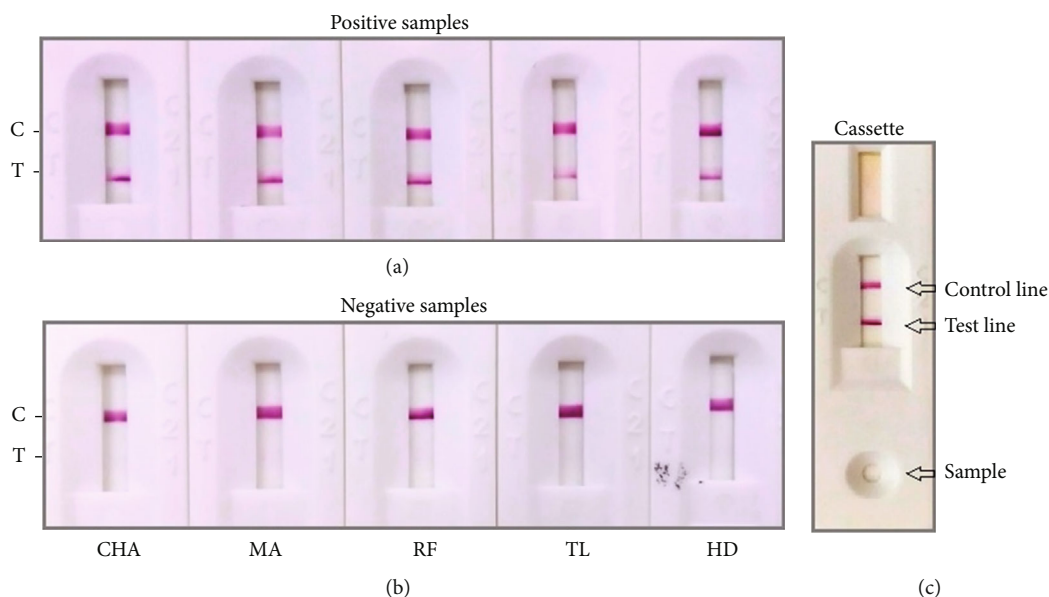


FIGURE 9: Illustrative results of detecting anti-*Leishmania* antibodies in sera and blood for VL diagnosis using the DTL-4-based ICT. (a) Sera samples from five VL different patients were included in this assay as a positive control (visible test and control line). (b) Sera samples from negative donors for LV with a previous diagnosis (ten samples of each disease) of Chagas' disease (CHA), malaria (MA), rheumatoid factor (RF), tegumentary leishmaniasis (TL), and healthy donor (HD) were tested. These assays presented negative results (only the control line was visible). (c) Representative test on the cassette. The sera sample from the VL patient was applied, and the control and test lines were visible.

system [41]. When evaluated in a panel of sera samples of VL cases from different Brazil regions, this test resulted in 92.1% sensitivity and 95.9% specificity, considering the IgG band. However, no VL case was positive on the IgM test, and one patient diagnosed with *Mycobacterium* infection was IgM positive [39], disclosing, there-

fore, the sensitivity and specificity of anti-*Leishmania* IgM antibodies for VL diagnosis. In 2019, Porcino et al. [42] also evaluated the ICT Kalazar Detect and Onsite *Leishmania* IgG/IgM Combo Rapid Test performance and obtained 76% and 64% sensitivities, respectively, in patients with active VL.

TABLE 5: Sensitivity, specificity, accuracy, and agreement of the VL-ICT versus the VL-ELISA using human samples from *L. infantum*-infected patients and healthy donors and VL/AIDS+), from panels 1 and 2.

VL (<i>n</i> = 87) and healthy donors (<i>n</i> = 85) (panel 1)		
Assay type	ELISA (+)	ELISA (-)
ICT (+)	80	02
ICT (-)	07	83
Accuracy = 94.80% (95% CI: 90.21–99.65%)	Sensitivity = 91.95% (95% CI: 84.12–96.70%)	Specificity = 97.65% (95% CI: 91.76–99.71%)
VL (<i>n</i> = 162) and healthy donors (<i>n</i> = 100) (panel 2)		
Assay type	ELISA (+)	ELISA (-)
ICT (+)	145	4
ICT (-)	9	104
Total	154	108
Accuracy = 95.14% (95% CI: 91.62–97.15%)	Sensitivity = 91.98% (95% CI: 86.65–95.39%)	Specificity = 100.00% (95% CI: 96.30–100.00%)
VL/AIDS+ (<i>n</i> = 46) and healthy donors (<i>n</i> = 64) (panel 2)		
Assay type	ELISA (+)	ELISA (-)
ICT (+)	34	6
ICT (-)	12	58
Total	46	64
Accuracy = 83.64% (IC 95%: 75.52–89.48%)	Sensitivity = 73.91% (IC 95%: 59.74–84.40%)	Specificity = 90.63% (IC 95%: 81.02–95.63%)
Concordance	Kappa index- <i>k</i> (95% CI)	Value <i>p</i> *
ELISA versus ICT (VL)	0.898 (0.844–0.952)	0.2673
ELISA versus ICT (VL/AIDS+)	0.657 (0.514–0.801)	0.2386

VL: visceral leishmaniasis; ELISA: enzyme-linked immunosorbent assay; ICT: immunochromatographic test; All the 46 VL/AIDS+ samples were positive by VL-ELISA. *McNemar test was used to estimate the statistical differences between ELISA and ICT. The differences were considered statistically significant when value $p < 0.05$.

Differences were observed for the sensitivity of the DTL-4-based tests when sera samples from patients living in different regions in Brazil were assayed. This finding may be attributed to the small sample size of some subset panels used. However, this result corroborates previous reports showing variations in sensitivity and specificity when similar antigens are tested with sera panels from people living in different regions [20, 43, 44]. These discrepant patterns may be attributed to differences in *Leishmania* strains causing infection or other epidemiological factors not very well understood, such as heterogeneity of populations, MHC molecules, age, and nutritional status. Nonetheless, additional epitopes present in chimeric recombinant proteins, such as DTL-4, may improve serodiagnosis performance.

The interference analysis performed to evaluate potential cross-reactivity showed that DTL-4, regardless of ICT and ELISA tests, very well discriminated VL from other diseases, including Chagas' disease, malaria, and tegumentary leishmaniasis, which are parasitic diseases also quite prevalent in different regions of Brazil. This finding indicated that DTL-4-ICT performed similarly to Kalazar Detect when tested with samples from the same diseases, as no cross-reactivity was observed in both studies [23]. Also, in samples from

Chagas disease, DTL-4-ICT was comparable to IT-LEISH [45]. On the other hand, Pedras et al. [37] reported lower specificity with malaria (85.0%) and Chagas' disease (83.3%) samples by using an rK39-based ELISA.

AIDS coinfection may impair the production of anti-*Leishmania* antibodies in patients with VL. Thus, a worrying aspect that still poses a significant challenge is the low sensitivity of serological tests in VL/AIDS coinfecting patients [46]. In Brazil, the prevalence of VL/AIDS is 9% [47]. However, the percentage of coinfection is underestimated because it considers only patients with VL manifestations. Also, around 40% of VL patients are negative by HIV serology, and both *Leishmania* and HIV infection may be asymptomatic [47]. Patients with negative results should undergo further investigation, such as direct detection of parasites in bone marrow aspirates. However, a positive result combined with clinical signs has a significant diagnostic value [48].

In this study, DTL-4-ELISA presented an overall sensitivity of 77.42% and DTL-4-ICT presented an overall sensitivity of 73.91% for diagnosing VL patients with HIV. Although sensitivity was lower in the group of coinfecting patients compared to that observed for the non-co-infected VL patients, it seems that DTL-4 may slightly improve VL serodiagnosis in

this patient group, as compared to other tests, including the commercially available kits. Freire et al. [36] reported the sensitivity values of 65.8% for NovaLisa *Leishmania infantum* IgG (ELISA) in HIV-coinfected patients from Brazil. These authors also reported that low sensitivity values were obtained with IT-LEISH (63.2%) and Kalazar Detect (47.4%). One possible alternative to improve the DTL-4-based test performance, which was not thoroughly investigated in the present work, would be to set up different conditions for DTL-4-based tests for samples from patients suspected of HVL/AIDS coinfection. Alterations may include changes in protein amounts, sera dilutions, or sample volume, which may be more sensitive for detecting anti-DTL-4 antibodies in HIV-coinfected patients. Additional studies may be performed to evaluate the use of DTL-4-based tests in epidemiological surveys, detect asymptomatic infection, and monitor *Leishmania* transmission through blood transfusion or treatment response.

In summary, the prototyped DTL-4-based ELISA or ICT displayed high accuracy and excellent performance compared to some in house or commercially available *Leishmania*-derived recombinant antigen-based ELISA or ICT tests. Although there is still much space for additional technical and product improvements, the DTL-4-based tests described herein represent improved alternative options for precise VL serological diagnosis.

Data Availability

The data used to support the findings of this study are available from the corresponding author upon request.

Conflicts of Interest

We declare that this work has not been influenced by any financial, personal, or professional interest.

Authors' Contributions

Maria Marta Figueiredo, Anna Raquel Ribeiro dos Santos, and Lara Carvalho Godoi performed the experiments and wrote the articles. Natália Salazar de Castro and Bruno Cas-saro de Andrade expressed and purified the protein. Sarah Aparecida Rodrigues Sergio helped in the execution of the ELISA experiments. Selma Maria Bezerra Jerônimo, Edward José de Oliveira, and Lucilândia Maria Bezerra offered sera samples of visceral leishmaniasis and helped in scientific discussions. Maria Marta Figueiredo and Ruth Tamara Valencia-Portillo helped in the execution of the ELISA and ICT experiments for external validation. Hiro Goto and Maria Carmen Arroyo Sanchez performed external validation and revised the article. Caroline Furtado Junqueira, Santuza Maria Ribeiro Teixeira, Flávio Guimarães Da Fonseca, Ricardo Tostes Gazzinelli, and Ana Paula Fernandes delineated the experiments, analyzed and discussed data, and wrote and revised the article.

Acknowledgments

We are grateful to BioClin Quibasa Ltda. for providing the rK39 protein. This work was supported by the Instituto Nacional de Ciência e Tecnologia em Vacinas (INCTv)/CNPq (grant nos. 573547/2008-4 and 465293/2014-0); Rede Mineira de Biomoléculas (FAPEMIG grant no. red001214); Conselho Nacional de Desenvolvimento Científico e Tecnológico (CNPq); Fundação de Amparo à Pesquisa do Estado de Minas Gerais (FAPEMIG); and Coordenação de Aperfeiçoamento de Pessoal de Nível Superior (CAPES).

References

- [1] J. Alvar, I. D. Vélez, C. Bern et al., "Leishmaniasis worldwide and global estimates of its incidence," *PLoS One*, vol. 7, no. 5, article e35671, 2012.
- [2] C. D. Mathers, M. Ezzati, and A. D. Lopez, "Measuring the burden of neglected tropical diseases: the global burden of disease framework," *PLoS Neglected Tropical Diseases*, vol. 1, no. 2, article e114, 2007.
- [3] J. Alvar, S. Yactayo, and C. Bern, "Leishmaniasis and poverty," *Trends in Parasitology*, vol. 22, no. 12, pp. 552–557, 2006.
- [4] Brasil, Ministério da Saúde, "Leishmaniose visceral: o que é, causas, sintomas, tratamento, diagnóstico e prevenção," 2020, <http://saude.gov.br/saude-de-a-z/leishmaniose-visceral>.
- [5] WHO, *Leishmaniasis*, World Health Organization, 2020, https://www.who.int/leishmaniasis/visceral_leishmaniasis/en/.
- [6] WHO, *Leishmaniasis*, World Health Organization, 2020, <http://www.who.int/news-room/fact-sheets/detail/leishmaniasis>.
- [7] D. Steverding, "The history of leishmaniasis," *Parasites & Vectors*, vol. 10, no. 1, p. 82, 2017.
- [8] G. Hiro and J. A. L. Lindoso, "Current diagnosis and treatment of cutaneous and mucocutaneous leishmaniasis," *Expert Review of Anti-Infective Therapy*, vol. 8, no. 4, pp. 419–433, 2010.
- [9] A. R. R. dos Santos, Â. V. Serufo, M. M. Figueiredo et al., "Evaluation of three recombinant proteins for the development of ELISA and immunochromatographic tests for visceral leishmaniasis serodiagnosis," *Mem Inst Oswaldo Cruz/Memórias do Instituto Oswaldo Cruz*, vol. 114, article e180405, 2019.
- [10] H. Sakkas, C. Gartzonika, and S. Levidiotou, "Laboratory diagnosis of human visceral leishmaniasis," *Journal of Vector Borne Diseases*, vol. 53, no. 3, pp. 8–16, 2016.
- [11] G. Srividya, A. Kulshrestha, R. Singh, and P. Salotra, "Diagnosis of visceral leishmaniasis: developments over the last decade," *Parasitology Research*, vol. 110, no. 3, pp. 1065–1078, 2012.
- [12] P. Srivastava, A. Dayama, S. Mehrotra, and S. Sundar, "Diagnosis of visceral leishmaniasis1," *Transactions of the Royal Society of Tropical Medicine and Hygiene*, vol. 105, 6 pages, 2011.
- [13] M. F. Zanette, V. M. Lima, M. D. Laurenti et al., "Serological cross-reactivity of *Trypanosoma cruzi*, *Ehrlichia canis*, *Toxoplasma gondii*, *Neospora caninum* and *Babesia canis* to *Leishmania infantum chagasi* tests in dogs," *Revista da Sociedade Brasileira de Medicina Tropical*, vol. 47, no. 1, pp. 105–107, 2014.

- [14] M. Mukhtar, A. Abdoun, A. E. Ahmed et al., "Diagnostic accuracy of rK28-based immunochromatographic rapid diagnostic tests for visceral leishmaniasis: a prospective clinical cohort study in Sudan," *Transactions of The Royal Society of Tropical Medicine and Hygiene*, vol. 109, no. 9, pp. 594–600, 2015.
- [15] S. Pattabhi, J. Whittle, R. Mohamath et al., "Design, development and evaluation of rK28-based point-of-care tests for improving rapid diagnosis of visceral leishmaniasis," *PLoS Neglected Tropical Diseases*, vol. 4, no. 9, article e822, 2010.
- [16] R. Porrozzio, M. V. S. Da Costa, A. Teva et al., "Comparative evaluation of enzyme-linked immunosorbent assays based on crude and recombinant leishmanial antigens for serodiagnosis of symptomatic and asymptomatic *Leishmania infantum* visceral infections in dogs," *Clinical and Vaccine Immunology*, vol. 14, no. 5, pp. 544–548, 2007.
- [17] E. M. Lemos, S. F. Guimarães Carvalho, R. Corey, and R. Dietze, "Avaliação do diagnóstico da leishmaniose visceral canina com a utilização de teste rápido com antígeno recombinante K39 em regiões," *Revista do Instituto Adolfo Lutz*, vol. 66, no. 2, pp. 185–193, 2007.
- [18] R. Badaró, D. Benson, M. C. Eulálio et al., "rK39: a cloned antigen of *Leishmania chagasi* that predicts active visceral leishmaniasis," *The Journal of Infectious Diseases*, vol. 173, no. 3, pp. 758–761, 1996.
- [19] B. Sarkari, R. E. Z. A. E. I. Zahra, and M. O. H. E. B. A. L. I. Mehdi, "Immunodiagnosis of visceral leishmaniasis: current status and challenges: a review article," *Iranian journal of parasitology*, vol. 13, no. 3, pp. 331–341, 2018.
- [20] J. Cunningham, E. Hasker, P. Das et al., "A global comparative evaluation of commercial immunochromatographic rapid diagnostic tests for visceral leishmaniasis," *Clinical Infectious Diseases*, vol. 55, no. 10, pp. 1312–1319, 2012.
- [21] M. M. Costa, H. M. Andrade, D. C. Bartholomeu et al., "Analysis of *Leishmania chagasi* by 2-D difference gel electrophoresis (2-D DIGE) and immunoproteomic: identification of novel candidate antigens for diagnostic tests and vaccine," *Journal of Proteome Research*, vol. 10, no. 5, pp. 2172–2184, 2011.
- [22] D. M. Resende, B. C. Caetano, M. S. Dutra et al., "Epitope mapping and protective immunity elicited by adenovirus expressing the *Leishmania* amastigote specific A2 antigen: correlation with IFN- γ and cytolytic activity by CD8+ T cells," *Vaccine*, vol. 26, no. 35, pp. 4585–4593, 2008.
- [23] S. F. G. Carvalho, E. M. Lemos, R. Corey, and R. Dietze, "Performance of recombinant K39 antigen in the diagnosis of Brazilian visceral leishmaniasis," *The American Journal of Tropical Medicine and Hygiene*, vol. 68, no. 3, pp. 321–324, 2003.
- [24] E. Ghedin, W. W. Zhang, H. Charest, S. Sundar, R. T. Kenney, and G. Matlashewski, "Antibody response against a *Leishmania donovani* amastigote-stage-specific protein in patients with visceral leishmaniasis," *Clinical and diagnostic laboratory immunology*, vol. 4, no. 5, pp. 530–535, 1997.
- [25] Brasil Ministério da Saúde, Secretaria de Vigilância em Saúde, Departamento de Vigilância Epidemiológica, *Manual de Vigilância e Controle da Leishmaniose Visceral*, Brasília, 2014.
- [26] E. Harith, A. H. J. Kolk, P. A. Kager et al., "A simple and economical direct agglutination test for serodiagnosis and seroepidemiological studies of visceral leishmaniasis," *Transactions of the Royal Society of Tropical Medicine and Hygiene*, vol. 80, no. 4, pp. 583–586, 1986.
- [27] Brasil Ministério da Saúde, Secretaria de Vigilância em Saúde, Departamento de DST, Aids e Hepatites Virais, *Manual Técnico para o Diagnóstico da Infecção pelo HIV*, Brasília, 2013.
- [28] A. P. M. M. Almeida, L. F. M. Machado, D. Doro et al., "New vaccine formulations containing a modified version of the amastigote 2 antigen and the non-virulent *Trypanosoma cruzi* CL-14 strain are highly antigenic and protective against *Leishmania infantum* challenge," *Frontiers in Immunology*, vol. 9, p. 465, 2018.
- [29] P. Matejtschuk and P. Phillips, "Product stability and accelerated degradation studies," in *Medicines from Animal Cell Culture*, G. Stacey and J. Davis, Eds., 2007.
- [30] J. Cohen, "A coefficient of agreement for nominal scales," *Educational and Psychological Measurement*, vol. 20, no. 1, pp. 37–46, 1960.
- [31] J. R. Landis and G. G. Koch, "The measurement of observer agreement for categorical data," *Biometrics*, vol. 33, no. 1, p. 159–174, 1977.
- [32] V. T. Coelho, J. S. Oliveira, D. G. Valadares et al., "Identification of proteins in promastigote and amastigote-like *Leishmania* using an immunoproteomic approach," *PLoS Neglected Tropical Diseases*, A. P. Fernandes and E. A. Coelho, Eds., vol. 6, no. 1, p. e1430, 2012.
- [33] A. S. Machado, F. F. Ramos, J. A. Oliveira-da-Silva et al., "An immunoproteomics approach to identify *Leishmania infantum* proteins to be applied for the diagnosis of visceral leishmaniasis and human immunodeficiency virus co-infection," *Parasitology*, vol. 147, no. 9, pp. 932–939, 2020.
- [34] B. Akhoundi, M. Mohebbali, S. Shojaei et al., "Rapid detection of human and canine visceral leishmaniasis: assessment of a latex agglutination test based on the A2 antigen from amastigote forms of *Leishmania infantum*," *Experimental Parasitology*, vol. 133, no. 3, pp. 307–313, 2013.
- [35] D. Lage, F. Ludolf, P. Silveira et al., "Screening diagnostic candidates from *Leishmania infantum* proteins for human visceral leishmaniasis using an immunoproteomics approach," *Parasitology*, vol. 146, no. 11, pp. 1467–1476, 2019.
- [36] M. L. Freire, T. M. de Assis, E. Oliveira et al., "Performance of serological tests available in Brazil for the diagnosis of human visceral leishmaniasis," *PLoS Neglected Tropical Diseases*, vol. 13, no. 7, article e0007484, 2019.
- [37] M. J. Pedras, V. L. de Gouvêa, E. J. de Oliveira, and A. Rabello, "Comparative evaluation of direct agglutination test, rK39 and soluble antigen ELISA and IFAT for the diagnosis of visceral leishmaniasis," *Transactions of the Royal Society of Tropical Medicine and Hygiene*, vol. 102, no. 2, pp. 172–178, 2008.
- [38] M. Boelaert, S. Bhattacharya, F. Chappuis et al., "Evaluation of rapid diagnostic tests: visceral leishmaniasis," *Nature Reviews Microbiology*, vol. 5, pp. S30–S39, 2007.
- [39] M. L. Freire, T. S. M. Assis, D. M. Avelar, A. Rabello, and G. Cota, "Evaluation of a new brand of immunochromatographic test for visceral leishmaniasis in Brazil made available from 2018," *Revista do Instituto de Medicina Tropical de São Paulo*, vol. 60, article e49, 2018.
- [40] K. Ritmeijer, Y. Melaku, M. Mueller, S. Kipngetich, C. O'keeffe, and R. N. Davidson, "Evaluation of a new recombinant K39 rapid diagnostic test for Sudanese visceral leishmaniasis," *The American Journal of Tropical Medicine and Hygiene*, vol. 74, no. 1, pp. 76–80, 2006.

- [41] Brasil Ministério da Saúde, “Coordenação Geral de Laboratórios de Saúde Pública–CGLAB, Brasília DF. Nota Informativa N° 3/2018-CGLAB/DEVIT/SVS/MS,” 2018, 2020, <https://www.saude.gov.br/images/pdf/2018/fevereiro/26/NOTA-INFORMATIVA-n3.pdf>.
- [42] G. N. Porcino, K. S. S. Carvalho, D. C. Braz, V. Costa Silva, C. H. N. Costa, and I. K. F. de Miranda Santos, “Evaluation of methods for detection of asymptomatic individuals infected with *Leishmania infantum* in the state of Piauí, Brazil,” *PLoS neglected tropical diseases*, vol. 13, no. 7, p. e0007493, 2019.
- [43] M. C. A. Sanchez, B. J. Celeste, J. A. L. Lindoso et al., “Performance of rK39-based immunochromatographic rapid diagnostic test for serodiagnosis of visceral leishmaniasis using whole blood, serum and oral fluid,” *PLoS One*, vol. 15, no. 4, p. e0230610, 2020, [published correction appears in *PLoS One*. 2020 Apr 29;15(4):e0232727].
- [44] E. K. Elmahallawy, A. Sampedro Martínez, J. Rodriguez-Granger et al., “Diagnosis of leishmaniasis,” *Journal of Infection in Developing Countries*, vol. 8, no. 8, pp. 961–972, 2014.
- [45] T. S. M. De Assis, A. S. C. Braga, M. J. Pedras et al., “Multi-centric prospective evaluation of rK39 rapid test and direct agglutination test for the diagnosis of visceral leishmaniasis in Brazil,” *Transactions of the Royal Society of Tropical Medicine and Hygiene*, vol. 105, no. 2, pp. 81–85, 2011.
- [46] WHO, 2020c World Health Organization, *Leishmaniasis. Leishmaniasis and HIV Coinfection* 2020, https://www.who.int/leishmaniasis/burden/hivcoinfection/burden_hiv_coinfection/en/.
- [47] J. A. Lindoso, C. H. Moreira, M. A. Cunha, and I. T. Queiroz, “Visceral leishmaniasis and HIV coinfection: current perspectives,” *HIV/AIDS-Research and Palliative Care*, vol. 10, pp. 193–201, 2018.
- [48] G. F. Cota, M. R. de Sousa, F. N. Demarqui, and A. Rabello, “The diagnostic accuracy of serologic and molecular methods for detecting visceral leishmaniasis in HIV infected patients: meta-analysis,” *PLoS Neglected Tropical Diseases*, vol. 6, no. 5, p. e1665, 2012.

Research Article

Invariant Natural Killer T Cells as Key Players in Host Resistance against *Paracoccidioides brasiliensis*

Joes Nogueira-Neto ¹, Flavio V. Loures ^{2,3}, Alessandra S. Schanoski ²,
David A. G. Andrade ¹, Michelangelo B. Gonzatti ¹, Tania A. Costa ², Bruno C. Vivanco ¹,
Patrícia Xander ⁴, Daniela S. Rosa ¹, Vera L. G. Calich ², and Alexandre C. Keller ¹

¹Departamento de Microbiologia, Imunologia e Parasitologia, Escola Paulista de Medicina, Universidade Federal de São Paulo, Brazil

²Departamento de Imunologia, Instituto de Ciências Biomédicas, Universidade de São Paulo, Brazil

³Instituto de Ciência e Tecnologia, Universidade Federal de São Paulo, Campus São José dos Campos, Brazil

⁴Departamento de Ciências Farmacêuticas, Instituto de Ciências Ambientais, Químicas e Farmacêuticas, Universidade Federal de São Paulo, Campus Diadema, Brazil

Correspondence should be addressed to Alexandre C. Keller; ackeller@unifesp.br

Received 23 December 2020; Revised 25 February 2021; Accepted 26 March 2021; Published 16 April 2021

Academic Editor: Luiz Felipe Domingues Passero

Copyright © 2021 Joes Nogueira-Neto et al. This is an open access article distributed under the Creative Commons Attribution License, which permits unrestricted use, distribution, and reproduction in any medium, provided the original work is properly cited.

Invariant Natural Killer T (iNKT) cells are key players in the immunity to several pathogens; however, their involvement in the resistance to *Paracoccidioides brasiliensis* infection remains unknown. Using splenocytes from CD1d (CD1d^{-/-}) and iNKT-deficient ($J\alpha 18^{-/-}$) mice, we found that iNKT cells are the innate source of IFN- γ after *P. brasiliensis* infection and are required to potentiate macrophage oxidative burst and control fungal growth. To determine whether iNKT cells contribute *in vivo* to host resistance against *P. brasiliensis* infection, we infected intratracheally wild-type and $J\alpha 18^{-/-}$ C57BL/6 mouse strains with the virulent Pb18 isolate. iNKT cell deficiency impaired the airway acute inflammatory response, resulting in decreased airway neutrophilia and reduced IFN- γ , KC, and nitric oxide (NO) production. The deficient innate immune response of $J\alpha 18^{-/-}$ mice to Pb18 infection resulted in increased fungal burden in the lungs and spleen. Besides, the activation of iNKT cells *in vivo* by administration of the exogenous iNKT ligand α -galactosylceramide (α -GalCer) improved host resistance to *P. brasiliensis* infection. Although the mechanisms responsible for this phenomenon remain to be clarified, α -GalCer treatment boosted the local inflammatory response and reduced pulmonary fungal burden. In conclusion, our study is the first evidence that iNKT cells are important for the protective immunity to *P. brasiliensis* infection and their activation by an exogenous ligand is sufficient to improve the host resistance to this fungal infection.

1. Introduction

Paracoccidioidomycosis (PCM) is caused by a fungus from the *Paracoccidioides* genus and is considered one of the highest causes of mortality among Brazilian systemic mycoses [1]. Clinical studies demonstrated a relationship between the characteristics of the immune response and disease severity [2]. In humans, a prominent Th1 response is associated with infection without disease, the chronic form of the disease with Th1/Th17 immunity, and the most severe manifestation, the acute or juvenile form, shows a prominent Th2/Th9

profile [1]. These data are supported by murine models of *P. brasiliensis* infection showing the association between the classical Th1 immune response, with high levels of IL-2 and IFN- γ , with resistance against the fungi [3, 4].

The lung is the primary site of fungal infection, where alveolar macrophages (M Φ) recognize Pathogen-Associated Molecular Patterns (PAMPs) through several Pattern Recognition Receptors (PRRs) [5]. Although *P. brasiliensis* proliferates in resident alveolar M Φ , these cells can inhibit fungal growth upon activation mediated by the synergistic action between lytic enzymes and metabolites from the oxidative

burst that mediate fungal killing [6, 7]. In parallel, these cells potentiate the immunity against the fungi by secreting cytokines and chemokines that coordinate the influx and activation of other immune cells, such as neutrophils and T lymphocytes, to the site of infection [8]. In this scenario, Th1-biased lymphocytes increase the fungicidal ability of phagocytes, promoting resistance against the pathogen [9, 10]. Although IFN- γ drives the quality of the inflammatory response during the acute phase of *P. brasiliensis* infection, the source of the early IFN- γ production remains unclear. Because invariant Natural Killer T (iNKT) lymphocytes are poised for the rapid production of IFN- γ , we hypothesized that they are important players in the immunity to *P. brasiliensis* infection [11].

The iNKT cells are a subpopulation of unconventional T lymphocytes that due to an invariant T cell receptor (TCR) promptly respond to lipid antigens presented in the context of CD1d molecules [12, 13]. In addition to this unique specificity, they can rapidly secrete several cytokines and chemokines, acting as a bridge between innate and adaptive immunity [14, 15]. This ability confers an essential immune regulatory function to these cells that participate in diverse types of immune responses, including those against pathogens [16, 17]. Although a previous study described that iNKT cells from both healthy controls and cured PCM patients have the same ability to expand and produce cytokines, there are no data regarding their role in *in vivo* models of *P. brasiliensis* infection [18]. Therefore, we used the intratracheal model of *P. brasiliensis* infection with the virulent Pb18 strain, and wild-type (WT) and iNKT-deficient ($J\alpha 18^{-/-}$) C57BL-6 mice to determine the role of these cells in host resistance to *P. brasiliensis* [13, 19].

Our findings show that iNKT lymphocytes are the primary innate source of IFN- γ , and their deficiency leads to impaired airway inflammation and increased pulmonary fungal burden. Furthermore, the specific activation of iNKT cells by α -galactosylceramide (α -GalCer) in an ongoing disease increased host resistance against this fungal pathogen. Therefore, iNKT cells were shown to play an essential role in shaping the protective immunity against the fungi, and the treatment with specific iNKT agonists potentiates host resistance to PCM.

2. Materials and Methods

2.1. Animals. Isogenic male C57Bl/6 mice from wild-type (WT), CD1d $^{-/-}$, and iNKT-deficient strain ($J\alpha 18^{-/-}$), aged 8–12 weeks, were obtained from the Animal Care Facility at the Federal University of São Paulo (UNIFESP). The C57Bl/6 $J\alpha 18^{-/-}$ strain was a gift from Dr. Masaru Taniguchi at the RIKEN Research Center for Allergy and Immunology (Japan) [13]. All animals were housed in individual standard cages and had free access to food and water. All procedures were previously reviewed and approved by the internal ethics committee of Universidade de São Paulo (USP-180/2011) and Universidade Federal de São Paulo (UNIFESP-CEP 0372/12).

2.2. Fungus. The virulent isolate Pb18 from *Paracoccidioides brasiliensis* was used throughout the experiments outlined

in this work [20]. Pb18 yeast cells were subcultivated every seven days in semisolid Fava-Netto culture medium at 37°C until use. The yeast cells were collected and washed with sterile phosphate-buffered saline (PBS, pH 7.2). Fungal viability was determined by the Janus Green B vital dye. All experimental procedures were carried out with fungal suspensions presenting viability between 90 and 95%.

2.3. Peritoneal M Φ , Splenocytes, and In Vitro Culture. A sterile solution of 3% thioglycolate was injected in the peritoneal cavity, and four days later, peritoneal leukocytes were collected, and thioglycolate-elicited peritoneal M Φ were isolated by adherence (2 h at 37°C in 5% CO₂) in plastic-bottom tissue-culture plates. Spleens were homogenized using the plunger end of a 3 mL syringe and a 70 μ m strainer, erythrocytes were removed using ACK solution (0.15 M NH₄Cl; 1 mM KHCO₃; 0.1 mM Na₂ EDTA), and cell viability was determined using trypan blue. After removing nonadherent cells, M Φ were cultivated alone or with *P. brasiliensis* yeasts in an M Φ : yeast ratio of 10:1 (2 h at 37°C in 5% CO₂) to allow fungi adhesion and ingestion. Supernatants were removed, and cells were gently washed with PBS to remove any noningested or nonadherent yeast. After that, splenocytes from WT, CD1d $^{-/-}$ or $J\alpha 18^{-/-}$ mice were added to the culture in an M Φ : splenocyte ratio of 1:10. After 48 h of coculture, supernatants were collected and analyzed for IFN- γ , IL-10, and NO production. After removing coculture supernatants, the wells were washed with distilled water to lyse the cells, and suspensions were collected in individual tubes. Cell homogenates were assayed for the presence of viable yeasts, as previously described [21].

2.4. Colony-Forming Units Assay. The number of viable Pb18 yeasts in cell cultures and infected organs was determined by counting the number of colony-forming units (CFU) as previously described [21].

2.5. Induction of Experimental PCM. Animals were deeply anesthetized and infected by intratracheal (i.t.) delivery of 1 x 10⁶ viable Pb yeast cells. Animals were euthanized 72 hours postinfection to assess iNKT cells' role in the acute phase of infection. Depending on the objective of the experiment, euthanasia occurred forty-five days or eight weeks postinfection to determine the severity of Pb infection.

2.6. Bronchoalveolar Lavage Fluid (BAL). To determine the content of inflammatory cells in the airways, mice were euthanized, the trachea was surgically exposed, and 0.5 mL of cold PBS was injected with a plastic cannula to obtain the BAL. After BAL collection, the total number of cells was determined in the Neubauer chamber and samples were centrifuged for supernatant analysis. Cellular precipitated was suspended in PBS for cytocentrifugation (Shandon, USA or Fanem, Br), and cellular populations were analyzed upon slides staining with hematoxylin/eosin.

2.7. Cytokine and Chemokine Production. IFN- γ and KC levels in BAL were analyzed with a multiplex kit (Millipore, USA) following the manufacturer's recommendations. The

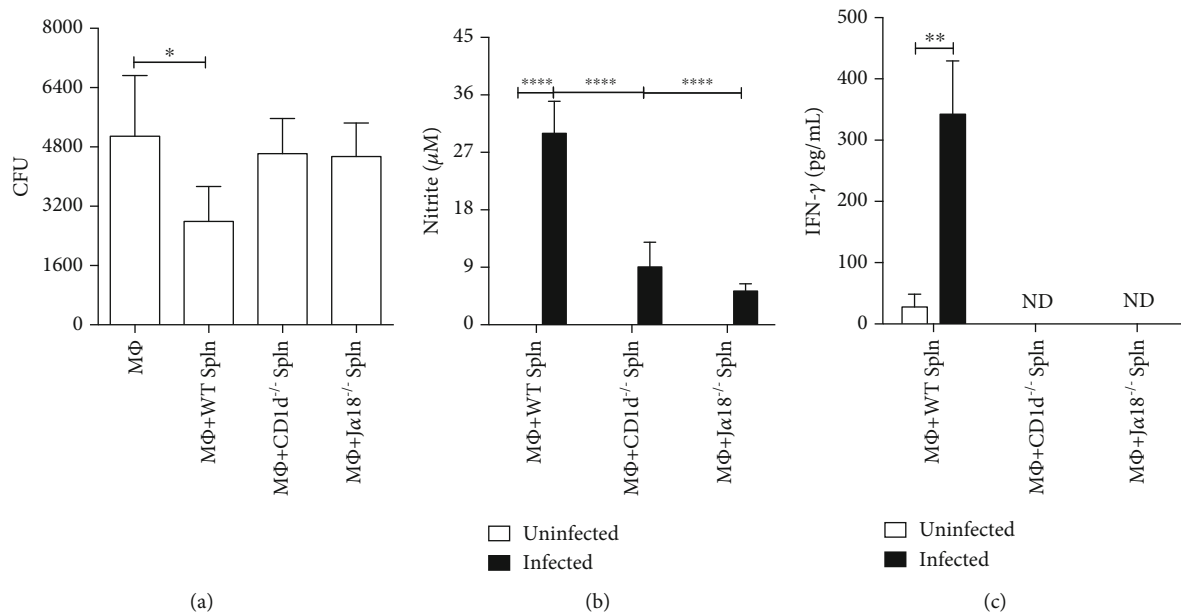


FIGURE 1: The invariant Natural Killer T cells drive *P. brasiliensis* killing by macrophages and respond for the innate source of IFN- γ upon fungal infection. Thioglycolate-elicited peritoneal M Φ from C57BL/6 mice were infected with Pb18 yeast (1:10) for 2 h. After washing, splenocytes (Spln) from WT, CD1d^{-/-}, or J α 18^{-/-} C57BL/6 mouse strains were added to the M Φ culture (10:1) for 48 h. After this period, supernatant was collected, and adherent cells were lysed with distilled water for fungal recovery. (a) Number of viable cell yeast obtained by colony-forming units assay (CFU). (b) NO levels in culture supernatants. (c) IFN- γ levels in the culture supernatants (ND = not detected). Data represent the mean \pm SD of quintuplicate samples from 1 of 2 independent experiments (a, b) and of 1 independent experiment (c). * $p < 0.05$; ** $p < 0.005$; **** $p < 0.0001$.

IFN- γ levels in culture supernatants were quantified using ELISA (R&D Systems, USA).

2.8. Nitric Oxide Production. Nitric oxide production in BAL was assessed using Nitrate/Nitrite Colorimetric Assay (Cayman Chemicals, USA) according to the manufacturer's recommendations. In culture supernatants, NO production was quantified by nitrite accumulation in the supernatants using a standard Griess reaction [22].

2.9. Flow Cytometry Assay. To determine the inflammatory state of lung parenchyma, the organs were digested with a DNase (1 mg/mL) and collagenase (2 mg/mL) solution (Invitrogen), homogenized, centrifuged in Percoll 35% (G&E, USA) solution, and stained for different surface markers (eBioscience, USA). The T lymphocyte population was analyzed according to the expression of CD3, CD4, CD8, and CD69. Myeloid-derived cells were analyzed according to the expression of GR1, CD11b, and MHC-II. All data concerning the FACS assays were analyzed using the FlowJo software (BD, USA), according to specific cell population characteristics. Further information about analysis strategy is presented in Supplementary Figures 1 and 2.

2.10. α -Galactosylceramide Treatment. At the week 4 after infection, mice were treated intravenously (i.v.) with 10 μ g of the NKT cell agonist α -GalCer (KRN7000, Cayman Chemical Company, USA) and euthanized four weeks later to determine the fungal burden in the lung.

2.11. Statistical Analysis. For the comparison between two groups, we used a 2-tailed unpaired *t*-test, and for multiple comparisons, we used a two-way ANOVA followed by Turkey's or Bonferroni's multiple comparison test. All statistical analyses were performed using the GraphPad Prism 7 software (San Diego, CA).

3. Results

3.1. Invariant Natural Killer T Cells Are the Innate Source of IFN- γ in Response to Fungal Infection and Are Required to Control *P. brasiliensis* Growth. To determine the role of the iNKT cells in the immunity against *P. brasiliensis*, we tested the ability of naive splenocytes from CD1d^{-/-} mouse, deficient in diverse CD1d-restricted cells, or J α 18^{-/-} mouse strain, which lacks only the CD1d-restricted iNKT cell subset, to respond to fungal infection [13, 23]. Thioglycolate-elicited peritoneal M Φ were exposed to Pb18 yeasts for 2 h, followed by coculture with 5×10^6 splenocytes from naive WT, CD1d^{-/-}, or J α 18^{-/-} mice. Two days later, culture supernatants were collected, and M Φ were lysed to determine the number of viable yeasts. Figure 1(a) demonstrates that the addition of naive WT splenocytes to M Φ culture increased the fungicidal activity of macrophages. In contrast, splenocytes from both CD1d^{-/-} and J α 18^{-/-} mice failed to increase M Φ killing capacity, indicating that the ability of naive splenocytes to control fungal growth depends on iNKT cells. In concordance, coculture with splenocytes from WT mice resulted in a higher NO production than those from CD1d^{-/-} and J α 18^{-/-} (Figure 1(b)).

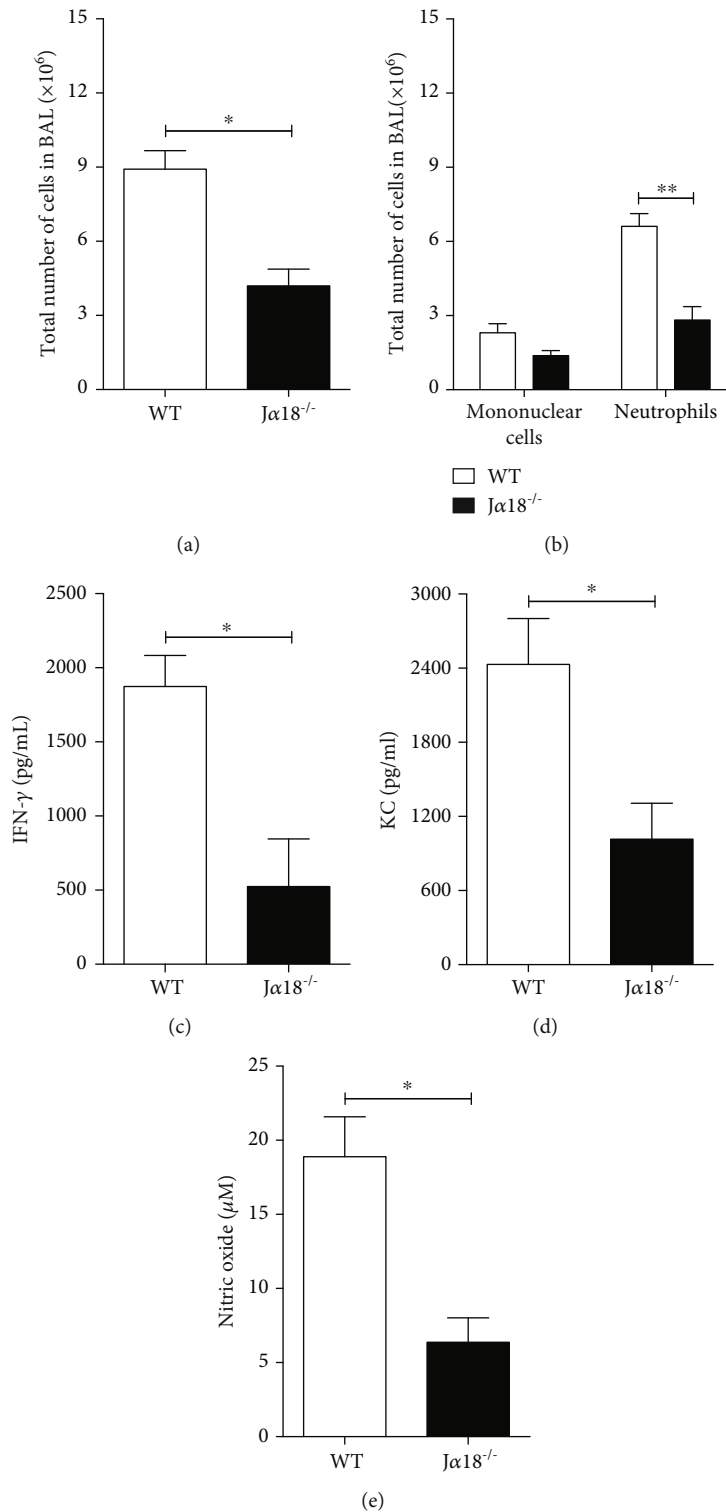


FIGURE 2: Deficiency in invariant Natural Killer T lymphocytes impairs the acute inflammatory response against *P. brasiliensis* infection. WT and $J\alpha 18^{-/-}$ C57BL/6 mouse strains were infected with 1×10^6 Pb18 yeasts, and 72 h later, the BAL content was analyzed for: (a) total number of cells; (b) presence of mononuclear cells and neutrophils; BAL levels of (c) IFN- γ , (d) KC, and (e) NO. Data represent the mean \pm SD from 1 of 2 independent experiments ($n = 4 - 5$ /group). * $p < 0.05$; ** $p < 0.005$.

Further analysis revealed that splenocytes from both $CD1d^{-/-}$ and $J\alpha 18^{-/-}$ failed to produce IFN- γ in response to fungal infection (Figure 1(c)). Therefore, these data show that among

$CD1d$ -restrict cells, the iNKT cell subset is the primary source of IFN- γ during *P. brasiliensis* infection and essential for early control of fungal growth.

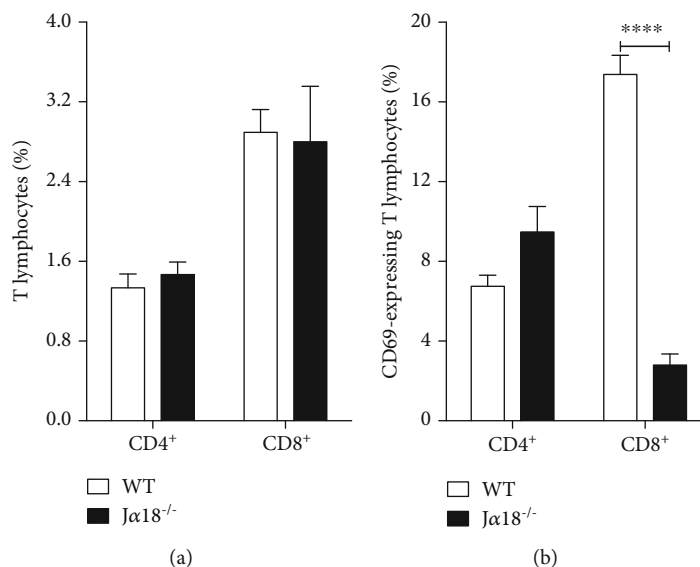


FIGURE 3: Deficiency in invariant Natural Killer T cells impairs early CD8 T lymphocyte activation during *P. brasiliensis* infection. WT and $J\alpha 18^{-/-}$ C57BL/6 mouse strains were infected with 1×10^6 Pb18 yeasts, and 72 h later, the lung parenchyma was analyzed for: (a) frequency of CD4⁺ and CD8⁺ T lymphocytes and (b) frequency of CD69-expressing CD4 and CD8 T cells. Data represent the mean \pm SD from 1 of 2 independent experiments ($n = 5$ /group). **** $p < 0.0001$.

3.2. Deficiency in iNKT Cells Impairs the Acute Airway Inflammation upon *P. brasiliensis* Infection. To determine the contribution of iNKT cells to the innate immune response against *P. brasiliensis* infection, we infected WT or $J\alpha 18^{-/-}$ C57BL/6 mice by intratracheal (i.t.) route with 1×10^6 living Pb18 yeast cells, and the BAL was collected 72 h later. $J\alpha 18^{-/-}$ mice presented a lower number of cells in the BAL compared to WT animals, which reflected an impaired airway neutrophilia (Figures 2(a) and 2(b), respectively). In accordance, the absence of iNKT cells resulted in lower levels of proinflammatory cytokines and chemokines, such as IFN- γ and KC in the airways (Figures 2(c) and 2(d), respectively). Moreover, NO levels in BAL were lower in the $J\alpha 18^{-/-}$ animals than in the WT group (Figure 2(e)). Therefore, these data demonstrate that iNKT cells play an important role in the acute phase of the inflammatory response following pulmonary Pb18 infection.

3.3. iNKT Cells Drive Early CD8 T Cell Activation and Influence the Presence of Distinct GRI^+CD11b^+ Cellular Population in the Lungs of Infected Mice. The flow cytometric analysis of lung parenchyma did not reveal any significant difference in the frequency of CD4⁺ and CD8⁺ T lymphocytes between WT and $J\alpha 18^{-/-}$ mice (Figure 3(a)). However, the frequency of CD8⁺CD69⁺ T cells in the $J\alpha 18^{-/-}$ was lower than observed in WT group (Figure 3(b)). Because CD69 molecule represents an early activation marker, this result indicates that iNKT cells are required for the early activation of CD8⁺ T cells [24]. No significant difference was observed regarding CD69 expression in the CD4⁺ subset.

Further analysis revealed the presence of distinct $GRI^+CD11b^+SSC^{high}$ and $GRI^+CD11b^+SSC^{low}$ cellular populations between WT and $J\alpha 18^{-/-}$ animals (Figure 4). We first found that the $GRI^+CD11b^+SSC^{high}$, but not the GRI^+

$CD11b^+SSC^{low}$, subset was significantly increased in the $J\alpha 18^{-/-}$ group versus WT animals (Figures 4(a) and 4(d), respectively). These cellular populations have been described as suppressor or effector myeloid cells according to their functional state [25]. Therefore, to better characterize their immunological status, we first determined the surface expression of the MHC-II molecule [26]. In the WT group, the frequency of MHC-II-expressing cells and its surface expression was higher in both $GRI^+CD11b^+SSC^{high}$ and $GRI^+CD11b^+SSC^{low}$ cells indicating a proinflammatory profile (Figures 4(b), 4(c), 4(e), and 4(f), respectively) [26]. This notion is corroborated by a higher surface expression of CD11b molecule, especially within the $GRI^+CD11b^+SSC^{low}$ subset (Figures 4(g) and 4(h)) [27].

3.4. Deficiency in iNKT Cells Impairs Host Resistance against *P. brasiliensis* Infection. Because iNKT deficiency impaired the early immune response against Pb18, we next determined their influence on a late phase of fungal infection. To this end, WT and $J\alpha 18^{-/-}$ mice were infected with 1×10^6 living Pb yeast cells, and 45 days later, the lungs, spleen, and liver were analyzed to determine fungal loads. Figures 5(a) and 5(b) demonstrate that $J\alpha 18^{-/-}$ mice presented a higher number of viable fungal cells in the lungs and spleen than WT animals. No differences in CFUs were detected in the livers (Figure 5(c)). These data indicate that the absence of iNKT cells increases the susceptibility of iNKT-deficient mice to Pb18 infection and support the idea that iNKT cells are important to control fungal growth at the site of infection and its dissemination to other organ.

3.5. Treatment of Mice with an iNKT Cells Agonist (α -GalCer) Confers Resistance to *P. brasiliensis* Infection. It is well described that activation of iNKT cells by exogenous ligands,

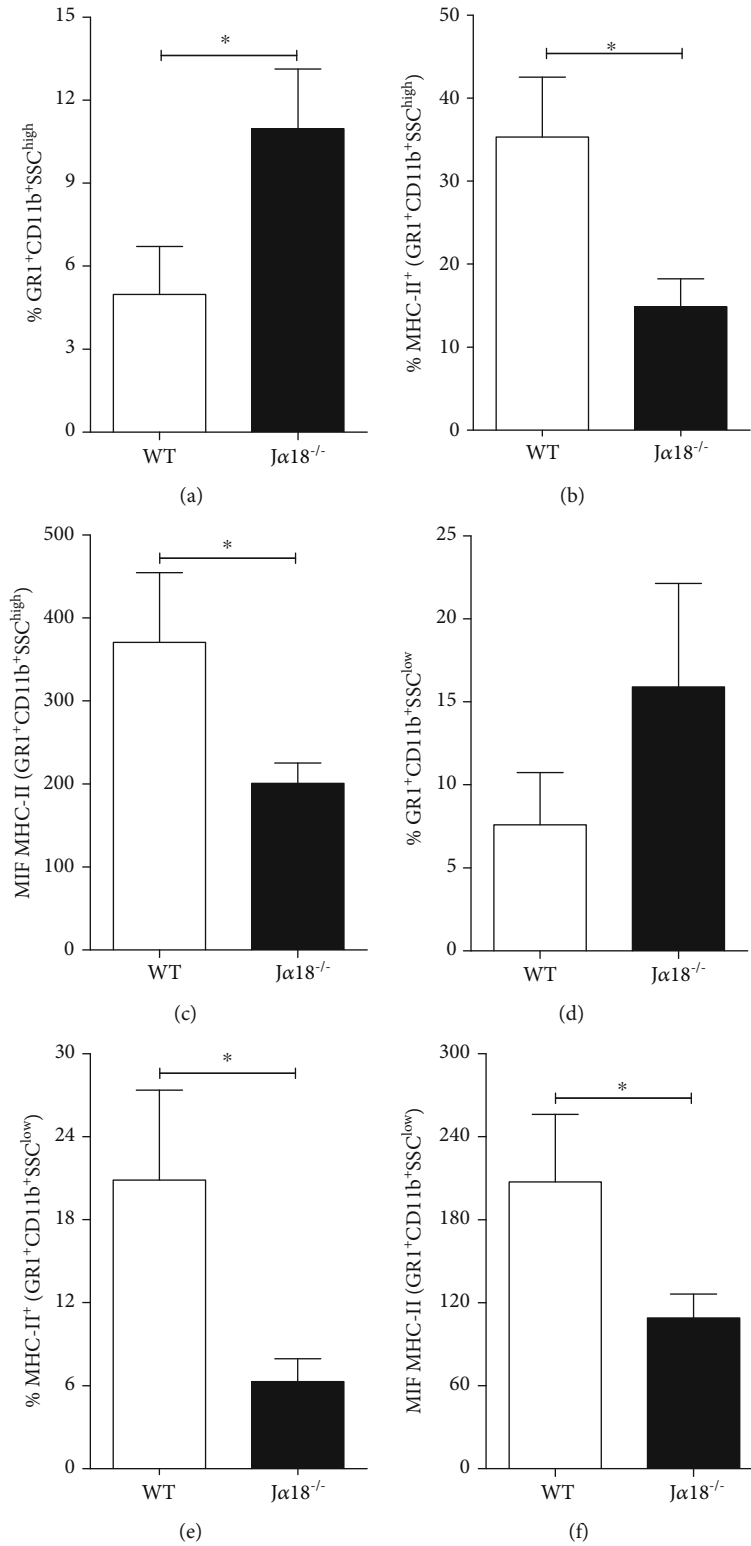


FIGURE 4: Continued.

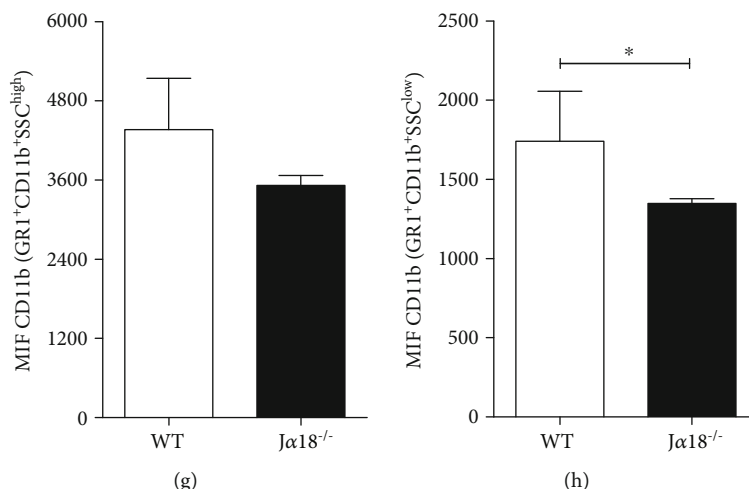


FIGURE 4: iNKT cells deficiency is associated with the accumulation of suppressor myeloid-derived cells in the lungs of *P. brasiliensis* infected mice. WT and Jα18^{-/-} C57BL/6 mouse strains were infected with 1×10^6 Pb18 yeasts, and 72 h later, the lung parenchyma was analyzed for: Frequency of (a) GR1⁺CD11b⁺SCC^{high} and (b) GR1⁺CD11b⁺SCC^{low} myeloid-derived cells. Frequency of MHC-II-expressing cells within (c) GR1⁺CD11b⁺SCC^{high} and (e) GR1⁺CD11b⁺SCC^{low} subsets and MHC-II surface expression level (c, f, respectively). Expression levels of CD11b molecules within the (g) GR1⁺CD11b⁺SCC^{high} and (h) GR1⁺CD11b⁺SCC^{low} myeloid-derived cells subsets. Data represent the mean \pm SD from 1 of 2 independent experiments ($n = 5/\text{group}$). * $p < 0.05$.

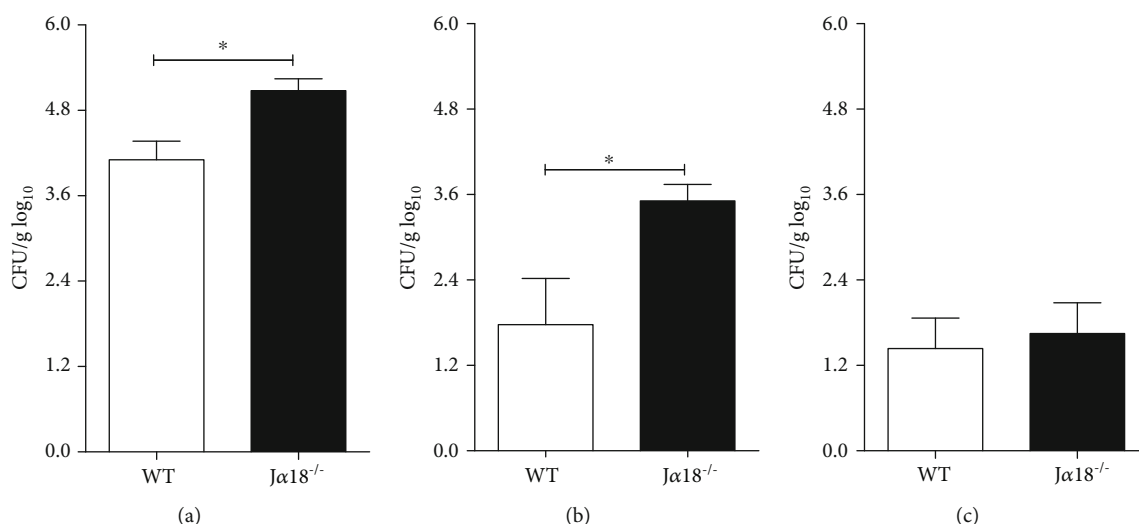


FIGURE 5: Invariant Natural Killer T cells restrain *P. brasiliensis* growth and dissemination. WT and Jα18^{-/-} C57BL/6 mouse strains were infected with 1×10^6 Pb18 yeast, and 45 days later, the fungal loads were determined in the lungs (a), spleen (b), and liver (c). Data represent the mean \pm SD from 1 of 2 independent experiments ($n = 5/\text{group}$). * $p < 0.05$.

especially α -GalCer, modulates different immune responses [28]. Thus, C57BL/6 WT mice were treated with $10 \mu\text{g}$ of α -GalCer at week four after infection to test its effect on the host resistance to *P. brasiliensis* infection. Briefly, four weeks after i.t. infection with 1×10^6 living yeasts, infected mice received one single i.v. injection of $10 \mu\text{g}$ of α -GalCer, and four weeks later, the influx of leukocytes to the airways and pulmonary fungal loads was determined.

The α -GalCer treatment resulted in a more intense inflammatory reaction against *P. brasiliensis* inoculation. The total number of cells and number of neutrophils were higher in the BAL of α -GalCer-treated mice compared to nontreated mice (Figures 6(a) and 6(b), respectively). This

increased inflammatory response was concomitant with lower fungal loads in the lungs of α -GalCer-treated mice (Figure 6(c)). Therefore, these data further indicate the protective role of iNKT cells and suggest that iNKT activation by specific agonist can be used as a possible therapeutic tool in pulmonary paracoccidioidomycosis.

4. Discussion

Paracoccidioides brasiliensis is an opportunistic fungus, which causes occasional, self-limited, infections in the majority of immunocompetent individuals. However, systemic spreading with severe clinical manifestations has been

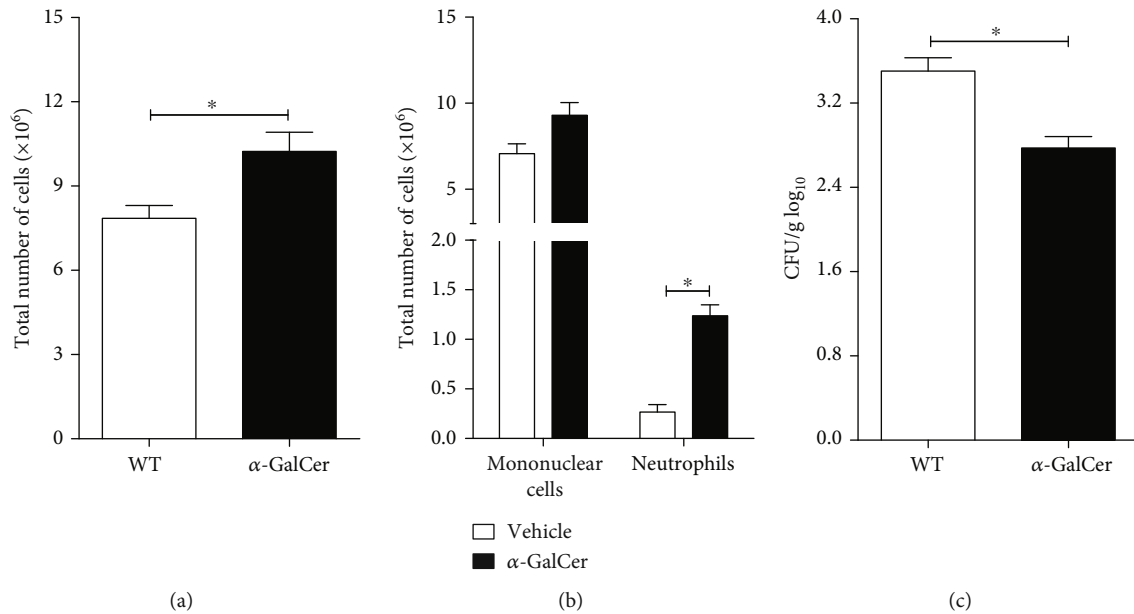


FIGURE 6: Treatment of *P. brasiliensis* infected mice with α -GalCer, an iNKT specific agonist, enhances host resistance to *P. brasiliensis* infection. WT C57BL/6 mice were infected with 1×10^6 Pb18 yeasts and treated four weeks later with $10 \mu\text{g}$ of α -GalCer by the i.v. route. At week 8 after infection, the number of inflammatory cells in the BAL and the number of viable yeasts in the lung parenchyma of α -GalCer-treated and untreated mice were determined. (a) Total number of inflammatory cells in BAL. (b) Mononuclear and neutrophil cell counts in the airways. (c) Fungal loads in lung parenchyma. Data represent the mean \pm SD from 1 independent experiment ($n = 5/\text{group}$). $*p < 0.05$.

correlated with intrinsic genetic characteristics of hosts, such as primary immunodeficiencies and individual lifestyle such as smoking, alcohol abuse, malnutrition, and treatment with immunosuppressive drugs [29, 30]. Despite the extensive literature about the importance of innate immunity in the acute host response to infection and fungal control, the role of iNKT cells remains unknown [31]. To determine the impact of invariant Natural Killer T cells in *P. brasiliensis* infection, we used animals that lack the CD1d molecule, which are deficient in diverse CD1d-restricted cells, or the $J\alpha 281$ TCR gene segment ($J\alpha 18^{-/-}$), which results in the specific depletion of the iNKT phenotype [13, 23].

In response to the contact with Pb-infected M Φ , naive splenocytes from WT mice produced high levels of IFN- γ , induced high levels of NO, and controlled fungal growth. These findings corroborate the notion that *in vitro* control of fungal growth by macrophages correlates with the ability of splenocytes to produce IFN- γ [32]. In contrast, splenic cells from CD1d $^{-/-}$ mice failed to produce IFN- γ , stimulate NO production, and control *P. brasiliensis* growth. Therefore, we could demonstrate that CD1d-restricted cells are responsible for the splenocytes IFN- γ production in response to *P. brasiliensis* infection and exerted an essential role for the early contention of fungal growth.

Several studies demonstrated that CD1d-restricted T cells comprise distinct cell subpopulations [23]. Thus, to demonstrate that it was specifically the iNKT cell subset, the one that exerted a regulatory role in pulmonary PCM, we used the $J\alpha 18^{-/-}$ mice strain, which lacks these cells due to the deletion of the $J\alpha 281$ gene segment [13]. Similar to CD1d $^{-/-}$ splenocytes, naive cells from $J\alpha 18^{-/-}$ mice failed to produce IFN- γ ,

induce NO production, and control fungal growth. Because no IFN- γ production was detected in the presence of naive splenocytes from both CD1d $^{-/-}$ or $J\alpha 18^{-/-}$ mice, it is conceivable to assume that the iNKT cells are responsible for the IFN- γ secretion and the control of fungal growth by *P. brasiliensis* infected M Φ .

To determine the *in vivo* influence of iNKT cells on host response to *P. brasiliensis*, we took advantage of the murine model of intratracheal fungal infection. The BAL analysis revealed that during the early phase of infection, the absence of iNKT cells impaired the migration of inflammatory cells to the airways, as determined by reduced airway neutrophilia. In parallel to this finding, iNKT cell deficiency also impaired KC production, a chemokine extensively described as a homing factor for neutrophils [33]. Although the mechanisms that control KC and neutrophilic inflammation are complex, it has been described that during *P. brasiliensis* infection, IFN- γ mediates diverse chemokines production, including KC [34]. Thus, it is pertinent to suppose that the lower levels of KC found in the BAL of $J\alpha 18^{-/-}$ -infected mice result from impaired IFN- γ production in the absence of iNKT cells. Although iNKT cells are rapid IFN- γ producing cells, neutrophils also seem to contribute for IFN- γ production during *P. brasiliensis* infection [35]. Thus, the reduced IFN- γ levels in $J\alpha 18^{-/-}$ mice during the acute responses may result from the absence of iNKT cells and the consequent impairment of neutrophil recruitment. The reduced ability to produce IFN- γ also impacted the secretion of fungicide, or fungistatic metabolites, such as nitric oxide (NO) [36].

The lung parenchyma analysis confirmed the *in vivo* inability of $J\alpha 18^{-/-}$ mice to mount a protective inflammatory

response. During the acute phase of the infection, iNKT deficiency was associated with a lower frequency of CD69-expressing CD8⁺, but not CD4⁺, T cells indicating their suboptimal activation. Although further experiments are required to better explore the relationship between iNKT and CD8⁺ cells during the acute phase of *P. brasiliensis* infection, the cross-talk between iNKT cells and CD8⁺ T lymphocytes is a phenomenon well recognized. The generation of short-lived effector cells in peripheral lymphoid organs depends on an initial short-lived interaction (0-6 h) followed by a prolonged-lasting contact (12-24 h) [37]. Also, IFN- γ production by iNKT cells is essential for the physiological induction of specific CD8 effector T cells [38]. Because the control of fungal loads has been associated with the CD8⁺ T lymphocyte subset, it is possible to propose that iNKT cells play an important role in generating effector CD8T⁺ cells during the beginning of *P. brasiliensis* infection [39, 40]. Furthermore, iNKT cell deficiency was also associated with the accumulation of myeloid-derived suppressor- (MDSC-) like cells. Although the interaction between iNKT lymphocytes and MDSC during infection remains unclear, there is evidence that activated iNKT cells can inhibit the immunosuppressive activity of MDSC [41, 42]. Myeloid cells expressing concomitantly the GR-1 and the CD11b markers represent a group of diverse polymorphonuclear (SSC^{high}) and monocytic (SSC^{low}) suppressor or effector cells [25, 26, 43]. Although a clear distinction between the suppressor or effector subsets requires very specific assays, the high expression of MHC-II and CD11b molecules may be used to distinguish between these cellular subsets [26, 27]. In this context, we found that during *P. brasiliensis* infection, the frequency of GR-1⁺CD11b⁺ cells expressing low MHC-II and CD11b levels increased in the *J α 18^{-/-}* animals, suggesting the appearance of the suppressive subset. Thus, it is reasonable to hypothesize that the early activation of iNKT cells in response to *P. brasiliensis* modulates the appearance of MDSC in the pulmonary environment.

The results discussed above support the idea that the absence of iNKT lymphocytes leads to an immunocompromised microenvironment that impairs host resistance against *P. brasiliensis* infection. Indeed, the importance of iNKT cells in the immunity against *P. brasiliensis* is evident when comparing fungal burdens between WT and *J α 18^{-/-}* mice. iNKT cell deficiency resulted in higher fungal loads in both lungs and spleen compared to the WT mice, indicating that these cells are key players in the control of fungus dissemination.

Finally, a previous study demonstrated that a single high dose of α -GalCer improved the outcome of *Mycobacterium tuberculosis* infection [44]. Thus, we next addressed the impact of α -GalCer administration on *P. brasiliensis*-infected mice. Animals treated with α -GalCer four weeks after fungal infection exhibited a significant reduction in the pulmonary fungal loads at week 8 after infection. Although the mechanisms involved in this phenomenon remain an object of study, fungal growth control was parallel to a more robust airway inflammatory response.

In conclusion, this study provides the first evidence of the contribution of iNKT cells to host resistance against *P. brasiliensis* infection and that their activation by exogenous ago-

nists could be considered a therapeutic tool to improve immunity to infection.

Data Availability

Data is available under reasonable request.

Conflicts of Interest

Although ACK is a member of the academic editorial board from the Journal of Immunology Research, he declares no conflict of interest. All the other authors declare that there is no conflict of interest.

Acknowledgments

This study was supported by research grants from Fundação de Amparo à Pesquisa do Estado de São Paulo (ACK: 2012/04692-1 and 2016/02189-1; VLGC: 2011/51258-2; and 2016/23189-0), and Coordenação de Aperfeiçoamento de Pessoal de Nível Superior—Brasil (CAPES)—Finance code 001. ACK, DSR, FVL and VLGC have personal scientific grants from Conselho Nacional de Pesquisa e Desenvolvimento (CNPq).

Supplementary Materials

Supplemental Figure 1: analysis of CD4 and CD8 T lymphocytes in lung parenchyma. After exclusion of dead cells, the CD3⁺ cells were analyzed for CD4 or CD8 expression and the frequency of CD69-expressing cells was determined within these populations. Supplemental Figure 2: analysis of GR-1⁺CD11b⁺ subsets in lung parenchyma. After exclusion of dead cells, the GR-1⁺ cells, within the CD11b⁺ subset, were analyzed according to SSC size (high or low). Next, both subsets were analyzed for MHC-II and CD11b expression. (*Supplementary Materials*)

References











- [1] M. A. Shikanai-Yasuda, R. P. Mendes, A. L. Colombo et al., "Brazilian guidelines for the clinical management of paracoccidioidomycosis," *Revista da Sociedade Brasileira de Medicina Tropical*, vol. 50, no. 5, pp. 715-740, 2017.
- [2] G. Benard, C. C. Romano, C. R. Cacere, M. Juvenale, M. J. Mendes-Giannini, and A. J. Duarte, "Imbalance of IL-2, IFN- γ and IL-10 secretion in the immunosuppression associated with human paracoccidioidomycosis," *Cytokine*, vol. 13, no. 4, pp. 248-252, 2001.
- [3] S. S. Kashino, R. A. Fazioli, C. Cafalli-Favati et al., "Resistance to Paracoccidioides brasiliensis infection is linked to a preferential Th1 immune response, whereas susceptibility is associated with absence of IFN-gamma production," *Journal of Interferon & Cytokine Research*, vol. 20, no. 1, pp. 89-97, 2000.
- [4] S. R. Almeida and J. D. Lopes, "The low efficiency of dendritic cells and macrophages from mice susceptible to Paracoccidioides brasiliensis in inducing a Th1 response," *Brazilian Journal of Medical and Biological Research*, vol. 34, no. 4, pp. 529-537, 2001.
- [5] V. L. Calich, A. Pina, M. Felonato, S. Bernardino, T. A. Costa, and F. V. Loures, "Toll-like receptors and fungal infections: the

- role of TLR2, TLR4 and MyD88 in paracoccidioidomycosis," *FEMS immunology and Medical Microbiology*, vol. 53, no. 1, pp. 1–7, 2008.
- [6] A. P. Moreira, L. A. Dias-Melicio, M. T. Peracoli, S. A. Calvi, and A. M. Victoriano de Campos Soares, "Killing of *Paracoccidioides brasiliensis* yeast cells by IFN- γ and TNF- α activated murine peritoneal macrophages: evidence of H₂O₂ and NO effector mechanisms," *Mycopathologia*, vol. 166, no. 1, pp. 17–23, 2008.
- [7] D. Lopera, B. H. Aristizabal, A. Restrepo, L. E. Cano, and A. Gonzalez, "Lysozyme plays a dual role against the dimorphic fungus *Paracoccidioides brasiliensis*," *Revista do Instituto de Medicina Tropical de Sao Paulo*, vol. 50, no. 3, pp. 169–175, 2008.
- [8] V. L. Calich, T. A. da Costa, M. Felonato et al., "Innate immunity to *Paracoccidioides brasiliensis* infection," *Mycopathologia*, vol. 165, no. 4-5, pp. 223–236, 2008.
- [9] E. Brummer, L. H. Hanson, and D. A. Stevens, "Gamma-interferon activation of macrophages for killing of *Paracoccidioides brasiliensis* and evidence for nonoxidative mechanisms," *International Journal of Immunopharmacology*, vol. 10, no. 8, pp. 945–952, 1988.
- [10] N. Kurita, S. K. Biswas, M. Oarada, A. Sano, K. Nishimura, and M. Miyaji, "Fungistatic and fungicidal activities of murine polymorphonuclear leucocytes against yeast cells of *Paracoccidioides brasiliensis*," *Medical Mycology*, vol. 37, no. 1, pp. 19–24, 1999.
- [11] D. B. Stetson, M. Mohrs, R. L. Reinhardt et al., "Constitutive cytokine mRNAs mark natural killer (NK) and NK T cells poised for rapid effector function," *Journal of Experimental Medicine*, vol. 198, no. 7, pp. 1069–1076, 2003.
- [12] T. Kawano, J. Cui, Y. Koezuka et al., "CD1d-restricted and TCR-mediated activation of α 14 NKT cells by glycosylceramides," *Science*, vol. 278, no. 5343, pp. 1626–1629, 1997.
- [13] J. Cui, T. Shin, T. Kawano et al., "Requirement for α 14 NKT cells in IL-12-mediated rejection of tumors," *Science*, vol. 278, no. 5343, pp. 1623–1626, 1997.
- [14] J. L. Matsuda, T. Mallevaey, J. Scott-Browne, and L. Gapin, "CD1d-restricted iNKT cells, the 'Swiss-Army knife' of the immune system," *Current Opinion in Immunology*, vol. 20, no. 3, pp. 358–368, 2008.
- [15] J. Klibi, L. Amable, and K. Benlagha, "A focus on NKT cell subset characterization and developmental stages," *Immunology and Cell Biology*, vol. 98, no. 7, p. 607, 2020.
- [16] S. J. McKee, S. R. Mattarollo, and G. R. Leggatt, "Immunosuppressive roles of natural killer T (NKT) cells in the skin," *Journal of Leukocyte Biology*, vol. 96, no. 1, pp. 49–54, 2014.
- [17] P. Arora, E. L. Foster, and S. A. Porcelli, "CD1d and natural killer T cells in immunity to *Mycobacterium tuberculosis*," *Advances in Experimental Medicine and Biology*, vol. 783, pp. 199–223, 2013.
- [18] V. G. Batista, L. Moreira-Teixeira, M. C. Leite-de-Moraes, and G. Benard, "Analysis of invariant natural killer T cells in human paracoccidioidomycosis," *Mycopathologia*, vol. 172, no. 5, pp. 357–363, 2011.
- [19] J. Defaveri, M. T. Rezkallah-Iwasso, and M. F. de Franco, "Experimental pulmonary paracoccidioidomycosis in mice: morphology and correlation of lesions with humoral and cellular immune response," *Mycopathologia*, vol. 77, no. 1, pp. 3–11, 1982.
- [20] S. S. Kashino, V. L. Calich, E. Burger, and L. M. Singer-Vermes, "In vivo and in vitro characteristics of six *Paracoccidioides brasiliensis* strains," *Mycopathologia*, vol. 92, no. 3, pp. 173–178, 1985.
- [21] L. M. Singer-Vermes, M. C. Ciavaglia, S. S. Kashino, E. Burger, and V. L. Calich, "The source of the growth-promoting factor(s) affects the plating efficiency of *Paracoccidioides brasiliensis*," *Journal of Medical and Veterinary Mycology*, vol. 30, no. 3, pp. 261–264, 1992.
- [22] A. H. Ding, C. F. Nathan, and D. J. Stuehr, "Release of reactive nitrogen intermediates and reactive oxygen intermediates from mouse peritoneal macrophages. Comparison of activating cytokines and evidence for independent production," *Journal of Immunology*, vol. 141, no. 7, pp. 2407–2412, 1988.
- [23] D. G. Pellicci and A. P. Uldrich, "Unappreciated diversity within the pool of CD1d-restricted T cells," *Seminars in Cell & Developmental Biology*, vol. 84, pp. 42–47, 2018.
- [24] R. Testi, J. H. Phillips, and L. L. Lanier, "Leu 23 induction as an early marker of functional CD3/T cell antigen receptor triggering. Requirement for receptor cross-linking, prolonged elevation of intracellular [Ca⁺⁺] and stimulation of protein kinase C," *Journal of Immunology*, vol. 142, no. 6, pp. 1854–1860, 1989.
- [25] A. Obregon-Henao, M. Henao-Tamayo, I. M. Orme, and D. J. Orday, "Gr1(int)CD11b+ myeloid-derived suppressor cells in *Mycobacterium tuberculosis* infection," *PLoS One*, vol. 8, no. 11, article e80669, 2013.
- [26] V. P. Makarenkova, V. Bansal, B. M. Matta, L. A. Perez, and J. B. Ochoa, "CD11b+/Gr-1+ myeloid suppressor cells cause T cell dysfunction after traumatic stress," *Journal of Immunology*, vol. 176, no. 4, pp. 2085–2094, 2006.
- [27] M. Duan, D. P. Steinfort, D. Smallwood et al., "CD11b immunophenotyping identifies inflammatory profiles in the mouse and human lungs," *Mucosal Immunology*, vol. 9, no. 2, pp. 550–563, 2016.
- [28] A. Schiefner, M. Fujio, D. Wu, C. H. Wong, and I. A. Wilson, "Structural evaluation of potent NKT cell agonists: implications for design of novel stimulatory ligands," *Journal of Molecular Biology*, vol. 394, no. 1, pp. 71–82, 2009.
- [29] R. Martinez, "New trends in paracoccidioidomycosis epidemiology," *Journal of Fungi*, vol. 3, no. 1, p. 1, 2017.
- [30] A. Restrepo, G. Benard, C. C. de Castro, C. A. Agudelo, and A. M. Tobon, "Pulmonary paracoccidioidomycosis," *Seminars in Respiratory and Critical Care Medicine*, vol. 29, no. 2, pp. 182–197, 2008.
- [31] F. Cezar-Dos-Santos, J. P. Assolini, N. C. M. Okuyama, K. F. Viana, K. B. de Oliveira, and E. N. Itano, "Unraveling the susceptibility of paracoccidioidomycosis: insights towards the pathogen-immune interplay and immunogenetics," *Infection, Genetics and Evolution*, vol. 86, p. 104586, 2020.
- [32] E. Brummer, L. H. Hanson, A. Restrepo, and D. A. Stevens, "In vivo and in vitro activation of pulmonary macrophages by IFN-gamma for enhanced killing of *Paracoccidioides brasiliensis* or *Blastomyces dermatitidis*," *Journal of Immunology*, vol. 140, no. 8, pp. 2786–2789, 1988.
- [33] Y. Kobayashi, "Neutrophil infiltration and chemokines," *Critical Reviews in Immunology*, vol. 26, no. 4, pp. 307–316, 2006.
- [34] J. T. Souto, J. C. Aliberti, A. P. Campanelli et al., "Chemokine production and leukocyte recruitment to the lungs of *Paracoccidioides brasiliensis*-infected mice is modulated by interferon- γ ," *The American Journal of Pathology*, vol. 163, no. 2, pp. 583–590, 2003.
- [35] P. A. Pino-Tamayo, J. D. Puerta-Arias, D. Lopera, M. E. UranJimenez, and A. Gonzalez, "Depletion of neutrophils

- exacerbates the early inflammatory immune response in lungs of mice infected with *Paracoccidioides brasiliensis*,” *Mediators of Inflammation*, vol. 2016, Article ID 3183285, 17 pages, 2016.
- [36] A. Gonzalez, W. de Gregori, D. Velez, A. Restrepo, and L. E. Cano, “Nitric oxide participation in the fungicidal mechanism of gamma interferon-activated murine macrophages against *Paracoccidioides brasiliensis* conidia,” *Infection and Immunity*, vol. 68, no. 5, pp. 2546–2552, 2000.
- [37] M. Valente, Y. Dolen, E. van Dinther et al., “Cross-talk between iNKT cells and CD8 T cells in the spleen requires the IL-4/CCL17 axis for the generation of short-lived effector cells,” *Proceedings of the National Academy of Sciences of the United States of America*, vol. 116, no. 51, pp. 25816–25827, 2019.
- [38] S. R. Mattarollo, M. Yong, L. Tan, I. H. Frazer, and G. R. Leggatt, “Secretion of IFN-gamma but not IL-17 by CD1d-restricted NKT cells enhances rejection of skin grafts expressing epithelial cell-derived antigen,” *The Journal of Immunology*, vol. 184, no. 10, pp. 5663–5669, 2010.
- [39] A. P. Chiarella, C. Arruda, A. Pina, T. A. Costa, R. C. Ferreira, and V. L. Calich, “The relative importance of CD4⁺ and CD8⁺T cells in immunity to pulmonary paracoccidioidomycosis,” *Microbes and Infection*, vol. 9, no. 9, pp. 1078–1088, 2007.
- [40] C. Paget, S. Ivanov, J. Fontaine et al., “Potential role of invariant NKT cells in the control of pulmonary inflammation and CD8⁺ T cell response during acute influenza A virus H3N2 pneumonia,” *Journal of Immunology*, vol. 186, no. 10, pp. 5590–5602, 2011.
- [41] H. J. Ko, J. M. Lee, Y. J. Kim, Y. S. Kim, K. A. Lee, and C. Y. Kang, “Immunosuppressive myeloid-derived suppressor cells can be converted into immunogenic APCs with the help of activated NKT cells: an alternative cell-based antitumor vaccine,” *Journal of Immunology*, vol. 182, no. 4, pp. 1818–1828, 2009.
- [42] D. Wu, Y. Shi, C. Wang et al., “Activated NKT cells facilitated functional switch of myeloid-derived suppressor cells at inflammation sites in fulminant hepatitis mice,” *Immunobiology*, vol. 222, no. 2, pp. 440–449, 2017.
- [43] V. Damuzzo, L. Pinton, G. Desantis et al., “Complexity and challenges in defining myeloid-derived suppressor cells,” *Cytometry Part B: Clinical Cytometry*, vol. 88, no. 2, pp. 77–91, 2015.
- [44] I. Sada-Ovalle, M. Skold, T. Tian, G. S. Besra, and S. M. Behar, “Alpha-galactosylceramide as a therapeutic agent for pulmonary *Mycobacterium tuberculosis* infection,” *American Journal of Respiratory and Critical Care Medicine*, vol. 182, no. 6, pp. 841–847, 2010.

Research Article

Macrophage Polarization in the Skin Lesion Caused by Neotropical Species of *Leishmania* sp

Carmen M. Sandoval Pacheco ¹, **Gabriela V. Araujo Flores** ¹, **Kadir Gonzalez** ²,
Claudia M. de Castro Gomes ¹, **Luiz F. D. Passero** ³, **Thaise Y. Tomokane** ¹,
Wilfredo Sosa-Ochoa,^{1,4} **Concepción Zúniga** ⁵, **Jose Calzada** ^{2,6}, **Azael Saldaña** ^{2,7},
Carlos E. P. Corbett,¹ **Fernando T. Silveira**,^{8,9} and **Marcia D. Laurenti** ¹

¹Departamento de Patologia, Laboratório de Patologia de Moléstias Infecciosas, Faculdade de Medicina, Universidade de São Paulo, Av. Doutor Arnaldo 455, 01246-903, Cerqueira César, São Paulo, SP, Brazil

²Departamento de Parasitología Molecular, Instituto Conmemorativo Gorgas de Estudios de la Salud, Ave. Justo Arosemena, 0816-02593 Calidonia, Panama

³São Paulo State University (UNESP), Institute of Biosciences and Institute for Advanced Studies of Ocean, São Vicente, SP, Brazil

⁴Instituto de Investigación en Microbiología, Universidad Nacional Autónoma de Honduras, Tegucigalpa, Honduras

⁵Departamento de Vigilancia de la Salud, Hospital Escuela, Tegucigalpa, Honduras

⁶Facultad de Medicina Veterinaria, Universidad de Panamá, Campus Harmodio Arias Madrid, Av. Juan Pablo II, Albrook, Panama

⁷Centro de Investigación y Diagnóstico de Enfermedades Parasitarias, Facultad de Medicina, Universidad de Panamá, Ave. Octavio Méndez Pereira, Panama

⁸Departamento de Parasitologia, Instituto Evandro Chagas, Belém, PA, Brazil

⁹Núcleo de Medicina Tropical, Universidade Federal de Pará, Belém, PA, Brazil

Correspondence should be addressed to Marcia D. Laurenti; mdlauren@usp.br

Received 20 February 2021; Revised 23 March 2021; Accepted 31 March 2021; Published 12 April 2021

Academic Editor: Alexandre Keller

Copyright © 2021 Carmen M. Sandoval Pacheco et al. This is an open access article distributed under the Creative Commons Attribution License, which permits unrestricted use, distribution, and reproduction in any medium, provided the original work is properly cited.

Macrophages play important roles in the innate and acquired immune responses against *Leishmania* parasites. Depending on the subset and activation status, macrophages may eliminate intracellular parasites; however, these host cells also can offer a safe environment for *Leishmania* replication. In this sense, the fate of the parasite may be influenced by the phenotype of the infected macrophage, linked to the subtype of classically activated (M1) or alternatively activated (M2) macrophages. In the present study, M1 and M2 macrophage subsets were analyzed by double-staining immunohistochemistry in skin biopsies from patients with American cutaneous leishmaniasis (ACL) caused by *L. (L.) amazonensis*, *L. (V.) braziliensis*, *L. (V.) panamensis*, and *L. (L.) infantum chagasi*. High number of M1 macrophages was detected in nonulcerated cutaneous leishmaniasis (NUCL) caused by *L. (L.) infantum chagasi* (M1 = 112 ± 12, M2 = 43 ± 12 cells/mm²). On the other side, high density of M2 macrophages was observed in the skin lesions of patients with anergic diffuse cutaneous leishmaniasis (ADCL) (M1 = 195 ± 25, M2 = 616 ± 114), followed by cases of localized cutaneous leishmaniasis (LCL) caused by *L. (L.) amazonensis* (M1 = 97 ± 24, M2 = 219 ± 29), *L. (V.) panamensis* (M1 = 71 ± 14, M2 = 164 ± 14), and *L. (V.) braziliensis* (M1 = 50 ± 13, M2 = 53 ± 10); however, low density of M2 macrophages was observed in NUCL. The data presented herein show the polarization of macrophages in skin lesions caused by different *Leishmania* species that may be related with the outcome of the disease.

1. Introduction

Macrophages have important roles in the immune system and play specific functions related to both innate and acquired immunity. During *Leishmania* infection, macrophages may have a dual role, killing or providing a safe environment for parasites. Thus, these host cells are fundamental in the progress or failure of the infection that relies on the type and magnitude of the host immune response [1–3].

In the vertebrate host, macrophages are found as naïve macrophages (M0), and the microenvironment where these cells survive provides different signals, leading to the development of different macrophage subsets, such as M1 (classically activated macrophages) and M2 macrophages (alternatively activated macrophages) [1, 4, 5]. These both macrophage subsets differ in cytokine production and, consequently, in their functions [6–8]. The microenvironment with IFN- γ and TNF- α presence may promote M1 subset differentiation, and this macrophage subset is able to present antigen, favoring the production of proinflammatory cytokines and reactive oxygen and nitrogen intermediates; besides, it aids the development of type 1 T helper lymphocytes (Th1). Phenotypically, M1 macrophage subsets express CD68 protein, which is a receptor for oxidized low-density lipoproteins (LDLs). Once CD68 binds to LDLs, M1 macrophages become able to phagocytose the pathogens and produce proinflammatory cytokines. Thus, M1 cells are crucial to eliminate intracellular pathogens, as well as *Leishmania*, by triggering an effective oxidative burst [2, 3, 6, 9–12].

On the other hand, microenvironment with high amounts of Th2 cytokines, such as IL-4, IL-10, and IL-13, favors the development of M2 macrophages. This macrophage subset has a low capacity for presenting antigens, has immunoregulatory properties, and reduces the inflammatory response by suppressing the proliferation and activity of T cells. Comparatively, M2 macrophages have opposed functions to M1 cells, being characterized by low production of IL-12 and high of IL-10, a cytokine associated with the development of adaptive Th2 immune responses. Additionally, M2 macrophages are involved in the remodeling of the extracellular matrix and angiogenesis, promoting tissue repair [2, 7].

Depending on the stimulus, M2 macrophages can be further divided into four subgroups: M2a macrophages that are induced by IL-4 or IL-13 produced mainly by Th2 cells, mast cells and basophils; M2b macrophages induced by immune complexes recognized by Fc receptors as well as agonists of Toll-like receptors (TLR) or IL-1; M2c macrophages induced by IL-10, TGF- β , and glucocorticoids that are considered deactivating macrophages; and finally, M2d macrophages induced by TLR agonists through the adenosine A2A receptor, once differentiated induce IL-10 and vascular endothelial growth factors releasing, additionally promote angiogenesis and tumor progression [2, 3, 6, 9–15].

It is well known that different *Leishmania* species trigger different immune responses [16, 17]. Based on the antigenic differences of the *Leishmania* species, a clinical and immunopathological spectrum of American cutaneous leishmaniasis has been described [18, 19]. The most common clinical form is named localized cutaneous leishmaniasis (LCL), which is

located in the center of the spectrum. This clinical form can be caused by several species of the subgenus *Leishmania* or *Viannia*, and from the histopathological point of view, this clinical form is characterized by an inflammatory infiltrate formed by lymphocytes, macrophages, and plasma cells with variable parasitism and a mixed cellular immune response. Mucocutaneous leishmaniasis (ML) has been considered the hyperreactive pole of the spectrum, and it is caused by parasites of the subgenus *Viannia*, mainly *L. (V.) braziliensis* and *L. (V.) panamensis* and histopathologically is characterized by the presence of lymphocytes with rare parasitism; additionally, a Th1-type cellular immune response with high amounts of proinflammatory cytokines can be identified in such cases. In contrast, the hyporeactive pole of this spectrum is anergic diffuse cutaneous leishmaniasis (ADCL), caused by parasites belonging to the subgenus *Leishmania*, mainly to *L. (L.) amazonensis* and *L. (L.) mexicana*, and it can be characterized by a plentiful Th2-type immune response and high amounts of circulating anti-inflammatory cytokines, and histopathologically, it is possible to observe high densities of heavily parasitized macrophages.

In experimental studies, M2 macrophages have been related to the development of pathology, and as a consequence, *L. (L.) major* and *L. (L.) amazonensis* survived and multiplied into macrophages [20, 21]. In contrast, M1 macrophages have been related to *in vivo* host resistance in *L. (L.) mexicana* and *L. (V.) braziliensis* infection [22, 23]. Therefore, the polarization of macrophages to M1 or M2 subsets is an important factor for the host in the final outcome of the disease; however, to the best of our knowledge, few reports performed a comparative analysis on the impact of macrophage subsets in human cutaneous leishmaniasis caused by different *Leishmania* species. Such study may shed further light on the importance and impact of macrophage subsets during the evolution of human cutaneous leishmaniasis in the American continent.

In this sense, the present study subpopulation of M1 and M2 macrophages were analyzed by double-staining immunohistochemistry in different clinical forms of human American cutaneous leishmaniasis (ACL) caused by *L. (L.) amazonensis*, *L. (V.) panamensis*, *L. (V.) braziliensis*, and *L. (L.) infantum chagasi*.

2. Materials and Methods

2.1. Human Skin Biopsies. Thirty-four skin biopsies from patients with ACL, previously diagnosed by clinical, parasitological, and molecular tests [24–26], were collected before treatment. Among them, five biopsies belonged to anergic diffuse cutaneous leishmaniasis (ADCL) caused by *L. (L.) amazonensis*, four to localized cutaneous leishmaniasis (LCL) caused by *L. (L.) amazonensis*, ten to LCL caused by *L. (V.) panamensis*, five to LCL caused by *L. (V.) braziliensis*, and ten to nonulcerated or atypical cutaneous leishmaniasis (NUCL) caused by *L. (L.) infantum chagasi* (Table 1).

All samples were obtained from the repository of the Laboratory of Pathology of Infectious Diseases, Medical School of University of São Paulo, previously approved by the Ethics of Research Committee of the Medical School,

TABLE 1: Characteristics of the samples used in the present study.

Clinical forms	<i>Leishmania</i> specie	N° of biopsy	Type of lesion	Endemic area
Anergic diffuse cutaneous leishmaniasis	<i>L. (L.) amazonensis</i>	5	Infiltrative/nodular	Brazil
Localized cutaneous leishmaniasis	<i>L. (L.) amazonensis</i>	4	Ulcerated	Brazil
Localized cutaneous leishmaniasis	<i>L. (V.) panamensis</i>	10	Ulcerated	Panamá
Localized cutaneous leishmaniasis	<i>L. (V.) braziliensis</i>	5	Ulcerated	Brazil
Nonulcerated or atypical cutaneous leishmaniasis	<i>L. (L.) infantum chagasi</i>	10	Nonulcerated	Honduras

University of São Paulo, Brazil (CAAE:83455317.9.0000.0065, CAAE:12861013.2.0000.0065, CAAE:25714814.0.0000.0065).

2.2. In Situ Detection of M1 and M2 Macrophages. Double-staining immunohistochemistry reaction was performed to observe M1 and M2 macrophage subsets. Both iNOS (polyclonal, ab15323) and CD68 antibodies (monoclonal, ab955) were used in double-staining immunohistochemistry reaction to identify the M1 subset while IL-10 (polyclonal, ab34843) and CD163 (monoclonal, ab156769) antibodies were used to identify M2 macrophages [2, 7, 11, 27, 28]. All primary antibodies were purchased from ABCAM.

Double-staining immunohistochemistry reaction was performed in two steps. Firstly, histological sections were deparaffinized in xylene for 15 minutes, followed by hydration in a descending series of alcohols. Then, endogenous peroxidase blockade was performed with 3% hydrogen peroxide solution. Antigen retrieval was performed using 10 mM/L citrate buffer pH 6.0 in a boiling water bath. After these steps, the following primary antibodies, produced in rabbits, added anti-iNOS (1 : 100) and anti-IL-10 (1 : 1500). As a negative control, a solution containing phosphate-buffered saline (PBS) and bovine serum albumin (BSA) with the omission of the primary antibody was used. The slides were incubated in a humidified chamber overnight at 4°C. To develop the reaction, a NOVOLINK™ polymer detection systems kit (RE7280-K, Leica Biosystems, Newcastle, UK) was used. The chromogenic substrate, DAB+H₂O₂ (diaminobenzidine with hydrogen peroxide, K3468, DakoCytomation), was added to the tissue, incubated for 5 minutes and briefly counterstained with Harris haematoxylin and immersed in TBS-T (Tris Buffered Saline with 0.05% Tween 20).

In the second step, the following primary antibodies, produced in mice, added anti-CD68 (1:400) and anti-CD163 (1:200). As a negative control, a solution containing phosphate-buffered saline and bovine serum albumin with the omission of the primary antibody was used. The slides were incubated in a humidified chamber overnight at 4°C; then, HRP mouse polymer (ABCAM, ab210061) was incubated for 30 minutes at room temperature. Slides were incubated with emerald chromogen (ABCAM, ab210061) for 5 minutes at room temperature; then, the slides were rinsed with distilled water, left to dry at room temperature to dehydrate the histological sections, and mounted with limonene mounting medium (ABCAM, ab104141).

2.2.1. Quantitative Morphometric Analysis. Ten sequential fields of each histological section using ×40 objective to give a final magnification of ×400 were photographed in an opti-

cal microscope coupled to the computer using the AxioVision 4.8.2 software (Zeiss, San Diego, CA, USA). The immunolabeled cells were quantified considering the pattern of staining as well as cell morphology. Immunostained cells were recorded in the dermal layer of the skin, the area where the inflammatory infiltrate was present. The determination of the cellular density (number of cells per square millimeter) of each marker was determined by the ratio between the immunostained cells and the area of each photo.

2.2.2. Statistical Analysis. Analysis of the data was performed using GraphPad Prism 8.0 software. The Kolmogorov-Smirnov test was employed to assess the normality of samples. *t*-test was used for data with a Gaussian distribution to compare the density of cellular markers. The results were expressed as the mean ± standard error. The one-way ANOVA test was used to compare CD68, CD163 markers, and subpopulations of macrophages (M1 and M2) between the different clinical forms. Differences were considered as statistically significant when $P < 0.05$. Graphics were made using the Origin 9.6.5.169 software.

3. Results

In the present study, M1 and M2 subsets of macrophages were analyzed by double-staining immunohistochemistry, being the M1 subset positive for both CD68 and iNOS markers while M2 macrophages positive for both CD163 and IL-10 markers.

M1 and M2 macrophages were observed in the dermis of the skin lesion from different clinical forms used in this study (Figures 1 and 2).

The quantitative morphometric analysis showed that the density of M1 macrophages was 195 ± 25 cells/mm² for ADCL caused by *L. (L.) amazonensis*, 97 ± 24 cell/mm² for LCL by *L. (L.) amazonensis*, 71 ± 14 cell/mm² for LCL by *L. (V.) panamensis*, 50 ± 13 cell/mm² for LCL by *L. (V.) braziliensis*, and 112 ± 12 cell/mm² for NUCL by *L. (L.) infantum chagasi*.

On the other hand, the cellular density of M2 macrophages was 616 ± 114 cell/mm² for ADCL caused by *L. (L.) amazonensis*, 219 ± 29 cell/mm² for LCL by *L. (L.) amazonensis*, 164 ± 14 cell/mm² for LCL by *L. (V.) panamensis*, 53 ± 10 cell/mm² for LCL by *L. (V.) braziliensis*, and 43 ± 12 cell/mm² for NUCL by *L. (L.) infantum chagasi* (Figure 3).

Comparatively, it was observed that the density of M2 macrophages was higher than M1 in ADCL by *L. (L.) amazonensis* and also in LCL caused by *L. (L.) amazonensis* and *L. (V.) panamensis* ($P < 0.05$). In contrast in NUCL, the density

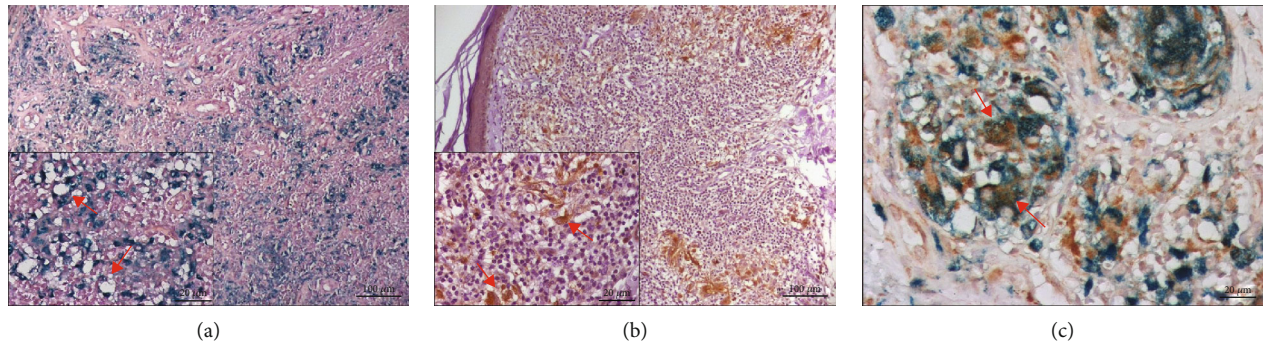


FIGURE 1: Histological sections of the skin lesion from nonulcerated or atypical cutaneous leishmaniasis (NUCL) processed by double-staining immunohistochemistry showing (a) CD68⁺ cells (blue), (b) iNOS⁺ cells (brown), and (c) M1 macrophages (CD68⁺/iNOS⁺) (×400). The red arrows show immunostained cells for the different markers.

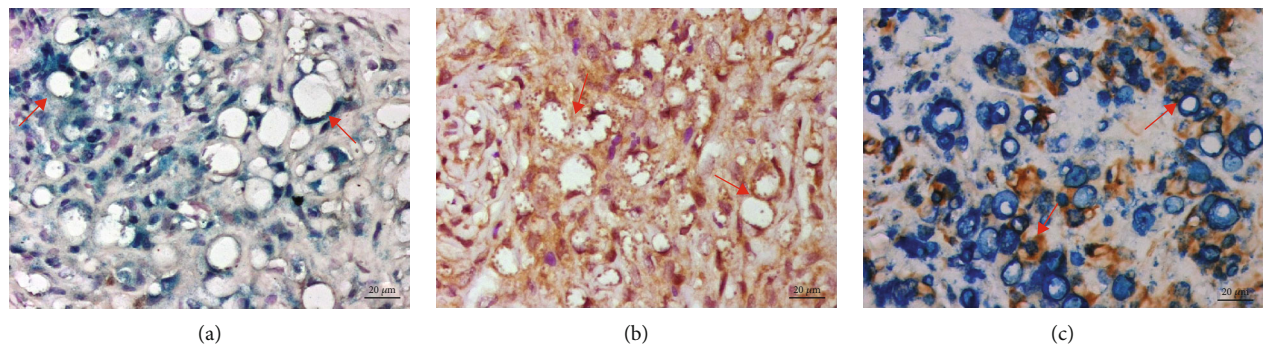


FIGURE 2: Histological sections of the skin lesion from anergic diffuse cutaneous leishmaniasis (ADCL) processed by double-staining immunohistochemistry showing (a) CD163⁺ cells (blue), (b) IL-10⁺ cells (brown), and (c) M2 macrophages (CD163⁺/IL-10⁺) (×400). The red arrows show immunostained cells for the different markers.

of M1 was higher than that M2 macrophages ($P < 0.001$). The LCL caused by *L. (V.) braziliensis* showed no statistical difference between M1 and M2 macrophage subsets ($P > 0.05$).

Additionally, the ratio between M1 and M2 macrophages was calculated, and it was observed that the M1:M2 ratio was higher in NUCL (2.605) than in the other clinical forms, ADCL (0.317) and LCL caused by *L. (L.) amazonensis* (0.443), *L. (V.) panamensis* (0.433), and *L. (V.) braziliensis* (0.943).

Considering the percentage of M1 and M2 cells inside to the macrophage population, it is possible to observe that the percentage of M1 cells is lower in ADCL (18%), LCL by *L. (L.) amazonensis* (21%), and LCL by *L. (V.) panamensis* (26%) compared to the percentage of M2 cells (57%, 48% and 59%, respectively). On the other side, in NUCL caused by *L. (L.) infantum chagasi*, the percentage of M1 (53%) is higher than M2 cells (20%) ($P < 0.01$). However, in LCL by *L. (V.) braziliensis*, the percentage of M1 and M2 cells was similar (26% and 28%, respectively) (Figure 4). Nevertheless, the absence of colocalization of the different markers in double-staining immunohistochemistry reaction, 25% of total macrophages in ADCL by *L. (L.) amazonensis*, 31% in LCL by *L. (L.) amazonensis*, 15% in LCL by *L. (V.) panamensis*, 46% in LCL by *L. (V.) braziliensis*, and 27% in NUCL by *L. (L.) infantum chagasi* was not characterized neither as M1 nor M2 cells (Supplementary Table (available here)).

4. Discussion

The final outcome of leishmaniasis is multifactorial and depends on the physiology of the host, type of immune response, specie, and virulence of *Leishmania* species. The entry of the parasite into the host cell, the establishment of infection, and the development of the disease involves different steps that may determine the success of the infection, as well as the development of different clinical forms of leishmaniasis [19, 29, 30].

Depending on the interaction between innate cells with T cells, the amount of cytokines produced, and the duration of exposure to parasitic antigens, macrophages can express different functional properties in response to this microenvironment, showing a polarization state that may be related to pathology or self-healing processes [6, 7, 31]. During *Leishmania* infection, macrophage subsets have opposed roles, and M1 macrophage is associated with the elimination of internalized parasites, while M2 is related to the maintenance of the parasite in the intracellular compartment [3]. Thus, in this study, the functional characteristics of macrophages were analyzed *in situ* in different clinical forms of cutaneous leishmaniasis caused by *L. (L.) amazonensis*, *L. (V.) panamensis*, *L. (V.) braziliensis*, and *L. (L.) infantum chagasi*, and their involvement with the development of different clinical forms was assessed.

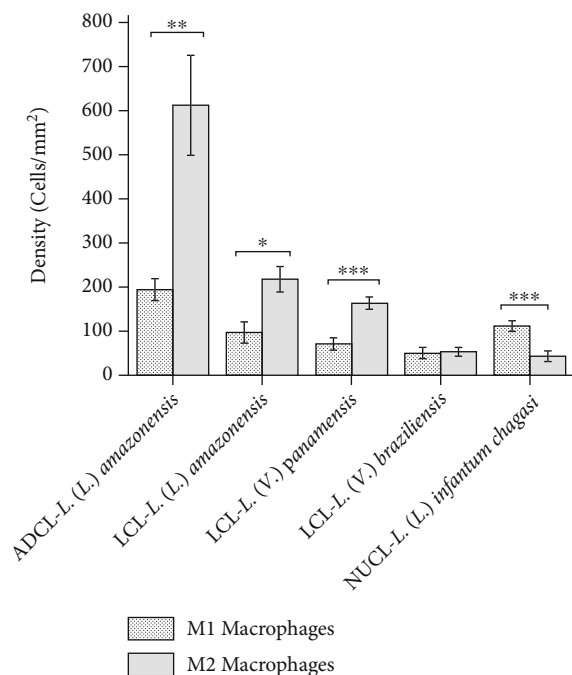


FIGURE 3: Cellular density (average \pm standard error) of M1 and M2 macrophages in the skin lesion of different clinical forms of American cutaneous leishmaniasis, anergic diffuse cutaneous leishmaniasis (ADCL) by *L. (L.) amazonensis*, localized cutaneous leishmaniasis (LCL) by *L. (L.) amazonensis*, *L. (V.) panamensis*, *L. (V.) braziliensis*, and nonulcerated cutaneous leishmaniasis (NUCL) by *L. (L.) infantum chagasi*. * $P < 0.05$; ** $P < 0.01$; *** $P < 0.001$.

Higher density of M2 than M1 macrophages was observed in the skin lesions of patients affected by ADCL caused by *L. (L.) amazonensis* and LCL caused by *L. (L.) amazonensis* and *L. (V.) panamensis*, as observed in Figure 3. Between *L. (L.) amazonensis* and *L. (V.) panamensis* infection, a higher amount of M2 macrophages was observed in the ADCL compared to the LCL caused by both species ($P < 0.05$). ADCL is a clinical form caused by *L. (L.) amazonensis* and *L. (L.) mexicana* in the New World. It is characterized by a primary lesion, which slowly spreads involving several areas of the skin. The inflammatory infiltrate displays a large number of highly parasitized and vacuolated macrophages, a histopathological characteristic also presented in the LCL caused by *L. (L.) amazonensis*; however, the intensity of the inflammatory process is lower than in ADCL, additionally in the histological section of the skin of patients with LCL it is possible to observe an inflammatory infiltrate characterized by both plasma cells and T lymphocytes, suggesting a better outcome than ADCL [32]. According to this, the results showed a high number of total macrophages in the ADCL, mainly the M2 subset, regarding the other clinical forms analyzed. In addition, it is possible to note that *L. (L.) amazonensis* is able to drive the infection from the center of the clinical spectrum that corresponds to the LCL towards the anergic pole of the infection spectrum that corresponds to the form of ADCL, which is one of the most severe clinical forms of leishmaniasis [24, 30]. Silveira et al. showed that

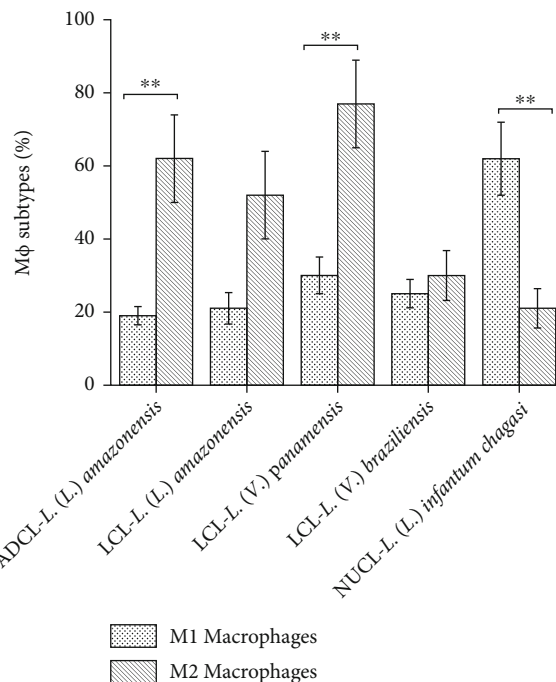


FIGURE 4: Percentage of M1 and M2 cells inside to total macrophages in the skin lesion of different clinical forms of American cutaneous leishmaniasis, anergic diffuse cutaneous leishmaniasis (ADCL) by *L. (L.) amazonensis*, localized cutaneous leishmaniasis (LCL) by *L. (L.) amazonensis*, *L. (V.) panamensis*, *L. (V.) braziliensis*, and nonulcerated cutaneous leishmaniasis (NUCL) by *L. (L.) infantum chagasi*.

ADCL represents the pole of cellular hyposensitivity, indicating that affected patients display cell-mediated immune responses incapable of controlling *Leishmania* spreading. Besides, ADCL patients have preferential activation of a Th2-type immune response resulting in the production of anti-inflammatory cytokines such as IL-4 and IL-10 [18, 19] which can be correlated with a large number M2 macrophages described in the present study. Similar results, high expression of M2 macrophages, were also observed in the anergic pole of leprosy, a chronic disease caused by *Mycobacterium leprae* that is characterized by the presence of vacuolated cells with variable amount of bacillus and development of Th2 immune response that stimulates a suppressive immune response [33].

On the other hand, patients with LCL caused by *L. (V.) panamensis* present ulcerated lesions and assembled a mixed cellular immune response, with the production of pro- and anti-inflammatory cytokines that is related to the pathology observed in this clinical form of the disease [34]. The inflammatory infiltrate in the LCL caused by this parasite is characterized by the presence of lymphocytes, macrophages, and plasma cells that have a correlation with a moderated size of the skin lesions and parasite density [35, 36]. Thus, in this study, a lower percentage of total macrophages was observed in LCL by *L. (V.) panamensis* than LCL by *L. (L.) amazonensis*. However, the results point to the predominance of M2 similar to that observed in the LCL caused by *L. (L.)*

amazonensis, suggesting that even with the presence of M1 macrophages, they are not enough to restrain parasite spreading.

The microenvironment in which macrophages are found provides different signals that activate them, leading to the development of functionally distinct macrophages. Therefore, the presence of Th2 lymphocytes producing IL-4, IL-10, and IL-13 cytokines in *L. (L.) amazonensis* and *L. (V.) panamensis* infections may stimulate the polarization macrophages toward the M2 subset, via activation of the enzyme arginase and production of urea and L-ornithine, favoring growth and survival of *Leishmania* in the macrophages and disease progression [1, 3, 37, 38]. The polarization of M2 macrophages in *Leishmania* infection can also be influenced by the parasite species [17]. Farrow et al. in an *in vitro* experimental study using *L. (L.) amazonensis* and *L. (L.) major* demonstrated that only M2 macrophages allow parasite growth. Besides, they showed that lipophosphoglycan (LPG) and gp63 from *Leishmania* surface act on M2 macrophages and suppresses the ncRNA genes leaving these cells permissive to infection [20]. In this sense, Lee et al. showed that the failure to cure the cutaneous lesion by *L. (L.) major* is related to an efficient interaction with M2 macrophages that facilitate the phagocytosis of the parasite suggesting that the preferential infection of this cell type plays a crucial role in the pathogenesis of the disease [21].

Regarding the LCL caused by *L. (V.) braziliensis*, our results did not show a statistical difference between M1 and M2 macrophages ($P > 0.05$). Despite the small number of macrophages present in these lesions, a similar number of M1 and M2 macrophages were observed. This finding can be associated to the characteristics of the inflammatory infiltrate presents in the lesion caused by *L. (V.) braziliensis* that is formed mainly by T lymphocytes and plasma cells, with a rare number of macrophages and scarce parasitism [18, 19]. Besides, patients have preferential activation of Th1 immune response, probably driven by parasite antigens [17], which is an important factor for controlling infection [39–43].

In NUCL caused by *L. (L.) infantum chagasi*, it was possible to identify a high density of M1 macrophages over M2, which could be associated to an efficient cellular immune response in the skin of patients. Such patients developed a robust response of CD8⁺ T lymphocytes and IFN- γ ⁺ cells [26, 44–46] that may control parasite spreading and polarize macrophages to a M1 pole. M1 macrophages have the ability to present antigens and produce and secrete proinflammatory cytokines; furthermore, these activated macrophages can kill *Leishmania* through toxic intermediates of nitrogen and oxygen. Remarkably, the M1 subset inhibits IL-10 production, favoring the development of Th1 lymphocyte response; thus, they are crucial for the elimination of *Leishmania* [2, 3, 6, 9–12, 38].

In post-Kala-azar Dermal Leishmaniasis (PKDL) caused by *L. (L.) donovani*, it was demonstrated that monocytes decreased the expression of TLR-2 and 4, as well as the production of reactive oxygen and nitrogen species. In addition, monocytes and intralesional macrophages presented high expression of CD206, arginase-1, and PPAR γ mRNA, suggesting that macrophage polarization follows to the M2 sub-

type, sustaining the chronicity in PKDL. However, after therapy, an immunological shift is observed, where macrophages display a profile of the M1 subset, suggesting that repolarization could be considered as a therapeutic approach [47].

Considering the percentage of M1 macrophages regarding the total of macrophage cells, a higher percentage of M1 cells in NUCL caused by *L. (L.) infantum chagasi* and a lower percentage of M1 cells in ADCL by *L. (L.) amazonensis* and LCL caused by *L. (L.) amazonensis* and *L. (V.) panamensis*. Interestingly, there were a considerable number of macrophages that was not characterized as M1 or M2 macrophages (Supplementary Table), suggesting that different subpopulations of macrophages could be related to the different clinical forms caused by different species of parasite. In this sense, depending on the stimulus, different subtypes of M2 macrophages can be observed. M2a subset can be induced by IL-4 or IL-13, M2b by immune complexes and IL-1, M2c by IL-10 and TGF- β , and M2d by TLR agonists [13, 20, 21, 38, 48–52]. Similarly, M1 macrophage subsets can also be categorized in M1a that is considered the classically activated macrophages and M1b the innate-activated macrophages, that is unable to fully develop into an M1a profile, failing to produce IL-12, an essential cytokine for triggering Th1 response [2].

Additionally, the M1:M2 ratio was lower than one in the skin lesions of ADCL patients, followed by LCL caused by *L. (L.) amazonensis* and *L. (V.) panamensis*, evidencing the preferential involvement of M2 macrophages in the more severe clinical form of infection (ADCL). However, the M1:M2 ratio in the skin lesions in NUCL caused by *L. (L.) infantum chagasi* was higher than one showing preferential involvement of M1 macrophages in the most benign clinical form of the disease. On the other hand, the ratio between M1 and M2 cells in LCL by *L. (V.) braziliensis* was close to one indicating a similar participation of these both cellular types in this skin lesion. These results correlate with the histopathological characteristics that may be responsible for differences in tissue parasitism and *in situ* cellular immune responses triggered by different species of parasites [18, 19, 26, 34].

5. Conclusions

Taking together, the results showed a polarization of the M1 and M2 macrophages according to the clinical forms of American cutaneous leishmaniasis with a predominance of M2 macrophages in the most severe clinical form, anergic diffuse cutaneous leishmaniasis caused by *L. (L.) amazonensis*, and a predominance of M1 macrophages in the most benign clinical form of disease, nonulcerated cutaneous leishmaniasis caused by *L. (L.) infantum chagasi*. The importance of the parasite species in the polarization of macrophage subpopulations must be considered.

Data Availability

The data used to support the findings of this study are available from the corresponding author upon request.

Conflicts of Interest

The authors declare that there is no conflict of interest regarding the publication of this paper.

Authors' Contributions

Carmen M. Sandoval Pacheco and Gabriela V. Araujo Flores equally contributed to this work.

Acknowledgments

We would like to thank to the Health Unit of the Municipality of Amapala Honduras, especially to Dr. Arnoldo Carranza (*in memoriam*) and Jessica Cardenas, to Hospital Santo Tomás and Instituto Conmemorativo Gorgas de los Estudios de la Salud, Panamá, to Parasitology Department, Evandro Chagas Institute, Brazil, and especially to Marliane Batista Campos for the sample collection and clinical and parasitological diagnosis. This study was supported by the Sao Paulo Research Foundation (FAPESP) grants #2014/50315-0, #2015/01154-7, #2017/24834-9, #2018/04698-6 and GVAF and CMSP Scholarship from CAPES (Social Demand) and Laboratório de Patologia de Moléstias Infecciosas (LIM50 HC-FMUSP). MDL is a research fellow from the National Research Council-CNPq, Brazil, grant #302174/2017-6.

Supplementary Materials

Supplementary 1: table–density of M1 and M2 macrophage subsets considering the total of macrophages and percentage of M1, M2, and non-M1/M2 macrophages in cutaneous leishmaniasis caused by different species of *Leishmania* parasites. (*Supplementary Materials*)

References

- [1] G. Arango Duque and A. Descoteaux, "Macrophage cytokines: involvement in immunity and infectious diseases," *Frontiers in Immunology*, vol. 5, p. 491, 2014.
- [2] F. O. Martinez, A. Sica, A. Mantovani, and M. Locati, "Macrophage activation and polarization," *Frontiers in Bioscience*, vol. 13, no. 13, pp. 453–461, 2008.
- [3] F. Tomiotto-Pellissier, B. T. S. Bortoleti, J. P. Assolini et al., "Macrophage polarization in Leishmaniasis: broadening horizons," *Frontiers in Immunology*, vol. 9, article 2529, 2018.
- [4] D. O. Adams, "Molecular interactions in macrophage activation," *Immunology Today*, vol. 10, no. 2, pp. 33–35, 1989.
- [5] C. F. Anderson and D. M. Mosser, "A novel phenotype for an activated macrophage: the type 2 activated macrophage," *Journal of Leukocyte Biology*, vol. 72, no. 1, pp. 101–106, 2002.
- [6] T. Lawrence and G. Natoli, "Transcriptional regulation of macrophage polarization: enabling diversity with identity," *Nature Reviews. Immunology*, vol. 11, no. 11, pp. 750–761, 2011.
- [7] D. M. Mosser, "The many faces of macrophage activation," *Journal of Leukocyte Biology*, vol. 73, no. 2, pp. 209–212, 2003.
- [8] P. J. Murray, J. E. Allen, S. K. Biswas et al., "Macrophage activation and polarization: nomenclature and experimental guidelines," *Immunity*, vol. 41, no. 1, pp. 14–20, 2014.
- [9] C. Guruvayoorappan, "Tumor versus tumor-associated macrophages: how hot is the link?," *Integrative Cancer Therapies*, vol. 7, no. 2, pp. 90–95, 2008.
- [10] A. Mantovani, A. Sica, S. Sozzani, P. Allavena, A. Vecchi, and M. Locati, "The chemokine system in diverse forms of macrophage activation and polarization," *Trends in Immunology*, vol. 25, no. 12, pp. 677–686, 2004.
- [11] J. G. Tidball and S. A. Villalta, "Regulatory interactions between muscle and the immune system during muscle regeneration," *American Journal of Physiology. Regulatory, Integrative and Comparative Physiology*, vol. 298, no. 5, pp. R1173–R1187, 2010.
- [12] N. G. Zanlucchi, P. F. Wolk, and P. Pinge Filho, "Macrophage polarization in Chagas disease," *Journal of Clinical and Cellular Immunology*, vol. 6, no. 2, 2015.
- [13] D. A. Chistiakov, Y. V. Bobryshev, N. G. Nikiforov, N. V. Elizova, I. A. Sobenin, and A. N. Orekhov, "RETRACTED: Macrophage phenotypic plasticity in atherosclerosis: the associated features and the peculiarities of the expression of inflammatory genes," *International Journal of Cardiology*, vol. 184, pp. 436–445, 2015.
- [14] Q. Wang, H. Ni, L. Lan, X. Wei, R. Xiang, and Y. Wang, "Fra-1 protooncogene regulates IL-6 expression in macrophages and promotes the generation of M2d macrophages," *Cell Research*, vol. 20, no. 6, pp. 701–712, 2010.
- [15] Y. Yao, X. H. Xu, and L. Jin, "Macrophage polarization in physiological and pathological pregnancy," *Frontiers in Immunology*, vol. 10, p. 792, 2019.
- [16] S. C. F. Mendonça, "Differences in immune responses against *Leishmania* induced by infection and by immunization with killed parasite antigen: implications for vaccine discovery," *Parasites and Vectors*, vol. 9, no. 1, p. 492, 2016.
- [17] F. T. Silveira, "What makes mucosal and anergic diffuse cutaneous leishmaniasis so clinically and immunopathologically different? A review in Brazil," *Transactions of the Royal Society of Tropical Medicine and Hygiene*, vol. 113, no. 9, pp. 505–516, 2019.
- [18] F. T. Silveira, R. Lainson, and C. E. Corbett, "Clinical and immunopathological spectrum of American cutaneous leishmaniasis with special reference to the disease in Amazonian Brazil: a review," *Memórias do Instituto Oswaldo Cruz*, vol. 99, no. 3, pp. 239–251, 2004.
- [19] F. T. Silveira, R. Lainson, C. M. de Castro Gomes, M. D. Laurenti, and C. E. P. Corbett, "Immunopathogenic competences of *Leishmania* (V.) *braziliensis* and *L. (L.) amazonensis* in American cutaneous leishmaniasis," *Parasite Immunology*, vol. 31, no. 8, pp. 423–431, 2009.
- [20] A. L. Farrow, T. Rana, M. K. Mittal, S. Misra, and G. Chaudhuri, "Leishmania-induced repression of selected non-coding RNA genes containing B-box element at their promoters in alternatively polarized M2 macrophages," *Molecular and Cellular Biochemistry*, vol. 350, no. 1-2, pp. 47–57, 2011.
- [21] S. H. Lee, M. Charmoy, A. Romano et al., "Mannose receptor high, M2 dermal macrophages mediate nonhealing *Leishmania* major infection in a Th1 immune environment," *The Journal of Experimental Medicine*, vol. 215, no. 1, pp. 357–375, 2018.
- [22] J. A. Díaz-Gandarilla, C. Osorio-Trujillo, V. I. Hernández-Ramírez, and P. Talamás-Rohana, "PPAR activation induces M1 macrophage polarization via cPLA2-COX-2 inhibition, activating ROS production against *Leishmania mexicana*," *BioMed Research International*, vol. 2013, Article ID 215283, 13 pages, 2013.

- [23] N. S. Vellozo, S. T. Pereira-Marques, M. P. Cabral-Piccin et al., "All-trans retinoic acid promotes an M1- to M2-phenotype shift and inhibits macrophage-mediated immunity to *Leishmania major*," *Frontiers in Immunology*, vol. 8, article 1560, 2017.
- [24] M. B. Campos, L. V. R. Lima, A. C. S. de Lima et al., "Toll-like receptors 2, 4, and 9 expressions over the entire clinical and immunopathological spectrum of American cutaneous leishmaniasis due to *Leishmania (V.) braziliensis* and *Leishmania (L.) amazonensis*," *PLoS One*, vol. 13, no. 3, p. e0194383, 2018.
- [25] K. Gonzalez, J. E. Calzada, R. Díaz et al., "Performance of immunohistochemistry as a useful tool for the diagnosis of cutaneous leishmaniasis in Panama, Central America," *Parasitology International*, vol. 71, pp. 46–52, 2019.
- [26] C. M. Sandoval Pacheco, G. V. Araujo Flores, A. Favero Ferreira et al., "Histopathological features of skin lesions in patients affected by non-ulcerated or atypical cutaneous leishmaniasis in Honduras, Central America," *International Journal of Experimental Pathology*, vol. 99, no. 5, pp. 249–257, 2018.
- [27] A. Sica and A. Mantovani, "Macrophage plasticity and polarization: *in vivo* veritas," *The Journal of Clinical Investigation*, vol. 122, no. 3, pp. 787–795, 2012.
- [28] T. H. Sulahian, P. Högger, A. E. Wahner et al., "Human monocytes express CD163, which is upregulated by il-10 and identical to p155," *Cytokine*, vol. 12, no. 9, pp. 1312–1321, 2000.
- [29] L. P. Carvalho, S. Passos, A. Schriefer, and E. M. Carvalho, "Protective and pathologic immune responses in human tegumentary leishmaniasis," *Frontiers in Immunology*, vol. 3, p. 301, 2012.
- [30] F. T. Silveira, S. R. Muller, A. A. A. de Souza et al., "Revisão sobre a patogenia da leishmaniose tegumentar americana na Amazônia, com ênfase à doença causada por *Leishmania (V.) braziliensis* e *Leishmania (L.) amazonensis*," *Revista Paraense de Medicina*, vol. 22, pp. 9–20, 2008.
- [31] C. Atri, F. Z. Guerfali, and D. Laouini, "Role of human macrophage polarization in inflammation during infectious diseases," *International Journal of Molecular Sciences*, vol. 19, no. 6, p. 1801, 2018.
- [32] F. T. Silveira, R. Lainson, J. J. Shaw, A. A. De Souza, E. A. Ishikawa, and R. R. Braga, "Cutaneous leishmaniasis due to *Leishmania (Leishmania) amazonensis* in Amazonian Brazil, and the significance of a negative Montenegro skin-test in human infections," *Transactions of the Royal Society of Tropical Medicine and Hygiene*, vol. 85, no. 6, pp. 735–738, 1991.
- [33] J. R. de Sousa, R. P. M. de Sousa, T. L. de Souza Aarão et al., "*In situ* expression of M2 macrophage subpopulation in leprosy skin lesions," *Acta Tropica*, vol. 157, pp. 108–114, 2016.
- [34] K. Gonzalez, J. E. Calzada, T. Y. Tomokane et al., "*In situ* study of cellular immune response in human cutaneous lesions caused by *Leishmania (Viannia) panamensis* in Panama," *Parasite Immunology*, vol. 43, no. 3, article e12801, 2020.
- [35] K. González, R. Diaz, A. F. Ferreira et al., "Histopathological characteristics of cutaneous lesions caused by *Leishmania Viannia panamensis* in Panama," *Revista do Instituto de Medicina Tropical de São Paulo*, vol. 60, article e8, 2018.
- [36] R. Restrepo, G. Caceres-Dittmar, F. J. Tapia, D. M. Isaza, and M. Restrepo, "Immunocytochemical and histopathologic characterization of lesions from patients with localized cutaneous leishmaniasis caused by *Leishmania panamensis*," *The American Journal of Tropical Medicine and Hygiene*, vol. 55, no. 4, pp. 365–369, 1996.
- [37] S. M. Muxel, J. I. Aoki, J. C. R. Fernandes et al., "Arginine and polyamines fate in *Leishmania* infection," *Frontiers in Microbiology*, vol. 8, article 2682, 2018.
- [38] L. Wang, S. Zhang, H. Wu, X. Rong, and J. Guo, "M2b macrophage polarization and its roles in diseases," *Journal of Leukocyte Biology*, vol. 106, no. 2, pp. 345–358, 2019.
- [39] O. Bacellar, H. Lessa, A. Schriefer et al., "Up-regulation of Th1-type responses in mucosal leishmaniasis patients," *Infection and Immunity*, vol. 70, no. 12, pp. 6734–6740, 2002.
- [40] T. M. Cardoso, Á. Machado, D. L. Costa et al., "Protective and pathological functions of CD8+ T cells in *Leishmania braziliensis* infection," *Infection and Immunity*, vol. 83, no. 3, pp. 898–906, 2015.
- [41] L. P. Carvalho, S. Passos, O. Bacellar et al., "Differential immune regulation of activated T cells between cutaneous and mucosal leishmaniasis as a model for pathogenesis," *Parasite Immunology*, vol. 29, no. 5, pp. 251–258, 2007.
- [42] C. I. de Oliveira and C. I. Brodsky, "The immunobiology of *Leishmania braziliensis* infection," *Frontiers in Immunology*, vol. 3, p. 145, 2012.
- [43] I. Follador, C. Araújo, O. Bacellar et al., "Epidemiologic and immunologic findings for the subclinical form of *Leishmania braziliensis* infection," *Clinical Infectious Diseases*, vol. 34, no. 11, pp. e54–e58, 2002.
- [44] G. V. Araujo Flores, C. M. Sandoval Pacheco, T. Y. Tomokane et al., "Evaluation of regulatory immune response in skin lesions of patients affected by nonulcerated or atypical cutaneous Leishmaniasis in Honduras, Central America," *Mediators of Inflammation*, vol. 2018, Article ID 3487591, 7 pages, 2018.
- [45] G. V. Araujo Flores, C. M. Sandoval Pacheco, W. H. Sosa Ochoa et al., "Th17 lymphocytes in atypical cutaneous leishmaniasis caused by *Leishmania (L.) infantum chagasi* in Central America," *Parasite Immunology*, vol. 42, no. 11, article e12772, 2020.
- [46] C. Sandoval, G. Araujo, W. Sosa et al., "*In situ* cellular immune response in non-ulcerated skin lesions due to *Leishmania (L.) infantum chagasi* infection," *Journal of Venomous Animals and Toxins including Tropical Diseases*, vol. 27, 2021.
- [47] D. Mukhopadhyay, S. Mukherjee, S. Roy et al., "M2 polarization of monocytes-macrophages is a Hallmark of Indian post Kala-Azar dermal Leishmaniasis," *PLoS Neglected Tropical Diseases*, vol. 9, no. 10, article e0004145, 2015.
- [48] A. Mantovani, S. Sozzani, M. Locati, P. Allavena, and A. Sica, "Macrophage polarization: tumor-associated macrophages as a paradigm for polarized M2 mononuclear phagocytes," *Trends in Immunology*, vol. 23, no. 11, pp. 549–555, 2002.
- [49] N. Wang, H. Liang, and K. Zen, "Molecular mechanisms that influence the macrophage M1-M2 polarization balance," *Frontiers in Immunology*, vol. 5, 2014.
- [50] C. D. Mills, "M1 and M2 macrophages: oracles of health and disease," *Critical Reviews in Immunology*, vol. 32, no. 6, pp. 463–488, 2012.
- [51] A. Shapouri-Moghaddam, S. Mohammadian, H. Vazini et al., "Macrophage plasticity, polarization, and function in health and disease," *Journal of Cellular Physiology*, vol. 233, no. 9, pp. 6425–6440, 2018.
- [52] D. Zhou, C. Huang, Z. Lin et al., "Macrophage polarization and function with emphasis on the evolving roles of coordinated regulation of cellular signaling pathways," *Cellular Signalling*, vol. 26, no. 2, pp. 192–197, 2014.

Research Article

Effect of Prophylactic Vaccination with the Membrane-Bound Acid Phosphatase Gene of *Leishmania mexicana* in the Murine Model of Localized Cutaneous Leishmaniasis

María Angélica Burgos-Reyes, Lidia Baylón-Pacheco, Patricia Espiritu-Gordillo, Silvia Galindo-Gómez, Víctor Tsutsumi, and José Luis Rosales-Encina 

Departamento de Infectómica y Patogénesis Molecular, Centro de Investigación y de Estudios Avanzados del Instituto Politécnico Nacional, México City, Mexico

Correspondence should be addressed to José Luis Rosales-Encina; ros-tal@hotmail.com

Received 18 December 2020; Revised 20 March 2021; Accepted 30 March 2021; Published 10 April 2021

Academic Editor: Márcia Laurenti

Copyright © 2021 María Angélica Burgos-Reyes et al. This is an open access article distributed under the Creative Commons Attribution License, which permits unrestricted use, distribution, and reproduction in any medium, provided the original work is properly cited.

Leishmaniasis is a disease caused by an intracellular protozoan parasite of the genus *Leishmania*. Current treatments for leishmaniasis are long, toxic, and expensive and are not available in some endemic regions. Attempts to develop an effective vaccine are feasible, but no vaccine is in active clinical use. In this study, the LmxMBA gene of *Leishmania mexicana* was selected as a possible vaccine candidate using the reverse vaccinology approach, and the prophylactic effect generated by DNA vaccination with this gene in a murine model of cutaneous leishmaniasis was evaluated. The results showed that prophylactic vaccination with pVAX1::LmxMBA significantly reduced the size of the lesion and the parasitic load on the footpad, compared to the control groups. At a histological level, a smaller number of parasites were evident in the dermis, as well as the absence of connective tissue damage. Mice immunized with plasmid pVAX1::LmxMBA induced immunity characterized by an increase in the IgG2a/IgG1 > 1 ratio and a higher rate of lymphocyte proliferation. In this study, immunization with the plasmid promoted an improvement in the macroscopic and microscopic clinical manifestations of the experimental infection by *L. mexicana*, with a T helper 1 response characterized by an IgG2a/IgG1 > 1 ratio and high lymphoproliferative response. These findings support immunization with the plasmid pVAX1::LmxMBA as a preventive strategy against cutaneous infection of *L. mexicana*.

1. Introduction

Leishmaniasis is an endemic disease in 97 countries and is considered a neglected tropical disease. A total of 1 billion people living in endemic areas are at risk of acquiring the disease, and it is estimated that there are at least 12 million cases of the various forms of leishmaniasis worldwide [1–3]. Cutaneous leishmaniasis (CL) caused by *L. mexicana*, *L. amazonensis*, *L. major*, and *L. braziliensis* is the most common form of leishmaniasis [4]. Visceral leishmaniasis (VL) caused by *L. donovani* and *L. infantum* is the most severe and fatal disease [5].

The immune cell response is essential in the control of *Leishmania* infection. The development of specific T helper 1 (Th1) response, based on the production of proinflamma-

tory cytokines, such as interferon-gamma (IFN- γ), interleukin 12 (IL-12), and tumor necrosis factor-alpha (TNF- α), can protect mammalian hosts from infection by the parasites. In contrast, a Th2 response supports the persistence of parasites and can cause an active disease [6, 7]. Over the past years, studies have been developed to identify new candidates for the prevention of leishmaniasis and generate protective immunity [8–10]. However, there is still no effective prophylactic vaccination against human disease. First-generation vaccines with attenuated parasites concern potential reversion to virulence and raise a risk of reversion to clinical disease in immunocompromised individuals. On the other hand, second-generation vaccines might induce mainly humoral responses and are poorly immunogenic when administered without the association of adjuvants [8, 11, 12].

Another approach is the use of antigen-encoding plasmid DNA as an efficient and practical method of antigen delivery and as induction of a protective immune response against various intracellular pathogens [13–15]. DNA vaccines have been used in experiments against human immunodeficiency virus, tuberculosis, Chagas disease, and leishmaniasis [16–23]. These plasmids contain cytosine-phosphate-guanosine (CpG) motifs, which bind and activate toll-like receptor 9 (TLR9), thus triggering the innate immune response and subsequent development of adaptive immunity, inducing the development of the Th1 response [24, 25]. In this context, this vaccination technology plays a promising role in the development of new candidates against CL, which requires Th1 cell immunity.

In the present work, the prophylactic potential of an intramuscular injection of plasmid DNA encoding the LmxMBA protein (membrane-bound acid phosphatase of *Leishmania mexicana*) was evaluated in BALB/c mice. Immunoinformatic tools selected the *L. mexicana* membrane-bound acid phosphatase (XP_003874608.1). LmxMBA protein was identified in the *L. mexicana* promastigote and amastigote stages by antibodies from mice immunized with recombinant protein. Due to the high conservation found in the amino acid sequence of this protein in different *Leishmania* species, the extramembrane region was cloned, purified, and evaluated as a DNA vaccine candidate in BALB/c mice against infection caused by this parasite. The vaccine efficacy was evaluated by measuring the size of the lesion in the footpad, the parasite load, and histopathological analysis of the lesion.

2. Materials and Methods

2.1. Cell Culture. *L. mexicana* promastigotes, strain MHOM/MX/92/UADY68, were axenically cultured at 28°C in RPMI-1640 medium (GIBCO), pH 7.4, supplemented with 10% fetal bovine serum and antibiotics (100 IU/ml penicillin and 50 µg/ml streptomycin).

2.2. Animals. Female BALB/c mice (4–6 weeks old) were provided by the Animal Production and Experimentation Unit (UPEAL-CINVESTAV) following the specifications of the Mexican National Norm (NOM-062-ZOO-1999) that is a version of the *Guide for the Care and Use of Laboratory Animals* 2011. The research protocol (no. 0216-16) was approved by CINVESTAV's Institutional Animal Care and Use Committee (CINVESTAV-IACUC).

2.3. In Silico Analysis. *L. mexicana* annotated proteins from the TriTryp databases consisted of 8250 open reading frames (ORFs) (TriTrypDB-6.0_LmexicanaMHOMGT2001U1103_AnnotatedProteins). The ORFs were analyzed for the identification of signal peptides and transmembrane helices by TMHMM (<http://www.cbs.dtu.dk/services/TMHMM/1>) and TOPCONS (<http://topcons.cbr.su.se/>). The expression sequence tags (EST) and mass spectrometry (MS) data from the TriTryp site (<https://tritrypdb.org/tritrypdb/>) were examined to define the expressed transmembrane proteins. Consensus subcellular localization was determined by Euk-

mPloc (<http://www.csbio.sjtu.edu.cn/bioinf/euk-multi-2/>), LocTree3 (<https://roslab.org/services/loctree3/>), DeepLoc (<http://www.cbs.dtu.dk/services/DeepLoc/>), and CELLO (<http://cello.life.nctu.edu.tw/>). Fold change in expressed genes between promastigotes, axenic amastigotes, and macrophage-derived amastigotes was identified based on RNA Seq Evidence (Transcriptomic in <https://tritrypdb.org/tritrypdb/>).

2.4. Construction of Recombinant Plasmids. The eukaryotic expression vector pVAX1 (Invitrogen, Carlsbad, CA, USA) and the bacterial expression vector pCR4-TOPO (Invitrogen, Carlsbad, CA, USA) were chosen to clone and express the LmxMBA gene. Briefly, the 1337 bp DNA fragment containing the LmxMBA gene (GenBank No. XM_003874559.1, sequence positions 94–1431), lacking the transmembrane regions, was obtained by polymerase chain reaction (PCR) (Thermal Cycler spp., Thermo Fisher Scientific) using the genomic DNA of *L. mexicana* promastigotes as the template and the primers LmxMBA F *HindIII* (5'-AAGCTTTCGCCA CCATGGACAAGGTGGAGCTGGTGCAG-3') and LmxMBA/R *EcoRI* (5'-CACGAATTCCTTACCCGCCGCTGGACATGGGCGAC-3'). The PCR reaction contained 1 µg of template, 2 mM MgCl₂, 0.2 mM of each dNTP, 1x PCR buffer, and 2.5 U of Taq DNA polymerase. PCR conditions involved initial denaturation at 94°C for 5 min, 35 cycles of primer annealing at 94°C for 1 min, 65°C for 30 s, and 72°C for 1 min and a final extension at 68°C for 7 min. The amplified fragment was purified (QIAEX II, Invitrogen, Carlsbad, CA USA), cloned into pCR4-TOPO vector and subcloned into pVAX1. The recombinant plasmid pVAX1::LmxMBA was confirmed by double restriction enzyme digestion (*HindIII/EcoRI*) and DNA sequencing.

The prokaryotic expression vector pRSET A (Invitrogen, Carlsbad, CA, USA) was chosen to clone and express the recombinant protein LmxMBA. The primers used were LmxMBAP/F *BamHI* (5'-CGGATCCTACAAGGTGGA GCTGGTGCAGGTG-3') and LmxMBAP/R *HindIII* (5'-GAAATATAAGCTTACCCGCCGCTGGACATGGGCG AC-3'). The content reaction and conditions of PCR reaction were previously described [26]. The amplified fragment was purified and inserted into the *BamHI* and *HindIII* restriction sites of pRSET A, obtaining the recombinant plasmid pRSETA::LmxMBA. The construct was sequenced to confirm the correct sequence of the gene after PCR and correct insertion of the gene in frame with the ATG of the plasmid.

2.5. DNA Purification. Plasmid pVAX1::LmxMBA was maintained and propagated in *E. coli* DH5. Endotoxin-free plasmid DNA was purified by anion-exchange chromatography using a PureLink™ HiPure Plasmid DNA Purification Kit (Invitrogen) according to instructions from the manufacturer, and DNA used for immunizations was resuspended in PBS pH 7.4. After purification, plasmid concentration was determined by absorbance at 260 nm and 280 nm. The OD 260/280 ratios for purified DNA were 1.8–2.0, indicating that preparations were free of major protein contamination.

2.6. Purification Recombinant Protein. To obtain the recombinant protein LmxMBA, *E. coli* BL21 pLysS cells were transformed with the recombinant plasmid pRSETA::LmxMBA and grown in Luria Bertani medium to an optical density of 0.6 at 540 nm. Cells were induced by incubation with 0.1 mM IPTG at 37°C/2 h. The cells were then harvested by centrifugation, washed in ice-cold 50 mM Tris HCl-buffer (pH 7.5), and suspended in extraction buffer (50 mM Tris HCl-buffer (pH 7.5), 150 mM NaCl, 10 mM MgCl₂, 5 mM B-mercaptoethanol, 3 M guanidinium chloride, and 2 M urea). After disruption by sonication, the crude extract was clarified by centrifugation at 30,000 × g for 30 min. The rLmxMBA was expressed as a fusion protein with an N-terminus six-histidine-residue affinity tag and was purified, under denatured conditions by affinity chromatography using Ni-agarose resin (Qiagen, Hilden, DE) according to the manufacturer instructions. The collected protein was dialyzed for 48 h at 4°C against PBS.

2.7. Anti-rLmxMBA Antibodies. The recombinant protein LmxMBA (rLmxMBA) was obtained as described above, and female BALB/c mice were immunized with 10 µg/dose. Animals received only two intraperitoneal (i.p.) doses with 15 days of interval; the immunization doses were administered in TiterMax adjuvant (1 : 1 mixture) (Sigma, St. Louis, MO, USA), and 30 days after the immunization scheme, mice were bled by cardiac puncture to obtain immune sera.

2.7.1. Expression of LmxMBA Antigen In Vitro. Mammalian cells were transfected with pVAX1::LmxMBA, using the XtremeGENE HP Transfection Reagent (Roche Diagnostics, Penzberg, DE), according to the manufacturer's instructions. The HeLa transfected cells were harvested 72 h later and washed three times with PBS. Total RNA was extracted with the TRIzol reagent (Invitrogen, Carlsbad, CA, USA). Complementary DNA (cDNA) was derived from RNA with the SuperScript™ First-Strand Synthesis System (Invitrogen, Carlsbad, CA, USA). LmxMBA cDNA was amplified by PCR using specific primers LmxMBA/F and LmxMBA/R, as described above. The amplified products were analyzed on a 1% agarose gel. In addition, the expression of LmxMBA was evaluated by immunoblotting of transfected cells. Glyceraldehyde-3-phosphate dehydrogenase (GAPDH) was used as a housekeeping control gene. The primers used were GAPDH/F (5'-GGTGCTAAGCAGTTGGTGGT-3') and GAPDH/R (5'-GAGTCAACGGATTTGGTCGT-3').

2.8. SDS-PAGE and Immunoblotting. Proteins were resolved on 12% SDS-PAGE and either visualized by Coomassie blue or electrophoretically transferred onto a nitrocellulose membrane for immunoblotting. Anti-histidine antibodies at 1 : 1000 dilution and anti-rLmxMBA antibodies at 1 : 200 dilution were used as primary antibodies in TBST (150 mM NaCl, 0.5% Tween 20, 2% skim milk, and 10 mM Tris HCl pH 7.4). Bound antibodies were detected using alkaline phosphatase-conjugated goat anti-mouse IgG (Zymed Labs, San Francisco, CA) diluted at 1 : 5000, and the blot was developed with NBT and BCIP (Invitrogen, Carlsbad, CA, USA).

2.9. Immunofluorescence Microscopy. *L. mexicana* promastigotes and amastigotes were washed 3 times in PBS and fixed in 4% paraformaldehyde (PFA) in filtered PBS pH 7.4 for 15 min at room temperature (RT). Following an additional PBS wash, the cells were resuspended in filtered PBS and then left to sediment and adhere to the surfaces glass slides for 30 min at RT. The fixed cells were permeabilized with cold methanol for 5 min and then labeled with mouse polyclonal anti-LmxMBA diluted 1 : 100 in PBS. A secondary FITC-conjugated goat anti-mouse IgG antibody was used for fluorescent detection of the LmxMBA protein. Slides were mounted with Vectashield and DAPI (4',6'-diamino-2-phenylindole).

2.10. Mouse Immunization and Experimental Infection. Four- to six-week-old female BALB/c mice (30 in total) were immunized intramuscularly. Plasmids were prepared as described and then dissolved in sterile PBS (pH 7.4) as DNA vaccines for immunization. Mice were divided randomly into three different groups of ten animals per group: one group was vaccinated with 100 µg of pVAX1::LmxMBA plasmid/per mice, and as controls, one group was vaccinated with the empty plasmid, pVAX1, and another was not immunized (PBS). A three-dose immunization scheme at 15-day intervals followed by parasite challenge was adopted.

Two weeks after the last immunization, the mice of each group were challenged at the right footpad subcutaneously. Cultured promastigotes were collected, centrifuged at 350 g/5 min, washed three times with PBS, and counted in a Neubauer chamber. The inoculum was prepared in a total volume of 25 µl of PBS containing 5 × 10⁶ promastigotes. The lesion size was determined weekly by measuring the thickness of the infected and healthy footpads, using a Vernier caliper, and calculating the size difference between the paw pads. The animals were sacrificed 105 days after infection, and the hind legs were amputated at the level of the subtalar joint to obtain skin tissue from the footpad. Mice were bled by cardiac puncture, and the spleens were collected for immunological purposes.

2.11. Determination of the Weight of Lesions and Parasite Burden. The parasite burden was quantified in skin tissue by limiting dilution culture [27]. Briefly, hind paws (infected and healthy) were removed aseptically and submerged in 3% ionized alcohol for up to 3 minutes to allow decontamination. The paws were weighed individually, and the difference between the infected and healthy paws of each mouse was taken as the net weight of the lesion. Skin sections of the footpad were obtained (approximately 20 mg), macerated in Eppendorf tubes with 1 ml of RPMI 1640 medium culture (medium containing 10% heat-inactivated SFB, 100 IU/ml penicillin, and 0.1 mg/ml streptomycin), and diluted with the same medium at a final concentration of 1 mg/ml. The material was tenfold serially diluted in RPMI 1640 medium supplemented with 10% FBS and cultured into 96-well flat-bottom plates, in duplicate. The plates were incubated at 26°C and observed under an inverted microscope (Nikon Diaphot, Nikon, Japan) every 3 days, up to a maximum of 20 days, to record the dilutions containing promastigotes.

The presence of mobile promastigotes was recorded at day 20 in each well, and the concentration of parasites per milligram of tissue was calculated as the reciprocal of the highest dilution that was positive for parasites. The total parasite load of the lesion was calculated with reference to the weight of the lesion. Each positive result is expressed as the log₁₀ number of promastigotes on the graph.

2.12. Cell Proliferation Assay. Mouse splenocytes were prepared as follows [28]. Spleens were taken from immunized/-challenge mice and control animals under sterile conditions, dissected, and resuspended in sterile, cold PBS (pH 7.4) containing FBS 2%. RBCs were disrupted with lysis buffer, and the single-cell suspensions were adjusted to 2×10^6 cells/ml with RPMI 1640 (HyClone, Logan, UT) containing 10% FBS. The diluted cell suspensions (100 μ l/well) were dispensed into 96-well flat-bottom culture plates (Thermo Fisher Scientific, Rochester, NY) and restimulated with 10 μ g/ml of rLmxMBA protein. Concanavalin A (2 μ g/ml), unstimulated wells, and complete culture medium were used as positive, negative, and blank controls, respectively. Each splenocyte sample was plated in triplicate. The proliferative response was measured by WST-1 (Roche Diagnostics, Mannheim, DE) according to fabricant instruction. After 72 h of culture, 10 μ l of WST-1 was added to each well and incubation continued for 4 h at 37°C and 5% CO₂. Following incubation, plates were read at 450 nm. The stimulation index (SI) was calculated as the ratio of average OD value of wells containing antigen-stimulated cells to average OD of wells containing only cells with the medium.

2.13. Histological Analysis. Slices taken from the skin of the footpad were rinsed with PBS and fixed with 10% formaldehyde for 24 h. Fixed sections were embedded in paraffin, sectioned (6 μ m), and stained with hematoxylin-eosin. The presence of amastigotes and histopathological alterations were examined under a light microscope (Nikon Eclipse 80i, Nikon, Japan). Semiquantification of parasites per field was expressed in ranges of parasites observed in 10 consecutive fields of the microscope under the 100x objective. At least 100 microscopic fields were examined before a sample was reported as negative.

2.14. Isotyping of Antibodies. The IgG1, IgG2a, IgG2b, IgG3, IgA, and IgM immunoglobulins from DNA-vaccinated mice were evaluated by indirect ELISA assays. Blood samples were collected ($n = 10$ animals/group) from the immunized mice 105 days after the infection. The sample was centrifuged for serum preparation. The 96-well microplates (Thermo Fisher Scientific, Rochester, NY) were coated with rLmxMBA (2 μ g/ml) in 100 mM carbonate-bicarbonate buffer (pH 9.6) and incubated overnight at 4°C. Plates were washed with PBS-0.05% Tween 20 (PBST) and incubated for 2 h at 37°C with blocking solution (PBS containing 5% skim milk). After washing with PBST, diluted serum samples (1 : 100) in PBST were added to each well and incubated at 37°C for 1 h and washed 3 times after the reaction. As a negative control, a pool of preimmune sera was used in all experiments. For isotyping, the plates were incubated with peroxidase-labeled

goat anti-mouse isotype antibodies (Abcam, Cambridge, UK) at 1 : 10000 dilution in PBS-T for 2 h at RT and then washed 4 times with PBST and PBS. The peroxidase activity was developed by 3-ethylbenzthiazoline-6-sulfonic acid (ABTS) substrate, and the optical density (OD) was read at 405 nm in an ELISA microplate reader (LabSystem Multiskan MS).

2.15. Statistical Analysis. The results were expressed as means \pm standard errors of the mean (SEM). All data in the study were compared using the Statistical Package for the Social Sciences (SPSS) 23.0 Data Editor (SPSS Inc., Chicago, Illinois, USA). Statistical analysis was performed using one-way analysis of variance (ANOVA) followed by a Tukey post hoc test to identify significantly different groups. Differences were considered statistically significant when the p value was <0.05 .

3. Results

3.1. Bioinformatic Analysis. We carried out a bioinformatic analysis of the *L. mexicana* ORF database to identify new proteins as potential candidates for the development of a vaccine. The main criterion was to select plasma membrane proteins. Analysis of the 8250 ORFs by using TMHMM [29] and TOPCONS [30] showed that 1543 proteins had transmembrane helices, and of the latter, 186 had the signal peptide. These membrane proteins were type I (112 proteins) and type III (74 proteins). Examination of the EST and MS/Tri-TrypDB databases indicated that 50 type I transmembrane proteins were expressed, and they presented the following subcellular location: 13 excreted, 7 in mitochondria, 8 in plasma membrane, 3 excreted/plasma membrane, 7 in endoplasmic reticulum, and 12 in various locations [31–34]. The transcriptomic analysis of the plasma membrane and plasma membrane-excreted proteins showed that the membrane-bound acid phosphatase is expressed at the same level in axenic amastigotes, macrophage-derived amastigotes, and promastigotes as compared with other proteins (Figure 1).

3.2. LmxMBA Localization in *Leishmania mexicana*. The subcellular location of LmxMBA was investigated in promastigotes and amastigotes by indirect immunofluorescence. Permeabilized and nonpermeabilized cells were incubated with the polyclonal anti-LmxMBA antibody, followed by a secondary antibody conjugated to FITC (green). As shown in Figure 2, green fluorescence was associated with the base of the flagellum in both permeabilized and nonpermeabilized promastigotes. Permeabilized promastigotes also showed green fluorescence between the nucleus and the kinetoplast. In amastigotes, green fluorescence was associated mainly towards one end of the parasite membrane.

3.3. LmxMBA Expression in Mammalian Cells. The recombinant plasmid pVAX1::LmxMBA was constructed to investigate the potential of the LmxMBA gene as a prophylactic DNA vaccine, in response to cutaneous leishmaniasis in the murine model. To ensure that LmxMBA could indeed be transcribed in mammalian cells, the presence of specific mRNA was established by RT-PCR from total RNA isolated

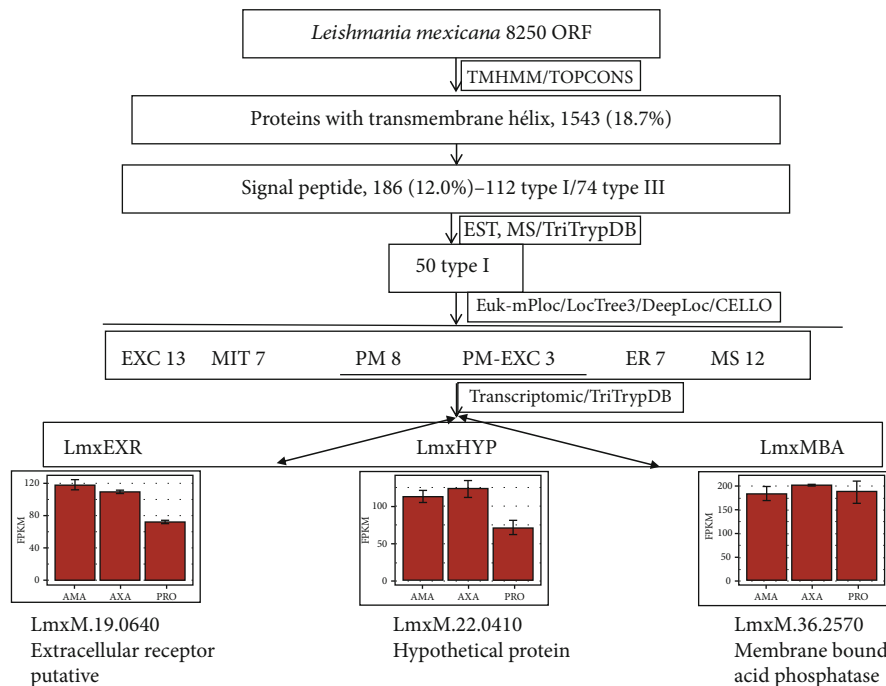


FIGURE 1: Strategy to identify putative vaccine candidates in *L. mexicana*. Abbreviations: EXC: excreted; MIT: mitochondria; PM: plasma membrane; ER: endoplasmic reticulum; MS: multiple sites.

from HeLa cells transfected with plasmid encoding the LmxMBA protein. RT-PCR showed amplification products at 400 bp for GAPDH in all the groups of cells (Figure 3(a)), while only the pVAX1::LmxMBA transfected cells showed amplification of the LmxMBA mRNA at 1337 bp, not so in untransfected cells or transfected with the empty vector (Figure 3(a)). In addition, the LmxMBA protein was detected in lysates of HeLa cells transfected with the plasmid encoding that protein by western blotting analysis (Figure 3(b)). The expected MW for LmxMBA protein is 49 kDa, and possibly, the lower and higher bands are degradation product and protein aggregate of the same protein, respectively.

3.4. Effect of DNA Vaccination on Lesion Development. Weekly measurements followed lesion development, and the lesion size kinetics showed that infection caused a progressive increase in footpad swelling in all mice from control groups. Mice immunized with plasmid encoding LmxMBA gene showed a delayed increase in lesion diameter compared to control mice, immunized with PBS ($p < 0.0001$) or pVAX1 ($p < 0.05$). In addition, statistical significance in the size of the lesion was found from 60 to 105 days after infection compared to the group immunized with PBS ($p < 0.0001$) and with pVAX1 ($p < 0.05$). Vaccination of mice with the empty plasmid pVAX1 showed continuous growth of the lesion at a slower rate than that observed in mice immunized with PBS ($p < 0.05$) (Figure 4(a)).

3.5. Determination of Parasite Load. There was a good correlation between lesion sizes and parasite loads. A significantly lesser amount of parasites was observed in footpad lesions of

mice vaccinated with pVAX1::LmxMBA plasmid, compared to the control groups inoculated with the empty vector ($p < 0.001$) or PBS ($p < 0.0001$). The footpad of mice immunized with the recombinant plasmid also showed lower lesion weights at 105 days compared to control mice immunized with PBS ($p < 0.01$) and compared to the group immunized with pVAX1. No statistically significant differences were found ($p > 0.05$) (Figures 4(b) and 4(c)).

3.6. Histopathological Study. Histopathological study showed a lesser amount of parasites in the tissue skin of mice immunized with the plasmid pVAX1::LmxMBA (Figure 5). 80% of the animals were negative in the microscopic examination of amastigotes, and the remaining 20% showed few parasites (0-20 per field) in the dermis. Mice immunized with PBS or with the empty plasmid, pVAX1, showed a high number of amastigotes (>200 per field) at the site of inoculation (Figures 5(a) and 5(b)). Besides, an infiltrate of inflammatory cells occupying the dermis and hypodermis with the presence of multiparasitic vacuolated macrophages was observed. A disorganized dermal region was also observed, with loss of normal morphology, filled by an intense infiltrate, rich in polymorphonuclear and mononuclear cells (Figures 5(a) and 5(b)). Mice immunized with the empty plasmid pVAX1 showed fewer vacuolated macrophages compared to nonimmunized mice. However, highly parasitized nonvacuolated macrophages were observed in mice immunized with the empty vector.

In contrast, immunized mice with pVAX1::LmxMBA plasmid showed a lower amount of parasitic structures per macrophage at the site of the lesion. The lesion of these animals showed a lower frequency of parasitized macrophages

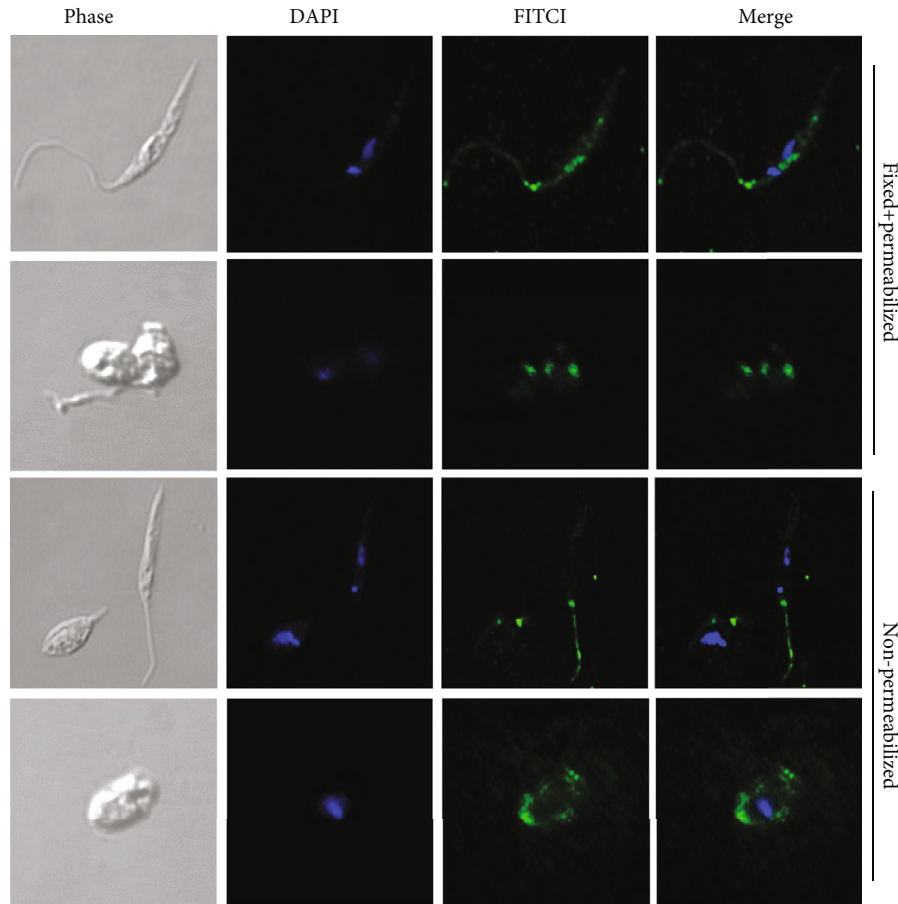


FIGURE 2: Subcellular localization of LmxMBA protein in *L. mexicana* promastigotes and amastigotes. Immunofluorescence microscopy utilizing serum anti-LmxMBA and secondary antibody coupled to FITC; nucleus and kinetoplast were marked with DAPI.

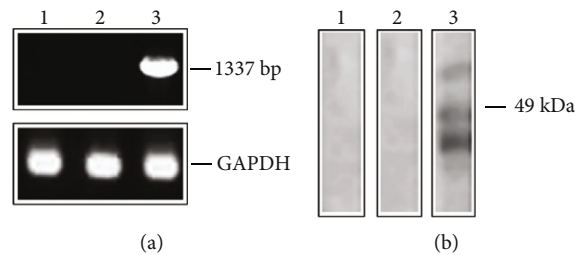


FIGURE 3: Expression of LmxMBA in transfected human HeLa cells. Nontransfected HeLa cells (1) and transfected with pVAX1 (2) or with pVAX1::LmxMBA (3) were assayed by RT-PCR (a) and immunoblotting (b) for the expression of LmxMBA 48 h posttransfection.

(20%) or total absence of them (80%) (Figure 5(c)). Vaccination with pVAX1::LmxMBA plasmid showed the typical histological characteristic in the infected footpad; a dermis with abundant collagen fibers was observed by microscopic examination, similar to control tissue (Figure 5(d)). Although there was still a mild inflammatory infiltrate in the dermis of some animals (30%) (including those with a low number of parasites per field), no damage or loss of the tissue microarchitecture was observed.

3.7. Lymphocyte Proliferation Assay. To further investigate the cellular immune response elicited by immunization with

pVAX1::LmxMBA, cellular proliferation assays were performed. As shown in Figure 6, mice immunized with pVAX1::LmxMBA induced a greater antigen-specific cell proliferation response, in contrast to the control groups ($p < 0.05$). This showed the ability of LmxMBA to induce spleen cell proliferation as a maker of memory T cell immune responses whereas no significant difference was observed between pVAX1 and PBS groups ($p > 0.05$).

3.8. Isotyping of Antibodies. In order to investigate the phenotype (Th1/Th2 pattern) of immune response elicited by immunization of pVAX1::LmxMBA, the isotype of

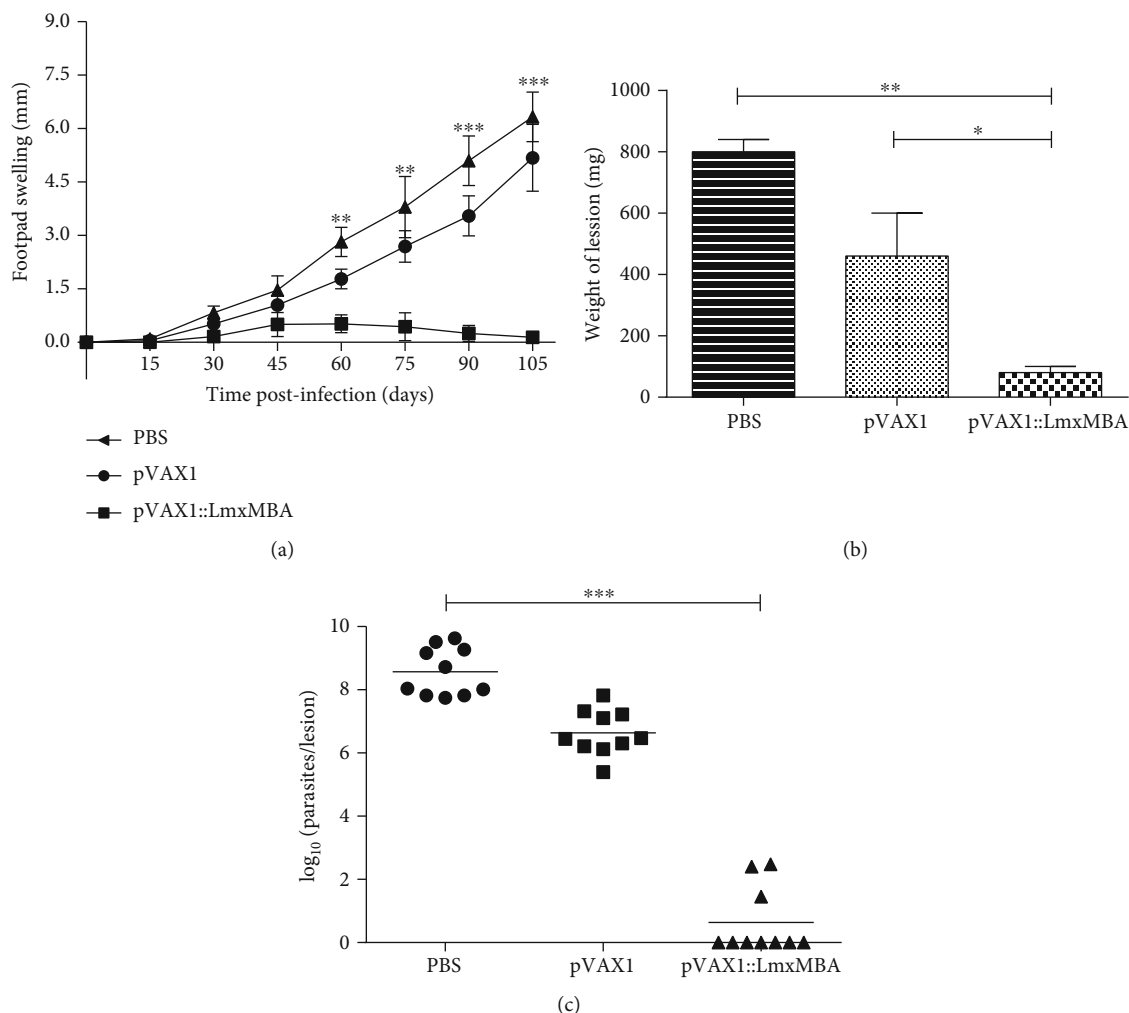


FIGURE 4: Footpad swelling (a), weight of lesions (b), and parasite burden (c) in BALB/c mice immunized and challenged with promastigotes of *L. mexicana*. Mice were immunized three times (intervals of 15 days between doses) with pVAX1::LmxMBA, pVAX1, or PBS. The results are expressed as means \pm standard errors of the mean (SEM) of ten mice per group (a). The weight of the lesion was determined by amputation of the paw 105 days after the infection; the difference between the infected and healthy paws was taken as the net weight of the lesion (b). The number of parasites in the lesion was determined by limiting dilution culture, and the results are expressed as \log_{10} (c). * $p < 0.05$.

antibodies was analyzed by an indirect ELISA method. As shown in Figure 7, anti-LmxMBA IgG+M+A values were significantly lower than the PBS control group ($p < 0.01$), and there was no statistically significant difference with the pVAX1 control group ($p > 0.05$). When comparing the immunoglobulin isotype levels from different groups of mice, we observed a low level of IgG1 in animals immunized with pVAX1::LmxMBA and the highest level in the control group immunized with PBS ($p < 0.001$) and pVAX1 ($p < 0.05$). On the other hand, a statistically significant difference in IgG2a levels was detected between mice immunized with pVAX1::LmxMBA and control mice, pVAX1 ($p < 0.001$) or PBS ($p < 0.001$). In all groups of mice, the levels of IgG3 and IgA remained low. The IgG2a/IgG1 ratio was >1 and higher in immunized mice with pVAX1::LmxMBA compared to control mice, PBS ($p < 0.05$) or pVAX1 ($p < 0.05$). This ratio does not differ significantly between mice immunized with PBS and pVAX1 ($p > 0.05$) (Figure 7).

4. Discussion

The control of leishmaniasis through vaccination is an increasing challenge. Although several attenuated and protein-based vaccines have protected against different species of *Leishmania* in different animal models, some of them have intrinsic disadvantages, such as the risk of reversion to virulence and the selection and use of adjuvants, respectively [8, 10, 34]. Vaccination with plasmid DNA is an active area of research applied to cancer and microbial pathogens associated with intracellular infections [19, 35]. DNA vaccines have been reported to persist in skeletal muscle for at least 19 months and are easy to produce in high purity [36, 37]. DNA vaccines are temperature stable (room temperature 2 to 8°C) over extended periods, enabling easier shipping and storage and allows to dispense with the cold chain used in conventional vaccines [37, 38]. Several plasmids used as DNA vaccines are stable for more than 3 years at 4°C, at least

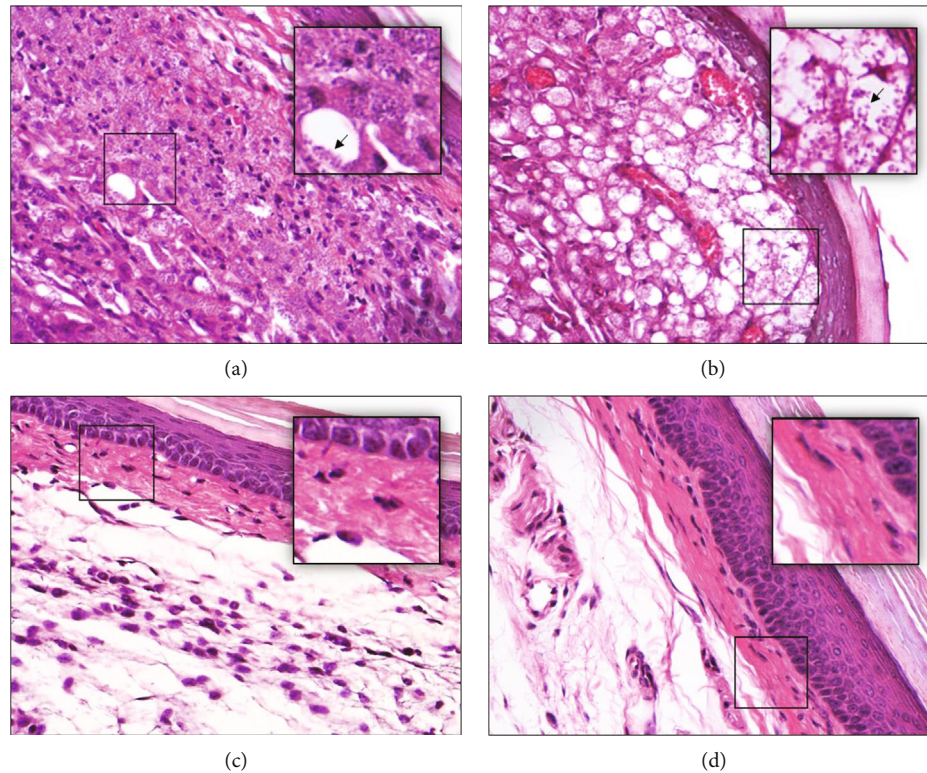


FIGURE 5: Histopathological analysis of the footpad of mice immunized with pVAX1::LmxMBA and challenged with promastigotes of *L. mexicana*. Tissues were collected 105 days after infection, and the sections were stained with hematoxylin and eosin. Vacuolated macrophages containing amastigotes were abundant in footpad lesions of mice immunized with PBS (b), as compared with mice immunized with the empty vector, pVAX1 (a); the dermis of control animals showed a massive infiltration with parasitized macrophages (arrows). In contrast, mice immunized with pVAX1::LmxMBA displayed more preserved skin with lymphocytes and macrophages containing few or no parasites (c). Microarchitecture of the dermis in mice immunized with pVAX1::LmxMBA was globally preserved in a similar manner to the healthy footpad (d).

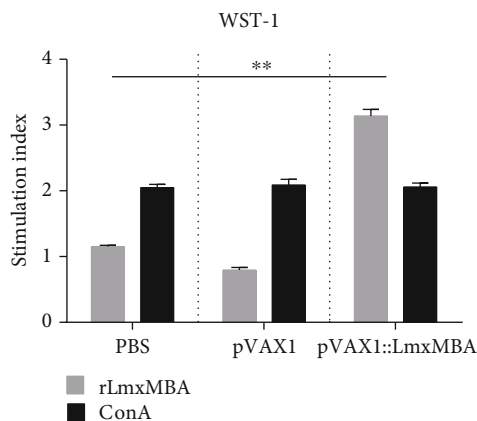


FIGURE 6: Proliferation of mononuclear cells in the spleen of mice immunized with PBS, pVAX1, or pVAX1::LmxMBA after stimulation with rLmxMBA. The mean stimulation index (SI) of vaccinated mice (injected with pVAX1::LmxMBA) was nearly 3 times greater than the mean SI of control mice (injected with PBS or pVAX1). ConA: concanavalin A. $*p < 0.05$.

1 year at 25°C, and 1 month at 37°C [39]. DNA vaccination has been used against different diseases due to its potential to induce both humoral and cellular immune responses and

together with reverse vaccinology represents a potentially new approach to design vaccines against leishmaniasis and other infectious diseases such as hepatitis B and C, malaria, and human papillomavirus infection [38, 39].

We identified a potential candidate for a protective vaccine by reverse vaccinology. The criteria by which we chose to select potential vaccine antigen initially included a focus on surface proteins and sequence conservation among *Leishmania* species. Other considerations were that the chosen candidate must lack sequence identity with human proteins and the ability to express the protein in a high-throughput manner for vaccine production, e.g., we discard insoluble proteins with more than two transmembrane helices. In this regard, the LmxMBA protein has a 26.9% identity with a human protein. However, importantly, it has no shared stretches greater than six amino acids and is therefore unlikely to contain any MHC I or II epitopes. Therefore, this protein is expected to have no safety concerns if administered during vaccine trials.

Infection with *L. mexicana* causes many CL cases in the Americas and, less frequently, diffuse cutaneous and mucocutaneous leishmaniasis, even more disfiguring forms of the disease. *L. major* can also cause CL in the old world, and on the other hand, the deadliest form of the disease, VL, is mainly caused by *L. donovani* and *L. infantum* [40–42].

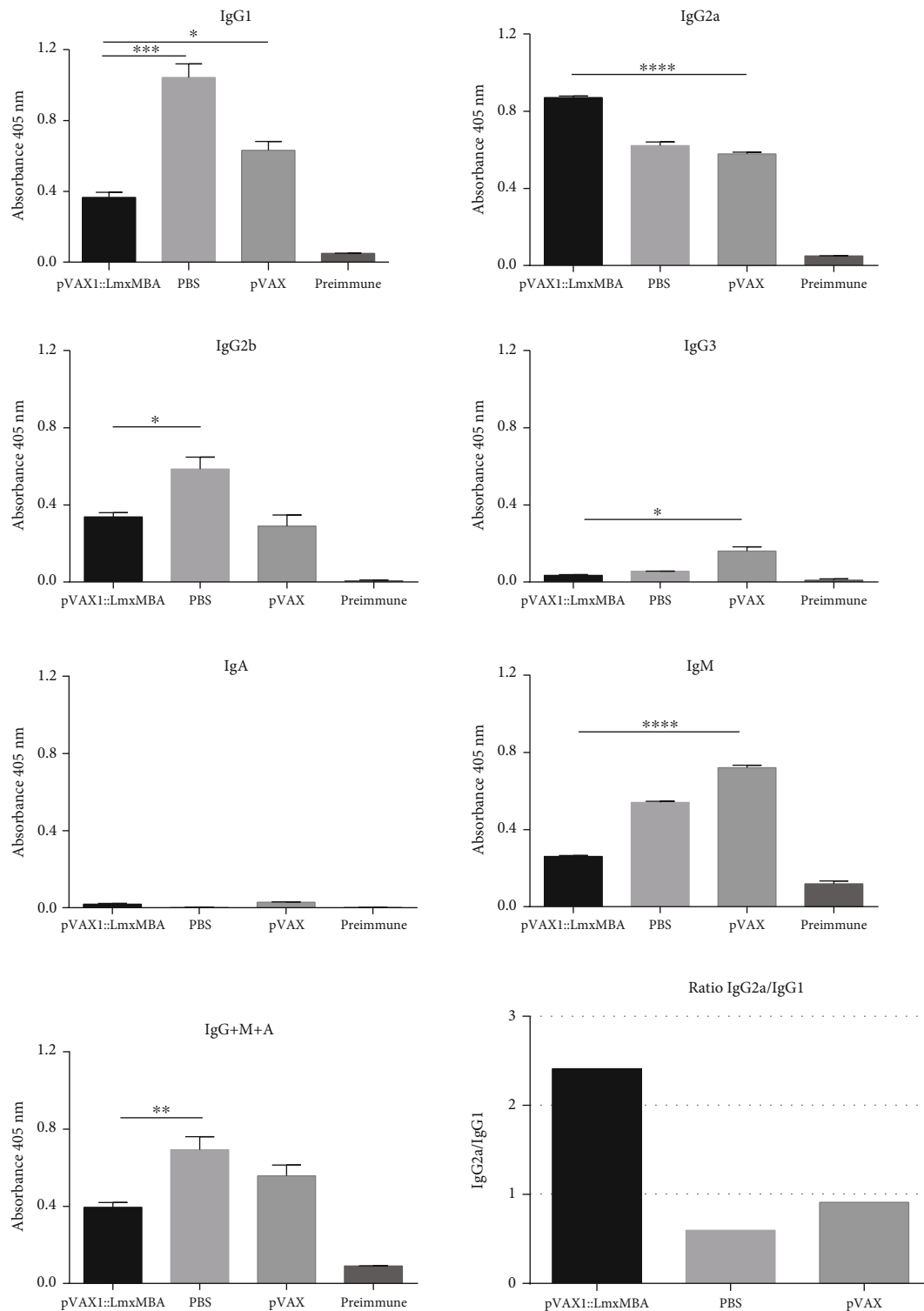


FIGURE 7: Vaccine-specific serological responses. Serum samples were collected by cardiac puncture on day 105 post infection. Plates were coated with $2 \mu\text{g/ml}$ of rLmxMBA, and serum samples were diluted 1 : 100. Each bar represents the average \pm standard deviation of optical densities. * $p < 0.05$.

Thus, when the selected antigen is conserved in the various *Leishmania* species, it is possible that a vaccine directed against CL could protect against these other forms of leishmaniasis. In this way, the candidate vaccine could confer cross-protection against other *Leishmania*

species because the extramembrane region of the LmxMBA protein has $>90\%$ identity with *L. major*, *L. donovani*, and *L. infantum* homologues. Even when considering the most distant species that belong to the alternated subgenus Viannia, the candidate antigen exhibits at

least 71% sequence conservation with *L. braziliensis*, *L. panamensis*, and *L. guyanensis* species.

LmxMBA is a protein exposed on the membrane of *L. mexicana* and belongs to the acid phosphatase expressed in the flagellar pocket in promastigotes and amastigotes. The LmxMBA gene [43] and its homologues in *Trypanosoma brucei* [44] encode proteins that have been observed in small vesicle-like structures close to the flagellar pocket, and protein overexpression in *L. mexicana* promastigotes leads to the translocation of the protein to the cell surface and the flagellar pocket membrane.

In this study, we found the LmxMBA protein is located mainly in the flagellar pocket membrane of wild-type promastigotes and amastigotes. It is less frequent on the surface or in organelles of the parasite, including the flagellum. Proteins exposed on the plasma membrane have been shown to represent the most accessible pool of potential vaccine targets for the development of vaccines. Therefore, LmxMBA as a membrane-bound protein may represent an ideal candidate for the development of a DNA vaccine against *L. mexicana*.

There are several key components involved in the immune response to *Leishmania* infection. The outcome of infection depends on the host's ability to mount a protective Th1 response versus the ability of the parasite to evade and manipulate the host's immune system [45]. Macrophages and effects molecules, dendritic cells, T helper cells, cytotoxic T cells, natural killer cells, and cytokines are all considered to play essential roles in the immune response to *Leishmania* infection [45]. In this study, DNA vaccine encoding LmxMBA of *L. mexicana* was able to promote humoral and cellular immune responses, reducing the clinical manifestations of the cutaneous disease in genetically susceptible mice. Most animals (70%) did not show any footpad swelling at 105 days after challenge, the parasites were cleared from the injection site, and the dermis was free of inflammatory infiltrates. The rest of the animals in this group (30%) showed minimal and transient swelling at the inoculation site and a low number of parasites and mild inflammatory infiltrates. A delay in the development of the disease was observed in all animals immunized with the LmxMBA gene. In cutaneous infection with *L. major*, vaccination with the divergent part of H2B protein confers clinical and parasitological protection against a virulent challenge, considered a protective effect when the size of the lesion and the parasite load in the vaccinated mice were significantly smaller than that observed in control animals [46]. In the experimental mouse model of visceral leishmaniasis caused by *L. donovani*, Melby et al. [47] showed that DNA vaccination using a cDNA library, containing notably H2B, partially protects BALB/c mice against a virulent challenge with *L. donovani*. The protective effect induced by the vaccine was partial since, during infection in this experimental model, vaccination was more efficient at clearing parasites from the liver than the spleen.

Immunization with the empty plasmid generated macroscopical lesions in all of this group's animals (100%). However, the size was smaller than the PBS control group's lesions, the parasite load remained high, and there was tissue damage with chronic inflammatory infiltrates. This apparent protective effect may be due to the CpG motif. The empty

vector has CpG motifs that act as a "danger signal" and as an enhancer of the Th1 immune response in DNA vaccination through interaction with TLR9-positive cells, and this could be activating a nonspecific immune response against infection [24, 25], thus inducing a lower swelling without reducing the parasite load.

As expected, parasites in the lesion were evident in all the animals in the control groups by staining tissue. However, in the group of animals immunized with the candidate antigen, only 20% showed parasites by stained skin and 10% more by limiting dilution culture; this is consistent with other studies in mice since limiting dilution culture allows quantification of parasite burdens at least 50- to 100-fold lower than the minimal parasite burdens quantifiable on stained organs [48]. Due to its high sensitivity, this method is particularly suitable for experimental situations in which parasites cannot be visualized in stained organs: e.g., after therapeutic intervention or a low parasite persistence. It would be interesting to extend the animals' monitoring time to observe the complete elimination of the parasite in the infected tissue or the persistence. Nevertheless, an essential characteristic of leishmaniasis is that residual parasites could remain in the host despite the lesion's disappearance, probably for a very long time [49].

The vaccine also showed that the control was given by a Th1-type response, since mice immunized with pVAX1::LmxMBA produced significantly higher levels of IgG2 compared to control mice, which conversely showed significantly high levels of IgG1. Many reports show that during *Leishmania* infection, higher amounts of the IgG1 isotype in comparison with IgG2a are associated with disease progression [50, 51]. This IgG2a/IgG1 > 1 ratio is representative of a Th1-type immune response because IFN- γ , produced by Th1-like cells, suppresses the induction of IgG1 and increases the production of IgG2 antibodies [52]. On the other hand, levels of IgM, IgG2b, and IgG3 were significantly lower in the experimental group compared to the control mice. Humoral immune response has been evaluated in different stages of the disease in humans with leishmaniasis. Elevated levels of IgM antibodies have been found in the serum of patients with visceral leishmaniasis who are in the acute phase of the disease, IgM levels remain high in patients resistant to sodium stibogluconate (SAG), and patients who respond to SAG showed a decrease in the levels of total IgG, IgM, and IgE [53].

It has been mentioned that the deletion mutant for this gene is able to infect BALB/c mice and peritoneal macrophages, thus suggesting that LmxMBA is neither involved in the infection process nor required for amastigote survival in the infected host cell [54]. It could be possible that the immune response induced by DNA vaccination with the LmxMBA gene affects the activity of LmxMBA or homologous proteins essential for the infection and survival of amastigotes within the host. The *L. mexicana* genome codifies for 3 membrane-bound acid phosphatases and 1 secreted histidine acid phosphatase with 53-56% homology to LmxMBA (data not shown).

In conclusion, immunization with the gene LmxMBA can induce partial protective immunity against *L. mexicana*

infection in the murine model. Until now, the efficacy of the single-dose vaccine candidate has not been evaluated. Future studies would be of great interest to test our DNA vaccine under additional conditions, mainly if lower doses of the vaccine or even a single dose is sufficient to reduce the clinical characteristics of visceral and cutaneous leishmaniasis in other animal models.

Our data identify a vaccine antigen that could potentially be used in target vaccination campings in *L. mexicana*-endemic regions. Due to possible cross-reactivity against other *Leishmania* species, it would be essential to evaluate the efficacy of this DNA vaccine against the parasitic challenge with species that cause visceral leishmaniasis in large animals, including dogs and also in humans, in order to find universal vaccine leishmaniasis.

Data Availability

The data that support the findings of this study are available from the corresponding author upon reasonable request.

Conflicts of Interest

The authors declare that they have no known competing financial interests or personal relationships that could have appeared to influence the work reported in this paper.

Authors' Contributions

María Angélica Burgos-Reyes handled investigation and writing (original draft). Lidia Baylón Pacheco worked on methodology and investigation. Patricia Espíritu-Gordillo took care of formal analysis and visualization. Silvia Galindo-Gómez managed the investigation. Víctor Tsutsumi secured the validation and resources. José Luis Rosales-Encina made bioinformatics analysis, conceptualization, validation, funding acquisition, writing (review and editing), and thesis director of Ph.D. student MABR.

Acknowledgments

We would like to thank Mr. Enrique Martínez de Luna for his technical assistance and María Guadalupe Aguilar González from the Departamento de Genética y Biología Molecular, CINVESTAV, México, for the DNA sequencing. MABR was a recipient of a Ph.D. fellowship from Consejo Nacional de Ciencia y Tecnología (CONACyT), México (CVU 636713). This work was supported by a grant from CONACyT, México (Grant CB 2014-240882-M), and a grant from Fondo SEP-Cinvestav (Application number 193) to JLRE.

References




- [1] J. Alvar, I. D. Vélez, C. Bern et al., "Leishmaniasis worldwide and global estimates of its incidence," *PLoS One*, vol. 7, no. 5, article e35671, 2012.
- [2] WHO, "Neglected tropical diseases. Leishmaniasis. Global Health Observatory (GHO) Data 2019," August 2020, https://www.who.int/gho/neglected_diseases/leishmaniasis/en/.
- [3] L. Kedzierski, "Leishmaniasis vaccine: where are we today?," *Journal of Global Infectious Diseases*, vol. 2, no. 2, pp. 177–185, 2010.
- [4] R. Reithinger, J.-C. Dujardin, H. Louzir, C. Pirmez, B. Alexander, and S. Brooker, "Cutaneous leishmaniasis," *The Lancet Infectious Diseases*, vol. 7, no. 9, pp. 581–596, 2007.
- [5] F. Chappuis, S. Sundar, A. Hailu et al., "Visceral leishmaniasis: what are the needs for diagnosis, treatment and control?," *Nature Reviews Microbiology*, vol. 5, no. 11, pp. 873–882, 2007.
- [6] J. Alexander and K. Bryson, "T helper (h)1/Th2 and *Leishmania* : paradox rather than paradigm," *Immunology Letters*, vol. 99, no. 1, pp. 17–23, 2005.
- [7] L. P. Carvalho, S. Passos, A. Schriefer, and E. M. Carvalho, "Protective and pathologic immune responses in human tegumentary leishmaniasis," *Frontiers in Immunology*, vol. 3, pp. 1–9, 2012.
- [8] J. Poot, K. Spreeuwenberg, S. J. Sanderson et al., "Vaccination with a preparation based on recombinant cysteine peptidases and canine IL-12 does not protect dogs from infection with *Leishmania infantum*," *Vaccine*, vol. 24, no. 14, pp. 2460–2468, 2006.
- [9] A. P. Fernandes, M. M. S. Costa, E. A. F. Coelho et al., "Protective immunity against challenge with *Leishmania (Leishmania) chagasi* in beagle dogs vaccinated with recombinant A2 protein," *Vaccine*, vol. 26, no. 46, pp. 5888–5895, 2008.
- [10] D. RIVIER, R. SHAH, P. BOVAY, and J. MAUEL, "Vaccine development against cutaneous leishmaniasis. Subcutaneous administration of radioattenuated parasites protects CBA mice against virulent *Leishmania* major challenge," *Parasite Immunology*, vol. 15, no. 2, pp. 75–84, 1993.
- [11] S. S. A. A. Hasson, J. K. Z. Al-Busaidi, and T. A. Sallam, "The past, current and future trends in DNA vaccine immunisations," *Asian Pacific Journal of Tropical Biomedicine*, vol. 5, no. 5, pp. 344–353, 2015.
- [12] S. Bhaumik, R. Basu, S. Sen, K. Naskar, and S. Roy, "KMP-11 DNA immunization significantly protects against *L. donovani* infection but requires exogenous IL-12 as an adjuvant for comparable protection against *L. major*," *Vaccine*, vol. 27, no. 9, pp. 1306–1316, 2009.
- [13] J. B. Alarcon, G. W. Waine, and D. P. McManus, "DNA vaccines: technology and application as anti-parasite and antimicrobial agents," *Advances in Parasitology*, vol. 42, pp. 343–410, 1999.
- [14] A. M. Watts and R. C. Kennedy, "DNA vaccination strategies against infectious diseases," *International Journal for Parasitology*, vol. 29, no. 8, pp. 1149–1163, 1999.
- [15] A. M. Watts, M. H. Shearer, H. I. Pass, R. K. Bright, and R. C. Kennedy, "Comparison of simian virus 40 large T antigen recombinant protein and DNA immunization in the induction of protective immunity from experimental pulmonary metastasis," *Cancer Immunology, Immunotherapy*, vol. 47, no. 6, pp. 343–351, 1999.
- [16] R. N. Coler, A. Campos-Neto, P. Ovendale et al., "Vaccination with the T cell antigen Mtb 8.4 protects against challenge with *Mycobacterium tuberculosis*," *The Journal of Immunology*, vol. 166, no. 10, pp. 6227–6235, 2001.
- [17] N. L. Letvin, "Progress in the development of an HIV-1 vaccine," *Science*, vol. 280, no. 5371, pp. 1875–1880, 1998.
- [18] D. B. Lowrie, "DNA vaccines against tuberculosis," *Current Opinion in Molecular Therapeutics*, vol. 1, no. 1, pp. 30–33, 1999.

- [19] J. D. Boyer, M. Chattergoon, K. Muthumani et al., "Next generation DNA vaccines for HIV-1," *Journal of Liposome Research*, vol. 12, no. 1-2, pp. 137–142, 2002.
- [20] B. Salgado-Jiménez, M. Arce-Fonseca, L. Baylón-Pacheco, P. Talamás-Rohana, and J. L. Rosales-Encina, "Differential immune response in mice immunized with the A, R or C domain from TcSP protein of *Trypanosoma cruzi* or with the coding DNAs," *Parasite Immunology*, vol. 35, no. 1, pp. 32–41, 2013.
- [21] M. Arce-Fonseca, M. A. Ballinas-Verdugo, E. R. A. Zenteno et al., "Specific humoral and cellular immunity induced by *Trypanosoma cruzi* DNA immunization in a canine model," *Veterinary Research*, vol. 44, no. 1, p. 15, 2013.
- [22] O. Rodríguez-Morales, S. C. Carrillo-Sánchez, H. García-Mendoza et al., "Effect of the plasmid-DNA vaccination on macroscopic and microscopic damage caused by the experimental chronic *Trypanosoma cruzi* infection in the canine model," *BioMed Research International*, vol. 2013, 8 pages, 2013.
- [23] O. Rodríguez-Morales, V. Monteón-Padilla, S. C. Carrillo-Sánchez et al., "Experimental vaccines against Chagas disease: a journey through history," *Journal of Immunology Research*, vol. 2015, Article ID 489758, 2015.
- [24] J. Mota-Sánchez, "Vacunas de ADN: Inducción de la respuesta inmunitaria," *Salud Publica de Mexico*, vol. 51, pp. 463–469, 2009.
- [25] B. Ferraro, M. P. Morrow, N. A. Hutnick, T. H. Shin, C. E. Lucke, and D. B. Weiner, "Clinical applications of DNA vaccines: current progress," *Clinical Infectious Diseases*, vol. 53, no. 3, pp. 296–302, 2011.
- [26] A. Carabarin-lima, M. C. González-vázquez, L. Baylon-pacheco, V. Tsutsumi, P. Talamás-rohana, and J. Luis, "Immunization with the recombinant surface protein rTcSP2 alone or fused to the CHP or ATPase domain of TcHSP70 induces protection against acute *Trypanosoma cruzi* infection," *Journal of Vaccines & Vaccination*, vol. 1, pp. 1–10, 2010.
- [27] P. C. Melby, B. Chandrasekar, W. Zhao, and J. E. Coe, "The hamster as a model of human visceral leishmaniasis: progressive disease and impaired generation of nitric oxide in the face of a prominent Th1-like cytokine response," *The Journal of Immunology*, vol. 166, no. 3, pp. 1912–1920, 2001.
- [28] F. Tabatabaie, M. Mahdavi, S. Faezi et al., "Th1 platform immune responses against *Leishmania major* induced by thiol-specific antioxidant-based DNA vaccines," *Jundishapur Journal of Microbiology*, vol. 7, pp. 1–8, 2014.
- [29] A. Krogh, È. Larsson, G. von Heijne, and E. L. L. Sonnhammer, "Predicting transmembrane protein topology with a hidden Markov model: application to complete genomes¹," *Journal of molecular biology*, vol. 305, no. 3, pp. 567–580, 2001.
- [30] K. D. Tsirigos, C. Peters, N. Shu, K. Lukas, and A. Elofsson, "The TOPCONS web server for consensus prediction of membrane protein topology and signal peptides," *Nucleic Acids Research*, vol. 43, pp. 401–407, 2015.
- [31] K. Chou and H. Shen, "A new method for predicting the subcellular localization of eukaryotic proteins with both single and multiple sites: Euk-mPLoc 2.0," *PLoS ONE*, vol. 5, no. 4, article e9931, 2010.
- [32] T. Goldberg, M. Hecht, T. Hamp et al., "LocTree3 prediction of localization," *Nucleic acids research*, vol. 42, pp. 350–355, 2014.
- [33] J. J. Almagro Armenteros, C. K. Sønderby, S. K. Sønderby, H. Nielsen, and O. Winther, "DeepLoc : prediction of protein subcellular localization using deep learning," *Bioinformatics*, vol. 33, no. 21, pp. 3387–3395, 2017.
- [34] C. Yu, Y. Chen, C. Lu, and J. Hwang, "Prediction of protein subcellular localization," *Proteins: Structure, Function, and Bioinformatics*, vol. 64, pp. 643–651, 2006.
- [35] A. Campos-Neto, R. Porrozzzi, K. Greeson et al., "Protection against cutaneous leishmaniasis induced by recombinant antigens in murine and nonhuman primate models of the human disease," *Infection and immunity*, vol. 69, no. 6, pp. 4103–4108, 2001.
- [36] D. J. Shedlock and D. B. Weiner, "DNA vaccination: antigen presentation and the induction of immunity," *Journal of Leukocyte Biology*, vol. 68, no. 6, pp. 793–806, 2000.
- [37] J. A. Wolff, J. J. Ludtke, G. Acsadi, P. Williams, and A. Jani, "Long-term persistence of plasmid DNA and foreign gene expression in mouse muscle," *Human Molecular Genetics*, vol. 1, no. 6, pp. 363–369, 1992.
- [38] S. Gurunathan, C. Y. Wu, B. L. Freidag, and R. A. Seder, "DNA vaccines: a key for inducing long-term cellular immunity," *Current Opinion in Immunology*, vol. 12, no. 4, pp. 442–447, 2000.
- [39] T. R. Smith, A. Patel, S. Ramos et al., "Immunogenicity of a DNA vaccine candidate for COVID-19," *Nature Communications*, vol. 11, pp. 1–13, 2020.
- [40] O. Billaut-Mulot, T. Idziorek, M. Loyens, A. Capron, and G. M. Bahr, "Modulation of cellular and humoral immune responses to a multiepitopic HIV-1 DNA vaccine by interleukin-18 DNA immunization/viral protein boost," *Vaccine*, vol. 19, no. 20-22, pp. 2803–2811, 2001.
- [41] C. Dye, "The leishmaniasis in biology and medicine: edited by W. Peters and R. Killick- Kendrick. Academic Press, 1987. Volumes I and II, £105.00/US\$190.50. ISBN 012552101 4/0 12 552102 2," *Parasitology Today*, vol. 4, no. 1, p. 28, 1988.
- [42] B. Alemayehu and M. Alemayehu, "Leishmaniasis: a review on parasite, vector and reservoir host," *Health Science Journal*, vol. 11, no. 4, 2017.
- [43] M. Wiese, O. Berger, Y. D. Stierhof, M. Wolfram, M. Fuchs, and P. Overath, "Gene cloning and cellular localization of a membrane-bound acid phosphatase of *Leishmania mexicana*," *Molecular and Biochemical Parasitology*, vol. 82, no. 2, pp. 153–165, 1996.
- [44] M. Engstler, F. Weise, K. Bopp et al., "The membrane-bound histidine acid phosphatase TbMBAP1 is essential for endocytosis and membrane recycling in *Trypanosoma brucei*," *Journal of Cell Science*, vol. 118, no. 10, pp. 2105–2118, 2005.
- [45] Y. Vanloubbeek and D. E. Jones, "The immunology of Leishmaniasis infection and the implications for vaccine development," *Annals of the New York Academy of Sciences*, vol. 1026, no. 1, pp. 267–272, 2004.
- [46] M. Chenik, H. Louzir, H. Ksontini, A. Dilou, I. Abdmouleh, and K. Dellagi, "Vaccination with the divergent portion of the protein histone H2B of *Leishmania* protects susceptible BALB/c mice against a virulent challenge with *Leishmania major*," *Vaccine*, vol. 24, no. 14, pp. 2521–2529, 2006.
- [47] P. C. Melby, G. B. Ogden, H. A. Flores et al., "Identification of vaccine candidates for experimental visceral leishmaniasis by immunization with sequential fractions of a cDNA expression library," *Infection and Immunity*, vol. 68, no. 10, pp. 5595–5602, 2000.
- [48] P. A. Buffet, A. Sulahian, Y. J. Garin, N. Nassar, and F. Derouin, "Culture microtitration: a sensitive method for

- quantifying *Leishmania infantum* in tissues of infected mice," *Antimicrobial agents and chemotherapy*, vol. 39, no. 9, pp. 2167-2168, 1995.
- [49] A. Schubach, F. Haddad, M. P. Neto et al., "Detection of *Leishmania* DNA by polymerase chain reaction in scars of treated human patients," *Journal of Infectious Diseases*, vol. 178, no. 3, pp. 911-914, 1998.
- [50] A. Thakur, H. Kaur, and S. Kaur, "Evaluation of the immunoprophylactic potential of a killed vaccine candidate in combination with different adjuvants against murine visceral leishmaniasis," *Parasitology International*, vol. 64, no. 1, pp. 70-78, 2015.
- [51] M. R. Jaafari, A. Ghafarian, A. Farrokh-Gisour et al., "Immune response and protection assay of recombinant major surface glycoprotein of *Leishmania* (rgp63) reconstituted with liposomes in BALB/c mice," *Vaccine*, vol. 24, no. 29-30, pp. 5708-5717, 2006.
- [52] C. Snapper and W. Paul, "Interferon-gamma and B cell stimulatory factor-1 reciprocally regulate Ig isotype production," *Science*, vol. 236, no. 4804, pp. 944-947, 1987.
- [53] K. Anam, F. Afrin, D. Banerjee et al., "Differential decline in *Leishmania* membrane antigen-specific immunoglobulin G (IgG), IgM, IgE, and IgG subclass antibodies in Indian Kala-Azar patients after chemotherapy," *Infection and immunity*, vol. 67, no. 12, pp. 6663-6669, 1999.
- [54] I. Benzel, F. Weise, and M. Wiese, "Deletion of the gene for the membrane-bound acid phosphatase of *Leishmania mexicana*," *Molecular and Biochemical Parasitology*, vol. 111, no. 1, pp. 77-86, 2000.

Review Article

Biomarkers and Their Possible Functions in the Intestinal Microenvironment of Chagasic Megacolon: An Overview of the (Neuro)inflammatory Process

José Rodrigues do Carmo Neto ¹, Yarlla Loyane Lira Braga,¹
Arthur Wilson Florêncio da Costa,¹ Fernanda Hélia Lucio,¹ Thais Cardoso do Nascimento,¹
Marlene Antônia dos Reis,² Mara Rubia Nunes Celes,¹ Flávia Aparecida de Oliveira,¹
Juliana Reis Machado ^{1,2} and Marcos Vinícius da Silva ³

¹Department of Bioscience and Technology, Institute of Tropical Pathology and Public Health, Federal University of Goiás, Goiânia, GO, Brazil

²Department of General Pathology, Federal University of Triângulo Mineiro, Uberaba, Minas Gerais, Brazil

³Department of Microbiology, Immunology and Parasitology, Institute of Biological and Natural Sciences, Federal University of Triângulo Mineiro, Uberaba, Minas Gerais, Brazil

Correspondence should be addressed to Juliana Reis Machado; juliana.patologiageral@gmail.com

Received 25 December 2020; Revised 8 March 2021; Accepted 19 March 2021; Published 8 April 2021

Academic Editor: Márcia Laurenti

Copyright © 2021 José Rodrigues do Carmo Neto et al. This is an open access article distributed under the Creative Commons Attribution License, which permits unrestricted use, distribution, and reproduction in any medium, provided the original work is properly cited.

The association between inflammatory processes and intestinal neuronal destruction during the progression of Chagasic megacolon is well established. However, many other components play essential roles, both in the long-term progression and control of the clinical status of patients infected with *Trypanosoma cruzi*. Components such as neuronal subpopulations, enteric glial cells, mast cells and their proteases, and homeostasis-related proteins from several organic systems (serotonin and galectins) are differentially involved in the progression of Chagasic megacolon. This review is aimed at revealing the characteristics of the intestinal microenvironment found in Chagasic megacolon by using different types of already used biomarkers. Information regarding these components may provide new therapeutic alternatives and improve the understanding of the association between *T. cruzi* infection and immune, endocrine, and neurological system changes.

1. Introduction

According to the World Health Organization (WHO), approximately 8 million people in the world are infected with *Trypanosoma cruzi* (*T. cruzi*), the etiological agent of Chagas disease (CD) (WHO, 2018). Most of these cases are concentrated in Latin America, where the number of new cases per year is estimated to be 300,000 [1]. In Brazil, at least one million people are infected with *T. cruzi*, and most of them are in the chronic phase [2]. Recently, the cases of acute CD have increased in Brazil, mainly owing to the consumption of food contaminated with parasites, such as açai and sugarcane juice [3, 4].

CD has two phases, acute and chronic. The acute phase is characterized by the high parasitic load with cellular destruction and extensive inflammatory foci [5]. Subsequently, the condition may progress to an undetermined or determined chronic phase of the disease, which may then lead to the development of severe cardiac and digestive dysfunctions and death [5]. The indeterminate chronic phase is characterized by positive serology and/or parasitology along with the absence of symptoms and/or signs caused by *T. cruzi* [5]. The symptomatic chronic phase can develop after few years to decades due to some unknown factors, in approximately 30% of the infected people. In this phase, mega syndromes could develop with cardiac (cardiomegaly) and/or digestive

(megaesophagus and/or megacolon) involvement, in addition to neurological damage [5].

The first suspected case of the digestive form of CD appeared in 1916, when Carlos Chagas observed that in the acute infection some adults presented marked dysphagia, which was perpetuated in the chronic phase, and he called this “Choking Disease” [6]. Patients with the digestive form of CD present with hypertrophic changes with esophagus (megaesophagus) and/or intestinal colon (megacolon) dilation, leading to dysphagia, regurgitation, and motor discoordination. The main cause of dilation of these organs is their denervation owing to the destruction of myenteric or Auerbach and submucosal or Meissner plexus [7]. Different mechanisms have been proposed to explain this neuronal destruction, such as the release of toxins during parasite fragmentation, direct neuronal injury through cell parasitism, and inflammatory damage triggered by the parasite [8].

This review focuses on the intestinal biomarkers of Chagasic megacolon and their possible functions in CD progression, especially those related to (neuro) inflammatory processes. Despite the advances in the understanding of the CD evolution, cell interactions and molecular pathways involved in megacolon development/progression are not completely clear. Thus, the investigation of biomarkers of altered intestinal structures is also fundamental to understand the rich microenvironment of Chagasic megacolon and its relationship with disease pathogenesis, especially those related to neuronal death.

2. An Immunological Overview of Chagasic Megacolon

Chagasic megacolon is characterized by a hollow viscera with chronic constipation, followed by permanent pathological dilation of the organ wall, which usually occurs in the rectus sigmoid portion, where the parasite is commonly found [5]. From the morphological point of view, patients with megacolon present histological changes such as organ wall thickening due to severe muscle fiber hypertrophy, especially in the circular layer; these changes are usually associated with an inflammatory process in addition to the presence of hypertrophied neurons in the submucous and myenteric plexus and/or with the signs of degeneration [7].

The myenteric plexus is severely affected by the inflammatory process triggered by *T. cruzi* infection, resulting in decreased number of nerve cells or even complete destruction of nerve ganglia [7, 9]. The *T. cruzi*-induced intestinal inflammation led to neuron degeneration in the gastrointestinal system [10, 11] and ganglionitis, peri-ganglionitis, neuritis, and peri-neuritis in the myenteric plexus [7]. These lesions begin to form in the acute phase and are prolonged and aggravated during the chronic phase [12]. The inflammatory process related to this neuron degeneration usually has a focal distribution. However, some neurons close to the injured neurons remain intact [7].

The phenotypic characterization of the inflammatory infiltrate components led to a better understanding of the pathophysiology of Chagasic megacolon, although the process is not yet completely understood. Eosinophils, mast cells

(MCs) and their proteases, CD68⁺ macrophages, CD57⁺ natural killer cells, and TIA-1⁺ cytotoxic lymphocytes in the affected intestine are factors related to inflammatory process maintenance and neuronal death during the CD chronic phase [8, 13–15].

Over the years, some theories attempted to explain neuronal destruction in the different phases of infection. During the acute phase, the high concentration of the protozoan has been suggested to participate in neuronal death [8]. In contrast, in the chronic phase, in which minimal amount of *T. cruzi* is clearly demonstrated in the injured organ, neuronal destruction process would be the consequence of the (auto) immune response following infection [8]. According to this idea, as indeterminate form progresses to digestive form, peripheral blood mononuclear produces higher levels of IFN- γ , inducing TNF- α augmentation and a proinflammatory milieu in the intestine [16].

Cytokines such as TNF- α and IFN- γ (produced mainly by Th1 lymphocytes) at the onset of infection are essential for parasites control as they are involved in the activation of microbicidal macrophages which produce reactive oxygen species (ROS) or nitric oxide (NO) [17, 18]. However, a balanced response is essential so that the infection is controlled and does not result in excessive tissue damage.

In addition to lymphocytes, central or peripheral glial cells are potential sources of NO. They have been reported to participate in neuropathologies, leading to the production of neuron protective or toxic molecules [19, 20]. In Chagasic megacolon, the alteration of the number of enteric glial cells, as well as glial activation markers, suggests that these cells participate in the inflammatory process and in the subsequent neuronal damage or protection [15, 21]. Actually, glial cells have been shown to be parasitized by *T. cruzi* in both the central nervous system (CNS) and the enteric nervous system (ENS) [7, 22–25].

3. Biomarkers in Chagasic Megacolon: Immune Response and Neuroinflammation

In addition to glial cells and traditional immune system components, other components are also associated with the progression of or protection against Chagasic megacolon. Possible interactions between the nervous and immune systems that may be associated with different CD progression events, particularly those related to the maintenance of the inflammatory process and tissue damage, especially in the ENS, are discussed below.

3.1. Protein Gene Product. Initially described in 1981, protein gene product (PGP 9.5) is a cytoplasmic protein produced by central and peripheral neurons [26]. It is highly concentrated in intact neurons and can be used as a specific neuronal marker and, consequently, for neuronal density evaluation [27]. The use of PGP 9.5 neuronal marker confirmed the participation of the ENS in the pathophysiology of diseases related to neuronal damage, such as Hirschsprung’s disease (HD) [28], ulcerative colitis [29], and intestinal neuronal dysplasia [30].

Due to the difficulty to establish experimental models for the digestive CD, divergent results regarding PGP 9.5 have been published. The C3H/He mice, 30 days after infection (acute phase) with Brazil *T. cruzi* strain, did not reduce the intestinal neuronal PGP 9.5 staining as compared with control mice [31]. Similarly, C57Bl/6 mice, seven days after infection (acute phase), also showed no decrease of immunoreactive neurons for PGP 9.5 (IR-PGP 9.5) [32]. In contrast, C57Bl/6 mice demonstrated a reduction in the neuron fibers and IR-PGP 9.5 neurons in the intestine, especially in the myenteric plexus, 10 days (acute phase) after infection with the Y strain [22].

Additionally, PGP 9.5 neuronal density was also investigated in chronic models of CD [33]. Infection of Swiss mice with Y strain for 11 days (acute phase) and 15 months (chronic phase, with the administration of a single dose of benznidazole at 11 days of infection) found that the infection reduced the density and number of IR-PGP 9.5 neurons in the intestine. Furthermore, the number of intramuscular IR-PGP 9.5 neuron fibers was lower in the chronic phase as compared to the acute phase [33].

Although most of the studies on PGP 9.5 neuronal density use the experimental models, da Silveira et al. [15] and Martins et al. [34] showed that patients chronically infected with megacolon presented reduced density of IR-PGP 9.5 nerve fibers in both, internal muscle layer and intestinal external muscle, as compared to nonmegacolon CD patients and noninfected.

3.2. Peripherin. Peripherin is a type III intermediate filament protein expressed in the cell body and axons of neurons, mainly in the peripheral nervous system [35–38]. Peripherin may play an important role in diseases such as amyotrophic lateral sclerosis [39–41] and type I diabetes mellitus [42–44]. In addition, peripherin plays a promising role as a pan-neural marker in the intestinal mucosa and submucosa [45].

Peripherin helps in the diagnosis of HD, as it is a part of the highly sensitive and specific ganglion cell identification protocol. Peripherin as neuronal biomarker is more sensitive and superior to microtubule-associated protein-2 (MAP-2) and calretinin in ganglion cell and nerve fibrillation marking in colon and rectum biopsies [46] so is specific method for identify HD patients [47].

The role of peripherin in CD, as well as in other pathological processes, is not completely elucidated, and despite the controversies, this protein has been used as a standard for pan-neuronal staining in intestinal diseases [45, 48, 49]. Morphometric analysis of immunoreactive neuronal ganglia for peripherin in the colon from CD patients with megacolon showed reduction in this protein compared to that in healthy people, as it is related to decreased number of neurons. In addition, neuronal ganglia marked with this protein in CD patients showed a deformed structure [50].

In addition, peripherin seems to play a role in neuronal apoptosis through the interaction with protein kinase C [51]. Considering that one of the hypotheses for the development of CD megacolon is the cell death of mucosal neurons, peripherin may have an additional role in the pathogenesis of this disease.

3.3. HuC/HuDa. HuC and HuDa are RNA-binding proteins that are obtained by the alternative splicing of Hu RNA [52], exclusively expressed in neurons. These proteins are considered potent ENS neuron markers [53–55]. Anti-HuC/HuDa antibodies were used as neuronal markers to determine the total number of cell bodies in the nerve plexus of CD patients, pointing that the dilated portion of CD patients with megacolon had fewer neuronal bodies in each ganglion [56]. Similarly, HuC/HuDa were also used as neuronal markers in the colon samples of CD patients in another study [57].

Thus, PGP 9.5, peripherin, and HuC/HuDa were used to evaluate intestinal neuronal loss, especially in Chagasic megacolon, in addition to evaluation of neuronal density, providing a better picture on neuronal regeneration, subpopulation proportion, and cell colocalization [58]. Furthermore, they represent an alternative to basic histological staining techniques, which are, in general, nonspecific [58].

3.4. Substance P. Substance P (SP) is a neuropeptide belonging to the tachykinin family [59, 60]. Expressed by several cell types, mainly neurons [61], this neuropeptide is involved in important inflammatory mechanisms, either in cell migration, where it acts directly, or through the induction of a series of chemokines, receptors and adhesion molecules in lymphocyte proliferation, and innate and adaptive immunity cell activation [62].

SP acts via the interaction with cell surface receptors NK1R, NK2, and NK3. NK1R has the greatest affinity for SP, as it is predominantly related to inflammatory processes, whereas NK2 and NK3 receptors are more related to gastrointestinal motility responses [63, 64]. In the intestine, SP regulates smooth muscle contractility, epithelial ion transport, vascular permeability, and gastrointestinal tract immune function [65, 66]. NK1R receptor density was found to increase significantly in patients with Crohn's disease and ulcerative colitis [67]. These levels correlate with a poor prognosis of CD [68–70].

Substance P can cause neuroinflammation, since neurons also produce and respond to SP [66]. Classical neuroinflammatory responses are characterized by glial activation, microglial proliferation, leukocyte recruitment, and positive inflammatory mediator regulation and secretion [71]. In infectious diseases, SP increases the severity of inflammation associated with *Trypanosoma brucei* infection, etiological agent of sleeping sickness, for example, and treatment with an NK1R antagonist reduced this effect [72]. Similarly, this neuropeptide also contributed to the development of *Taenia crassiceps* infection in a neurocysticercosis model. Knockout mice for the SP precursor or its NK1 receptor had reduced granuloma volume and lower IL-1 β , TNF- α , IL-6, and IFN- γ expression [73]. NK1R inhibition was also promising for the treatment of experimental autoimmune encephalomyelitis (EAE) [74], head trauma [75], and meningitis caused by *S. pneumoniae* [76]. NK1R inhibition is a promising treatment for neuroinfectious and neuroinflammatory processes, with positive immune response effects in the nervous tissue, and several antagonists are being developed.

The SP expression has also been shown to be directly correlated with the severity of Chagasic megacolon. The SP

expression has been shown to be high in the submucosa and myenteric plexus neurons in the dilated portion of Chagasic megacolon compared to that in the nondilated portions and noninfected people [56]. Moreover, in contrast to the high SP level, low NK1R receptor levels were observed in the dilated portion [77]. Conversely, other studies described lower myenteric and submucous plexus SP concentration in the rectum samples from CD patients. The authors associated this finding with the destruction of intestinal nerve ganglia [78]. Corroborating this study, SP staining activity was reduced in the neurons of the myenteric plexus of the colon in experimental models of acute and chronic infection with the Y [79, 80].

In general, the role of SP in the immune response to *T. cruzi* infection is particularly remarkable. The increase of this neuropeptide in patients with megacolon may be related to the elimination of the parasite, which somehow accelerates the progression of the megaesophagus or colon due to increased inflammatory response. Besides, SP may have the ability to modulate the production of a wide range of cytokines. SP stimulates the production of proinflammatory cytokines such as IL-1 β , IL-6, and TNF- α by human peripheral mononuclear cells, inducing lymphocyte proliferation and immunoglobulin production [62, 65, 81]. This situation probably occurs due to positive NK1R regulation, since, while IL-12, IL-18, and TNF- α induce the NK1R expression in T cells [82]; IL-10 and TGF- β decrease the NK1R expression [83]. The release of SP-induced inflammatory mediators potentiates tissue injury and stimulates leukocyte recruitment, amplifying the inflammatory response [84]. Thus, these studies suggest that the SP/NK1R axis maintains the inflammatory response to *T. cruzi* infection in CD, but no study has analyzed the effects of SP on intestinal Chagas neuroinflammation.

3.5. Growth-Associated Protein 43. Growth-associated protein-43 (GAP-43) is a marker of neuronal plasticity in embryogenesis processes, axonal growth and regeneration, and subsequent neurite branching [85]. GAP-43 has already been used in several intestinal disease models to evaluate neuronal plasticity, such as HD [86, 87], inflammatory bowel disease (IBD) [88], appendicitis [89], intestinal neuronal dysplasia [90], and *Nippostrongylus brasiliensis* infection [91]. These conditions are characterized by neuronal loss and establish an intestinal inflammatory process, which are also essential factors for the progression of Chagasic megacolon.

In fact, evidence shows that the neuronal regenerative process, evaluated using GAP-43 expression, occurs in the intestinal nervous plexus in Chagasic megacolon [50, 92]. Neuronal destruction mediated by the inflammatory process in the most affected areas is suggested to induce neurons to extend their projections into the destroyed areas to maintain intestinal homeostasis [50, 92]. However, this regeneration would be restricted only to the most destroyed neural subpopulations in the intestinal form of CD, corresponding to inhibitory motor neurons characterized by the expression of intestinal vasoactive peptide and NO synthase [50]. The same reestablishment would not occur for other subpopulations such as intrinsic primary afferent neurons, excitatory

motor neurons, and interneurons since they are not considerably destroyed by the infectious process [50].

Although no studies have focused on GAP-43-related pathways in Chagasic megacolon, other axon injury models have been evaluated [93–96]. Some studies have shown that GAP-43 inhibition decreases axon regenerative capacity after injury [93]. In addition, the use of blockers to inhibit the GAP-43 process, such as Nogo-A-dependent processes, represents an alternative to induce increased axon regeneration [97–99]. Thus, studies on neuronal regeneration and plasticity in Chagasic megacolon may establish new mechanisms to control progression in the early stages of this form of CD.

3.6. S-100 Proteins and Glial Fibrillary Acidic Protein: Enteric Glial Cells. S-100 is a family of approximately 21 proteins characterized as small calcium-binding proteins [100]. Besides participating in Ca₂⁺ homeostasis, S-100 proteins have intracellular and extracellular functions, acting in an autocrine and/or paracrine manner in target cells [101] and act in cell proliferation, differentiation, and migration as well as inflammatory processes [102], and as cell markers, mainly of glial cells [103].

Although S-100 proteins are mainly used as a CNS astrocyte biomarker [104, 105], glial components of the ENS also showed reactivity for these proteins, which was not observed for intestinal neurons [106, 107]. Thus, S-100 was characterized as a pan-glial marker also for the intestine.

Another important marker to visualize glial components, specifically astrocytes, is the glial fibrillary acidic protein (GFAP) [108]. Classified as the main intermediate filament protein of class III astrocytes, GFAP is related to the maintenance of cell structure and signal transduction [109]. In general, GFAP has been shown to play a role in cell motility, migration, and proliferation processes; chaperone-mediated autophagy; synaptic plasticity; neuronal damage or protection; and inflammation [108, 110]. Initially described as a CNS astrocyte marker, astrocyte-like enteric glial cells were also found to be immunoreactive for GFAP, especially in the intestinal nerve ganglia [103, 104, 111].

Chagasic megacolon was characterized by decreased S-100 glial-IR cells in different intestinal nerve plexuses [15, 112, 113]. In addition, the dilated portion of the intestinal form of CD is described as having greater glial destruction (IR-S-100) than the nondilated one [15, 21, 114]. Interestingly, the GFAP marker increased the number of glial cell immunoreactive for this protein in *T. cruzi* infection, regardless of intestinal involvement [15, 21]. However, the number of IR-GFAP glial cells in CD patients without megacolon or in the nondilated part of the intestine of CD patients was higher than that in the affected part [15, 21]. Thus, considering that unaffected intestinal segments would have greater glial cell preservation, the presence of these cells has been suggested to protect ENS components from the inflammatory process established by *T. cruzi* infection [15, 21].

In fact, enteric glial cells and their products participate in intestinal homeostasis, especially in neuronal survival. Thus, the reduction of these cells has already been suggested to be associated with infectious [115, 116] and noninfectious intestinal diseases [117–119], which are characterized by

neurodegeneration, like in CD. Evidence shows a glial cell and neuron network owing to the production of NTs such as NGF, NT-3/4/5, and glial cell line-derived neurotrophic factor (GDNF). These neurotrophic factors directly and positively affect neuronal growth, maturation, and survival [120, 121]. Whether these molecules could protect neurons was also evaluated in the digestive form of CD [112]. Interestingly, the levels of NT-3, NGF, and GDNF were higher in the intestine of CD patients without megacolon, and this increase was correlated with the increase in the number of IR-GFAP glial cells and ENS cell protection [112]. In addition, along with the glial system, neurons and inflammatory infiltrate also increased NT production, increasing the relationship between the immune and nervous systems [112]. Thus, the authors suggested that the inflammation found in the intestine of CD patients without megacolon is determinant for NT production and that the increased enteric glial cells would facilitate the reestablishment of the integrity and functioning of the intestine after *T. cruzi* infection and the regulation of the established inflammatory process.

Similar to CNS astrocytes, enteric glial cells are sensitive to the stimuli of inflammatory processes. Proinflammatory cytokines such as IL-1 β , TNF- α , and IFN- α can induce GFAP [122, 123] and NT production [124] and act on *in vitro* proliferation of these cells, which could justify the results found in the intestine of patients infected with *T. cruzi*. Additionally, experimental models of intestinal inflammation showed that inflammation induces enteric glial cell proliferation in the myenteric plexus and that the lack of these cells results in severe tissue inflammation and intestinal necrosis [125, 126]. Conversely, enteric glial cells (EGCs) can also produce inflammatory mediators and exacerbate the intestinal inflammatory process [122, 127–129].

In fact, the microglia phenotype in the CNS is directly related to the microenvironment to which these cells are exposed [130]. When these cells are stimulated with proinflammatory components such as IFN- γ , TNF- α , and IL-17, the microglia polarize to the M1-like profile and can produce NO, ROS, and proinflammatory cytokines (IL-1, IL-12, and TNF- α) related to neurotoxicity and neuronal death. In contrast, once IL-4 and IL-13 stimulate these cells, the M2-like profile is established in the microglia. This activation profile is related to IL-10, TGF- β , and NT production (NT-3, NGF, and GDNF), which is related to neuroprotection and neuronal survival. Although this classification was not noted for EGCs, evaluating intestinal subpopulations and glial plasticity in CD, especially comparing infected patients with and without megacolon, is important.

In addition, analysis of neurodegeneration and inflammatory processes showed that CNS microglia cells express molecules originally found in macrophages, such as class II HLA-DR, B7.1, and B7.2, indicating how these cells interact with the immune system as antigen-presenting cells. In fact, in CD patients with megacolon, EGCs begin to express class II HLA-DR and B7 costimulating molecules [49]. These results suggest that the established inflammatory process would affect the profile of EGCs that could act on lymphocyte activation in the intestine of patients with megacolon [49]. The presence of macrophages and lymphocytes was often

associated with the severity of Chagasic megacolon [13]. Thus, EGCs also influence the progression of chronic digestive CD as antigen-presenting cells, consequently acting on lymphocyte activation [49].

These results suggest that the progression of intestinal CD depends on the microenvironment of the intestinal segment (with or without megacolon; Figure 1). The presence of a greater inflammatory infiltrate, a higher level of proinflammatory cytokines, and tissue destruction may indicate that EGCs would maintain the inflammatory process and neuronal destruction in Chagasic megacolon. The opposite could be assumed for patients without the digestive form, with lower organ involvement and greater quantity of enteric glia reestablishing the intestinal homeostasis. Further studies are needed to determine the role of EGCs in the acute phase of the disease and to elucidate whether this phase would be the determinant for the activation, destruction, and subsequent participation of the glia in the development of Chagasic megacolon, as well as whether the activation profile of these cells in the intestine of *T. cruzi*-infected patients in the chronic phase is M1- or M2-like.

3.7. Tryptase and Chymase: Mast Cells. Tryptase and chymase are the main serine proteases secreted by MCs; they mainly act as a factor to evaluate MC activation and classification in humans and mice [131, 132]. In general, tryptase and chymase are mainly involved in extracellular matrix degradation processes, tissue remodeling, and fibrosis [133–136] and have a dualistic role in inflammatory processes [137].

In fact, MCs play an important role in megacolon pathophysiology. Evidence shows that the concentration of these cells is increased regardless of the affected intestine layer [13, 34, 138, 139]; the same has been observed in a murine chronic phase model [140]. The increase in chymase-IR and tryptase-IR MCs has been shown to be correlated with decreased PGP 9.5-IR neurons in Chagasic megacolon [34]. In addition, only increased tryptase-IR MCs (and not chymase-IR MCs) were correlated with decreased PAR2-IR neurons. This receptor is cleaved by tryptase and participates in hyperactivation and neuronal death, triggering chronic intestinal function changes [141]. Also, there is a proximity between MCs in active degranulation (fragmented and anaphylactic) and intestinal nerve fibers, and the subsequent neuronal death could be partially mediated by the tryptase enzyme released through MC degranulation in Chagasic megacolon, and both proteases would be involved in the maintenance of the inflammatory process in the organ [34].

The communication between MCs and neurons in the intestine has already been reported in other studies [141–144], suggesting an important interface between the immune and nervous systems [145]. MC degranulation was found to be associated with nerve fiber network disintegration and loss of neuronal cell bodies in a coculture model between myenteric neurons and peritoneal MCs isolated from rats [146], and besides tryptase, other proinflammatory MC mediators such as IL-6 and prostaglandin 2 could induce neuronal death. The same was observed when a PAR2 agonist was used [146], corroborating what was suggested by Martins et al. [34] in Chagasic megacolon.

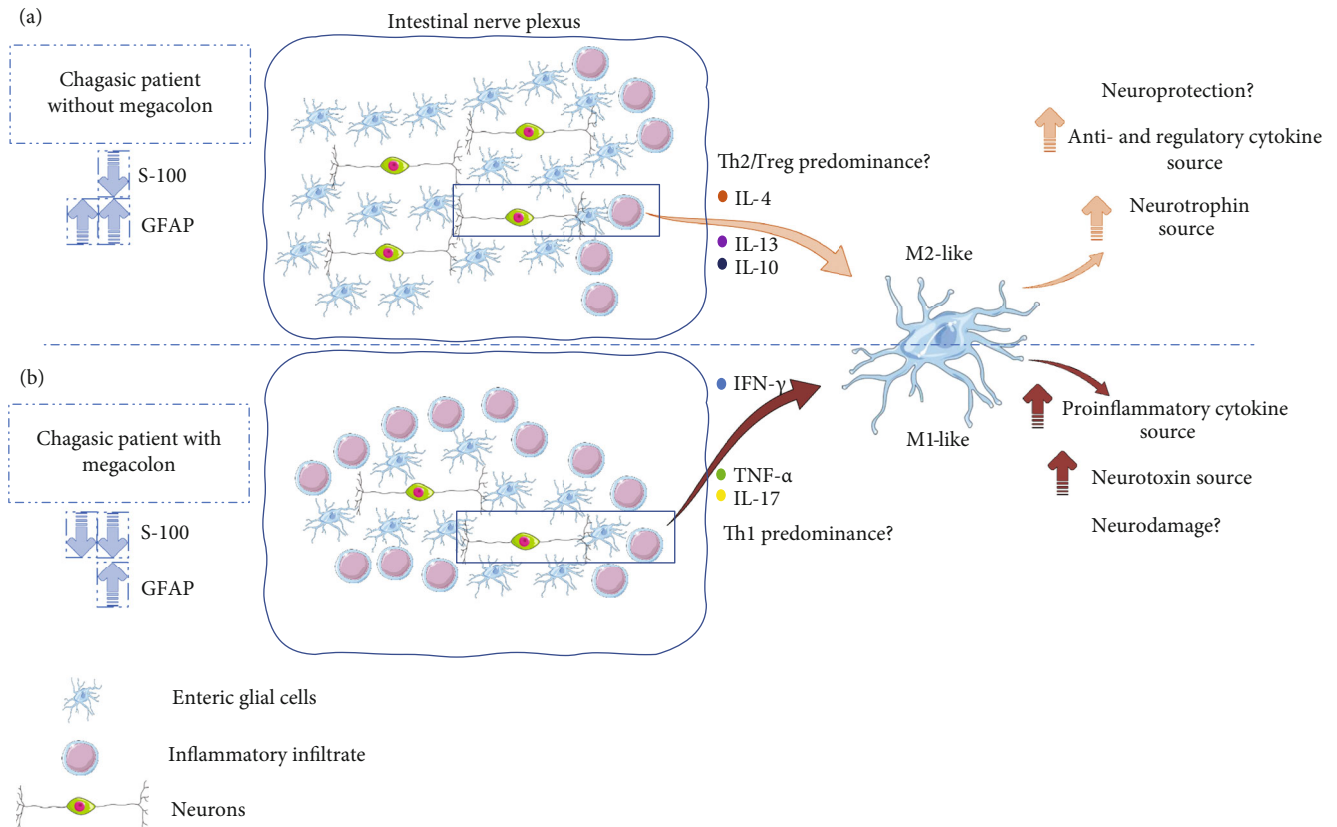


FIGURE 1: Hypothetical scheme of the differential behavior of enteric glial cells in the intestine of infected patients without megacolon (a) and with megacolon (b). This work, “Hypothetical scheme of the differential behavior of enteric glial cells in the intestine of infected patients without megacolon (a) and with megacolon (b),” is a derivative of “Servier Medical Art” by Servier, used under CC BY 3.0.

Neuropeptides have also been shown to activate MCs, which further confirms the participation of this cellular type in nervous system inflammation [147], such as SP in experimental dermatitis model [148] and irritable bowel syndrome [149]. Thus, the increased SP-IR neurons found in Chagasic megacolon are thought to be correlated with MC degranulation in the affected organ, subsequently releasing proinflammatory mediators such as TNF- α , IL-1 β , and tryptase, which reinforced the relation between MCs, tryptase, neuroinflammation, and neuronal death.

Moreover, tryptase was suggested to participate in the inflammatory cell transmigration process [150–153]. Lung allergy [154, 155], psoriasis [156], asthma [157], and CD models [158] showed that this protease is a potential component in eosinophilic infiltration. The increased tryptase-IR MCs in the myenteric plexus and internal muscle layer were positively correlated with increased eosinophils in the same regions in Chagasic megacolon [158] and showed cell proximity under electron microscopy, suggesting a possible communication between MCs and eosinophils via PAR2. The role of MCs–eosinophil communication during the *T. cruzi* infection is unknown, but MCs are believed to participate in eosinophil survival in Chagasic megacolon [158]. However, MCs–eosinophil cells interact through the production of mediators such as histamine, eotaxin, and tryptase produced by MCs [159] and via physical contact in other intestinal diseases [160]. A decreased eosinophil infiltration

was also observed under MC deficiency conditions [161], which reinforces the communication between these two cell types.

The presence of eosinophils in the *in vitro* and/or *in vivo* CD study models in humans was associated with protozoan destruction and control, tissue damage, and inflammatory process maintenance in both the acute and chronic phases of the disease [162–168]. In addition, this cell type was correlated with intestinal fibrosis in the nerve plexus and muscle layers of patients with megacolon, regions that showed an increased level of eosinophils compared to that in noninfected people and infected patients without megacolon [13]. The dual role of these cells in the affected intestine has been discussed. Increased eosinophils would allow (1) returning to intestinal homeostasis or/and (2) controlling the infection and consequently resulting in tissue damage.

The role of chymase in the inflammatory process is not yet clear. Evidence suggests that it participates in the pathophysiology of intestinal inflammatory diseases such as IBD [169] and protozoan [170] and helminth infections [171]. Therefore, the blockade of this protease is related to an improved intestinal inflammatory status [172, 173], which was related to increased IL-10, TGF- β , IL-17A, and T regulatory lymphocyte production in experimental IBD in rats [174].

In contrast, the expression of mast cell chymase gene (CMA1) was shown to be associated with increased IL-10

in an experimental chronic intestinal stress model [175], suggesting its regulatory role in the inflammatory process. In addition, a murine sepsis model showed that the mast cell protease 4 (corresponding to chymase in humans) degrades TNF- α , limiting the proinflammatory effect of this cytokine, which increased the survival of the animals [176]. The functions of these proteases are apparently dependent on the location of MCs producing it, which also varies according to the pathophysiology of each disease studied.

Besides the inflammatory process, chymase participates in tissue remodeling via TGF- β and metalloproteinases in different organs and pathological conditions [177, 178]. The presence of intestinal MCs in Chagasic megacolon is positively correlated with organ fibrosis [13]. Thus, increased chymase in the chronic phase of CD may represent a pathway for intestinal collagen deposition according to disease progression. However, little is known about this function in Chagasic megacolon.

Proteases produced by enteric MCs represent a source of therapeutic targets for Chagasic megacolon. Thus, further studies are needed to elucidate more completely the mechanisms involving these cells and their products since they can be related to several processes that affect the progression of Chagasic megacolon (Figure 2).

3.8. Galectins. Galectins are proteins of the lectin family that have high affinity for the β -galactoside residues present in the components of the extracellular matrix (ECM). Although all cells express galectins, the amount expressed varies according to cell type, tissue, and microenvironment. Approximately 15 types of galectins have been reported in vertebrates, with different body functions [179]. In general, these proteins are related to homeostasis conditions, inflammatory processes, and interactions with ECM components and between cells, cell adhesion, and fibrogenesis.

Changes in galectin levels were correlated with the progression and worse prognosis of intestinal diseases such as colorectal cancer, colorectal adenoma, rectal cancer, and Crohn's disease [180]. In CD, galectin-1 (gal-1) and galectin-3 (gal-3) production was analyzed in experimental *in vitro* cardiac form models and in infected patients with Chagas heart disease in the acute and chronic phases [181]. Information regarding the profile and function of these proteins in the megacolon is lacking.

Beghini et al. [182] were the first to show changed gal-1, gal-3, and gal-9 levels in the intestine of *T. cruzi*-infected patients with megacolon. The authors reported that these three galectins were highly expressed only in the myenteric plexus of patients with the digestive form of CD compared to those who were not infected. In addition, to better establish the gal-3 profile in Chagasic megacolon, Garvil et al. [183] analyzed the protein expression in the intestine of megacolon patients with intact or injured mucosa and in people without infection with an intact mucosa. Regardless of mucosal integrity, patients with Chagasic megacolon had more gal-3-marked cells [183]. Both studies suggested the potential functions of galectin in Chagasic megacolon.

Studies have shown that gal-1 has an ambiguous role in the course of *T. cruzi* infection, either acting in a protective

or detrimental manner. An *in vitro* cardiomyocyte infection model showed that the use of endogenous gal-1 inhibited *T. cruzi* infection [184]. The same study showed that gal-1-deficient mice had higher parasitemia, less tissue inflammation, and lower survival than wild mice, suggesting an important role of gal-1 in protection against infection [184]. In contrast, another study showed that this galectin can induce anergy and form dendritic and T regulatory tolerogenic lymphocyte cells in mice with acute *T. cruzi* infection. This would impair Th1 response, which is important for controlling infection, thereby increasing parasite persistence in the tissues [185].

Besides its impact on the course of infection, gal-1 was also found to be related to neuroprotection in neuroinflammatory diseases [186]. Thus, the increase of this galectin in Chagasic megacolon could be to protect the ENS and control the neuroinflammatory process. In a murine multiple sclerosis model knockout for gal-1, extracellular gal-1 and also gal-9 could induce Th1 and Th17 lymphocyte apoptosis, which decreased the established inflammatory process [187, 188]. In addition, the administration of endogenous gal-1 in this same wild murine model inhibited microglia activation for the M1-like profile (important in EAE pathophysiology), favoring M2-like polarization and neuroprotection in this pathology [189]. Gal-1 also induces macrophages to produce NTs, stimulates the regenerative process of axons, and facilitates Schwann cell migration to injured peripheral nerves [190]. Thus, future studies need to elucidate the role of gal-1 in the inflammatory process in the chronic phase of CD and its relationship with ENS components.

Considering that Gal-3 level increases in the myenteric plexus of CD patients with megacolon, its role in facilitating the establishment of cell invasion at the early stages of infection, maintenance of the inflammatory process, and induction of fibrosis in the intestine has been discussed [182, 183]. In fact, these processes were already revealed in experimental Chagas cardiopathy models, in which the increase of this lectin was found to be directly related to increased inflammatory processes and cardiac fibrosis. Gal-3 also has a relationship with MCs by inducing their degranulation, a process involved in collagen fiber formation and tissue remodeling by tryptase [191]. Thus, gal-3 could have a detrimental role in the Chagasic megacolon and could be involved in the progression of the digestive form in both the persistence of the inflammatory process and the induction of tissue remodeling.

Gal-3 also plays an essential role in neuroinflammation [186], a process that may represent a new pathway for the maintenance of the neural inflammatory process in Chagasic megacolon. An experimental EAE model with a knockout phenotype for gal-3 suggested that this lectin would exacerbate the inflammatory process of the disease by increasing IL-17 and IFN- γ and decreasing IL-10 [192]. As for the ENS, a murine stroke model (middle cerebral artery occlusion) showed that serum from C57Bl/6 mice overexpressing gal-3 decreased the *in vitro* survival of intestinal myenteric neurons [193]. The same was observed when these cells were exposed to purified gal-3 [193]. Finally, the authors concluded that gal-3 release in the central and peripheral

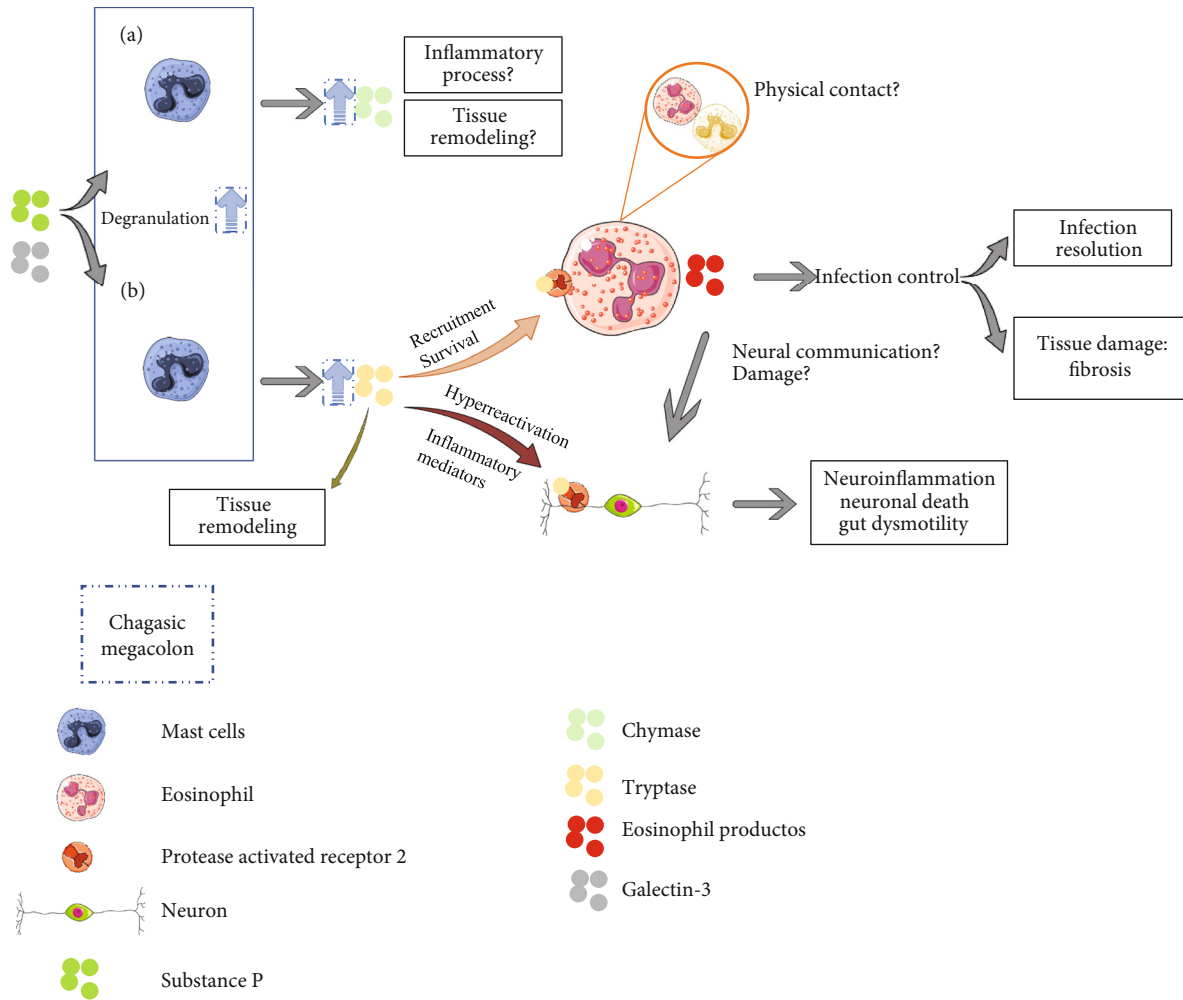


FIGURE 2: Possible functions of mast cells and chymase (a) and tryptase (b) proteases in Chagasic megacolon. This work, “Possible functions of mast cells and chymase (a) and tryptase (b) proteases in Chagasic megacolon,” is a derivative of “Servier Medical Art” by Servier, used under CC BY 3.0.

nervous systems would be directly related to intestinal neuronal death via toll-like receptor 4, an innate immunity receptor previously related to death induction in neurons [193]. Future studies need to focus on identifying gal-3 inhibitors for the control and treatment of CNS neuroinflammatory pathologies [194]. Thus, the use and search for these inhibitors may also represent alternatives for ENS-related diseases such as Chagasic megacolon.

Further studies are needed to elucidate the role of galectins in the digestive form of CD, as most of the studies available are related to cardiac changes. In general, these lectins may also mediate the interaction between the immune and nervous systems, suggesting new therapeutic targets based on gal-3 blockade or even gal-1 or gal-9 administration [186].

3.9. Serotonin and Receptors. Serotonin, or 5-hydroxytryptamine (5-HT), was initially discovered as a part of the coagulation process [195] and was later described in the homeostasis of several tissues such as the CNS [196] and the intestine [197, 198]. Enterochromaffin cells (ECs) of the intestinal mucosa synthesize, store, and release most of the serotonin in the body near the terminal of intestinal

nerves [199, 200]. Other intestinal components such as enteric neurons and myenteric plexus cells also produce serotonin [201]. In addition, immune cells, enterocytes, and enteric neurons can express different subtypes of 5-HT receptors activated by 5-HT, which reveals the connection between the three systems: neuronal, immune, and endocrine [202]. Serotonin is known to be important in the modulation of the inflammatory process.

Changes in serotonin levels and metabolism receptors and intermediates were related to the progression of gastrointestinal diseases such as irritable bowel syndrome [203], IBD [204], celiac disease [205], and intestinal infectious diseases such as *Vibrio cholerae* [206, 207], *Salmonella typhimurium* [208], and *Trichinella spiralis* [209] infections. Changes in serotonin metabolism were shown to be related to the induction of inflammation and intestinal physiological changes [210].

Discordant evidence shows that the role of serotonin in CD depends on the progression of the digestive form. Some studies suggest that serotonin plays an anti-inflammatory role in the intestine of *T. cruzi*-infected patients without organ involvement, in which serotonin level is high and B

TABLE 1: Intestinal microenvironment and biological behavior of the components involved in the pathophysiology of Chagasic megacolon.

Biomarker or techniques	Markers	Behavior	Supposed participation in the pathogenesis	References
PGP 9.5	Pan-neural	↓	Destruction induced by the parasite and the inflammatory process established in the intestine. It affects intestinal motility and is involved with fecal stasis, organ dilation, and Chagasic megacolon progression.	[15, 34]
Peripherin	Pan-neural	↓		[50, 112]
	Disregarded	-		[48, 57]
HuC/HuDa	Pan-neural	↓		[56]
Substance P	Excitatory motor neurons (SP)	↑	Maintenance of the intestinal proinflammatory profile.	[56, 77]
GAP-43	Excitatory motor neuron regeneration (GAP-43/SP and GAP-43/cCHAT)	=	The greatest regeneration found in the subpopulations of inhibitory motor neurons (GAP-43/VIP and GAP-43/NO) is related to the greater destruction of these cell types when compared to the other subpopulations, which do not suffer reduction. Thus, through compensatory mechanisms, the subpopulation of inhibitory neurons tries to be reestablished, and due to this, there is only an increase in this subpopulation.	[50]
	Inhibitory motor neuron regeneration (GAP-43/VIP and GAP-43/NO)	↑		
	Intrinsic primary afferent neuron regeneration (GAP-43/calretinin)	=		
	Interneuron regeneration (GAP-43/neuropeptide Y)	=		
S-100	Enteric glial cells	↓	Infection focus in the intestine.	[15, 21, 114]
GFAP	Enteric activated glial cells	↑	Increased activation of this cell type in an attempt to control the infection through the production of proinflammatory and microbicidal components, which leads to neurotoxicity or/and increased activation of this cell type in an attempt to control the inflammatory process through the production of anti and regulatory cytokines and neuroprotective components.	[15, 21]
CD3 ⁺	T lymphocyte	↑	Participation of the immune response in neuronal loss.	[8, 15]
CD20 ⁺	B lymphocyte	↑		
CD68 ⁺	Macrophage	↑		
CD57 ⁺	Natural killer cell	↑		
TIA-1+	Cytotoxic lymphocyte	↑		
Hematoxylin-eosin section	Eosinophil	↑	Participation of the immune response in neuronal loss and intestinal remodeling.	[13]
Giemsa/toluidine blue section	Mast cell	↑		[13, 139]
Serotonin	Serotonin-producing cells	↓	Duality between the anti-inflammatory and proinflammatory role of the components.	[138, 211]
5-HT3a receiver	Lymphocytes producing 5-HT3a receptor	↓		[32]
Tryptase	Tryptase-producing mast cells	↑		[212]
Chymase	Chymase-producing mast cells	↑	Participation in neuronal damage, maintenance of the inflammatory process, and tissue remodeling in the intestine.	[34, 158]
Galectin-1 and -9	Galectins	↑	Neuroprotection and infection control.	[34]
Galectin-3	Galectins	↑	Maintenance of the inflammatory process, neuroinflammation, and fibrosis.	[182]

↑: increased component compared to healthy intestine without *T. cruzi* infection; ↓: decreased component compared to healthy intestine without *T. cruzi* infection; =: no component change compared to healthy intestine without *T. cruzi* infection.

and T lymphocyte [211] and MC [138] levels are low. The opposite was observed in megacolon, in which the amount of these inflammatory cells was higher than that of serotonin [138, 211]. In contrast, the serotonergic activity was greater in the intestinal crypt cells in Chagasic megacolon than in noninfected people and patients with idiopathic megacolon [32].

The anti-inflammatory function of serotonin was reinforced by showing that lymphocytes present in the intestine of infected patients without megacolon expressed greater amount of serotonin's 5-HT3A receptor than those in patients with megacolon [212]. In addition, CD8⁺ and CD20⁺ lymphocytes were higher in the most severe form than in the nondigestive form of CD [212]. These results

corroborate the initial discussion on the immune suppressor role of serotonin [138, 211]. They also contribute to the development of a new pathway, in which this molecule would act on lymphocytes via the 5-HT_{3A} receptor, leading to the inhibition of these cells. This would prevent the exacerbated immune response in CD patients without megacolon [212].

However, more information regarding the role of serotonin in the acute and chronic phases of CD is needed. The diversity of results found with either increased or decreased serotonin in Chagasic megacolon can be attributed to the methodological differences related to the phase of the disease, comparative groups, and experimental models used in each study.

A summary of biomarkers potentially involved in digestive CD establishment and/or progression is presented in Table 1.

4. Outstanding Questions for Further Scrutiny

The data discussed in this review raises the following questions to help clarify the several components involved in the intestinal form of CD:

- (i) Does the activation of ECGs with a proinflammatory profile precede neural destruction in Chagasic megacolon? What is the behavior of ECGs in the acute phase of CD?
- (ii) Do ECGs influence intestinal motility and mucosal changes in Chagasic megacolon?
- (iii) Are ECGs protective or harmful in the progression of Chagasic megacolon?
- (iv) Would it be possible to stimulate neuronal regeneration in the intestine of CD patients with megacolon?
- (v) Does serotonin have different effects in acute and chronic phases of *T. cruzi* infection? What is the relationship between serotonin and immune system activation or inhibition in Chagasic megacolon?
- (vi) Would MC enzymes, such as tryptase, be another neuronal cell death mechanism and maintaining the inflammatory perfil in Chagasic megacolon?
- (vii) What is the function of chymase in intestinal tissue remodeling in Chagasic megacolon?
- (viii) Would galectins be involved in the maintenance of the inflammatory process and intestinal remodeling in CD patients with megacolon?
- (ix) What is the role of galectins in the protection or intestinal neuronal damage in CD?

The answer to any of these questions may be related to the development of new therapies to prevent, improve, or even reverse the severity of Chagasic megacolon.

5. Conclusion

Although over 100 years have passed since the discovery of CD, little is known about the specific mechanism of Chagasic

megacolon pathogenesis. This review shows that Chagasic patients with or without megacolon have a rich and differentiated intestinal microenvironment. Additionally, the participation of neurons, glial cells, MCs, eosinophils, and proteins addressed in this review reveals the high complexity of Chagasic megacolon pathology. The progression of the digestive form of *T. cruzi* infection is associated with different components that circulate and interact with the immunological, endocrine, and neurological systems. Glial cells and MCs are potential participants in its systems since they are sensitive to stimuli such as proinflammatory cytokines, serotonin, and galectins. Thus, a more profound analysis of these components could contribute to clinical management and the identification of new therapeutic targets.

Data Availability

All the data used to support the findings of this study are included within the article and references.

Conflicts of Interest

The authors declare that there is no conflict of interest regarding the publication of this review article.

References

- [1] M. C. P. Nunes, A. Beaton, H. Acquatella et al., "Chagas cardiomyopathy: an update of current clinical knowledge and management: a scientific statement from the American Heart Association," *Circulation*, vol. 138, no. 12, pp. e169–e209, 2018.
- [2] A. da Silva Sousa Júnior, V. R. d. C. M. Palácios, C. d. S. Miranda et al., "Análise espaço-temporal da doença de Chagas e seus fatores de risco ambientais e demográficos no município de Barcarena, Pará, Brasil," *Revista Brasileira de Epidemiologia*, vol. 20, no. 4, pp. 742–755, 2017.
- [3] A. Vargas, J. M. A. S. Malta, V. M. Costa et al., "Investigação de surto de doença de Chagas aguda na região extra-amazônica, Rio Grande do Norte, Brasil, 2016," *Cadernos de Saúde Pública*, vol. 34, no. 1, 2018.
- [4] G. H. F. Sampaio, A. N. B. da Silva, C. R. D. N. Brito et al., "Epidemiological profile of acute Chagas disease in individuals infected by oral transmission in Northern Brazil," *Revista da Sociedade Brasileira de Medicina Tropical*, vol. 53, 2020.
- [5] J. A. Pérez-Molina and I. Molina, "Chagas disease," *The Lancet*, vol. 391, no. 10115, pp. 82–94, 2018.
- [6] C. Chagas, "Processos patojenicos da tripanozomiasis americana," *Memórias do Instituto Oswaldo Cruz*, vol. 8, no. 2, pp. 5–36, 1916.
- [7] W. L. Tafuri, "Light and electron microscope studies of the autonomic nervous system in experimental and human American trypanosomiasis," *Virchows Archiv Abteilung A Pathologische Anatomie*, vol. 354, no. 2, pp. 136–149, 1971.
- [8] C. E. P. Corbett, U. Ribeiro, M. G. Prianti, A. Habr-Gama, M. Okumura, and J. Gama-Rodrigues, "Cell-mediated immune response in megacolon from patients with chronic Chagas' disease," *Diseases of the Colon & Rectum*, vol. 44, no. 7, pp. 993–998, 2001.

- [9] S. J. Adad, D. C. S. Andrade, E. R. Lopes, and E. Chapadeiro, "Pathological anatomy of chagasic megaesophagus," *Revista do Instituto de Medicina Tropical de São Paulo*, vol. 33, no. 6, pp. 443–450, 1991.
- [10] M. M. De Souza, S. G. Andrade, A. A. Barbosa Jr, R. T. M. Santos, V. A. F. Alves, and Z. A. Andrade, "Trypanosoma cruzi strains and autonomic nervous system pathology in experimental Chagas disease," *Memórias do Instituto Oswaldo Cruz*, vol. 91, no. 2, pp. 217–224, 1996.
- [11] S. J. Adad, C. G. Cançado, R. M. Etchebehere et al., "Neuron count reevaluation in the myenteric plexus of chagasic megacolon after morphometric neuron analysis," *Virchows Archiv*, vol. 438, no. 3, pp. 254–258, 2001.
- [12] Z. A. Andrade and S. G. Andrade, "Immunochemical study of experimental Chagas' disease," *Revista do Instituto de Medicina Tropical de São Paulo*, vol. 11, no. 1, pp. 44–47, 1969.
- [13] A. B. M. da Silveira, S. J. Adad, R. Correa-Oliveira, J. B. Furness, and D. D'Avila Reis, "Morphometric study of eosinophils, mast cells, macrophages and fibrosis in the colon of chronic chagasic patients with and without megacolon," *Parasitology*, vol. 134, no. 6, pp. 789–796, 2007.
- [14] A. B. M. da Silveira, R. M. E. Arantes, A. R. Vago et al., "Comparative study of the presence of Trypanosoma cruzi DNA, inflammation and denervation in chagasic patients with and without megaesophagus," *Parasitology*, vol. 131, no. 5, pp. 627–634, 2005.
- [15] A. B. M. da Silveira, E. M. Lemos, S. J. Adad, R. Correa-Oliveira, J. B. Furness, and D. D'Avila Reis, "Megacolon in Chagas disease: a study of inflammatory cells, enteric nerves, and glial cells," *Human Pathology*, vol. 38, no. 8, pp. 1256–1264, 2007.
- [16] B. M. Ribeiro, E. Crema, and V. Rodrigues Jr., "Analysis of the cellular immune response in patients with the digestive and indeterminate forms of Chagas' disease," *Human Immunology*, vol. 69, no. 8, pp. 484–489, 2008.
- [17] M. M. Camargo, A. C. Andrade, I. C. Almeida, L. R. Travassos, and R. T. Gazzinelli, "Glycoconjugates isolated from Trypanosoma cruzi but not from Leishmania species membranes trigger nitric oxide synthesis as well as microbicidal activity in IFN-gamma-primed macrophages," *Journal of Immunology*, vol. 159, no. 12, 1997.
- [18] B. Basso, "Modulation of immune response in experimental Chagas disease," *World J Exp Med*, vol. 3, no. 1, pp. 1–10, 2013.
- [19] J. E. Yuste, E. Tarragon, C. M. Campuzano, and F. Ros-Bernal, "Implications of glial nitric oxide in neurodegenerative diseases," *Frontiers in Cellular Neuroscience*, vol. 9, p. 322, 2015.
- [20] F. Ochoa-Cortes, F. Turco, A. Linan-Rico et al., "Enteric glial cells: a new frontier in neurogastroenterology and clinical target for inflammatory bowel diseases," *Inflamm Bowel Dis*, vol. 22, no. 2, pp. 433–449, 2016.
- [21] A. B. M. da Silveira, M. A. R. Freitas, E. C. de Oliveira et al., "Glial fibrillary acidic protein and S-100 colocalization in the enteroglial cells in dilated and nondilated portions of colon from chagasic patients," *Hum Pathol*, vol. 40, no. 2, pp. 244–251, 2009.
- [22] R. M. E. Arantes, H. H. F. Marche, M. T. Bahia, F. Q. Cunha, M. A. Rossi, and J. S. Silva, "Interferon- γ -induced nitric oxide causes intrinsic intestinal denervation in Trypanosoma cruzi-infected mice," *Am J Pathol*, vol. 164, no. 4, pp. 1361–1368, 2004.
- [23] J. R. da, M. E. R. S. Camargos, E. Chiari, and C. R. S. Machado, "Trypanosoma cruzi infection and the rat central nervous system: proliferation of parasites in astrocytes and the brain reaction to parasitism," *Brain Res Bull*, vol. 53, no. 2, pp. 153–162, 2000.
- [24] J. E. H. Pittella, "Central nervous system involvement in experimental Trypanosomiasis cruzi," *Memórias do Instituto Oswaldo Cruz*, vol. 86, no. 2, pp. 141–145, 1991.
- [25] E. Villela and E. Villela, "Elementos do sistema nervoso central parasitados pelo Trypanosoma cruzi," *Mem Inst Oswaldo Cruz*, vol. 26, no. 1, pp. 77–81, 1932.
- [26] P. Jackson and R. J. Thompson, "The demonstration of new human brain-specific proteins by high-resolution two-dimensional polyacrylamide gel electrophoresis," *J Neurol Sci*, vol. 49, no. 3, pp. 429–438, 1981.
- [27] R. J. Thompson, J. F. Doran, P. Jackson, A. P. Dhillon, and J. Rode, "PGP 9.5—a new marker for vertebrate neurons and neuroendocrine cells," *Brain Res*, vol. 278, no. 1–2, pp. 224–228, 1983.
- [28] Y. Watanabe, F. Ito, H. Ando et al., "Morphological investigation of the enteric nervous system in Hirschsprung's disease and hypoganglionosis using whole-mount colon preparation," *J Pediatr Surg*, vol. 34, no. 3, pp. 445–449, 1999.
- [29] D. de Fontgalland, S. J. Brookes, I. Gibbins, T. C. Sia, and D. A. Wattchow, "The neurochemical changes in the innervation of human colonic mesenteric and submucosal blood vessels in ulcerative colitis and Crohn's disease," *Neurogastroenterol Motil*, vol. 26, no. 5, pp. 731–744, 2014.
- [30] H. J. Krammer, W. Meier-Ruge, W. Sigge, R. Eggert, and W. Kühnel, "Histopathological features of neuronal intestinal dysplasia of the plexus submucosus in whole mounts revealed by immunohistochemistry for PGP 9.5," *Eur J Pediatr Surg*, vol. 4, no. 6, pp. 358–361, 1994.
- [31] L. Ny, K. Persson, B. Larsson et al., "Localization and activity of nitric oxide synthases in the gastrointestinal tract of Trypanosoma cruzi-infected mice," *J Neuroimmunol*, vol. 99, no. 1, pp. 27–35, 1999.
- [32] V. Kannen, J. Y. Sakita, Z. A. Carneiro et al., "Mast cells and serotonin synthesis modulate Chagas disease in the colon: clinical and experimental evidence," *Dig Dis Sci*, vol. 63, no. 6, pp. 1473–1484, 2018.
- [33] C. F. Campos, S. D. Cangussú, A. L. C. Duz et al., "Correction: Enteric neuronal damage, intramuscular denervation and smooth muscle phenotype changes as mechanisms of chagasic megacolon: evidence from a long-term murine model of Tripanosoma cruzi infection," *PLoS One*, vol. 12, no. 4, article e0176224, 2017.
- [34] P. R. Martins, R. D. Nascimento, A. T. dos Santos, E. C. de Oliveira, P. M. Martinelli, and D. d'Avila Reis, "Mast cell-nerve interaction in the colon of Trypanosoma cruzi-infected individuals with chagasic megacolon," *Parasitol Res*, vol. 117, no. 4, pp. 1147–1158, 2018.
- [35] A. Moncla, F. Landon, M. G. Mattei, and M. M. Portier, "Chromosomal localisation of the mouse and human peripherin genes," *Genet Res*, vol. 59, no. 2, pp. 125–129, 1992.
- [36] L. M. Parysek and R. D. Goldman, "Characterization of intermediate filaments in PC12 cells," *J Neurosci*, vol. 7, no. 3, pp. 781–791, 1987.
- [37] B. A. Brody, C. A. Ley, and L. M. Parysek, "Selective distribution of the 57 kDa neural intermediate filament protein in the rat CNS," *J Neurosci*, vol. 9, no. 7, pp. 2391–2401, 1989.
- [38] E. M. Hol and Y. Capetanaki, "Type III intermediate filaments desmin, glial fibrillary acidic protein (GFAP),

- vimentin, and peripherin," *Cold Spring Harbor Perspectives in Biology*, vol. 9, no. 12, 2017.
- [39] S. Xiao, J. McLean, and J. Robertson, "Neuronal intermediate filaments and ALS: a new look at an old question," *Biochimica et Biophysica Acta - Molecular Basis of Disease*, vol. 1762, no. 11-12, pp. 1001-1012, 2006.
- [40] R. K. H. Liem and A. Messing, "Dysfunctions of neuronal and glial intermediate filaments in disease," *Journal of Clinical Investigation*, vol. 119, no. 7, pp. 1814-1824, 2009.
- [41] J. McLean, H. N. Liu, D. Miletic et al., "Distinct biochemical signatures characterize peripherin isoform expression in both traumatic neuronal injury and motor neuron disease," *J Neurochem*, vol. 114, no. 4, pp. 1177-1192, 2010.
- [42] K. S. Eriksson, S. Zhang, L. Lin, R. C. Larivière, J. P. Julien, and E. Mignot, "The type III neurofilament peripherin is expressed in the tuberomammillary neurons of the mouse," *BMC Neurosci*, vol. 9, no. 1, p. 26, 2008.
- [43] C. M. Leeth, J. Racine, H. D. Chapman et al., "B-lymphocytes expressing an Ig specificity recognizing the pancreatic β -cell autoantigen peripherin are potent contributors to type 1 diabetes development in NOD mice," *Diabetes*, vol. 65, no. 7, pp. 1977-1987, 2016.
- [44] T. M. Doran, J. Morimoto, S. Simanski et al., "Discovery of phosphorylated peripherin as a major humoral autoantigen in type 1 diabetes mellitus," *Cell Chem Biol*, vol. 23, no. 5, pp. 618-628, 2016.
- [45] A. Brehmer, H. Rupprecht, and W. Neuhuber, "Two submucosal nerve plexus in human intestines," *Histochem Cell Biol*, vol. 133, no. 2, pp. 149-161, 2010.
- [46] K. M. Chisholm and T. A. Longacre, "Utility of peripherin versus MAP-2 and calretinin in the evaluation of Hirschsprung disease," *Appl Immunohistochem Mol Morphol*, vol. 24, no. 9, pp. 627-632, 2016.
- [47] S. K. Holland, R. B. Hessler, M. D. Reid-Nicholson, P. Ramalingam, and J. R. Lee, "Utilization of peripherin and S-100 immunohistochemistry in the diagnosis of Hirschsprung disease," *Mod Pathol*, vol. 23, no. 9, pp. 1173-1179, 2010.
- [48] K. Kramer, A. B. M. da Silveira, S. Jabari, M. Kressel, M. Raab, and A. Brehmer, "Quantitative evaluation of neurons in the mucosal plexus of adult human intestines," *Histochemistry and Cell Biology*, vol. 136, no. 1, pp. 1-9, 2011.
- [49] A. Barcelos Morais da Silveira, E. C. de Oliveira, S. G. Neto et al., "Enteroglial cells act as antigen-presenting cells in chagasic megacolon," *Hum Pathol*, vol. 42, no. 4, pp. 522-532, 2011.
- [50] M. D. Moreira, A. Brehmer, E. C. de Oliveira et al., "Regenerative process evaluation of neuronal subclasses in chagasic patients with megacolon," *Hum Immunol*, vol. 74, no. 2, pp. 181-188, 2013.
- [51] L. Sunesson, U. Hellman, and C. Larsson, "Protein kinase Ce binds peripherin and induces its aggregation, which is accompanied by apoptosis of neuroblastoma cells," *J Biol Chem*, vol. 283, no. 24, pp. 16653-16664, 2008.
- [52] H. J. Okano and R. B. Darnell, "A hierarchy of Hu RNA binding proteins in developing and adult neurons," *J Neurosci*, vol. 17, no. 9, pp. 3024-3037, 1997.
- [53] M. D. Gershon, "Behind an enteric neuron there may lie a glial cell," *Journal of Clinical Investigation*, vol. 121, no. 9, pp. 3386-3389, 2011.
- [54] Z. Lin, N. Gao, H. Z. Hu et al., "Immunoreactivity of Hu proteins facilitates identification of myenteric neurones in guinea-pig small intestine," *Neurogastroenterol Motil*, vol. 14, no. 2, pp. 197-204, 2002.
- [55] R. de Giorgio, M. Bovara, G. Barbara et al., "Anti-HuD-induced neuronal apoptosis underlying paraneoplastic gut dysmotility," *Gastroenterology*, vol. 125, no. 1, pp. 70-79, 2003.
- [56] A. B. M. da Silveira, D. D'Avila Reis, E. C. de Oliveira et al., "Neurochemical coding of the enteric nervous system in chagasic patients with megacolon," *Dig Dis Sci*, vol. 52, no. 10, pp. 2877-2883, 2007.
- [57] S. Jabari, A. B. M. da Silveira, E. C. de Oliveira et al., "Selective survival of calretinin- and vasoactive-intestinal-peptide-containing nerve elements in human chagasic submucosa and mucosa," *Cell Tissue Res*, vol. 349, no. 2, pp. 473-481, 2012.
- [58] P. Vento and S. Soynila, "Quantitative comparison of growth-associated protein GAP-43, neuron-specific enolase, and protein gene product 9.5 as neuronal markers in mature human intestine," *J Histochem Cytochem*, vol. 47, no. 11, pp. 1405-1415, 2016.
- [59] U. S. V. Euler and J. H. Gaddum, "An unidentified depressor substance in certain tissue extracts," *J Physiol*, vol. 72, no. 1, pp. 74-87, 1931.
- [60] C. Severini, G. Improta, G. Falconieri-Ersamer, S. Salvadori, and V. Ersamer, "The tachykinin peptide family," *Pharmacological Reviews*, vol. 54, no. 2, pp. 285-322, 2002.
- [61] J. C. Ansel, A. H. Kaynard, C. A. Armstrong, J. Olerud, N. Bunnett, and D. Payan, "Skin-nervous system interactions," *J Invest Dermatol*, vol. 106, no. 1, pp. 198-204, 1996.
- [62] A. Mashaghi, A. Marmalidou, M. Tehrani, P. M. Grace, C. Pothoulakis, and R. Dana, "Neuropeptide substance P and the immune response," *Cellular and Molecular Life Sciences*, vol. 73, no. 22, pp. 4249-4264, 2016.
- [63] W. K. Hon and C. Pothoulakis, "Immunomodulatory properties of substance P: the gastrointestinal system as a model," in *Annals of the New York Academy of Sciences*, pp. 23-40, Blackwell Publishing Inc., 2006.
- [64] M. G. Vannucchi and S. Evangelista, "Neurokinin receptors in the gastrointestinal muscle wall: cell distribution and possible roles," *Biomolecular Concepts*, vol. 4, no. 3, pp. 221-231, 2013.
- [65] T. M. O'Connor, J. O'Connell, D. I. O'Brien, T. Goode, C. P. Bredin, and F. Shanahan, "The role of substance P in inflammatory disease," *Journal of Cellular Physiology*, vol. 201, no. 2, pp. 167-180, 2004.
- [66] M. B. Johnson, A. D. Young, and I. Marriott, "The therapeutic potential of targeting substance P/NK-1R interactions in inflammatory CNS disorders," *Front Cell Neurosci*, vol. 10, 2017.
- [67] D. Renzi, B. Pellegrini, F. Tonelli, C. Surrenti, and A. Calabrò, "Substance P (neurokinin-1) and neurokinin A (neurokinin-2) receptor gene and protein expression in the healthy and inflamed human intestine," *Am J Pathol*, vol. 157, no. 5, pp. 1511-1522, 2000.
- [68] T. R. Koch, J. A. Carney, and L. W. Vay Go, "Distribution and quantitation of gut neuropeptides in normal intestine and inflammatory bowel diseases," *Dig Dis Sci*, vol. 32, no. 4, pp. 369-376, 1987.
- [69] J. V. Weinstock, "Substance P and the regulation of inflammation in infections and inflammatory bowel disease," *Acta Physiologica*, vol. 213, no. 2, pp. 453-461, 2015.
- [70] N. M. Delvalle, C. Dharshika, W. Morales-Soto, D. E. Fried, L. Gaudette, and B. D. Gulbransen, "Communication

- between enteric neurons, glia, and nociceptors underlies the effects of tachykinins on neuroinflammation," *Cell Mol Gastroenterol Hepatol*, vol. 6, no. 3, pp. 321–344, 2018.
- [71] J. M. Ziebell and M. C. Morganti-Kossmann, "Involvement of pro- and anti-inflammatory cytokines and chemokines in the pathophysiology of traumatic brain injury," *Neurotherapeutics*, vol. 7, no. 1, pp. 22–30, 2010.
- [72] P. G. E. Kennedy, J. Rodgers, F. W. Jennings, M. Murray, S. E. Leeman, and J. M. Burke, "A substance P antagonist, RP-67,580, ameliorates a mouse meningoencephalitic response to *Trypanosoma brucei brucei*," *Proceedings of the National Academy of Sciences of the United States of America*, vol. 94, no. 8, pp. 4167–4170, 1997.
- [73] A. Garza, J. Weinstock, and P. Robinson, "Absence of the SP/SP receptor circuitry in the substance P-precursor knockout mice or SP receptor, neurokinin (NK)1 knockout mice leads to an inhibited cytokine response in granulomas associated with murine *Taenia crassiceps* infection," *J Parasitol*, vol. 94, no. 6, pp. 1253–1258, 2008.
- [74] E. K. Reinke, M. J. Johnson, C. Ling et al., "Substance P receptor mediated maintenance of chronic inflammation in EAE," *J Neuroimmunol*, vol. 180, no. 1–2, pp. 117–125, 2006.
- [75] Q. Li, X. Wu, Y. Yang et al., "Tachykinin NK1 receptor antagonist L-733,060 and substance P deletion exert neuroprotection through inhibiting oxidative stress and cell death after traumatic brain injury in mice," *Int J Biochem Cell Biol*, vol. 107, pp. 154–165, 2019.
- [76] V. S. Chauhan, J. M. Kluttz, K. L. Bost, and I. Marriott, "Prophylactic and therapeutic targeting of the neurokinin-1 receptor limits neuroinflammation in a murine model of pneumococcal meningitis," *J Immunol*, vol. 186, no. 12, pp. 7255–7263, 2011.
- [77] A. B. M. da Silveira, M. A. R. Freitas, E. C. de Oliveira et al., "Substance P and NK1 receptor expression in the enteric nervous system is related to the development of chagasic megacolon," *Trans R Soc Trop Med Hyg*, vol. 102, no. 11, pp. 1154–1156, 2008.
- [78] R. G. Long, A. J. Barnes, D. J. O'Shaughnessy et al., "Neural and hormonal peptides in rectal biopsy specimens from patients with Chagas' disease and chronic autonomic failure," *Lancet*, vol. 315, no. 8168, pp. 559–562, 1980.
- [79] H. O. Almeida, W. L. Tafuri, J. R. Cunha-Melo, L. Freire-Maia, P. Raso, and Z. Brener, "Studies on the vesicular component of the Auerbach's plexus and the substance P content of the mouse colon in the acute phase of the experimental *Trypanosoma cruzi* infection," *Virchows Arch A Pathol Anat Histol*, vol. 376, no. 4, pp. 353–360, 1977.
- [80] L. B. M. Maifrino, E. A. Liberti, and R. R. de Souza, "Vasoactive-intestinal-peptide- and substance-P-immunoreactive nerve fibres in the myenteric plexus of mouse colon during the chronic phase of *Trypanosoma cruzi* infection," *Ann Trop Med Parasitol*, vol. 93, no. 1, pp. 49–56, 1999.
- [81] C. A. Maggi, "The effects of tachykinins on inflammatory and immune cells," *Regulatory Peptides*, vol. 70, no. 2-3, pp. 75–90, 1997.
- [82] J. V. Weinstock, A. Blum, A. Metwali, D. Elliott, and R. Arsenescu, "IL-18 and IL-12 signal through the NF- κ B pathway to induce NK-1R expression on T cells," *J Immunol*, vol. 170, no. 10, pp. 5003–5007, 2003.
- [83] M. Beinborn, A. Blum, L. Hang et al., "TGF- β regulates T-cell neurokinin-1 receptor internalization and function," *Proceedings of the National Academy of Sciences*, vol. 107, no. 9, pp. 4293–4298, 2010.
- [84] P. Holzer and U. Holzer-Petsche, "Tachykinins in the gut. Part II. Roles in neural excitation, secretion and inflammation," *Pharmacology and Therapeutics*, vol. 73, no. 3, pp. 219–263, 1997.
- [85] M. R. Holahan, "A shift from a pivotal to supporting role for the growth-associated protein (GAP-43) in the coordination of axonal structural and functional plasticity," *Frontiers in Cellular Neuroscience*, vol. 11, 2017.
- [86] D. Grynspan, A. C. C. Giassi, R. Cadonic et al., "Growth-associated protein-43 (GAP-43) expression in ganglionic and aganglionic colon," *Pediatric and Developmental Pathology*, vol. 15, 2012.
- [87] A. Saeed, L. Barreto, S. G. Neogii, A. Loos, I. Mcfarlane, and A. Aslam, "Identification of novel genes in Hirschsprung disease pathway using whole genome expression study," *Journal of Pediatric Surgery*, vol. 47, no. 2, pp. 303–307, 2012.
- [88] L. CMY, R. K. Kumar, D. Z. Lubowski, and E. Burcher, "Neuropeptides and nerve growth in inflammatory bowel diseases: a quantitative immunohistochemical study," *Digestive Diseases and Sciences*, vol. 47, no. 3, pp. 495–502, 2002.
- [89] P. Di Sebastiano, T. Fink, F. F. di Mola et al., "Neuroimmune appendicitis," *The Lancet*, vol. 354, no. 9177, pp. 461–466, 1999.
- [90] H. Kobayashi, H. Hirakawa, and P. Puri, "Is intestinal neuronal dysplasia a disorder of the neuromuscular junction?," *Journal of Pediatric Surgery*, vol. 31, no. 4, pp. 575–579, 1996.
- [91] R. H. Stead, U. Kosecka-Janiszewska, A. B. Oestreicher, M. F. Dixon, and J. Bienenstock, "Remodeling of B-50 (GAP-43)- and NSE-immunoreactive mucosal nerves in the intestines of rats infected with *Nippostrongylus brasiliensis*," *The Journal of Neuroscience*, vol. 11, no. 12, pp. 3809–3821, 1991.
- [92] A. B. M. da Silveira, M. A. R. Freitas, E. C. de Oliveira et al., "Neuronal plasticity of the enteric nervous system is correlated with chagasic megacolon development," *Parasitology*, vol. 135, no. 11, pp. 1337–1342, 2008.
- [93] A. L. A. Mascaro, P. Cesare, L. Sacconi et al., "In vivo single branch axotomy induces GAP-43-dependent sprouting and synaptic remodeling in cerebellar cortex," *Proceedings of the National Academy of Sciences*, vol. 110, no. 26, 2013.
- [94] W. H. Gispen, J. Boonstra, P. N. E. De Graan et al., "B-50/GAP-43 in neuronal development and repair," *Restorative Neurology and Neuroscience*, vol. 1, no. 3,4, pp. 237–244, 1990.
- [95] C. J. Woolf, M. L. Reynolds, C. Molander, C. O'Brien, R. M. Lindsay, and L. I. Benowitz, "The growth-associated protein gap-43 appears in dorsal root ganglion cells and in the dorsal horn of the rat spinal cord following peripheral nerve injury," *Neuroscience*, vol. 34, no. 2, pp. 465–478, 1990.
- [96] P. Yang, H. Wen, S. Ou, J. Cui, and D. Fan, "IL-6 promotes regeneration and functional recovery after cortical spinal tract injury by reactivating intrinsic growth program of neurons and enhancing synapse formation," *Experimental Neurology*, vol. 236, no. 1, pp. 19–27, 2012.
- [97] F. Liu, F. Liao, W. Li, Y. Han, and D. Liao, "Progesterone alters Nogo-A, GFAP and GAP-43 expression in a rat model of traumatic brain injury," *Molecular Medicine Reports*, vol. 9, no. 4, pp. 1225–1231, 2014.
- [98] N. Marklund, F. M. Bareyre, N. C. Royo et al., "Cognitive outcome following brain injury and treatment with an inhibitor

- of Nogo-A in association with an attenuated downregulation of hippocampal growth-associated protein-43 expression," *Journal of Neurosurgery*, vol. 107, no. 4, pp. 844–853, 2007.
- [99] Y. Yang, Y. Liu, P. Wei et al., "Silencing Nogo-A promotes functional recovery in demyelinating disease," *Annals of Neurology*, vol. 67, no. 4, pp. 498–507, 2010.
- [100] D. B. Zimmer, J. O. Eubanks, D. Ramakrishnan, and M. F. Criscitiello, "Evolution of the S100 family of calcium sensor proteins," *Cell Calcium*, vol. 53, no. 3, pp. 170–179, 2013.
- [101] A. R. Bresnick, "S100 proteins as therapeutic targets," *Biophysical Reviews*, vol. 10, no. 6, pp. 1617–1629, 2018.
- [102] R. Donato, B. R. Cannon, G. Sorci et al., "Functions of S100 proteins," *Current Molecular Medicine*, vol. 13, no. 1, pp. 24–57, 2012.
- [103] D. Grundmann, E. Loris, S. Maas-Omlor et al., "Enteric glia: S100, GFAP, and beyond," *The Anatomical Record*, vol. 302, no. 8, pp. 1333–1344, 2019.
- [104] A. E. Bishop, F. Carlei, V. Lee et al., "Combined immunostaining of neurofilaments, neuron specific enolase, GFAP and S-100 - a possible means for assessing the morphological and functional status of the enteric nervous system," *Histochemistry*, vol. 82, no. 1, pp. 93–97, 1985.
- [105] L. Ariel Gomez, A. Brusco, and J. P. Saavedra, "Immunocytochemical study of S-100 positive glial cells in the brainstem and spinal cord of the rat embryo," *International Journal of Developmental Neuroscience*, vol. 8, no. 1, pp. 55–64, 1990.
- [106] G. L. Ferri, L. Probert, D. Cocchia, F. Michetti, P. J. Marangos, and J. M. Polak, "Evidence for the presence of S-100 protein in the glial component of the human enteric nervous system," *Nature*, vol. 297, no. 5865, pp. 409–410, 1982.
- [107] H. J. Krammer, S. T. Karahan, W. Sigge, and W. Kühnel, "Immunohistochemistry of markers of the enteric nervous system in whole-mount preparations of the human colon," *European Journal of Pediatric Surgery*, vol. 4, no. 5, pp. 274–278, 1994.
- [108] D. Li, X. Liu, T. Liu et al., "Neurochemical regulation of the expression and function of glial fibrillary acidic protein in astrocytes," *GLIA*, vol. 68, no. 5, pp. 878–897, 2020.
- [109] L. F. Eng, R. S. Ghirnikar, and Y. L. Lee, "Glial fibrillary acidic protein: GFAP-thirty-one years (1969–2000)," *Neurochemical Research*, vol. 25, no. 9/10, pp. 1439–1451, 2000.
- [110] J. Middeldorp and E. M. Hol, "GFAP in health and disease," *Progress in Neurobiology*, vol. 93, no. 3, pp. 421–443, 2011.
- [111] K. R. Jessen and R. Mirsky, "Glial cells in the enteric nervous system contain glial fibrillary acidic protein," *Nature*, vol. 286, no. 5774, pp. 736–737, 1980.
- [112] M. A. R. Freitas, N. Segatto, Pedro et al., "Neurotrophin expression in chagasic megacolon," *JSM Atherosclerosis*, vol. 1, no. 3, p. 1013, 2016.
- [113] G. Iantorno, G. Bassotti, Z. Kogan et al., "The enteric nervous system in chagasic and idiopathic megacolon," *American Journal of Surgical Pathology*, vol. 31, no. 3, pp. 460–468, 2007.
- [114] S. Jabari, A. B. M. da Silveira, E. C. de Oliveira et al., "Interstitial cells of Cajal: crucial for the development of megacolon in human Chagas' disease?," *Colorectal Disease*, vol. 15, no. 10, pp. e592–e598, 2013.
- [115] A. R. Trevizan, L. C. L. Schneider, E. J. de Almeida Araújo et al., "Acute *Toxoplasma gondii* infection alters the number of neurons and the proportion of enteric glial cells in the duodenum in Wistar rats," *Neurogastroenterology & Motility*, vol. 31, no. 3, p. e13523, 2019.
- [116] M. F. Pavanelli, C. M. Colli, R. C. Bezagio et al., "Assemblages A and B of *Giardia duodenalis* reduce enteric glial cells in the small intestine in mice," *Parasitology Research*, vol. 117, no. 7, pp. 2025–2033, 2018.
- [117] C. Cirillo, G. Sarnelli, G. Esposito et al., "Increased mucosal nitric oxide production in ulcerative colitis is mediated in part by the enteroglia-derived S100B protein," *Neurogastroenterology & Motility*, vol. 21, no. 11, 2009.
- [118] G. D. P. Bossolani, B. T. Silva, J. V. C. M. Perles et al., "Rheumatoid arthritis induces enteric neurodegeneration and jejunal inflammation, and quercetin promotes neuroprotective and anti-inflammatory actions," *Life Sciences*, vol. 238, article 116956, 2019.
- [119] G. B. T. Von Boyen, N. Schulte, C. Pflüger, U. Spaniol, C. Hartmann, and M. Steinkamp, "Distribution of enteric glia and GDNF during gut inflammation," *BMC Gastroenterology*, vol. 11, no. 1, p. 3, 2011.
- [120] S. J. Allen, J. J. Watson, D. K. Shoemark, N. U. Barua, and N. K. Patel, "GDNF, NGF and BDNF as therapeutic options for neurodegeneration," *Pharmacology & Therapeutics*, vol. 138, no. 2, pp. 155–175, 2013.
- [121] R. Soret, S. Schneider, G. Bernas et al., "Glial cell-derived neurotrophic factor induces enteric neurogenesis and improves colon structure and function in mouse models of Hirschsprung disease," *Gastroenterology*, vol. 159, no. 5, pp. 1824–1838.e17, 2020.
- [122] C. Cirillo, G. Sarnelli, F. Turco et al., "Proinflammatory stimuli activates human-derived enteroglia cells and induces autocrine nitric oxide production," *Neurogastroenterology & Motility*, vol. 23, no. 9, pp. e372–e382, 2011.
- [123] G. B. T. Von Boyen, M. Steinkamp, M. Reinshagen, K. H. Schäfer, G. Adler, and J. Kirsch, "Proinflammatory cytokines increase glial fibrillary acidic protein expression in enteric glia," *Gut*, vol. 53, no. 2, pp. 222–228, 2004.
- [124] G. B. von Boyen, M. Steinkamp, I. Geerling et al., "Proinflammatory cytokines induce neurotrophic factor expression in enteric glia," *Inflammatory Bowel Diseases*, vol. 12, no. 5, pp. 346–354, 2006.
- [125] T. G. Bush, T. C. Savidge, T. C. Freeman et al., "Fulminant jejuno-ileitis following ablation of enteric glia in adult transgenic mice," *Cell*, vol. 93, no. 2, pp. 189–201, 1998.
- [126] A. Cornet, T. C. Savidge, J. Cabarocas et al., "Enterocolitis induced by autoimmune targeting of enteric glial cells: a possible mechanism in Crohn's disease?," *Proceedings of the National Academy of Sciences*, vol. 98, no. 23, pp. 13306–13311, 2001.
- [127] F. Turco, G. Sarnelli, C. Cirillo et al., "Enteroglia-derived S100B protein integrates bacteria-induced Toll-like receptor signalling in human enteric glial cells," *Gut*, vol. 63, no. 1, pp. 105–115, 2014.
- [128] M. Murakami, T. Ohta, and S. Ito, "Lipopolysaccharides enhance the action of bradykinin in enteric neurons via secretion of interleukin-1 β from enteric glial cells," *Journal of Neuroscience Research*, vol. 87, no. 9, pp. 2095–2104, 2009.
- [129] A. Rühl, S. Franzke, S. M. Collins, and W. Stremmel, "Interleukin-6 expression and regulation in rat enteric glial cells," *American Journal of Physiology-Gastrointestinal and Liver Physiology*, vol. 280, no. 6, pp. G1163–G1171, 2001.
- [130] Y. Yuan, C. Wu, and E.-A. Ling, "Heterogeneity of microglia phenotypes: developmental, functional and some therapeutic

- considerations," *Current Pharmaceutical Design*, vol. 25, no. 21, pp. 2375–2393, 2019.
- [131] D. Atiakshin, I. Buchwalow, V. Samoilova, and M. Tiemann, "Tryptase as a polyfunctional component of mast cells," *Histochemistry and Cell Biology*, vol. 149, no. 5, pp. 461–477, 2018.
- [132] D. Atiakshin, I. Buchwalow, and M. Tiemann, "Mast cell chymase: morphofunctional characteristics," *Histochemistry and Cell Biology*, vol. 152, no. 4, pp. 253–269, 2019.
- [133] J. Li, S. Jubair, S. P. Levick, and J. S. Janicki, "The autocrine role of tryptase in pressure overload-induced mast cell activation, chymase release and cardiac fibrosis," *IJC Metabolic & Endocrine*, vol. 10, pp. 16–23, 2016.
- [134] H. Tan, Z. Chen, F. Chen et al., "Tryptase promotes the profibrotic phenotype transfer of atrial fibroblasts by PAR2 and PPAR γ pathway," *Archives of Medical Research*, vol. 49, no. 8, pp. 568–575, 2018.
- [135] M. W. Kofford, L. B. Schwartz, N. M. Schechter, D. R. Yager, R. F. Diegelmann, and M. F. Graham, "Cleavage of type I procollagen by human mast cell chymase initiates collagen fibril formation and generates a unique carboxyl-terminal propeptide," *Journal of Biological Chemistry*, vol. 272, no. 11, pp. 7127–7131, 1997.
- [136] D. Kosanovic, H. Luitel, B. K. Dahal et al., "Chymase: a multifunctional player in pulmonary hypertension associated with lung fibrosis," *European Respiratory Journal*, vol. 46, no. 4, pp. 1084–1094, 2015.
- [137] G. H. Caughey, "Mast cell proteases as protective and inflammatory mediators," *Advances in Experimental Medicine and Biology*, vol. 716, pp. 212–234, 2011.
- [138] M. A. R. Freitas, N. Segatto, N. Tischler, E. C. de Oliveira, A. Brehmer, and A. B. M. Da Silveira, "Relation between mast cells concentration and serotonin expression in chagasic megacolon development," *Parasite Immunology*, vol. 39, no. 3, article e12414, 2017.
- [139] S. W. Pinheiro, A. M. de Oliveira Rua, R. M. Etchebehere et al., "Morphometric study of the fibrosis and mast cell count in the circular colon musculature of chronic Chagas patients with and without megacolon," *Revista da Sociedade Brasileira de Medicina Tropical*, vol. 36, no. 4, pp. 461–466, 2003.
- [140] C. F. Campos, S. D. Cangussú, A. L. C. Duz et al., "Enteric neuronal damage, intramuscular denervation and smooth muscle phenotype changes as mechanisms of chagasic megacolon: evidence from a long-term murine model of *Trypanosoma cruzi* infection," *PLoS One*, vol. 11, no. 4, 2016.
- [141] D. E. Reed, C. Barajas-Lopez, G. Cottrell et al., "Mast cell tryptase and proteinase-activated receptor 2 induce hyperexcitability of guinea-pig submucosal neurons," *The Journal of Physiology*, vol. 547, no. 2, pp. 531–542, 2003.
- [142] L. Zhang, J. Song, T. Bai, R. Wang, and X. Hou, "Sustained pain hypersensitivity in the stressed colon: role of mast cell-derived nerve growth factor-mediated enteric synaptic plasticity," *Neurogastroenterology & Motility*, vol. 30, no. 9, article e13430, 2018.
- [143] D. Ostertag, A. Annahazi, D. Krueger et al., "Tryptase potentiates enteric nerve activation by histamine and serotonin: relevance for the effects of mucosal biopsy supernatants from irritable bowel syndrome patients," *Neurogastroenterology & Motility*, vol. 29, no. 9, article e13070, 2017.
- [144] K. Mueller, K. Michel, D. Krueger et al., "Activity of protease-activated receptors in the human submucous plexus," *Gastroenterology*, vol. 141, no. 6, pp. 2088–2097.e1, 2011.
- [145] F. Wang, T. L. B. Yang, and B. S. Kim, "The return of the mast cell: new roles in neuroimmune itch biology," *Journal of Investigative Dermatology*, vol. 140, no. 5, pp. 945–951, 2020.
- [146] E. Sand, A. Themner-Persson, and E. Ekblad, "Mast cells reduce survival of myenteric neurons in culture," *Neuropharmacology*, vol. 56, no. 2, pp. 522–530, 2009.
- [147] M. Kulka, C. H. Sheen, B. P. Tancowny, L. C. Grammer, and R. P. Schleimer, "Neuropeptides activate human mast cell degranulation and chemokine production," *Immunology*, vol. 123, no. 3, pp. 398–410, 2008.
- [148] S. Ständer, H. Ständer, S. Seeliger, T. A. Luger, and M. Steinhoff, "Topical pimecrolimus and tacrolimus transiently induce neuropeptide release and mast cell degranulation in murine skin," *British Journal of Dermatology*, vol. 156, no. 5, pp. 1020–1026, 2007.
- [149] X. Pang, W. Boucher, G. Triadafilopoulos, G. R. Sant, and T. C. Theoharides, "Mast cell and substance P-positive nerve involvement in a patient with both irritable bowel syndrome and interstitial cystitis," *Urology*, vol. 47, no. 3, pp. 436–438, 1996.
- [150] J. Cairns and A. Walls, "Mast cell tryptase is a mitogen for epithelial cells. Stimulation of IL-8 production and intercellular adhesion molecule-1 expression," *The Journal of Immunology*, vol. 156, no. 1, pp. 275–283, 1996.
- [151] N. Vergnolle, M. D. Hollenberg, K. A. Sharkey, and J. L. Wallace, "Characterization of the inflammatory response to proteinase-activated receptor-2 (PAR2)-activating peptides in the rat paw," *British Journal of Pharmacology*, vol. 127, no. 5, pp. 1083–1090, 1999.
- [152] M. C. Meyer, M. H. Creer, and J. McHowat, "Potential role for mast cell tryptase in recruitment of inflammatory cells to endothelium," *American Journal of Physiology-Cell Physiology*, vol. 289, no. 6, pp. C1485–C1491, 2005.
- [153] M. E. M. S. Khedr, A. M. Abdelmotelb, S. L. F. Pender, X. Zhou, and A. F. Walls, "Neutrophilia, gelatinase release and microvascular leakage induced by human mast cell tryptase in a mouse model: lack of a role of protease-activated receptor 2 (PAR2)," *Clinical & Experimental Allergy*, vol. 48, no. 5, pp. 555–567, 2018.
- [154] N. A. Matos, J. F. Silva, T. C. Matsui et al., "Mast cell tryptase induces eosinophil recruitment in the pleural cavity of mice via proteinase-activated receptor 2," *Inflammation*, vol. 36, no. 6, pp. 1260–1267, 2013.
- [155] F. Schmidlin, S. Amadesi, K. Dabbagh et al., "Protease-activated receptor 2 mediates eosinophil infiltration and hyperreactivity in allergic inflammation of the airway," *The Journal of Immunology*, vol. 169, no. 9, pp. 5315–5321, 2002.
- [156] M. R. Namazi, "Possible molecular mechanisms to account for the involvement of tryptase in the pathogenesis of psoriasis," *Autoimmunity*, vol. 38, no. 6, pp. 449–452, 2005.
- [157] G. Lezmi, L. Galmiche-Rolland, S. Rioux et al., "Mast cells are associated with exacerbations and eosinophilia in children with severe asthma," *European Respiratory Journal*, vol. 48, no. 5, pp. 1320–1328, 2016.
- [158] P. R. Martins, R. D. Nascimento, J. G. Lopes et al., "Mast cells in the colon of *Trypanosoma cruzi*-infected patients: are they involved in the recruitment, survival and/or activation of eosinophils?," *Parasitology Research*, vol. 114, no. 5, pp. 1847–1856, 2015.
- [159] M. R. Galdiero, G. Varricchi, M. Seaf, G. Marone, F. Levi-Schaffer, and G. Marone, "Bidirectional mast cell-eosinophil

- interactions in inflammatory disorders and cancer,” *Frontiers in Medicine*, vol. 4, 2017.
- [160] M. Elishmereni, H. T. Alenius, P. Bradding et al., “Physical interactions between mast cells and eosinophils: a novel mechanism enhancing eosinophil survival *in vitro*,” *Allergy*, vol. 66, no. 3, pp. 376–385, 2011.
- [161] J. D. de Boer, J. Yang, F. E. van den Boogaard et al., “Mast cell-deficient KitW-sh mice develop house dust mite-induced lung inflammation despite impaired eosinophil recruitment,” *Journal of Innate Immunity*, vol. 6, no. 2, pp. 219–226, 2014.
- [162] H. A. Molina, K. J. Hamann, G. J. Gleich, and F. Kierszenbaum, “Toxic effects produced or mediated by human eosinophil granule components on *Trypanosoma cruzi*,” *The American Journal of Tropical Medicine and Hygiene*, vol. 38, no. 2, pp. 327–334, 1988.
- [163] H. A. Molina and F. Kierszenbaum, “Immunohistochemical detection of deposits of eosinophil-derived neurotoxin and eosinophil peroxidase in the myocardium of patients with Chagas’ disease,” *Immunology*, vol. 64, no. 4, pp. 725–731, 1988.
- [164] H. A. Molina and F. Kierszenbaum, “Interaction of human eosinophils or neutrophils with *Trypanosoma cruzi in vitro* causes bystander cardiac cell damage,” *Immunology*, vol. 66, no. 2, pp. 289–295, 1989.
- [165] F. Villalta and F. Kierszenbaum, “Role of inflammatory cells in Chagas’ disease. I. Uptake and mechanism of destruction of intracellular (amastigote) forms of *Trypanosoma cruzi* by human eosinophils,” *The Journal of Immunology*, vol. 132, no. 4, pp. 2053–2058, 1984.
- [166] F. Kierszenbaum, G. J. Gleich, and S. J. Ackerman, “Destruction of bloodstream forms of *Trypanosoma cruzi* by eosinophil granule major basic protein,” *The American Journal of Tropical Medicine and Hygiene*, vol. 30, no. 4, pp. 775–779, 1981.
- [167] M. C. Nakhle, M. D. C. S. de Menezes, and I. Irulegui, “Eosinophil levels in the acute phase of experimental Chagas’ disease,” *Revista do Instituto de Medicina Tropical de São Paulo*, vol. 31, no. 6, pp. 384–391, 1989.
- [168] G. A. N. Nascentes, W. S. F. Meira, E. Lages-Silva, and L. E. Ramírez, “Immunization of mice with a *Trypanosoma cruzi*-like strain isolated from a bat: predictive factors for involvement of eosinophiles in tissue damage,” *Vector-Borne and Zoonotic Diseases*, vol. 10, no. 10, pp. 989–997, 2010.
- [169] A. Andoh, Y. Deguchi, O. Inatomi et al., “Immunohistochemical study of chymase-positive mast cells in inflammatory bowel disease,” *Oncology Reports*, vol. 16, no. 1, pp. 103–107, 2006.
- [170] Z. Li, D. Peirasmaki, S. Svärd, and M. Åbrink, “The chymase mouse mast cell protease-4 regulates intestinal cytokine expression in mature adult mice infected with *Giardia intestinalis*,” *Cells*, vol. 9, no. 4, p. 925, 2020.
- [171] C. E. Lawrence, Y. Y. W. Paterson, S. H. Wright, P. A. Knight, and H. R. P. Miller, “Mouse mast cell protease-1 is required for the enteropathy induced by gastrointestinal helminth infection in the mouse,” *Gastroenterology*, vol. 127, no. 1, pp. 155–165, 2004.
- [172] H. Serna, M. Porras, and P. Vergara, “Mast cell stabilizer ketotifen [4-(1-methyl-4-piperidylidene)-4H-benzo[4,5]cyclohepta[1,2-b]thiophen-10(9H)-one fumarate] prevents mucosal mast cell hyperplasia and intestinal dysmotility in experimental *Trichinella spiralis* inflammation in the rat,” *Journal of Pharmacology and Experimental Therapeutics*, vol. 319, no. 3, pp. 1104–1111, 2006.
- [173] E.-Y. Cho, S.-C. Choi, S.-H. Lee et al., “Nafamostat mesilate attenuates colonic inflammation and mast cell infiltration in the experimental colitis,” *International Immunopharmacology*, vol. 11, no. 4, pp. 412–417, 2011.
- [174] W. X. Liu, Y. Wang, L. X. Sang et al., “Chymase inhibitor TY-51469 in therapy of inflammatory bowel disease,” *World Journal of Gastroenterology*, vol. 22, no. 5, pp. 1826–1833, 2016.
- [175] Y. Li, Z. Song, K. A. Kerr, and A. J. Moeser, “Chronic social stress in pigs impairs intestinal barrier and nutrient transporter function, and alters neuro-immune mediator and receptor expression,” *PLoS One*, vol. 12, no. 2, 2017.
- [176] A. M. Piliponsky, C.-C. Chen, E. J. Rios et al., “The chymase mouse mast cell protease 4 degrades TNF, limits inflammation, and promotes survival in a model of sepsis,” *The American Journal of Pathology*, vol. 181, no. 3, pp. 875–886, 2012.
- [177] S. Takai, D. Jin, and M. Miyazaki, “Multiple mechanisms for the action of chymase inhibitors,” *Journal of Pharmacological Sciences*, vol. 118, no. 3, pp. 311–316, 2012.
- [178] L. J. Dell’Italia, J. F. Collawn, and C. M. Ferrario, “Multifunctional role of chymase in acute and chronic tissue injury and remodeling,” *Circulation Research*, vol. 122, no. 2, pp. 319–336, 2018.
- [179] G. G. Caballero, H. Kaltner, T. J. Kutzner et al., “How galectins have become multifunctional proteins,” *Histology and Histopathology*, vol. 35, no. 6, pp. 509–539, 2020.
- [180] P. Demetter, N. Nagy, B. Martin et al., “The galectin family and digestive disease,” *The Journal of Pathology*, vol. 215, no. 1, pp. 1–12, 2008.
- [181] C. G. Barbosa, T. M. C. Costa, C. S. Desidério et al., “*Trypanosoma cruzi* mexican strains differentially modulate surface markers and cytokine production in bone marrow-derived dendritic cells from C57BL/6 and BALB/c mice,” *Mediators of Inflammation*, vol. 2019, Article ID 7214798, 14 pages, 2019.
- [182] M. Beghini, M. F. de Araújo, V. O. Severino, R. M. Etchebere, D. B. Rocha Rodrigues, and S. A. de Lima Pereira, “Evaluation of the immunohistochemical expression of Gal-1, Gal-3 and Gal-9 in the colon of chronic chagasic patients,” *Pathology - Research and Practice*, vol. 213, no. 9, pp. 1207–1214, 2017.
- [183] M. P. Garvil, T. C. de Souza Furtado, N. B. de Lima et al., “Although with intact mucosa at colonoscopy, chagasic megacolons have an overexpression of Gal-3,” *Einstein*, vol. 18, article eAO5105, 2020.
- [184] A. F. Benatar, G. A. García, J. Bua et al., “Galectin-1 prevents infection and damage induced by *Trypanosoma cruzi* on cardiac cells,” *PLOS Neglected Tropical Diseases*, vol. 9, no. 10, article e0004148, 2015.
- [185] C. V. Poncini, J. M. Illarregui, E. I. Batalla et al., “*Trypanosoma cruzi* infection imparts a regulatory program in dendritic cells and T cells via galectin-1-dependent mechanisms,” *The Journal of Immunology*, vol. 195, no. 7, pp. 3311–3324, 2015.
- [186] H.-L. Chen, F. Liao, T.-N. Lin, and F.-T. Liu, “Galectins and neuroinflammation,” Springer, New York, NY, USA, 2014.
- [187] M. A. Toscano, G. A. Bianco, J. M. Illarregui et al., “Differential glycosylation of TH1, TH2 and TH-17 effector cells selectively regulates susceptibility to cell death,” *Nature Immunology*, vol. 8, no. 8, pp. 825–834, 2007.
- [188] C. Zhu, A. C. Anderson, A. Schubart et al., “The Tim-3 ligand galectin-9 negatively regulates T helper type 1 immunity,” *Nature Immunology*, vol. 6, no. 12, pp. 1245–1252, 2005.

- [189] S. C. Starossom, I. D. Mascanfroni, J. Imitola et al., "Galectin-1 deactivates classically activated microglia and protects from inflammation-induced neurodegeneration," *Immunity*, vol. 37, no. 2, pp. 249–263, 2012.
- [190] H. Horie, T. Kadoya, N. Hikawa et al., "Oxidized galectin-1 stimulates macrophages to promote axonal regeneration in peripheral nerves after axotomy," *Journal of Neuroscience*, vol. 24, no. 8, pp. 1873–1880, 2004.
- [191] H.-Y. Chen, B. B. Sharma, L. Yu et al., "Role of galectin-3 in mast cell functions: galectin-3-deficient mast cells exhibit impaired mediator release and defective JNK expression," *The Journal of Immunology*, vol. 177, no. 8, pp. 4991–4997, 2006.
- [192] H.-R. Jiang, Z. Al Rasebi, E. Mensah-Brown et al., "Galectin-3 deficiency reduces the severity of experimental autoimmune encephalomyelitis," *The Journal of Immunology*, vol. 182, no. 2, pp. 1167–1173, 2009.
- [193] X. Cheng, A. Boza-Serrano, M. F. Turesson, T. Deierborg, E. Ekblad, and U. Voss, "Galectin-3 causes enteric neuronal loss in mice after left sided permanent middle cerebral artery occlusion, a model of stroke," *Scientific Reports*, vol. 6, no. 1, 2016.
- [194] I. Srejavic, D. Selakovic, N. Jovicic, V. Jakovljević, M. L. Lukic, and G. Rosic, "Galectin-3: roles in neurodevelopment, neuroinflammation, and behavior," *Biomolecules*, vol. 10, no. 5, p. 798, 2020.
- [195] G. Reid and M. Rand, "Physiological actions of the partially purified serum vasoconstrictor (serotonin)," *Australian Journal of Experimental Biology and Medical Science*, vol. 29, no. 6, pp. 401–415, 1951.
- [196] J. Lv and F. Liu, "The role of serotonin beyond the central nervous system during embryogenesis," *Frontiers in Cellular Neuroscience*, vol. 11, 2017.
- [197] M. D. Gershon, "Serotonin: its role and receptors in enteric neurotransmission," *Advances in Experimental Medicine and Biology*, vol. 294, pp. 221–230, 1991.
- [198] R. Mittal, L. H. Debs, A. P. Patel et al., "Neurotransmitters: the critical modulators regulating gut-brain axis," *Journal of Cellular Physiology*, vol. 232, no. 9, pp. 2359–2372, 2017.
- [199] M. D. Gershon, A. B. Drakontides, and L. L. Ross, "Serotonin: synthesis and release from the myenteric plexus of the mouse intestine," *Science*, vol. 149, no. 3680, pp. 197–199, 1965.
- [200] M. D. Gershon and J. Tack, "The serotonin signaling system: from basic understanding to drug development for functional GI disorders," *Gastroenterology*, vol. 132, no. 1, pp. 397–414, 2007.
- [201] P.-L. Yu, M. Fujimura, K. Okumiya, M. Kinoshita, H. Hasegawa, and M. Fujimiya, "Immunohistochemical localization of tryptophan hydroxylase in the human and rat gastrointestinal tracts," *The Journal of Comparative Neurology*, vol. 411, no. 4, pp. 654–665, 1999.
- [202] M. S. Shajib and W. I. Khan, "The role of serotonin and its receptors in activation of immune responses and inflammation," *Acta Physiologica*, vol. 213, no. 3, pp. 561–574, 2015.
- [203] A. Y. Thijssen, Z. Mujagic, D. M. A. E. Jonkers et al., "Alterations in serotonin metabolism in the irritable bowel syndrome," *Alimentary Pharmacology & Therapeutics*, vol. 43, no. 2, pp. 272–282, 2016.
- [204] M. S. Shajib, U. Chauhan, S. Adeeb et al., "Characterization of serotonin signaling components in patients with inflammatory bowel disease," *Journal of the Canadian Association of Gastroenterology*, vol. 2, no. 3, pp. 132–140, 2019.
- [205] N. S. Coleman, S. Foley, S. P. Dunlop et al., "Abnormalities of serotonin metabolism and their relation to symptoms in untreated celiac disease," *Clinical Gastroenterology and Hepatology*, vol. 4, no. 7, pp. 874–881, 2006.
- [206] C. P. Bearcroft, D. Perrett, and M. J. Farthing, "5-Hydroxytryptamine release into human jejunum by cholera toxin," *Gut*, vol. 39, no. 4, pp. 528–531, 1996.
- [207] J. L. Turvill, P. Connor, and M. J. G. Farthing, "The inhibition of cholera toxin-induced 5-HT release by the 5-HT₃ receptor antagonist, granisetron, in the rat," *British Journal of Pharmacology*, vol. 130, no. 5, pp. 1031–1036, 2000.
- [208] M. L. Grøndahl, G. M. Jensen, C. G. Nielsen, E. Skadhauge, J. E. Olsen, and M. B. Hansen, "Secretory pathways in *Salmonella Typhimurium*-induced fluid accumulation in the porcine small intestine," *Journal of Medical Microbiology*, vol. 47, no. 2, pp. 151–157, 1998.
- [209] J. Wheatcroft, D. Wakelin, A. Smith, C. R. Mahoney, G. Mawe, and R. Spiller, "Enterochromaffin cell hyperplasia and decreased serotonin transporter in a mouse model of postinfectious bowel dysfunction," *Neurogastroenterology and Motility*, vol. 17, no. 6, pp. 863–870, 2005.
- [210] R. Spiller, "Serotonin and GI clinical disorders," *Neuropharmacology*, vol. 55, no. 6, pp. 1072–1080, 2008.
- [211] M. A. R. de Freitas, E. C. de Oliveira, F. C. de Oliveira, S. Jabari, A. Brehmer, and A. B. M. da Silveira, "Is the increased presence of CD8 T-lymphocytes related to serotonin levels in Chagas disease?," *Colorectal Disease*, vol. 17, no. 3, pp. 268–269, 2015.
- [212] J. A. de Oliveira, M. A. R. Freitas, E. C. de Oliveira, S. Jabari, A. Brehmer, and A. B. M. Da Silveira, "5-HT_{3A} serotonin receptor in the gastrointestinal tract: the link between immune system and enteric nervous system in the digestive form of Chagas disease," *Parasitology Research*, vol. 118, no. 4, pp. 1325–1329, 2019.

Research Article

Antiviral Efficacy of the Anesthetic Propofol against Dengue Virus Infection and Cellular Inflammation

Ting-Jing Shen ^{1,2}, Chia-Ling Chen,³ Ming-Kai Jhan,^{1,2} Po-Chun Tseng,^{2,4}
Rahmat Dani Satria,^{2,5,6,7} Chung-Hsi Hsing ^{8,9} and Chiou-Feng Lin ^{1,2,4,10}

¹Graduate Institute of Medical Sciences, College of Medicine, Taipei Medical University, Taipei 110, Taiwan

²Department of Microbiology and Immunology, School of Medicine, College of Medicine, Taipei Medical University, Taipei 110, Taiwan

³School of Respiratory Therapy, College of Medicine, Taipei Medical University, Taipei 110, Taiwan

⁴Core Laboratory of Immune Monitoring, Office of Research & Development, Taipei Medical University, Taipei 110, Taiwan

⁵International Ph.D. Program in Medicine, College of Medicine, Taipei Medical University, Taipei 110, Taiwan

⁶Department of Clinical Pathology and Laboratory Medicine, Faculty of Medicine, Public Health and Nursing, Universitas Gadjah Mada, Yogyakarta 55281, Indonesia

⁷Clinical Laboratory Installation, Dr. Sardjito Central General Hospital, Yogyakarta 55281, Indonesia

⁸Department of Medical Research, Chi-Mei Medical Center, Tainan 710, Taiwan

⁹Department of Anesthesiology, Chi-Mei Medical Center, Tainan 710, Taiwan

¹⁰Center of Infectious Diseases and Signaling Research, National Cheng Kung University, Tainan 701, Taiwan

Correspondence should be addressed to Chung-Hsi Hsing; hsing@mail.chimei.org.tw and Chiou-Feng Lin; cflin2014@tmu.edu.tw

Received 10 October 2020; Revised 28 February 2021; Accepted 21 March 2021; Published 1 April 2021

Academic Editor: Luiz Felipe Domingues Passero

Copyright © 2021 Ting-Jing Shen et al. This is an open access article distributed under the Creative Commons Attribution License, which permits unrestricted use, distribution, and reproduction in any medium, provided the original work is properly cited.

Propofol, 2,6-diisopropylphenol, is a short-acting intravenous sedative agent used in adults and children. Current studies show its various antimicrobial as well as anti-inflammatory effects. Dengue virus (DENV) is an emerging infectious pathogen transmitted by mosquitoes that causes mild dengue fever and progressive severe dengue diseases. In the absence of safe vaccines and antiviral agents, adjuvant treatments and supportive care are generally administered. This study investigated the antiviral effects of propofol against DENV infection and cellular inflammation by using an *in vitro* cell model. Treatment with propofol significantly inhibited DENV release 24 h postinfection in BHK-21 cells. Furthermore, it also blocked viral protein expression independent of the translational blockade. Propofol neither caused inhibitory effects on endosomal acidification nor prevented dsRNA replication. Either the proinflammatory TNF- α or the antiviral STAT1 signaling was reduced by propofol treatment. These results provide evidence to show the potential antiviral effects of the sedative propofol against DENV infection and cellular inflammation.

1. Introduction

The anesthetic propofol is routinely used in the short term to provide a rapid onset and offset of sedation in critically ill patients under intensive care [1]. Treatment with propofol confers a range of pharmacodynamic effects from amnestic, muscle relaxant, and hypnotic effects to anesthesia. In addition to its neuropharmacological properties, propofol has immunomodulating actions through its negative regulation

of proinflammatory cytokine/chemokine production and immune cell activation [2, 3]. Additionally, general anesthetics, including propofol, remifentanyl, and ketamine, exert antimicrobial and microbial growth-promoting effects against bacterial infection [4, 5].

Dengue, an arthropod-borne viral disease, is caused by the dengue virus (DENV), a flavivirus transmitted by *Aedes* mosquitoes [6]. Globally, infection with DENV affects more than 100 countries, with an estimated 400 million new

infections and 25,000 deaths annually [7]. Clinical presentations of DENV infection range from mild dengue fever to severe dengue diseases, including dengue hemorrhagic fever/dengue shock syndrome (DHF/DSS) and multiorgan involvement. Without appropriate medication, severe dengue has a mortality rate ranging from 5 to 20%. Due to its emerging disease status, safe and long-term protective DENV vaccines and anti-DENV drugs are essential for dengue prevention and treatment.

For severe dengue management, some sedative agents are used in patients [8, 9]. An innovative patent describes the application of propofol as an antiviral medication for preventing and treating infections caused by influenza A viruses (EP2590637A1; European Patent Office). However, its pharmacological effects on viral replication as well as viral inflammation remain undefined. In this study, we first investigated the possible effects of propofol on DENV infection and replication and DENV-induced cellular inflammation by using an *in vitro* cell model.

2. Materials and Methods

2.1. Cells and Virus. The process of cell culture and virus preparation was according to our previous study [10]. Briefly, baby hamster kidney- (BHK-) 21 fibroblasts (ATCC, CCL10) were maintained in Dulbecco's modified Eagle's medium (DMEM; Thermo Fisher Scientific) containing 10% heat-inactivated fetal bovine serum (FBS, Biological Industries) and 1% penicillin-streptomycin (Thermo Fisher Scientific) at 37°C in 5% CO₂. BHK-21 cells harboring a luciferase-expressing DENV replicon (BHK-D2-Fluc-SGR-Neo-1) were maintained in DMEM with 10% heat-inactivated FBS, 1% penicillin-streptomycin, and 0.4 mg/ml G418 agent (Cat# A1720, Sigma-Aldrich) at 37°C in 5% CO₂. The *Aedes albopictus* clone mosquito C6/36 cells (ATCC, CRL1660) were maintained in Minimum Essential Medium (MEM; Thermo Fisher Scientific) containing 10% heat-inactivated FBS, 1% penicillin-streptomycin (Thermo Fisher Scientific), 1% sodium pyruvate (Cat# 11360-070, Thermo Fisher Scientific), 1% 4-(2-hydroxyethyl)-1-piperazineethanesulfonic acid (HEPES; Cat# 15630-080, Thermo Fisher Scientific), and 1% nonessential amino acids (NEAA; Cat# 11140-035, Thermo Fisher Scientific) at 28°C in 5% CO₂. Dengue virus serotype 2 (DENV2, strain PL046) was obtained from Center for Disease Control in Taiwan and propagated in a C6/36 cell monolayer at a multiplicity of infection (MOI) of 0.01. After incubation (28°C in 5% CO₂) for 5 days, the viral supernatants were collected and filtered with a 0.22 μm filter and then stored at -80°C until use. Viral titers were determined by plaque assay using BHK-21 cells.

2.2. Agents and Antibodies. Propofol (2,6-diisopropylphenol) was purchased from Sigma-Aldrich (St. Louis, MO, USA). An antibody against DENV NS1 (Cat# GTX124280) was purchased from GeneTex (San Antonio, TX); antibodies against phospho-STAT1^{Tyr701} (Cat# 9167; clone 58D6), STAT1 (Cat# 9172), horseradish peroxidase- (HRP-) conjugated goat anti-rabbit IgG (Cat# 7074S), and HRP-conjugated horse anti-mouse IgG (Cat# 7076S) were pur-

chased from Cell Signaling Technology (Beverly, MA); Alexa Fluor 488-conjugated goat anti-mouse antibody (Cat# A-11029) and Hoechst 33258 (Cat# H3569) were purchased from Thermo Fisher Scientific (Pittsburgh, PA, USA); antibody against dsRNA (Cat# 10010200) was purchased from SCICONS; antibody against mouse β-actin (Cat# A5441), 4,6-diamidino-2-phenylindole (DAPI; Cat# D9542), the V-ATPase inhibitor bafilomycin A1 (Baf A1; Cat# 19-148), and acridine orange hemi (zinc chloride) salt (Cat# A6014) were purchased from Sigma-Aldrich (St. Louis, MO). According to the manufacturer's instructions, cell cytotoxicity was assessed using Cytotoxicity Detection Kit assays (Roche Diagnostics, Lewes, UK).

2.3. Western Blotting. Accordingly [10], cells were collected and extracted with lysis buffer containing a protease inhibitor cocktail (Sigma-Aldrich). The processed proteins were separated by 10% SDS-polyacrylamide gel electrophoresis followed by transfer to a polyvinylidene difluoride (PVDF) membrane (Millipore). Then, the PVDF membrane was blocked with 5% nonfat milk in 0.05% Tween-20-containing Tris-buffer-based saline (TBS-T) at room temperature for 1 h. Next, the membrane was washed three times with TBS-T buffer and immunohybridized with the indicated primary antibodies at 4°C overnight. Then, the membrane was washed with TBS-T buffer three times, followed by incubation with the indicated HRP-conjugated secondary antibodies at room temperature for 1 h. The antibody-protein complexes on the PVDF membrane were detected using an ECL Western blot detection kit (PerkinElmer). The signals of the identified proteins were captured with a film exposure system.

2.4. Plaque Assay. BHK-21 cells were grown in a monolayer in a 12-well plate at 7 × 10⁴ cells/well. Serially diluted viral solutions were added to infect cells for 2 h and then replaced with fresh DMEM containing 4% FBS and 0.5% methylcellulose (Sigma-Aldrich) for 5 days. Next, wells were washed with 2 ml PBS twice and stained with crystal violet solution containing 1% crystal violet (Sigma-Aldrich), 0.64% NaCl, and 2% paraformaldehyde (Sigma-Aldrich) overnight. Subsequently, wells were washed with water and air-dried to count the number of plaque-forming units (PFU).

2.5. Reporter Assay. BHK-D2-Fluc-SGR-Neo-1 cells (replis) were seeded in 96-well plates at 3,000 cells/well overnight. After the treatments, luciferase activity was detected using the Dual-Glo® Luciferase Assay System (Cat# E2940, Promega) and a spectral scanning multimode reader (Thermo Varioskan Flash).

2.6. Double-stranded RNA (dsRNA) Staining. Cells were washed with ice-cold PBS 3 times and fixed with 4% paraformaldehyde (Sigma-Aldrich) at room temperature for 15 minutes. Then, the cells were washed 3 times with ice-cold PBS and permeabilized with permeabilization buffer (PBS containing 1% Triton X-100) at room temperature for 5 minutes. The cells were then washed 3 times with ice-cold PBS and immunoblocked with blocking buffer (PBS containing 1% BSA and 0.01% Triton X-100) at 4°C for 30 minutes.

Next, the cells were washed 3 times with ice-cold PBS and immunohybridized with mouse anti-dsRNA J2 primary antibody at 4°C overnight. Subsequently, the cells were washed 3 times with ice-cold PBS and stained with Alexa Fluor 488-conjugated goat anti-mouse antibody (Thermo Fisher Scientific) at room temperature for 15 minutes. The cells were washed 3 times with ice-cold PBS and then visualized with fluorescence or confocal microscopy. DAPI (Sigma-Aldrich) was used for nuclear staining.

2.7. Acridine Orange Staining. Cells were washed with HBSS (Thermo Fisher Scientific) once and then stained with acridine orange agent (Sigma-Aldrich) and Hoechst 33258 (Thermo Fisher Scientific) in an incubator at 37°C in 5% CO₂. After 45 minutes, the cells were washed with HBSS once and rinsed with HBSS. Subsequently, cells were visualized with a fluorescence microscope (EVOS). Hoechst 33258 was used for nuclear staining.

2.8. Enzyme-Linked Immunosorbent Assay (ELISA). According to the manufacturer's instruction, samples were harvested, and the concentration of mouse TNF α was determined using ELISA kit (Cat# 88-7324-88, eBioscience).

2.9. Statistical Analysis. GraphPad Prism (version 8.3.0) was applied to analyze the experimental data. One-way ANOVA (Tukey's multiple comparison test) was used to determine experiments involving numerous groups. Values are means \pm standard deviation (SD). All *p* values were obtained from two-tailed significance tests. A *p* value of <0.05 was considered statistically significant.

3. Results

3.1. Propofol Treatment Inhibits DENV Infection. Several antiviral drugs have been designed and repurposed to reduce DENV infection [11]. Here, we examined propofol, a short-term anesthetic, for its antiviral activity. The LDH assay showed that propofol did not cause cytotoxicity at testing dosages ranging from 1 to 50 μ g/ml (Figure 1(a)). Based on these results, BHK-21 cells were pretreated with propofol for 1 h and then infected with DENV for an additional 24 h. In this DENV infection model, 24 h postinfection showed a significant viral replication as demonstrated by using plaque assay. The results showed that propofol significantly (*p* < 0.001) reduced DENV virion release, as demonstrated by the viral titer, at doses of 5, 10, 25, and 50 μ g/ml (Figure 1(b)). These results indicate that propofol treatment effectively blocks DENV infection.

3.2. Propofol Reduces DENV Viral Protein Expression but Does Not Affect Viral Translation. To assess propofol's inhibitory activity on DENV infection, we next used BHK-21-SGR cells, a cellular replicon-based reporter assay, to examine propofol's translational targets. The luciferase activity showed no remarkable difference in replicons treated with or without propofol (Figure 2(a)), indicating that a protein translation-independent route mediates the propofol-induced antiviral effect. By western blot analysis, we found that viral NS1 protein expression was effectively increased 24 h postinfection

and was decreased in a dose-dependent manner under propofol treatment (Figure 2(b)). Overall, propofol inhibits DENV viral protein expression independent of the translational blockade.

3.3. Propofol Does Not Affect DENV-Induced Endosomal Acidification. The endosomal acidification step is critical for DENV uncoating to release the viral genome for further replication in the cytoplasm [6]. Therefore, the pH-sensitive dye acridine orange (AO) was used to explore whether propofol affects the early stages of DENV infection accordingly [12]. After a 2-hour infection, images of AO-stained BHK-21 cells showed a low pH in the endosomes (red) of DENV-infected cells compared with mock-infected cells. Cells treated with bafilomycin (Baf) A1, a V-ATPase inhibitor [12], were intensely stained green, indicating that endosome acidification was blocked. Notably, cells treated with propofol exhibited a red color attenuated by cotreatment with Baf A1 (Figure 3). These results reveal that propofol does not affect endosomal acidification during DENV infection.

3.4. Propofol Does Not Inhibit dsRNA Replication at the Early Infectious Stage. Following endocytosis, the viral genome is released into the cytoplasm and undergoes genome replication [6]. To investigate propofol's inhibitory effect on viral RNA replication, cells were pretreated with the indicated drugs for 1 h and then infected with DENV for an additional 6 h. Images of dsRNA immunostaining showed that dsRNA expression occurred, as demonstrated by positive staining (green), in both cells treated with and without propofol under DENV infection. However, cells pretreated with Baf A1 as a positive control then treated with propofol showed reduced dsRNA expression in the infected cells (Figures 4(a) and 4(b)). The data demonstrate that propofol does not affect blocking DENV viral dsRNA replication at early infection.

3.5. Propofol Impedes Proinflammatory Cytokine Responses. DENV infection induces robust cytokine productions, such as TNF- α , which is immunopathogenic *in vivo* and *in vitro*, to defeat hosts [13–15]. Although propofol is typically used as an anesthetic agent, it also functions to eliminate inflammation. Propofol reduces both the gene and cytokine productions of TNF- α in not only CoCl₂-treated hypoxic BV2 microglia but also cecal ligation and puncture-administrated rat liver [16, 17]. In this study, RAW 264.7 cells were pretreated with or without propofol (10 or 25 μ g/ml) followed by infected with DENV for 24 h. ELISA analysis showed that DENV infection significantly increased mouse TNF- α production; however, propofol treatment reduced the cytokine levels in a dose-dependent manner (Figure 5(a)). Regarding propofol treatment that inhibits DENV replication, it is hypothesized that propofol may enhance antiviral interferon (IFN) responses. The protein expressions of phospho-STAT1 and STAT1, the expected transcription factor of antiviral IFN signaling, were increased following DENV infection but inhibited by propofol treatment (Figure 5(b)). Thus, it is suggested that propofol has

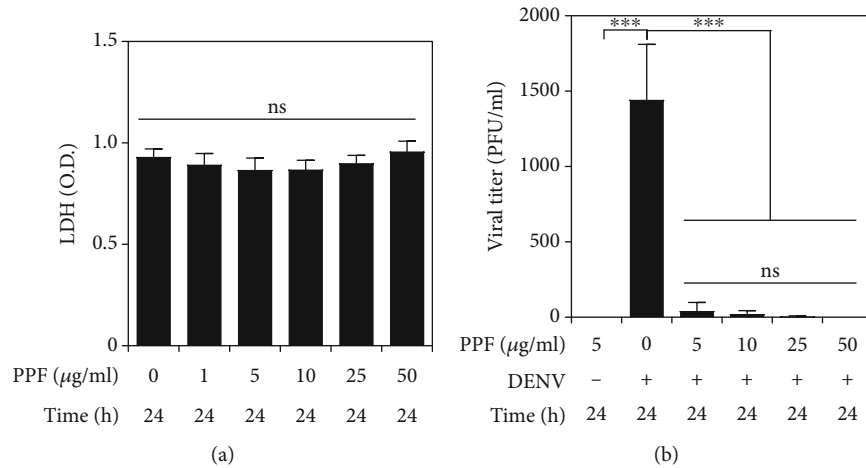


FIGURE 1: Propofol treatment inhibits DENV virion production. (a) The LDH assay showed the cytotoxicity of BHK-21 cells cultured in a medium containing propofol for 24 h. (b) Plaque assay determined the viral titer in BHK-21 cells pretreated with propofol for 1 h followed by DENV2 (MOI = 1) infection for 24 h. Quantitative data are presented as the mean \pm SD of at least three independent experiments ($n = 3$). *** $p < 0.001$. ns: not significant.

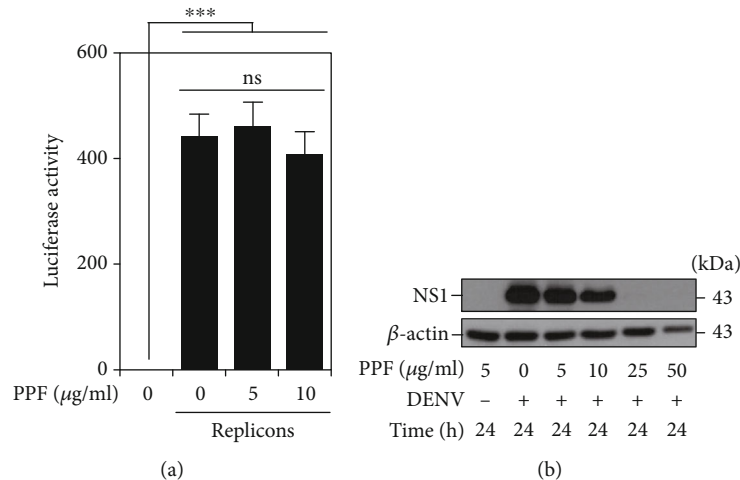


FIGURE 2: Propofol treatment reduces DENV viral NS1 protein expression but does not affect viral protein translation. (a) Luciferase activities of BHK-21 cells and replicons treated with or without propofol were used to determine viral protein translation. (b) Western blot analysis showed viral NS1 protein expression in BHK-21 cells pretreated with propofol for 1 h and then infected with DENV2 (MOI = 1) for 24 h. Quantitative data are presented as the mean \pm SD of at least three independent experiments ($n = 3$). *** $p < 0.001$. ns: not significant.

anti-inflammation activity against DENV-induced cellular inflammation.

4. Discussion

As a sedative agent, the anesthetic propofol is usually used in critically ill patients [1]. Although it is not a standard medication used in severe dengue patients, its immunomodulatory effects have been reported to inhibit inflammation. Regarding its dual antimicrobial [4] and promicrobial impact [18], this compound confers intense antiviral action against enveloped viruses, especially the influenza viruses (EP2590637A1; European Patent Office). However, propofol is an emulsion of soybean oil, glycerol, and egg lecithin that may prolong the environmental stability to sustain the survival of the hepatitis C virus under this lipid-based formula-

tion [19]. Therefore, the treatment time and the dosage of propofol used for antimicrobial therapy need full consideration. As demonstrated in this *in vitro* cell model, our study is the first to report an antiviral effect of propofol against flavivirus DENV infection.

To date, no licensed antiviral drugs are available for treating DENV. Several potential agents, including chloroquine (a 9-aminoquinoline), balapiravir (4'-azidocytidine), prednisolone, lovastatin, and the α -glucosidase inhibitor celgosivir, are relatively limited by their unusable antiviral effects in dengue patients [20–22]. To speed the development of antiviral agents against DENV infection, repurposing FDA-approved agents is an alternative strategy to target DENV infection and replication [23]. Host factor cyclooxygenase- (COX-) 2 can facilitate DENV replication, and pharmacologically inhibiting its kinase activity has been

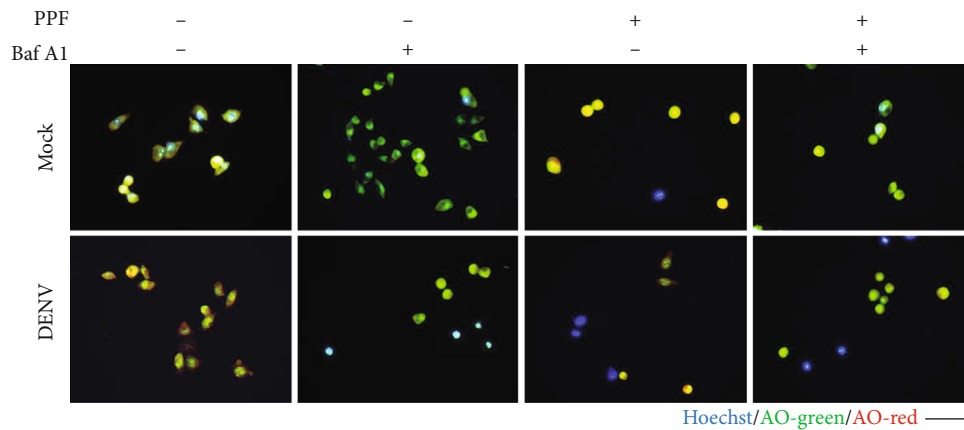
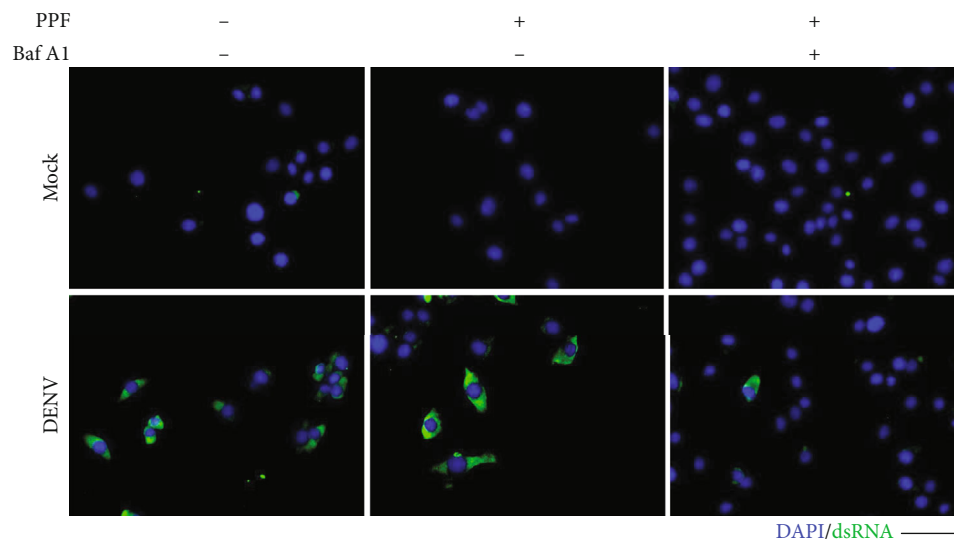


FIGURE 3: Propofol treatment does not affect endosomal acidification during DENV infection. The fluorescent images of acridine orange-stained BHK-21 cells pretreated with or without Baf A1 and propofol for 1 h showed endosomal acidification during mock and DENV infection for 2 h. Hoechst (blue) was used to label nuclear DNA. Scale bar: 100 μ m.



(a)

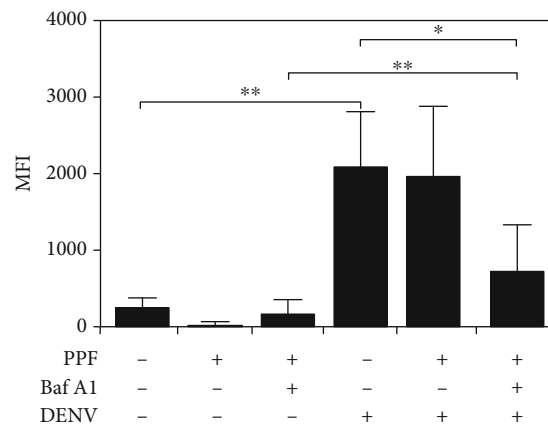


FIGURE 4: Propofol treatment has no blocking effect on viral dsRNA replication during DENV infection. (a) Images of immunocytochemistry staining showed viral dsRNA (green) expression 6 h postinfection in mock- and DENV2-infected BHK-21 cells pretreated with or without Baf A1 and propofol for 1 h. DAPI (blue) was used to label nuclear DNA. (b) Statistical analysis of the staining presented as mean fluorescent intensity (MFI). Quantitative data are presented as the mean \pm SD of the experiments ($n = 3$). * $p < 0.05$; ** $p < 0.01$. Scale bar: 100 μ m.

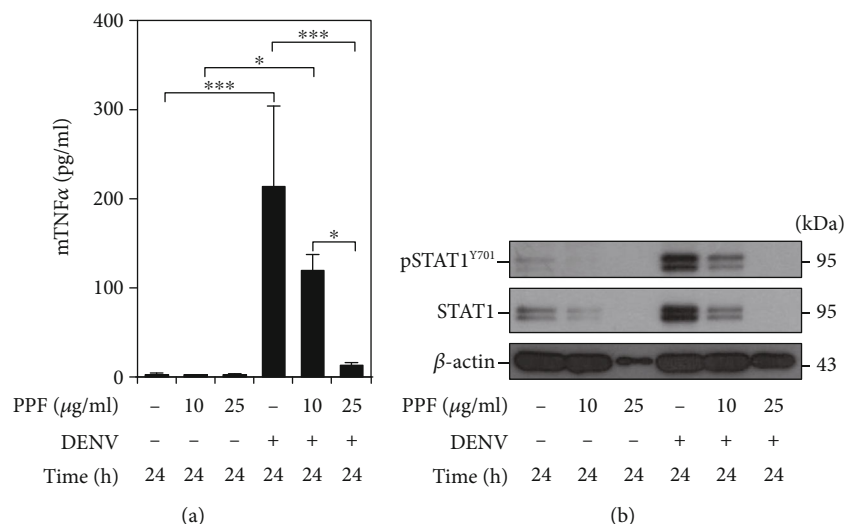


FIGURE 5: Propofol treatment reduces proinflammatory TNF- α production and type I IFN signaling. RAW 264.7 cells were pretreated without or with propofol (10 or 25 μ g/ml) followed by infection with DENV2 (MOI = 10) for 24 h. (a) The ELISA analysis determined mouse TNF- α production. (b) Western blot analysis showed protein expressions of phospho-STAT1 and STAT1. Quantitative data are presented as the mean \pm SD of the experiments ($n = 3$). * $p < 0.05$; *** $p < 0.001$.

demonstrated as a potential antiviral strategy [24]. Significantly, treating macrophages with propofol could modulate cellular inflammation via COX activity suppression [25, 26]. It is speculated that the antiviral activity of propofol is mediated by targeting the COX signaling pathway.

Administration of propofol significantly inhibits virion release following the inhibition of viral protein expression; however, propofol treatment does not block DENV-induced endosomal acidification or viral dsRNA replication. Based on our findings, as demonstrated by using a replicon-based reporter system, propofol did not interfere with viral protein translation. All these results indicate a possible effect initiated by propofol targeting protein posttranslational modification. Although a COX-regulated viral infection may act on viral gene transcription, protein expression, and viral genome replication [27], its possible interaction with host factors may also control the posttranslational regulation of viral proteins [28]. Further investigations for exploring propofol-mediated inhibition on the DENV infectious cycle, such as viral protein posttranslational modification, virion assemble, and release, are needed to identify propofol's antiviral actions.

In addition to the modulation of cellular inflammation through suppressing COX activity in macrophages, propofol attenuates neuroinflammation. Peng et al. found that propofol treatment blocks NF- κ B/Hif-1 α signaling and reduces the gene expressions and cytokine secretions of TNF- α , IL-1 β , and IL-6 in hypoxic BV2 microglia [16]. Propofol treatment also could remarkably inhibit gene expressions of TNF- α , TLR-4, CD14, and GM-CSF in cultured hepatocytes under LPS stimulation [29]. Besides, propofol exposure causes the reductive numbers of TNF- α and inducible nitric oxide synthase-producing dendritic cells in *Listeria monocytogenes*-infected mouse spleens, which therefore reduces the sufficient bacterial clearance [30]. Proinflammatory cyto-

kines such as TNF- α are positively associated with severe dengue disease [31]. Jhan et al. further revealed that the blockade of TNF- α by knocking the TNF- α gene or neutralizing TNF- α could reduce the disease severity and mortality in DENV-infected mice [15]. Therefore, in consideration of propofol's inhibition activity on TNF- α production, propofol treatment may be a considerable agent to prohibit dengue disease progression.

In conclusion, by using an *in vitro* cell model of DENV infection, for the first time, we demonstrate the antiviral capacity of propofol against DENV infection, which probably occurs through a mechanism involving the blockade of viral protein expression independent of translational inhibition as well as the increase in an antiviral interferon response. While propofol is used as a sedative agent, this study's findings further provide evidence to show the potential antiviral and anti-inflammatory application of propofol in patients with DENV infection. In considering safe dose used in the clinic, an *in vivo* model of DENV infection is essential for evaluating its antiviral and anti-inflammatory effects.

Data Availability

The data used to support the findings of this study are available from the corresponding author upon request.

Conflicts of Interest

The authors declare that they have no conflicts of interest.

Acknowledgments

This work was supported by grants from the Ministry of Science and Technology (MOST) (108-2320-B-038-026, 109-2320-B-038-050, 109-2327-B-006-010, and 109-2320-B-038-

070), Chi Mei Medical Center, and Taipei Medical University (105CM-TMU-03, 106CM-TMU-09, and 107CM-TMU-10), Taiwan. We thank the Core Facility Center of Taipei Medical University (TMU) for providing technical support.

References

- [1] G. Angelini, J. T. Ketzler, and D. B. Coursin, "Use of propofol and other nonbenzodiazepine sedatives in the intensive care unit," *Critical Care Clinics*, vol. 17, no. 4, pp. 863–880, 2001.
- [2] S. L. Anderson, T. Duke-Novakovski, and B. Singh, "The immune response to anesthesia: part 2 sedatives, opioids, and injectable anesthetic agents," *Veterinary Anaesthesia and Analgesia*, vol. 41, no. 6, pp. 553–566, 2014.
- [3] S. A. K. Helmy and R. J. al-Attayah, "The immunomodulatory effects of prolonged intravenous infusion of propofol versus midazolam in critically ill surgical patients," *Anaesthesia*, vol. 56, no. 1, pp. 4–8, 2001.
- [4] T. Z. Apan, A. Apan, S. Sahin, and M. Cakirca, "Antibacterial activity of remifentanyl and mixtures of remifentanyl and propofol," *Journal of Clinical Anesthesia*, vol. 19, no. 5, pp. 346–350, 2007.
- [5] Z. Begec, A. Yucel, Y. Yakupogullari et al., "The antimicrobial effects of ketamine combined with propofol: an in vitro study," *Brazilian Journal of Anesthesiology*, vol. 63, no. 6, pp. 461–465, 2013.
- [6] T. Solomon and M. Mallewa, "Dengue and other emerging flaviviruses," *The Journal of Infection*, vol. 42, no. 2, pp. 104–115, 2001.
- [7] J. D. Stanaway, D. S. Shepard, E. A. Undurraga et al., "The global burden of dengue: an analysis from the Global Burden of Disease Study 2013," *The Lancet Infectious Diseases*, vol. 16, no. 6, pp. 712–723, 2016.
- [8] C. J. Gregory and K. M. Tomashek, "Management of severe dengue," *Pediatric Critical Care Medicine*, vol. 13, no. 1, pp. 125–125; author reply 126, 2012.
- [9] L. C. Lum, S. K. Lam, R. George, and S. Devi, "Fulminant hepatitis in dengue infection," *The Southeast Asian Journal of Tropical Medicine and Public Health*, vol. 24, no. 3, pp. 467–471, 1993.
- [10] T. J. Shen, C. L. Chen, M. K. Jhan, P. C. Tseng, and C. F. Lin, "CNS immune profiling in a dengue virus-infected immunocompetent outbred ICR mice strain," *Frontiers in Cellular and Infection Microbiology*, vol. 10, article 557610, 2020.
- [11] E. G. Acosta and R. Bartenschlager, "The quest for host targets to combat dengue virus infections," *Current Opinion in Virology*, vol. 20, pp. 47–54, 2016.
- [12] J. C. Kao, W. C. HuangFu, T. T. Tsai et al., "The antiparasitic drug niclosamide inhibits dengue virus infection by interfering with endosomal acidification independent of mTOR," *PLoS Neglected Tropical Diseases*, vol. 12, no. 8, article e0006715, 2018.
- [13] H. C. Chen, F. M. Hofman, J. T. Kung, Y. D. Lin, and B. A. Wu-Hsieh, "Both virus and tumor necrosis factor alpha are critical for endothelium damage in a mouse model of dengue virus-induced hemorrhage," *Journal of Virology*, vol. 81, no. 11, pp. 5518–5526, 2007.
- [14] Y. L. Cheng, Y. S. Lin, C. L. Chen et al., "Activation of Nrf2 by the dengue virus causes an increase in CLEC5A, which enhances TNF- α production by mononuclear phagocytes," *Scientific Reports*, vol. 6, no. 1, article 32000, 2016.
- [15] M. K. Jhan, W. C. HuangFu, Y. F. Chen et al., "Anti-TNF- α restricts dengue virus-induced neuropathy," *Journal of Leukocyte Biology*, vol. 104, no. 5, pp. 961–968, 2018.
- [16] X. Peng, C. Li, W. Yu et al., "Propofol attenuates hypoxia-induced inflammation in BV2 microglia by inhibiting oxidative stress and NF- κ B/Hif-1 α signaling," *BioMed Research International*, vol. 2020, Article ID 8978704, 11 pages, 2020.
- [17] G. J. Wu, Y. W. Lin, H. C. Tsai, Y. W. Lee, J. T. Chen, and R. M. Chen, "Sepsis-induced liver dysfunction was ameliorated by propofol via suppressing hepatic lipid peroxidation, inflammation, and drug interactions," *Life Sciences*, vol. 213, pp. 279–286, 2018.
- [18] S. Nseir, D. Makris, D. Mathieu, A. Durocher, and C. H. Marquette, "Intensive care unit-acquired infection as a side effect of sedation," *Critical Care*, vol. 14, no. 2, article R30, 2010.
- [19] E. Steinmann, S. Ciesek, M. Friesland, T. J. Erichsen, and T. Pietschmann, "Prolonged survival of hepatitis c virus in the anesthetic propofol," *Clinical Infectious Diseases*, vol. 53, no. 9, pp. 963–964, 2011.
- [20] V. C. Gan, "Dengue: moving from current standard of care to state-of-the-art treatment," *Current Treatment Options in Infectious Diseases*, vol. 6, no. 3, pp. 208–226, 2014.
- [21] V. Tricou, N. N. Minh, T. P. Van et al., "A randomized controlled trial of chloroquine for the treatment of dengue in vietnamese adults," *PLoS Neglected Tropical Diseases*, vol. 4, no. 8, article e785, 2010.
- [22] J. Whitehorn, C. V. V. Nguyen, L. P. Khanh et al., "Lovastatin for the treatment of adult patients with dengue: a randomized, double-blind, placebo-controlled trial," *Clinical Infectious Diseases*, vol. 62, no. 4, pp. 468–476, 2015.
- [23] C. Cruz-Oliveira, J. M. Freire, T. M. Conceicao, L. M. Higa, M. A. R. B. Castanho, and A. T. Da Poian, "Receptors and routes of dengue virus entry into the host cells," *FEMS Microbiology Reviews*, vol. 39, no. 2, pp. 155–170, 2015.
- [24] C. K. Lin, C. K. Tseng, Y. H. Wu et al., "Cyclooxygenase-2 facilitates dengue virus replication and serves as a potential target for developing antiviral agents," *Scientific Reports*, vol. 7, no. 1, article 44701, 2017.
- [25] T. Inada, K. Kubo, T. Kambara, and K. Shingu, "Propofol inhibits cyclo-oxygenase activity in human monocytic THP-1 cells," *Canadian Journal of Anaesthesia*, vol. 56, no. 3, pp. 222–229, 2009.
- [26] T. Inada, K. Kubo, H. Ueshima, and K. Shingu, "Intravenous anesthetic propofol suppresses prostaglandin E2 production in murine dendritic cells," *Journal of Immunotoxicology*, vol. 8, no. 4, pp. 359–366, 2011.
- [27] S. A. Steer and J. A. Corbett, "The role and regulation of COX-2 during viral infection," *Viral Immunology*, vol. 16, no. 4, pp. 447–460, 2003.
- [28] A. Alexanian and A. Sorokin, "Cyclooxygenase 2: protein-protein interactions and posttranslational modifications," *Physiological Genomics*, vol. 49, no. 11, pp. 667–681, 2017.
- [29] B. Jawan, Y. H. Kao, S. Goto et al., "Propofol pretreatment attenuates LPS-induced granulocyte-macrophage colony-stimulating factor production in cultured hepatocytes by suppressing MAPK/ERK activity and NF- κ B translocation," *Toxicology and Applied Pharmacology*, vol. 229, no. 3, pp. 362–373, 2008.

- [30] L. Visvabharathy, B. Xayarath, G. Weinberg, R. A. Shilling, and N. E. Freitag, "Propofol increases host susceptibility to microbial infection by reducing subpopulations of mature immune effector cells at sites of infection," *PLoS One*, vol. 10, no. 9, article e0138043, 2015.
- [31] L. Kittigul, W. Temprom, D. Sujirarat, and C. Kittigul, "Determination of tumor necrosis factor-alpha levels in dengue virus infected patients by sensitive biotin-streptavidin enzyme-linked immunosorbent assay," *Journal of Virological Methods*, vol. 90, no. 1, pp. 51–57, 2000.

Research Article

Nanoemulsified Butenafine for Enhanced Performance against Experimental Cutaneous Leishmaniasis

Adriana Bezerra-Souza,¹ Jéssica A. Jesus ,¹ Márcia D. Laurenti ,¹ Aikaterini Lalatsa ,² Dolores R. Serrano,³ and Luiz Felipe D. Passero ^{4,5}

¹Laboratory of Pathology of Infectious Diseases (LIM-50), Medical School, University of São Paulo, Avenida Dr. Arnaldo 455, 01246903 Cerqueira César, SP, Brazil

²Biomaterials, Bio-engineering and Nanomedicines (BioN) Laboratory, Institute of Biomedical and Biomolecular Sciences, School of Pharmacy and Biomedical Sciences, University of Portsmouth, White Swan Road, Portsmouth PO1 2DT, UK

³Department of Pharmaceutics and Food Technology and Instituto Universitario de Farmacia Industrial (IUFI), School of Pharmacy, Complutense University, Avenida Complutense, 28040 Madrid, Spain

⁴Institute of Biosciences, São Paulo State University (UNESP), São Vicente, Praça Infante Dom Henrique, s/n, 11330-900 São Vicente, SP, Brazil

⁵São Paulo State University (UNESP), Institute for Advanced Studies of Ocean, São Vicente, Av. João Francisco Bendorp, 1178, 11350-011 São Vicente, SP, Brazil

Correspondence should be addressed to Luiz Felipe D. Passero; felipepassero@yahoo.com.br

Received 28 August 2020; Revised 7 October 2020; Accepted 23 March 2021; Published 31 March 2021

Academic Editor: Carlo Cavaliere

Copyright © 2021 Adriana Bezerra-Souza et al. This is an open access article distributed under the Creative Commons Attribution License, which permits unrestricted use, distribution, and reproduction in any medium, provided the original work is properly cited.

The production of ergosterol lipid involves the activity of different enzymes and is a crucial event for the *Leishmania* membrane homeostasis. Such enzymes can be blocked by azoles and allylamines drugs, such as the antifungal butenafine chloride. This drug was active on parasites that cause cutaneous and visceral leishmaniasis. Based on the leishmanicidal activity of butenafine chloride and considering the absence of reports about the therapeutic potential of this drug in cutaneous leishmaniasis, the present work is aimed at analyzing the efficacy of butenafine formulated in two different topical delivery systems, the self-nanoemulsifying drug delivery systems (BUT-SNEDDS) and in a SNEDDS-based nanogel (BUT-SNEDDS gel) as well as in the free form in experimental cutaneous leishmaniasis. Physical studies showed that both formulations were below 300 nm with low polydispersity (<0.5) and good colloidal stability (around -25 mV). Increased steady-state flux was reported for nanoenabled butenafine formulations with reduced lag time in Franz cell diffusion assays across Strat-M membranes. No toxic or inflammatory reactions were detected in animals treated with BUT-SNEDDS, BUT-SNEDDS gel, or butenafine. Animals topically treated with butenafine (free or nanoformulated) showed small dermal lesions and low tissue parasitism. Furthermore, BUT-SNEDD gel and butenafine presented similar efficacy than the standard drug Glucantime given by the intralésional route. Increased levels of IFN- γ were observed in animals treated with BUT-SNEDDS gel or butenafine. Based on these data, the antifungal drug butenafine chloride can be considered an interesting repurposed drug for the treatment of cutaneous leishmaniasis.

1. Introduction

Leishmaniasis is an infectious disease caused by protozoans from the Trypanosomatidae family, Kinetoplastida order, and *Leishmania* genus, that affect humans, wild and domestic animals, and invertebrates belonging to the *Lutzomyia* and *Phlebotomus* genera [1, 2]. Leishmaniasis is considered a

complex of diseases with important clinical-immunological spectrum and epidemiological diversity. Depending on the infecting species and the intrinsic features of the host, cutaneous or visceral leishmaniasis can be clinically characterized. The cutaneous form of leishmaniasis is caused by different *Leishmania* species; therefore, a spectrum of clinical signs can be found, ranging from a single localized skin

lesion, that can heal spontaneously, to multiple ulcerated or nonulcerated lesions in the skin and/or mucosa; these types of lesions frequently require a more complex treatment [3]. In spite of that, the treatment of all clinical forms of leishmaniasis is based on few therapeutic alternatives, such as pentavalent antimonials and amphotericin B [4].

Pentavalent antimonials remain the first choice of treatment for all clinical forms leishmaniasis, mainly in Latin America [5]. Additionally, pentavalent antimonials induce significant side effects such as gastrointestinal intolerance and cardiotoxicity, resulting in low patient compliance and termination of therapy prior to achieving therapeutic outcomes [6]. In some geographic areas, such as in India, drug-resistant parasites have been frequently detected [7]. In such situations, amphotericin B is used as the second-line drug. Amphotericin B is effective in treating leishmaniasis [8], but it interacts with the host cell membrane inducing mild to severe adverse effects in patients, including fever and renal and gastrointestinal toxicities [9, 10]. Moreover, amphotericin B-resistant parasites have been isolated [11]. To mitigate toxicity of amphotericin B micellar formulation, liposomal formulations of amphotericin B are clinically indicated [12], but their use is limited in developing countries due to high cost and temperature instability [12, 13]. An amphotericin B cream (3% w/w, Anfoleish) is currently under clinical trials, but preliminary results have shown variable efficacy in patients with CL as a result of limited skin permeability [14], while a range of adverse effects such as itching, redness, peeling dryness, and irritation of the skin were observed in patients [15]. Miltefosine, the only orally bioavailable licensed treatment for leishmaniasis, has shown different levels of efficacy [16]. Paromomycin, only available licensed formulation, has shown poor efficacy in treating post-kala-azar dermal leishmaniasis in India; however in the New World, it shows variable efficacy in cutaneous leishmaniasis [17, 18]. Altogether, the prevalence of the disease with distinct outcomes, the ineffectiveness, and toxicity of the available drugs emphasizes the need for more active and less toxic treatments based on natural or synthetic molecules [19–21].

The sterol biosynthesis pathway is shared by fungi and *Leishmania* sp. [22, 23]. Molecules generated in this biochemical pathway, such as ergosterol and other 24-methyl sterols, are important for the maintenance of the cell membrane homeostasis. In fact, studies already showed that antifungal drugs are active on *Leishmania* parasites, and these drugs can be selective toward parasites, since host cells do not produce ergosterol, and depending on the drug, the impact towards the homeostasis of the host can be absent or tolerable [24, 25]. The class of the antifungal azoles such as ketoconazole, fenticonazole and tioconazole, that were previously shown to inhibit the C14 α -demethylase enzyme, was able to eliminate promastigote and amastigote of *Leishmania* sp. *in vitro* and *in vivo* [26, 27]. Additionally, squalene epoxidase enzyme, that converts squalene to lanosterol, an important precursor of ergosterol, has also been successfully inhibited by antifungal drugs belonging to the allylamine class [28, 29]. The most studied allylamine drug so far is terbinafine that was active on promastigote and amastigote forms of *Leishmania* sp. [30, 31]. Additionally, patients with

CL treated with terbinafine by the oral route showed partial to full recovery [32], while cutaneous lesions of patients treated with topical terbinafine (32.25–75.5 mg/day depending on the size of the skin lesion) plus Glucantime (20 mg/kg by intramuscular route) during 20 days showed faster improvement in comparison to patients treated with placebo ointment [33].

Besides terbinafine, other antifungal drugs that target squalene epoxidase enzyme impacted *Leishmania* sp. survival. Butenafine hydrochloride and tolnaftate drugs, that are traditionally indicated for the topical treatment of superficial mycosis, were active on promastigote and amastigote forms of *L. (L.) amazonensis*, *L. (V.) braziliensis*, and *L. (L.) infantum* [34, 35], and by morphological and/or physiological studies, the lipids from parasites were affected during the *in vitro* treatments. These and other studies highlight that squalene epoxidase enzyme is an attractive target to be inhibited aiming at impairing the parasite viability.

In spite of elegant works on drug repurposing in leishmaniasis, few reports provided *in vivo* validation of drug candidates. To the best of our knowledge, this is the first study to demonstrate the *in vivo* efficacy of butenafine in cutaneous leishmaniasis. Here, we present a topical butenafine formulation that involves loading butenafine in self-nanoemulsifying drug delivery systems (SNEDDS) and SNEDDS-enabled hydrogels in an attempt to improve butenafine permeation across the skin and localize effective concentrations butenafine within the dermis, increasing the efficacy of butenafine in American cutaneous leishmaniasis.

2. Material and Methods

2.1. Materials. Butenafine hydrochloride (>98%, HPLC) was obtained from Kemprotec Ltd. (Smailthorn, Middleton-in-Lonsdale, Cumbria, UK). Labrasol (caprylocaproyl macrogol-8 glycerides), Transcutol P (diethylene glycol monoethyl ether), and Capryol 90 (propylene glycol monocaprylate) were a gift from Gattefosse (Alpha Chemicals, Berkshire, UK). Carbopol 940 and all other chemicals were purchased from Fisher Scientific UK (Loughborough, UK).

2.2. Preparation of Butenafine Nanoformulations. BUT-SNEDDS (2.125% w/w) were prepared by dispersing BUT (0.0425 g) within an isotropic mixture of Labrasol (0.6 g), Capryol 90 (0.2 g), and Transcutol P (1.2 g), respectively [36, 37]. The ratio of oil:surfactant and solvent was optimized in terms of particle size using tertiary diagrams, and choice of surfactants and solvents was based on solubility studies [36, 37]. The BUT-SNEDDS were magnetically stirred for 15 minutes and left under stirring in a water bath (50 rpm, Kotterman D1365, Hanigsen, Germany) at 37°C overnight for 16 hours [20]. Blank SNEDDS were produced using the same methodology but without adding BUT.

To prepare BUT-SNEDDS gel (0.70% w/w), Carbopol 940 (1 g) was added in deionized water (25 mL) and left to swell overnight. The pH of the swollen gel (10 g) was then adjusted to pH 6.5 by addition of sodium hydroxide (~0.78 mL, 5 M). Neutralised Carbopol 940 gel (10 g) and BUT-SNEDDS (2.125% w/w, 5 g) (final pH: 6.5 \pm 0.1,

Accumet AB200 pH meter, Fisher Scientific, Loughborough, UK) were mixed to obtain BUT-SNEDDS gel.

2.3. Characterization of Prepared SNEDDS and SNEDDS Gel in terms of Particle Size and Colloidal Stability. Blank and butenafine-loaded SNEDDS and SNEDDS gels were diluted with deionized water ($\text{pH } 6.5 \pm 0.1$) (5 mg in 30 mL of water and 16.8 mg in 1.5 mL of water, respectively). SNEDDS samples were vortexed and left to stand for 15 minutes prior to analysis. Gels were diluted and centrifuged (5,000 rpm, 5 minutes, SciSpin, Micro Centrifuge, Shropshire, UK) to remove carbomer, which is insoluble in water, and the supernatant was left to stand for 15 minutes prior to analysis. Particle size and zeta potential were measured as previously described [13, 20, 36, 38] using a Nano-ZS Zetasizer (Malvern Instruments, Worcestershire, UK). The data were analyzed using the Contin method of data analysis [36]. The accuracy of the instrument was assessed periodically using a drop of latex beads (polystyrene, mean size $0.1 \mu\text{m}$) in 50 mM sodium chloride (dispersed phase). All measurements ($n = 13$) were performed in triplicate, and results presented as the mean \pm SD were reported.

Zeta potential (Malvern Nano-Zs, Malvern Instruments, UK) was measured for the diluted formulations using the Doppler electrophoresis technique. Analysis of the Doppler shift (Fourier transformed) was done by using mixed-mode measurement phase analysis light scattering (M3-Pals). The viscosity of the sample was hypothesized to be the viscosity of water at 25°C . All measurements were performed in triplicate, and results presented as the mean \pm SD were reported [20].

2.4. Franz Cell Diffusion Studies. Franz cells (of 12 mL capacity) were mounted with a semisolid Teflon holder with a diffusional area of 1.327 cm^2 . Compartments were rinsed with deionized water and methanol, and a stirrer bar ($3 \times 6 \text{ mm}$) was placed inside. To ensure sink conditions, the receptor compartment was filled with a mixture of 0.1% v/v trimethylamine buffer (adjusted to $\text{pH } 5.00 \pm 0.1$ using 1 M hydrochloric acid and 1 M sodium hydroxide when needed) and methanol (9:1 v/v), preheated to 37°C . Strat-M membranes for transdermal diffuse testing (Millipore) were mounted to adequately cover the receptor chambers. The donor compartment and the receptor compartment were tightly sealed using a thin layer of KORASILON Paste silicone grease (Mittelviskos Kurt Obermeier GmbH & Co. KG) and Parafilm™ prior to being clamped together. The donor chamber was filled with 0.1% trimethylamine buffer (0.4 mL) and covered with Parafilm™ prior to being placed in a water bath at 37°C (RCT basic, IKA® England Ltd., Oxford, UK). After 0.5 h, the buffer was removed from the receptor chamber and was collected for analysis. The receptor chamber was refilled with fresh trimethylamine buffer and methanol mixture prewarmed to 37°C . The trimethylamine buffer in the donor chamber was removed, and the formulations (BUT SNEDDS 1% or BUT SNEDDS gel 1%; 0.4 g) or butenafine solubilized in PBS plus 1% DMSO (10 mg/mL; 0.4 mL/chamber) was added to the donor chamber ensuring it was in contact with the Strat-M membranes. Samples (0.3 mL) were withdrawn

at predetermined times (5 min, 10 min, 15 min, 30 min, 60 min, 120 min, 180 min, 240 min, 360 min, and 480 min) from the receptor chamber using a 1 mL syringe with a 21 g needle (38 mm in length), and samples were analyzed by HPLC as described below. The receptor chamber was immediately replenished with prewarmed trimethylamine buffer and methanol mixture (0.3 mL).

Collected samples were analyzed by HPLC which was equipped with a Jasco PU-1580 pump, a Jasco AS-2050 Plus autosampler, and a Jasco UV-1575 UV-visible detector. Integration of the peaks was performed with the program Borwin 1.5 for PC (JMBS Developments). A Phenomenex LiChrosorb C18 reverse phase HPLC column ($250 \times 2.6 \text{ mm}$, $5 \mu\text{m}$, 100 \AA) was used for analysis. An isocratic elution was used with a mobile phase consisting of freshly prepared and $0.45 \mu\text{m}$ nylon filtered 0.1% v/v trimethylamine buffer (adjusted to $\text{pH } 5.00 \pm 0.1$ using 1 M hydrochloric acid and 1 M sodium hydroxide when needed) and HPLC grade acetonitrile (25:75 v/v). The flow rate was set at 1.2 mL/min, and the injection volume was $40 \mu\text{L}$. Detection was carried at 282 nm and a linear calibration curve was achieved between 0.1 and $100 \mu\text{g mL}^{-1}$ ($R^2 > 0.999$).

Regression analysis was used to calculate the slopes and intercepts of the linear portion of each graph. The steady-state flux (JSS), permeability coefficient (P), the diffusion coefficient, and the lag time were estimated as previously described in Lalatsa et al. [36]. Each formulation was tested at least in triplicate.

2.5. Animals. Six- to eight-week-old female BALB/c mice were obtained from Medical School of São Paulo University. This study was carried out in strict accordance with the recommendations in the *Guide for the Care and Use of Laboratory Animals* of the Brazilian National Council of Animal Experimentation (<http://www.cobea.org.br>). The protocol was approved by the Committee on the Ethics of Animal Experiments of the Institutional Animal Care and Use Committee at the Medical School of São Paulo University (CEP 322/12). For all experimental procedures, mice were anaesthetized or euthanized with thiopental (50 and 150 mg/kg, respectively).

2.6. Histological Changes in the Skin of Healthy BALB Mice Treated with Butenafine-Containing Nanoformulations. Thirty-five female BALB/c mice were divided into seven groups: group 1 was treated topically with SNEDDS (containing 10 mg of butenafine); group 2 was treated topically with BUT-SNEDDS gel (containing 10 mg of butenafine), group 3 was treated topically with butenafine solubilized in DMSO (10 mg of butenafine), and group 4 was injected intralesionally with 100 mg/kg of Glucantime. Groups 5 and 6 were topically treated with blank SNEDDS or blank SNEDDS gels, respectively. Group 7 was topically treated with vehicle solution (PBS plus 1% DMSO). Animals were treated once a day for 15 days. Animals were physically examined weekly. Forty-eight hours after the last application, animals were euthanized with thiopental. Skin fragments were collected, fixed in formalin, and stained with hematoxylin and eosin to analyze histological changes.

2.7. Parasites. *L. (L.) amazonensis* parasite (MHOM/BR/73/M2269) was kindly provided by Prof. Dr. Fernando T. Silveira from the criobank of “Leishmaniasis Laboratory Prof. Dr. Ralph Laison”, Department of Parasitology, Evandro Chagas Institute, Ministry of Health, Belém, Pará, Brazil. The parasite was identified using monoclonal antibodies and isoenzyme electrophoretic profiles at the Leishmaniasis Laboratory of the Evandro Chagas Institute (Belém, Pará State, Brazil). This parasite was grown in Roswell Park Memorial Institute-1640 medium—RPMI 1640 (Gibco®, Life Technologies, Carlsbad, CA, USA), supplemented with 10% heat-inactivated fetal bovine serum, 10 µg/mL of gentamicin, and 1,000 U/mL of penicillin (R10) at 25°C. Promastigote forms in the stationary phase were used.

2.8. Infection and Experimental Treatment. Thirty-five male BALB/c mice were subcutaneously infected in the base of tail with 10^6 promastigote forms of *L. (L.) amazonensis*, and five BALB/c mice received only sodium chloride 0.9% (*w/v*) under the same route (healthy group). Four weeks after infection, *L. (L.) amazonensis*-infected BALB/c mice were divided into seven groups: group 1 (G1) was constituted by infected animals that received only vehicle solution (PBS plus 1% DMSO); groups 2 (G2) and 3 (G3) were treated with blank SNEDDS or blank SNEDDS gels, respectively; group 4 (G4) was treated with BUT-SNEDDS (containing 10 mg of butenafine); group 5 (G5) was treated topically with BUT-SNEDDS gel (containing 10 mg of butenafine), group 6 (G6) was treated topically with butenafine (10 mg of butenafine) solubilized in PBS plus 1% of DMSO, and group 7 (G7) was injected intralesionally with 100 mg/kg of Glucantime. Groups 1 to 6 were treated topically with butenafine-containing formulations, blank formulations, butenafine, or vehicle solution, while G7 was injected intralesionally. Group 8 was constituted by noninfected, nontreated animals. Animals were treated for 15 consecutive days once daily. The physical conditions of the animals were monitored once a week. Two weeks after the last application, animals were euthanized with thiopental. Skin fragments were collected, fixed in formalin, and stained with hematoxylin and eosin to analyze histological changes. There was no dead prior to the endpoint. In all experiments, parasites were in stationary phase of growth, and never exceeded three passages *in vitro*.

2.9. Clinical Course of Lesion Development and Determination of Parasite Burden in the Skin of Infected and Treated Animals. The clinical course of lesion development was evaluated weekly by recording the average diameter of the tail measured as the mean of tail base diameters in horizontal and vertical directions using a caliper. The parasite load in the skin was determined using the quantitative limiting dilution assay, as previously described [39]. Briefly, a skin fragment from the base of tail was aseptically excised, weighed, and homogenized in Schneider’s medium. The skin suspensions were subjected to 12 serial dilutions with four replicate wells. The number of viable parasites was determined based on the highest dilution that promastigotes could be grown after 10 days of incubation at 25°C.

2.10. Cytokine Production Studies. The subiliac and popliteal lymph nodes from the different groups were aseptically collected and macerated in R10 medium, and the number of cells estimated under trypan blue exclusion dye. Cells were adjusted at 5×10^5 cells/well and stimulated with 5.0 µg of whole antigen of *L. (L.) amazonensis* or 1.0 µg of concanavalin A, as a positive control; negative controls were cultivated only with R10 medium during 72 h in a humidified incubator, 37°C, 5% CO₂. Following this experimental time, supernatants were collected, and the amounts of IL-4 and IFN-γ (BD, Franklin Lakes, NJ, USA) were quantified by sandwich enzyme-linked immunosorbent assay (ELISA) in accordance with the manufacturer’s recommendations.

2.11. Statistical Analysis. The results were expressed as the mean ± standard deviation of three independent experiments, and the nonparametric Mann–Whitney *U* test was used to compare results among groups. Differences were considered statistically significant at 5% significance level ($p < 0.05$). GraphPad Prism 5 (GraphPad Software, Inc., La Jolla, CA, USA) was used to analyze the results.

3. Results

3.1. Measurement of Particle Size and Zeta Potential of Nanoformulations. Prepared BUT-SNEDDS and BUT-SNEDDS gel illustrated sizes consistently below 300 nm (Table 1) with good colloidal stability. The particle size of BUT-SNEDDS and BUT-SNEDDS gel was similar indicating the ability of nanoparticles forming after dilution of the gels in aqueous environments. Viscosity of the prepared hydrogels was appropriate for skin application avoiding running [36].

3.2. Franz Cell Diffusion Studies. In the permeability studies, it was observed that butenafine-containing formulations displayed higher flux rate, permeability, and diffusion coefficients through the Strat membrane in comparison to the butenafine solubilized in DMSO ($p < 0.05$). Additionally, the formulations showed a significant lower lag time compared to free butenafine which can be explained for the slower release of the drug ($p < 0.05$). These data are summarized in Table 2.

3.3. Histological Changes in the Skin of Healthy BALB Mice Treated with Butenafine-Containing Nanoformulations. BALB/c mice were treated topically with formulations containing butenafine (10 mg of butenafine), butenafine solubilized in DMSO (10 mg), and blank formulations or intralesionally treated with Glucantime (100 mg/kg) once a day during 15 days. Forty-eight hours later, animals were euthanized and fragments of the skin were collected.

The histological section of the skin from nontreated BALB/c mice showed no morphological changes in the epidermis and dermis layers (Figure 1(a)). Similarly, skin from animals treated with blank SNEDDS and blank SNEDDS gels (Figures 1(b) and 1(c), respectively), BUT-SNEDDS and BUT-SNEDDS gel (Figures 1(d) and 1(e), respectively), or butenafine solubilized in DMSO (Figure 1(f)) showed normal morphology of the epidermis and dermis; additionally, no signs of inflammation were observed. Animals treated with Glucantime (Figure 1(g)) did not show changes in the

TABLE 1: Mean particle size, polydispersity, and zeta potential of prepared batches of BUT-SNEDDS and BUT-SNEDDS gel ($n = 4$).

Formulation	Particle size (nm)	Polydispersity	Zeta potential (mV)
BUT-SNEDDS	185 ± 2	0.343 ± 0.024	-20.3 ± 3.0
BUT-SNEDDS gel	235 ± 11	0.458 ± 0.032	-24.3 ± 1.5
Blank SNEDDS	245 ± 27	0.578 ± 0.011	-14.8 ± 2.3
Blank SNEDDS gels	294 ± 85	0.605 ± 0.032	-22.6 ± 1.9

epidermis; however, a diffuse inflammatory infiltrate was identified in the dermis, mainly composed of mononuclear cells (Figure 1(g), white arrow).

3.4. Clinical Course of the Lesion Development and Determination of Parasite Burden in the Skin of Infected and Treated Animals. All the infected control groups [infected nontreated (G1), treated with blank SNEDDS (G2), or blank SNEDDS gel (G3)] showed similar growth of lesions that increased over eight weeks of postinfection (Figure 2(a)). Skin lesions in animals treated with BUT-SNEDDS (G4) and BUT-SNEDDS gel (G5) as well as butenafine (G6) and Glucantime (G7) significantly decreased in size after 6 weeks of postinfection and remained significantly smaller until the end of the experiment (8 weeks) compared to the control groups ($p < 0.05$, Figure 2(a)).

In comparison to the controls, animals treated topically with nanoenabled butenafine formulations or butenafine presented lower tissue parasitism ($p < 0.05$). Additionally, animals treated with Glucantime (G7) by the intralésional route also showed low parasitism in the skin compared to the controls ($p < 0.05$). Furthermore, BUT-SNEDDS gel (G5) was more efficient at decreasing tissue parasitism in infected animals than blank SNEDDS gel (G3). Although efficient at decreasing the lesion size, BUT-SNEDDS (G4) displayed similar ability to decrease parasite load than blank SNEDDS (G2) ($p > 0.05$). Treatment with BUT-SNEDDS gel (G5) and butenafine (G6) demonstrated comparable efficacy to intralésional administration of Glucantime (G7) ($p > 0.05$), as shown in Figure 2(b).

3.5. Histological Changes in Infected Animals Treated with Free or Nanoformulated Butenafine. Histological sections from the skin of infected control animals, i.e., infected nontreated (G1), treated with blank SNEDDS (G2), or with blank SNEDDS gels (G3) as in Figures 3(a)–3(c), respectively, displayed complete disruption of the epidermis and dermis. Macrophages were highly infected with amastigotes in such control groups; additionally, neutrophil and eosinophil immune cells were detected throughout these sections. Histological sections from animals treated with BUT-SNEDDS (G4) displayed lower tissue parasitism compared to the controls (G1, G2, and G3), but mixed inflammatory infiltrate still persisted, with the involvement of mononuclear and polymorphonuclear immune cells (Figure 3(d)). On the other hand, lesions from animals treated topically with BUT-SNEDDS gel (G5) (Figure 3(e)) or intralésionally with Glucantime (G7) (Figure 3(g)) showed inflammatory infiltrates

characterized by the presence of lymphocytes and few infected macrophages (inset in the respective figures). In the histological section of the skin from BALB/c mice treated with free butenafine (G6) (Figure 3(f)), inflammatory infiltrate was constituted of mononuclear cells, mainly with the involvement of few polymorphonuclear cells. Figure 3(h) shows histological section from the skin of healthy BALB/c mice (G8). Black arrows indicate amastigote forms.

3.6. Cytokine Production Studies. Mononuclear cells from animals treated with blanks (G2 and G3), BUT-SNEDDS (G4), SNEDDS gel (G5), and butenafine (G6) produced similar amounts of IL-4 (Figure 4(a)) in comparison to the infected control animals (G1). Cells from animals treated with Glucantime (G7) produced significant low levels of IL-4 in comparison with the infected control group ($p < 0.05$).

In comparison with infected control (G1), mononuclear cells from animals treated with BUT-SNEDDS gel (G5) or butenafine (G6) produced significant high levels of IFN- γ ($p < 0.05$). Cells from animals treated with blanks (G2 and G3), BUT-SNEDDS (G4), or Glucantime (G7) did not alter the amounts of IFN- γ produced ($p > 0.05$, Figure 4(b)). Animals treated with BUT-SNEDDS gel (G5) produced higher amounts of IFN- γ than animals treated with blank SNEDDS gel (G3) ($p < 0.05$).

Furthermore, it was possible to observe that the control groups (G1, G2, and G3) showed an elevated IL-4/IFN- γ ratio, demonstrating that these animals from an immunological point of view developed an expressive Th2 immune response, although the G4 group, treated with BUT-SNEDDS, also developed a Th2 response. In contrast, animals treated with BUT-SNEDDS gel (G5), butenafine (G6), and Glucantime (G7) were able to inhibit the production of Th2 immune response, and especially, G5 and G6 upregulated Th1 immune response.

Lymph node cells stimulated with concanavalin A produced high amounts of both cytokines (data not shown), while negative controls (cells cultured with R10 only) did not produce quantifiable levels of both cytokines (data not shown).

4. Discussion

The cell membrane physiology of *Leishmania* parasites is dependent on the formation of ergosterol and other 24-alkyl sterols; furthermore, this biochemical route is complex and different leishmanial enzymes take part of this process. Thus, the inhibition of key molecules may disrupt the balance of the cell membrane and induce death in *Leishmania* sp., caused by depletion of ergosterol precursors [40]. Butenafine, an antifungal drug, has been shown to eliminate promastigote and intracellular amastigote forms of *L. (L.) amazonensis* and *L. (V.) braziliensis* selectively, while being able to induce structural changes associated with lipid recycling and programmed cell death in promastigote forms of *L. (L.) amazonensis* [34]. Possibly, the leishmanicidal activity of butenafine relies on the fact that it is able to inhibit squalene epoxidase enzyme, and once inhibited, squalene as well as other intermediated molecule will not be produced,

TABLE 2: Permeation parameters for butenafine and butenafine nanoenabled formulations across Strat membrane.

Parameter	BUT-SNEDDS gel	BUT-SNEDDS	Butenafine
Steady-state flux ($\mu\text{g}/\text{cm}^2/\text{h}$)	$52.2 \pm 2.7^*$	$51.29 \pm 0.34^*$	35.60 ± 12.10
Lag time (min)	$2.14 \pm 0.01^*$	2.60 ± 0.01	5.28 ± 0.01
Permeability coefficient (cm^2/h)	$5.22 \pm 0.27^*$	$5.13 \pm 0.03^*$	3.56 ± 1.21
Diffusion coefficient (cm/h)	$0.57 \pm 0.03^*$	$0.56 \pm 0.01^*$	0.39 ± 0.27

* $p < 0.05$ indicates statistical significance in comparison to the permeation parameters for butenafine.

resulting in a deficiency in basic processes required for *Leishmania* sp. survival, such as membrane recycling and cell division [29].

Although butenafine is active on *Leishmania* sp. parasites [41], there are not available clinical formulations to support its topical use for the treatment of cutaneous leishmaniasis. Thus, this study demonstrated for the first time that applying butenafine in the infected skin of BALB/c mice decreased the size of the skin lesion as well as parasitism. Additionally, butenafine was formulated in cost-effective, easily scalable nanosystems prepared from generally regarded as safe excipients that were highly efficient at killing tissue amastigotes. These data provided preclinical proof of concept of the butenafine, administered in formulations or in the free form, which is effective in cutaneous leishmaniasis caused by *L. (L.) amazonensis*.

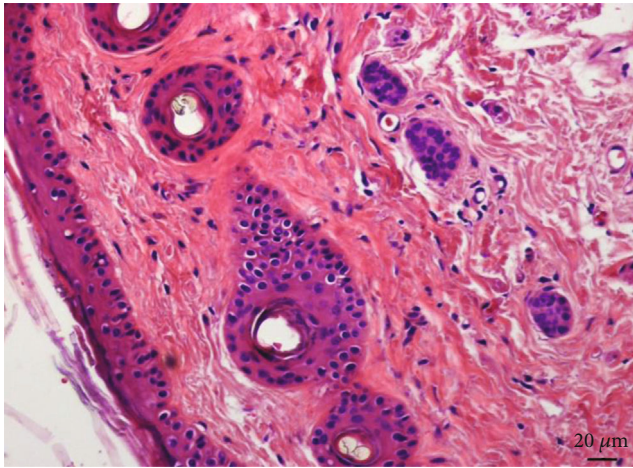
Physical data obtained demonstrated that both BUT-SNEEDS and BUT-SNEDDS gel have the potential to penetrate through the skin, since their particle sizes are 235 nm or below, with a low polydispersity index (<0.5) and a zeta potential around -24 mV. Previous studies showed that formulations containing particles with size lower than 300 nm, presenting low polydispersity (~ 0.4) and zeta potential below -25 mV, have high degree of stability, present low tendency to form aggregates, and have potential to penetrate through biological systems, such as the skin [42]. Thus, physical features suggested that both BUT-SNEEDS and BUT-SNEDDS gel are suitable formulations to be employed in studies aiming at analyzing butenafine efficacy by the topical route. In fact, studies employing Strat-M artificial membranes, that mimic the skin and transcutaneous permeation, showed that butenafine formulated into SNEDDS and SNEDDS gel presented high steady-state flux, permeability, and diffusion coefficients suggesting a faster permeability through the membrane than butenafine solubilized in PBS plus 1% DMSO; additionally, a lower lag time observed in both formulations showed that butenafine formulated into SNEDDS and SNEDDS gel diffused faster than butenafine through artificial membranes.

Healthy BALB/c mice were treated with BUT-SNEDDS and BUT-SNEDDS gel to analyze possible toxic effects of formulation in the skin of animals. In this case, no histological changes were observed in animals treated with butenafine, butenafine loaded in nanoenabled formulations, or blank formulations. Altogether, data suggested that free and nanoenabled formulations are not toxic to BALB/c skin after topical application for 15 consecutive days. In spite of that, it is important to point out that an inflammatory infiltrate was detected in the dermis of animals injected with Glucan-

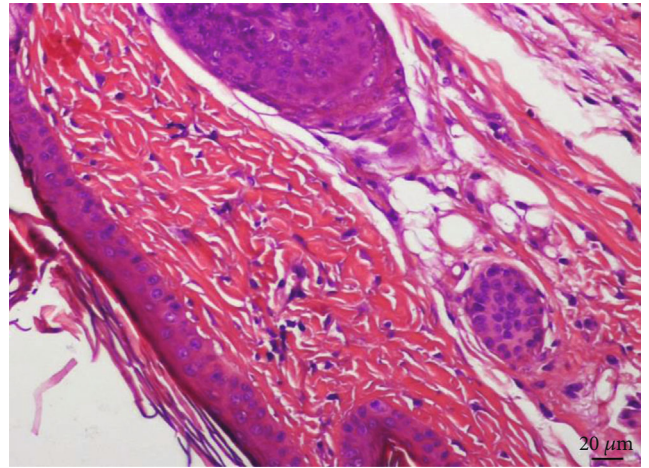
time. The severe side effects induced by Glucantime can be avoided by applying it intralesionally; however, some patients can experience local inflammatory reactions, associated with the type IV hypersensitivity [43, 44], and a similar process may take place in BALB/c mice.

Butenafine, BUT-SNEDDS, and BUT-SNEDDS gel were able to decrease the size of the skin lesions in BALB/c mice. Blank formulations did not alter the course of the infection. BUT-SNEDDS gel was more efficient in reducing parasite load in the lesions compared to BUT-SNEDDS. According to data on artificial membrane permeation, both BUT-SNEDDS and BUT-SNEDDS gel have the same potential to permeate by membranes; however, BUT-SNEDDS has higher viscosity (data not shown), favoring the draining out of this formulation, that can alter the efficacy of this formulation. Moreover, animals treated with BUT-SNEDDS gel or butenafine demonstrated similar lesion size and tissue parasitism in comparison to the animals treated with Glucantime. In previous studies with terbinafine, the latter also was able to inhibit the development of the skin lesion in BALB/c mice infected with *L. (L.) major* [45], and humans naturally infected with *Leishmania* sp. receiving terbinafine by oral route or topically associated with Glucantime had improvements in the skin lesions [32, 33], suggesting that inhibitors of squalene epoxidase enzyme can be interesting targets to characterize new classes of leishmanicidal drugs. In addition to the therapeutic activity of butenafine, the topical route of application offers many advantages compared to injections, such as the possibility of self-administration, pain-free, no need for patient hospitalization, enable to bypass the liver metabolism of drugs, and more importantly is noninvasive; thus, this can be considered a useful nanomedicine to treat cutaneous leishmaniasis. By contrast, Glucantime, the first-line drug, although effective in the present study, for human treatment has been considered outdated, highly toxic, invasive, and painful, and more importantly, some patients are refractory to this treatment [46–48], which in fact can limit its efficacy.

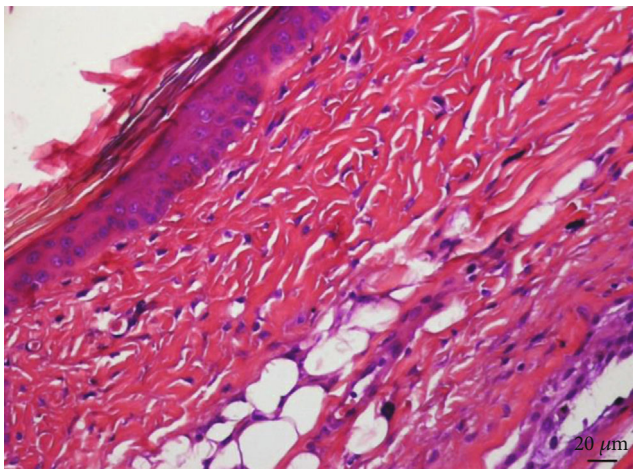
The same pattern observed in the studies of the skin parasitism was found in the histological analysis. In the skin of the control groups [infected and nontreated (G1), infected and treated with blank SNEDDS (G2), or blank SNEDDS gels (G3)], an intense inflammatory infiltrate was observed and it was mainly composed by heavily infected macrophages. In the skin of animals treated topically with BUT-SNEDD (G4), intermediate number of amastigote forms was observed along with an intense inflammatory infiltrate composed by polymorphonuclear and mononuclear cells; in the skin of animals treated with BUT-SNEDD gel (G5), few amastigote



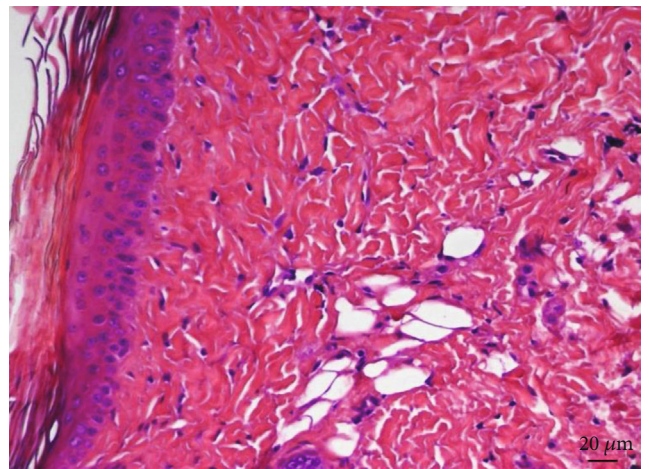
(a)



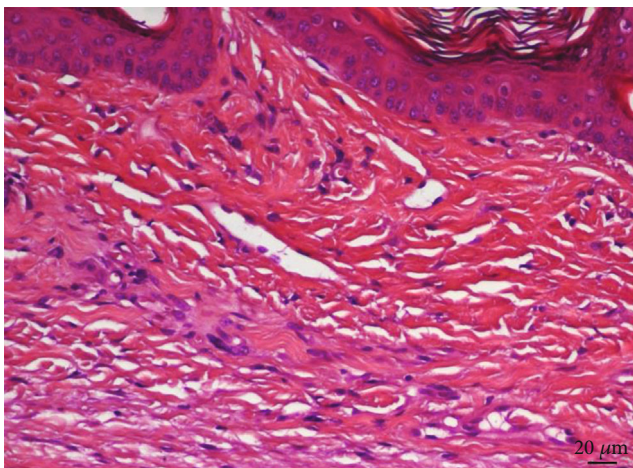
(b)



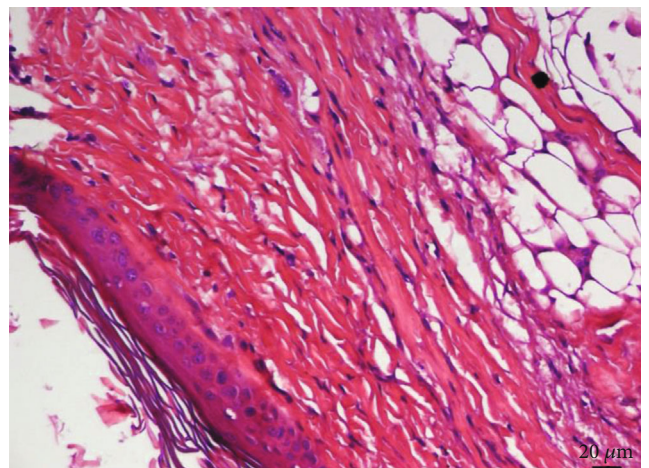
(c)



(d)

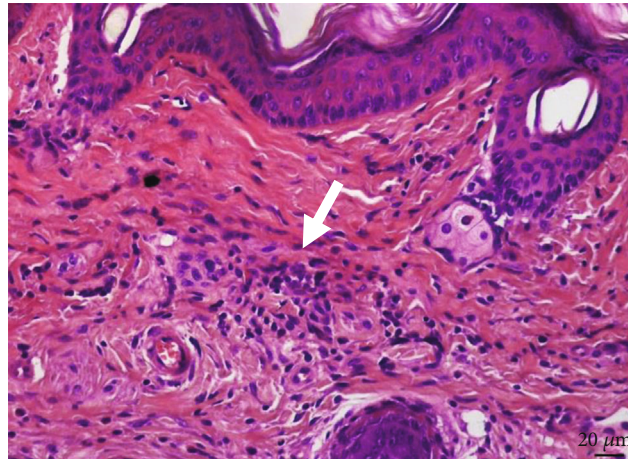


(e)



(f)

FIGURE 1: Continued.



(g)

FIGURE 1: BALB/c mice were treated topically with butenafine chloride formulated in the self-nanoemulsifying drug delivery system (SNEDDS) or in a SNEDDS-based nanogel (SNEDDS gel) containing butenafine (10 mg of butenafine per dose), butenafine solubilized in DMSO (10 mg/dose), and blank formulations of the nanosystems or intralesionally treated with Glucantime (100 mg/kg/dose) once a day during 15 days. Forty-eight hours after the last dose, fragments of the skin from BALB/c mice were collected and analyzed by histology. Histological section of the skin from (a) nontreated animals, (b) blank SNEDDS, (c) blank SNEDDS gel, (d) BUT-SNEDDS, (e) BUT-SNEDDS gel, (f) butenafine, and (g) Glucantime. White arrow shows an area of inflammatory infiltrate.

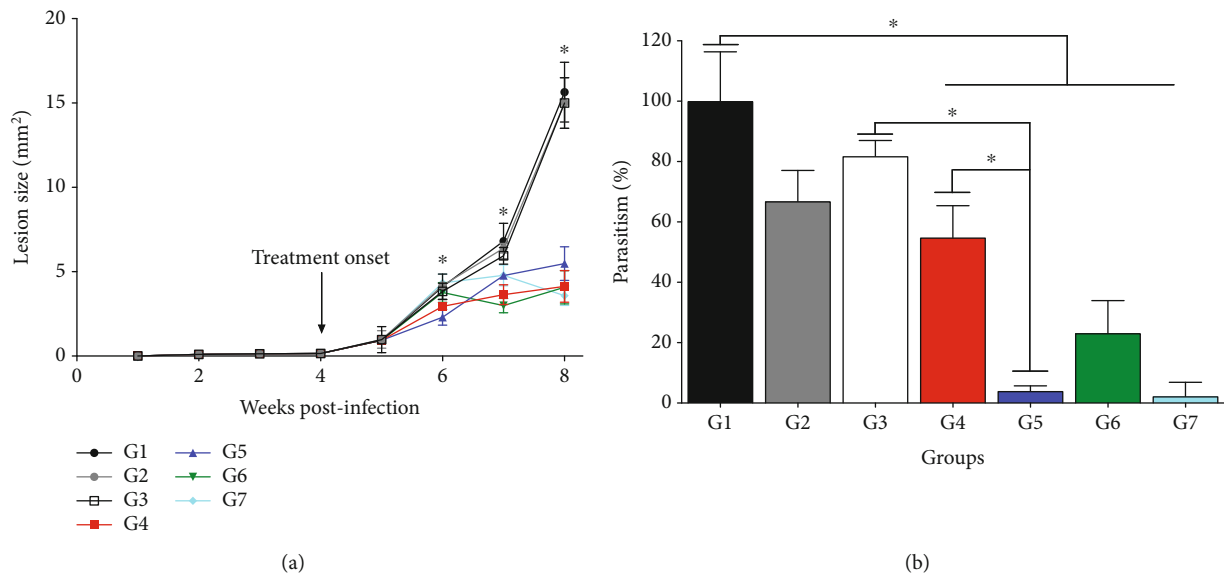
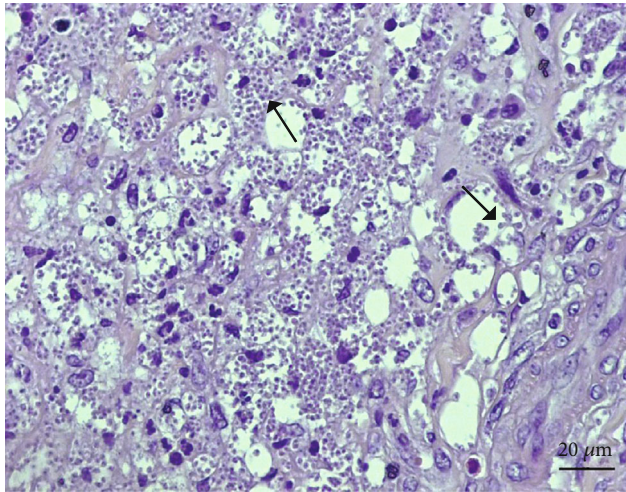


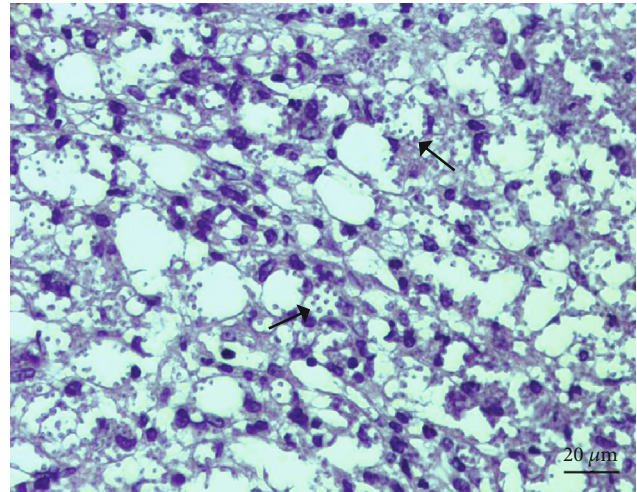
FIGURE 2: *In vivo* efficacy of butenafine and nanoenabled formulations in experimental cutaneous leishmaniasis. BALB/c mice were infected into the base of the tail with 10^6 promastigote forms of *L. (L.) amazonensis* in stationary phase of growth. Four weeks after, infected animals were topically treated once daily for 15 days with blank SNEDDS, blank SNEDDS gel, BUT-SNEDDS, BUT-SNEDDS gel, butenafine, and Glucantime. Lesion sizes were analyzed weekly (a), and the skin parasitism from the base of tail, quantified by limiting dilution assay, was analyzed at 8 weeks of postinfection (b). * $p < 0.05$ indicates statistical significance. G1: infected control; G2 and G3: animals treated with blank SNEDDS or blank SNEDDS gels, respectively; G4: animals treated with BUT-SNEDDS; G5: animals treated BUT-SNEDDS gel; G6: animals treated with butenafine; G7: animals treated with Glucantime.

forms were identified (inset in Figure 3(e)), and mononuclear cells were the main cells identified in the inflammatory infiltrate; additionally, fibroblasts were observed around the inflammatory cells that may be associated with the process of skin remodeling [49], suggesting a superior therapeutic activity of such formulation compared to BUT-SNEDD. A low number of amastigote forms inside big intracellular vacuoles from macrophages were observed in the skin of animals

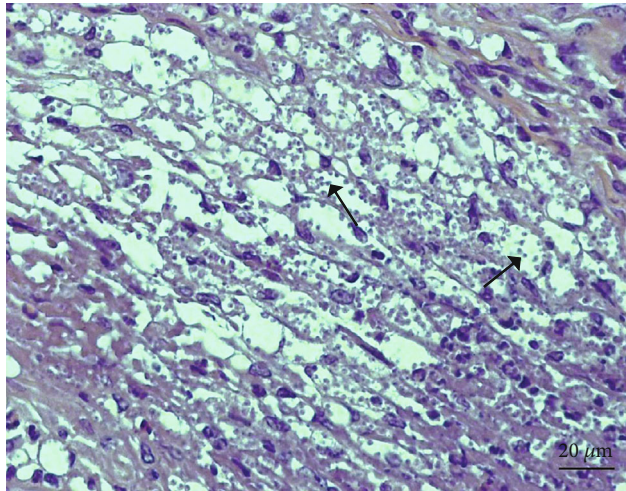
with butenafine (G6); furthermore, an inflammatory process composed by both mononuclear and polymorphonuclear cells was identified in focal areas of the skin. The features associated with the low number of parasitism along with focal areas suggested that butenafine was active in the experimental model cutaneous leishmaniasis. The skin of animals treated by intralesional route with Glucantime (G7) presented similar features than the skin from G4, since few



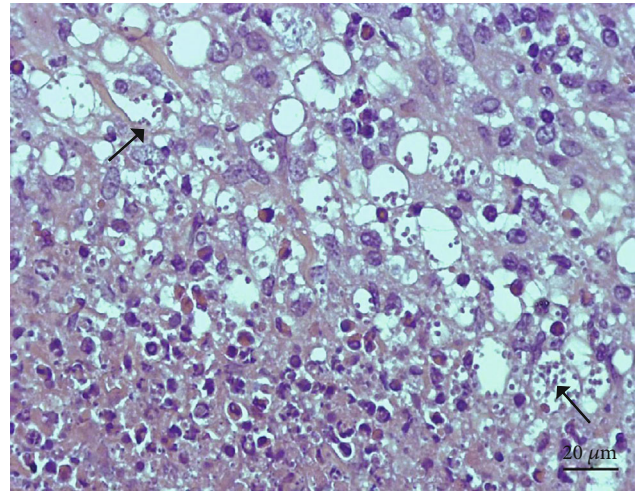
(a)



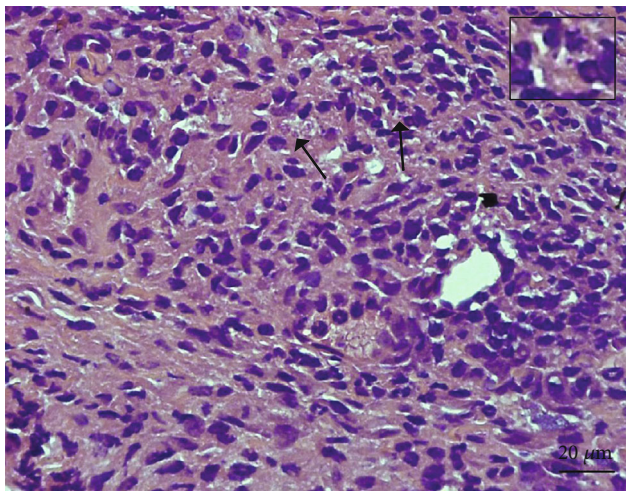
(b)



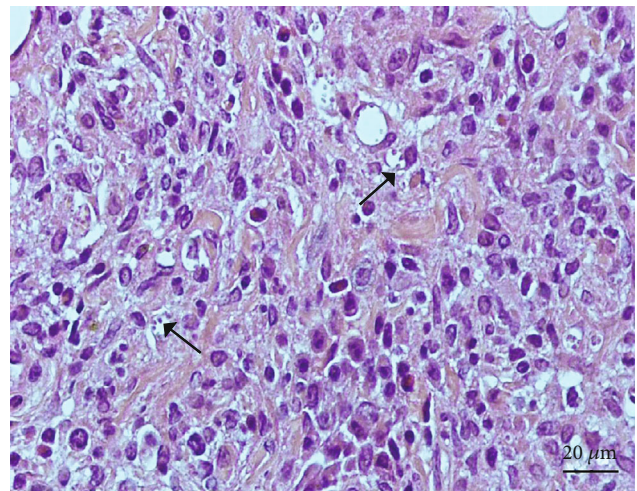
(c)



(d)



(e)



(f)

FIGURE 3: Continued.

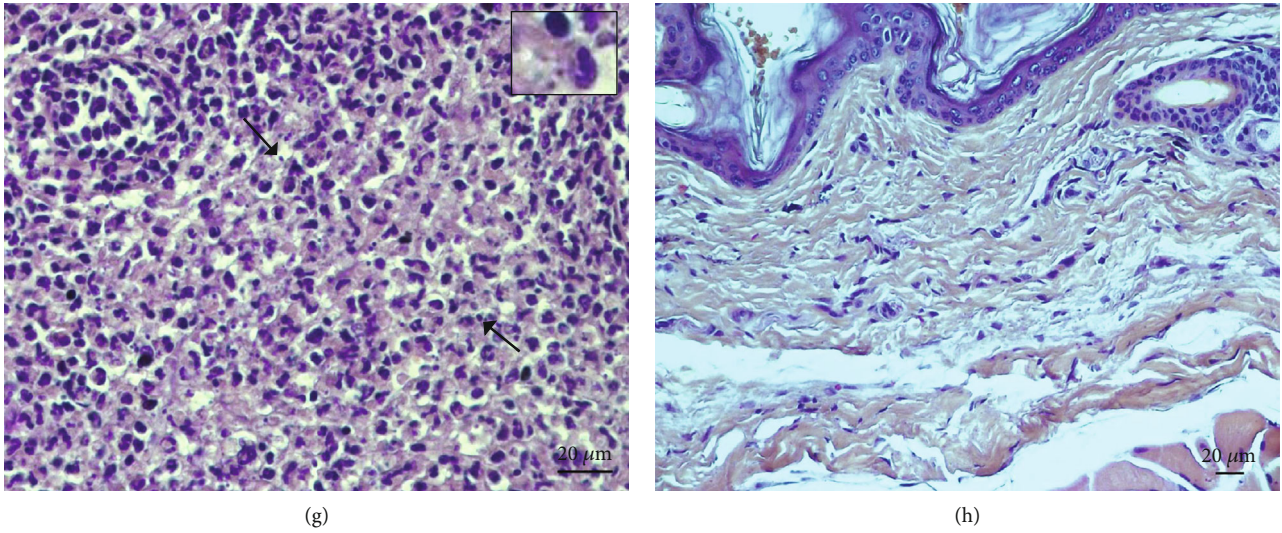


FIGURE 3: Skin histological section from infected controls: (a) infected, nontreated, (b, c) infected and treated with blank SNEDDS or blank SNEDDS gel, respectively, and animals treated with BUT-SNEDDS or BUT-SNEDDS gel (d, e, respectively), butenafine (f), or Glucantime (g). Skin histological section from healthy animals is shown in (h). Black arrows indicate intracellular amastigote forms. Insets show in details amastigote forms of the skin histological sections from animals treated with butenafine loaded in gel (e) or Glucantime (g).

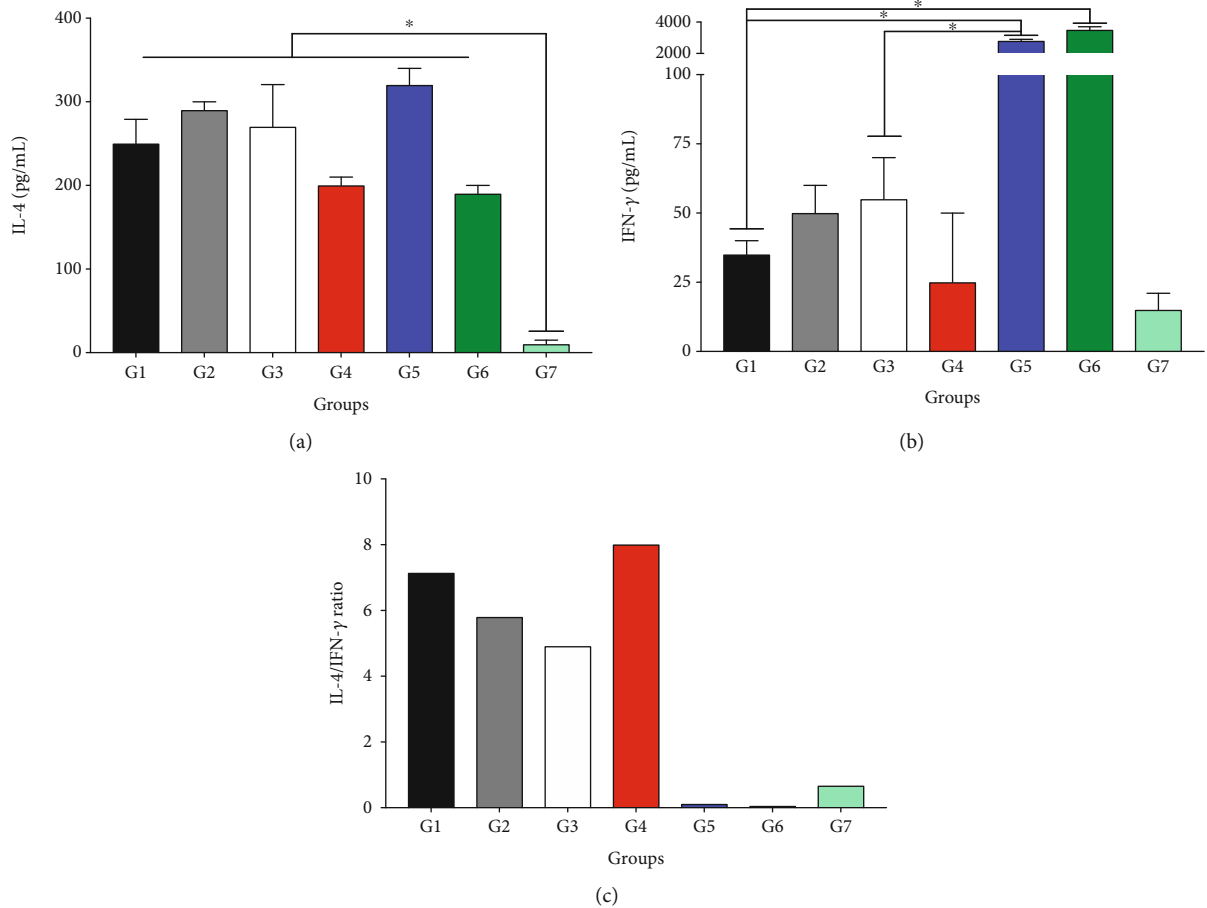


FIGURE 4: Mononuclear cells from lymph nodes of treated and control BALB/c mice were isolated and cultured by 72 h under specific stimulation with the whole antigen of *L. (L.) amazonensis*, following the levels of IL-4 (a) and IFN- γ cytokines (b) which were quantified by ELISA. (c) IL-4/IFN- γ ratio. * $p < 0.05$ indicates statistical significance. G1: infected control; G2 and G3: animals treated with blank SNEDDS or blank SNEDDS gels, respectively; G4: animals treated with BUT-SNEDDS; G5: animals treated with BUT-SNEDDS gel; G6: animals treated with butenafine; G7: animals treated with Glucantime.

amastigote forms were detected (inset in Figure 3(g)), but the inflammatory infiltrate persisted that can be an effect of low number of amastigote forms or even an effect of the drug, since Glucantime triggered an inflammatory response in the skin of healthy animals (Figure 1(g)) and humans [44].

In cutaneous leishmaniasis, IL-4 and IFN- γ cytokines play antagonistic roles, as IFN- γ is capable of activating macrophages that, in turn, will produce reactive species of nitrogen and oxygen and eliminate intracellular amastigote forms [50]. On the other hand, IL-4 aids CD4⁺ Th2 lymphocyte differentiation and inhibits Th1 generation [51]. In the present study, the level of IL-4 in treated animals was unaltered when compared to the control, suggesting differentiation of IL-4-producing cells stimulated by the parasite antigens. Conversely, high levels of IFN- γ were detected in animals treated with BUT-SNEDDS gel and butenafine, suggesting that butenafine has immunomodulatory activity, and at least partially, the leishmanicidal activity of this drug can be accounted due to its immunomodulation [52]. Surprisingly, cells from animals treated with SNEDDS did not change the profile of cytokine production. This can be explained by the low viscosity of SNEDDS compared to SNEDDS gels and the inability of SNEDDS to remain on the skin. On the other hand, mononuclear cells from animals treated with Glucantime produced low levels of both IL-4 and IFN- γ cytokines. Possibly, Glucantime eliminates high number of parasites quickly and the remaining ones are not able to induce the differentiation of specific Th1 or Th2 anti-*Leishmania* T lymphocyte clones. However, it was shown *in vitro* that butenafine, as well as other squalene epoxidase inhibitors [26, 34, 35], was able to eliminate amastigote forms after 24 h; thus, parasites can be eliminated slower, allowing antigens to circulate and maintaining clones of T cells. Recently, Yamamoto et al. [53] observed that cells from BALB/c mice infected with *L. (L.) amazonensis* and treated with amphotericin B also produced low amounts of IL-4 and IFN- γ cytokines, pointing out to the fact that low parasite numbers cannot stimulate a specific immune response, and in fact, a minimum level is needed to maintain an efficient inflammatory response. In addition, it was possible to observe that groups treated with BUT-SNEDDS gel or butenafine enhanced the efficacy of the immune response, since a strong Th1 immune response was triggered upon treatment, and as expected, the control groups produced high levels of IL-4 and developed an increased Th2 immune response.

In conclusion, butenafine chloride was successfully formulated as nanoenabled stable gels for topical administration. BUT-SNEDDS gel showed high flux across healthy mouse skin without causing any toxic, inflammatory, or allergic reactions. Additionally, infected BALB/c mice topically treated with BUT-SNEDDS gel or butenafine (vehicle) showed reduced lesion size and parasite load similar to that elicited by intralesional administration of Glucantime and these effects were associated with increase in IFN- γ levels. Taken together, transcutaneous drug delivery of butenafine can offer advantages over other invasive routes of administration currently in use towards a cost-effective, easily scalable, and safe topical repurposed therapy for leishmaniasis.

Data Availability

The data are available from the corresponding author upon request.

Conflicts of Interest

The authors declare no conflicts of interest.

Acknowledgments

This work was supported by the São Paulo Research Foundation (2016/00468-0, 2017/09405-4, and 2018/24077-6), the Royal Society (RG130542), the Ibero-American Universities Union Research Collaboration Fund (Unión Iberoamericana de Universidades; ENF03-2017), and the Hospital das Clínicas da Faculdade de Medicina da Universidade de São Paulo (LIM50).

References

- [1] P. Kaye and P. Scott, "Leishmaniasis: complexity at the host-pathogen interface," *Nature Reviews. Microbiology*, vol. 9, no. 8, pp. 604–615, 2011.
- [2] R. S. Lana, É. M. Michalsky, C. L. Fortes-Dias et al., "Phlebotomine sand fly fauna and leishmania infection in the vicinity of the Serra do Cipó National Park, a natural Brazilian heritage site," *BioMed Research International*, vol. 2015, Article ID 385493, 9 pages, 2015.
- [3] R. Reithinger, J.-C. Dujardin, H. Louzir, C. Pirmez, B. Alexander, and S. Brooker, "Cutaneous leishmaniasis," *The Lancet Infectious Diseases*, vol. 7, no. 9, pp. 581–596, 2007.
- [4] L. F. D. Passero, L. A. Cruz, G. Santos-Gomes, E. Rodrigues, M. D. Laurenti, and J. H. G. Lago, "Conventional versus natural alternative treatments for leishmaniasis: a review," *Current Topics in Medicinal Chemistry*, vol. 18, no. 15, pp. 1275–1286, 2018.
- [5] S. H. Carvalho, F. Frézard, N. P. Pereira et al., "American tegumentary leishmaniasis in Brazil: a critical review of the current therapeutic approach with systemic meglumine antimoniate and short-term possibilities for an alternative treatment," *Tropical Medicine & International Health*, vol. 24, no. 4, pp. 380–391, 2019.
- [6] F. Frézard, C. Demicheli, and R. R. Ribeiro, "Pentavalent antimonials: new perspectives for old drugs," *Molecules*, vol. 14, no. 7, pp. 2317–2336, 2009.
- [7] S. Sundar, "Drug resistance in Indian visceral leishmaniasis," *Tropical Medicine & International Health*, vol. 6, no. 11, pp. 849–854, 2001.
- [8] F. Chappuis, S. Sundar, A. Hailu et al., "Visceral leishmaniasis: what are the needs for diagnosis, treatment and control?," *Nature Reviews. Microbiology*, vol. 5, no. 11, pp. 873–882, 2007.
- [9] S. Sundar and A. Singh, "Chemotherapeutics of visceral leishmaniasis: present and future developments," *Parasitology*, vol. 145, pp. 481–489, 2017.
- [10] A. Lemke, A. F. Kiderlen, and O. Kayser, "Amphotericin B," *Applied Microbiology and Biotechnology*, vol. 68, no. 2, pp. 151–162, 2005.
- [11] B. Purkait, A. Kumar, N. Nandi et al., "Mechanism of amphotericin B resistance in clinical isolates of *Leishmania*

- donovani," *Antimicrobial Agents and Chemotherapy*, vol. 56, no. 2, pp. 1031–1041, 2012.
- [12] D. R. Serrano and A. Lalatsa, "Oral amphotericin B: the journey from bench to market," *Journal of Drug Delivery Science and Technology*, vol. 42, pp. 75–83, 2017.
- [13] D. R. Serrano, A. Lalatsa, M. A. Dea-Ayuela et al., "Oral particle uptake and organ targeting drives the activity of amphotericin B nanoparticles," *Molecular Pharmaceutics*, vol. 12, no. 2, pp. 420–431, 2015.
- [14] L. López, I. Vélez, C. Asela et al., "A phase II study to evaluate the safety and efficacy of topical 3% amphotericin B cream (Anfoleish) for the treatment of uncomplicated cutaneous leishmaniasis in Colombia," *PLoS Neglected Tropical Diseases*, vol. 12, no. 7, article e0006653, 2018.
- [15] A. Ganeshpurkar, P. Vaishya, S. Jain, V. Pandey, D. Bansal, and N. Dubey, "Delivery of amphotericin B for effective treatment of *Candida albicans* induced dermal mycosis in rats via emulgel system: formulation and evaluation," *Indian Journal of Dermatology*, vol. 59, no. 4, pp. 369–374, 2014.
- [16] S. Sundar, A. Singh, M. Rai et al., "Efficacy of miltefosine in the treatment of visceral leishmaniasis in India after a decade of use," *Clinical Infectious Diseases*, vol. 55, no. 4, pp. 543–550, 2012.
- [17] F. A. Neva, C. Ponce, E. Ponce, R. Kreutzer, F. Modabber, and P. Olliaro, "Non-ulcerative cutaneous leishmaniasis in Honduras fails to respond to topical paromomycin," *Transactions of the Royal Society of Tropical Medicine and Hygiene*, vol. 91, no. 4, pp. 473–475, 1997.
- [18] N. Sosa, J. M. Pascale, A. I. Jiménez et al., "Topical paromomycin for New World cutaneous leishmaniasis," *PLoS Neglected Tropical Diseases*, vol. 13, no. 5, article e0007253, 2019.
- [19] E. J. G. Silva, A. Bezerra-Souza, L. F. D. Passero et al., "Synthesis, leishmanicidal activity, structural descriptors and structure-activity relationship of quinoline derivatives," *Future Medicinal Chemistry*, vol. 10, no. 17, pp. 2069–2085, 2018.
- [20] L. Smith, D. R. Serrano, M. Mauger, F. Bolás-Fernández, M. A. Dea-Ayuela, and A. Lalatsa, "Orally bioavailable and effective buparvaquone lipid-based nanomedicines for visceral leishmaniasis," *Molecular Pharmaceutics*, vol. 15, no. 7, pp. 2570–2583, 2018.
- [21] M. L. A. C. Bordon, M. D. Laurenti, S. P. Ribeiro, M. H. Toyama, D. de Toyama, and L. F. D. Passero, "Effect of phospholipase A2 inhibitors during infection caused by *Leishmania (Leishmania) amazonensis*," *Journal of Venomous Animals and Toxins including Tropical Diseases*, vol. 24, no. 1, p. 21, 2018.
- [22] S. S. Braga, "Multi-target drugs active against leishmaniasis: a paradigm of drug repurposing," *European Journal of Medicinal Chemistry*, vol. 183, p. 111660, 2019.
- [23] G. I. Lepesheva, L. Friggeri, and M. R. Waterman, "CYP51 as drug targets for fungi and protozoan parasites: past, present and future," *Parasitology*, vol. 145, no. 14, pp. 1820–1836, 2018.
- [24] L. J. Goad, R. L. Berens, J. J. Marr, D. H. Beach, and G. G. Holz, "The activity of ketoconazole and other azoles against *Trypanosoma cruzi*: biochemistry and chemotherapeutic action in vitro," *Molecular and Biochemical Parasitology*, vol. 32, no. 2–3, pp. 179–189, 1989.
- [25] D. T. Hart, W. J. Lauwers, G. Willemsens, H. Vanden Bossche, and F. R. Opperdoes, "Perturbation of sterol biosynthesis by itraconazole and ketoconazole in *Leishmania mexicana mexicana* infected macrophages," *Molecular and Biochemical Parasitology*, vol. 33, no. 2, pp. 123–134, 1989.
- [26] M. A. Vannier-Santos, J. A. Urbina, A. Martiny, A. Neves, and W. Souza, "Alterations induced by the antifungal compounds ketoconazole and terbinafine in leishmania," *The Journal of Eukaryotic Microbiology*, vol. 42, no. 4, pp. 337–346, 1995.
- [27] E. S. Yamamoto, J. A. Jesus, A. Bezerra-Souza, M. D. Laurenti, S. P. Ribeiro, and L. F. D. Passero, "Activity of fenticonazole, tioconazole and nystatin on New World leishmania species," *Current Topics in Medicinal Chemistry*, vol. 18, no. 27, pp. 2338–2346, 2018.
- [28] X. Serrano-Martín, Y. García-Marchan, A. Fernandez et al., "Amiodarone destabilizes intracellular Ca²⁺ homeostasis and biosynthesis of sterols in *Leishmania mexicana*," *Antimicrobial Agents and Chemotherapy*, vol. 53, no. 4, pp. 1403–1410, 2009.
- [29] N. S. Ryder, "Squalene epoxidase — enzymology and inhibition," in *Biochemistry of Cell Walls and Membranes in Fungi*, pp. 189–203, Springer Berlin Heidelberg, Berlin, Heidelberg, 1990.
- [30] H. A. Zakai, S. K. Zimmo, and M. A. H. Fouad, "Effect of itraconazole and terbinafine on *Leishmania promastigotes*," *Journal of the Egyptian Society of Parasitology*, vol. 33, no. 1, pp. 97–107, 2003.
- [31] E. Shekhova, O. Kniemeyer, and A. A. Brakhage, "Induction of mitochondrial reactive oxygen species production by itraconazole, terbinafine, and amphotericin B as a mode of action against *Aspergillus fumigatus*," *Antimicrobial Agents and Chemotherapy*, vol. 61, no. 11, 2017.
- [32] K. Bahamdan, T. Tallab, H. Johargi et al., "Terbinafine in the treatment of cutaneous leishmaniasis: a pilot study," *International Journal of Dermatology*, vol. 36, no. 1, pp. 59–60, 1997.
- [33] S. Farajzadeh, A. Heshmatkhan, B. Vares et al., "Topical terbinafine in the treatment of cutaneous leishmaniasis: triple blind randomized clinical trial," *Journal of Parasitic Diseases*, vol. 40, no. 4, pp. 1159–1164, 2016.
- [34] A. Bezerra-Souza, E. S. Yamamoto, M. D. Laurenti, S. P. Ribeiro, and L. F. D. Passero, "The antifungal compound butenafine eliminates promastigote and amastigote forms of *Leishmania (Leishmania) amazonensis* and *Leishmania (Viannia) braziliensis*," *Parasitology International*, vol. 65, no. 6, pp. 702–707, 2016.
- [35] E. S. Yamamoto, J. A. de Jesus, A. Bezerra-Souza et al., "Tolnafate inhibits ergosterol production and impacts cell viability of *Leishmania sp.*," *Bioorganic Chemistry*, vol. 102, p. 104056, 2020.
- [36] A. Lalatsa, P. V. Patel, Y. Sun et al., "Transcutaneous anaesthetic nano-enabled hydrogels for eyelid surgery," *International Journal of Pharmaceutics*, vol. 577, p. 119003, 2020.
- [37] A. Lalatsa, K. Emeriewen, V. Protopsalti, G. Skelton, and G. M. Saleh, "Developing transcutaneous nanoenabled anaesthetics for eyelid surgery," *The British Journal of Ophthalmology*, vol. 100, no. 6, pp. 871–876, 2016.
- [38] A. Lalatsa, N. L. Garrett, T. Ferrarelli, J. Moger, A. G. Schätzlein, and I. F. Uchegbu, "Delivery of peptides to the blood and brain after oral uptake of quaternary ammonium palmitoyl glycol chitosan nanoparticles," *Molecular Pharmaceutics*, vol. 9, no. 6, pp. 1764–1774, 2012.
- [39] L. F. D. Passero, M. L. A. D. C. Bordon, A. K. De Carvalho, L. M. Martins, C. E. P. Corbett, and M. D. Laurenti, "Exacerbation of *Leishmania (Viannia) shawi* infection in BALB/c mice after immunization with soluble antigen from amastigote forms," *APMIS*, vol. 118, no. 12, pp. 973–981, 2010.

- [40] S. T. de Macedo Silva, G. Visbal, J. L. P. Godinho, J. A. Urbina, W. de Souza, and J. C. F. Rodrigues, "In vitro antileishmanial activity of ravuconazole, a triazole antifungal drug, as a potential treatment for leishmaniasis," *The Journal of Antimicrobial Chemotherapy*, vol. 73, no. 9, pp. 2360–2373, 2018.
- [41] A. Bezerra-Souza, R. Fernandez-Garcia, G. F. Rodrigues et al., "Repurposing butenafine as an oral nanomedicine for visceral leishmaniasis," *Pharmaceutics*, vol. 11, no. 7, p. 353, 2019.
- [42] R. Fernández-García, A. Lalatsa, L. Statts, F. Bolás-Fernández, M. P. Ballesteros, and D. R. Serrano, "Transferosomes as nano-carriers for drugs across the skin: quality by design from lab to industrial scale," *International Journal of Pharmaceutics*, vol. 573, p. 118817, 2020.
- [43] S. Córdoba, M. G. Cano, M. Aguado et al., "Delayed allergic skin reactions due to intralesional meglumine antimoniate therapy for cutaneous leishmaniasis," *Allergy*, vol. 67, no. 12, pp. 1609–1611, 2012.
- [44] A. Brasileiro, G. Martín-Ezquerria, P. García-Martínez, R. M. Pujol, and A. M. Giménez-Arnau, "Allergic reactions to meglumine antimoniate while treating cutaneous leishmaniasis," *Journal of the European Academy of Dermatology and Venereology*, vol. 31, no. 1, pp. e59–e60, 2017.
- [45] H. A. Zakai and S. K. Zimmo, "Effects of itraconazole and terbinafine on *Leishmania major* lesions in BALB/c mice," *Annals of Tropical Medicine and Parasitology*, vol. 94, no. 8, pp. 787–791, 2000.
- [46] R. Rojas, L. Valderrama, M. Valderrama, M. X. Varona, M. Ouellette, and N. G. Saravia, "Resistance to antimony and treatment failure in human *Leishmania* (*Viannia*) infection," *The Journal of Infectious Diseases*, vol. 193, no. 10, pp. 1375–1383, 2006.
- [47] A. K. Haldar, P. Sen, and S. Roy, "Use of antimony in the treatment of leishmaniasis: current status and future directions," *Molecular Biology International*, vol. 2011, Article ID 571242, 23 pages, 2011.
- [48] C. T. Trinconi, J. Q. Reimão, V. I. Bonano et al., "Topical tamoxifen in the therapy of cutaneous leishmaniasis," *Parasitology*, vol. 145, no. 4, pp. 490–496, 2018.
- [49] M. D. Laurenti, L. F. Passero, T. Y. Tomokane et al., "Dynamic of the cellular immune response at the dermal site of *Leishmania* (*L.*) *amazonensis* and *Leishmania* (*V.*) *braziliensis* infection in *Sapajus apella* primate," *BioMed Research International*, vol. 2014, Article ID 134236, 8 pages, 2014.
- [50] L. F. D. Passero, A. K. Carvalho, M. L. A. C. Bordon et al., "Proteins of *Leishmania* (*Viannia*) *shawi* confer protection associated with Th1 immune response and memory generation," *Parasites and Vectors*, vol. 5, no. 1, 2012.
- [51] I. Okwor and J. Uzonna, "Persistent parasites and immunologic memory in cutaneous leishmaniasis: implications for vaccine designs and vaccination strategies," *Immunologic Research*, vol. 41, no. 2, pp. 123–136, 2008.
- [52] B. L. S. Campos, T. N. Silva, S. P. Ribeiro et al., "Analysis of iron superoxide dismutase-encoding DNA vaccine on the evolution of the *Leishmania amazonensis* experimental infection," *Parasite Immunology*, vol. 37, no. 8, pp. 407–416, 2015.
- [53] E. S. Yamamoto, B. L. S. Campos, M. D. Laurenti et al., "Treatment with triterpenic fraction purified from *Baccharis uncinella* leaves inhibits *Leishmania* (*Leishmania*) *amazonensis* spreading and improves Th1 immune response in infected mice," *Parasitology Research*, vol. 113, no. 1, pp. 333–339, 2014.

Research Article

Dual Role of Insulin-Like Growth Factor (IGF)-I in American Tegumentary Leishmaniasis

Carolina de O Mendes-Aguiar ^{1,2}, Camilla Lopes-Siqueira,¹ Fabrício Pettito-Assis ³,
Márcia Pereira-Oliveira ¹, Manoel Paes de Oliveira-Neto,⁴ Claude Pirmez ¹,
Alda Maria Da-Cruz ^{1,5} and Hiro Goto ³

¹Laboratório Interdisciplinar de Pesquisas Médicas, Instituto Oswaldo Cruz, FIOCRUZ, Rio de Janeiro, Brazil

²Instituto de Medicina Tropical do Rio Grande do Norte, Universidade Federal do Rio Grande do Norte, RN, Brazil

³Instituto de Medicina Tropical de São Paulo, Faculdade de Medicina, Universidade de São Paulo, São Paulo, Brazil

⁴Instituto Nacional de Infectologia Evandro Chagas, FIOCRUZ, Rio de Janeiro, Brazil

⁵Disciplina de Parasitologia, DMIP, Faculdade de Ciências Médicas, Universidade do Estado do Rio de Janeiro, Brazil

Correspondence should be addressed to Hiro Goto; hgoto@usp.br

Received 21 December 2020; Revised 12 February 2021; Accepted 10 March 2021; Published 30 March 2021

Academic Editor: Luiz Felipe Domingues Passero

Copyright © 2021 Carolina de O Mendes-Aguiar et al. This is an open access article distributed under the Creative Commons Attribution License, which permits unrestricted use, distribution, and reproduction in any medium, provided the original work is properly cited.

Background. Cytokines and growth factors involved in the tissue inflammatory process influence the outcome of *Leishmania* infection. Insulin-like growth factor (IGF-I) constitutively present in the skin may participate in the inflammatory process and parasite-host interaction. Previous work has shown that preincubation of *Leishmania (Leishmania) amazonensis* with recombinant IGF-I induces accelerated lesion development. However, in human cutaneous leishmaniasis (CL) pathogenesis, it is more relevant to the persistent inflammatory process than progressive parasite proliferation. In this context, we aimed to investigate whether IGF-I was present in the CL lesions and if this factor may influence the lesions' development acting on parasite growth and/or on the inflammatory/healing process. **Methodology.** Fifty-one CL patients' skin lesion samples from endemic area of *L. (Viannia) braziliensis* infection were submitted to histopathological analysis and searched for *Leishmania* and IGF-I expression by immunohistochemistry. **Results.** In human CL lesions, IGF-I was observed preferentially in the late lesion (more than 90 days), and the percentage of positive area for IGF-I was positively correlated with duration of illness ($r = 0.42$, $P < 0.05$). IGF-I was highly expressed in the inflammatory infiltrate of CL lesions from patients evolving with good response to therapy ($2.8\% \pm 2.1\%$; median = 2.1%; $n = 18$) than poor responders ($1.3\% \pm 1.1\%$; median: 1.05%; $n = 6$; $P < 0.05$). **Conclusions.** It is the first time that IGF-I was detected in lesions of infectious cutaneous disease, specifically in American tegumentary leishmaniasis. IGF-I was related to chronicity and good response to treatment. We may relate this finding to the efficient anti-inflammatory response and the known action of IGF-I in wound repair. The present data highlight the importance of searching nonspecific factors besides adaptive immune elements in the study of leishmaniasis' pathogenesis.

1. Introduction

Leishmaniasis are diseases caused by protozoan parasites of the genus *Leishmania*, endemic in around 88 countries. In Brazil, *L. (Viannia) braziliensis* is the main species for American tegumentary leishmaniasis (ATL), causing injuries ranging from benign cutaneous to disfiguring mucosal lesions [1]. After promastigote inoculation in the skin, these parasites interact primarily with innate host elements and growth fac-

tors present in this site. Once established the infection, the inflammatory infiltrate in the cutaneous leishmaniasis (CL) is characterized as chronic inflammation, with granuloma with or without necrosis, and the presence of macrophages, plasma cells, and lymphocytes [2]. The disease's progression is not directly correlated to progressive parasite growth in the lesion site, with few parasites being detected mainly in chronic cases [3]. Instead, cell-mediated immunity has essential participation in CL pathogenesis. Chronic CL lesions are

composed of an increased number of activated CD69⁺ T [4] and regulatory CD4⁺CD25⁺FOXP3⁺ IL-10-producing T cells [5, 6], granzyme A CD8⁺ cytotoxic T cells, or even proinflammatory CD4⁺ IFN- γ -producing T cells [6]. Further, in a recent transcriptomic study in skin samples of ATL patients, delayed or no cure was correlated to the higher expression of gene sets related to the cytolytic pathway [7]. These findings exemplify the complexity of CL immunopathogenesis.

In the skin, different innate elements and growth factors participate at the inoculation site of the parasite. Insulin-like growth factor (IGF)-I is one of them, and we have been studying its participation in *Leishmania*-vertebrate host interaction. It is a hormone that acts as an autocrine and/or paracrine element, being essential to maintain body homeostasis. It can be detected in the serum, but it has a widespread distribution in tissues [8]. Many cells, including macrophages, produce IGF-I [8–10]. Different IGF-I serum levels were associated with the pathogenesis of melanomas [11], HPV infection [12], and psoriasis [13]. In cutaneous tissues, IGF-I has a central role in wound healing [14]. In leishmaniasis, previous studies have demonstrated the effect of IGF-I in inducing *in vitro* proliferation of different species of *Leishmania* [15, 16]. *In vivo*, in mouse model of CL, an increase in lesion size and the number of viable parasites after infection with IGF-I preactivated promastigotes of *L. amazonensis* was observed [17]. IGF-I induces arginase activation, which in turn activates *Leishmania* promastigotes [18]. Moreover, infection with IGF-I-preactivated *Leishmania* leads to an increase in lesion size in mice, due to the expansion of the inflammatory infiltrate and parasite growth, suggesting that IGF-I may contribute to cell migration besides parasite proliferation [17]. However, in ATL patients with mucosal and disseminated forms, IGF-I serum levels were lower than in simple CL and healthy controls [19].

IGF-I can potentially interact with *Leishmania* parasites in the initial phase of infection. Nevertheless, it is still unknown whether IGF-I has any role in the later stages of infection and whether this growth factor may contribute to leishmaniasis' pathogenesis. Therefore, we aimed to investigate whether IGF-I was present in the CL lesions and if this factor may influence the development of the lesion acting on parasite growth and/or on the inflammatory/healing process.

2. Subjects and Methods

2.1. Growth Curve of *Leishmania* spp. in the Presence of IGF-I. *L. (V.) braziliensis* (MHOM/BR/1975/M2903) promastigotes were maintained at 25°C, in Schneider's insect medium (Gibco, Thermo Fisher Scientific Inc, MA, USA) supplemented with 10% heat-inactivated fetal calf serum (Gibco, USA) and 200 IU of penicillin per mL, and 200 μ g of streptomycin (Sigma Chemical Company, St. Louis, Mo, USA) per mL, and grown until stationary phase before using in *Leishmania* growth curve analysis. The stationary phase promastigotes were distributed in triplicate into 24-well plates (5×10^5 parasites/well) in a final volume of 1.0 mL of Schneider's insect medium (Gibco, USA) supplemented with 2% FCS and antibiotics, with or without 50 ng/mL recombi-

nant human IGF-I (rIGF-I, R&D Systems, USA) and maintained during the experimental period.

2.2. Patients. The patient groups were composed of 37 men and 14 women, all of them living in endemic area of *L. braziliensis* transmission. The median age was 35 [18–57] years. The patients were classified according to the duration of illness at the moment of diagnosis as early group when the appearance of the lesions was less than 30 days before; intermediate, in the 30–60-day interval; late, more than 90 days. The patients were also grouped by having a good response (complete epithelization three months after the end of therapy) or poor response (no complete healing of lesions three months after the end of treatment or development of secondary lesions).

The following criteria were used for leishmaniasis diagnosis: (i) type of lesion and epidemiological data compatible with ATL; (ii) positive delayed-type hypersensitivity reaction to leishmanial antigens; (iii) detection of serum anti-*Leishmania* antibodies; and (iv) detection of *Leishmania* parasites in lesion by microscopic examination of histological sections or by culture in NNN-modified medium. Patients were treated with pentavalent antimony (*N*-methyl-glucamine, Glucantime). All procedures were approved by the Ethical Committee of the Fundação Oswaldo Cruz, Ministério da Saúde, Rio de Janeiro, Brazil, and informed consent was obtained from each subject.

The skin fragment was obtained for diagnosis before treatment, and it was taken from the border of the cutaneous lesion. The fragment was divided into three parts: one was fixed for histopathology analysis, the second one was cryopreserved for immunohistochemistry analysis, and the last one was used for *Leishmania* DNA detection by PCR. Fragments of skin lesions were not taken sequentially after treatment for ethical reasons.

2.3. Immunohistochemistry. Skin fragments were frozen in OCT resin (Tissue Tek; Sakura Finetek, Torrance, CA, U.S.A.), were cut into 3–4 μ m thick sections and mounted on microscope slides (silanized slides; DakoCytomation, Carpinteria, CA, USA). To detect IGF-I expression, the slides were fixed in acetone:methanol:formalin (19:19:2) and rehydrated in Tris-Saline Buffer (TBS) pH 7.6. The procedure was performed according to the Envision Double Staining kit (Dako, USA) manual. Briefly, endogenous enzymes were blocked with Endogenous Enzyme Block reagent, and then, the slides were incubated with the first primary polyclonal rabbit anti-human IGF-I antibody (1:200; GroPep Limited–Adelaide, Australia) followed by incubation with the mouse and rabbit antibody conjugated to Polymer/HRP reagent. This first antibody was developed by DAB+ Chromogen. For the second part of immunostaining, beginning with the blocking step, the Doublestain Block reagent was used. The anti-*Leishmania* mouse serum was used as a second antibody and was added diluted 1:8000. This anti-*Leishmania* serum was obtained at two months of infection from BALB/c mice infected in the footpad with 10^6 stationary phase *L. amazonensis* promastigotes [20]. Then, mouse and rabbit antibodies conjugated to Polymer/AP reagent were

used, and permanent Red Chromogen developed the second reaction. Between the steps, the slides were washed with TBS pH 7.6, and the antibodies were diluted in BSA 2%-Tris-HCL 0.01M pH 7.6 and incubated for 30 minutes, at room temperature each. At the end of the procedure, the slides were counterstained with Meyer's hematoxylin (Merck, Germany). For control purposes, the specific antibodies were omitted. The slides were examined under a light microscope (Nikon, Nikon, Eclipse E600, Japan).

2.3.1. Immunohistochemistry Analysis. Two independent observers analyzed the slides. All fragment area was analyzed, and the IGF-I and anti-*Leishmania* staining were classified in only IGF-I detection, IGF-I and *Leishmania* antigen coexpression, or only *Leishmania* antigen detection. Twenty-five cases in which IGF-I was present were photographed. Five representative areas were photographed using Cool Snap-Pro Color (Media Cybernetics Inc, USA), and the photos were analyzed by Image-Pro Plus® Software (Media Cybernetics Inc, USA). The percentage of the positive area was measured for IGF-I and *Leishmania* sp. antigen staining.

2.4. Statistical Analysis. Mann-Whitney test, Kruskal-Wallis test, and Spearman correlation were utilized (GraphPad Software; San Diego, CA, USA) using the software GraphPad Prism version 6. Results were considered statistically different when the P value was ≤ 0.05 .

3. Results

3.1. *Leishmania (Viannia) braziliensis* in vitro Growth upon IGF-I Stimulus. In a previous study, the effect of IGF-I on parasite growth in vitro *L. braziliensis*-infected human monocytic cell line THP1 was inconclusive [19]; thus, we first investigated whether IGF-I can influence the *L. braziliensis* growth in vitro. The addition of rIGF-I in promastigote cultures in physiological concentration increased the *L. braziliensis* proliferation compared with controls without IGF-I (Figure 1).

3.2. IGF-I Was Present in Cutaneous Leishmaniases Lesions. Next, we investigated the presence of IGF-I in fifty-one CL lesions by immunohistochemistry. IGF-I was present in 70.5% of cases ($n = 36$). Histologically, IGF-I was spread in the dermis and epidermal basal lamina (Figures 2(b) and 2(c)). In normal skin (control; $n = 3$), IGF-I was seen only in the basal lamina (Figure 2(a)).

Concomitantly with IGF-I immunostaining, we carried out the *Leishmania* antigen detection. *Leishmania* antigens were detected in 84.3% of cases ($n = 43$). Isolated *Leishmania* antigen detection was found in 29.5% of cases ($n = 15$). *Leishmania* antigens were observed in the extracellular matrix and cell foci in the dermis (Figure 2(d)). *Leishmania* antigen detection decreased with chronicity: 92.8% of patients (13/14) in the early group; in 89.4% of patients (17/19) in the intermediate group; and in 72.2% of patients (13/18) in the late lesion group (Table 1). IGF-I and *Leishmania* antigens were observed in the dermis of the same lesion area in 28 cases. However, IGF-I and *Leishmania* antigens' colocalization was not observed.

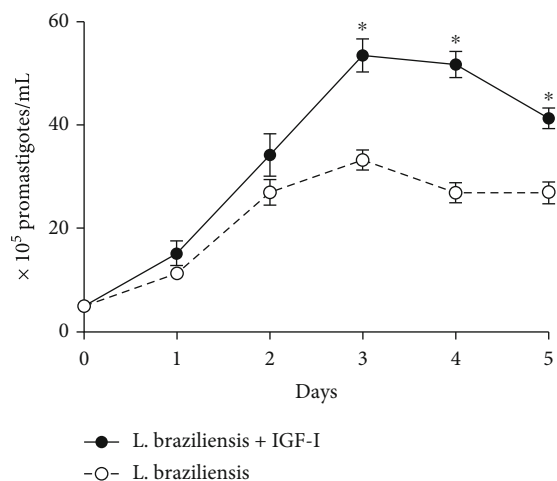


FIGURE 1: Effect of insulin-like growth factor (IGF)-I on *Leishmania (Viannia) braziliensis* promastigote proliferation. In vitro *L. braziliensis* growth curve in the presence (black circle) or absence (white circle) of 50 ng/mL rIGF-I. Live promastigotes were counted every day for five days. The points represent the mean of the three experiments, and the bars represent standard deviation. * $P < 0.05$.

3.3. The Duration of Illness and Treatment Response in relation to the Area of Expression of IGF-I. To evaluate the relationship of the presence of IGF-I with clinical parameters, 36 IGF-I positive cases were grouped according to the duration of illness or treatment response.

IGF-I seems to have a relationship to the chronicity of the lesions since the number of cases expressing IGF-I increases with the disease's progression. The IGF-I was detected in 64.2% of patients (9/14) in the early lesion group, in 68.4% of patients (13/19) in the intermediate group, and in 77.7% of patients (14/18) in the late lesion group (Table 1). Moreover, percentage of positive area of IGF-I was also correlated with duration of illness (early lesion group: mean = $1.52\% \pm 1.12$, median = 1.47%, $n = 7$; intermediate group: mean = $2.32\% \pm 2.47$, median = 1.5, $n = 10$; late lesion group: mean = $3.18\% \pm 1.9$, median = 3.12, $n = 8$; $r = 0.42$, $P = 0.023$) (Table 2).

To assess the relationship of IGF-I expression with treatment response ($n = 24$), we grouped patients in those having a good response (complete epithelization three months after the end of therapy) or having a poor response (no complete healing of lesions three months after the end of treatment or development of secondary lesions). IGF-I was detected in 75% of patients with good therapeutic response. Those with good response showed higher percentage of positive areas for IGF-I (good responder: mean = $2.8\% \pm 2.1$, median = 2.1%, $n = 18$) when compared with poor response (poor responder: mean: $1.3\% \pm 1.1$, median = 1.05%, $n = 6$; $P = 0.03$) (Table 2).

4. Discussion

In this work, we initially showed the enhanced proliferation of *L. braziliensis* promastigotes in the presence of IGF-I. Further, IGF-I was detected in human CL lesions, and for the first time, it was shown in lesions of an infectious cutaneous

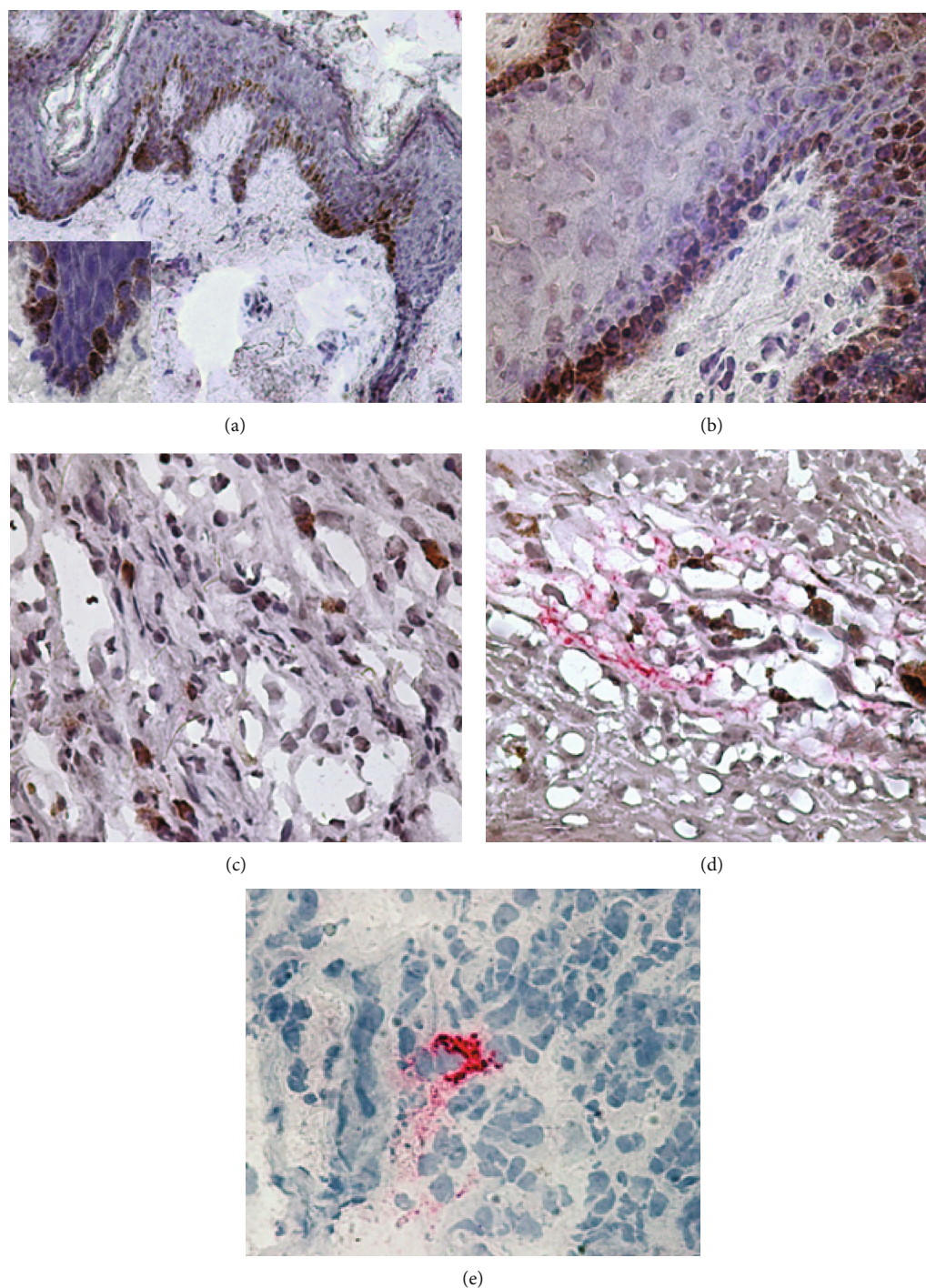


FIGURE 2: *In situ* detection of insulin-like growth factor (IGF)-I and *Leishmania* antigens in the inflammatory infiltrate of cutaneous leishmaniases lesions caused by *L. (Viannia) braziliensis*. IGF-I (brown) and *Leishmania* antigens (red) are expressed in normal skin (a) and cutaneous leishmaniases lesions (b–e). IGF-I is present in the basal layer in normal skin (a) and in CL lesions (b). In CL lesions, IGF-I is present in the dermis (c). IGF-I was observed close to *Leishmania* antigens in the dermis (d). *Leishmania* antigens were observed in the dermis (e). Representative photos of immunohistochemical analysis. Original magnification $\times 400$.

disease. A limitation of this study was the unfeasibility to obtain sequential material from individual patients due to ethical issues, and further, we had patients who had a different time of development of the overt disease at the moment of diagnosis. However, we were able to analyze the histopathological alterations relating them to the duration of disease

and also to response to treatment. Then, the percentage of patients presenting IGF-I detectable in the lesion was higher in chronic lesions. It was also higher among good responders for treatment.

IGF-I interacts with several *Leishmania* promastigote species inducing proliferation [15–17]. This effect did not

TABLE 1: Insulin-like growth factor (IGF)-I or *Leishmania* antigen detection in lesions of cutaneous leishmaniasis patients according to the duration of illness.

	% of positive cases	Duration of illness	% detection (n/n_{total})
Leishmanial antigens	84.3% ($n = 43$)	Early	92.8% (13/14)
		Intermediate	89.4% (17/19)
		Late	72.2% (13/18)
IGF-I	70.5% ($n = 36$)	Early	64.2% (9/14)
		Intermediate	68.4% (13/19)
		Late	77.7% (14/18)

Duration of illness: early = lesions with less than 30 days; intermediate = lesions with 30-60 days; late = lesions with more than 90 days.

TABLE 2: Area of expression of insulin-like growth factor (IGF)-I in the lesions of cutaneous leishmaniasis patients according to the duration of illness and response to treatment.

	Groups	IGF-I-area %		P
		Median	Mean \pm SD	
Duration of illness	Early lesion ($n = 7$)	1.47	1.52 \pm 1.12	** $r = 0.42$ 0.023
	Intermediate ($n = 10$)	1.50	2.32 \pm 2.47	
	Late lesion ($n = 8$)	3.12	3.18 \pm 1.90	
Treatment response	Good responder ($n = 18$)	2.10	2.80 \pm 2.10	#0.03
	Poor response ($n = 6$)	1.05	1.30 \pm 1.10	

**Spearman correlation, #Mann-Whitney test.

occur with IGF-II polypeptide, which shares 60% of similarity with IGF-I [15]. Here, we showed *L. braziliensis* promastigote growth in culture in the presence of a physiological concentration of IGF-I as previously observed for other *Leishmania* species. Thus, we would suggest that IGF-I might act at the beginning of infection interacting with promastigotes at the moment of *Leishmania* inoculation in the host's skin. With other species, amastigotes were also shown to proliferate in the presence of physiological concentrations of IGF-I [16] but inconclusive with *L. braziliensis* [19]. IGF-I binds to a receptor expressed on the *Leishmania* parasite surface, causing phosphorylation of certain proteins and increase the replicative rate of both parasite forms (promastigote and amastigote) in culture [16].

In this work, we analyzed the presence of IGF-I in CL lesions. It is the first data on the presence and influence of *in situ* IGF-I in human cutaneous infectious disease. In CL lesions, IGF-I was found spread throughout the dermis, basal lamina, and epidermis differing from normal skin where it was seen only in basal lamina. IGF-I's capacity to continuously stimulate keratinocyte growth [9] may contribute to altering the tissue architecture and, at first glance, maybe connected to acanthosis often present in CL lesions [21]. In psoriasis, a cutaneous inflammatory disease, IGF-I contributes to lesion severity stimulating continuous keratinocyte growth [22]. Thus, we hypothesize that the presence of IGF-I in CL lesions may influence the disease outcome.

IGF-I presence in CL lesions with different distribution and a constitutive presence of IGF-I in normal skin leads us to ask whether this factor could act in different phases of *Leishmania* infection. To address this question, we have

performed a double immunostain to IGF-I and *Leishmania* antigens by immunohistochemistry. *Leishmania* antigens were detected mainly in recent lesions confirming previous observations [23]. In the mouse model, the infection with IGF-I preactivated *L. amazonensis* promastigotes induced larger lesions than non-pre-activated parasites [17]. The aggravation of mice CL lesions was due to an increase in the number of parasites along with intense cell migration. However, in the present study, we could not observe colocalization of IGF-I and *Leishmania* antigens in CL lesions suggesting another role for IGF-I in human ATL other than on parasite proliferation. In *in vitro* study, it was shown intrinsic IGF-I surrounding *L. major* within infected macrophages [24], but it could be due to the differences among *Leishmania* species and in this particular experimental conditions, very far from the lesion pathogenic process in the skin.

Here, we also correlated IGF-I expression with lesion chronicity and treatment response. Our results showed that area of IGF-I expression was positively correlated with duration of illness (chronicity). Many immune factors can contribute to chronic CL lesions in humans [6], where the lesion development is related instead to hypersensitivity than to susceptibility to parasite growth [25, 26]. In this context, increasing concentration of IGF-I in chronic lesions may suggest IGF-I's known participation in anti-inflammatory response [27, 28], counteracting persistent, and intense inflammation.

Analyzing the IGF-I area concerning treatment response, we observed higher IGF-I expression areas in patients with good response to the treatment. We may relate this finding to the efficient anti-inflammatory response and the known

action of IGF-I in wound repair in the reepithelialization [29]. Retarded wound healing in mice diabetic lesions was associated with a delay in IGF-I expression [30]. In humans, a lack of IGF-I expression in diabetes mellitus ulcer contributes to a retarded wound repair [31]. Besides, IGF-I treatment helped to restore the normal expression of both matrix metalloproteinase (MMP)-9 and tissue inhibitors of metalloproteinase (TIMP)-1 in diabetic rats with skin ulcers [32], indicating an important role of IGF-I in healing. Furthermore, in CL patients, MMP-2 was associated with a satisfactory response to antimicrobial therapy, in conjunction with moderate amounts of IFN- γ , IL-10, and TGF- β [33]. It is conceivable to argue that IGF-I present in CL lesions can act in this net of soluble factors comprising cytokines and hormones involved in the homeostatic process, thus influencing the healing process.

In the pathogenesis of lesion in cutaneous leishmaniasis, inflammatory cytokines [34] and cytotoxic mechanisms [7] are involved that are modulated during development to cure. In this context, the interplay between interferon-gamma (IFN- γ) and IGF-I may determine the outcome of the disease. IFN- γ decreases IGF-I expression through inhibition of transcription of IGF-I mRNA [35], and IFN- γ is a cytokine that is important for parasite control but implicated in the lesion pathogenesis. In patients with CL in Brazil, expression of IFN- γ tends to decrease during the time, mainly in subjects with good response to treatment [36]. Thus, we may speculate that it may result in higher expression of IGF-I in patients with chronic evolution and a good response to treatment.

Our results suggest that IGF-I can play a dual role in CL lesions. IGF-I was detected more in chronic ulcers where may act as an anti-inflammatory factor and in lesions of good responders to treatment where the contribution of this hormone on wound healing would prevail. IGF-I's dual role in CL lesions could be explained by the complex pathogenesis of CL lesions, whereas in the same lesion, we can find areas of an intense inflammatory response and wound repair [34]. It is also observed regions with synthesis besides degradation of extracellular matrix granuloma, compatible with transient or reversible histopathological features occurring in CL lesions [37]. The interplay between IGF-I and other immune-inflammatory elements present in CL lesions may influence the disease outcome.

In the study of leishmaniasis' immunity and pathogenesis, most approaches focus on the adaptive immune response that is undoubtedly relevant. However, the present data highlight the importance of searching nonspecific factors such as growth factors besides adaptive immune elements in the study of leishmaniasis' pathogenesis.

Data Availability

The data used to support the findings of this study are included within the article.

Conflicts of Interest

There is no conflict of interest.

Acknowledgments

This work was supported by IOC/FIOCRUZ internal funds, FAPERJ (E-26/102.457/2010), FAPESP (2005/52271-1 and 2018/14398-0), and Laboratório de Investigação Médica (LIM-38), HC-FMUSP. COM-A was a postdoctoral fellow sponsored by FAPERJ/CAPEs, Brazil. AMD-C is a CNPq and FAPERJ (CNE) researcher fellow. HG is CNPq research fellow.






References

- [1] M. P. Oliveira-Neto, M. S. Mattos, M. A. Perez et al., "American tegumentary leishmaniasis (ATL) in Rio de Janeiro State, Brazil: main clinical and epidemiologic characteristics," *International Journal of Dermatology*, vol. 39, no. 7, pp. 506–514, 2000.
- [2] A. V. Magalhães, M. A. Moraes, A. N. Raick et al., "Histopathology of cutaneous leishmaniasis by *Leishmania braziliensis* braziliensis. 1. Histopathological patterns and study of the course of the lesions," *Revista do Instituto de Medicina Tropical de São Paulo*, vol. 28, no. 4, pp. 253–262, 1986.
- [3] M. N. Sotto, E. H. Yamashiro-Kanashiro, V. L. da Matta, and T. de Brito, "Cutaneous leishmaniasis of the New World: diagnostic immunopathology and antigen pathways in skin and mucosa," *Acta Tropica*, vol. 46, no. 2, pp. 121–130, 1989.
- [4] N. L. Diaz, O. Zerpa, L. V. Ponce, J. Convit, A. J. Rondon, and F. J. Tapia, "Intermediate or chronic cutaneous leishmaniasis: leukocyte immunophenotypes and cytokine characterisation of the lesion," *Experimental Dermatology*, vol. 11, no. 1, pp. 34–41, 2002.
- [5] E. Bourreau, C. Ronet, E. Darsissac et al., "In leishmaniasis due to *Leishmania guyanensis* infection, distinct intralesional interleukin-10 and Foxp3 mRNA expression are associated with unresponsiveness to treatment," *The Journal of Infectious Diseases*, vol. 199, no. 4, pp. 576–579, 2009.
- [6] D. R. Faria, P. E. Souza, F. V. Duraes et al., "Recruitment of CD8⁺ T cells expressing granzyme A is associated with lesion progression in human cutaneous leishmaniasis," *Parasite Immunology*, vol. 31, no. 8, pp. 432–439, 2009.
- [7] C. F. Amorim, F. O. Novais, B. T. Nguyen et al., "Variable gene expression and parasite load predict treatment outcome in cutaneous leishmaniasis," *Science Translational Medicine*, vol. 11, no. 519, 2019.
- [8] R. E. Humbel, "Insulin-like growth factors I and II," *European Journal of Biochemistry*, vol. 190, no. 3, pp. 445–462, 1990.
- [9] S. R. Edmondson, S. P. Thumiger, G. A. Werther, and C. J. Wraight, "Epidermal homeostasis: the role of the growth hormone and insulin-like growth factor systems," *Endocrine Reviews*, vol. 24, no. 6, pp. 737–764, 2003.
- [10] J. I. Jones and D. R. Clemmons, "Insulin-like growth factors and their binding proteins: biological actions," *Endocrine Reviews*, vol. 16, no. 1, pp. 3–34, 1995.
- [11] S. L. Park, V. W. Setiawan, P. A. Kanetsky et al., "Serum insulin-like growth factor-I and insulin-like growth factor binding protein-3 levels with risk of malignant melanoma," *Cancer Causes & Control*, vol. 22, no. 9, pp. 1267–1275, 2011.
- [12] T. G. Harris, R. D. Burk, H. Yu et al., "Insulin-like growth factor axis and oncogenic human papillomavirus natural history," *Cancer Epidemiology Biomarkers & Prevention*, vol. 17, no. 1, pp. 245–248, 2008.

- [13] M. El-Komy, I. Amin, A. Zidan, D. Kadry, O. A. Zeid, and O. Shaker, "Insulin-like growth factor-1 in psoriatic plaques treated with PUVA and methotrexate," *Journal of the European Academy of Dermatology and Venereology*, vol. 25, no. 11, pp. 1288–1294, 2011.
- [14] A. Toulon, L. Breton, K. R. Taylor et al., "A role for human skin-resident T cells in wound healing," *Journal of Experimental Medicine*, vol. 206, no. 4, pp. 743–750, 2009.
- [15] C. M. Gomes, H. Goto, C. E. Corbett, and M. Gidlund, "Insulin-like growth factor-1 is a growth promoting factor for *Leishmania* promastigotes," *Acta Tropica*, vol. 64, no. 3-4, pp. 225–228, 1997.
- [16] H. Goto, C. M. Gomes, C. E. Corbett, H. P. Monteiro, and M. Gidlund, "Insulin-like growth factor I is a growth-promoting factor for *Leishmania* promastigotes and amastigotes," *Proceedings of the National Academy of Sciences of the United States of America*, vol. 95, no. 22, pp. 13211–13216, 1998.
- [17] C. M. Gomes and H. Goto, "Insulin-like growth factor (IGF)-I affects parasite growth and host cell migration in experimental cutaneous leishmaniasis," *International Journal of Experimental Pathology*, vol. 81, no. 4, pp. 249–255, 2000.
- [18] C. M. Vendrame, M. D. Carvalho, F. J. Rios, E. R. Manuli, F. Petitto-Assis, and H. Goto, "Effect of insulin-like growth factor-I on *Leishmania amazonensis* promastigote arginase activation and reciprocal inhibition of NOS2 pathway in macrophage *in vitro*," *Scandinavian Journal of Immunology*, vol. 66, no. 2-3, pp. 287–296, 2007.
- [19] L. D. de Souza, C. M. Vendrame, A. R. de Jesus et al., "Insulin-like growth factor-I serum levels and their biological effects on *Leishmania* isolates from different clinical forms of American tegumentary leishmaniasis," *Parasites & Vectors*, vol. 9, no. 1, p. 335, 2016.
- [20] F. A. Costa, H. Goto, L. C. Saldanha et al., "Histopathologic patterns of nephropathy in naturally acquired canine visceral leishmaniasis," *Veterinary Pathology*, vol. 40, no. 6, pp. 677–684, 2003.
- [21] K. González, R. Diaz, A. F. Ferreira et al., "Histopathological characteristics of cutaneous lesions caused by *Leishmania Viannia panamensis* in Panama," *Revista do Instituto de Medicina Tropical de São Paulo*, vol. 60, article e8, 2018.
- [22] H. Miura, S. Sano, M. Higashiyama, K. Yoshikawa, and S. Itami, "Involvement of insulin-like growth factor-I in psoriasis as a paracrine growth factor: dermal fibroblasts play a regulatory role in developing psoriatic lesions," *Archives of Dermatological Research*, vol. 292, no. 12, pp. 590–597, 2000.
- [23] G. Salinas, L. Valderrama, G. Palma, G. Montes, and N. G. Saravia, "Detection of amastigotes in cutaneous and mucocutaneous leishmaniasis using the immunoperoxidase method, using polyclonal antibody: sensibility and specificity compared with conventional methods of diagnosis," *Memórias do Instituto Oswaldo Cruz*, vol. 84, no. 1, pp. 53–60, 1989.
- [24] L. C. Reis, E. M. Ramos-Sanchez, and H. Goto, "The interactions and essential effects of intrinsic insulin-like growth factor-i on *Leishmania (Leishmania) major* growth within macrophages," *Parasite Immunology*, vol. 35, no. 7-8, pp. 239–244, 2013.
- [25] L. P. Carvalho, S. Passos, O. Bacellar et al., "Differential immune regulation of activated T cells between cutaneous and mucosal leishmaniasis as a model for pathogenesis," *Parasite Immunology*, vol. 29, no. 5, pp. 251–258, 2007.
- [26] O. Bacellar, H. Lessa, A. Schriefer et al., "Up-regulation of Th1-type responses in mucosal leishmaniasis patients," *Infection and Immunity*, vol. 70, no. 12, pp. 6734–6740, 2002.
- [27] S. Sukhanov, Y. Higashi, S. Y. Shai et al., "IGF-1 reduces inflammatory responses, suppresses oxidative stress, and decreases atherosclerosis progression in ApoE-deficient mice," *Arteriosclerosis, Thrombosis, and Vascular Biology*, vol. 27, no. 12, pp. 2684–2690, 2007.
- [28] W. J. Lee, "IGF-I exerts an anti-inflammatory effect on skeletal muscle cells through down-regulation of TLR4 signaling," *Immune Network*, vol. 11, no. 4, pp. 223–226, 2011.
- [29] G. Kratz, M. Lake, and M. Gidlund, "Insulin like growth factor-1 and -2 and their role in the re-epithelialisation of wounds; interactions with insulin like growth factor binding protein type 1," *Scandinavian Journal of Plastic and Reconstructive Surgery and Hand Surgery*, vol. 28, no. 2, pp. 107–112, 1994.
- [30] D. L. Brown, C. D. Kane, S. D. Chernausek, and D. G. Greenhalgh, "Differential expression and localization of insulin-like growth factors I and II in cutaneous wounds of diabetic and nondiabetic mice," *The American Journal of Pathology*, vol. 151, no. 3, pp. 715–724, 1997.
- [31] R. Blakytyn, E. B. Jude, J. Martin Gibson, A. J. Boulton, and M. W. Ferguson, "Lack of insulin-like growth factor 1 (IGF1) in the basal keratinocyte layer of diabetic skin and diabetic foot ulcers," *The Journal of Pathology*, vol. 190, no. 5, pp. 589–594, 2000.
- [32] F. Gong, F. Zhao, S. L. Cheng et al., "Effect of insulin-like growth factor-1 on promoting healing of skin ulcers in diabetic rats," *Journal of Biological Regulators and Homeostatic Agents*, vol. 33, no. 3, pp. 687–694, 2019.
- [33] A. C. Maretti-Mira, M. P. de Oliveira-Neto, A. M. Da-Cruz, M. P. de Oliveira, N. Craft, and C. Pirmez, "Therapeutic failure in American cutaneous leishmaniasis is associated with gelatinase activity and cytokine expression," *Clinical and Experimental Immunology*, vol. 163, no. 2, pp. 207–214, 2011.
- [34] A. L. Bittencourt and A. Barral, "Evaluation of the histopathological classifications of American cutaneous and mucocutaneous leishmaniasis," *Memórias do Instituto Oswaldo Cruz*, vol. 86, no. 1, pp. 51–56, 1991.
- [35] S. Arkins, N. Rebeiz, D. L. Brunke-Reese, A. Biragyn, and K. W. Kelley, "Interferon-gamma inhibits macrophage insulin-like growth factor-I synthesis at the transcriptional level," *Molecular Endocrinology*, vol. 9, no. 3, pp. 350–360, 1995.
- [36] F. Conceição-Silva, J. Leite-Silva, and F. N. Morgado, "The binomial parasite-host immunity in the healing process and in reactivation of human tegumentary leishmaniasis," *Frontiers in Microbiology*, vol. 9, p. 1308, 2018.
- [37] P. Esterre, J. P. Dedet, S. Guerret, M. Chevallerier, C. Frenay, and J. A. Grimaud, "Matrix remodelling and fibroblast phenotype in early lesions of human cutaneous leishmaniasis," *Pathology, Research and Practice*, vol. 187, no. 8, pp. 924–930, 1991.

Research Article

Evaluation of the PE Δ III-LC3-KDEL3 Chimeric Protein of *Entamoeba histolytica*-Lectin as a Vaccine Candidate against Amebic Liver Abscess

Sandra L. Martínez-Hernández ¹, Viridiana M. Becerra-González,¹
Martín H. Muñoz-Ortega ², Víctor M. Loera-Muro,³ Manuel E. Ávila-Blanco ¹,
Marina N. Medina-Rosales ¹ and Javier Ventura-Juárez ¹

¹Departamento de Morfología, Centro de Ciencias Básicas, Universidad Autónoma de Aguascalientes, C. P. 20131., Aguascalientes, Ags., Mexico

²Departamento de Química, Centro de Ciencias Básicas, Universidad Autónoma de Aguascalientes, C. P. 20131., Aguascalientes, Ags., Mexico

³Departamento de Fisiología y Farmacología, Centro de Ciencias Básicas, Universidad Autónoma de Aguascalientes, C. P. 20131., Aguascalientes, Ags., Mexico

Correspondence should be addressed to Javier Ventura-Juárez; jventur@correo.uaa.mx

Received 5 October 2020; Revised 24 February 2021; Accepted 6 March 2021; Published 22 March 2021

Academic Editor: Gabriela Santos-Gomes

Copyright © 2021 Sandra L. Martínez-Hernández et al. This is an open access article distributed under the Creative Commons Attribution License, which permits unrestricted use, distribution, and reproduction in any medium, provided the original work is properly cited.

Entamoeba histolytica is an intestinal parasite that causes dysentery and amebic liver abscess. *E. histolytica* has the capability to invade host tissue by union of virulence factor Gal/GalNAc lectin; this molecule induces an adherence-inhibitory antibody response as well as to protect against amebic liver abscess (ALA). The present work showed the effect of the immunization with PE Δ III-LC3-KDEL3 recombinant protein. *In vitro*, this candidate vaccine inhibited adherence of *E. histolytica* trophozoites to HepG2 cell monolayer, avoiding the cytolysis, and in a hamster model, we observed a vaccine-induced protection against the damage to tissue liver and the inhibition of uncontrolled inflammation. PE Δ III-LC3-KDEL3 reduced the expression of TNF- α , IL-1 β , and NF- κ B in all immunized groups at 4- and 7-day postinfection. The levels of IL-10, FOXP3, and IFN- γ were elevated at 7 days. The immunohistochemistry assay confirmed this result, revealing an elevated quantity of +IFN- γ cells in the liver tissue. ALA formation in hamsters immunized was minimal, and few trophozoites were identified. Hence, immunization with PE Δ III-LC3-KDEL3 herein prevented invasive amebiasis, avoided an acute proinflammatory response, and activated a protective response within a short time. Finally, this recombinant protein induced an increase of serum IgG.

1. Introduction

Entamoeba histolytica is an enteric protozoan parasite and the etiologic agent of amebiasis [1]. This disease is a worldwide health problem that affects an estimated 50 million people and causes over 100,000 deaths annually (primarily in developing countries) [2]. Children exposed to repeated infections can suffer malnourishment and the stunting of growth [3]. Whereas about 90% of amebic infections are asymptomatic, the other 10% display a spectrum of diseases: acute diarrhea, dysentery, amebic colitis, and amebic liver

abscess (ALA); the latter is the most common extraintestinal manifestation of amebiasis [4], triggered by the capacity of *E. histolytica* to produce host cell death and a destructive inflammatory response [5]. Invasive amebiasis is treated with nitroimidazoles, which have toxic side effects and require complementary drugs to cure the infection in 40–60% of patients [6]. Despite the medical importance of this parasite, an effective vaccine to prevent amebiasis has not yet to become available. In the search for alternative treatments, the amebic galactose-binding lectin is today among the most commonly used antigens for carrying out exploratory assays.

This complex protein is located on the surface of the parasite and consists of three subunits. The main component, the heavy subunit of 170 kDa, is one of the most immunogenic *E. histolytica* molecules [7], bearing a carbohydrate recognition domain rich in cysteines (LC3) [8].

In one of our previous studies, a chimeric vaccine (PE Δ III-LC3-KDEL3) was elaborated that contained the *Entamoeba histolytica* LC3 fragment fused to domains I and II of exotoxin A of *Pseudomonas aeruginosa* (*P. aeruginosa*) and the carboxy-terminal signal KDEL3 [9]; this chimeric molecule was evaluated in capability to raise antibodies in sera from animals immunized; it was detected a raised serum IgG at 2.03- to 2.1-fold greater concentration in immunized versus nonimmunized animals [9]. The aim of the present study was to evaluate the effect of PE Δ III-LC3-KDEL3 as a recombinant vaccine through analysis of its immunogenic activity (antibody production and modulation of inflammation), inhibition of cytotoxicity, and protection against the development of ALA.

2. Materials and Methods

2.1. Animals. Male golden hamsters (*Mesocricetus auratus*) weighing 80-100 g were used in this study. The animals were dewormed by ivermectin 5 mg in 500 ml of distilled water during the first week, after that, were maintained on standard diet with drinking water *ad libitum*. All animals received human care according to the guidelines of the Committee on Bioethics in the animal facilities of the Autonomous University of Aguascalientes, Aguascalientes, Mexico, which is based on the guidelines for animal research published by the National Institute of Health (National Research Council (US) Committee for the Update of the Guide for the Care and Use of Laboratory Animals, 2011) and the Mexican Official Norm: NOM-062-ZOO-1999 [10].

2.2. *E. histolytica* Culture. *E. histolytica* HM-1:IMSS trophozoites were grown axenically in TYI-S-33 [11]. Trophozoites were harvested at 72 h for use in all experiments.

2.3. Vaccine Antigen PE Δ III-LC3-KDEL3. Recombinant vaccine was designed, purified, and analyzed by Martínez-Hernández et al. [9] and detected with a rabbit polyclonal anti-6X His tag antibody (Ab1187, Abcam, Cambridge, UK) and a rabbit polyclonal antibody monospecific to *E. histolytica* [12].

2.4. Immunization. Hamsters were divided into five groups ($n = 5$ each), intact and sham as a control and three experimental. The former was healthy intact (no treatment nor infection) and sham, administered the vehicle (sterile PBS 1x, 100 μ l) intramuscularly with a 0.40 mm \times 1/2 inch needle. The three experimental groups were immunized intramuscularly with PE Δ III-LC3-KDEL3 at doses of 50, 75, and 100 μ g/animal. The PE Δ III-LC3-KDEL3 and the vehicle were applied on days 1, 7, and 14.

2.5. Experimental Hepatic Amebiasis. One week after the last immunization, amoebic liver abscesses were induced by direct hepatic inoculation as previously described [13]. On

day 4 or 7 postinfection, the animals were anaesthetized with sodium pentobarbital and sacrificed. To evaluate the development of ALAs, liver samples were taken from all the animals and fixed with 4% paraformaldehyde processed in paraffin and submitted to hematoxylin and eosin (H&E) staining. The tissue sections were stored in RNA later at -81°C to await analysis.

2.6. Antibody Detection by ELISA. Serum was examined *in vitro* by ELISA for the identification of antibodies against *E. histolytica* elicited by treatment with PE Δ III-LC3-KDEL3, by a slightly modified method [14], using *E. histolytica* membrane protein antigen [12], then, HRP-conjugated anti-hamster IgG antibody (H1643, SIGMA, San Luis Missouri, USA) (1:1000). After that, it was developed with orthophenyldiamine (Thermo Scientific 34005, MA USA) and read at 490 nm on an iMark-microplate-reader (Bio-Rad, Hercules, California, USA).

2.7. Cytotoxicity Assay. 2×10^4 trophozoites of *E. histolytica* were resuspended in TYI-S-33 medium; they were treated with dilutions (1:100) of immune serum (from the 50, 75, and 100 μ g groups) and sham serum at 37°C for 1 h. For a positive control, trophozoites were left untreated. Simultaneous with the preincubation, 2×10^5 HepG2 cells were seeded in 24-well plates. Once they get confluence, trophozoites were added, and interaction between HepG2 cells and *E. histolytica* took place at 37°C for 2 h. After that, wells were washed, fixed with 2% PFA, stained with 0.1% methylene blue in 10 mM borate buffer for 15 min, and finally washed 3 times. Subsequently, 0.1 M HCl was added, and each well was left at 37°C for 30 min to extract the stain. Absorbance was then read on a spectrometer at 655 nm (OD_{655}). The percentage of monolayer destruction was calculated as follows: $[(\text{OD}_{655} \text{ of control wells}) - (\text{OD}_{655} \text{ of experimental wells})] / (\text{OD}_{655} \text{ of control wells}) \times 100$.

2.8. Analysis of Cytokine Expression by RT-qPCR. The RNA extracted from the liver tissue from the immunized and nonimmunized animals was analyzed by RT-qPCR using specific primers for cytokine genes (Table 1). Total RNA was isolated from 100 mg of liver tissue of control and experimental animals using the SV Total RNA Isolation System (Z3100, Promega, Madison, Wisconsin, USA), according to the manufacturer's protocol, then quantified with a Biodrop (Biochrom, Waterbeach Cambridge, United Kingdom) and stored at -80°C until needed. Reverse transcription was performed with 1 μ g of total RNA and the GoScript Reverse Transcription System (A5001, Promega, Madison, Wisconsin, USA). Quantitative PCR was carried out with the Maxima SYBR Green/ROX qPCR Master Mix (2x) (K0221, Thermo Fisher Scientific, Waltham, Massachusetts, USA) in a StepOne System (Applied Biosystems, Foster City, California, USA), utilizing the following programming: 50°C for 2 min, 95°C for 3 min, 40 cycles of 95°C for 45 sec, and 60°C for 35 sec. Oligonucleotides were designed to target the cytokine genes. Relative expression was normalized to that of β -actin, and the differences were determined using the $2^{-\Delta\Delta\text{C}_q}$ relative method [15].

TABLE 1: Primers used for RT-qPCR.

Target	Oligonucleotides		Amplicon size
	Sense	Antisense	
IL-10	CAACTGCAGCGTGT CATCGATTT	AGTGCCTGAAGACG CCTTTCTCT	175
IL-1 β	TTT CCA CAG CGA TGA GAA TG	GCCACAATGACTGAC ACCAC	217
IFN- γ	CAGCAGCATGGAAAA ACTGA	GCTCGCCAGAATGTT TTTGT	220
NF- κ B	CAGGAGCCTCAAACC TGAAG	CGTCTGTG GAGAGA AGTCC	174
FoxP3	AAGTCTGGCCACAT CTACG	GTCTGTGCCATT TCCCA CT	246
TNF- α	CCTCCTGTCCGCCAT CAAG	CACTGAGTCGGTCAC CTTTC	246
β -Actin	TGTCACCAACTGGGA CGATA	GGGGTGTGAAGGTC TCAAA	120

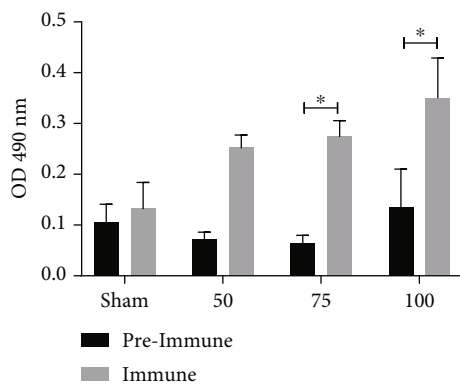


FIGURE 1: The PE Δ III-LC3-KDEL3 vaccine induced IgG antibody production. Serum samples were evaluated by ELISA. Bars represent the mean \pm SEM of three independent assays. Statistical analysis was performed with one-way ANOVA ($p < 0.05$).

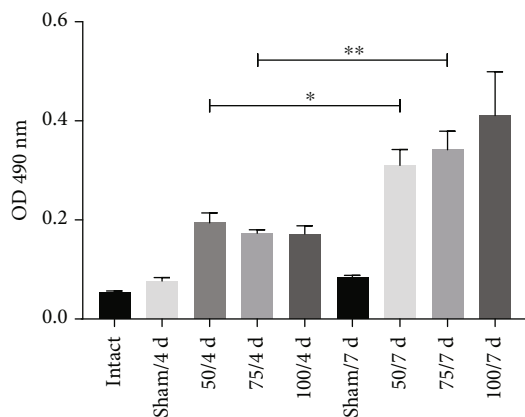


FIGURE 2: The antibody levels were elevated in the animals receiving the PE Δ III-LC3-KDEL3 vaccine even in the postinfection period.

2.9. Immunohistochemistry. IFN- γ -positive cells and *E. histolytica* trophozoites were identified in liver tissue by immunohistochemistry as done by Ventura-Juárez et al. [16]. Briefly, we used primary rabbit polyclonal anti-IFN- γ antibody (500-P32, Pepro-Tech, Cranbury, NJ, USA) diluted 1:200, 1 h at 37°C. As a secondary antibody, Dako Envision system AP (IgG rabbit-mouse, K4065, DAKO, DNK) for 2 h and peroxidase activity were developed with diaminobenzidine for 5 min. Images were captured and analyzed with the Image

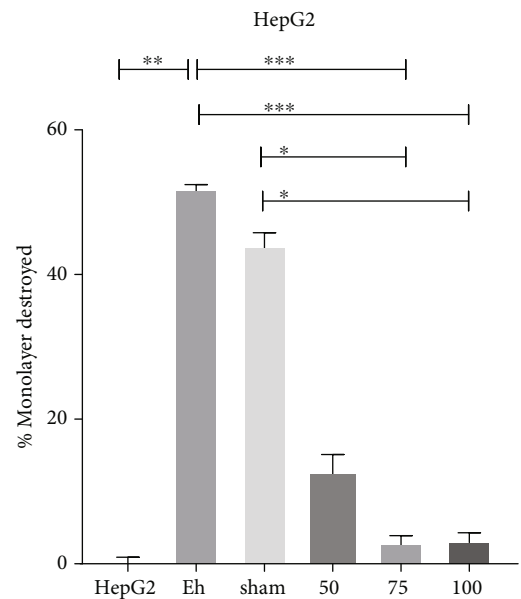


FIGURE 3: Inhibition of cytopathic effect of *E. histolytica* on HepG2 cells. Serum from the immunized groups inhibits destruction. Serum from sham animals generated a high percentage of destruction, similar to the positive control. HepG2 cells not exposed to *E. histolytica* represented the negative control. Data are expressed as the mean \pm SEM of three independent assays, no parametric test Dunn's post hoc. * $p < 0.05$; ** $p < 0.01$; *** $p < 0.001$.

Pro Plus Software 4.5.1 (Media Cybernetics, Bethesda, Maryland, USA) in a Zeiss Axioscop 40/40L microscope (Zeiss, Oberkochen, DEU).

2.10. Statistical Analysis. Differences between groups were assessed with one-way analysis of variance (ANOVA), followed by Tukey's and Dunn's *post hoc* test, using GraphPad Prism version 8.0 for Windows (GraphPad Software, San Diego, California, USA). Data are expressed as the mean \pm SEM of the values from three independent experiments. Significance was considered at $p < 0.05$.

3. Results

3.1. PE Δ III-LC3-KDEL3 Increased Serum Antibody Levels. The levels of the specific antibodies elicited by the

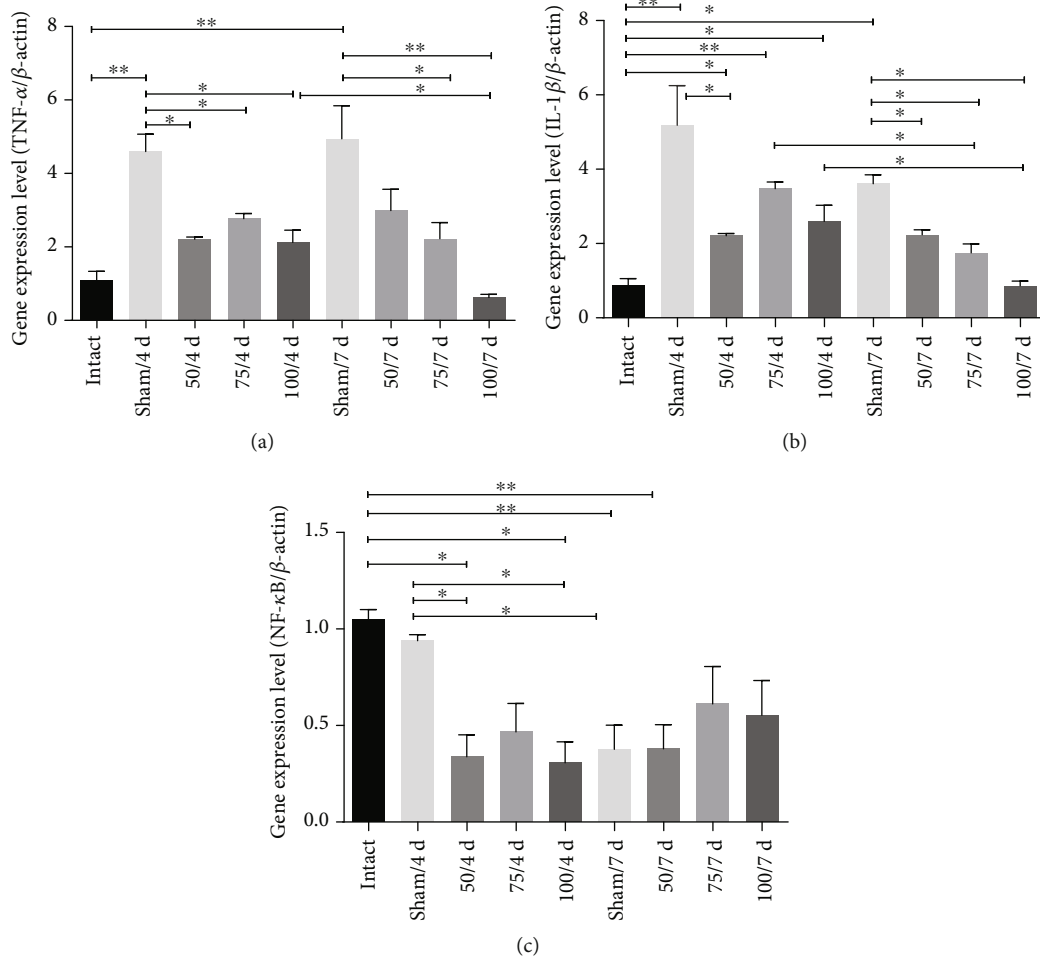


FIGURE 4: The vaccine reduced the expression of the proinflammatory genes. (a, b) TNF- α and IL-1 β in all immunized hamsters at 4- and 7-day postinfection were downregulated. (c) The NF- κ B gene expression was also diminished in all immunized animals. Comparisons among groups: * $p < 0.05$ and ** $p < 0.01$.

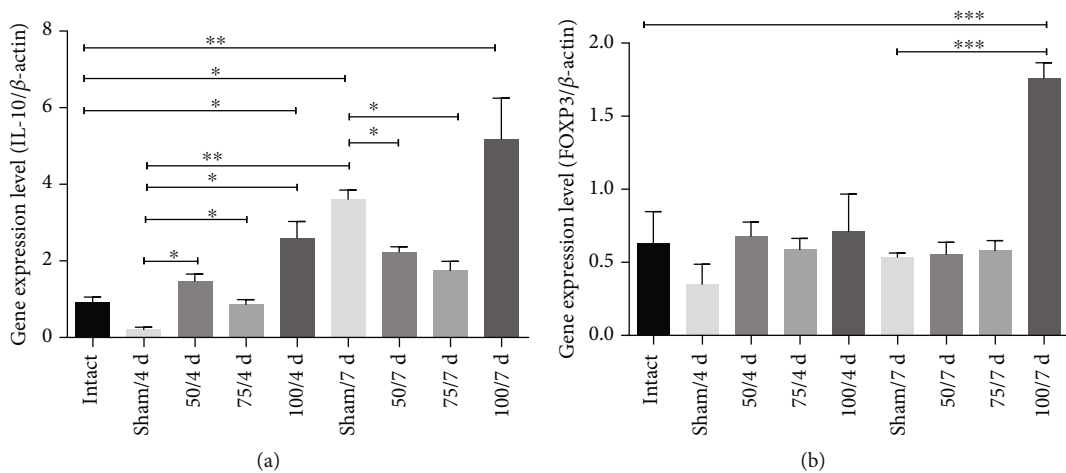


FIGURE 5: The PE Δ III-LC3-KDEL3 vaccine upregulated IL-10 and FOXP3. (a, b) The 100 μ g concentration of the vaccine induced a greater IL-10 and FOXP3 gene expression at 7-day postinfection. (b) Comparisons between groups: * $p < 0.05$, ** $p < 0.01$, and *** $p < 0.001$.

recombinant vaccine were determined in the serum from animals before and after immunization. All immunized hamsters developed a greater quantity of IgG antibodies than nonimmunized animals (Figure 1), although the difference was significant only for the 75 and 100 μg groups. Immunized hamsters were infected 7-day postimmunization, then sacrificed at 4- and 7-day postinfection. Compared to the sham animals at day 7 postinfection, the antibody level in the 50 and 75 μg groups showed a significant increase, while the level in the 100 μg group was not significantly higher (Figure 2).

3.2. Immune Sera Inhibit *E. histolytica* Cytopathic Activity on HepG2 Cells. The ability of *E. histolytica* trophozoites to recognize and adhere to cells leads to cell death followed by phagocytosis [17]. Thus, HepG2 liver cells were herein exposed to trophozoites previously incubated for 1 h with the serum from immunized or nonimmunized animals. The virulent trophozoites without pretreatment and pretreated with serum from nonimmunized hamsters generated a high percentage of destruction of HepG2 cells (51% and 44%, respectively). The trophozoites pretreated with the serum from immunized animals inhibit destruction of the HepG2 cell monolayer, being 12.3% with 50 μg and only 3.0% with both 75 and 100 μg (Figure 3). This indicate that antibodies from vaccine-immunized hamsters recognized the LC3 fragment of trophozoites and interfered with the ability of the parasite to bind to and destroy the HepG2 cells.

3.3. Gene Expression of *TNF- α* , *IL-1 β* , *IFN- γ* , *NF- κ B*, *FOXP3*, and *IL-10* in Vaccinated Hamsters. Compared to the sham group, the gene expression for the proinflammatory cytokine *TNF- α* was significantly lower at 4- and 7-day postinfection for the hamsters receiving 50, 75, and 100 μg ($p < 0.05$, $p < 0.01$) is important to realize that 100 μg at 7 days was even more low than at 4 days (Figure 4(a)). The *IL-1 β* gene expression was diminished at 4 and 7 days in the 50 μg group ($p < 0.05$); likewise, gene expression of this cytokine was low at 75 and 100 μg at 7 days compared those to 4 days. Anterior results show a diminish timeline of the *IL-1 β* gene expression (Figure 4(b)). To corroborate these results, the gene expression for nuclear factor kappa B (*NF- κ B*) was also examined, finding it to be downregulated in all immunized hamsters ($p < 0.05$, $p < 0.01$), except 75 and 100 μg at 7 days (Figure 4(c)).

IL-10 participates in downregulating the inflammatory process. The gene expression of *IL-10* increases at all doses at 4 days ($p < 0.05$ and $p < 0.01$, respectively) compared to sham (Figure 5(a)). No significant difference existed among immunized groups (50, 75, and 100 μg) and intact hamsters, at 7 days only increase *IL-10* gen in sham and 100 μg (Figure 5(a)). Regarding *FOXP3*, the gene expression increased only in 100 μg at 7-day postinfection ($p < 0.001$) (Figure 5(b)). Additionally, the expression of *INF- γ* gene in all immunized animals was significantly increased until 7-day postinfection ($p < 0.05$, $p < 0.01$, $p < 0.001$) (Figure 6).

The immunohistochemistry assay confirmed this result, revealing an elevated quantity of +*IFN- γ* cells in liver tissue

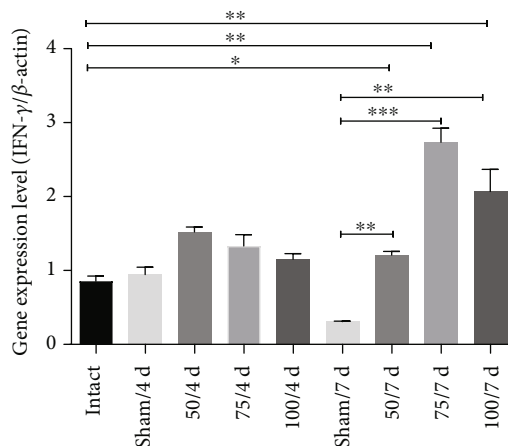


FIGURE 6: The PE Δ III-LC3-KDEL3 vaccine promoted the expression of *IFN- γ* . The *IFN- γ* gene expression in the 50, 75, and 100 μg groups was only elevated at 7-day postinfection. Comparisons between groups: * $p < 0.05$, ** $p < 0.01$, and *** $p < 0.001$.

from animals immunized with 75 μg (Figures 7(g), 7(h), and 7(k)). As can be appreciated, the PE Δ III-LC3-KDEL3 vaccine had a downregulatory influence on the hamster immune response, which included anti-inflammatory effects.

3.4. Effects of the PE Δ III-LC3-KDEL3 Vaccine on ALA Formation. Male hamsters were inoculated with 5×10^5 virulent *E. histolytica* trophozoites 7 days after vaccination. The liver tissue of the sham group showed characteristic ALA lesions: large, pale hemorrhagic zones located at the site of inoculation and were larger on 7 days than 4 days (Figures 8(a), (D) and 8(a), (C)). Compared to the sham hamsters, a considerable decrease in liver damage was found in all immunized groups; the liver tissue of the 50 μg group displayed a small white lesion without hemorrhagic borders at 4 and 7 days (Figures 8(a), (E) and 8(a), (F)). The liver from inoculated with 75 μg group exhibited a small lesion (at 4 days Figure 8(a), (G)) with a hemorrhagic area (at 7 days) (Figure 8(a), (H)). Surprisingly, evaluation of the liver tissue of the 100 μg group revealed the absence of any lesion or hemorrhagic areas (at days 4 and 7; Figures 8(a), (I) and 8(a), (J)). Histological analysis evidenced necrosis of the liver parenchyma (asterisks) and inflammatory infiltrate in the sham (arrows in Figure 8(b), (B)), and in 50 and 75 μg groups, contrarily, there was a better architecture of the parenchyma without any tissue necrosis, although inflammatory infiltrate was detected (arrowheads, Figures 8(b), (C) and 8(b), (D)). Surprisingly, the architecture of the liver parenchyma was similar for the 100 μg (Figure 8(b), (E)) and intact group (Figure 8(b), (A)), with no tissue disruption or inflammatory infiltrate.

3.5. Detection and Quantification of *E. histolytica* Trophozoites by Immunohistochemistry. We observed in the sham group the abundant trophozoites in liver parenchyma (arrowheads in Figures 9(c) and 9(d)); however, in hamsters immunized with 50 μg , fragments of trophozoites were

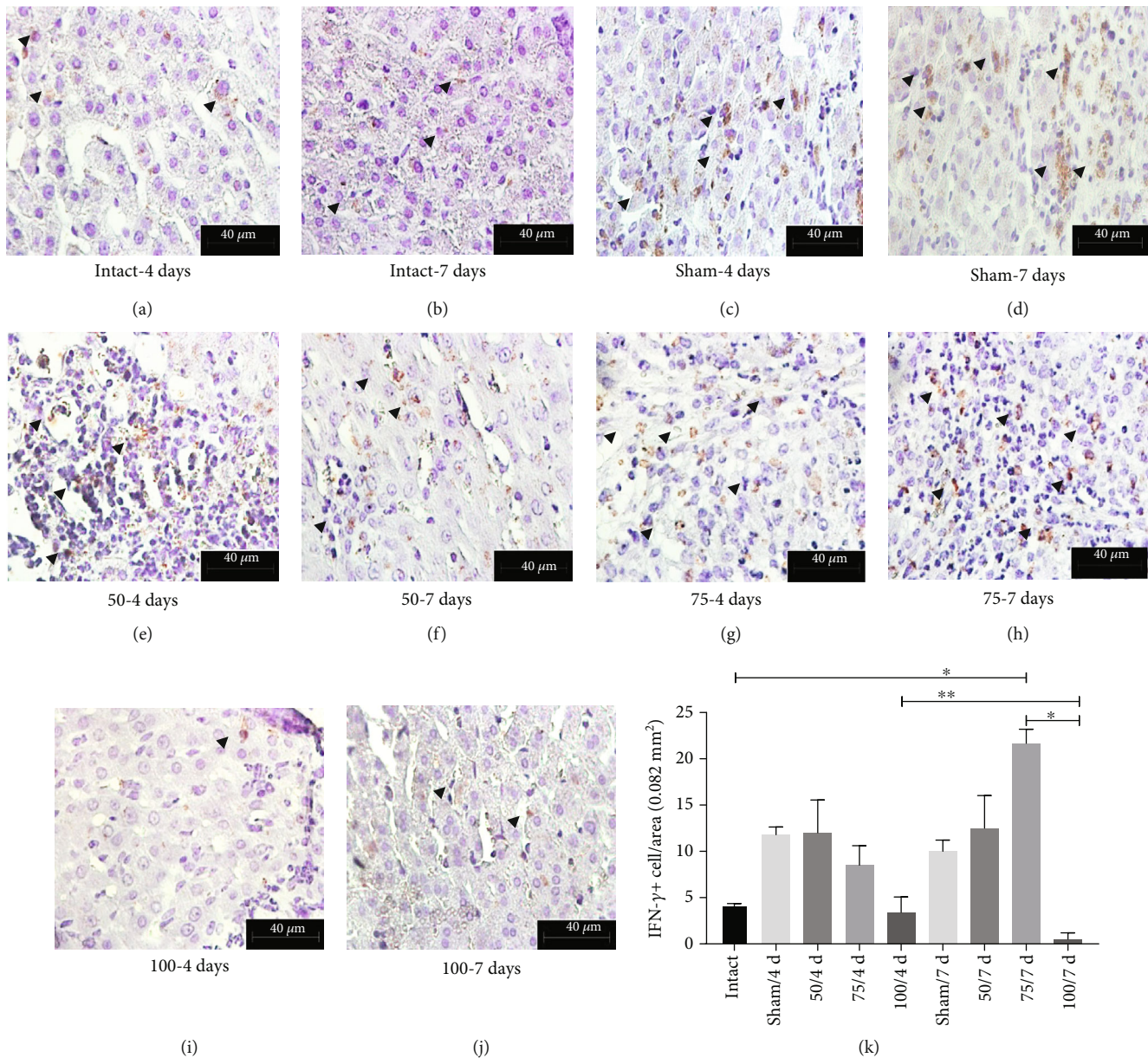


FIGURE 7: Immunohistochemical analysis of +IFN- γ hepatic cells. Original magnification 400x. (a–j) Based on the immunohistochemistry assay, the quantity of +IFN- γ cells was determined in the liver tissue of hamsters (arrowhead). (k) The cells were abundant in 75 μ g group at 7 days.

identified (light brown, arrowheads in Figures 9(e) and 9(f)); in hamsters immunized with 75 μ g, very few trophozoites invaded by inflammatory cells (arrowheads in Figures 9(g) and 9(h)) can be identified; likewise, in hamsters immunized with 100 μ g, at 4 days, small areas of inflammatory infiltrate are observed with few fragments of trophozoites (arrowheads in Figure 9(i)); finally, at 7 days, the tissue liver is seen healthy, and fragments of trophozoites are seen sporadically (arrowhead in Figure 9(j)).

4. Discussion

Amebiasis is a neglected disease that requires a solution, having widespread prevalence, and a significant annual

mortality. The main treatment (nitroimidazole) for invasive amebiasis has serious adverse effects and in many cases requires the complement of additional medications. The vaccines elaborated to date induce only partial protection of the acquired immunity of the host, and the relative importance of mucosal, cellular, and humoral immunity in protection is still undetermined [18].

The amebic antigen most frequently investigated for the development of a vaccine is the galactose-binding lectin. Vaccines based on the native or recombinant form of the Gal/GalNAc lectin proteins are the most promising, with reports of success in protecting animals against intestinal amebiasis and ALA [7, 19–21]. Clinical trials will be required to validate its efficacy in humans [18].

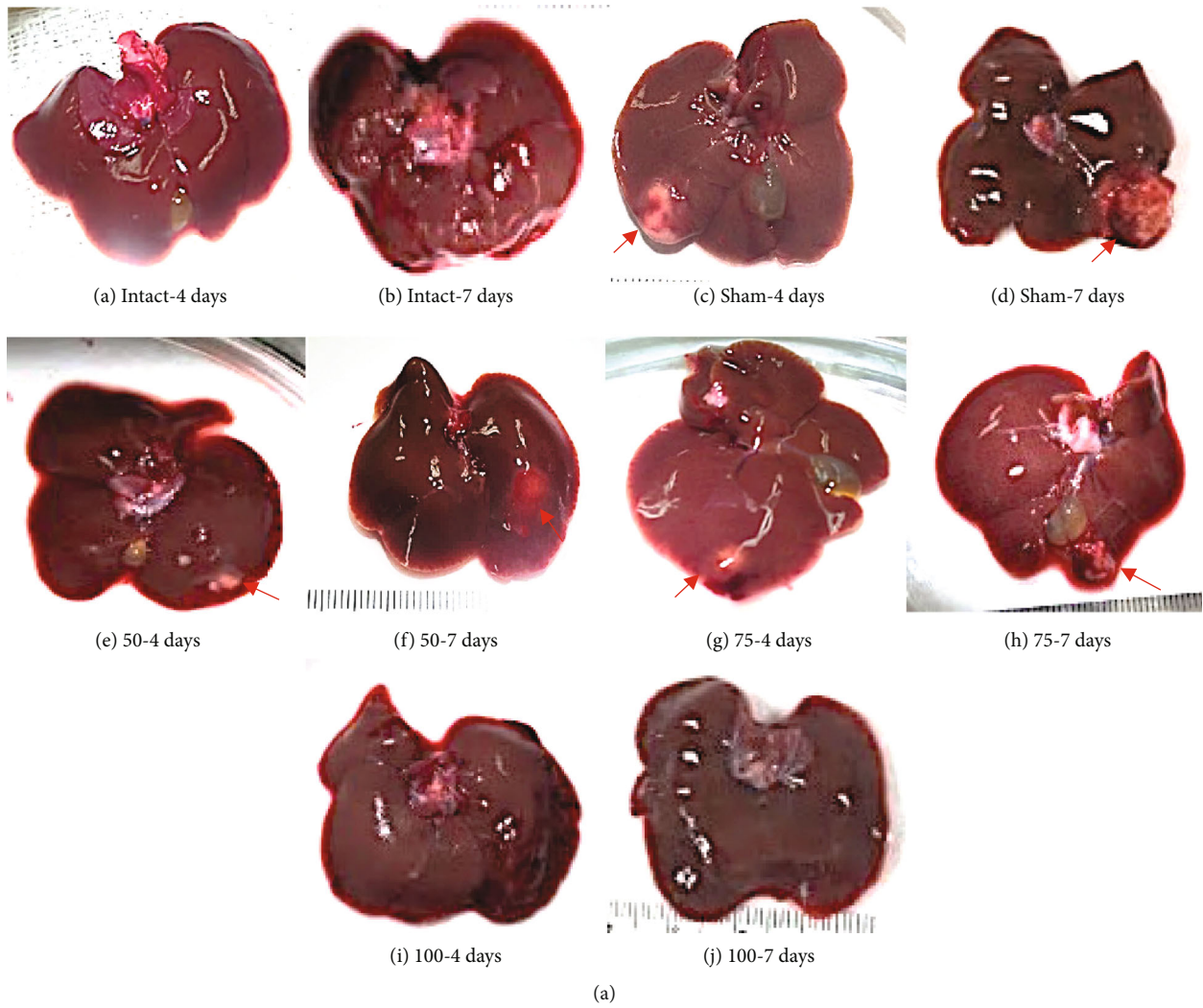


FIGURE 8: Continued.

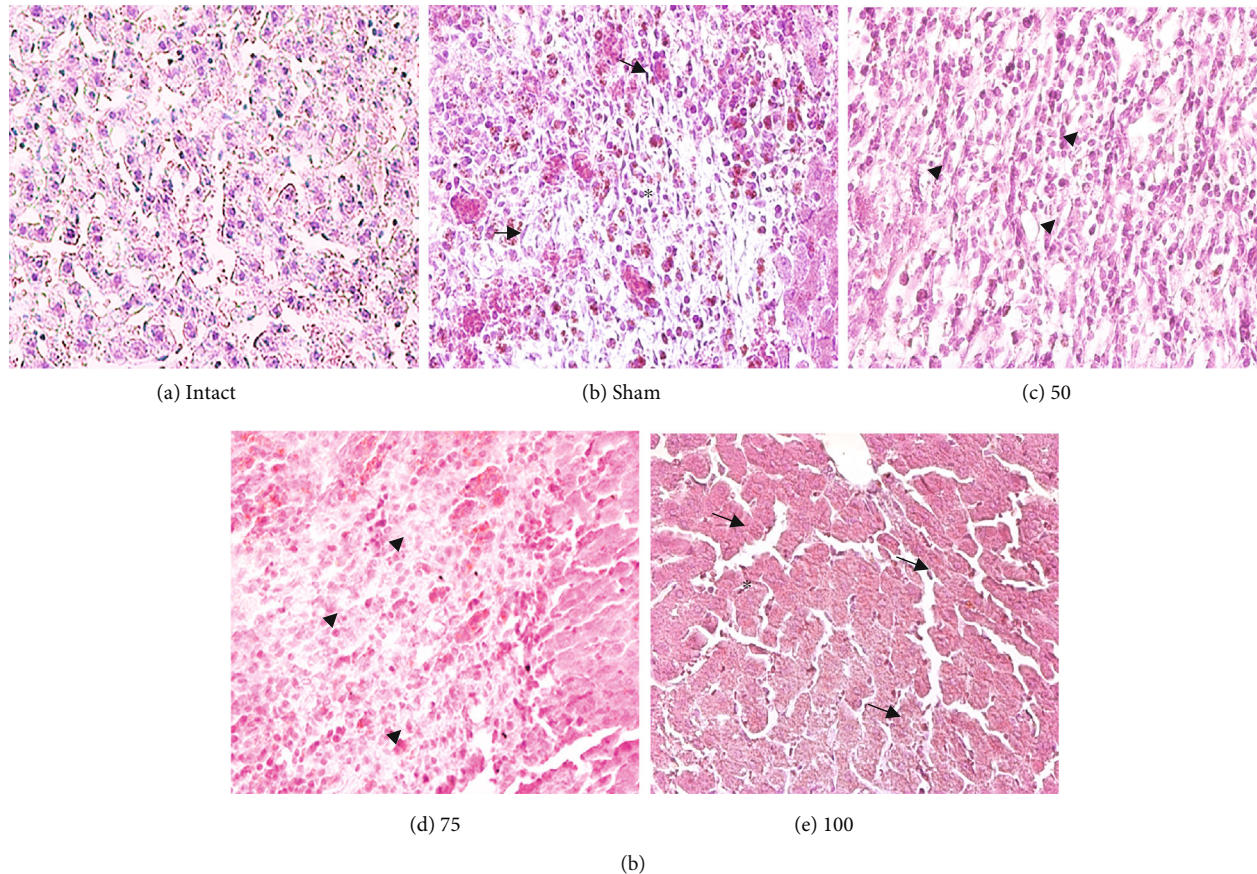


FIGURE 8: (a) Macroscopic analysis of amoebic liver abscess formation. (A, B) No abscesses were detected in the liver of uninfected hamsters. (C, D) The liver of the sham group showed the characteristic ALA lesions. (E, F) The 50 μg group exhibited smaller lesions on day 7 than day 4 than sham. (G, H) A single small lesion is seen in the liver of the 75 μg group (arrows). (I, J) No lesion was detected in the liver of the 100 μg group. (b) Light microscopy of paraffin histological technique of amoebic liver abscess. Original magnification 400x. (A) In the intact hamsters, normal architecture was found in the liver tissue. (B, C) In two of the infected groups, sham and vaccinated with 50 μg , a necrotic area was observed in the liver parenchyma, accompanied by inflammatory infiltrate (arrows, asterisk). (D) In the 75 μg group, the parenchyma displayed no tissue necrosis (arrowhead). (E) In the 100 μg group, the parenchyma was similar to the intact animals, and there was no tissue necrosis or inflammation (arrows, cross).

The aim of the present study was to test a recombinant vaccine based on the Gal-lectin antigen in a hamster model. This vaccine has better immunostimulatory characteristics [22, 23]. The most important findings of the current contribution in regard to the PE Δ III-LC3-KDEL3 vaccine are its effective liver tissue protection and ability to inhibit important amoebic virulent functions. The latter is related to the stimulation of antibody production and the inhibition of the inflammatory response.

In response to the vaccine, the animals generated IgG-type antibodies in serum. The lectin Gal/GalNAc is by itself a highly antigenic molecule [24] that promotes the production of specific antibodies against *E. histolytica* in gerbil and mouse models of amoebiasis [16]. The antibodies elicited by the vaccine were able to inhibit the cytotoxicity of virulent *E. histolytica* on HepG2 cells. This effect is especially important because the adhesion of trophozoites to host cells is a prerequisite for their capacity to destroy cells [17, 25]. A hallmark of *E. histolytica*-induced damage to host tissue is the presence of excessive inflammation, which is triggered by

the activation of transcriptional factors that elicit the production and release inflammatory mediators [26–28]. For instance, TNF- α and IL-1 β stimulate an inflammatory response and contribute to tissue damage [29, 30]. Additionally, TNF- α foments the migration of trophozoites [31]. In the current study, all animals immunized with PE Δ III-LC3-KDEL3 showed an attenuation of inflammatory factors in the liver microenvironment.

PE Δ III-LC3-KDEL3 herein promoted IL-10 cytokine gene expression, which may contribute to protection. For example, this cytokine with powerful anti-inflammatory properties [32] is related to the resistance of animals to an invasive *E. histolytica* infection by avoiding damage to host tissue and maintaining tissue homeostasis [33, 34] limiting like this an excessive inflammation, thus protecting the hamsters from ALA formation. Accordingly, there was an increase for FOXP3 in immunized groups; as a consequence, it was a decrease for NF- κ B.

On the other hand, some studies focusing on animal models and on human infection have established that

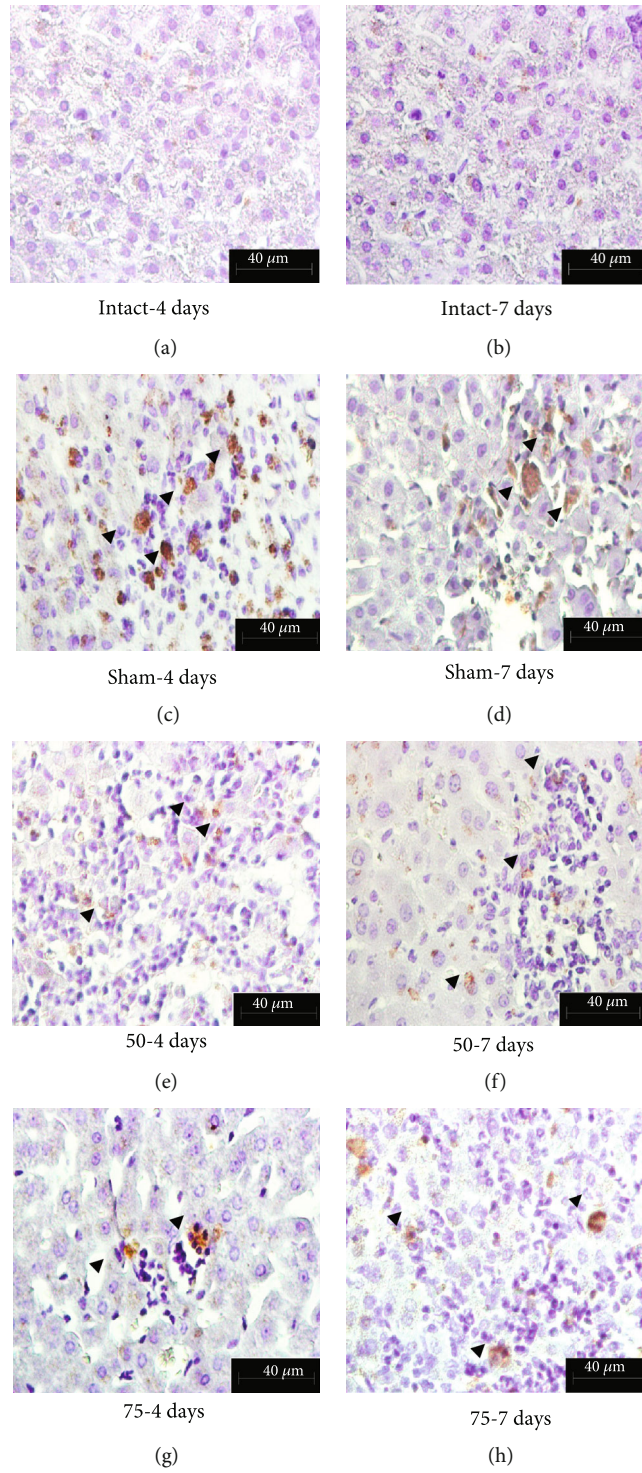


FIGURE 9: Continued.

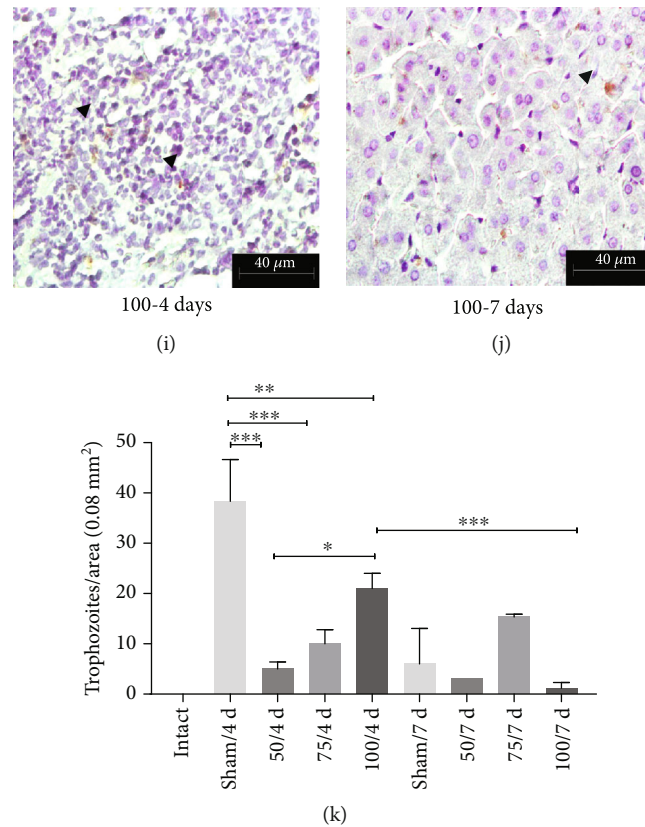


FIGURE 9: Immunohistochemistry detection for *E. histolytica* trophozoites. Original magnification 400x. (c, d) Trophozoites and their fragments (e–j) can be seen by the light brown color (arrowheads). The number of trophozoites was lower as the vaccine dose increased (e–j). (k) Graphical expression of the quantity of *E. histolytica* trophozoites per tissue area (* $p < 0.05$, ** $p < 0.01$, *** $p < 0.001$).

amebiasis vaccines require a Th1 response [35]. Our results evidence an elevated expression of the IFN- γ gene at the last period analyzed (at 7 days). IFN- γ reportedly plays an important role in the host defense against *E. histolytica* [36, 37]. One mechanism described in the literature is its activation of macrophages to produce reactive oxygen species (ROS) and reactive nitrogen species (RNS), which are cytotoxic to the parasite [38].

The ALA lesion induced in the animals was minimal. This panorama was also observed by Meneses-Ruiz [39], who described “sterile protection against ALA.” The protection provided by the PE Δ III-LC3-KDEL3 vaccine likely stems in part from its upregulation of IFN- γ , leading to an effective Th1 response against *E. histolytica* and the downregulation of the immune response through IL-10 and FOXP3.

This vaccine represents a successful example of a recombinant protein that utilizes domains of a bacterial toxin for the development of a potent vaccine against *E. histolytica* [16, 40]. PE Δ III-LC3-KDEL3 was presently administered in the absence of adjuvants, unlike the majority of studies on vaccine candidate proteins, including serine-rich protein (SREHP) [41], Gal/GalNac lectin [19], 112 kDa [42], and peroxiredoxin [43]. Many authors have reported that adjuvants induce focal necrosis and a granulomatous inflammatory response, with the predominance of macrophages at the injection site (elicited by Freund’s adjuvant) [44, 45].

5. Conclusions

PE Δ III-LC3-KDEL3 recombinant protein prevents invasive amebiasis, inhibiting an excessive inflammatory response and activating a protective response in a short time.

Further research is underway to attain a more in-depth understanding of the immunological activity of this vaccine with the aim of allowing for its use in clinical trials.

Data Availability

The data used to support the findings of this study were supplied by Sandra Luz Martínez-Hernández under license and so cannot be made freely available. Requests for access to these data should be made to Sandra Luz Martínez-Hernández, email: lilith3050@hotmail.com. Previously reported data for design of an amoebic recombinant vaccine were used to support this study and are available at DOI 10.1007/s10529-017-2341-2. These prior studies are cited at relevant places within the text as references [# 9].

Conflicts of Interest

The authors declare that there is no conflict of interest regarding the publication of this paper.

Authors' Contributions

SLMH designed, obtained, and evaluated the PEΔIII-LC3-KDEL3 vaccine. VMBG developed the histological technique in the liver tissues. MHMO contributed with the analysis of RT-qPCR. VMLM and MEAB contributed with the microscopy analysis and the statistical analysis of the data. MNRM contributed with the maintenance of trophozoites and HepG2 cells. JVJ contributed to the conception, design, writing, and revision of the manuscript. All of the authors have approved the final manuscript.

Acknowledgments

The present study was financed by grant PIBB16-2 from the Universidad Autónoma de Aguascalientes and Grant 286184 from the Consejo Nacional de Ciencia y Tecnología (CONACYT). Sandra Luz Martínez-Hernández was granted a fellowship by CONACYT (244835) as part of the doctorate program in Biological Sciences in the Universidad Autónoma de Aguascalientes.

References

- [1] C. Jiménez, R. Cerritos, L. Rojas et al., "Human amebiasis: breaking the paradigm?," *International Journal of Environmental Research and Public Health*, vol. 7, no. 3, pp. 1105–1120, 2010.
- [2] WHO, "A moebiasis," *Releve Epidemiologique*, vol. 72, no. 14, pp. 97–99, 1997.
- [3] R. B. Sack, R. Haque, D. Mondal, W. A. Petri, and B. D. Kirkpatrick, "Attribution of malnutrition to cause-specific diarrheal illness: evidence from a prospective study of preschool children in Mirpur, Dhaka, Bangladesh," *The American Journal of Tropical Medicine and Hygiene*, vol. 80, no. 5, pp. 824–826, 2009.
- [4] R. Haque, C. D. Huston, M. Hughes, E. Houpt, and W. A. Petri Jr., "Amoebiasis: review article," *The New England Journal of Medicine*, vol. 348, no. 16, pp. 1565–1573, 2003.
- [5] S. Ghosh, J. Padalia, and S. Moonah, "Tissue destruction caused by *Entamoeba histolytica* parasite: cell death, inflammation, invasion, and the gut microbiome," *Current Clinical Microbiology Reports*, vol. 6, no. 1, pp. 51–57, 2019.
- [6] W. A. Petri Jr., "Therapy of intestinal protozoa," *Trends in Parasitology*, vol. 19, no. 11, pp. 523–526, 2003.
- [7] H. Lotter, T. Zhang, and K. B. Seydel, "Identification of an epitope on the *Entamoeba histolytica* 170-kDa lectin conferring antibody-mediated protection against invasive amebiasis," *Journal of Experimental Medicine*, vol. 185, no. 10, pp. 1793–1801, 1997.
- [8] B. J. Mann, B. E. Torian, T. S. Vedvick, and W. A. Petri, "Sequence of a cysteine-rich galactose-specific lectin of *Entamoeba histolytica*," *Proceedings of the National Academy of Science of the United States of America*, vol. 88, no. 8, pp. 3248–3252, 1991.
- [9] S. L. Martínez-Hernández, D. Cervantes-García, M. H. Muñoz-Ortega et al., "An anti-amoebic vaccine: generation of the recombinant antigen LC3 from *Entamoeba histolytica* linked to mutated exotoxin A (PEΔIII) via the *Pichia pastoris* system," *Biotechnology Letters*, vol. 39, no. 8, pp. 1149–1157, 2017.
- [10] L. I. O. Muñoz, *Norma Oficial Mexicana NOM-062-ZOO-1999, especificaciones técnicas*, Diario Oficial De La Federacion, Mexico, 2007.
- [11] L. S. Diamond, D. R. Harlow, and C. C. Cunnick, "A new medium for the axenic cultivation of *Entamoeba histolytica* and other *Entamoeba*," *Transaction of The Royal Society of Tropical Medicine and Hygiene*, vol. 72, no. 4, pp. 431–432, 1978.
- [12] J. Ventura-Juárez, R. Campos-Rodríguez, and V. Tsutsumi, "Early interactions of *Entamoeba histolytica* trophozoites with parenchymal and inflammatory cells in the hamster liver: an immunocytochemical study," *Canadian Journal of Microbiology*, vol. 48, no. 2, pp. 123–131, 2002.
- [13] C. P. Ivory, K. Keller, and K. Chadee, "CpG-oligodeoxynucleotide is a potent adjuvant with an *Entamoeba histolytica* Gal-inhibitable lectin vaccine against amoebic liver abscess in gerbils," *Infection and Immunity*, vol. 74, no. 1, pp. 528–536, 2006.
- [14] P. K. Vaz, C. A. Hartley, and G. F. Browning, "Marsupial and monotreme serum immunoglobulin binding by proteins A, G and L and anti-kangaroo antibody," *Journal of Immunological Methods*, vol. 427, pp. 94–99, 2015.
- [15] K. J. Livak and T. D. Schmittgen, "Analysis of relative gene expression data using real-time quantitative PCR and the $2^{-\Delta\Delta C_T}$ method," *Methods*, vol. 25, no. 4, pp. 402–408, 2001.
- [16] S. L. Stanlejr Jr., "Progress towards development of a vaccine for amebiasis," *Clinical Microbiology Reviews*, vol. 10, no. 4, pp. 637–649, 1997.
- [17] U. Katz, S. Ankri, T. Stolarsky, Y. Nuchamowitz, and D. Mirelman, "*Entamoeba histolytica* expressing a dominant negative N-truncated light subunit of its gal-lectin are less virulent," *Molecular Biology of the Cell*, vol. 13, no. 12, pp. 4256–4265, 2002.
- [18] D. T. Shirley, K. Watanabe, and S. Moonah, "Significance of amebiasis: 10 reasons why neglecting amebiasis might come back to bite us in the gut," *PLoS Neglected Tropical Diseases*, vol. 13, no. 11, article e0007744, 2019.
- [19] W. A. Petri Jr. and J. I. Ravdin, "Protection of gerbils from amebic liver abscess by immunization with the galactose-specific adherence lectin of *Entamoeba histolytica*," *Infection and Immunity*, vol. 59, no. 1, pp. 97–101, 1991.
- [20] E. C. Roncolato, J. E. Teixeira, J. E. Barbosa, L. N. Zambelli Ramalho, and C. D. Huston, "Immunization with the *Entamoeba histolytica* surface metalloprotease EhMSP-1 protects hamsters from amebic liver abscess," *Infection and Immunity*, vol. 83, no. 2, pp. 713–720, 2015.
- [21] Y. Jinno, M. Ogata, V. K. Chaudhary et al., "Domain II mutants of pseudomonas exotoxin deficient in translocation," *The Journal of Biological Chemistry*, vol. 264, no. 27, pp. 15953–15959, 1989.
- [22] J. Fominaya and W. Wels, "Target cell-specific DNA transfer mediated by a chimeric multidomain protein: novel non-viral gene delivery system," *The Journal of Biological Chemistry*, vol. 271, no. 18, pp. 10560–10568, 1996.
- [23] C. W. Liao, C. A. Chen, C. N. Lee et al., "Fusion protein vaccine by domains of bacterial exotoxin linked with a tumor antigen generates potent immunologic responses and antitumor effects," *Cancer Research*, vol. 65, no. 19, pp. 9089–9098, 2005.
- [24] W. A. Petri Jr., J. Broman, G. Healy, T. Quinn, and J. I. Ravdin, "Antigenic stability and immunodominance of the Gal/GalNAc adherence lectin of *Entamoeba Histolytica*," *The*

- American Journal of the Medical Sciences*, vol. 297, no. 3, pp. 163–165, 1989.
- [25] K. S. Ralston and W. A. Petri Jr., “Tissue destruction and invasion by *Entamoeba histolytica*,” *Trends in Parasitology*, vol. 27, no. 6, pp. 254–263, 2011.
- [26] K. B. Seydel, E. Li, P. Swanson, and S. L. Stanley Jr., “Human intestinal epithelial cells produce proinflammatory cytokines in response to infection in a SCID mouse-human intestinal xenograft model of amebiasis,” *Infection and Immunity*, vol. 65, no. 5, pp. 1631–1639, 1997.
- [27] K. B. Seydel, E. Li, Z. Zhang, and S. L. Stanley Jr., “Epithelial cell-initiated inflammation plays a crucial role in early tissue damage in amebic infection of human intestine,” *Gastroenterology*, vol. 115, no. 6, pp. 1446–1453, 1998.
- [28] S. Blazquez, M. C. Rigotherier, M. Huerre, and N. Guillen, “Initiation of inflammation and cell death during liver abscess formation by *Entamoeba histolytica* depends on activity of the galactose/*N*-acetyl-d- galactosamine lectin,” *International Journal of Parasitology*, vol. 37, no. 3–4, pp. 425–433, 2007.
- [29] S. N. Moonah, N. M. Jiang, and W. A. Petri Jr., “Host immune response to intestinal amebiasis,” *PLoS Pathogens*, vol. 9, no. 8, article e10034899:8, 2013.
- [30] Z. Zhang, S. Mahajan, X. Zhang, and S. L. Stanley Jr., “Tumor necrosis factor alpha is a key mediator of gut inflammation seen in amebic colitis in human intestine in the SCID mouse-human intestinal xenograft model of disease,” *Infection and Immunity*, vol. 71, no. 9, pp. 5355–5359, 2003.
- [31] S. Blazquez, C. Zimmer, G. Guigon, J. C. Olivo-Marin, N. Guillén, and E. Labruyère, “Human tumor necrosis factor is a chemoattractant for the parasite *Entamoeba histolytica*,” *Infection and Immunity*, vol. 74, no. 2, pp. 1407–1411, 2006.
- [32] R. Sabat, G. Grütz, K. Warszawska et al., “Biology of interleukin-10,” *Cytokine and Growth Factor Reviews*, vol. 21, no. 5, pp. 331–344, 2010.
- [33] M. E. Quintanar-Quintanar, A. Jarillo-Luna, and V. Rivera-Aguilar, “Immunosuppressive treatment inhibits the development of amebic liver abscesses in hamsters,” *Medical Science Monitor*, vol. 10, no. 9, pp. 317–324, 2004.
- [34] A. Asgharpour, C. Gilchrist, D. Baba, S. Hamano, and E. Houpt, “Resistance to intestinal *Entamoeba histolytica* infection is conferred by innate immunity and Gr1+ cells,” *Infection and Immunity*, vol. 73, no. 8, pp. 4522–4529, 2005.
- [35] L. Guo, X. Barroso, S. M. Becker et al., “Protection against intestinal amebiasis by a recombinant vaccine is transferable by T cells and mediated by gamma interferon,” *Infection and Immunity*, vol. 77, no. 9, pp. 3909–3918, 2009.
- [36] E. A. García-Zepeda, M. E.-V. Rojas-López, and P. Ostoa-Saloma, “Regulation of the inflammatory immune response by the cytokine/chemokine network in amoebiasis,” *Parasite Immunology*, vol. 29, no. 12, pp. 679–684, 2007.
- [37] W. A. Petri, S. Roy, P. Duggal et al., “Correlation of interferon- γ production by peripheral blood mononuclear cells with childhood malnutrition and susceptibility to amebiasis,” *American Journal of Tropical Medicine and Hygiene*, vol. 76, no. 2, pp. 340–344, 2007.
- [38] I. Bruchhaus, S. Richter, and E. Tannich, “Removal of hydrogen peroxide by the 29 kDa protein of *Entamoeba histolytica*,” *The Biochemical Journal*, vol. 326, no. 3, pp. 785–789, 1997.
- [39] D. M. Meneses-Ruiz, H. Aguilar-Díaz, R. J. Bobes et al., “Protection against amoebic liver abscess in hamster by intramuscular immunization with an *Autographa californica* Baculovirus driving the expression of the Gal-lectin LC3 fragment,” *BioMed Research International*, vol. 2015, Article ID 760598, 10 pages, 2015.
- [40] C. F. Hung, K. F. Hsu, W. F. Cheng et al., “Enhancement of DNA vaccine potency by linkage of antigen gene to a gene encoding the extracellular domain of Fms-like tyrosine kinase 3-ligand,” *Cancer Research*, vol. 61, no. 3, pp. 1080–1088, 2001.
- [41] T. Zhang, P. R. Cieslak, and S. L. Stanley Jr., “Protection of gerbils from amebic liver abscess by immunization with a recombinant *Entamoeba histolytica* antigen,” *Infection and Immunity*, vol. 62, no. 4, pp. 1166–1170, 1994.
- [42] C. Martínez-López, E. Orozco, T. Sánchez, R. M. García-Pérez, F. Hernández-Hernández, and M. A. Rodríguez, “The EhADH112 recombinant polypeptide inhibits cell destruction and liver abscess formation by *Entamoeba histolytica* trophozoites,” *Cell Microbiology*, vol. 6, no. 4, pp. 367–376, 2004.
- [43] B. Jiménez-Delgadillo, P. P. Chaudhuri, L. Baylón-Pacheco, A. López-Monteon, P. Talamás-Rohana, and J. L. Rosales-Encina, “*Entamoeba histolytica*: cDNAs cloned as 30 kDa collagen-binding proteins (CBP) belong to an antioxidant molecule family.: protection of hamsters from amoebic liver abscess by immunization with recombinant CBP,” *Experimental Parasitology*, vol. 108, no. 1–2, pp. 7–17, 2004.
- [44] P. P. A. M. Leenaars, M. A. Koedam, P. W. Wester et al., “Assessment of side effects induced by injection of different adjuvant/antigen combinations in rabbits and mice,” *Laboratory Animals*, vol. 32, no. 4, pp. 387–406, 1998.
- [45] H. F. Stils Jr., “Adjuvants and antibody production: dispelling the myths associated with Freund’s complete and other adjuvants,” *ILAR Journal*, vol. 46, no. 3, pp. 280–293, 2005.

Research Article

Related Pentacyclic Triterpenes Have Immunomodulatory Activity in Chronic Experimental Visceral Leishmaniasis

Jéssica Adriana de Jesus,¹ Márcia Dalastra Laurenti ,¹ Leila Antonangelo,^{2,3}
Caroline Silvério Faria,³ João Henrique Ghilardi Lago,⁴
and Luiz Felipe Domingues Passero ^{5,6}

¹Laboratory of Pathology of Infectious Diseases (LIM50), Department of Pathology, Medical School of São Paulo University, Av. Dr. Arnaldo, 455 Cerqueira César, São Paulo, 01246-903 SP, Brazil

²Laboratório de Patologia Clínica, Departamento de Patologia, Hospital das Clínicas, Faculdade de Medicina, Universidade de São Paulo, São Paulo, SP, Brazil

³Laboratório de Investigação Médica (LIM03), Hospital das Clínicas, Faculdade de Medicina, Universidade de São Paulo, São Paulo, SP, Brazil

⁴Centre of Natural and Human Sciences, Federal University of ABC (UFABC), Santo André 09210-580, Brazil

⁵São Paulo State University (UNESP), Institute of Biosciences, São Vicente, Praça Infante Dom Henrique s/n, 11330-900 São Vicente, SP, Brazil

⁶São Paulo State University (UNESP), Institute for Advanced Studies of Ocean, São Vicente, João Francisco Bendorp 1178, 11350-011 São Vicente, SP, Brazil

Correspondence should be addressed to Luiz Felipe Domingues Passero; felipepassero@yahoo.com.br

Received 11 December 2020; Revised 25 January 2021; Accepted 4 February 2021; Published 18 February 2021

Academic Editor: Elizabeth Soares Fernandes

Copyright © 2021 Jéssica Adriana de Jesus et al. This is an open access article distributed under the Creative Commons Attribution License, which permits unrestricted use, distribution, and reproduction in any medium, provided the original work is properly cited.

Leishmaniasis is a neglected tropical disease caused by the flagellated protozoa of the genus *Leishmania* that affects millions of people around the world. Drugs employed in the treatment of leishmaniasis have limited efficacy and induce local and systemic side effects to the patients. Natural products are an interesting alternative to treat leishmaniasis, because some purified molecules are selective toward parasites and not to the host cells. Thus, the aim of the present study was to compare the *in vitro* antileishmanial activity of the triterpenes betulin (Be), lupeol (Lu), and ursolic acid (UA); analyze the physiology and morphology of affected organelles; analyze the toxicity of selected triterpenes in golden hamsters; and study the therapeutic activity of triterpenes in hamsters infected with *L. (L.) infantum* as well as the cellular immunity induced by studied molecules. The triterpenes Lu and UA were active on promastigote ($IC_{50} = 4.0 \pm 0.3$ and $8.0 \pm 0.2 \mu M$, respectively) and amastigote forms ($IC_{50} = 17.5 \pm 0.4$ and $3.0 \pm 0.2 \mu M$, respectively) of *L. (L.) infantum*, and their selectivity indexes (SI) toward amastigote forms were higher (≥ 13.4 and 14, respectively) than SI of miltefosine (2.7). *L. (L.) infantum* promastigotes treated with Lu and UA showed cytoplasmic degradation, and in some of these areas, cell debris were identified, resembling autophagic vacuoles, and parasite mitochondria were swelled, fragmented, and displayed membrane potential altered over time. Parasite cell membrane was not affected by studied triterpenes. Studies of toxicity in golden hamster showed that Lu did not alter blood biochemical parameters associated with liver and kidney functions; however, a slight increase of aspartate aminotransferase level in animals treated with 2.5 mg/kg of UA was detected. Lu and UA triterpenes eliminated amastigote forms in the spleen (87.5 and 95.9% of reduction, respectively) and liver of infected hamster (95.9 and 99.7% of reduction, respectively); and UA showed similar activity at eliminating amastigote forms in the spleen and liver than amphotericin B (99.2 and 99.8% of reduction). The therapeutic activity of both triterpenes was associated with the elevation of IFN- γ and/or iNOS expression in infected treated animals. This is the first comparative work showing the *in vitro* activity, toxicity, and therapeutic activity of Lu and UA in the chronic model of visceral leishmaniasis caused by *L. (L.) infantum*; additionally, both triterpenes activated cellular immune response in the hamster model of visceral leishmaniasis.

1. Introduction

Leishmaniasis is a neglected tropical disease and a public health problem worldwide, affecting vulnerable people in 98 countries, with 12 million cases detected worldwide per year; additionally, 1 billion people live in areas at risk of transmission [1]. The most severe form of the disease is visceral leishmaniasis (VL), also known as kala-azar, and in Latin America, it is caused by *L. (L.) chagasi* or *L. (L.) infantum* [2]. VL has an incidence of 1.6 cases per 100,000 inhabitants and is considered fatal if not properly treated. The main compromised organs are the spleen, liver, and bone marrow. Hepatomegaly, splenomegaly, pancytopenia, prolonged fever, and weight loss are the main clinical signs of manifested disease [3].

The therapeutic arsenal available for the treatment of leishmaniasis is scarce, and it is based on the use of the first-line drug, pentavalent antimonial [4]. Second-line drugs, such as amphotericin B, and its liposomal formulation AmBisome, paromomycin, and more recently, miltefosine, have also been used with different degrees of effectivity worldwide [4, 5]. Additionally, all these second-line drugs have limitations, such as long duration of treatment, high costs, local and systemic side effects that include pain in the local of application, nephrotoxicity, cardiotoxicity, gastrointestinal events, and teratogenic effects [6, 7].

Based on the aforementioned comments, it becomes clear the importance of identifying new leishmanicidal drugs. According to DNDi (Drugs for Neglected Diseases initiative), new prototype drugs need to be safe and affordable. In this sense, different studies have shown that natural molecules have these characteristics and can be considered prototype antileishmanial drugs [8]. Furthermore, these natural products are active and selective toward pathogens; additionally, the selectivity can be improved after synthetic modifications [9, 10].

Triterpenes are the most representative group of phytochemicals, comprising more than 20,000 recognized compounds, and are biosynthesized in plants through the cyclization of squalene [11]. Due to the structural diversity associated with their pharmacological effects, these compounds are considered interesting candidates for the development of new drugs [12, 13]. Moreover, in some Asian countries, triterpenes are used as anti-inflammatory, analgesic, hepatoprotectant, cardiotoxic agents, and sedatives [14, 15].

Betulin (Be), lupeol (Lu), and ursolic acid (UA) are pentacyclic triterpenoids widely distributed in nature and exhibit important pharmacological effects such as antioxidant, anti-allergic, antipruritic, antiangiogenic, and antimicrobial agents [16–18]. Additionally, these pentacyclic triterpenes have immunomodulatory activity and depending on the dose employed and route of administration Th1-associated cytokines as well as specific mediators of inflammation can be produced by innate or acquired immune cells [19]. In visceral leishmaniasis, antigen-specific immune suppression is caused by *L. (L.) infantum* [20, 21] and thus becomes essential to identify immunomodulatory-leishmanicidal prototype drugs that are able to reverse the immunosuppression caused

by parasites. Considering such inherent properties of pentacyclic triterpenes on the immunity, the scarcity of drugs available to treat leishmaniasis, the severe side effects of antimonial and amphotericin B, and the emergence of resistance in *Leishmania* sp., the present study was aimed at analyzing the activity and selectivity of Be, Lu, and UA on an American strain of *L. (L.) infantum*, as well as the possible target organelles. Additionally, the toxicity, therapeutic, and immunomodulatory activities of these triterpenes were studied in the experimental model of chronic visceral leishmaniasis.

2. Material and Methods

2.1. Chemical Analysis of the Triterpenes Be, Lu, and UA. Be, Lu, and UA triterpenes were purchased from Cayman Chemicals (USA). ^1H and ^{13}C nuclear magnetic resonance (NMR) spectra were recorded, respectively, at 300 and 75 MHz in a DPX-300 spectrometer (Bruker, USA) using deuteriochloroform (CDCl_3), deuterated dimethyl sulfoxide (DMSO-d_6), or deuterated methanol (CD_3OD) as solvents and internal standard (Merck, Germany). Elemental analysis was obtained in an Elemental Analyzer 2400 CHN (Perkin-Elmer, USA).

2.2. Animals and Ethical Considerations. Golden hamsters (*Mesocricetus auratus*), 8 weeks old, were obtained from Anilab (Paulinia, São Paulo, Brazil). This study was carried out in strict accordance with the recommendations of the guide for the Care and Use of Laboratory Animals of the Brazilian National Council of Animal Experimentation (<http://www.cobea.org.br>). The protocol was approved by the Ethics Committee of Animal Experiments of the Institutional Committee of Animal Care and Use at the Medical School of São Paulo University (056/16). Hamsters were housed in the Animal Experimental Institute of Tropical Medicine of São Paulo (IMT-USP), according to the standards of the Committee of Animal Welfare, and allowed access to food and water ad libitum throughout the study under a 12 h light cycle. The animals were anesthetized with intraperitoneal sodium thiopental at 1 mg/200 μL (Cristália, Brazil).

2.3. Cytotoxicity Assay. Peritoneal macrophages from golden hamsters (*Mesocricetus auratus*) (10^6 macrophages/well) were cultured in 96-well plates in RPMI medium supplemented with 10% of fetal bovine serum (Thermo Fisher, USA), 2 mM L-glutamine (Sigma-Aldrich, USA), 10 mM Hepes (Sigma-Aldrich, USA), 1 mM sodium pyruvate, 1% *v/v* nonessential amino acid solution (Thermo Fisher, USA), 10 $\mu\text{g}/\text{mL}$ of gentamicin (Thermo Fisher, USA), and 1000 U/mL of penicillin (Thermo Fisher, USA) (R10) along with triterpenes Be, Lu, and UA or the standard drug miltefosine (2.0 to 240 μM). The plates were incubated at 37°C, 5% CO_2 , for 24 h and then centrifuged at 400 \times g for 10 min at 4°C and washed 3 times, followed by addition of 9.6 μM of 3-(4,5-dimethylthiazol-2-yl)-2,5-diphenyltetrazolium bromide (MTT) (Sigma-Aldrich, USA). Four hours later, 50 μL of 10% sodium dodecyl sulfate (SDS) was added to each well. The plates were further incubated for 18 h and read in an ELISA reader at 595 nm. Cytotoxic concentration

50% (CC_{50}) was estimated using the nonlinear regression test with GraphPad Prism 5.0 software. The index of selectivity (SI) was estimated according to Passero and collaborators [22], and essentially, it is the ratio between CC_{50} and IC_{50} .

2.4. Promastigote Assay. Promastigote forms of *L. (L.) infantum* (MHOM/BR/72/46) were incubated in a 96-well culture plate in Schneider's medium (Sigma-Aldrich, USA) supplemented with 10% heat-inactivated fetal bovine serum and 50,000 IU/mL penicillin and 50 mg/mL streptomycin (S10), at 2×10^6 promastigotes/well with the triterpenes Be, Lu, and UA or standard drug miltefosine from 2.0 to 240 μ M (Sigma-Aldrich, USA). The negative control group was cultivated in medium and vehicle solution (PBS plus 1% DMSO). The parasites were incubated for 24 h at 25°C, then washed with 200 μ L of PBS three times with centrifugation at $1200 \times g$, 10 min at 4°C, followed by addition of 9.6 μ M of MTT. Four hours later, 50 μ L of 10% sodium dodecyl sulfate (SDS) was added to each well [23]. The plates were further incubated for 18 h and read in an ELISA reader at 595 nm. Inhibitory concentration 50% (IC_{50}) was estimated using GraphPad Prism 5.0 software.

2.5. Activity of Triterpenes in Intracellular Amastigotes, Nitric Oxide, and Hydrogen Peroxide Production. Peritoneal macrophages from golden hamsters (10^6 macrophages) were collected and cultured on round coverslips in 24-well plates during 4 h in R10, and then, cells were infected with *L. (L.) infantum* promastigotes (10 parasites per 1 peritoneal macrophage). The plates were incubated overnight at 5% CO_2 at 37°C. Then, the triterpenes Be (14 to 113 μ M), Lu (12 to 96 μ M), and UA (2 to 22 μ M) were added to the infected macrophages. Of note, the highest concentration used was always below the values of the respective CC_{50} values. Miltefosine (18 to 74 μ M) was used as the positive control. After 24 hours, macrophage supernatants were collected and stored at -80°C for quantifications of nitric oxide (NO) (Life Technologies, USA) and hydrogen peroxide (H_2O_2) (Life Technologies, USA) according to the manufacturer's instructions of the respective kits. The coverslips were dried at room temperature, fixed in methanol, and stained by Giemsa (Sigma-Aldrich, USA). The number of infected macrophages and of parasites per macrophage was determined at least in 100 cells. The infection index (II) was expressed as the percentage of infected macrophages multiplied by the average number of amastigotes per macrophage according to Passero and collaborators [24], and the inhibitory concentration that inhibit 50% (IC_{50}) of the infection index was estimated using GraphPad Prism 5.0. As a positive control for NO and H_2O_2 , macrophages were incubated with 100 ng/mL LPS (Sigma-Aldrich, USA) according to Passero et al. [22].

2.6. Ultrastructural Alterations Induced by Triterpenes in *L. (L.) infantum*. Promastigote forms of *L. (L.) infantum* (2×10^6 promastigotes/well) were incubated in a 24-well culture plate in S10 with Lu and UA at EC_{50} for 24 h, 25°C. The control group was cultivated with medium and vehicle solution. The plate was centrifuged at $1200 \times g$, 4°C, for 10 min and washed three times with 200 μ L of PBS. Then, the pellets

were resuspended in glutaraldehyde 2% (Sigma-Aldrich, USA), pH 7.2, and incubated at 4°C, during 60 min. Parasites were postfixed in 1% osmium tetroxide (Sigma-Aldrich, USA), and further incubated with 0.5% aqueous uranyl acetate overnight, and dehydrated in a graded series of ethanol. Then, samples were embedded in a polyester resin, thin sectioned with Reichert ultramicrotome, double stained by uranyl acetate and lead citrate (Ladd Research Industries), and examined with a Jeol 1010 (Tokyo, Japan) transmission electron microscope (TEM).

2.7. Cell Membrane Integrity and Mitochondrial Membrane Potential Assays. Promastigote forms of *L. (L.) infantum* (2×10^6 promastigotes/well) were incubated in 96-well black culture plate (Corning Inc., USA) in S10 with the IC_{50} of triterpenes Lu and UA as well as miltefosine for 0, 10, 20, 30, 40, 50, 60, 120, and 1440 minutes. At each time point, the probes SYTOX Green at 0.5 μ M/well (Life Technologies, USA) or Rhodamine 123 at 3 μ M/well (Sigma-Aldrich, USA) were added in the parasite culture in order to evaluate cell membrane damage or mitochondrial membrane potential, respectively. Parasites were placed in the dark for 15 minutes at 25°C, then centrifuged at 1200 g, 5 min at 10°C, and washed three times with 200 μ L of PBS. Plates containing parasites stained with SYTOX Green were read in a fluorescence reader using 530 nm emission wavelength and 490 nm excitation, and parasites stained with Rhodamine 123 read with 520 nm emission wavelength and 485 nm excitation. Results were normalized in relation to the control, nontreated parasites. Triton X-100 (0.05 μ L) (Sigma-Aldrich, USA) was used as a positive control for cell membrane damage and oligomycin at 0.1 μ M/well (Cayman Chemicals, USA) as positive control of mitochondrial membrane potential inhibition.

2.8. Hepatic and Renal Biochemical Parameters. Healthy golden hamsters (8 weeks old) were divided into four groups containing 5 animals/group. The experimental groups were arranged as follows: groups 1 and 2 were treated with 2.5 mg/kg of UA or Lu, respectively. Group 3 was treated with 5.0 mg/kg of amphotericin B [25] (Cristália, Brazil), and group 4 was constituted by animals that received only the vehicle solution (control). Animals were treated by the intraperitoneal route, once a day, during 10 days. One week after the last injection, the animals were euthanized, sera collected, and the following biochemical parameters quantified: serum alanine transaminase (ALT), aspartate aminotransferase (AST), urea, and creatinine by colorimetric method on COBAS C111 equipment (Roche, USA).

2.9. Therapeutic Activity of Triterpenes in Visceral Leishmaniasis. Golden hamsters were infected intraperitoneally with 2×10^7 *L. (L.) infantum* promastigotes (MHOM/BR/72/46). The noninfected control group was injected with PBS alone. Infected hamsters were divided into 4 groups, with 5 animals each. After 60 days of infection, animals were treated with UA, Lu, or AmB and the last group was constituted by animals that received only the vehicle solution (control). The protocol of the treatment is described in the Section 2.8. One week after the last injection, animals

TABLE 1: Leishmanicidal and cytotoxic activity and selective index of betulin (Be), lupeol (Lu), and ursolic acid (UA). Results are expressed by mean and standard error of triplicates from three different experiments.

Compound	IC ₅₀ (μ M) promastigotes	IC ₅₀ (μ M) amastigotes	CC ₅₀ (μ M)	SI promastigotes	SI amastigotes
Be	133.0 \pm 3.0	NA	170.4 \pm 0.5	1.3	NA
Lu	4.0 \pm 0.3	17.5 \pm 0.4	\geq 240	\geq 58.5	\geq 13.4
UA	8.0 \pm 0.2	3.0 \pm 0.2	42.1 \pm 0.2	5.3	14.0
Miltefosine	13.5 \pm 0.9	33.4 \pm 2.0	89.3 \pm 8.3	6.6	2.7

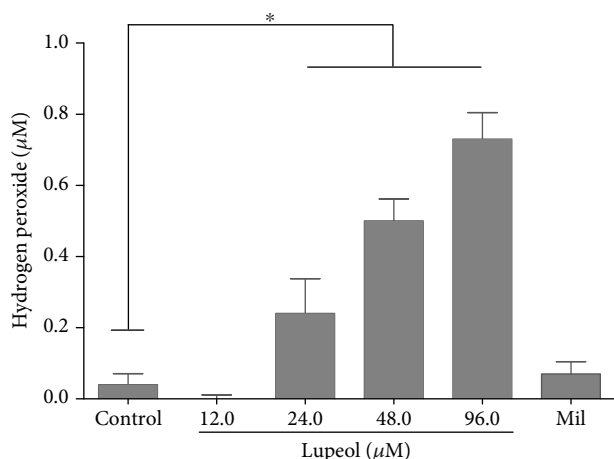


FIGURE 1: Hydrogen peroxide production. Macrophages infected with *L. (L.) infantum* were incubated with different concentrations of betulin (Be), lupeol (Lu), ursolic acid (UA), and miltefosine. After 24 h, the supernatants were collected and the NO and H₂O₂ levels were quantified. Only infected macrophages treated with Lu produced H₂O₂. * $p < 0.05$ compared to control.

were euthanized and the spleen and liver were collected to quantify the splenic and hepatic parasitism by limiting-dilution assay [26]. Additionally, amastigote forms in such organs were demonstrated by immunohistochemistry technique [27].

2.10. Cell Immune Response. RNA from hamster spleen fragments (~10 mg) was extracted using the commercial RNeasy Mini Kit (Qiagen, Germany) according to the manufacturer's protocol. cDNA was synthesized with the SuperScript[®]-VILO™ cDNA synthesis kit (Life Technologies, USA). Amplification consisted of an initial denaturation phase at 95°C for 10 min, followed by 40 amplification cycles consisting of 95°C for 15 s, 61°C for 90s, and 72°C for 30 s, using a thermocycler (Eppendorf, Germany). Prior to quantification, the efficiency of each reaction was verified using cDNA from the spleens of a healthy animal; it was always above 95%. Expression levels of genes of interest were normalized to β -actin (endogenous control). Quantitative PCR (qPCR) reaction was carried out using the GoTaq[®] 1-Step RT-qPCR System (Promega Corporation, Madison, WI, USA) and 75 nM of primers. The primer sequences (Sigma-Aldrich, USA) were as follows (5' to 3'): IFN- γ forward: GACAACCAG GCCATCC and reverse: CAAAACAGCACCGACT; IL-10 forward: TGGACAACATACTACTACTG and reverse:

GATGTCAAATTCATTCATGGC; iNOS forward: CGAC GGCACCATCAGAGG and reverse: AGGATCAGAGG CAGCACATC; and β -actin forward: TCCTGTGGCAT CCACGAAACTACA and reverse: ACAGCACTGTGTTG GCATAGAGGT. Quantification results are expressed in fold changes of 2^{- Δ Ct} over the infected control group. PCR products were electrophoresed on 2% agarose gels to confirm amplification of products with the correct size; one single amplification product of predicted size, according to Lafuse et al. [28], was always obtained for such reactions.

2.11. Statistical Analysis. All data obtained have been reported as the mean of three independent assays. Values are expressed as mean \pm standard error. Statistical analyses were performed using GraphPad Prism 5.0 software, and the ANOVA test was used to assess the differences between groups. Statistical significance was set at a p value < 0.05 .

3. Results

3.1. Chemical Analysis of the Triterpenes. NMR (¹H and ¹³C) data triterpenes betulin (Be), lupeol (Lu), and ursolic acid (UA) were recorded, and obtained data were compared with those reported in the literature [29–31]. These data, in association with elemental analysis, indicated that tested compounds exhibited more than 99.5% of purity (supplementary material 1).

3.2. Effect of Triterpenes on Promastigotes, Amastigotes, and Host Cells. Promastigote forms of *L. (L.) infantum* were incubated with the triterpenes during 24 h, and the inhibitory 50% concentration (IC₅₀) for each compound was estimated. All triterpenes were active against promastigote forms of *L. (L.) infantum*, being Lu (IC₅₀ = 4.0 \pm 0.3 μ M) more effective at inhibiting promastigote form growth, followed by UA (IC₅₀ = 8.0 \pm 0.2 μ M) and Be (IC₅₀ = 133.0 \pm 3.0 μ M). Miltefosine, used as positive control, showed an IC₅₀ of 13.5 \pm 0.9 μ M (Table 1). Regarding the cytotoxic potential of triterpenes on peritoneal macrophages of golden hamsters, it was verified that Lu presented CC₅₀ above 200 μ M. Triterpenes Be and UA displayed a CC₅₀ of 170.4 \pm 0.5 μ M and 42.1 \pm 0.2 μ M, respectively. Miltefosine eliminated 50% of the cell population with 89.3 \pm 8.3 μ M (Table 1).

Based on the ratio between IC₅₀ and CC₅₀, it was possible to calculate the SI of the triterpenes toward *L. (L.) infantum*. In this regard, compound Lu was 58.5 times more selective to promastigote forms than the host macrophages, followed by triterpenes UA and Be (SI = 5.3 and 1.3, respectively).

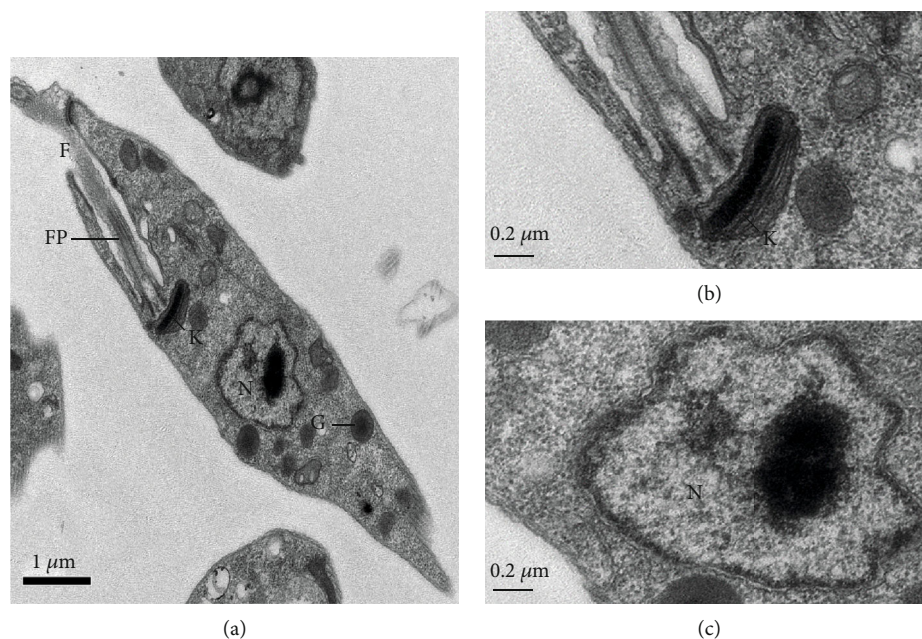


FIGURE 2: Ultrastructure of promastigote forms of *L. (L.) infantum*: (a) general morphology of *L. (L.) infantum* promastigote ($\times 25K$); (b) detail of flagellar pocket (FP) and kinetoplast (K) of control untreated ($\times 80K$); glycosome (G); (c) nucleus (N), membrane, and chromatin without changes in untreated control ($\times 80K$).

Miltefosine presented a SI of 6.6. These data are summarized in Table 1.

Macrophages infected with *L. (L.) infantum* and treated with triterpenes Lu and UA exhibited significant decrease in the parasitism, as demonstrated by the respective IC_{50} values. As shown in Table 1, the most active triterpene was UA followed by Lu, with IC_{50} values of $3.0 \pm 0.2 \mu M$ and $17.5 \pm 0.4 \mu M$. Be was inactive on amastigote forms of *L. (L.) infantum*. Miltefosine killed amastigote forms with an IC_{50} of $33.4 \pm 2.0 \mu M$. Comparatively, Lu and UA triterpenes were more effective at killing intracellular amastigote forms compared to the standard drug miltefosine. Selectivity indexes of analyzed triterpenes over amastigote forms of *L. (L.) infantum* were higher than those determined to miltefosine (SI = 2.7).

3.3. Quantification of Nitric Oxide and Hydrogen Peroxide.

Macrophages infected with *L. (L.) infantum* and treated with triterpenes Be, Lu, and UA did not produce quantifiable levels of NO. By the other side, macrophages infected and treated with Lu increased the levels of H_2O_2 in a dose-dependent manner when compared to the control group ($p < 0.05$), as indicated in Figure 1. Infected macrophages treated with triterpenes Be, UA, or miltefosine did not produce quantifiable H_2O_2 . Noninfected macrophages did not produce measurable levels of H_2O_2 . Macrophages treated with LPS produced high amounts of NO ($17.1 \pm 2.2 \mu M$) and H_2O_2 ($213.1 \pm 24.4 \mu M$).

3.4. Ultrastructural Changes in Promastigote Forms Treated with Triterpenes Lu and UA. Control promastigote forms showed a well-preserved external structure, with fusiform shape and intact cell membrane (Figure 2(a)). The cyto-

plasm, flagellum (F), and flagellar pocket (FP) exhibited regular morphology (Figures 2(a) and 2(b)). The kinetoplast (K), presented in detail in Figure 2(b), and the nucleus (N) (Figure 2(c)) displayed normal morphology.

Promastigote forms treated with Lu at the IC_{50} for 24 h showed major changes in the morphology (Figure 3(a)). Cell membrane protrusions were detected (arrowhead); the cytoplasm presented areas of cytoplasm degradation (*), resembling autophagic vacuoles (Figure 3(a)). The complex mitochondria (M)–kinetoplast (K) was swelled, and disruption of the mitochondrial cristae (Figures 3(a) and 3(b)) was observed. Parasite nucleus (N) seems to be degraded and fragmented (Figures 3(a) and 3(c)).

Figure 4(a) shows parasites treated with UA during 24 h. Parasites lost the fusiform shape (Figure 4(a)); the cytoplasm seems degraded showing changes resembling autophagic vacuoles (*) (Figures 4(a) and 4(b)); myelin-like figures (MF) were detected (Figure 4(b)). Blebs were identified in the outer cell membrane of promastigote forms treated with UA (Figure 4(c), arrowhead). Moreover, mitochondrial bleb containing DNA was identified in the kDNA of parasites treated with UA (Figure 4(a), arrowhead). The nucleus (N) of promastigote forms presented with dense and peripheral chromatin that appears to be fragmented (Figure 4(a)).

L. (L.) infantum treated with miltefosine lost the fusiform morphology, and the cytoplasm was degraded, showing structures resembling autophagic vacuoles (*). Nuclear membrane detachment was observed (Figure 5(a), black arrow); additionally, fragmentation of chromatin was detected in the nucleus (Figures 5(a) and 5(c)). The complex kDNA-mitochondria (M) was swelled (Figure 5(a)) and fragmented, cristae were disrupted, and blebs were observed (Figure 5(b)).

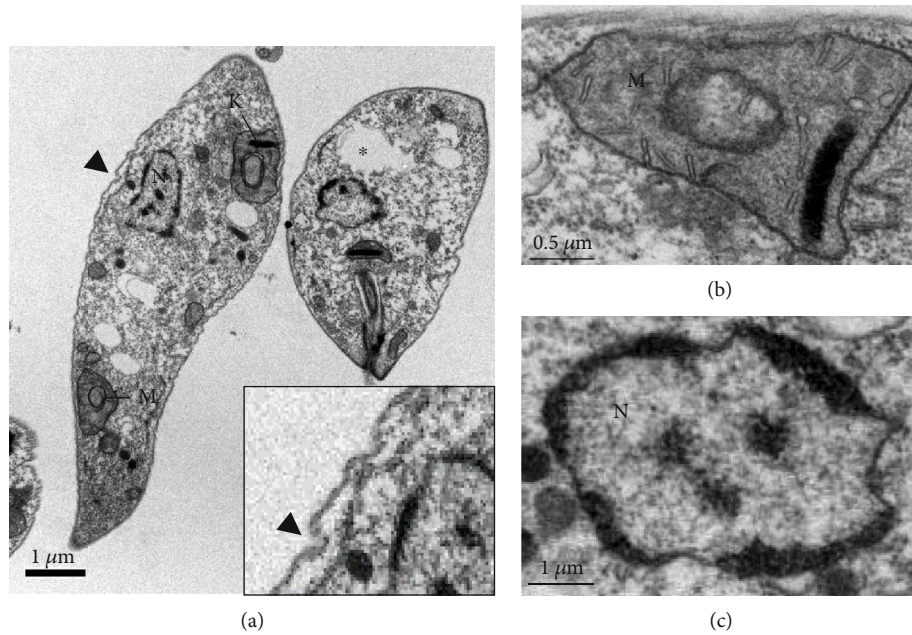


FIGURE 3: Ultrastructure of promastigote forms of *L. (L.) infantum* treated with IC_{50} of lupeol (Lu) for 24 h: (a) parasites treated with lupeol lost the fusiform shape, displayed cell membrane protrusions (arrowhead) and areas of cytoplasm degradation (*); (b) detail of the mitochondria and kinetoplast from parasites treated with Lu ($\times 50K$); (c) nucleus showing condensed and fragmented chromatin after Lu treatment ($\times 50K$).

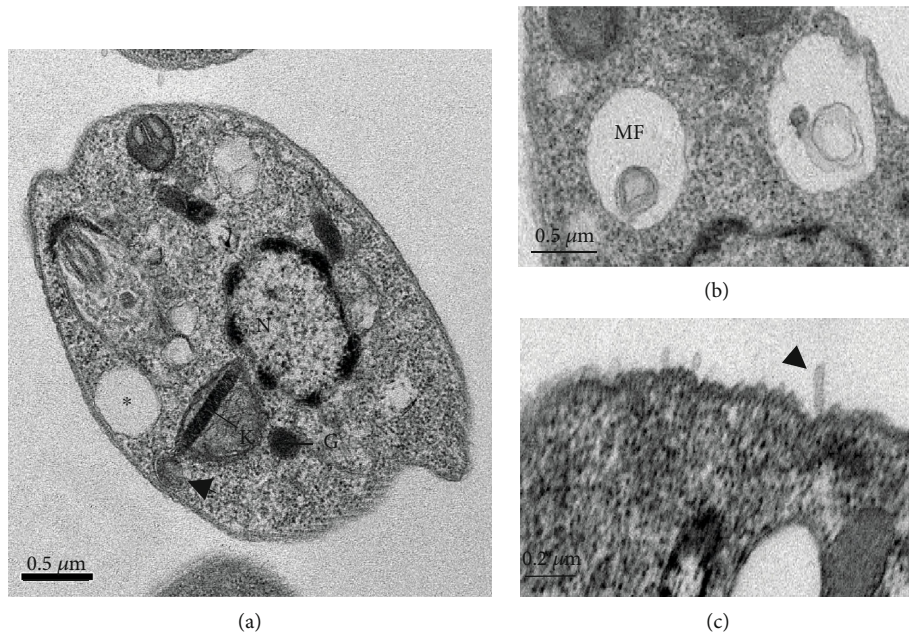


FIGURE 4: Ultrastructure of promastigote forms of *L. (L.) infantum* treated with IC_{50} of ursolic acid (UA) for 24 h: (a) parasite showing round shape morphology, with areas of cytoplasm degradation (*) and nucleus with condensed and peripheral chromatin; the kinetoplast was swollen, and a bleb was identified (arrowhead) ($\times 30K$); (b) parasite treated with UA displayed myelin-like figures (MF) ($\times 25K$); (c) blebbing in the cell membrane (arrowhead) of promastigote forms treated with UA ($\times 80K$).

3.5. Cell Membrane Integrity and Mitochondrial Membrane Potential Assays. Corroborating the morphological changes, it was observed that the triterpenes Lu and UA as well as miltefosine did not damage the cell membrane of promastigote forms of *L. (L.) infantum* (Figures 6(a)–6(c)). In addition, parasites reduced the emission of fluorescence by 50% at

1440, and it is associated with the reduction of the parasite population by 50%. Parasites incubated with Triton X-100 emitted high levels of fluorescence (Figures 6(a)–6(c)).

As observed in the TEM images, treated parasites showed morphological changes in the mitochondrial-kDNA complex, and to validate such alterations, the mitochondrial

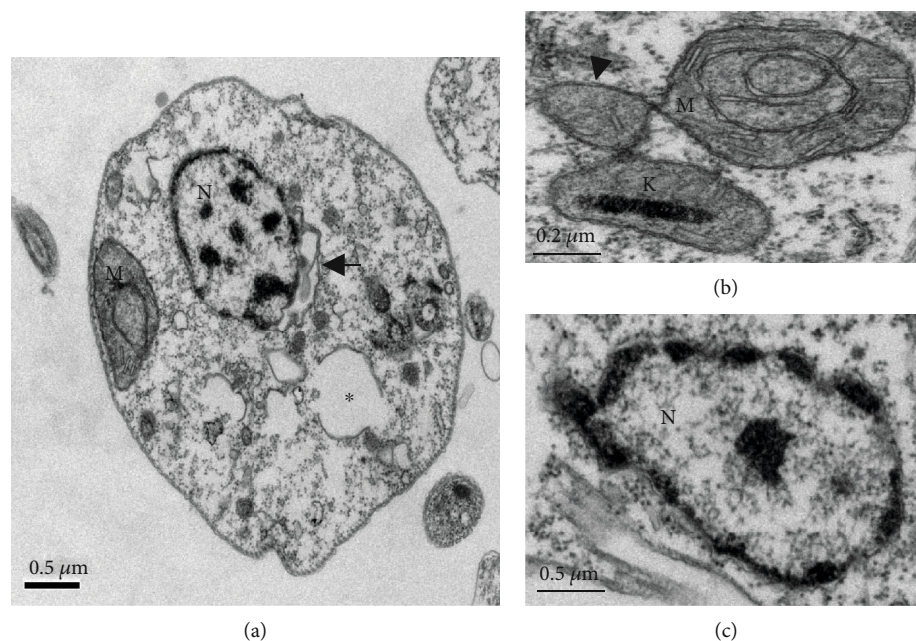


FIGURE 5: Ultrastructure of promastigote forms of *L. (L.) infantum* treated with EC_{50} of miltefosine during 24h: (a) parasites treated with miltefosine lost its fusiform morphology; areas of cytoplasm degradation (*) and detachment of nuclear membrane were observed (black arrow) ($\times 30K$); (b) miltefosine altered the morphology of the kDNA (k)-mitochondria (M) complex that presented to be fragmented and with blebs (arrowhead) ($\times 80K$); (c) nucleus (N) with condensed chromatin in parasites treated with miltefosine ($\times 50K$).

membrane potential of treated parasites was analyzed. Triterpenes Lu and UA as well as positive control miltefosine (Figures 6(d)–6(f)) decreased the mitochondrial membrane potential ($\Delta\Psi_m$) in a time-dependent manner at 30 minutes of incubation. Additionally, at 45 minutes, a hyperpolarization was detected in parasites treated with UA and miltefosine. Parasites treated with triterpenes Lu and UA displayed complete inhibition of the mitochondrial membrane potential at 60 and 1440 minutes of incubation (Figures 6(d) and 6(e), respectively). The mitochondria of parasites treated with miltefosine showed complete inhibition of the mitochondrial membrane potential at 1440 minutes (Figure 6(e)). Oligomycin (positive control) inhibited the mitochondrial membrane potential over time.

3.6. Hepatic and Renal Biochemical Parameters. Deficiencies in the metabolism and excretion of triterpenes were analyzed by hepatic and renal functions, respectively. In respect to hepatic function, it was verified that UA treatment caused a significant increase in the level of AST (Figure 7(a)) but not ALT (Figure 7(b)). Lu and AmB did not change the biochemical parameters of the liver. Animals treated with Lu and UA did not change renal functions, as the levels of urea and creatinine were similar to the healthy group (Figures 7(c) and 7(d)). By the other side, animals treated with AmB significantly increased the level of serum creatinine, as demonstrated in Figure 7(d).

3.7. Therapeutic Activity of Triterpenes in Visceral Leishmaniasis. Infected hamsters treated with 2.5 mg/kg of UA or Lu showed significant reduction in the splenic and hepatic parasitism (Figures 8(a) and 8(b), respectively) in

comparison to infected control ($p < 0.05$), as demonstrated by limiting-dilution assay. In addition, tissue amastigote forms were stained by immunohistochemistry, and it is possible to observe that the treatment carried out with UA or Lu drastically decreased the number of parasites in comparison to the spleen and liver of infected control.

3.8. Cell Immune Response. Analysis of cellular immune response in the spleen of *L. (L.) infantum*-infected hamsters showed that animals treated with 2.5 mg/kg of UA or Lu expressed higher levels of $IFN-\gamma$ compared to the infected control (Figure 9(a), $p < 0.05$). Animals treated with amphotericin B expressed lower levels of $IFN-\gamma$ in comparison to the infected control, and it was similar to the healthy control. In respect to iNOS gene expression, only animals treated with lupeol showed significant elevation in the expression of this mediator of inflammation compared to the infected control (Figure 9(b), $p < 0.05$). Animals treated with 5 mg/kg of amphotericin B exhibited a significant decrease expression of IL-10 in comparison to the infected control (Figure 9(c), $p < 0.05$).

4. Discussion

The quality of drugs is a fundamental factor to ensure pharmacological activity and minimize the occurrence of unwanted effects resulting from the presence of impurities and/or degradation products. Thus, according to the nuclear magnetic resonance, associated with the elemental analysis, it was possible to confirm the purity degree of all studied triterpene (see supplementary material 1). Additionally, NMR spectral analysis was useful to confirm the identity of

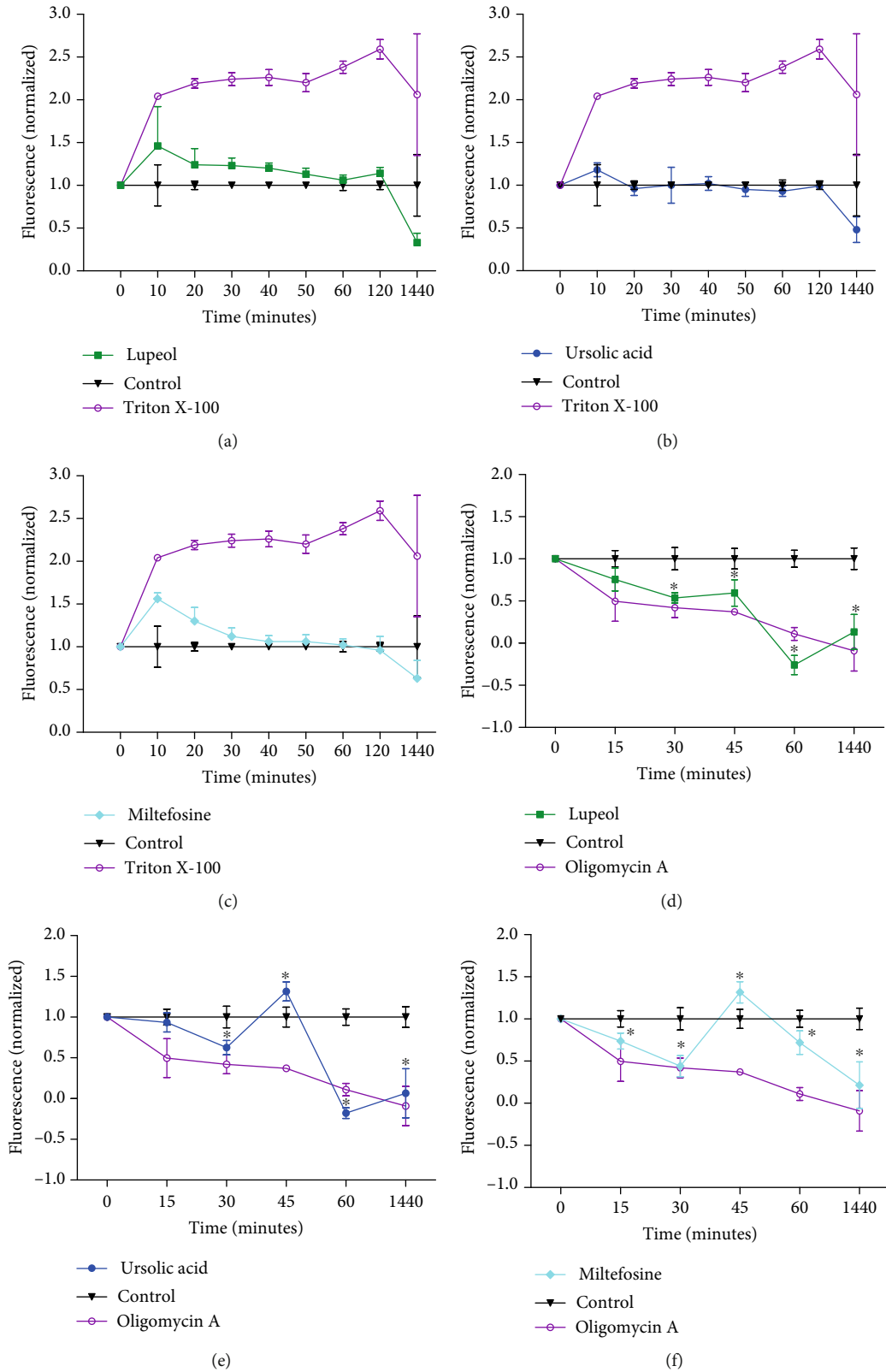


FIGURE 6: Cell membrane integrity and mitochondrial membrane potential assays of *L. (L.) infantum* promastigotes. Parasites were treated with Lu (a), UA (b), and miltefosine (c) at the IC₅₀ and at different time points, the probe SYTOX® Green (0.5 μM) was added, and the fluorescence intensity was analyzed. Triton X-100 was used as a positive control. In (d-f), promastigote forms were incubated with the IC₅₀s of the Lu, UA, and miltefosine, respectively, and at different time points, Rhodamine 123 probe (3 μM) was added to the parasites, and the fluorescence intensity was analyzed. Oligomycin A was used as a positive control. Fluorescence was normalized relative to the control parasites.

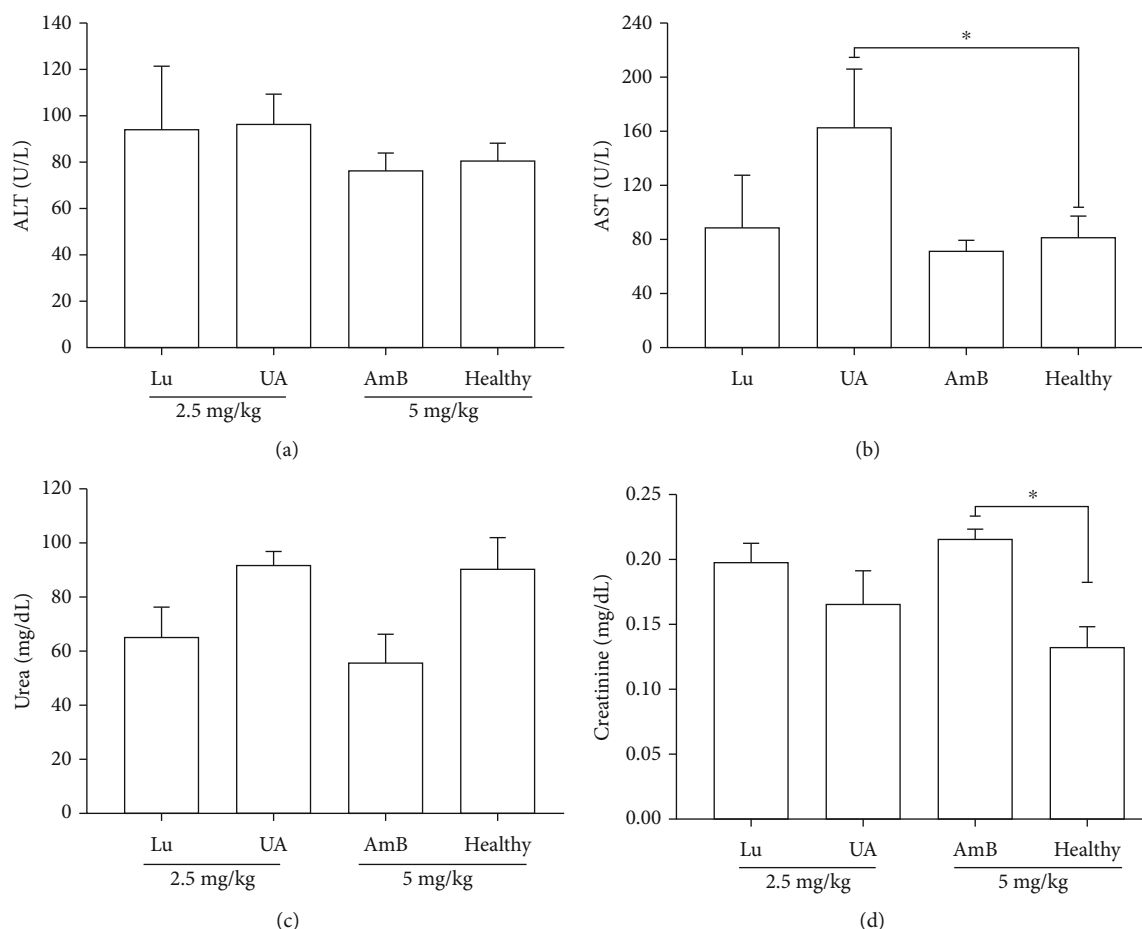


FIGURE 7: Blood biochemical parameters of hamster treated with lupeol (Lu), ursolic acid (UA), and amphotericin B (AmB). Levels of ALT (a), AST (b), urea (c), and creatinine (d) were quantified in the serum of animals treated with 2.5 mg/kg of lupeol (Lu), ursolic acid (UA), or 5 mg/kg of amphotericin B (AmB) during 10 consecutive days by intraperitoneal route. * $p < 0.05$ indicates statistical significance.

triterpenes such as betulin (Be), lupeol (Lu), and ursolic acid (UA). These triterpenes showed *in vitro* leishmanicidal activity on promastigote forms of *L. (L.) infantum* that were more sensitive to Lu, followed by UA and Be. However, Lu and UA impacted the survival of intracellular amastigote forms, while Be was inactive. Although triterpenes presented similar structures, they also displayed different activities on promastigote and amastigote forms. Possibly, the liposolubility [32] is one factor associated with the biological activities found herein, since to interact with the cell membrane, molecules need to present hydrophobic groups, allowing their uptake by the cell [33]. The lipophilicity of a compound can be characterized by its partition coefficient ($\log P$) between octanol and water, octanol being assumed to have a similar lipophilicity to cell membranes [32]. This coefficient may be used as one of the predictors of drug absorption by passive diffusion [34]. Lu is the triterpene with the highest lipophilicity, with a $\log P$ of 7.67 [35], followed by the UA and Be with $\log P$ values determined, respectively, as 6.43 [36] and 6.17 [32], suggesting that these triterpenes have intermediate lipophilicity to interact with the cell membranes and access to the intracellular environment.

Additionally, minor structural differences among studied triterpenes can determine the potency of leishmanicidal

effect. Considering Be structure, the presence of two hydroxyl groups at positions C-3 and C-28 should be crucial to the absence of the leishmanicidal activity of this triterpene. By the other side, Lu exhibits only one hydroxyl group at position C-3 and it is 33 times more effective at killing promastigote forms than Be. Additionally, on amastigote forms, this difference is higher, since Be was inactive, while Lu showed high activity and selectivity toward intracellular forms. UA was the most active at killing amastigote forms (5.8 times) in comparison to Lu, and such pharmacological activity has been related to the presence of the carboxylic acid at the position C-28 in the structure of compound UA that was not observed in the structure of Lu. By comparing the structure of all studied triterpenes, the presence of the hydroxyl group at the position C-28 found in the structure of Be may determine the low or absent leishmanicidal activity found herein. Additionally, it is important to note that Lu and UA showed higher activity and selectivity toward parasites than miltefosine, and thus, these molecules should be considered to develop new leishmanicidal drugs. Additionally, previous studies have been verified that both Lu and UA are active on promastigote and amastigote forms of different *Leishmania* species [26, 37–39], suggesting that besides high

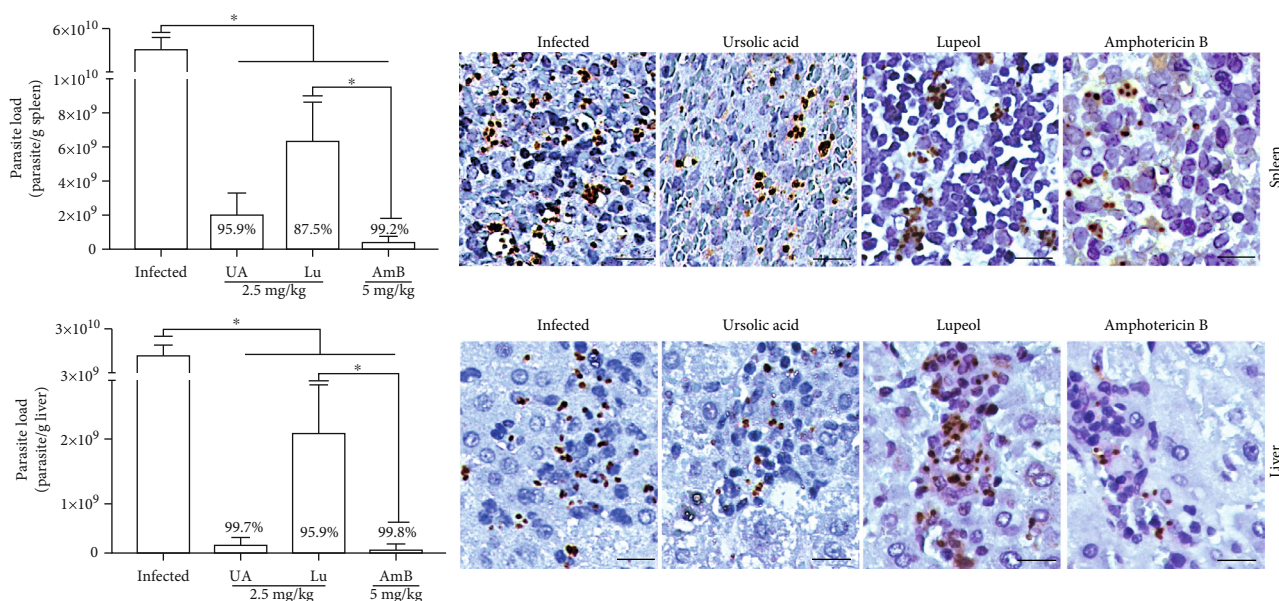


FIGURE 8: Splenic and hepatic parasitism from hamsters infected with *L. (L.) infantum* and treated with triterpenes. Hamsters were infected with promastigote forms of *L. (L.) infantum*, and four weeks after infection, animals were intraperitoneally treated once daily during 10 days with 2.5 mg/kg of ursolic acid (UA), lupeol (Lu), or 5 mg/kg of amphotericin B (AmB). The splenic and hepatic parasitism was quantified by limiting-dilution assay; additionally, amastigote forms were stained by immunohistochemistry technique.

selectivity, both triterpenes have multispectral activity that needs to be considered for drug development.

Regarding cytotoxic potential of triterpenes on peritoneal macrophages of golden hamsters, it is important to note that Lu had CC_{50} above 240 μ M that was higher than that of miltefosine. UA showed the highest toxic potential toward macrophage, and it was associated with the presence of carboxylic acid at C-28 and hydroxyl group at C-3 position. In spite of showing some toxicity to the host cell, the selectivity toward amastigote forms (SI~14) suggests that this triterpene is still an important leishmanicidal agent. Moreover, other studies have already shown that these triterpenes have absent or low cytotoxic effects on different cell lineages [40–43], suggesting the applicability of such molecules in therapeutic studies.

During infection, *Leishmania* sp. suppresses respiratory burst in the host macrophages, so compounds able to increase macrophage respiratory activity can aid the parasite elimination. In this regard, it was observed that infected macrophages treated with Lu produced elevated amounts of H_2O_2 that is able to trigger programmed cell death in *Leishmania* sp. [42, 44, 45]. Thus, Lu was able to activate infected host macrophages to a leishmanicidal state, and such activity, triggered by Lu, can be an additive mechanism to eliminate parasites [41].

In order to analyze major morphological changes induced by triterpenes, promastigote forms of *L. (L.) infantum* were analyzed by transmission electron microscopy, followed by physiological changes in the plasma and mitochondrial membranes. In general, parasites showed altered morphology, intracellular disorganization, blebs, chromatin condensation, nuclear fragmentation, and different cytoplasmic alterations, mainly related to the cytoplasmic extraction. Additionally, changes in the parasite mitochondria and nucleus suggest that triterpenes act on the parasite's bioener-

getics or even inducing programmed cell death [46–48]. In fact, Lu and UA were able to inhibit mitochondrial transmembrane potential after 30 minutes of incubation, suggesting that the mitochondria can be the target organelle of these triterpenes. Additionally, parasites treated with UA showed a transient recovery of the mitochondrial membrane potential that may be associated with a hyperpolarization of this organelle as previously mentioned by Bilbao-Ramos and collaborators [38], suggesting that UA triggers programmed cell death in *L. (L.) infantum*. According to Vannier-Santos and Castro [49], pyknosis and nuclear fragmentation observed in parasites treated with drugs can be considered a morphological indicator of programmed cell death. In parasites incubated with miltefosine, shrinkage of the cell surface was observed, presence of myelin-like figures, and fragmentation of mitochondria and nuclear DNA suggests the occurrence of programmed cell death, as previously demonstrated [50, 51], suggesting that miltefosine can be a good control of programmed cell death in *Leishmania* sp. Previous studies have shown that programmed cell death may be a common mechanism of cell death in *Trypanosoma* sp. [52–54] and *Leishmania* [53, 55] in response to chemotherapeutic agents such as miltefosine [50] and triterpenes [39, 42, 43]. Thus, the leishmanicidal activity of triterpenes can be associated with the major changes in the mitochondria, in the nucleus, and in the intracellular compartments that might be related to programmed cell death in *L. (L.) infantum*.

Despite cell protrusions and blebs observed in the cell membrane of promastigote forms treated with Lu or UA, cell membrane lysis was not detected by morphology and physiology studies. Protrusions and blebs observed in the cell membrane of treated parasites can be the effect of the triterpenes on the cytoskeleton of promastigote forms [49]. Similar morphological changes were also observed in *Trypanosoma cruzi*

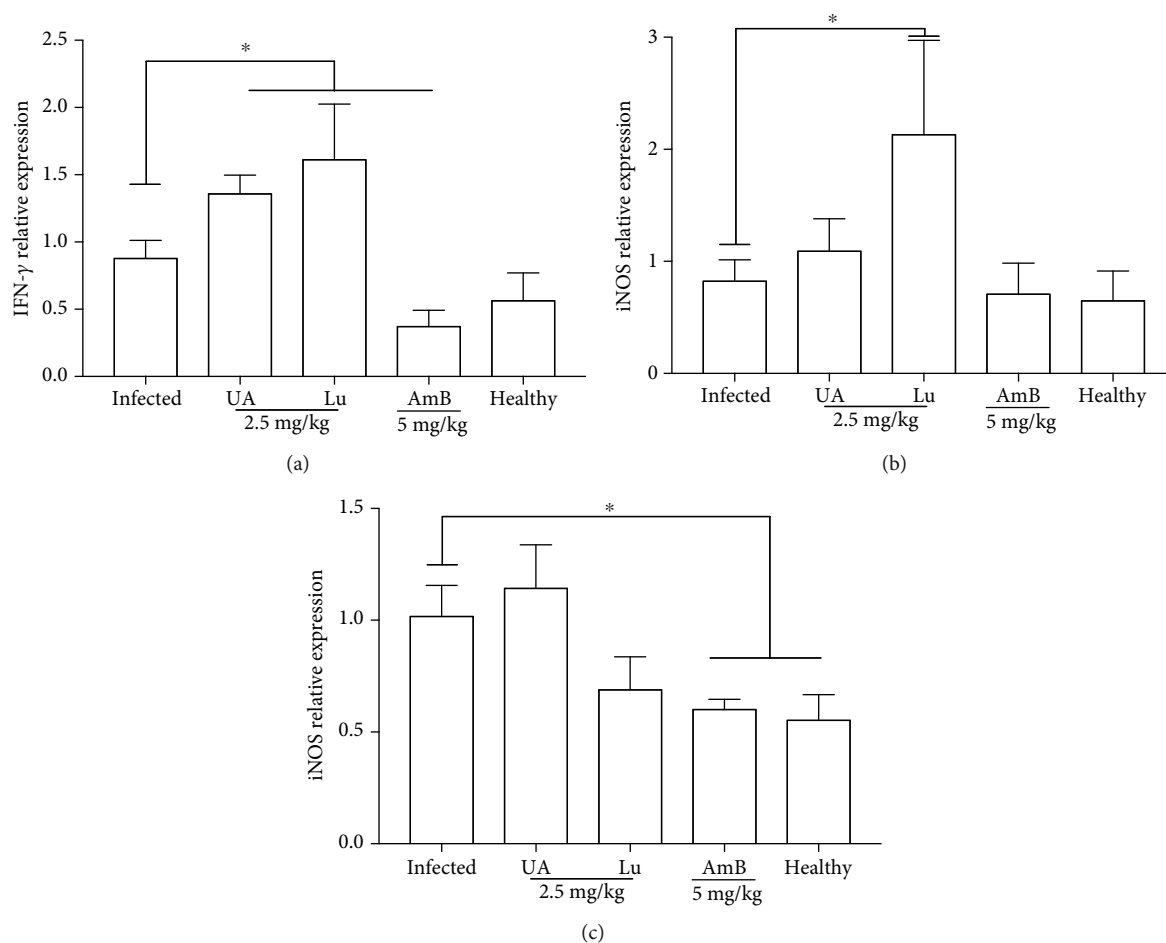


FIGURE 9: Cell immune response of hamsters infected with *L. (L.) infantum* and treated with triterpenes and amphotericin B. IFN- γ (a), iNOS (b, and IL-10 (c) relative gene expression in the spleen of infected golden hamsters treated with 2.5 mg/kg of ursolic acid (UA) or lupeol (Lu) and 5 mg/kg of amphotericin B (AmB). Relative gene expression was estimated by quantitative PCR. The expression levels of genes of interest were normalized to β -actin. * $p < 0.05$ indicates statistical significance.

treated with lysophospholipid analogues, such as edelfosine, ilmofosine, and miltefosine [56]. In addition to these changes, membrane debris were observed in areas resembling autophagic vacuoles. Previous works demonstrated that parasites recycle abnormal structures during an autophagic process [49, 57, 58]; besides targeting mitochondria, both triterpenes may also trigger autophagy in promastigote forms.

Both triterpenes showed promising *in vitro* activity and selectivity toward *L. (L.) infantum* amastigotes, and thus, golden hamsters were injected with Lu or UA to evaluate hepatic and renal functions after treatment. Healthy golden hamsters treated with UA showed a significant increase of aspartate transaminase (AST) compared to the healthy animals. Both ALT and AST are produced by hepatocytes; therefore, increased levels of ALT and AST indicate hepatocellular injury. In the present study, UA-treated hamsters showed elevation only in AST, suggesting an initial hepatocellular injury. Previous studies already showed that low doses of UA are safe for BALB/c mice, and golden hamster treated with 2 mg/kg showed no changes in serum ALT or AST; furthermore, no morphological changes in the liver structure were observed; however, higher doses of UA (150 mg/kg)

administered with a diet over 6 weeks can cause hepatic damage [59]. By the other side, UA can be found in fruits and vegetables present in the human diet; furthermore, this triterpene also is used as a dietary supplement for humans [60]. Thus, UA hepatotoxicity may be related to the dosage, duration of treatment, and route of administration. In contrast, Lu did not cause changes in the levels of ALT or AST.

Golden hamsters treated with Lu or UA did not change the levels of urea and creatinine, suggesting that both triterpenes are not nephrotoxic. By the other side, animals treated with 5 mg/kg of amphotericin B showed an increase in the creatinine level, suggesting that AmB caused renal toxicity in golden hamsters. Previous study already showed that hamsters treated with 5.0 mg/kg/day of AmB during 16 days displayed morphological changes compatible with acute renal toxicity [26]. AmB also induced nephrotoxicity in patients that presented reduced glomerular filtration rate and tubular dysfunction [61], reinforcing that one of the main side effects of AmB in vertebrates is renal failure.

Although the treatment with UA at 2.5 mg/kg induced toxicity to the liver, its efficacy in the model of visceral leishmaniasis was assessed, since only the levels of AST marker

increased after treatment. In fact, UA and Lu were able to eliminate amastigotes forms in the spleen and liver of *L. (L.) infantum*-infected hamsters; however, UA treatment showed higher efficacy at eliminating hepatic parasites than Lu treatment; moreover, UA showed similar efficacy than AmB treatment. Lu, as well as UA, was poorly investigated concerning the leishmanicidal effect, and few available works showed the therapeutic activity of this triterpene only in the murine model of visceral leishmaniasis that mimics the acute phase of infection; thus, currently, this is the first work showing that Lu is able to decrease amastigote forms in the spleen and liver from hamsters in the chronic phase of visceral leishmaniasis.

In leishmaniasis, resistance to infection has been associated with the development of a Th1 immune response, with remarkable amounts of interferon gamma (IFN- γ) cytokine that can be mainly produced by NK and T cells [62–64]. As phagocytes are exposed to IFN- γ , classical activation and induction of microbicidal mechanisms can occur, with the participation of inducible nitric oxide synthase enzyme (iNOS), as well as nitric oxide (NO), a mediator of inflammation, that along with other reactive oxygen and nitrogen species can kill intracellular parasites [64–66]. In the present study, an association between leishmanicidal activity *in vivo* and increased IFN- γ expression was observed, suggesting that both these triterpenes may direct the immune response to a Th1 immune response, emphasizing that besides a direct activity on parasites, the therapeutic activity of triterpenes is mediated by immune response activation [26, 39].

In contrast to resistance, the susceptibility in visceral leishmaniasis has been accompanied by elevation in the levels of IL-10, a cytokine with anti-inflammatory activity and suppressive effects on the Th1 immune response. Thus, elevation in the level of IL-10 frequently results in parasite proliferation as well as chronification of *Leishmania* infection [67, 68]. UA or Lu treatment did not inhibit IL-10 expression. Possibly, in this chronic model of visceral leishmaniasis, where the disease is fully manifested, both Lu and UA lose the ability to restrain IL-10 expression and/or production, as mentioned previously [26], maintaining a small number of parasites in the spleen and liver of hamsters. Despite that, it is still important to note that both triterpenes eliminated high amounts of amastigote forms in the spleen and liver of infected animals, and even Lu is being less potent than UA and AmB, it was not toxic for hamsters and should be viewed as an important target to develop new leishmanicidal drugs.

Previous studies already discussed the *in vitro* and *in vivo* activities of both Lu and UA [26, 37, 69]; however, this is the first comparative work showing the leishmanicidal activity of related pentacyclic triterpenes in association with their structures, as well as morphological and physiological changes that took place in *L. (L.) infantum*. In addition, this is the first work showing the comparative therapeutic activity of both Lu and UA in the experimental model of chronic visceral leishmaniasis that is the most suitable model of natural infection. Taken together, data showed herein demonstrates that UA and Lu triterpenes were able to promote effective and selective antileishmanial activity on promastigote and amastigote forms of *L. (L.) infantum*, and possibly, the parasite

mitochondria may be the target organelle, since impairment of transmembrane potential was observed after 30 minutes of incubation; furthermore, morphological studies showed a complete disorganization of such organelle. Both triterpenes increased the cellular immune response in hamsters with visceral leishmaniasis, and it was associated with amastigote elimination in the spleen and liver, suggesting that the leishmanicidal activity is mediated by immunomodulation of both innate and acquired immune systems.

Data Availability

The data used to support the findings of this study are available from the corresponding author upon request.

Conflicts of Interest

The authors declare that they have no conflict of interest.

Acknowledgments

The authors would like to thank the São Paulo Research Foundation (FAPESP) for the support (Grants 2015/17623-6, 2016/00468-0, 2018/07885-1, and 2016/10324-6), HCFMUSP-LIM50, and CNPq scientific research award to JHGL and MDL.

Supplementary Materials

Figure 1: molecular structure of betulin, lupeol, and ursolic acid. Table 1: ^{13}C NMR of botulin, lupeol, and ursolic acid. Figure 2: ^1H NMR spectrum (δ , $\text{CDCl}_3+\text{CD}_3\text{OD}$, 300 MHz) of betulin (Be). Figure 3: ^{13}C NMR spectrum (δ , $\text{CDCl}_3+\text{CD}_3\text{OD}$, 75 MHz) of betulin (Be). Figure 4: ^1H NMR spectrum (δ , $\text{CDCl}_3+\text{CD}_3\text{OD}$, 300 MHz) of lupeol (Lu). Figure 5: ^{13}C NMR spectrum (δ , $\text{CDCl}_3+\text{CD}_3\text{OD}$, 75 MHz) of lupeol (Lu). Figure 6: ^1H NMR spectrum (δ , $\text{DMSO}-d_6$, 300 MHz) of ursolic acid (UA). Figure 7: ^{13}C NMR spectrum (δ , $\text{DMSO}-d_6$, 75 MHz) of ursolic acid (UA). Table 2: elemental analysis results. (*Supplementary Materials*)

References

- [1] WHO, *Leishmaniasis* October 2020, <https://www.who.int/leishmaniasis/en/>.
- [2] F. T. Silveira and C. E. P. Corbett, “Leishmania chagasi Cunha & Chagas, 1937: indigenous or introduced? A brief review,” *Revista Pan-Amazônica de Saúde*, vol. 1, no. 2, pp. 143–147, 2010.
- [3] F. Tajebe, M. Getahun, E. Adem et al., “Disease severity in patients with visceral leishmaniasis is not altered by coinfection with intestinal parasites,” *PLoS Neglected Tropical Diseases*, vol. 11, no. 7, article e0005727, 2017.
- [4] N. K. Copeland and N. E. Aronson, “Leishmaniasis,” *Current Opinion in Infectious Diseases*, vol. 28, no. 5, pp. 426–437, 2015.
- [5] F. Chappuis, S. Sundar, A. Hailu et al., “Visceral leishmaniasis: what are the needs for diagnosis, treatment and control?,” *Nature Reviews Microbiology*, vol. 5, no. 11, pp. 873–882, 2007.

- [6] A. K. Haldar, P. Sen, and S. Roy, "Use of antimony in the treatment of leishmaniasis: current status and future directions," *Molecular Biology International*, vol. 2011, 23 pages, 2011.
- [7] A. Maheshwari, A. Seth, S. Kaur et al., "Cumulative cardiac toxicity of sodium stibogluconate and amphotericin b in treatment of kala-azar," *The Pediatric Infectious Disease Journal*, vol. 30, no. 2, pp. 180-181, 2011.
- [8] S. L. Croft, E. Chatelain, and M. P. Barrett, "Antileishmanial and antitrypanosomal drug identification," *Emerging Topics in Life Sciences*, vol. 1, no. 6, pp. 613-620, 2017.
- [9] M. B. Isah, M. A. Ibrahim, A. Mohammed, A. B. Aliyu, B. Masola, and T. H. T. Coetzer, "A systematic review of pentacyclic triterpenes and their derivatives as chemotherapeutic agents against tropical parasitic diseases," *Parasitology*, vol. 143, no. 10, pp. 1219-1231, 2016.
- [10] N. Ullah, A. Nadhman, S. Siddiq et al., "Plants as antileishmanial agents: current scenario," *Phytotherapy Research*, vol. 30, no. 12, pp. 1905-1925, 2016.
- [11] E. Oldfield and F.-Y. Lin, "Terpene biosynthesis: modularity rules," *Angewandte Chemie (International Ed. in English)*, vol. 51, no. 5, pp. 1124-1137, 2012.
- [12] Z. Baharum, A. M. Akim, T. Y. Y. Hin, R. A. Hamid, and R. Kasran, "Theobroma cacao: review of the extraction, isolation, and bioassay of its potential anti-cancer compounds," *Tropical Life Sciences Research*, vol. 27, no. 1, pp. 21-42, 2016.
- [13] J. Favela-Hernández, O. González-Santiago, M. Ramírez-Cabrera, P. Esquivel-Ferriño, and M. Camacho-Corona, "Chemistry and pharmacology of Citrus sinensis," *Molecules*, vol. 21, no. 2, p. 247, 2016.
- [14] T. Geetha and P. Varalakshmi, "Anti-inflammatory activity of lupeol and lupeol linoleate in rats," *Journal of Ethnopharmacology*, vol. 76, no. 1, pp. 77-80, 2001.
- [15] R. A. Hill and J. D. Connolly, "Triterpenoids," *Natural Product Reports*, vol. 29, no. 7, pp. 780-818, 2012.
- [16] L. Wei, W. Zhang, L. Yin, F. Yan, Y. Xu, and F. Chen, "Extraction optimization of total triterpenoids from *Jatropha curcas* leaves using response surface methodology and evaluations of their antimicrobial and antioxidant capacities," *Electronic Journal of Biotechnology*, vol. 18, no. 2, pp. 88-95, 2015.
- [17] J. A. Jesus, J. H. G. Lago, M. D. Laurenti, E. S. Yamamoto, and L. F. D. Passero, "Antimicrobial activity of oleanolic and ursolic acids: an update," *Evidence-Based Complementary and Alternative Medicine*, vol. 2015, Article ID 620472, 14 pages, 2015.
- [18] A. Kishikawa, Y. Amen, and K. Shimizu, "Anti-allergic triterpenes isolated from olive milled waste," *Cytotechnology*, vol. 69, no. 2, pp. 307-315, 2017.
- [19] M. Laszczyk, "Pentacyclic triterpenes of the lupane, oleanane and ursane group as tools in cancer therapy," *Planta Medica*, vol. 75, no. 15, pp. 1549-1560, 2009.
- [20] H. Goto and J. A. L. Lindoso, "Immunity and immunosuppression in experimental visceral leishmaniasis," *Brazilian Journal of Medical and Biological Research*, vol. 37, no. 4, pp. 615-623, 2004.
- [21] H. Goto and M. . G. Prianti, "Immunoactivation and immunopathogeny during active visceral leishmaniasis," *Revista do Instituto de Medicina Tropical de São Paulo*, vol. 51, no. 5, pp. 241-246, 2009.
- [22] L. F. D. Passero, R. R. Assis, T. N. F. da Silva et al., "Differential modulation of macrophage response elicited by glycoinositol-phospholipids and lipophosphoglycan from *Leishmania (Viannia) shawi*," *Parasitology International*, vol. 64, no. 4, pp. 32-35, 2015.
- [23] E. S. Yamamoto, J. A. de Jesus, A. Bezerra-Souza et al., "Tolnafate inhibits ergosterol production and impacts cell viability of *Leishmania sp.*," *Bioorganic Chemistry*, vol. 102, p. 104056, 2020.
- [24] L. F. D. Passero, J. V. Sacomori, T. Y. Tomokane, C. E. P. Corbett, F. T. da Silveira, and M. D. Laurenti, "Ex vivo and in vivo biological behavior of *Leishmania (Viannia) shawi*," *Parasitology Research*, vol. 105, no. 6, pp. 1741-1747, 2009.
- [25] M. J. Corral, D. R. Serrano, I. Moreno, J. J. Torrado, M. Dominguez, and J. M. Alunda, "Efficacy of low doses of amphotericin B plus allicin against experimental visceral leishmaniasis," *The Journal of Antimicrobial Chemotherapy*, vol. 69, no. 12, pp. 3268-3274, 2014.
- [26] J. A. Jesus, T. N. Fragoso, E. S. Yamamoto et al., "Corrigendum to "Therapeutic effect of ursolic acid in experimental visceral leishmaniasis" [Int. J. Parasitol. Drugs Drug Resist. 7 (2017) 1-11]," *International Journal for Parasitology: Drugs and Drug Resistance*, vol. 7, no. 2, p. 250, 2017.
- [27] M. D. Laurenti, L. F. D. Passero, T. Y. Tomokane et al., "Dynamic of the cellular immune response at the dermal site of *Leishmania (L.) amazonensis* and *Leishmania (V.) braziliensis* infection in *Sapajus apella* primate," *BioMed Research International*, vol. 2014, Article ID 134236, 8 pages, 2014.
- [28] W. P. Lafuse, R. Story, J. Mahylis et al., "Leishmania donovani infection induces anemia in hamsters by differentially altering erythropoiesis in bone marrow and spleen," *PLoS One*, vol. 8, no. 3, article e59509, 2013.
- [29] S. B. Mahato and A. P. Kundu, "¹³C NMR spectra of pentacyclic triterpenoids—a compilation and some salient features," *Phytochemistry*, vol. 37, no. 6, pp. 1517-1575, 1994.
- [30] W. Hou, Y. Li, Q. Zhang et al., "Triterpene acids isolated from *Lagerstroemia speciosa* leaves as α -glucosidase inhibitors," *Phytotherapy Research*, vol. 23, no. 5, pp. 614-618, 2009.
- [31] L. G. Verdi, I. M. C. Brighente, and M. G. Pizzolatti, "Gênero *Baccharis* (Asteraceae): aspectos químicos, econômicos e biológicos," *Química Nova*, vol. 28, no. 1, pp. 85-94, 2005.
- [32] N. J. C. Furtado, L. Pirson, H. Edelberg et al., "Pentacyclic triterpene bioavailability: an overview of in vitro and in vivo studies," *Molecules*, vol. 22, no. 3, p. 400, 2017.
- [33] R. Di Pasqua, G. Betts, N. Hoskins, M. Edwards, D. Ercolini, and G. Mauriello, "Membrane toxicity of antimicrobial compounds from essential oils," *Journal of Agricultural and Food Chemistry*, vol. 55, no. 12, pp. 4863-4870, 2007.
- [34] P. Artursson, K. Palm, and K. Luthman, "Caco-2 monolayers in experimental and theoretical predictions of drug transport¹," *Advanced Drug Delivery Reviews*, vol. 46, no. 1-3, pp. 27-43, 2001.
- [35] M. Malinowska, B. Miroslaw, E. Sikora et al., "New lupeol esters as active substances in the treatment of skin damage," *PLoS One*, vol. 14, no. 3, article e0214216, 2019.
- [36] C. Béragère, N. Caussarieu, P. Morin, L. Morin-Allory, and M. Lafosse, "Rapid analysis of triterpenic acids by liquid chromatography using porous graphitic carbon and evaporative light scattering detection," *Journal of Separation Science*, vol. 27, no. 12, pp. 964-970, 2004.
- [37] A. Das, J. J. Jawed, M. C. Das et al., "Antileishmanial and immunomodulatory activities of lupeol, a triterpene compound



- isolated from *Sterculia villosa*,” *International Journal of Antimicrobial Agents*, vol. 50, no. 4, pp. 512–522, 2017.
- [38] P. Bilbao-Ramos, D. R. Serrano, H. K. Ruiz Saldaña, J. J. Torrado, F. Bolás-Fernández, and M. A. Dea-Ayuela, “Evaluating the potential of ursolic acid as bioproduct for cutaneous and visceral leishmaniasis,” *Molecules*, vol. 25, no. 6, p. 1394, 2020.
- [39] G. Kaur, K. Chauhan, and S. Kaur, “Lupeol induces immunity and protective efficacy in a murine model against visceral leishmaniasis,” *Parasitology*, vol. 146, no. 11, pp. 1440–1450, 2019.
- [40] M. Saleem, “Lupeol, a novel anti-inflammatory and anti-cancer dietary triterpene,” *Cancer Letters*, vol. 285, no. 2, pp. 109–115, 2009.
- [41] S. Das, S. Ghosh, A. K. De, and T. Bera, “Oral delivery of ursolic acid-loaded nanostructured lipid carrier coated with chitosan oligosaccharides: development, characterization, in vitro and in vivo assessment for the therapy of leishmaniasis,” *International Journal of Biological Macromolecules*, vol. 102, pp. 996–1008, 2017.
- [42] E. S. Yamamoto, B. L. S. Campos, J. A. Jesus et al., “The effect of ursolic acid on *Leishmania (Leishmania) amazonensis* is related to programmed cell death and presents therapeutic potential in experimental cutaneous leishmaniasis,” *PLoS One*, vol. 10, no. 12, article e0144946, 2015.
- [43] P. Saudagar and V. K. Dubey, “Molecular mechanisms of in vitro betulin-induced apoptosis of *Leishmania donovani*,” *The American Journal of Tropical Medicine and Hygiene*, vol. 90, no. 2, pp. 354–360, 2014.
- [44] M. Das, S. B. Mukherjee, and C. Shaha, “Hydrogen peroxide induces apoptosis-like death in *Leishmania donovani* promastigotes,” *Journal of Cell Science*, vol. 114, Part 13, pp. 2461–2469, 2001.
- [45] C. Bruno de Sousa, K. N. Gangadhar, T. R. Morais et al., “Antileishmanial activity of meroditerpenoids from the macroalgae *Cystoseira baccata*,” *Experimental Parasitology*, vol. 174, pp. 1–9, 2017.
- [46] J. Fernandes Rodrigues and W. Souza, “Ultrastructural alterations in organelles of parasitic protozoa induced by different classes of metabolic inhibitors,” *Current Pharmaceutical Design*, vol. 14, no. 9, pp. 925–938, 2008.
- [47] M. C. Duarte, G. S. V. Tavares, D. G. Valadares et al., “Antileishmanial activity and mechanism of action from a purified fraction of *Zingiber officinalis* Roscoe against *Leishmania amazonensis*,” *Experimental Parasitology*, vol. 166, pp. 21–28, 2016.
- [48] A. C. Marques, “Contributions of ultrastructural studies to the cell biology of trypanosomatids: targets for anti-parasitic drugs,” *The Open Parasitology Journal*, vol. 4, no. 1, pp. 178–187, 2010.
- [49] M. A. Vannier-Santos and S. L. De Castro, “Electron microscopy in antiparasitic chemotherapy: a (close) view to a kill,” *Current Drug Targets*, vol. 10, no. 3, pp. 246–260, 2009.
- [50] C. Paris, P. M. Loiseau, C. Bories, J. Bréard, J. Bréard, and J. Bréard, “Miltefosine induces apoptosis-like death in *Leishmania donovani* promastigotes,” *Antimicrobial Agents and Chemotherapy*, vol. 48, no. 3, pp. 852–859, 2004.
- [51] N. K. Verma, G. Singh, and C. S. Dey, “Miltefosine induces apoptosis in arsenite-resistant *Leishmania donovani* promastigotes through mitochondrial dysfunction,” *Experimental Parasitology*, vol. 116, no. 1, pp. 1–13, 2007.
- [52] A. Debrabant, N. Lee, S. Bertholet, R. Duncan, and H. L. Nakhasi, “Programmed cell death in trypanosomatids and other unicellular organisms,” *International Journal for Parasitology*, vol. 33, no. 3, pp. 257–267, 2003.
- [53] S. Kaczanowski, M. Sajid, and S. E. Reece, “Evolution of apoptosis-like programmed cell death in unicellular protozoan parasites,” *Parasites & Vectors*, vol. 4, no. 1, p. 44, 2011.
- [54] A. Szallies, B. K. Kubata, and M. Duzenko, “A metacaspase of *Trypanosoma brucei* causes loss of respiration competence and clonal death in the yeast *Saccharomyces cerevisiae*,” *FEBS Letters*, vol. 517, no. 1–3, pp. 144–150, 2002.
- [55] D. Arnoult, K. Akarid, A. Grodet, P. X. Petit, J. Estaquier, and J. C. Ameisen, “On the evolution of programmed cell death: apoptosis of the unicellular eukaryote *Leishmania major* involves cysteine proteinase activation and mitochondrion permeabilization,” *Cell Death and Differentiation*, vol. 9, no. 1, pp. 65–81, 2002.
- [56] R. M. Santa-Rita, H. Santos Barbosa, M. Meirellesde, and S. L. de Castro, “Effect of the alkyl-lysophospholipids on the proliferation and differentiation of *Trypanosoma cruzi*,” *Acta Tropica*, vol. 75, no. 2, pp. 219–228, 2000.
- [57] E. S. Yamamoto, J. A. Jesus, A. Bezerra-Souza, M. D. Laurenti, S. P. Ribeiro, and L. F. D. Passero, “Activity of fenticonazole, tioconazole and nystatin on new world *Leishmania* species,” *Current Topics in Medicinal Chemistry*, vol. 18, no. 27, pp. 2338–2346, 2019.
- [58] S. Orenes Lorente, J. C. F. Rodrigues, C. Jimenez Jimenez et al., “Novel azasterols as potential agents for treatment of leishmaniasis and trypanosomiasis,” *Antimicrobial Agents and Chemotherapy*, vol. 48, no. 8, pp. 2937–2950, 2004.
- [59] S. Wüpper, A. Fischer, K. Lüersen et al., “High dietary Kudung tea extract supplementation induces hepatic xenobiotic-metabolizing enzymes—a 6-week feeding study in mice,” *Nutrients*, vol. 12, no. 1, p. 40, 2020.
- [60] Q. Sun, M. He, M. Zhang et al., “Ursolic acid: a systematic review of its pharmacology, toxicity and rethink on its pharmacokinetics based on PK-PD model,” *Fitoterapia*, vol. 147, p. 104735, 2020.
- [61] R. H. Berdichevski, L. B. Luis, L. Crestana, and R. C. Manfro, “Amphotericin B-related nephrotoxicity in low-risk patients,” *Brazilian Journal of Infectious Diseases*, vol. 10, no. 2, 2006.
- [62] I. Ghersetich, G. Menchini, P. Teofoli, and T. Lotti, “Immune response to *Leishmania* infection in human skin,” *Clinics in Dermatology*, vol. 17, no. 3, pp. 333–338, 1999.
- [63] Y. Vanloubbeek and D. E. Jones, “The immunology of *Leishmania* infection and the implications for vaccine development,” *Annals of the New York Academy of Sciences*, vol. 1026, no. 1, pp. 267–272, 2004.
- [64] K. Schroder, P. J. Hertzog, T. Ravasi, and D. A. Hume, “Interferon- γ : an overview of signals, mechanisms and functions,” *Journal of Leukocyte Biology*, vol. 75, no. 2, pp. 163–189, 2004.
- [65] T. Decker, S. Stockinger, M. Karaghiosoff, M. Müller, and P. Kovarik, “IFNs and STATs in innate immunity to microorganisms,” *The Journal of Clinical Investigation*, vol. 109, no. 10, pp. 1271–1277, 2002.
- [66] C. K. Prajeeth, S. Haeberlein, H. Sebald, U. Schleicher, and C. Bogdan, “*Leishmania*-infected macrophages are targets of NK cell-derived cytokines but not of NK cell cytotoxicity,” *Infection and Immunity*, vol. 79, no. 7, pp. 2699–2708, 2011.
- [67] H. W. Murray, A. L. Moreira, C. M. Lu et al., “Determinants of response to interleukin-10 receptor blockade immunotherapy

in experimental visceral leishmaniasis," *The Journal of Infectious Diseases*, vol. 188, no. 3, pp. 458–464, 2003.

- [68] M. L. Murphy, U. Wille, E. N. Villegas, C. A. Hunter, and J. P. Farrell, "IL-10 mediates susceptibility to *Leishmania donovani* infection," *European Journal of Immunology*, vol. 31, no. 10, pp. 2848–2856, 2001.
- [69] J. A. Jesus, T. N. Fragoso da Silva, E. S. Yamamoto, J. H. G. Lago, M. Dalastra Laurenti, and L. F. D. Passero, "Ursolic acid potentializes conventional therapy in experimental leishmaniasis," *Pathogens*, vol. 9, no. 10, p. 855, 2020.

Research Article

Schistosoma japonicum Infection in Treg-Specific USP21 Knockout Mice

Youxiang Zhang,¹ De-Hui Xiong,² Yangyang Li,³ Guina Xu,⁴ Baoxin Zhang,⁵ Yang Liu,⁶ Shan Zhang,¹ Qing Huang,¹ Simin Chen,¹ Fansheng Zeng,⁴ Jingyi Guo,⁷ Bin Li,³ Zhiqiang Qin¹ ,⁷ and Zuping Zhang¹ 

¹Department of Pathogen Biology, School of Basic Medical Science, Central South University, Changsha 410078, China

²Molecular Biology Research Center, School of Life Science, Central South University, 110 Xiangya Road, Changsha, Hunan 410078, China

³Department of Microbiology and Immunology, Shanghai Institute of Immunology, Shanghai Jiao Tong University School of Medicine, Shanghai 200025, China

⁴Key Laboratory of Control Technique for *Schistosoma* and Pathogen Infection for Dongting Lake Region, Yiyang Medical College, Yiyang 413002, China

⁵Department of Epidemic Prevention, Armed Police Hospital of Hunan Province, Changsha, 410008 Hunan, China

⁶Sichuan Center for Disease Control and Prevention, Chengdu, 610041 Sichuan, China

⁷Key Laboratory of Parasite and Vector Biology, Ministry of Health; National Institute of Parasitic Diseases, Chinese Center for Disease Control and Prevention, Chinese Center for Tropical Diseases Research, Shanghai 200025, China

Correspondence should be addressed to Zhiqiang Qin; qinzq@nipd.chinacdc.cn and Zuping Zhang; zhangzuping@csu.edu.cn

Received 26 November 2020; Revised 11 January 2021; Accepted 21 January 2021; Published 9 February 2021

Academic Editor: Luiz Felipe Domingues Passero

Copyright © 2021 Youxiang Zhang et al. This is an open access article distributed under the Creative Commons Attribution License, which permits unrestricted use, distribution, and reproduction in any medium, provided the original work is properly cited.

The E3 deubiquitinating enzyme ubiquitin-specific proteolytic enzyme 21 (USP21) plays vital roles in physiological activities and is required for Treg-cell-mediated immune tolerance. Using a murine model infected with *Schistosoma japonicum*, we observed that there were more cercariae developed into adults and more eggs deposited in the livers of the USP21^{fl/fl}FOXP3^{Cre} (KO) mice. However, immunohistochemistry showed that the degree of egg granuloma formation and liver fibrosis was reduced. In USP21^{fl/fl}FOXP3^{Cre} mice, levels of IFN- γ , IL-4, anti-soluble egg antigen (SEA) IgG and anti-soluble worm antigen preparation (SWAP) IgG increased in blood, as determined using ELISAs and multiplex fluorescent microsphere immunoassays, while the levels of IL-10, IL-17A, IL-23, IL-9, and anti-SEA IgM decreased. In addition, the levels of the USP21 protein and mRNA in the liver and spleen of KO mice decreased. We further observed increased Th1 responses amplified by Tregs (regulatory T cells) and compromised Th17 responses, which alleviated the liver immunopathology. We speculated that these changes were related to polarization of Th1-like Tregs. Our results revealed the roles of USP21 in Treg-cell-mediated regulation of immune interactions between *Schistosoma* and its host. USP21 may have potential for regulating hepatic fibrosis in patients with schistosomiasis.

1. Introduction

Schistosomiasis is an acute and chronic parasitic disease caused by blood flukes (trematode worms) of the genus *Schistosoma*. According to the WHO Report 2017, schistosomiasis transmission was reported by 78 countries, and at least 220.8

million people required preventive treatment in 2017. Schistosomiasis affects almost 240 million people worldwide, and more than 700 million people live in endemic areas, mostly in sub-Saharan Africa [1]. People become infected when the larval form of the parasite penetrates the skin (during contacting with infested water) after being released from

freshwater snails. The larvae develop into adult schistosomes inside the body. Adult worms live in the blood vessels, where the females release eggs. Some of the eggs are passed out of the body in the feces or urine to continue the parasite lifecycle. Other eggs are trapped in body tissues, causing immune reactions and progressive damage to organs [2].

The immune system of infected hosts encounters parasites in several stages of its life cycle: penetrating cercariae, migrating schistosomula, adult worms, and eggs produced by adult worm pairs. Parasites in the developmental stages express hundreds of antigenic moieties, many of which stimulate strong humoral and cellular immune responses [3]. Some of these responses continue to increase during chronic infection, and others are substantially reduced [4]. Observations in experimental mouse models of infection have elucidated the mechanisms governing the development and regulation of the pathogenic immune response in schistosomiasis [5]. Some factors, including IL-10, Tregs, B cells, antibodies, T cell anergy, macrophages, and microRNAs, are related to the pathogenic immune response in schistosomiasis [6]. In addition, several studies have suggested that Th17 cells are involved in the pathogenesis of both *Schistosoma mansoni* and *Schistosoma japonicum* infection [7].

Tregs have an immunosuppressive capacity that is essential for maintaining immune homeostasis and controlling immune tolerance. The induction of Tregs inhibits the development of granuloma pathology [8]. FOXP3 is a crucial factor involved in producing the immunosuppressive phenotype of Tregs. Unstable FOXP3 makes the Treg-cell phenotype unstable and may bias the generation of different T helper cell phenotypes under different inflammatory conditions [9]. Furthermore, studies conducted with a conditional knockout mouse model suggested that USP21 stabilized the expression of the FOXP3 protein in Tregs by deubiquitination, thereby regulating the function of Tregs. A Th1-like sputum cell response, as observed with USP21-deficient Tregs, preferentially transforms into a Th2 cell-like phenotype in a host with a severe Th2-type disorder, whereas under arthritic conditions, Tregs may lose FOXP3 expression and transform into cells with a Th17 cell-like phenotype [10]. More importantly, FOXP3, GATA3, and USP21 are closely associated with Tregs. In Tregs, FOXP3 binds to the promoter region of USP21 and activates its transcription, and USP21 interacts with GATA3 and deubiquitinates it, thus inhibiting its degradation by the proteasome and maintaining its stability.

Moreover, GATA3 regulates the function of T cells in the inflammatory response by stabilizing the expression of FOXP3. Thus, in Tregs, the three proteins described above form a positive feedback pathway. Furthermore, studies conducted with conditional knockout mouse models suggested that USP21 regulated the expression of the FOXP3 protein in Tregs by deubiquitination, thereby regulating the function of Tregs [9]. In antiviral responses, USP21 binds to and deubiquitinates RIG-I in the cytoplasm to exert an immunomodulatory effect; USP21 can also hydrolyzes the K27/63-linked polyubiquitin chain on STING to

negatively regulate DNA virus-induced type I interferon production [11].

Although Tregs may play an essential role in the regulation of the immune response during schistosome infection, the molecular mechanisms are not yet precisely defined. Therefore, this study is aimed at exploring the mechanism of action of USP21 in the regulation of the immune response during schistosome infection using the USP21 gene knockout mouse model. This study will describe the regulatory role of USP21 in the USP21 knockout mice infected with *S. japonicum* and related immune responses; we will further study the molecular mechanism underlying the effect of USP21 on the immune response to *S. japonicum*.

2. Materials and Methods

2.1. Ethics Statement. We carried out all the animal experiments in strict accordance with the Laboratory Animal Regulation (1988.11.1) and made every effort to minimize suffering. The IACUC of the National Institution of Parasitic Diseases of Chinese Center for Diseases Control and Prevention and Control approved all the procedures related to the use of experimental animals (License No. NJMU 07-0137). We used humane endpoints in this study. Due to the needs of the experiment, all experimental animals were euthanized on the 42nd day after infection. We monitored the health of the animals daily. Tissues were harvested after animals were euthanized by CO₂ exposure, which was confirmed by decapitation (to minimize the animal's suffering and distress). No animals died unexpectedly in this study. These animals were housed in groups of two to three per cage with free access to food and water on a 12 h light/dark cycle. Every effort was made to minimize the number and suffering of animals. The number of mice used in each test is listed in Table S1.

2.2. Experimental Animals, Parasites, and Establishment of Infection Models. Two strains of female mice, FOXP3^{Cre} (WT) and USP21^{fl/fl}FOXP3^{Cre} (KO), were provided by Shanghai Institute of Bioscience, Chinese Academy of Sciences. The *S. japonicum* cercariae (Chinese mainland strain) were released from naturally infected *Oncomelania hupehensis* snails from the National Institute of Parasitic Diseases of Chinese Center for Diseases Control and Prevention (Shanghai, China). Mice from the two strains were divided into a normal control (NC/uninfected) group ($n = 2$) and an infection (INF) group ($n = 10 \pm 2$) and were housed under specific pathogen-free conditions. All experimental animals were used at 6 to 8 weeks of age. Then, the mice in the INF group were infected with 25 ± 2 cercariae through the shaved abdominal skin. All experimental animals were sacrificed on the 42nd day after infection [12]. The animals were included in the study if they were successfully infected with *S. japonicum*. If the animal died prematurely, follow-up experiment data were unable to be collected. Fifty-six animals were ultimately included in this study, and all met our inclusion and exclusion criteria. Serum, which was stored at -80°C and used for ELISAs, was separated from mouse blood that was collected from the tail vein at different times, namely, before infection, 20 days and 30 days after infection,

and 42 days after infection. Blood was collected by eyeball enucleation. The animal experiments were conducted strictly with blinded protocols according to the Laboratory Animal Regulation, and we made every effort to minimize pain. The animals' cages were placed on the same shelf, and the feeding conditions and environment were as controlled as much as possible. For each animal, four different investigators were involved as follows: a first investigator (ZZP or QZQ) assigned the group based on the randomization table. This investigator was the only person aware of the group allocation. A second investigator (ZS, CSM, or HQ) was responsible for the normal feeding stage, whereas a third investigator (ZYY, LYY, XGN or XDH) performed the experimental procedures. Finally, a fourth investigator (LB, GJY, ZBX, ZFS or LY) (also unaware of treatment) assessed all experimental data. The mouse model of *S. japonicum* infection was repeated three times.

2.3. Collection of *S. japonicum* Worms and Measurement of the Weight of the Spleen and Liver of the Infected Mice. The mice were sacrificed by the cervical dislocation method 42 days after infection. The worms were collected from the portal vein by a cardiac infusion of saline, and the numbers of male and female adult worms and worm pairs were determined [12]. The spleens and livers of the mice were weighed and photographed.

2.4. HE and Masson Trichrome Staining. HE staining and Masson's trichrome staining have been previously described [13]. The remaining right liver lobe of each mouse was fixed with 4% paraformaldehyde and embedded in a paraffin block. We stained a section (5 μm thick) with hematoxylin-eosin and performed the analysis with an inverted microscope (magnification 100x). The areas of single liver egg granulomas ($n \geq 5$ per mouse) were measured using ImageJ software (NIH, Bethesda, USA), and the average number of eggs in a randomly selected visual field ($n \geq 5$ per mouse) was counted at 40x magnification to evaluate the pathological changes and the number of eggs in the groups. Similarly, the same site of the liver from each mouse was stained with Masson's trichrome. We measured and analyzed the ratio of the collagen area ($n \geq 5$ per mouse) using ImageJ software to evaluate the degree of hepatic fibrosis in the two groups.

2.5. Isolation of Peripheral Blood Mononuclear Cells (PBMCs) and Culture In Vitro. The cell preparation and cell culture methods have been previously described [14]. Blood (0.5–1 ml) was collected from the mice following eyeball enucleation at 42 days after infection. The serum and plasma were separated, and the serum was stored at -80°C until analysis. We mixed the plasma with sterile PBS at a ratio of 1 : 1, and the mixture was gently inverted approximately ten times. We then gently added the same volume of lymphocyte separation solution to form stratified layers. After centrifugation, we collected the middle layer, added red blood cell lysis buffer, and conducted another centrifugation step to obtain PBMCs. PBMCs were resuspended in complete culture medium containing 5 $\mu\text{g}/\text{ml}$ ConA to stimulate lymphocyte proliferation and maintain cell activity. The cell density, as

determined under a microscope, was adjusted to 2×10^6 cells/ml, and the cells were seeded into culture plates or dishes and cultured at 37°C with 5% CO_2 for 72 h under sterile conditions. We then stored the culture supernatant after centrifugation at -80°C .

2.6. Spleen Cell Isolation and Culture In Vitro. Forty-two days after the infection, the mice were sacrificed by cervical dislocation method and the spleen was harvested [12]. The spleen was passed through a 100 μm cell strainer to obtain a tissue homogenate, and red blood cell lysis buffer was repeatedly added until no red blood cells remained. Then, complete culture medium composed of RPMI 1640 medium supplemented with 10% fetal bovine serum (FBS) (GIBCO) and 1% Pen/Strep (GIBCO) was added to resuspend the cells. The cell density, as determined under a microscope, was adjusted to $2 \times 10^5 - 10^6$ cells/ml, and the cells were seeded in culture plates or dishes and cultured with 5 $\mu\text{g}/\text{ml}$ ConA to stimulate the cells at 37°C with 5% CO_2 for 72 h under sterile conditions. We then stored the culture supernatant after centrifugation at -80°C .

2.7. Flow Cytometry. The flow cytometry method has been previously described [9]. For the cell surface marker and Tregs analysis, lymphocytes were isolated from the spleen, and the CD4^+ T cells were enriched with CD4 (L3T4) MicroBeads mouse isolation kits (Miltenyi Biotec Inc., Auburn, CA 95602, USA). For the analysis of surface markers, the CD4^+ T cells were stained with APC-conjugated anti-mouse CD4 (GK1.5, 1 : 100), PE-conjugated anti-mouse CD25 (PC61.5, 1 : 100), and FITC-conjugated anti-mouse FOXP3 (3G3, 1 : 100) antibodies from Tonbo Biosciences in PBS containing 2% FBS. The cell membranes were permeabilized, and the nuclear transcription factor FOXP3 was stained using the Transcription Factor Staining Buffer Kit (Tonbo Biosciences, San Diego, CA, USA) according to the manufacturer's instructions. Compensation was performed with a BD LSRFortessa (BD Biosciences). The data were acquired and analyzed with FlowJo software (Tree Star, Ashland, OR, USA).

2.8. RNA Extraction and RT-PCR. The RNA extraction and RT-PCR have been previously described [15]. We extracted the total RNA from 30 mg of liver and spleen tissues with TRIzol according to the manual. The quality and quantity of the RNA were then evaluated using an ultramicronucleic acid protease analyzer. The total RNA (1 μg) was reverse transcribed with a RevertAid First-Strand cDNA Synthesis Kit (K1622, Thermo Fisher Scientific). The expression of USP21 , IL-10 , IL-17 , and FOXP3 in the liver and spleen and α -Smooth muscle actin (α -SMA), collagen, and Collagen III in the liver was detected using the iTaq™ Universal SYBR® Green super mixture (1725121, Bio-Rad) and a fluorescence quantitative PCR 7500 system (Applied Biosystems, USA). The data were quantitatively analyzed using the $2^{-\Delta\Delta\text{Ct}}$ method with glyceraldehyde-3-phosphate dehydrogenase (GAPDH) as a control. The PCR cycling conditions were as follows: 40 cycles of 95°C for 30 s, 95°C for 5 s, and 60°C for 34 s, followed by 95°C for 15 s, 60°C for 60 s, 95°C for 15 s,

TABLE 1: Primers used for the mRNA analysis.

Gene	Forward primer (5'→3')	Reverse primer (5'→3')
GAPDH	ACTCCACTCACGGCAAATTC	TCTCCATGGTGGTGAAGACA
USP21	ACCCAGGAAAGACAGCAACC	CTCGAAGACCTTCTCACAACCA
FOXP3	GTGATTTTAATAAGCTCCAAGACCA	GATCATCATGTATGCTTCTATGCAG
IL-10	TATCCCTCTGTGATCTGGGAAG	ATCTTCTCGACCCTGAAAGTGA
IL-17	CACAGCCCTGGTGTGCGACAAT	TTGCTCTGGGCTTCATCCCCCA
α -SMA	TCCTGCGCCTAATGTCCACCGA	AAGCGACTGTTGCCTTCGCCTC
Collagen I	TCCTGGTGGCAAGGGTGATCGT	TGGAGCACCAGAAGGACCAGCA
Collagen III	GCTCACCACACACTGCTTCT	GGATTCACAGCTTCACAGGA

and 60°C for 60 s. All the primers were subjected to a blast search with NCBI to ensure their specificity. All the primers are shown in Table 1.

2.9. Western Blotting. The Western blotting procedure has been previously described [16]. Liver tissue (30–50 mg) from each mouse was lysed on ice in cold RIPA lysis buffer (1–1.2 ml) containing a protease inhibitor cocktail (B14001, Bimake) for 3 to 4 h. After centrifugation at 14000 \times g/min for 15 min, the supernatant was transferred to another tube to determine the total protein concentration using the BCA protein detection kit (P0010, Beyotime, China). The protein samples were boiled for 3 min, loaded onto a 10% polyacrylamide gel, electrophoresed, and transferred to a PVDF membrane (Millipore MA, USA). The proteins were separated using SDS-gel electrophoresis. The protein bands were detected by incubating the membrane with polyclonal primary antibodies against GAPDH (sc-32233, Santa Cruz), USP21 (ab171028, Abcam), α -SMA (no. 19245T, Cell Signaling Technology), Collagen I (BA0325, Boster), and Collagen III (sc-271249, Santa Cruz) for 12–16 h at 4°C, followed by an incubation with HRP-goat anti-rabbit IgG (ab97080, Abcam) and HRP-rabbit anti-mouse IgG (ab6728, Abcam) secondary antibodies. The immune complexes were visualized with the WesternBright™ ECL substrate (K-12045-D10, Advansta), and the luminescent signal was recorded with a chemiluminescence imaging system (Bio-Rad, USA) to determine the expression of the proteins. The expression of USP21, α -SMA, Collagen I, and Collagen III was quantified using GAPDH as a reference for relative quantification. ImageJ analysis software was applied to calculate the grayscale values of the bands on the images, which were used for statistical analysis (NIH, Bethesda, USA).

2.10. ELISA. The ELISA technique has been previously described [17]. Briefly, for the *S. japonicum*-SEA and *S. japonicum*-SWAP ELISAs, all the native antigens were diluted to a final concentration of 1 μ g/ml with coating buffer; for the *S. japonicum*-SEA and *S. japonicum*-SWAP ELISAs, 50 ng of each antigen in 100 μ l was added to each well and incubated at 4°C overnight. After blocking with blocking buffer (1% BSA in PBST) at 37°C for one hour, the serum samples diluted 1:250 with blocking buffer were added (100 μ l/well) and incubated for one hour at 37°C. HRP-goat anti-mouse IgM (ab97230, Abcam) and HRP-rabbit anti-mouse IgG

(ab6728, Abcam) were used as the secondary antibodies (1:20000, 100 μ l/well), and the samples were incubated for one hour at 37°C. Streptavidin-HRP (BD Pharmingen, CA, USA) (1:10000) was then applied to each well (100 μ l/well). The wells were washed with PBST five times for 2 min each after each step. The reactions were developed using TMB as a substrate (100 μ l/well) for 5 min, and this development was stopped using 2 M sodium hydroxide (50 μ l/well). The optical density (OD) values were recorded at 450 nm using a microplate reader, and all the tests were performed in duplicate on each test plate.

2.11. Cytokine Detection (Multiplex Fluorescent Microsphere Immunoassay). The mouse serum and cell culture samples were prepared according to the manufacturer's instructions (Laizee Biotech Co. Ltd., ppx-6, China). Fifty microliters of premixed beads was added to each of the 96 wells and then incubated with the samples. The detection antibodies (IFN- γ , IL-4, IL-10, IL-17A, IL-23, and IL-9) were added after an initial wash, followed by a second wash and the addition of SA-PE. The clean and dried 96-well plate was placed in the Bio-Plex 200 instrument for detection. The standard curve was fitted using a five-parameter nonlinear regression method, and the concentration was calculated. The results included the label, the median of the fluorescence intensity, and the concentration [18].

2.12. Statistical Analyses. Statistical comparisons were performed with Prism 7.0 (GraphPad Prism.) and SPSS 18.0 software using a *t*-test for comparisons of two datasets and ANOVA for multiple comparisons. All the data are presented as the $\bar{x} \pm$ S.D., and the differences were considered statistically significant at $p \leq 0.05$.

3. Results

3.1. Depletion of USP21 in Treg Cells Weakens the Resistance to *S. japonicum* in Infected Mice. Both WT and KO mice were infected with *S. japonicum*, and the adult parasites were recovered (according to the steps described below) to observe the differences between the mouse strains. The number of total adult parasites (females and males combined) recovered from KO mice was significantly greater than the number recovered (Figure 1(a)). However, no difference was found in the development of cercariae between male and female

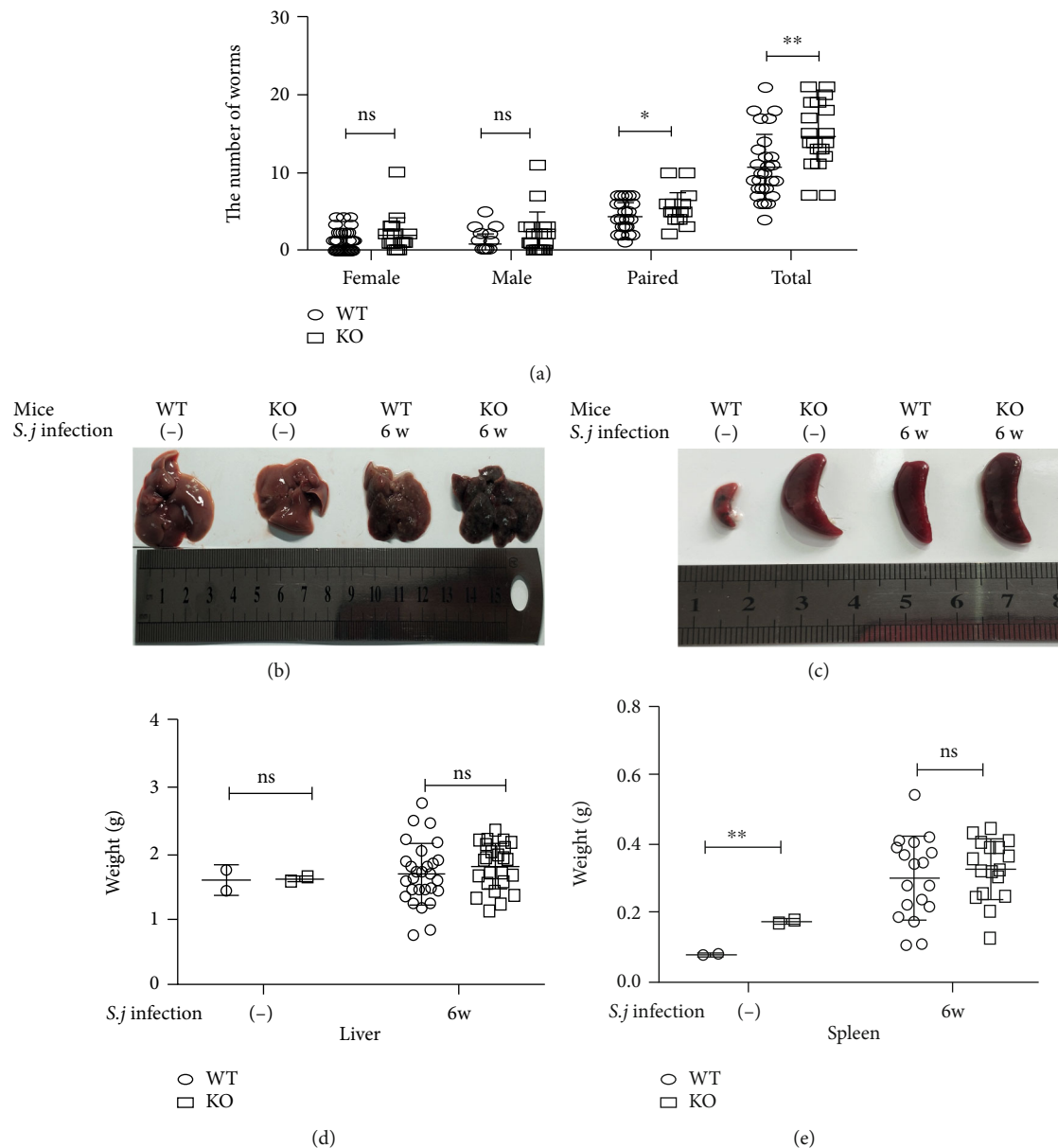


FIGURE 1: Deletion of USP21 in Tregs reduces the resistance to *S. japonicum* in infected mice. (a–e) FOXP3^{Cre} (WT) and USP21^{fl/fl}FOXP3^{Cre} (KO) mice ($n = 26 \pm 2/\text{group}$) were infected with 25 ± 2 cercariae through the abdomen and were sacrificed 6 weeks after infection. The liver and spleen tissues were collected, and the adults were recovered. (a) Comparison of the number of females, males, pairs, and adults recovered from the WT- and KO-infected (INF) groups ($n = \text{mean} \pm \text{SD}$), $*p = 0.01$ for the total number of adults and $**p = 0.036$ for the total number of worm pairs. (b) Representative images of the livers of the WT and KO mice from the NC and INF groups. (c) Liver weight of the WT and KO mice in the NC and INF groups (weight = mean \pm SD); $p > 0.05$ was considered a difference that was not statistically significant between the normal control group and the infected group. (d) Representative images of the spleens of the WT and KO mice in the NC and INF groups. (e) Spleen weight of the WT and KO mice in the NC and INF groups (weight = mean \pm SD); $**p = 0.007$ compared with the normal control group; $p > 0.05$ represented a difference that was not statistically significant compared with the infected group.

adult parasites. The numbers of single males, single females, and pairs and the total number of adults were counted. We weighed the liver and spleen of the mice and observed changes in their color, shape, and texture. The color and size of the liver and spleen of the KO-INF group were slightly darker and larger than the WT group, and the KO mice suffer from splenomegaly even if they were uninfected (Figures 1(b)–1(e)).

3.2. Effect of USP21 on *S. japonicum* Eggs during Infection in KO Mice. A portion of the liver obtained from the mice 42 days after infection was used for HE staining to observe the pathological changes in egg granuloma formation. We analyzed the granuloma area and egg number in the KO mice and WT mice using ImageJ software. A significantly greater number of eggs was observed in the KO mice than in the WT mice (Figure 2(a)), but the number of inflammatory cells

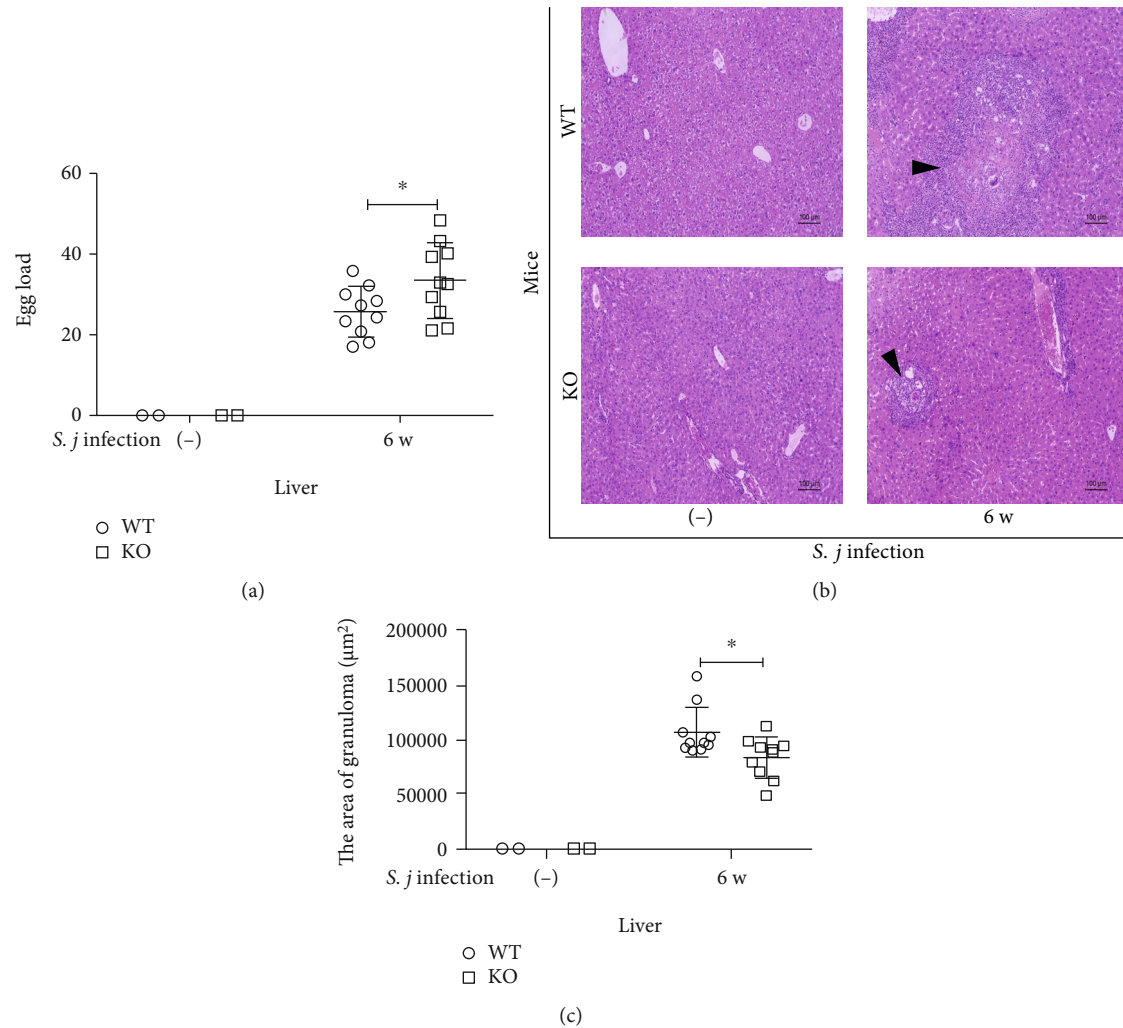


FIGURE 2: Effect of USP21 on *S. japonicum* eggs in infected KO mice. (a–c) The livers were harvested from the mice on the 42nd day after the infection for HE staining, and the number of eggs was counted under the microscope ($n = 2$ from the uninfected group and $n = 10$ from the infected group). (a) Statistical graph of the eggs in the livers of the WT-INF group and the KO-INF group (the data are presented as the means \pm SD, $*p = 0.043$). (b) Representative images of HE staining in the livers of WT-INF and KO-INF groups (original magnification: 100x). The arrows indicate the granulomas. (c) Comparison of the liver egg granuloma areas between the WT-INF and KO-INF groups. The data are presented as the means \pm SD, $*p = 0.022$.

in the egg granulomas of the KO mice was lower than in the WT mice, and lighter HE staining was observed in the KO mice (Figure 2(b)). The areas of the liver egg granulomas in the KO mice were significantly smaller than those in the WT mice (Figure 2(c)).

3.3. Changes in Liver Fibrosis in *USP21^{fl/fl}FOXP3^{cre}* Mice Infected with *S. japonicum*. The expansion of collagen fibers, which reflects the severity of hepatic fibrosis, was observed using Masson's trichrome staining (Figure 3(a)). α -SMA is a hallmark of activated myofibroblasts and has been extensively used to indicate the occurrence and severity of fibrosis in individuals with liver diseases [13]. In hepatic fibrosis associated with schistosomiasis, the expression level of α -SMA is elevated [13]. Therefore, the expression of the α -SMA, Collagen I, and Collagen III mRNAs was detected

using RT-PCR, and the protein expression of these factors was analyzed using Western blotting. Fewer collagen fibers with a lighter staining intensity were observed in the KO mice than in the WT mice, and these differences were statistically significant (Figure 3(b)). Significantly lower levels of the α -SMA, Collagen I, and Collagen III mRNAs and proteins were detected in the KO mice than in the WT mice (Figures 3(c)–3(e)).

3.4. Hepatic Immunity in *USP21^{fl/fl}FOXP3^{cre}* Mice Infected with *S. japonicum*. We detected the expression of the IL-10, IL-17, and FOXP3 mRNAs in the liver to determine whether the immune status of the liver was consistent with the condition of the spleen. We also detected the expression levels of the USP21 protein and mRNA. Lower expression levels of the USP21 protein and mRNA were detected in the liver of

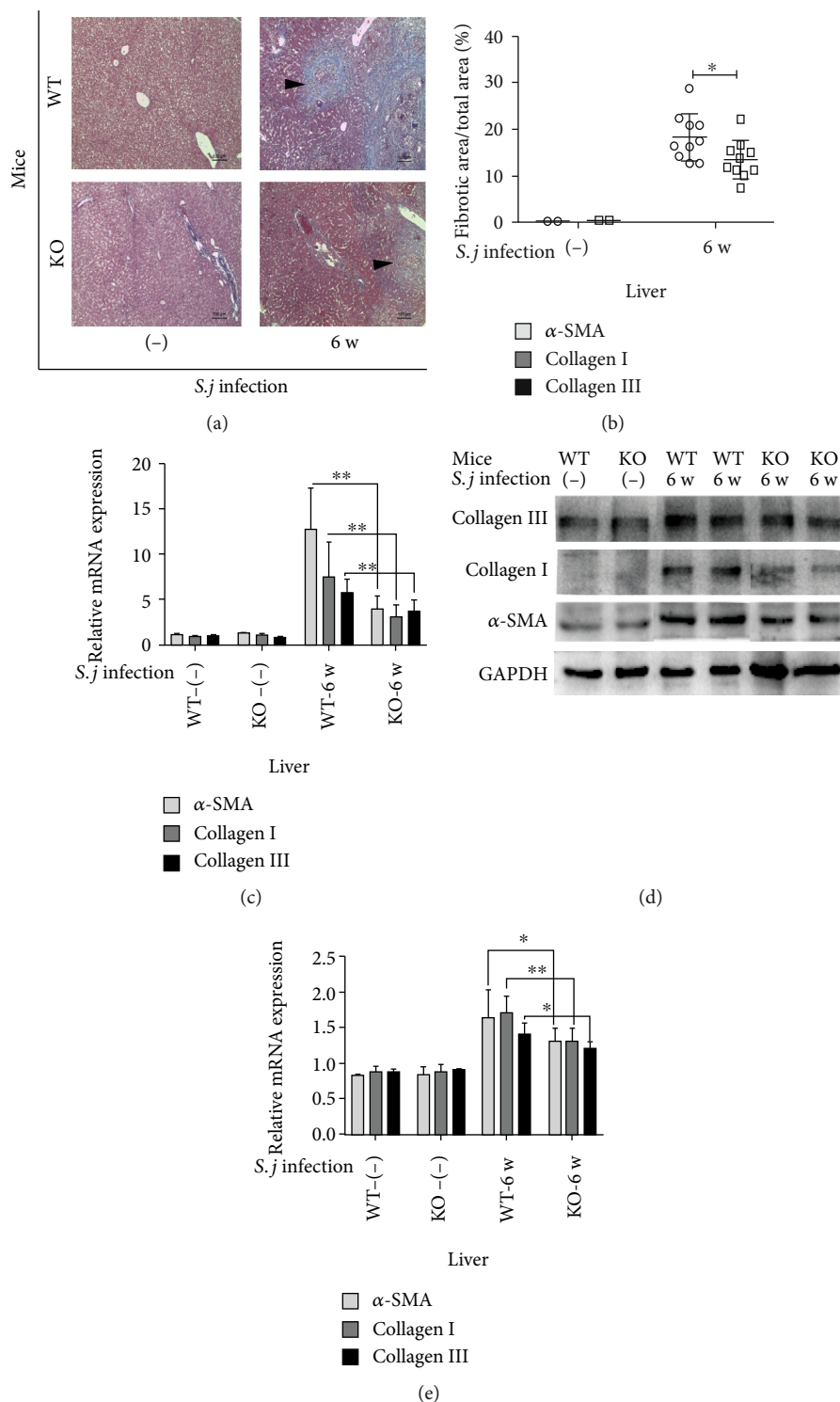


FIGURE 3: Changes in liver fibrosis in USP21^{fl/fl}FDX3^{cre} mice infected with *S. japonicum*. (a–e) The livers were harvested from the mice on the 42nd day after the infection and stained with Masson’s trichrome ($n = 10$ animals/group). (a) Representative images of collagen deposition in the WT-INF and KO-INF mice (original magnification: 100x) were obtained. The blue areas are collagen granules. (b) Comparison of the percentages of the hepatic fibrosis area between the WT-INF and KO-INF groups. The data are presented as the means \pm SD, $*p = 0.039$. (c) Comparison of the levels the α -SMA, Collagen I, and Collagen III mRNAs in the WT and KO mice in the NC and INF groups. The data are presented as the means \pm SD. Comparison of the levels of the α -SMA, Collagen I, and Collagen III mRNAs between the infected groups. The data are presented as the means \pm SD. In the infection group, α -SMA: $**p < 0.001$; collagen I: $**p = 0.008$, and Collagen III: $**p = 0.006$. (d) Representative images of SMA, Collagen I, and Collagen III protein expression in the WT and KO mice from the NC and INF groups, as determined by Western blotting. (e) Comparison of protein expression between WT and KO mice in the NC and INF groups. The data are presented as the means \pm SD. In the infection group, α -SMA: $*p = 0.034$, Collagen I: $**p = 0.006$, and Collagen III: $*p = 0.03$.

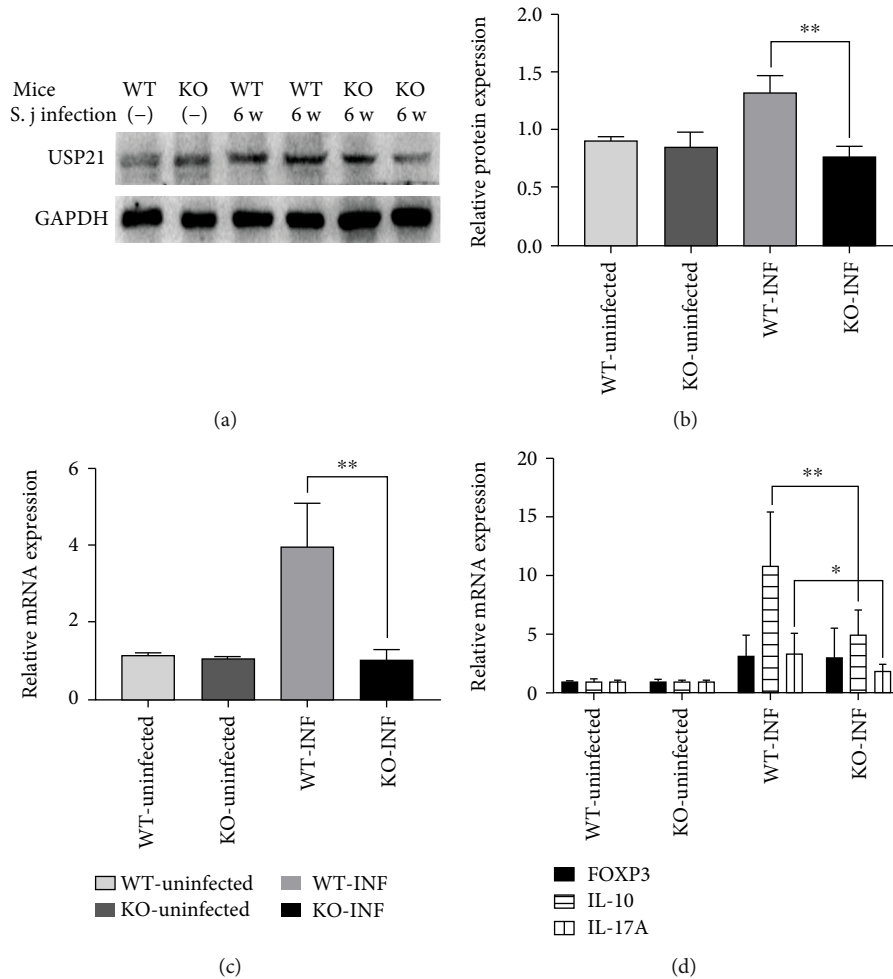


FIGURE 4: Liver immunity in *USP21^{fl/fl}FOXP3^{cre}* mice infected with *S. japonicum*. (a) Representative images of USP21 protein expression in the in WT and KO mice in the NC and INF groups determined using Western blotting ($n = 6$ mice/group). (b) Comparison of protein expression in the WT and KO mice in the NC and INF groups ($n = 6$ mice/group). The data are presented as the means \pm SD, and the difference between the infection groups was significant (** $p < 0.001$). (c) Comparison of the USP21 mRNA levels between WT and KO mice in the NC and INF groups ($n = 6$ mice/group). The data are presented as the means \pm SD, ** $p = 0.001$ for the comparison between the infection groups. (d) Comparison of the levels of the FOXP3, IL-10, and IL-17 mRNAs in the WT and KO mice from the NC and INF groups ($n = 6$ mice/group). The data are presented as the means \pm SD; for the comparison between the infection groups: IL-10 ** $p = 0.003$ and IL-17 * $p = 0.026$.

KO mice than in WT mice (Figures 4(a)–4(c)). Significantly lower expression of the IL-10 and IL-17 mRNAs was observed in the KO mice than in the WT mice (Figure 4(d)).

3.5. Changes in Spleen Immunity in *USP21^{fl/fl}FOXP3^{cre}* Mice Infected with *S. japonicum*. In an attempt to understand the differences in the splenic immune cells between the KO and WT mice after infection with *S. japonicum*, splenic cells from the two groups, including the NC group, were collected, isolated, and cultured *in vitro* to detect and analyze the number of Tregs and the percentage of CD4⁺CD25⁺FOXP3^{high} cells among the CD4⁺ cell population. The comparison of the proportion of CD4⁺CD25⁺FOXP3^{high} cells among the CD4⁺ T cell population in the WT and KO mice from the NC and INF groups is shown in Figure 5(a). The percentage of FOXP3^{high}Tregs in the KO-uninfected group and WT-uninfected group was not significantly different, while the percentage of FOXP3^{high}Tregs in the KO-INF

group was significantly lower than in the WT-INF group. The changes in the types of T cells were revealed by detecting the relative mRNA expression of IL-10, IL-17, FOXP3, and USP21 in the spleen using RT-PCR and by the detection of the levels of IFN-gamma, IL-4, IL-10, IL-17A, IL-23, and IL-9 in the splenocytes using a multiplex fluorescent microsphere immunoassay. Lower levels of the IL-10, IL-17, FOXP3, and USP21 mRNAs were detected in the KO mice than in the WT mice (Figure 5(b)). The results of splenic cell culture cytokine production showed significantly higher levels of IFN-gamma and IL-4 in the KO-uninfected group than in the WT-uninfected group. In the comparison between the two INF groups, the IFN-gamma and IL-4 contents in KO mice were also higher than in WT mice, and the content of IL-10 was higher in WT mice (Figure 5(c)).

3.6. Specific Antibody Responses in *USP21^{fl/fl}FOXP3^{cre}* Mice Infected with *S. japonicum*. Serum samples were collected

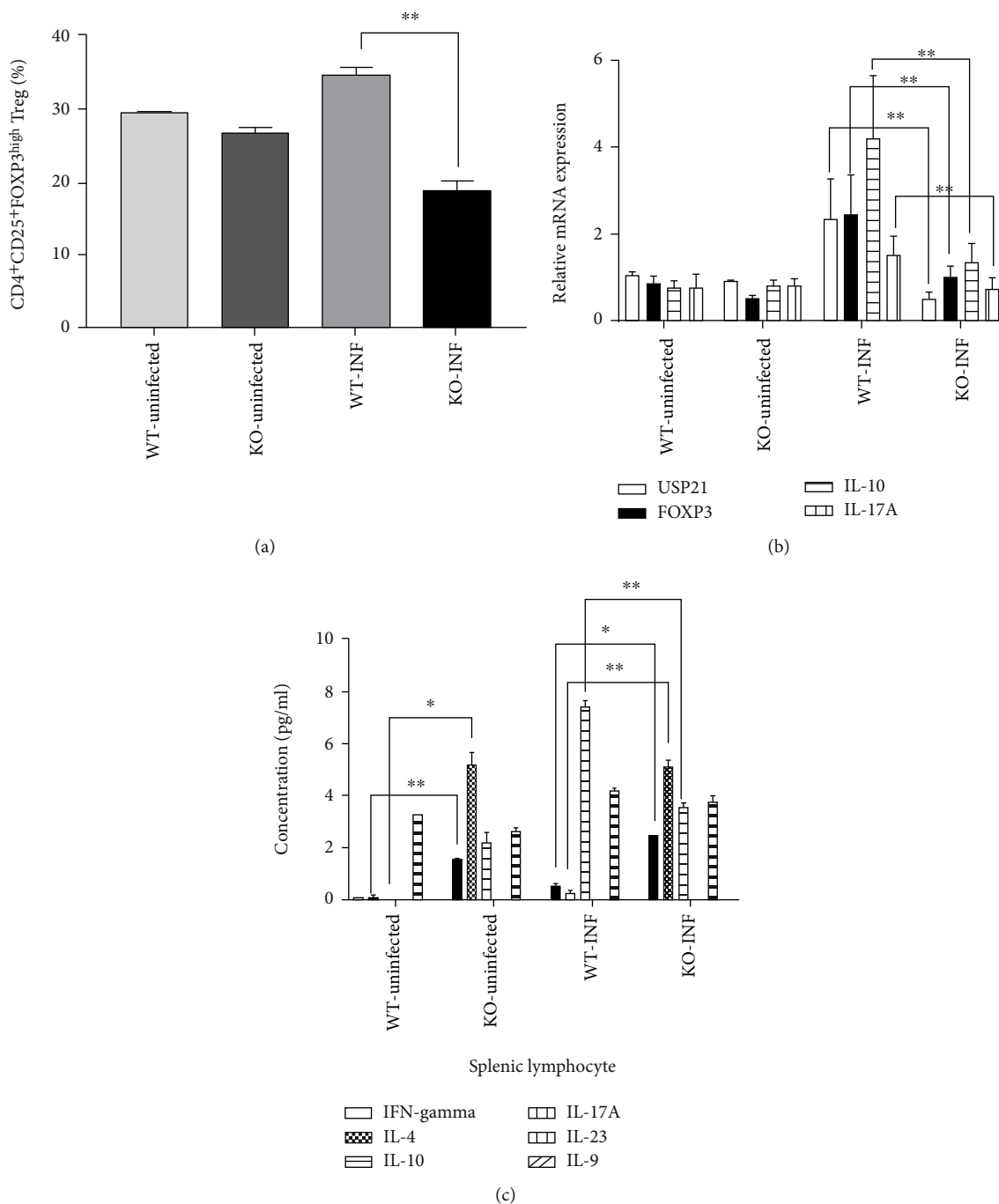


FIGURE 5: Changes in splenic immunity in USP21^{fl/fl}FOXP3^{cre} mice infected with *S. japonicum*. (a–c) The spleens were harvested from the mice on the 42nd day after the infection. (a) CD4⁺CD25⁺FOXP3^{high} cells directly isolated from the spleens of WT and KO mice in the NC and INF groups were identified using flow cytometry at 42 days after the infection with *S. japonicum*. Comparison of the proportion of CD4⁺CD25⁺FOXP3^{high} cells among the CD4⁺ T cell population in the WT and KO mice in the NC and INF groups. The data are presented as the means ± SD, infection groups: ***p* = 0.007. (b) Comparison of the mRNA levels of FOXP3, IL-10, IL-17, and USP21 in the WT and KO mice in the NC and INF groups, and the data are presented as the means ± SD. For the comparison between the infection groups, FOXP3 ***p* = 0.001, IL-10 ***p* < 0.001, IL-17 ***p* < 0.001, and USP21 ***p* < 0.001. (c) The splenic cells were cultured *in vitro* (*n* = 6 /group). Comparison of the levels of IFN-gamma, IL-4, IL-10, IL-17A, IL-23, and IL-9 in cultured spleen cells from the WT and KO mice in the NC and INF groups. The data are presented as the means ± SD. In the NC group, IFN-gamma ***p* = 0.002 and IL-4 **p* = 0.002; for the comparison between the infection groups, IFN-gamma **p* = 0.013, IL-4 ***p* = 0.005, and IL-10 ***p* = 0.004.

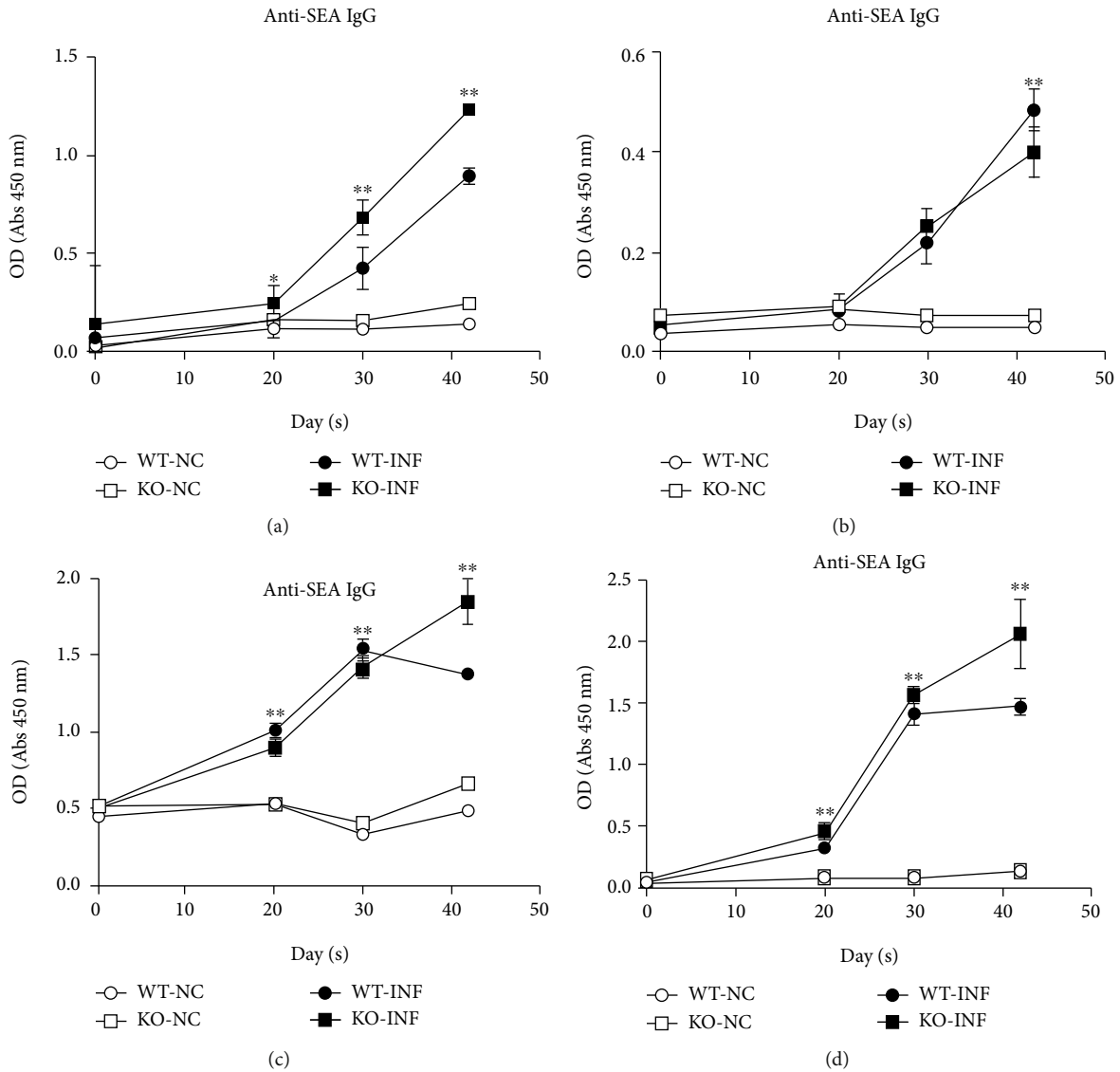


FIGURE 6: Specific antibody responses in USP21^{fl/fl}FOXP3^{Cre} mice infected with *S. japonicum*. (a–d) Serum collected from the WT and KO mice in the NC and INF groups ($n = 26 \pm 2/\text{group}$) at different stages of the infection (uninfected, day 20, day 30, day 42). (a) Comparison of the changes in the anti-SEA IgG content. The data are presented as the means \pm SD. For the comparison between infection groups, $*p = 0.01$ on day 20, $**p < 0.001$ on day 30, and $**p < 0.001$ on day 42. (b) Comparison of the anti-SEA IgM content. The data are presented as the means \pm SD, and $**p = 0.002$ on day 42 when comparing between the infection groups. (c) Comparison of the anti-SWAP IgG contents. The data are presented as the means \pm SD; for the comparison between infection groups, $**p < 0.001$ on day 20, $**p = 0.003$ on day 30, and $**p < 0.001$ on day 42. (d) Comparison of the anti-SWAP IgM contents. The data are presented as the means \pm SD. For the comparison between infection groups, $**p < 0.001$ on day 20, $**p = 0.004$ on day 30, and $**p < 0.001$ on day 42.

from the KO and WT mice to measure the contents of anti-SEA and anti-SWAP IgG/IgM antibodies at different stages of the infection and to better understand the specific antibody responses of USP21^{fl/fl}FOXP3^{Cre} mice to *S. japonicum*.

The analysis of the anti-SEA content revealed a higher level of anti-SEA IgG secretion in the KO-INF group than in the WT-INF group at all stages of infection, and the trends of the two groups were consistent and increased (Figure 6(a)). Meanwhile, the level of anti-SEA IgM secretion in the KO-INF group was lower than that in the WT-INF group beginning on the 30th day after *S. japonicum* infection

to the 42nd day, and the trend of the changes in the two groups was basically the same (Figure 6(b)).

The anti-SWAP IgG level in the WT-INF group decreased beginning on the 30th day, and the level of IgG secretion in the preceding 30 days was higher than in the KO-INF group. The level of secreted IgG in the KO-INF group increased until the 42nd day after *S. japonicum* infection (Figure 6(c)). Based on the graph showing the change in the secretion of anti-SWAP IgM, the level in the KO-INF also increased until the 42nd day after *S. japonicum* infection and was always higher than the level

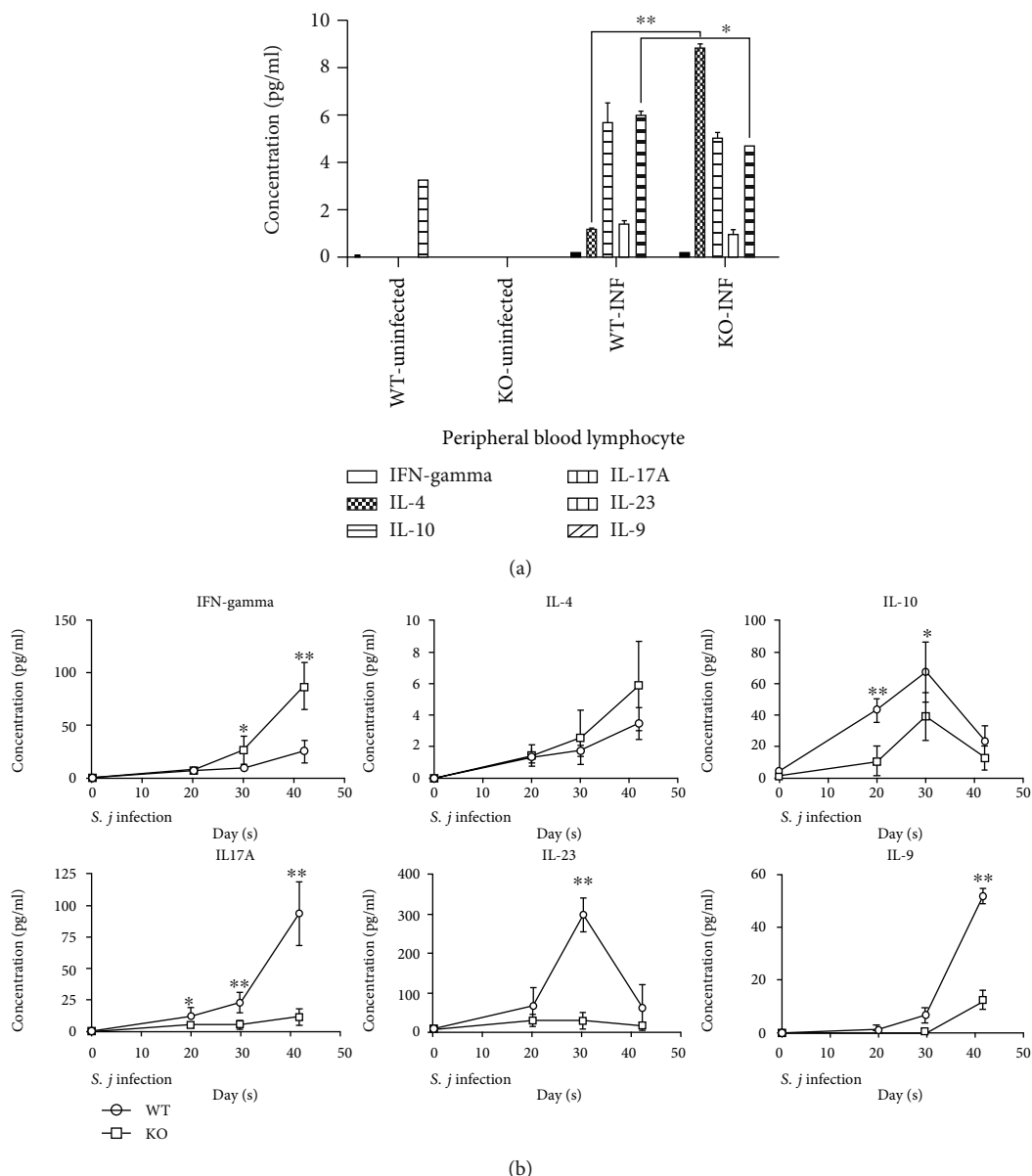


FIGURE 7: Serum cytokines in $USP21^{fl/fl}FOXP3^{Cre}$ mice infected with *S. japonicum*. (a) Comparison of the concentrations of IFN-gamma, IL-4, IL-10, IL-17A, IL-23, and IL-9 in the cultures of peripheral blood lymphocytes isolated from the WT and KO mice in the NC and INF groups 42 days after the infection ($n = 10$ mice/group). The data are presented as the means \pm SD, IL-4 $**p = 0.008$, and IL-23 $*p = 0.035$ for the comparison between the infection groups. (b) Comparison of the serum IFN-gamma, IL-4, IL-10, IL-17A, IL-23, and IL-9 levels in the WT- and KO-INF groups ($n = 26 \pm 2$ /group) at different time points (uninfected, 20th day after infection, 30th day after infection, and 42nd day after infection). The data are presented as the means \pm SD. IFN- γ $*p = 0.024$ on day 20 and $**p < 0.001$ on day 42; IL-10 $**p < 0.001$ on day 20 and $*p = 0.017$ on day 30; IL-17A $*p = 0.026$ on day 20, $*p < 0.001$ on day 30, and $**p < 0.001$ on day 42; IL-23 $**p < 0.001$ on day 30; and IL-9 $**p < 0.001$ on day 42.

in the WT-INF group. However, the anti-SWAP IgM level in the WT-INF group remained basically unchanged after the 30th day (Figure 6(d)).

3.7. Serum Cytokine Levels in $USP21^{fl/fl}FOXP3^{Cre}$ Mice Infected with *S. japonicum*. We measured the levels of IFN-gamma, IL-4, IL-10, IL-17A, IL-23, and IL-9 in the serum samples and PBMCs from the KO and WT mice at different stages of infection to conduct an extensive analysis of how

USP21-deficient Tregs affect the resistance of mice to *S. japonicum*.

In the peripheral blood lymphocyte culture, the concentration of each cytokine in the KO-uninfected group was basically the same as the WT-uninfected group. The IL-4 level was significantly increased in the KO-INF group compared with the WT-INF group, whereas a lower IL-23 level was detected in the KO-INF group than in the WT-INF group. The concentrations of other cytokines in the

KO-INF group were higher than those in the WT-INF group, but the differences were not statistically significant (Figure 7(a)).

Serum measurements performed at different stages of the *S. japonicum* infection revealed similar trends for the changes in the IFN- γ , IL-4, IL-10, IL-17A, and IL-9 levels in the WT-INF and KO-INF groups. The levels of secreted IFN- γ and IL-4 in the WT-INF and KO-INF groups increased, and the level in the KO-INF group was significantly higher than that in the WT-INF group. Although the levels of IL-17A and IL-9 increased, the level in the KO-INF group was significantly lower than that in the WT-INF group. The level of secreted IL-10 in the two groups decreased on the 30th day, and the level secreted in the KO-INF group was always lower than that in the WT-INF group. Interestingly, the levels of IL-23 differed between the WT-INF and KO-INF group. The level in the KO-INF group remained basically unchanged, while the level in the WT-INF group increased from day 0 to day 30 of infection, and its concentration decreased rapidly from day 30 to day 42, with statistically significant differences (Figure 7(b)).

4. Discussion

In mammalian hosts, *S. japonicum* stimulates immune responses during all stages of its life cycle, which are activated by Th1, Th2, and Th17 cells [19]. Meanwhile, Tregs play an essential immunomodulatory role in curbing overactive T cell responses [20, 21]. USP21 is a member of the ubiquitin-specific proteolytic enzyme (USP) family that exerts different biological functions. For example, USP21 regulates gene expression in hepatocytes during liver regeneration by catalyzing the hydrolysis of ubH2A [22]. During inflammation, USP21 negatively regulates RIPK1 to inhibit its activity downstream of TNFR1 [23], and the USP21-mediated deubiquitination of IL-33 promotes the transcription of NF- κ B p65 [24]. Additionally, USP21 binds to and deubiquitinates RIG-I in the cytoplasm to play an immunomodulatory role in antiviral responses [25]. More recently, USP21 was shown to regulate the expression of factors related to cell cycle, proliferation, and craniofacial development by deubiquitinating FOXM1 and gooseoid (GSC) [26, 27].

Previously, researchers used a USP21 knockout mouse model to explore its biological role in the differentiation of lymphocytes and hematopoietic stem cells [28]. They found that elderly USP21 knockout mice exhibited spontaneous T cell activation and splenomegaly. Furthermore, another study showed that the depletion of USP21 induces the production of Th1-like Tregs as a result of unstable FOXP3 expression, leading to severe autoimmune systemic disorders [9]. Thus, we used the model of USP21 knockout mice with *S. japonicum* infection to illustrate the role of unstable Tregs in *S. japonicum* infection.

Schistosome infection can be divided into three stages, namely, acute infection, active infection, and late chronic infection, and these stages present different clinical symptoms and immune mechanisms [2]. Differences in clinical symptoms and immune mechanisms of these stages have

been identified. In the present study, after *S. japonicum* infection, there was a greater number of pairs and adult parasites recovered from the KO mice than that from the WT mice, and a similar trend was noted for the number of eggs recovered. In addition, no difference was observed between the female and male adults recovered from the two groups. *Schistosoma* depends on host signals, such as TGF- β and TNF- α , to maintain its proper development and maturation [29, 30]. We speculated that the changes in the immune microenvironment in the host were potentially caused by the absence of USP21 and Treg dysfunction, which might promote the development of cercariae and the male and female combination of *S. japonicum*. Considering that protection from *S. japonicum* infection mainly depends on the clearance of *S. japonicum* in the early stage of infection, USP21^{-/-} Tregs might inhibit the ability of mice to cause the death of *S. japonicum*. These two theories require further evaluation in the future.

According to recent studies, liver egg granuloma and fibrosis are the main pathogenic pathological responses, and the severity of these symptoms is usually related to the intensity of infection [2]. The major mechanism of liver fibrosis is the abnormal expression of collagen and the excessive deposition of ECM (Extracellular matrix) caused by the activation of HSCs (hepatic stellate cells). Normally, the HSCs are mainly distributed in the hepatic sinusoid space to store vitamin A in a resting state [31, 32]. When chronic liver damage occurs, resting HSCs are activated and converted into myofibroblasts that then secrete a large amount of ECM and many fibrogenic cytokines, such as α -SMA and transforming growth factor- β 1 (TGF- β 1) [33, 34]. The deposition of ECM containing collagen fibers leads to the imbalance of ECM degradation and the synthesis, eventually leading to damage to the liver structure and liver fibrosis [35]. Studies have confirmed that HSC activation critically regulates the development of liver fibrosis, and HSC inhibition improves the process of liver fibrosis, thereby reducing the degree of liver fibrosis.

In our study, the diameter of the egg granulomas in the KO mice was smaller than that of the egg granulomas in the WT mice at six weeks, the levels of proinflammatory cytokines/chemokines and infiltrating neutrophils were reduced, and the HE staining was lighter. The degree of hepatic fibrosis in the KO mice was also lower than that in the WT mice, as determined using RT-PCR, Western blotting, and Masson's trichrome staining. Therefore, USP21-deficient Tregs might inhibit HSC overactivation and further reduce pathological liver damage. The liver fibrosis and splenic diseases caused by *S. japonicum* are associated with the great number of FOXP3⁺ Tregs in the blood [7]. According to previous studies, Th17 cells might play an essential role in the immunopathology in the liver and the formation of egg granulomas, and the development of severe schistosomiasis in mice is associated with high levels of IL-17A [36, 37]. IL-17-deficient mice showed higher IFN- γ levels and reduced immunopathology [38], similar to the USP21 KO mice with downregulated IL-17, increased IFN- γ and reduced immunopathology. The results from this previous study further suggested that IL-17 may affect these changes in infected KO

mice. The results of the present study also confirmed that the IL-17A in the KO group was lower than that in the WT group, but a similar trend was noted for the content of IL-10. Therefore, we speculated that the absence of USP21 might inhibit the Th17-type immune response, which exerted a positive effect on the reduction of liver immunopathological damage and might also lead to immune dysfunction in the host. The number of Tregs was decreased in KO mice; however, the hepatic immunopathology was suppressed. We speculated that upon *S. japonicum* infection, Tregs were overactivated in mice lacking USP21, although unstable Tregs lose their immunosuppressive effects, disrupting the host immune mechanism and weakening the related immune pathology caused by eggs. However, more in-depth researches are needed on the specific mechanism to determine which pathway affects liver immunopathology.

Additionally, the expression of the USP21 mRNA was detected in the liver and spleen. The decrease in USP21 expression in the spleen of KO mice might be associated with overactivation of Tregs. The absence of USP21 destabilized the expression of FOXP3 and led to increased T cells. The percentage of FOXP3⁺ Tregs was reduced in KO mice due to the degradation of FOXP3. Meanwhile, we speculated that unstable FOXP3 led to the generation of T helper-like Tregs. The higher expression of USP21 in liver of the WT mice was related to the excessive activation of Tregs. In the WT mice, liver inflammation and liver fibrosis were more serious, and the number of parasites recovered from tissues and cells was increased, and the hepatocyte activity and USP21 expression were increased.

Soluble egg antigen (SEA) and adult worm antigen (SWA) are the main soluble proteins that are targeted by the adaptive immune response induced by *S. japonicum* infection. Related studies have shown that a high level of anti-*Schistosoma* IgG is associated with increased susceptibility to parasites and that anti-*Schistosoma* IgG, especially the IgG4 response [39], is positively correlated with severe schistosomiasis. In this study, anti-SEA and anti-SWA IgG in the USP21 knockout mice infected with *S. japonicum* were higher than those in the WT mice, while the IgM levels were not significantly different between the two groups. Based on this finding, USP21-deficient Tregs increased the susceptibility of mice to schistosomiasis.

Previous studies have shown that the immunologic process of *S. japonicum* infection is an initial short-lived increase in the number IFN- γ -producing Th1 cells, resulting in a mostly host-protective, Th2- (IL-4, IL-5, and IL-13) dominated environment [40, 41]. Cytokines, such as IL-4, IL-10, IFN- γ , IL-17, and IL-9, have been reported to be key signals in the immune cells involved in schistosomiasis. IL-4, a typical type 2 immune factor, attenuates Tregs function in type 2 inflammatory diseases through IL-4 receptor α (IL-4R α) signaling. Increased IL-4R α levels, through mutations in their functional domains or chronic inflammation of type 2 immune responses, leads to a rapid reduction in the FOXP3⁺ Treg population and the impairment of Tregs function, driving the polarization of Tregs to Th2- or Th17-like cells [42, 43]. Other studies have shown that Tregs need IL-4R α to

control inflammation during worm infection [44]. IL-10 has been reported to have dual functions, namely, proinflammatory and anti-inflammatory effects, which, on the one hand, might inhibit Th1-type autoimmune diseases and aggravate autoantibody-mediated autoimmune diseases, such as lupus erythematosus and myasthenia gravis, and, on the other hand, ameliorate parasite-mediated autoimmune disease [45]. Tregs are important components of the immunomodulatory network in chronic worm infection, especially the immunosuppression of chronic schistosomiasis, which is characterized by an independent downregulation of IL-10 produced by Th2 cytokines [46, 47].

Higher levels of IFN- γ and IL-4 were detected in the KO mice than those in the WT mice in the present study, while lower IL-10, IL-17A, IL-23, and IL-9 levels were observed in the KO mice than those in the WT mice. After different durations of infection, the trends of the changes in the serum cytokine levels in the two groups were approximately the same. These results are consistent with previous findings [9] and prompted us to speculate that the depletion of USP21 transforms Tregs to Th1-like cells. In the later stage of *S. japonicum* infection, IFN- γ levels remained stable, while IL-4 levels increased. However, this result was different from those mentioned above, which showed that the IL-4 was higher in the KO mice than that in the WT mice. The unstable Tregs might exhibit different differentiation patterns because of the different microenvironments present during schistosome infection. A series of T cell activation steps and long-term stimulation of chronic inflammatory factors might result in low reactivity, which was basically consistent with the results from the present study [9, 48]. This phenomenon was consistent with the reduced levels of secreted factors, in addition to IFN- γ and IL-4. The result also suggested that Th1 and Th2 cells are the main immune cell types involved in schistosomiasis. IL-23 is one of the driving factors that induce IL-17A expression [21]. We also observed that IL-17A was related to IL-23, both of which were downregulated and present at lower levels in the KO group than those in the WT group.

Worms live for a long time in the host, and accumulating evidence suggests that they can manipulate the host immune system through the host immunomodulatory network [47, 49]. As shown in our study, unstable Tregs in mice infected with *S. japonicum* might allow the host to benefit from the excessive inflammatory responses. This study still has some limitations. In particular, the eventual survival status of the mice was not considered.

In conclusion, USP21 is an important immunomodulatory molecule in the host that plays an important role in host immunity to *S. japonicum* infection. Our study might provide a theoretical basis for further analysis of the USP21-mediated regulation of different immune cell types activated by *S. japonicum*.

Data Availability

All relevant data are within the manuscript and its Supporting Information files.

Disclosure

The funders had no role in the study design, data collection and analysis, decision to publish, or preparation of the manuscript.

Conflicts of Interest

The authors declare that no conflicts of interest exist regarding the publication of this paper.

Authors' Contributions

Youxiang Zhang and De-Hui Xiong contributed equally to this work and co-first authors.

Acknowledgments

We thank Professor Qingren Zeng and Dr. Adiele Onyeye for their thorough reviews that greatly improved the manuscript. This study was completely or partially supported by the Key Techniques in Collaborative Prevention and Control of Major Infectious Diseases in the Belt and Road (<http://www.most.gov.cn/>) (Grant No. 2018ZX10101002-005 to ZQ) and the National Natural Science Foundation of China (<http://www.nsf.gov.cn/>) (Grant Nos. 81830051, 31525008, and 31961133011 to BL and 81372183 to ZZ).

Supplementary Materials

Table S1: number of mice used in each test. (*Supplementary Materials*)

References

- [1] F. Mutapi, R. Maizels, A. Fenwick, and M. Woolhouse, "Human schistosomiasis in the post mass drug administration era," *The Lancet Infectious Diseases*, vol. 17, no. 2, pp. e42–e48, 2017.
- [2] D. P. McManus, D. W. Dunne, M. Sacko, J. Utzinger, B. J. Vennervald, and X. N. Zhou, "Schistosomiasis," *Nature Reviews Disease Primers*, vol. 4, no. 1, p. 13, 2018.
- [3] J. E. Allen and R. M. Maizels, "Diversity and dialogue in immunity to helminths," *Nature Reviews Immunology*, vol. 11, no. 6, pp. 375–388, 2011.
- [4] Q. Yang, J. Qu, C. Jin et al., "Schistosoma japonicum infection promotes the response of Tfh cells through down-regulation of caspase-3-mediated apoptosis," *Frontiers in Immunology*, vol. 10, article 2154, 2019.
- [5] T. Zhan, H. Ma, S. Jiang et al., "Interleukin-9 blockage reduces early hepatic granuloma formation and fibrosis during Schistosoma japonicum infection in mice," *Immunology*, vol. 158, no. 4, pp. 296–303, 2019.
- [6] B. R. Giri and G. Cheng, "Host _miR-148_ regulates a macrophage-mediated immune response during _Schistosoma japonicum_ infection," *International Journal for Parasitology*, vol. 49, no. 13-14, pp. 993–997, 2019.
- [7] A. Romano, X. Hou, M. Sertorio et al., "FOXP3+ regulatory T cells in hepatic fibrosis and splenomegaly caused by Schistosoma japonicum: the spleen may be a major source of Tregs in subjects with splenomegaly," *PLOS Neglected Tropical Diseases*, vol. 10, no. 1, article e0004306, 2016.
- [8] M. D. Taylor, N. van der Werf, and R. M. Maizels, "T cells in helminth infection: the regulators and the regulated," *Trends in Immunology*, vol. 33, no. 4, pp. 181–189, 2012.
- [9] Y. Li, Y. Lu, S. Wang et al., "USP21 prevents the generation of T-helper-1-like Treg cells," *Nature Communications*, vol. 7, article 13559, 2016.
- [10] A. Levescot, N. Nelson-Maney, A. Morris, R. G. Bouyer, P. Lee, and P. Nigrovic, "Autoimmune arthritis in IL-1 receptor antagonist-deficient mice is associated with a pathogenic conversion of Foxp3+ regulatory T cells into Th17 cells," *Arthritis & Rheumatology*, vol. 69, 2017.
- [11] Y. Chen, L. Wang, J. Jin et al., "p38 inhibition provides anti-DNA virus immunity by regulation of USP21 phosphorylation and STING activation," *Journal of Experimental Medicine*, vol. 214, no. 4, pp. 991–1010, 2017.
- [12] B. M. Tebeje, M. Harvie, H. You, V. Rivera, and D. P. McManus, "T cell-mediated immunity in CBA mice during Schistosoma japonicum infection," *Experimental Parasitology*, vol. 204, article 107725, 2019.
- [13] B. Zhang, X. Wu, J. Liu et al., "β-Actin: not a suitable internal control of hepatic fibrosis caused by Schistosoma japonicum," *Frontiers in Microbiology*, vol. 10, p. 66, 2019.
- [14] B. N. Ondigo, E. M. Ndombi, S. C. Nicholson et al., "Functional studies of T regulatory lymphocytes in human Schistosomiasis in Western Kenya," *The American Journal of Tropical Medicine and Hygiene*, vol. 98, no. 6, pp. 1770–1781, 2018.
- [15] P. He, W. Wang, B. Sanogo et al., "Molluscicidal activity and mechanism of toxicity of a novel salicylanilide ester derivative against Biomphalaria species," *Parasites & Vectors*, vol. 10, no. 1, p. 383, 2017.
- [16] L. Ma, W. R. Zhao, X. Y. Hou et al., "Identification of linear epitopes in SjSP-13 of Schistosoma japonicum using a GST-peptide fusion protein microplate array," *Parasites & Vectors*, vol. 12, no. 1, 2019.
- [17] P. Cai, K. G. Weerakoon, Y. Mu et al., "A parallel comparison of antigen candidates for development of an optimized serological diagnosis of Schistosomiasis japonica in the Philippines," *eBioMedicine*, vol. 24, pp. 237–246, 2017.
- [18] S. A. Hall, S. H. Ison, C. Owles, J. Coe, D. A. Sandercock, and A. J. Zanella, "Development and validation of a multiplex fluorescent microsphere immunoassay assay for detection of porcine cytokines," *MethodsX*, vol. 6, pp. 1218–1227, 2019.
- [19] M. S. Wilson, M. M. Mentink-Kane, J. T. Pesce, T. R. Ramalingam, R. Thompson, and T. A. Wynn, "Immunopathology of schistosomiasis," *Immunology and Cell Biology*, vol. 85, no. 2, pp. 148–154, 2007.
- [20] C. L. Tang, J. Yang, L. Y. Cheng, L. F. Cheng, and Z. M. Liu, "Anti-CD25 monoclonal antibody enhances the protective efficacy of Schistosoma japonicum GST vaccine via inhibition of CD4+CD25+Foxp3+ regulatory T cells," *Parasitology Research*, vol. 116, no. 10, pp. 2727–2732, 2017.
- [21] B. Zheng, J. Zhang, H. Chen et al., "T lymphocyte-mediated liver immunopathology of schistosomiasis," *Frontiers in Immunology*, vol. 11, p. 61, 2020.
- [22] T. Nakagawa, T. Kajitani, S. Togo et al., "Deubiquitylation of histone H2A activates transcriptional initiation via trans-histone cross-talk with H3K4 di- and trimethylation," *Genes & Development*, vol. 22, no. 1, pp. 37–49, 2008.

- [23] J. Zhang, C. Chen, X. X. Hou et al., "Identification of the E3 deubiquitinase ubiquitin-specific peptidase 21 (USP21) as a positive regulator of the transcription factor GATA3," *Journal of Biological Chemistry*, vol. 288, no. 13, pp. 9373–9382, 2013.
- [24] L. Q. Tao, C. Chen, H. H. Song, M. Piccioni, G. Shi, and B. Li, "Deubiquitination and stabilization of IL-33 by USP21," *International Journal of Clinical and Experimental Pathology*, vol. 7, no. 8, pp. 4930–4937, 2014.
- [25] Y. H. Fan, R. F. Mao, Y. Yu et al., "USP21 negatively regulates antiviral response by acting as a RIG-I deubiquitinase," *Journal of Experimental Medicine*, vol. 211, no. 2, pp. 313–328, 2014.
- [26] A. Arceci, T. Bonacci, X. Wang et al., "FOXO1 deubiquitination by USP21 regulates cell cycle progression and paclitaxel sensitivity in basal-like breast cancer," *Cell Reports*, vol. 26, no. 11, pp. 3076–3086.e6, 2019.
- [27] F. W. Liu, Q. Fu, Y. P. Li et al., "USP21 modulates Goosecoid function through deubiquitination," *Bioscience Reports*, vol. 39, no. 7, 2019.
- [28] J. Pannu, J. I. Belle, M. Forster et al., "Ubiquitin specific protease 21 is dispensable for normal development, hematopoiesis and lymphocyte differentiation," *PLoS One*, vol. 10, no. 2, 2015.
- [29] P. Amiri, R. M. Locksley, T. G. Parslow et al., "Tumour necrosis factor α restores granulomas and induces parasite egg-laying in schistosome-infected SCID mice," *Nature*, vol. 356, no. 6370, pp. 604–607, 1992.
- [30] T. C. Freitas, E. Jung, and E. J. Pearce, "TGF- β signaling controls embryo development in the parasitic flatworm *Schistosoma mansoni*," *PLoS Pathogens*, vol. 3, no. 4, article e52, 2007.
- [31] Y. S. Lee, S. Y. Kim, E. Ko et al., "Exosomes derived from palmitic acid-treated hepatocytes induce fibrotic activation of hepatic stellate cells," *Scientific Reports*, vol. 7, no. 1, article 3710, 2017.
- [32] C. Y. Zhang, W. G. Yuan, P. He, J. H. Lei, and C. X. Wang, "Liver fibrosis and hepatic stellate cells: etiology, pathological hallmarks and therapeutic targets," *World Journal of Gastroenterology*, vol. 22, no. 48, pp. 10512–10522, 2016.
- [33] H. Xin, F. Wang, Y. Li et al., "Secondary release of exosomes from astrocytes contributes to the increase in neural plasticity and improvement of functional recovery after stroke in rats treated with exosomes harvested from microRNA 133b-overexpressing multipotent mesenchymal stromal cells," *Cell Transplantation*, vol. 26, no. 2, pp. 243–257, 2017.
- [34] J. Luo, Y. Liang, F. Kong et al., "Vascular endothelial growth factor promotes the activation of hepatic stellate cells in chronic schistosomiasis," *Immunology and Cell Biology*, vol. 95, no. 4, pp. 399–407, 2017.
- [35] J. P. Carson, G. A. Ramm, M. W. Robinson, D. P. McManus, and G. N. Gobert, "Schistosome-induced fibrotic disease: the role of hepatic stellate cells," *Trends in Parasitology*, vol. 34, no. 6, pp. 524–540, 2018.
- [36] L. I. Rutitzky and M. J. Stadecker, "CD4 T cells producing pro-inflammatory interleukin-17 mediate high pathology in schistosomiasis," *Memórias do Instituto Oswaldo Cruz*, vol. 101, Supplement 1, pp. 327–330, 2006.
- [37] X. Y. Wen, L. He, Y. Chi et al., "Dynamics of Th17 cells and their role in *Schistosoma japonicum* infection in C57BL/6 mice," *PLoS Neglected Tropical Diseases*, vol. 5, no. 11, 2011.
- [38] L. I. Rutitzky and M. J. Stadecker, "Exacerbated egg-induced immunopathology in murine *Schistosoma mansoni* infection is primarily mediated by IL-17 and restrained by IFN- γ ," *European Journal of Immunology*, vol. 41, no. 9, pp. 2677–2687, 2011.
- [39] D. Negrão-Corrêa, J. F. Fittipaldi, J. R. Lambertucci, M. M. Teixeira, C. M. de Figueiredo Antunes, and M. Carneiro, "Association of *Schistosoma mansoni*-specific IgG and IgE antibody production and clinical schistosomiasis status in a rural area of Minas Gerais, Brazil," *PLoS One*, vol. 9, no. 2, article e88042, 2014.
- [40] B. M. Larkin, P. M. Smith, H. E. Ponichtera, M. G. Shainheit, L. I. Rutitzky, and M. J. Stadecker, "Induction and regulation of pathogenic Th17 cell responses in schistosomiasis," *Seminars in Immunopathology*, vol. 34, no. 6, pp. 873–888, 2012.
- [41] X. He, R. Tang, Y. Sun et al., "MicroR-146 blocks the activation of M1 macrophage by targeting signal transducer and activator of transcription 1 in hepatic schistosomiasis," *EBioMedicine*, vol. 13, pp. 339–347, 2016.
- [42] M. N. Rivas, O. T. Burton, P. Wise et al., "Regulatory T cell reprogramming toward a Th2-cell-like lineage impairs oral tolerance and promotes food allergy," *Immunity*, vol. 42, no. 3, pp. 512–523, 2015.
- [43] A. H. Massoud, L. M. Charbonnier, D. Lopez, M. Pellegrini, W. Phipatanakul, and T. A. Chatila, "An asthma-associated IL4R variant exacerbates airway inflammation by promoting conversion of regulatory T cells to T_H17-like cells," *Nature Medicine*, vol. 22, no. 9, pp. 1013–1022, 2016.
- [44] N. A. Aziz, J. K. Nono, T. Mpotje, and F. Brombacher, "The Foxp3+ regulatory T-cell population requires IL-4R α signaling to control inflammation during helminth infections," *PLoS Biology*, vol. 16, no. 10, article e2005850, 2018.
- [45] Y. Nagayama, K. Watanabe, M. Niwa, S. M. McLachlan, and B. Rapoport, "Schistosoma mansoni and alpha-galactosylceramide: prophylactic effect of Th1 immune suppression in a mouse model of Graves' hyperthyroidism," *Journal of Immunology*, vol. 173, no. 3, pp. 2167–2173, 2004.
- [46] R. M. Maizels, A. Balic, N. Gomez-Escobar, M. Nair, M. D. Taylor, and J. E. Allen, "Helminth parasites - masters of regulation," *Immunological Reviews*, vol. 201, no. 1, pp. 89–116, 2004.
- [47] M. Baumgart, F. Tompkins, J. Leng, and M. Hesse, "Naturally occurring CD4+Foxp3+ regulatory T cells are an essential, IL-10-independent part of the immunoregulatory network in *Schistosoma mansoni* egg-induced inflammation," *Journal of Immunology*, vol. 176, no. 9, pp. 5374–5387, 2006, Epub 2006/04/20.
- [48] E. El-Ahwany, I. R. Bauomy, F. Nagy, R. Zalot, O. Mahmoud, and S. Zada, "T regulatory cell responses to immunization with a soluble egg antigen in *Schistosoma mansoni*-infected mice," *The Korean Journal of Parasitology*, vol. 50, no. 1, pp. 29–35, 2012.
- [49] D. P. McManus, R. Bergquist, P. Cai, S. Ranasinghe, B. M. Tebeje, and H. You, "Schistosomiasis-from immunopathology to vaccines," *Seminars in Immunopathology*, vol. 42, no. 3, pp. 355–371, 2020.

Research Article

New Biomarker in Chagas Disease: Extracellular Vesicles Isolated from Peripheral Blood in Chronic Chagas Disease Patients Modulate the Human Immune Response

Rafael Pedro Madeira ^{1,2}, Lavinia Maria Dal'Mas Romera,² Paula de Cássia Buck,³ Charles Mady,³ Barbara Maria Ianni,³ and Ana Claudia Torrecilhas ²

¹Disciplina de Infectologia, Departamento de Medicina, Universidade Federal de São Paulo (UNIFESP), São Paulo, Brazil

²Laboratório de Imunologia Celular e Bioquímica de Fungos e Protozoários, Departamento de Ciências Farmacêuticas, Universidade Federal de São Paulo (UNIFESP), Diadema, Brazil

³Unidade Clínica de Miocardiopatias, Instituto do Coração, Universidade de São Paulo (USP), São Paulo, Brazil

Correspondence should be addressed to Ana Claudia Torrecilhas; ana.torrecilhas@unifesp.br

Received 9 November 2020; Revised 21 December 2020; Accepted 30 December 2020; Published 12 January 2021

Academic Editor: Luiz Felipe Domingues Passero

Copyright © 2021 Rafael Pedro Madeira et al. This is an open access article distributed under the Creative Commons Attribution License, which permits unrestricted use, distribution, and reproduction in any medium, provided the original work is properly cited.

Chagas disease, a neglected tropical disease (NTD) caused by the flagellated protozoan *Trypanosoma cruzi* (*T. cruzi*), is a major public health problem. It was initially restricted to Latin America, but it is now expanding globally. Host and pathogen interactions are crucial in the establishment of disease, and since 1970, it has been known that eukaryotic cells release extracellular vesicles (EVs), which in turn have an important role in intercellular communication in physiological and pathological conditions. Our study proposed to characterize and compare circulating EVs isolated from the plasma of chronic Chagas disease (CCD) patients and controls. For this, peripheral blood was collected from patients and controls, and mononuclear cells (PBMCs) were isolated and stimulated with parasite EVs, showing that patient cells released fewer EVs than control cells. Then, after plasma separation followed by EV total shedding enrichment, the samples were subjected to ultracentrifugation to isolate the circulating EVs, which then had their size and concentration characterized by nanoparticle tracking analysis (NTA). This showed that patients had a lower concentration of circulating EVs while there were no differences in size, corroborating the *in vitro* data. Additionally, circulating EVs were incubated with THP-1 cells (macrophages) that, after the interaction, had their supernatant analyzed by ELISA for cytokine detection. In relation to their ability to induce cytokine production, the CCD patient EVs were able to induce a differential production of IFN- γ and IL-17 in relation to controls, with differences being more evident in earlier/less severe stages of the disease. In summary, a decreased concentration of circulating EVs associated with differential activation of the immunological system in patients with CCD is related to parasite persistence and the establishment of chronic disease. It is also a potential biomarker for monitoring disease progression.

1. Introduction

Trypanosoma cruzi is a protozoan parasite and the causative agent of Chagas disease (CD), also called American trypanosomiasis. CD is a systemic and chronic disease that is considered one of the 13 most Neglected Tropical Diseases (NTD) worldwide by the World Health Organization [1]. These diseases persist exclusively in the poorest and most marginalized populations, living without adequate sanitation and in close

contact with infected vectors and reservoirs. The disease affects 8 million people in Latin America from Mexico to Argentina, and there is a potential public health problem in the USA, as well as Europe and Asia, due to increasing immigration from endemic countries [2, 3].

In its chronic phase, the clinical presentations range from the absence of signs and symptoms (the indeterminate form) to a severe cardiac, digestive, or cardiodigestive burden with high morbidity and mortality [3–5]. The gold standard for

CCD diagnosis is a combination of two different serological assays, enzyme-linked immunosorbent assays (ELISA), hemagglutination inhibition assays (HAI), or indirect immunofluorescence (IIF), with the addition of a third test if the first two have discrepant results [6]. This combination approach is due to the reduced specificity of the tests based on the type of antigen used, which may lead to cross-reactivity with other parasitic diseases such as leishmaniasis [7]. There are still no available methodologies for the prognosis of confirmed chronic patients, although some studies using molecular and imaging approaches have shown some degree of correlation with the disease severity [8–10].

Once referred to as “platelet dust” by Wolf in 1967, extracellular vesicles (EVs) have now been extensively studied due to their role in intercellular communication and physiological and pathological conditions [11–13]. Their role in assessing disease progression as well as in establishing a prognosis suggests a potential use for them as biomarkers in noncommunicable diseases, such as cancer, but also in infectious diseases such as latent tuberculosis infection [14–16].

In a previous work by our group, we showed that *T. cruzi* trypomastigotes derived from infected mammalian cells released vesicles into the medium and that EVs of different sizes were associated with both the parasite membrane and the culture medium ([17]; [18]). These EVs carry glycoproteins are responsible for cell activation via TLR2, and it modulates the host innate immune response and increases the number of cell infections and intracellular parasites [19, 20]. The major glycoproteins from parasite surface, such as TS/gp85 glycoproteins and mucins, were found in EVs release by infective trypomastigote forms of *T. cruzi*. The mucins are the major surface glycoproteins from *T. cruzi* cell surface and are rich in O-linked α -galactosyl (α Gal) epitope-containing oligosaccharides [21]. These α -Gal epitopes are the major target of lytic anti- α Gal antibodies, which are the predominant IgG during Chagas’ disease and have the ability to control parasitic infection [21]. Furthermore, the addition of sialic acid residues confers a protection to the parasite against the anti- α Gal antibodies [22]. In fact, a proteomic analysis of this EVs isolated from trypomastigotes forms show that about 60% of the hits correspond to proteins of the 85 K Daltons family (gp85/TS) and mucins of the protozoa parasite [20]. Those glycoproteins are involved in the parasite host interaction and invasion by the parasite ([23–27]; [18, 28]). EVs contain virulence factors involved in pathogenesis and immunopathology, suggesting their ability to modulate host immune responses and inflammation.

In vivo, EVs increase the number of amastigote nests in heart tissue and carry virulence factors that are important for pathogenesis ([18–20, 29]).

The applications of EVs in clinical therapy have rapidly advanced in the past decade. The main challenges in clinical investigation are to promote the use of EVs in clinical trials and during the follow-up of many inflammatory and infectious diseases, as there is still no biomarker for infectious disease progression. Since EVs were demonstrated to be important for the development of heart parasitism and inflammation in animal models of infection, we proposed

to characterize the peripheral blood circulating population of EVs in CCD patients as well as their immunomodulatory capacity *in vitro*.

2. Materials and Methods

2.1. Ethics Statement. All of the experiments in this work were approved by the Federal University of São Paulo Ethics Committee in Research, CEP/UNIFESP (CAAE: 70749317.2.0000.5505), and samples from both patient and healthy controls were only collected after individuals agreed to participate and signing a written informed consent form.

2.2. Participants. The study included 70 individuals, 40 chronic Chagas disease patients and 30 healthy controls, selected from two university outpatient clinics (infected) and laboratory staff (noninfected) between January 2019 and May 2019. All patients, despite being in different disease stages, had a positive serological diagnosis for Chagas disease using ELISA and IIF. The patients were further divided into groups according to disease stage, degree of cardiac burden, and functional classification by New York Heart Association parameters as described in Table 1.

2.3. Obtaining and Isolating EVs Released by Trypanosoma Cruzi. *T. cruzi* culture (Y strain) was maintained by infection of green monkey kidney LLC-MK2 epithelial cells (ATCC, Manassas, VA) in Dulbecco’s modified eagle (DME) medium supplemented with 10% fetal bovine serum (FBS) at 37°C, under 5% CO₂ atmosphere, as described elsewhere [29]. Total *T. cruzi* shed vesicles were obtained from the culture medium supernatant of tissue culture cell-derived trypomastigotes (TCTs), which were harvested 5 to 9 days after the infection of LLC-MK2 cells. Parasites were counted, centrifuged (15 min, 1,500–2,000g, 10°C), and resuspended in DME medium supplemented with 5% FBS, at a concentration of 1×10^9 parasites/mL of medium. After incubation for 2–3 h at 37°C, under 5% CO₂ atmosphere, trypomastigotes were removed by centrifugation (10 min, 3000 g, 10°C), and the supernatant containing the total shed material was filtered through a 0.45 μ m cartridge [20, 29].

2.4. Fractionation of T. cruzi Vesicles. The total shed material was 2-fold diluted with 200 mM ammonium acetate (pH 6.5) and loaded onto a Sepharose CL-4B column (1 \times 40 cm, GE Healthcare, Piscataway, NJ) preequilibrated with 100 mM ammonium acetate (pH 6.5). The column was eluted with the equilibration buffer, in a flow rate of 0.2 mL/min using a peristaltic pump (GE Healthcare). Fractions ($N = 80$) of 1 mL were collected and then screened by chemiluminescent enzyme-linked immunosorbent assay (CL-ELISA) as described elsewhere [20], using anti-*T. cruzi* membrane polyclonal antibody (mouse) or anti-Alpha Gal purified from sera of chronic Chagasic patients (human Ch anti- α Gal), as described [21]. The most reactive fractions being pooled and concentrated in a vacuum centrifuge and then resuspended in filtered PBS for further analysis by nanoparticle tracking analysis (NTA) as previously described [20, 29, 30].

TABLE 1: Patients' and controls' baseline and clinical characteristics. Chronic Chagas disease patients (CCD; $n = 40$) and controls (CTRL; $n = 30$).

		Chronic Chagas disease (CCD)	Healthy controls (CTRL)
Sex	Male	17	10
	Female	23	20
Age	<20	0	1
	20-39	1	27
	40-59	18	2
	60-80	20	0
	>80	1	0
Clinical stage of cardiac burden	Indeterminate	10	—
	ECG alteration	15	—
	ECG alteration + ventricular dysfunction	15	—
NYHA functional classification	I	28	—
	II	8	—
	IV	4	—
		160	60

ECG: electrocardiogram; NYHA: New York Heart Association.

2.5. Blood Collection and Sample Preparation. Blood from the CCD samples was collected in lithium heparin for peripheral blood mononuclear cell (PBMC) isolation in a Ficoll-Paque (GE Healthcare) density gradient according to the manufacturer's instructions. Additionally, blood collected in sodium EDTA tubes was left at ambient temperature for 4 h and then incubated overnight at 4°C for plasma separation, which was used as the starting material for the isolation of circulating EVs.

2.6. Isolation of EVs from CCD Patient Plasma. After plasma separation from the blood, it was submitted to centrifugation at 100,000g for 1 h in a Thermo Scientific™ Sorvall™ WX100 Ultra Centrifuge using a fixed angle rotor (Thermo Scientific™ T-8100 Fixed Angle Rotor). The pellets were resuspended in filtered PBS (0.2 μm syringe filter) and then analyzed by NTA.

2.7. Scanning Electron Microscopy (SEM). PBMCs, after incubation for 24 and 48 h with and without EVs isolated from parasites, were fixed in a 2.5% glutaraldehyde solution, post-fixed with osmium tetroxide, treated with tannic acid, and dehydrated with ethanol [29]. The samples were observed in a field emission FEI Quanta 250 FEG scanning electron microscope (FEI, OR, USA).

2.8. PBMC-Parasite EV Interaction Assay. Following isolation, 1×10^5 PBMCs were seeded on 24-well plates and incubated for 24 h in culture medium. After 24 h, the cells were washed with PBS and then incubated with parasite EVs at a 1:100 (cell:EV) ratio, parasite extract (obtained from freeze-thawing and filtering an equivalent of 10^8 parasites), and culture medium for another 24 h at 37°C and 5% CO₂. Supernatants were centrifuged for 10 minutes at 750g and then analyzed by NTA.

2.9. Nanoparticle Tracking Analysis (NTA). EVs isolated from parasites and samples from patients were diluted in filtered PBS and then loaded into the NanoSight NS300 equipment (Malvern Panalytical) coupled to an sCMOS camera at a 532 nm wavelength, camera level set to auto, threshold and focus set manually to optimize readings as per the manufacturer's instructions. Readings were taken in triplicate for 30 seconds at 25 frames per second, and the data were analyzed using Nanoparticle Tracking Analysis software (NTA version 3.2 Dev Build 3.2.16).

2.10. Immunological Assays. THP-1 cells (ATCC® TIB-202™ Cell Type: monocyte) (10^7 cells) were differentiated with macrophages. Fifty ng/mL phorbol 12-myristate 13-acetate was primed with 10 ng/mL human recombinant interferon-gamma (IFN-γ, GenScript). The cells were then incubated with EVs isolated from plasma patients in a 1:100 (cell:EV) ratio. All incubations were performed at 37°C in 5% CO₂ for 24 h. Supernatants were collected for cytokine assays. Culture medium alone was used as a negative control.

2.11. Cytokine Measurements. For the ELISA cytokine detection, supernatants were collected, and cytokines were determined using Human Cytokine assay kits (Human DuoSet ELISA, R&D Systems) according to the manufacturer's specifications. The cytokines TNF-α, IFN-γ, IL-4, IL-5, IL-6, IL-10, IL12p70, and IL-17 were assessed and, when detected in the supernatant, had their concentration measured and compared to controls and between subgroups of patients.

2.12. Statistical Analysis. All data sets were assessed using GraphPad Prism 7.0 software (GraphPad Software Inc., San Diego, USA) and Orange (University of Ljubljana, Slovenia). As appropriate, Spearman's correlation, unpaired *t*-tests with Welch's correction, and ordinary one-way ANOVA followed by Dunnett's multiple comparisons test were performed, and

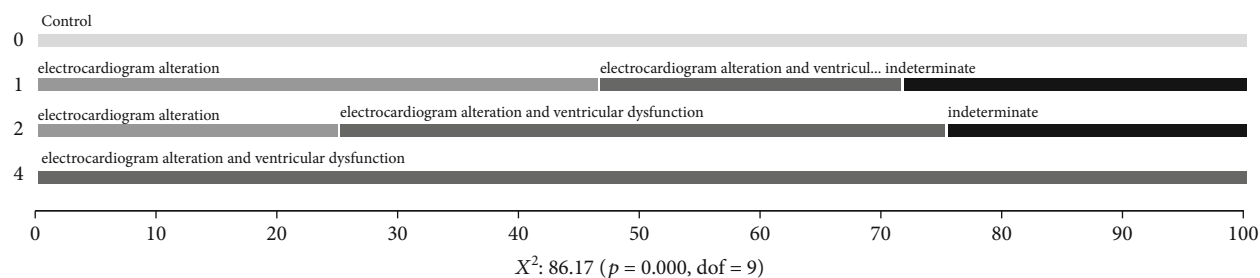


FIGURE 1: CCD patients' clinical data analysis. Frequency of patients by the stage of cardiac burden in relation to the NYHA functional classification.

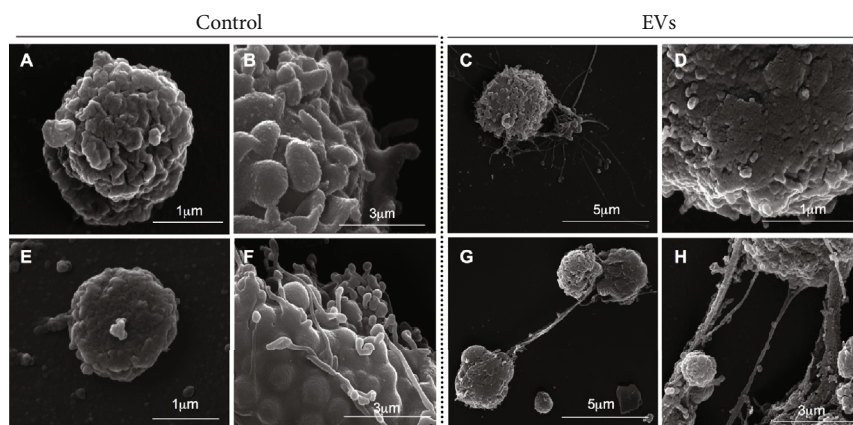


FIGURE 2: Scanning electron microscopy (SEM) of CCD PBMCs releasing EVs after 24 and 48 h of parasite EV stimulus. 24 h control in (a, b), 48 h control in (e, f), 24 h parasite EV stimulus in (c, d), and 48 h parasite EV stimulus in (g, h).

the results are presented as the means \pm 95% confidence intervals.

3. Results

3.1. Patient Distribution among Subgroups and Analysis of Clinical Data. Our cohort of patients was evenly distributed between male and female individuals as well as disease stage and degree of cardiac burden, with the majority (39 out of 40) of patients being over 40 years old and in NYHA class I (Table 1). Additionally, there was a correlation between a higher degree of cardiac burden and NYHA functional classification (Figure 1). Full clinical data from the patients are presented in Supplementary Table 1.

3.2. PBMC Purification from Chronic Chagas Disease Patients Releases Fewer EVs Than from Healthy Individuals. PBMCs isolated from chronic Chagas disease patients' blood can constitutively release EVs, as shown by scanning electron microscopy (Figure 2). When stimulated with *T. cruzi* extract or *T. cruzi* EVs, PBMC EVs presented a similar size dispersion but a smaller mean particle size than healthy individuals (Figure 3, top and center). For their mean concentration, even though they were larger in size, they were fewer in quantity when compared to healthy individuals (Figure 3, bottom).

3.3. Chronic Chagas Disease Patients Have Fewer Total Circulating EVs in Plasma Than Healthy Individuals (Control). After isolation from plasma, nanoparticle tracking analysis revealed that patients with chronic Chagas disease had a lower concentration of total circulating EVs when compared to healthy individuals, corroborating the observed results from peripheral blood mononuclear cells (Figure 4(a)). When analyzing the frequencies of the concentration values throughout subgroups of patients, it was observed that reduced concentrations of circulating EVs were associated with alterations in cardiac clinical parameters (Figure 4(b)), but this phenomenon was not observed when assessing EV size (Figure 4(c)).

3.4. EVs from Chronic Chagas Disease Patients Induce Differential Cytokine Production and Release from THP-1 Cells (Macrophages). After EV stimulation, differentiated and activated THP-1 cells (macrophages) exhibited differential production and release of cytokines in the supernatant. In general, cells that interacted with chronic Chagas patient EVs exhibited a higher production of IFN- γ but a lower production of IL-17 (Figure 5). When the data were analyzed based on the different patient subgroups, IFN- γ differential production was maintained throughout every subset analyzed, while IL-17 only presented a tendency toward a reduction in patient samples. Taking into consideration the clinical stage of cardiac burden, IFN- γ production is higher due to

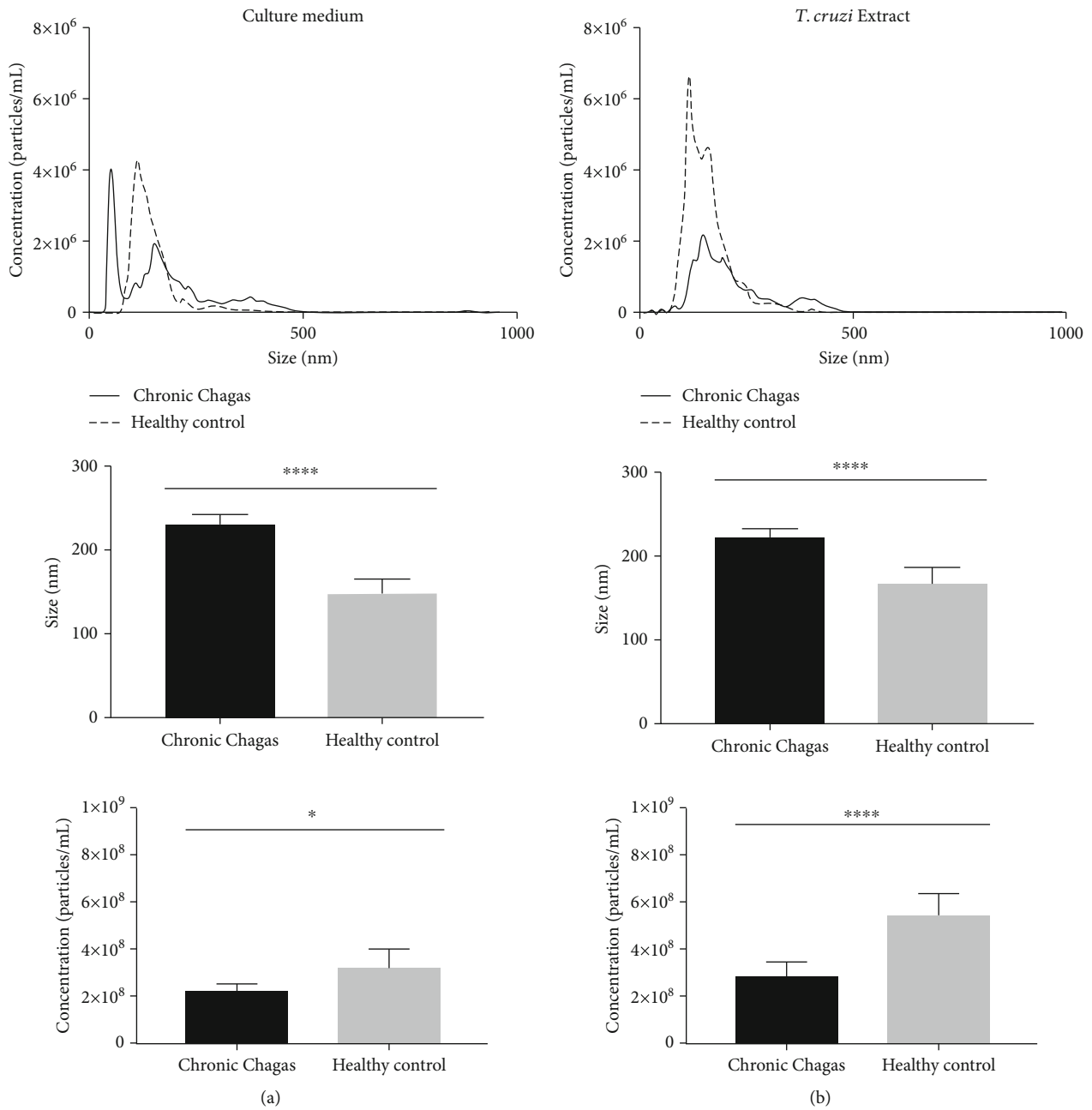


FIGURE 3: Continued.

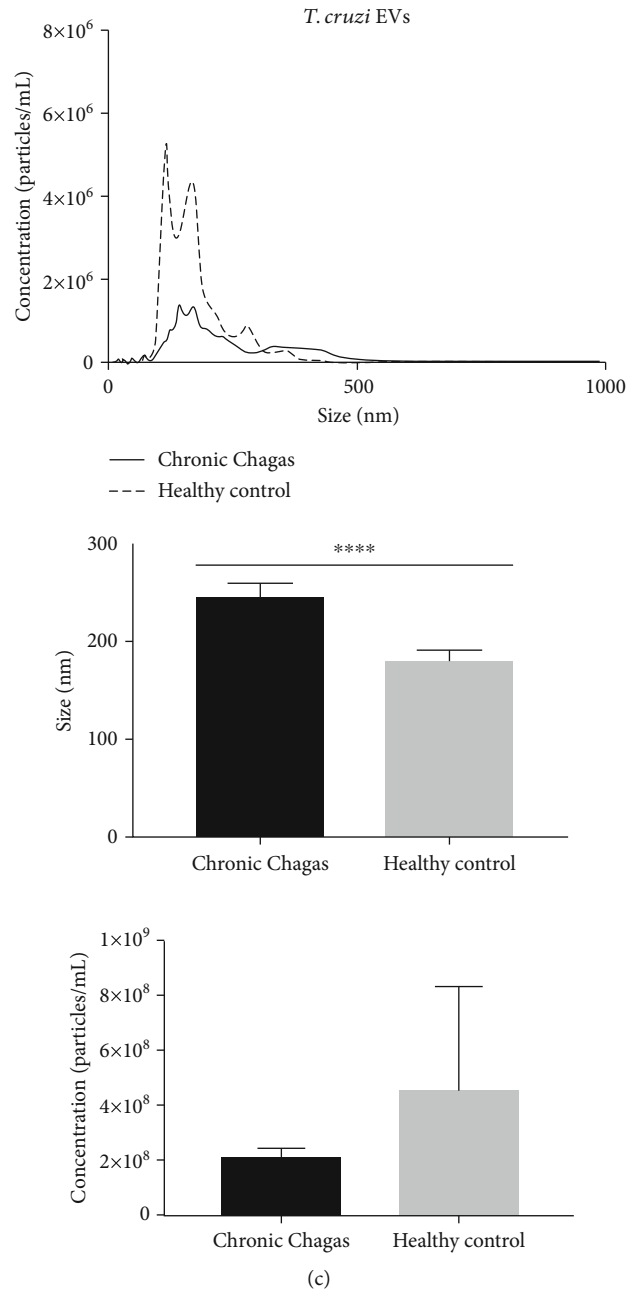


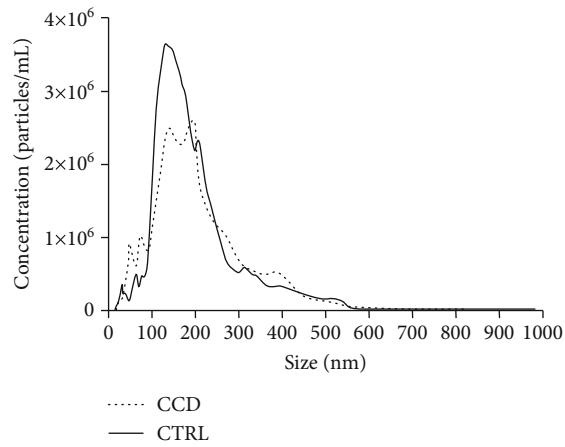
FIGURE 3: Comparison of EV profiles from CCD and CTRL PBMCs after a 24 h incubation. Concentration/size distribution (top), mean size \pm 95%CI (center) and mean concentration \pm 95%CI (bottom) after (a) culture medium (* $p = 0.0326$ and **** $p < 0.0001$), (b) *T. cruzi* extract (** $p = 0.0003$ and **** $p = 0.0002$), or (c) *T. cruzi* EV stimuli (**** $p < 0.0001$).

interaction with EVs from patients with the indeterminate form and decreases as the severity of cardiac burden increases (Figure 6(a)), a phenomenon that is clearly observed when the frequencies of each subgroup are plotted against the IFN- γ concentration (Figure 6(b)). On the other hand, IL-17 production after EV stimuli showed no significant difference, with only a tendency toward lower levels of this cytokine in the patients (Figures 6(c) and 6(d)). When the data were analyzed based on the New York Heart Association (NYHA) Functional Classification, only EVs from patients included in Class I induced higher IFN- γ production (Figure 7(a)) and lower IL-17 production (Figure 7(c)) than

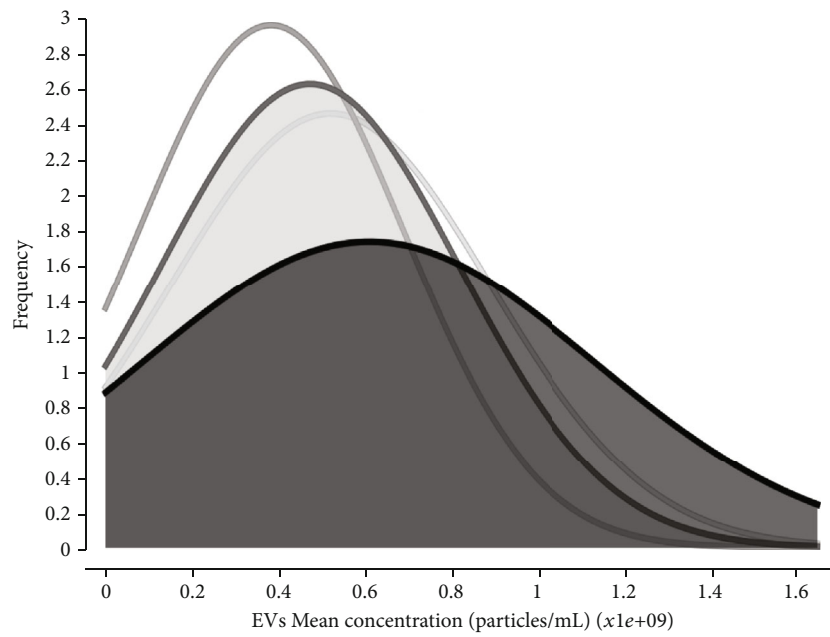
the control EVs, as was also seen on the overlapping curves of frequency by cytokine concentration (Figures 7(b) and 7(d), respectively). In addition to the clinical parameters, age showed a positive correlation with IFN- γ production (Figure 8(a)) and a negative correlation with IL-17 (Figure 8(b)), but in neither case was sex relevant to the results obtained.

4. Discussion

Extracellular vesicles are released from a wide array of cells ranging from prokaryotic organisms to higher eukaryotes



(a)



- Control ($\mu = 521203333.33, \sigma = 369134052.87$)
- Electrocardiogram alteration ($\mu = 521203333.33, \sigma = 369134052.87$)
- Electrocardiogram alteration and ventricular dysfunction ($\mu = 473606666.67, \sigma = 345704410.28$)
- Indeterminate ($\mu = 611272000, \sigma = 523468182.28$)

(b)

FIGURE 4: Continued.

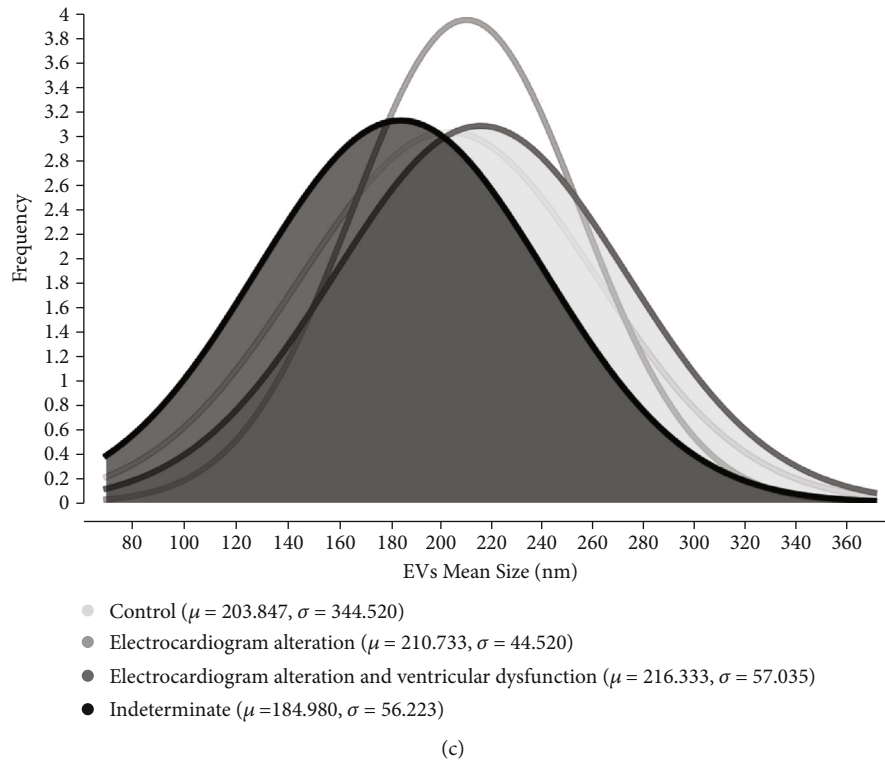


FIGURE 4: Comparison of circulating EV profiles in CCD patients in relation to CTRL. (a) Concentration (particles/mL) \times size (nm) profile. (b) Frequency of EV concentration among different degrees of cardiac burden. (c) Frequency of EV size among different stages of cardiac burden.

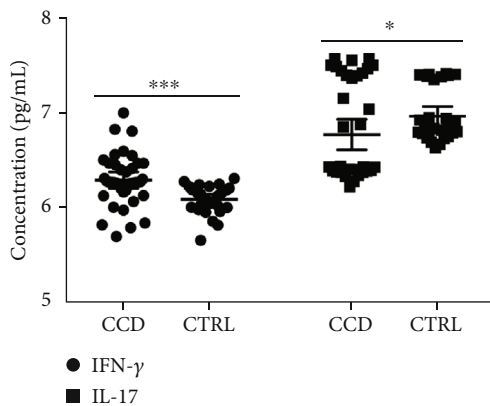


FIGURE 5: Cytokine production by THP-1 cells (macrophages) quantified in the supernatant by ELISA after 24 h of stimulation with CCD or CTRL EVs. (* $p = 0.0438$ and *** $p = 0.0002$).

and are found in virtually all body fluids in humans [13, 31, 32]. They have important roles in intercellular signaling during physiological processes, such as in kidney physiology, where urinary EVs may play a role in the renin-angiotensin system by carrying angiotensin-converting enzyme and being able to interact with cells in the renal tubule lumen [33]. Another important example of EVs helping to maintain homeostasis is in modulating chemotaxis, signaling, and the proliferation of hematopoietic cells by platelet-derived microparticles [34].

Due to the many different cells circulating in blood, we first wanted to assess whether the mononuclear cell EV-releasing behavior in chronic Chagas disease patients was compatible with what was observed in healthy individuals. Peripheral blood mononuclear cells from chronic Chagas patients released a lower quantity of EVs than cells from healthy individuals when cultivated *in vitro*, and this phenomenon was also observed when quantifying EVs directly from peripheral blood plasma.

The alteration of body fluid EV concentrations in pathological states has been described in both infectious and inflammatory models [35, 36]. In patients with periodontitis, there is a higher concentration of EVs in gingival crevicular fluid, which correlates with the clinical inflammatory periodontal parameters [37]. A similar phenomenon is observed in patients with human African trypanosomiasis, where late stage patients have a higher concentration of EVs in cerebrospinal fluid when compared to early and intermediate stages, with these EVs also showing different functional properties such as altering astrocyte protein expression *in vitro* [38]. In our study, as the EV concentration in patients was lower than that in controls, we hypothesized that this might have led to a loss of function in the human immune response, which in turn contributed to infection persistence and severity, as in a previously described *in vitro* model of *Pseudomonas aeruginosa* infection where the infected cells released fewer EVs that, in turn, carried less CCL4 mRNA, contributing to a less effective immune response [39].

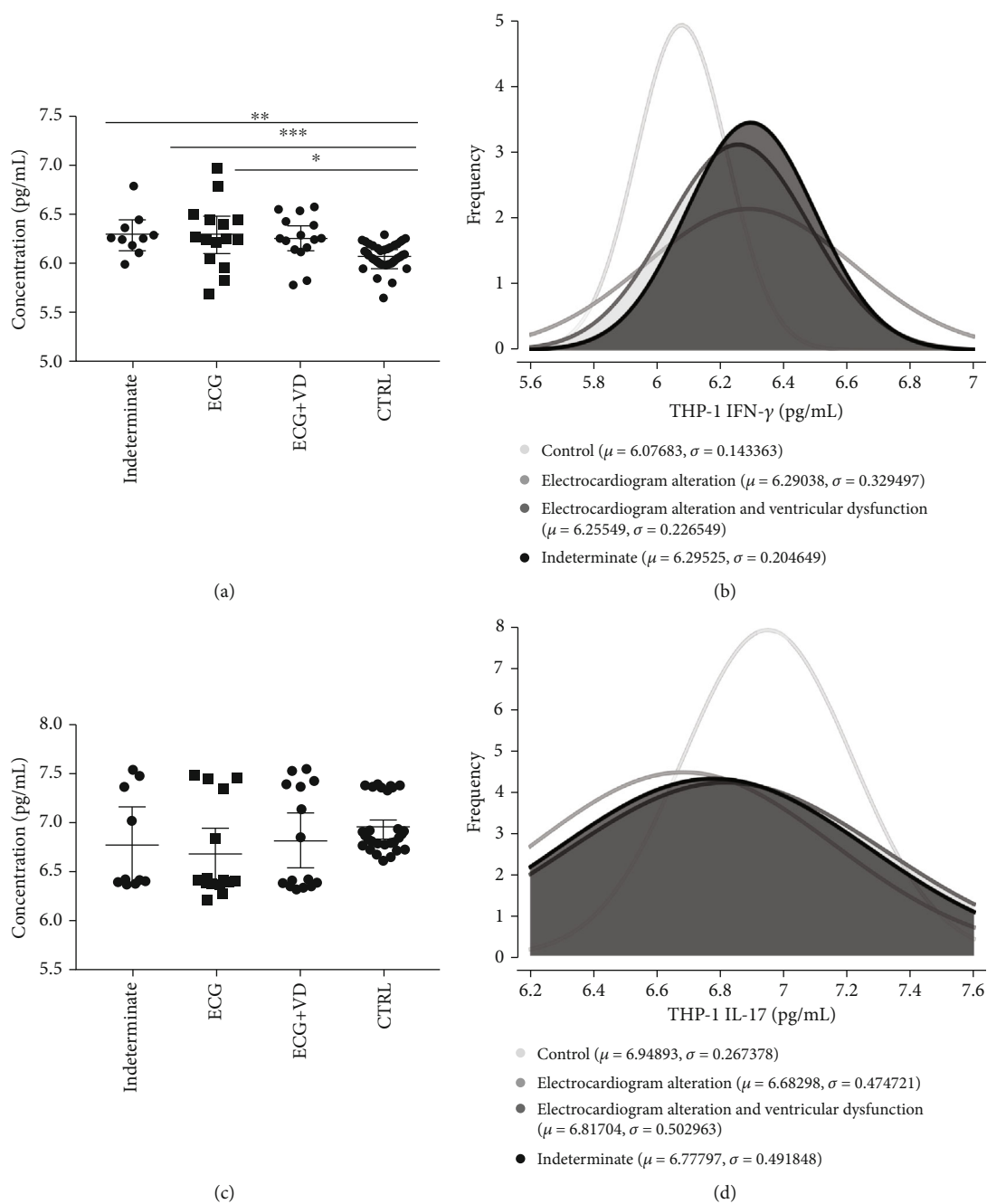


FIGURE 6: Cytokine production by THP-1 cells (macrophages) quantified in the supernatant by ELISA after 24 h of stimulation with CCD or CTRL EVs among patients grouped based on the clinical stage of the cardiac burden and controls. (a) IFN- γ concentration in pg/mL ($*p = 0.0420$, $**p = 0.0291$, and $***p = 0.0118$). (b) Frequency of IFN- γ concentration values. (c) IL-17 concentration in pg/mL. (d) Frequency of IL-17 concentration values.

To assess the impact of circulating EVs on the human immune response, despite their decreased number in chronic Chagas patients, we incubated macrophage (THP-1) cells, which were previously differentiated and activated, with EVs and quantified an array of cytokines in the culture supernatant. The importance of studying cytokines in Chagas disease can be exemplified by polymorphisms in genes related to Th1-type T cell differentiation playing a role in genetic susceptibility to chronic Chagas cardiomyopathy [40]. In our model, we observed that while most cytokines analyzed could

not be detected or showed no differences among the groups, both IFN- γ and IL-17 presented a differential profile when comparing chronic Chagas patients and healthy controls.

We observed that in samples from patients, circulating EVs induced a higher production of IFN- γ , corroborating data available from an in vivo chronic model of benznidazole treatments where the treated mice had fewer IFN- γ -producing cells as well as an improvement in electrocardiographic alterations. Additionally, circulating IFN- γ was positively correlated with the cardiac inflammatory process and

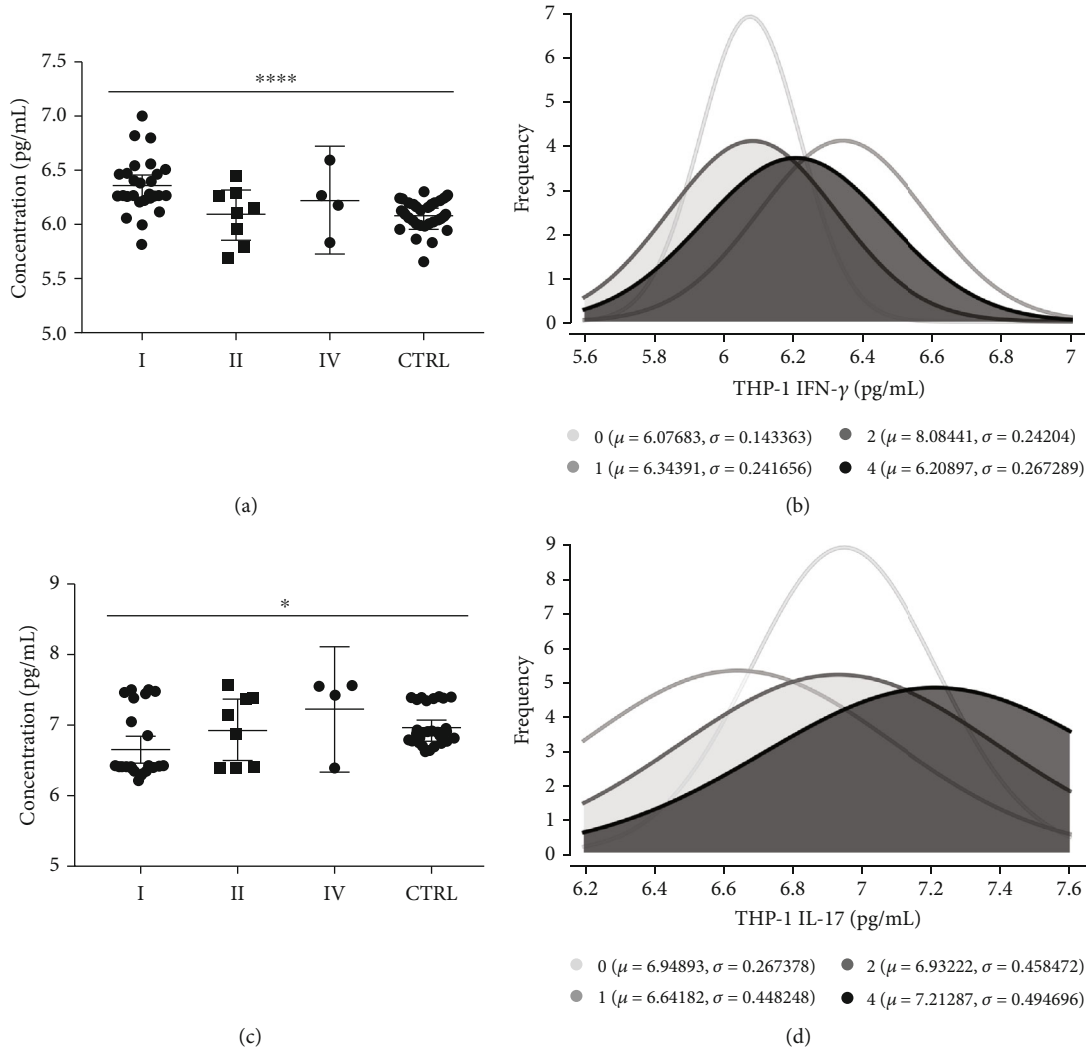


FIGURE 7: Cytokine production by THP-1 cells (macrophages) quantified in the supernatant by ELISA after 24 h of stimulation with CCD or CTRL EVs among patients grouped based on NYHA functional classification and controls. (a) IFN- γ concentration in pg/mL (**** $p = 0.0001$). (b) Frequency of IFN- γ concentration values (0: CTRL). (c) IL-17 concentration in pg/mL (* $p = 0.0125$). (d) Frequency of IL-17 concentration values (0: CTRL).

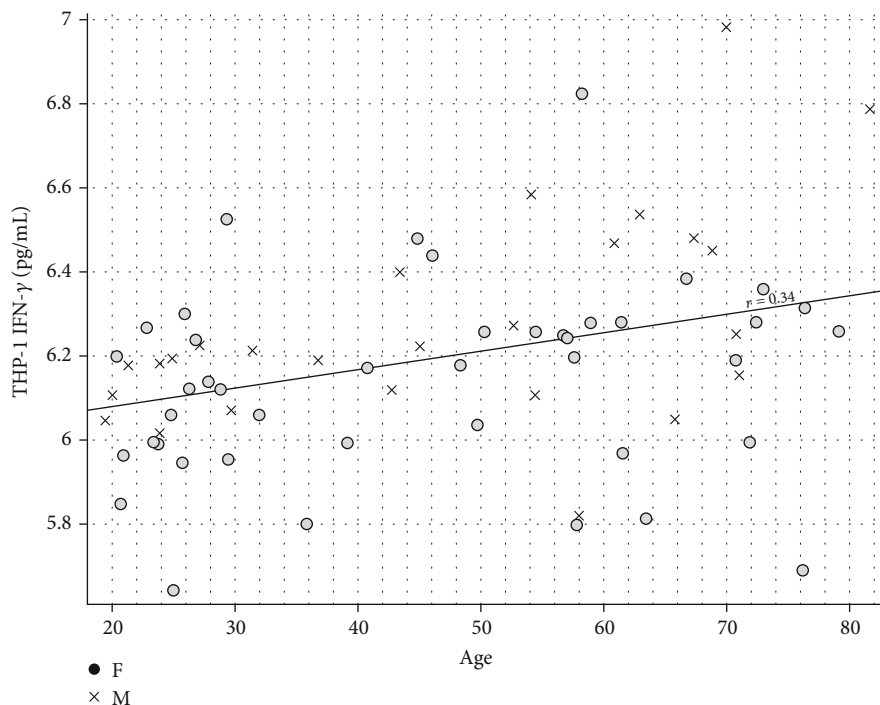
parasite burden [41, 42]. In contrast to IFN- γ , IL-17 production was diminished after stimulation with patient EVs, which in murine models is associated with compromised parasite control and a reduction of the response magnitude and survival of CD8⁺ T cells [43]. This combination of augmented IFN- γ and reduced IL-17 may play an important role in parasite persistence in chronic disease as well as tissue damage in target organs due to continuous inflammatory signaling.

In an attempt to evaluate whether the alterations in circulating EV concentration and subsequent immune activation would be associated with Chagas disease chronification and progression, we stratified our cohort of patients by sex, age, degree of cardiac burden, and functional classification.

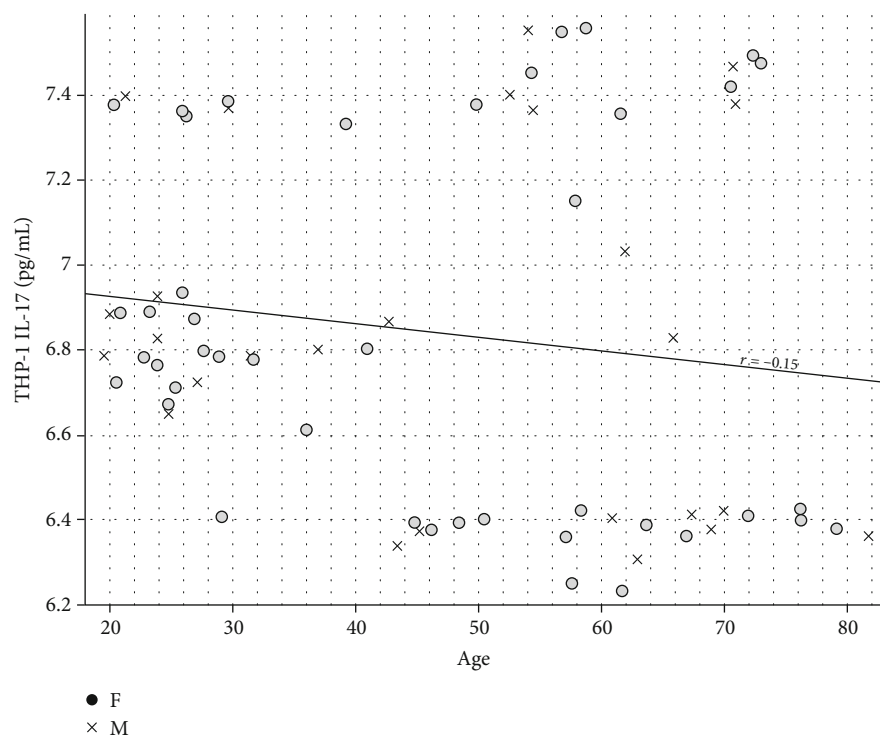
Sex can be an important factor in inflammation pathophysiology. In athletes who suffered a concussion, while men have a positive correlation of IFN- γ levels with the severity of their symptoms, women have a negative correlation of IFN- γ levels and symptom severity [44]. However,

apart from a slight difference in healthy individuals, sex was not a factor that could interfere with IFN- γ production after stimulus with EVs from chronic Chagas disease patients.

While sex represented no interfering factor with IFN- γ production, age proved itself a much more complex factor. During aging, a process called immunosenescence takes place and it is characterized by a decrease in the acute inflammatory response combined with a persistent low-grade inflammatory profile that may lead to a higher risk of infection development as well as participate in the pathogenesis of chronic noncommunicable diseases such as osteoporosis, rheumatoid arthritis, and coronary heart disease [45–47]. After incubation with circulating EVs from patients, macrophages produced more IFN- γ than healthy controls. Another point to take into consideration is that almost all of the patients were older than the controls, so a combination of both age and infection might be responsible for the increase in IFN- γ levels and the establishment of a basal proinflammatory environment, which in turn could be related to



(a)



(b)

FIGURE 8: Correlation of age (*X* axis), cytokine production by THP-1 cells (macrophages) quantified in the supernatant by ELISA after 24 h of stimulation with CCD or CTRL EVs (*Y* axis) and sex (●: female; X: male). (a) IFN- γ ($r = 0.34$). (b) IL-17 ($r = -0.15$).

cardiac tissue damage characteristic of chronic symptomatic Chagas disease [48, 49].

IFN- γ production represents a major factor in Chagas disease pathogenesis. When we compared different degrees of cardiac damage, clinically assessed by electrocardiography

(ECG), we observed that only EVs from patients in the indeterminate stage or with only ECG alterations were able to induce IFN- γ production, as EVs from patients with ECG alterations combined with ventricular dysfunction could not. This might suggest that an increase in IFN- γ production,

and consequently more inflammation, is crucial in the establishment of chronic disease more than in the final stages, where the severity of symptoms is more due to a loss of organ function [50, 51].

In addition to the cardiac burden, the overall effects on its function could also be related to immunological EV-mediated signaling [52, 53]. Corroborating the data derived from patients grouped by ECG, when we looked at the loss of cardiac function, we observed that IFN- γ production was also increased when using EVs from patients with no loss of function, validating our hypothesis that a proinflammatory environment is a key point in the establishment of chronic disease. Another important point is that in functionally normal patients, their EVs also led to a decrease in IL-17. A follow-up study in school-aged children with Chagas disease found that higher IL-17A levels were associated with the persistence of infection after treatment with benznidazole, suggesting this cytokine could be a possible biomarker for nonresponse to treatment and the persistence of infection [54]. However, when we analyzed our data under this hypothesis, in contrast to what was previously described, EVs from chronic patients with no cardiac function loss induced a lower production of IL-17, suggesting that in patients who did not receive benznidazole treatment, this cytokine might have another role, even a protective one.

The observed important role of EVs in Chagas disease pathogenesis and chronic disease combined with their altered quantity when compared to healthy individuals suggests EVs are a possible biomarker for disease progression. Even though other situations may alter the concentration of circulating EVs, their differential effect on target cells suggests a composition unlike that seen for healthy individuals' vesicles. Proteomics studies using primary murine or immortalized human cells infected with parasites such as *Plasmodium yoelii* and *Trypanosoma cruzi* demonstrated that EVs released from infected cells carry parasite molecules as well their own cargo, but none showed this phenomenon using circulating EVs or EVs from patients [55, 56].

In the case of Chagas disease, some highly expressed parasite molecules are important for infection, such as the virulence factors *trans*-sialidase and cruzipain [57]. These molecules are able to induce a humoral immune response that can be detected and used for diagnostics and treatment monitoring, even though cross-reactivity with other infections also exists [57–59]. Considering the demonstrated importance of EVs in the modulation of the immune response of infection and their altered concentration in circulation, EVs present themselves as promising candidates for biomarkers of disease progression in Chagas disease.

Data Availability

Data are available on request.

Conflicts of Interest

No potential conflict of interest was reported by the authors.

Authors' Contributions

RPM, BMI, and ACT conceived and designed the experiments. RPM, LMDR, PCB, and ACT performed most of the experiments. RPM, BMI, and ACT wrote the manuscript. RPM, BMI, CM, and ACT contributed to the final manuscript. All of the authors reviewed the manuscript.

Acknowledgments

We thank all colleagues from the Laboratório de Imunologia Celular e Bioquímica de fungos e protozoários (LICBfp), Departamento de Ciências Farmacêuticas, UNIFESP, who provided helpful technical advice and expertise that greatly assisted the research. This work was supported by FAPESP Regular (2016/01917-3) and CNPq Universal (408186/2018-6) grants and a CAPES doctoral fellowship (Financial Code 001).

Supplementary Materials

Supplementary Table 1: full clinical data from patients and controls. (*Supplementary Materials*)

References

- [1] P. J. Hotez, D. H. Molyneux, A. Fenwick et al., "Control of neglected tropical diseases," *The New England Journal of Medicine*, vol. 357, pp. 1018–1027, 2007.
- [2] J. R. Coura and P. A. Vias, "Chagas disease: a new worldwide challenge," *Nature*, vol. 465, pp. S6–S7, 2010.
- [3] A. Rassi, A. Rassi, and J. A. Marin-Neto, "Chagas disease," *Lancet*, vol. 375, pp. 1388–1402, 2010.
- [4] N. G. Echavarría, L. E. Echeverría, M. Stewart, C. Gallego, and C. Saldarriaga, "Chagas disease: chronic Chagas cardiomyopathy," *Current Problems in Cardiology*, vol. 1, no. article 100507, 2020.
- [5] L. E. Echeverría, R. Marcus, G. Novick et al., "WHF IASC roadmap on Chagas disease," *Global Heart*, vol. 15, p. 26, 2020.
- [6] Organización Panamericana de la Salud, *Guía para el diagnóstico y el tratamiento de la enfermedad de Chagas*, 2018.
- [7] Z. C. Caballero, O. E. Sousa, W. P. Marques, A. Saez-Alquezar, and E. S. Umezawa, "Evaluation of serological tests to identify *Trypanosoma cruzi* infection in humans and determine cross-reactivity with *Trypanosoma rangeli* and *Leishmania* spp," *Clinical and Vaccine Immunology*, vol. 14, pp. 1045–1049, 2007.
- [8] T. F. Cianciulli, M. C. Saccheri, A. Papantoniou et al., "Use of tissue Doppler imaging for the early detection of myocardial dysfunction in patients with the indeterminate form of Chagas disease," *Revista da Sociedade Brasileira de Medicina Tropical*, vol. 53, 2020.
- [9] N. Cortes-Serra, I. Losada-Galvan, M. J. Pinazo, C. Fernandez-Becerra, J. Gascon, and J. Alonso-Padilla, "State-of-the-art in host-derived biomarkers of Chagas disease prognosis and early evaluation of anti-*Trypanosoma cruzi* treatment response," *Biochimica et Biophysica Acta - Molecular Basis of Disease*, vol. 1866, article 165758, 2020.
- [10] C. K. Nonaka, B. R. Cavalcante, A. C. Alcántara et al., "Circulating miRNAs as potential biomarkers associated with cardiac remodeling and fibrosis in Chagas disease cardiomyopathy," *International Journal of Molecular Sciences*, vol. 20, p. 4064, 2019.

- [11] J. H. Campos, R. P. Soares, K. Ribeiro, A. Cronemberger Andrade, W. L. Batista, and A. C. Torrecilhas, "Extracellular vesicles: role in inflammatory responses and potential uses in vaccination in cancer and infectious diseases," *Journal of Immunology Research*, vol. 2015, 14 pages, 2015.
- [12] A. C. Torrecilhas, R. I. Schumacher, M. J. M. Alves, and W. Colli, "Vesicles as carriers of virulence factors in parasitic protozoan diseases," *Microbes and Infection*, vol. 14, pp. 1465–1474, 2012.
- [13] M. Yáñez-Mó, P. R. Siljander, Z. Andreu et al., "Biological properties of extracellular vesicles and their physiological functions," *Journal of extracellular vesicles*, vol. 4, article 27066, 2015.
- [14] J. J. Castellano, R. M. Marrades, L. Molins et al., "Extracellular vesicle lincRNA-p21 expression in tumor-draining pulmonary vein defines prognosis in NSCLC and modulates endothelial cell behavior," *Cancers*, vol. 12, p. 734, 2020.
- [15] E. Le Rhun, J. Seoane, M. Salzet, R. Soffietti, and M. Weller, "Liquid biopsies for diagnosing and monitoring primary tumors of the central nervous system," *Cancer Letters*, vol. 480, pp. 24–28, 2020.
- [16] C. Mehaffy, N. A. Kruh-Garcia, B. Graham et al., "Identification of *Mycobacterium tuberculosis* peptides in serum extracellular vesicles from persons with latent tuberculosis infection," *Journal of Clinical Microbiology*, vol. 58, 2020.
- [17] M. F. Gonçalves, E. S. Umezawa, A. M. Katzin et al., "Trypanosoma cruzi : shedding of surface membrane vesicles antigens as," *Experimental Parasitology*, vol. 53, pp. 43–53, 1991.
- [18] A. C. Torrecilhas, R. R. Tonelli, W. R. Pavanelli et al., "Trypanosoma cruzi: parasite shed vesicles increase heart parasitism and generate an intense inflammatory response," *Microbes and Infection*, vol. 11, pp. 29–39, 2009.
- [19] A. Cronemberger-Andrade, P. Xander, R. P. Soares et al., "Trypanosoma cruzi-infected human macrophages shed proinflammatory extracellular vesicles that enhance host-cell invasion via toll-like receptor 2," *Frontiers in Cellular and Infection Microbiology*, vol. 10, 2020.
- [20] K. S. Ribeiro, C. I. Vasconcellos, R. P. Soares et al., "Proteomic analysis reveals different composition of extracellular vesicles released by two Trypanosoma cruzi strains associated with their distinct interaction with host cells," *Journal of extracellular vesicles*, vol. 7, 2018.
- [21] I. C. Almeida, M. A. J. Ferguson, S. Schenkman, and L. R. Travassos, "Lytic anti- α -galactosyl antibodies from patients with chronic Chagas' disease recognize novel O-linked oligosaccharides on mucin-like glycosyl-phosphatidylinositol-anchored glycoproteins of Trypanosoma cruzi," *The Biochemical Journal*, vol. 304, pp. 793–802, 1994.
- [22] V. L. Pereira-Chioccola, A. Acosta-Serrano, I. C. De Almeida et al., "Mucin-like molecules form a negatively charged coat that protects Trypanosoma cruzi trypomastigotes from killing by human anti- α -galactosyl antibodies," *Journal of cell science*, vol. 113, pp. 1299–1307, 2000.
- [23] R. Giordano, D. L. Fouts, D. Tewari, W. Colli, J. E. Manning, and M. J. M. Alves, "Cloning of a surface membrane glycoprotein specific for the infective form of Trypanosoma cruzi having adhesive properties to laminin," *The Journal of Biological Chemistry*, vol. 274, pp. 3461–3468, 1999.
- [24] M. H. Magdesian, R. Giordano, H. Ulrich et al., "Infection by Trypanosoma cruzi: identification of a parasite ligand and its host cell receptor," *The Journal of Biological Chemistry*, vol. 276, pp. 19382–19389, 2001.
- [25] K. A. Norris, B. Bradt, N. R. Cooper, and M. So, "Characterization of a Trypanosoma cruzi C3 binding protein with functional and genetic similarities to the human complement regulatory protein, decay-accelerating factor," *Journal of Immunology*, vol. 147, 1991.
- [26] S. Schenkman, D. Eichinger, M. E. A. Pereira, and V. Nussenzweig, "Structural and functional properties of Trypanosoma trans-sialidase," *Annual Review of Microbiology*, vol. 48, pp. 499–523, 1994.
- [27] S. Schenkman, M. S. Jiang, G. W. Hart, and V. Nussenzweig, "A novel cell surface trans-sialidase of trypanosoma cruzi generates a stage-specific epitope required for invasion of mammalian cells," *Cell*, vol. 65, pp. 1117–1125, 1991.
- [28] A. C. Torrecilhas, R. P. Soares, S. Schenkman, C. Fernández-Prada, and M. Olivier, "Extracellular vesicles in trypanosomatids: host cell communication," *Frontiers in Cellular and Infection Microbiology*, vol. 10, p. 750, 2020.
- [29] P. M. Nogueira, K. Ribeiro, A. C. Silveira et al., "Vesicles from different Trypanosoma cruzi strains trigger differential innate and chronic immune responses," *Journal of extracellular vesicles*, vol. 4, article 28734, 2015.
- [30] C. Théry, K. W. Witwer, E. Aikawa et al., "Minimal information for studies of extracellular vesicles 2018 (MISEV2018): a position statement of the International Society for Extracellular Vesicles and update of the MISEV2014 guidelines," *Journal of extracellular vesicles*, vol. 7, 2018.
- [31] M. Colombo, G. Raposo, and C. Théry, "Biogenesis, secretion, and intercellular interactions of exosomes and other extracellular vesicles," *Annual Review of Cell and Developmental Biology*, vol. 30, pp. 255–289, 2014.
- [32] M. Tkach and C. Théry, "Communication by extracellular vesicles: where we are and where we need to go," *Cell*, vol. 164, pp. 1226–1232, 2016.
- [33] T. Pisitkun, R. F. Shen, and M. A. Knepper, "Identification and proteomic profiling of exosomes in human urine," *Proceedings of the National Academy of Sciences of the United States of America*, vol. 101, pp. 13368–13373, 2004.
- [34] M. Baj-Krzyworzeka, M. Majka, D. Pratico et al., "Platelet-derived microparticles stimulate proliferation, survival, adhesion, and chemotaxis of hematopoietic cells," *Experimental Hematology*, vol. 30, pp. 450–459, 2002.
- [35] F. Shiri, B. K. Gale, H. Sant, G. T. Bardi, J. L. Hood, and K. E. Petersen, "Characterization of human glioblastoma versus normal plasma-derived extracellular vesicles preisolated by differential centrifugation using cyclical electrical field-flow fractionation," *Analytical Chemistry*, vol. 92, no. 14, pp. 9866–9876, 2020.
- [36] A. Ł. Zadka, A. Piotrowska, and A. Opalińska, "Comparative analysis of exosome markers and extracellular vesicles between colorectal cancer and cancer-associated normal colonic mucosa," *Polish Archives of Internal Medicine*, vol. 4, 2020.
- [37] A. Chaparro Padilla, L. Weber Aracena, O. Realini Fuentes et al., "Molecular signatures of extracellular vesicles in oral fluids of periodontitis patients," *Oral Diseases*, vol. 26, pp. 1318–1325, 2020.
- [38] V. Dozio, V. Lejon, D. Mumba Ngoyi, P. Büscher, J. C. Sanchez, and N. Tiberti, "Cerebrospinal fluid-derived microvesicles from sleeping sickness patients alter protein expression in human astrocytes," *Frontiers in Cellular and Infection Microbiology*, vol. 9, 2019.

- [39] L. B. Jones, S. Kumar, C. R. Bell et al., "Effects of *Pseudomonas aeruginosa* on microglial-derived extracellular vesicle biogenesis and composition," *Pathogens*, vol. 8, 2019.
- [40] A. F. Frade-Barros, B. M. Ianni, S. Cabantous et al., "Polymorphisms in genes affecting interferon- γ production and Th1 T cell differentiation are associated with progression to Chagas disease cardiomyopathy," *Frontiers in Immunology*, vol. 11, pp. 1–12, 2020.
- [41] M. S. Rial, E. C. Arrúa, M. A. Natale et al., "Efficacy of continuous versus intermittent administration of nanoformulated benznidazole during the chronic phase of *Trypanosoma cruzi* Nicaragua infection in mice," *The Journal of Antimicrobial Chemotherapy*, vol. 75, pp. 1906–1916, 2020.
- [42] B. C. de Carvalho, M. Wesley, A. Moraes et al., "Correlation of parasite burden, kDNA integration, autoreactive antibodies, and cytokine pattern in the pathophysiology of Chagas disease," *Frontiers in Microbiology*, vol. 10, p. 1856, 2019.
- [43] J. Tosello Boari, C. L. Araujo Furlan, F. Fiocca Vernengo et al., "IL-17RA-signaling modulates CD8⁺ T cell survival and exhaustion during *Trypanosoma cruzi* infection," *Frontiers in Immunology*, vol. 9, p. 2347, 2018.
- [44] A. P. Di Battista, N. Churchill, S. G. Rhind, D. Richards, and M. G. Hutchison, "The relationship between symptom burden and systemic inflammation differs between male and female athletes following concussion," *BMC Immunology*, vol. 21, no. 1, article 11, 2020.
- [45] C. Franceschi, M. Bonafè, S. Valensin et al., "Inflamm-aging: an evolutionary perspective on immunosenescence," *Annals of the New York Academy of Sciences*, vol. 908, pp. 244–254, 2000.
- [46] G. R. Mundy, "Osteoporosis and inflammation," *Nutrition Reviews*, vol. 65, pp. S147–S151, 2008.
- [47] P. Sarzi-Puttini, F. Atzeni, A. Doria, L. Iaccarino, and M. Turiel, "Tumor necrosis factor- α , biologic agents and cardiovascular risk," *Lupus*, vol. 14, pp. 780–784, 2005.
- [48] L. Koelman, O. Pivovarova-Ramich, A. F. H. Pfeiffer, T. Grune, and K. Aleksandrova, "Cytokines for evaluation of chronic inflammatory status in ageing research: reliability and phenotypic characterisation," *Immunity & Ageing*, vol. 16, 2019.
- [49] M. Meuser-Batista, N. Vacani-Martins, C. M. Cascabulho, D. G. Beghini, and A. Henriques-Pons, "In the presence of *Trypanosoma cruzi* antigens, activated peripheral T lymphocytes retained in the liver induce a proinflammatory phenotypic and functional shift in intrahepatic T lymphocyte," *Journal of Leukocyte Biology*, vol. 107, pp. 695–706, 2020.
- [50] É. Santos and L. Menezes Falcão, "Chagas cardiomyopathy and heart failure: from epidemiology to treatment," *Revista Portuguesa de Cardiologia*, vol. 39, pp. 279–289, 2020.
- [51] L. E. Villanueva-Lizama, J. V. Cruz-Chan, L. Versteeg et al., "TLR4 agonist protects against *Trypanosoma cruzi* acute lethal infection by decreasing cardiac parasite burdens," *Parasite Immunology*, vol. 42, 2020.
- [52] R. Almeida Paiva, T. Martins-Marques, K. Jesus et al., "Ischaemia alters the effects of cardiomyocyte-derived extracellular vesicles on macrophage activation," *Journal of Cellular and Molecular Medicine*, vol. 23, pp. 1137–1151, 2019.
- [53] J. Zhang, X. Cui, J. Guo et al., "Small but significant: insights and new perspectives of exosomes in cardiovascular disease," *Journal of Cellular and Molecular Medicine*, vol. 24, 2020.
- [54] C. Vásquez Velásquez, G. Russomando, E. E. Espínola et al., "IL-17A, a possible biomarker for the evaluation of treatment response in *Trypanosoma cruzi* infected children: a 12-months follow-up study in Bolivia," *PLoS Neglected Tropical Diseases*, vol. 13, article e0007715, 2019.
- [55] L. Martin-Jaular, E. S. Nakayasu, M. Ferrer, I. C. Almeida, and H. A. del Portillo, "Exosomes from *Plasmodium yoelii*-infected reticulocytes protect mice from lethal infections," *PLoS One*, vol. 6, article e26588, 2011.
- [56] M. I. Ramirez, P. Deolindo, I. J. de Messias-Reason et al., "Dynamic flux of microvesicles modulate parasite-host cell interaction of *Trypanosoma cruzi* in eukaryotic cells," *Cellular Microbiology*, vol. 19, article e12672, 2017.
- [57] C. Y. Chain, D. E. Pires Souto, M. L. Sbaraglini et al., "*Trypanosoma cruzi* virulence factors for the diagnosis of Chagas' disease," *ACS infectious diseases*, vol. 5, pp. 1813–1819, 2019.
- [58] V. L. Pereira-Chioccola, A. A. Fragata-Filho, A. M. De Aparecida Levy, M. M. Rodrigues, and S. Schenkman, "Enzyme-linked immunoassay using recombinant trans-sialidase of *Trypanosoma cruzi* can be employed for monitoring of patients with Chagas' disease after drug treatment," *Clinical and Diagnostic Laboratory Immunology*, vol. 10, pp. 826–830, 2003.
- [59] E. S. Saba, L. Gueyffier, M. L. Dichtel-Danjoy et al., "Anti-*Trypanosoma cruzi* cross-reactive antibodies detected at high rate in non-exposed individuals living in non-endemic regions: seroprevalence and association to other viral serologies," *PLoS One*, vol. 8, article e74493, 2013.